Aus dem GKSS Forschungszentrum Geesthacht GmbH, Institut für Chemie, Teltow

Die Bedeutung der Volumen- und Oberflächeneigenschaften von Biomaterialien für die Adsorption von Proteinen und nachfolgende zelluläre Reaktionen

Habilitationsschrift

Zur Erlangung des akademischen Grades Doktor rerum naturalium habilitatus

(Dr. rer. nat. habil.)

In der Wissenschaftsdisziplin „Biotechnologie – Biomaterialien“

eingereicht an der

Mathematisch-Naturwissenschaftlichen Fakultät

der Universität Potsdam

Von Dr. Thomas Groth

Geboren am 21.04.1956 in Berlin

Teltow, im Mai 2002

Für meine Ehefrau Karin, meine Kinder Julius und Maximilian, und

meine Mutter Elisabeth Groth

Inhaltsverzeichnis

Danksagung

Mein ganz besonderer Dank gehört Herrn Professor Dieter Paul, der mich in den vergangenen Jahren in meiner Arbeit gefördert und unterstützt hat, und ohne dessen Bereitschaft Biokompatibilitätsstudien am Institut für Chemie des GKSS Forschungszentrums in diesem Umfange wohl nicht zustande gekommen wären.

Großer Dank gilt auch Herrn Professor Günter von Sengbusch, der sich für die Wiederetablierung der Biomaterialforschung am Institut für Chemie in Teltow sehr eingesetzt hat, und seiner Unterstützung unserer Arbeiten auf diesem Gebiet.

Herrn Professor Steup danke ich sehr herzlich für sein Interesse und sein Entgegenkommen, dass ich als externer Habilitand diese Habilitationsschrift an der Universität Potsdam einreichen konnte.

Herrn Professor Burkhardt Micheel danke ich für die Möglichkeit, die Habilitation auf dem Lehrgebiet Biotechnologie-Biomaterialien verteidigen zu können.

Meiner langjährigen Kollegin Barbara Seifert danke ich sehr für die gute Zusammenarbeit, die eine Reihe von Publikationen in der vorliegenden Schrift zum Ergebnis hatte. Ganz besonders danke ich ihr auch für ihre Unterstützung bei der Betreuung von Diplomanden, Doktoranden und Gästen, die gemeinsam mit uns experimentelle Arbeiten am Institut für Chemie durchgeführt haben.

Meiner Mitarbeiterin Ruth Hesse möchte ich ganz besonders für Ihre Geduld und ihre engagierte Mitwirkung an einer Reihe der hier beschriebenen Arbeiten danken. Auch für ihr Organisationstalent, das Labor trotz vieler Mitarbeiter und Gäste immer mit allen notwendigen Ausrüstungsgegenständen und Verbrauchsmitteln am Leben zu erhalten, danke ich ihr sehr.

Meinen Kollegen Wolfgang Albrecht und Günter Malsch bin ich dankbar für die fruchtbare Zusammenarbeit bei der Entwicklung von Copolymeren und Membranen für Biohybrid-Organe.

Meine ganz besonderer und herzlicher Dank gilt meinem Freund und Kollegen George Altankov vom Institut für Biophysik der Bulgarischen Akademie der Wissenschaften, mit dem ich die wohl fruchtbarste Zusammenarbeit über die Jahre hatte, und der damit einen wesentlichen Beitrag zum Zustandekommen dieser Habilitationsschrift geleistet hat. Dies gilt auch für meine Kollegen Mathias Ulbricht und Volkmar Thom.

Ich danke auch allen Gästen, die über kürzere oder längere Zeit mit mir gearbeitet und durch gemeinsame Publikationen zum Werden dieser Schrift beitrugen, wie Nikoletta Katsala, Anelia Kostadinova, Natalia Krasteva, Georgios Mihanetzis und Andreas Podias.

Bedanken möchte ich mich auch bei den Drittmittelgebern, die durch ihre finanzielle Unterstützung die Gastaufenthalte von Wissenschaftlern in meinem Labor ermöglicht haben und zur Finanzierung der Forschungsvorhaben beitrugen. Das waren die Deutsche Forschungsgemeinschaft mit der Projektförderung (Gr 1290/4-1 und 4-2) und der Finanzierung mehrerer Gastaufenthalte bulgarischer Wissenschaftler. Das BMBF hat die bilaterale Zusammenarbeit mit Bulgarien und Griechenland über mehrere Jahre gefördert (Gr 180 und BUL 001/98). Durch das NATO Science Programme wurde ein Linkage Grant mit Bulgarien gefördert (CLG.LST 975147). Die Europäische Union hat im Rahmen des Brite/EuRam III Programms Arbeiten zur Entwicklung von Membranen für Biohybrid-Organe gefördert (BE 97-4329).

Nicht zuletzt möchte ich sehr meiner Familie dafür danken, dass sie über die Jahre, in denen ich mich mit der dieser Arbeit zugrunde liegenden Thematik beschäftigt habe, viel Geduld und Verständnis aufgebracht hat.

0 Motivation für die durchgeführten Untersuchungen

Die in der vorliegenden Habilitationsschrift zusammengefassten Publikationen wurden seit Beginn der neunziger Jahre erarbeitet. Zu diesem Zeitpunkt war der Autor am Universitätsklinikum Charité, in der Abteilung für Biomaterialforschung beschäftigt. Der Arbeitsschwerpunkt bestand in der Untersuchung der Blutverträglichkeit von Materialien. In Zusammenarbeit mit Partnern aus chemischen Instituten wurde an der Entwicklung hämokompatibler Materialien gearbeitet. Eine Reihe der in dieser Habilitationsschrift beschriebenen Arbeiten, wie die Entwicklung blutverträglicher Polyurethane oder die Immobilisierung gerinnungshemmender Substanzen auf Polymeren, entstanden im Ergebnis dieser Kooperationen.

Nach dem Wechsel zum GKSS Forschungszentrum verlagerte sich der Schwerpunkt der Arbeiten auf die Entwicklung von Polymermembranen für biohybride Organe zum Ersatz von Leber und Niere. Für diese Anwendungen muss der Erhalt der Entgiftungsfunktion von immobilisierten Zellen gewährleistet werden. Dies beinhaltet einerseits einen engen Kontakt zwischen Material und zu entgiftendem Blut, stellt aber andererseits die Aufgabe brauchbare Eigenschaften des Substrates für eine erfolgreiche Ansiedlung von Zellen zu entwickeln. Um der Frage nachzugehen, wie sich die Materialeigenschaften auf die Adsorption von Proteinen und nachfolgenden zellulären Reaktionen auswirken, wurden deshalb neben Untersuchungen mit Polymeren auch solche an Modellsubstraten durchgeführt. Hierfür wurden silanisierte Glasoberflächen verwendet, die leicht und reproduzierbar herstellbar sind und eine Reihe methodischer Vorteile für die Untersuchung von Zellen aufweisen. Erkenntnisse sowie Methoden aus diesen Grundlagenuntersuchungen wurden auf die Entwicklung von Materialien für Biohybrid-Organe und die Oberflächenmodifizierung von Polysulfon mit Polyethylenglykol erfolgreich übertragen.

Die Erfahrungen auf dem Gebiet der Entwicklung blutverträglicher und gewebekompatibler Materialien sowie das damit verfügbare Methodenspektrum zur Charakterisierung der Biokompatibilität wurden genutzt, um Membranen für die Herstellung von Biohybrid-Organen zu entwickeln. Dabei standen Membranen auf denen Hepatozyten und Nierenepithelzellen immobilisiert werden können, im Mittelpunkt des Interesses. Zudem wurde auch die Blutverträglichkeit solcher Polymere optimiert.

In der vorliegenden Habilitationsschrift wurde der Versuch unternommen, einen Teil der zu dieser Thematik publizierten Arbeiten in den allgemeinen Kontext von Biomaterialien und Biokompatibilität zu stellen. Dabei wurde, ausgehend von den Eigenschaften der Polymere bzw. deren Grenzflächencharakteristika, der Adsorption von Proteinen und den nachfolgenden Reaktionen des biologischen Systems besondere Aufmerksamkeit gewidmet.

1 Einleitung

1.1 Biomaterialien – Werkstoffe für den Einsatz in der modernen Medizin

Fremdmaterialien wurden bereits im Altertum für den Verschluss von Wunden oder die Füllung von Kavitäten in Zähnen eingesetzt. Eine wirkliche Nutzung von körperfremden Werkstoffen in der Medizin wurde jedoch erst mit der Einführung aseptischer Operationstechniken durch J. Lister und I. Semmelweis in der zweiten Hälfte des 19. Jahrhunderts möglich. Zuvor waren alle Versuche der Implantation von Fremdmaterialien durch die dabei verursachten Infektionen zum Scheitern verurteilt. Die ersten sterilen Implantationen von Fremdmaterialien erfolgten zur Behandlung von Defekten des Stützsystems. Dabei wurden zu Beginn des 20. Jahrhunderts metallische Implantate zur Fixierung von Knochenfrakturen verwendet. Jedoch waren auch diese Versuche zunächst wegen der ungenügenden mechanischen und Korrosionsstabilität der eingesetzten Materialien nicht erfolgreich. Erst mit der fortschreitenden Entwicklung von rostfreiem Stahl und Kobalt-Vanadium-Legierungen in den dreißiger Jahren des vergangenen Jahrhunderts konnten bessere Erfolge bei der Fixierung komplizierter Knochenfrakturen erreicht werden (Park 1995). Die während des 2. Weltkrieges gemachte Beobachtung, dass Flugzeugpiloten, die durch Splitter des Kanzelmaterials Polymethylmethacrylat (PMMA) verletzt wurden, keine chronischen Abwehrreaktionen nach Verbleib des Kunststoffes im Körper zeigten, öffnete auch den Weg für die Anwendung von Polymeren als Implantatwerkstoffe. So wurde PMMA auch bald zum Ersatz der Kornea oder von Teilen des Schädelknochens verwendet (Lendlein 1999). Durch Wilhelm Kolff wurde bereits im Jahre 1944 der erste Versuch unternommen, den Verlust der Nierenfunktion durch die Anwendung einer Cellulose-Membran (Cellophan) im Verfahren der Hämodialyse zu ersetzen, wobei Giftstoffe und Salze aus dem Blut durch die Membran in eine Dialyseflüssigkeit übertreten sollten (Kolff 1944). Diese wenigen Beispiele verdeutlichen, dass erst die im vergangenen Jahrhundert gemachten Fortschritte auf dem Gebiet der Werkstoffwissenschaften und die Möglichkeit der industriellen Herstellung von Metallen, Keramiken und Kunststoffen in hoher Reinheit, verbunden mit der Weiterentwicklung von Operationstechniken, einer breiteren Anwendung von Fremdmaterialien in der Medizin den Weg bereitet haben.

Aus den oben angeführten Beispielen zeigt sich sowohl die Bandbreite der möglichen Anwendungen, als auch die Nutzung verschiedener Werkstoffklassen in der Medizin. Materialien für den medizinischen Einsatz werden als Biomaterialien bezeichnet, wenn diese in zeitweiliger oder dauerhafter Wechselwirkung mit dem biologischen System zur Diagnostik, Behandlung, Unterstützung oder dem Ersatz von Geweben, Organen und

Körperfunktionen dienen sollen (Williams 1987). Andere Definitionen beschränken sich auf die Aussage, dass Biomaterialien unbelebte Materialien repräsentieren, die in Wechselwirkung mit dem biologischen System treten (Black 1992). Eine etwas detailliertere Definition umschreibt den Begriff des Biomaterials als einen Werkstoff synthetischen, aber auch natürlichen Ursprungs, der in Kontakt mit Gewebe, Blut und Körperflüssigkeiten kommt oder für deren Lagerung dient oder für prothetische, therapeutische und diagnostische Anwendungen benutzt wird, ohne den Organismus oder dessen Komponenten zu schädigen (Bruck 1980).

Biomaterialien finden in der modernen Medizin zur Diagnostik und vor allem zur Therapie in allen Körpersystemen Anwendung. So werden Biomaterialien im Stützapparat zum Ersatz von Gelenken und Knochen oder als Nahtmaterial für Binde- und Muskelgewebe eingesetzt (Bayer und Meier 1988). Im Herz-Kreislaufsystem verwendet man Biomaterialien als Herzklappen, Stents oder künstliche Blutgefäße, bis hin zum Linksherz- und Totalherzersatz (Helmus und Hubbell 1993, Ratner 1993). Das Atmungssystem kann zumindest zeitweilig durch einen aus Membranen bestehenden extrakorporalen Oxygenator ersetzt werden (Alpard und Zwischenberger 1998). Bei schweren Verbrennungen kommen spezielle Wundabdeckungen zum Einsatz, oder es wird zunehmend ein künstlich generierter Hautersatz verwendet, der eine Kombination von Biomaterial und Zellen darstellt (Dvorankova et al. 1998). Im Urogenitalsystem werden Katheter und Stents genutzt (Denstedt et al. 2000, Lendlein 1999). Die Nierenfunktion kann über Zeiträume von Jahren bis Jahrzehnten durch die Hämodialyse zumindest teilweise ersetzt werden (Klinkmann und Viencken 1995). Das Nervensystem kann durch die Anwendung von Biomaterialien unterstützt werden, wie bei der Ableitung von überschüssigem Liquor beim Hydrocephalus, beim Herzschrittmacher oder zur Unterstützung der Regeneration peripherer Nerven (Hudson et al. 2000, Park 1995). Endokrine Funktionen versucht man durch die Verkapselung von Drüsenzellen und deren Implantation zu ersetzen (Park 1995). Diese sehr kurze und bei weitem nicht vollständige Zusammenfassung zeigt die Anwendung von Biomaterialien in unterschiedlichen Organsystemen, mit sich daraus ergebenden sehr unterschiedlichen Anforderungen an die physikalisch-chemischen Eigenschaften dieser Werkstoffe.

Um solchen Anforderungen an Biomaterialien für eine spezifische Anwendung, wie ausreichende mechanische Festigkeit und Korrosionsstabilität, gerecht zu werden, wurden die aus technischen Anwendungen verfügbaren Materialklassen wie Metalle, Keramiken und Polymere in der Medizin eingesetzt. Dabei sollte unterstrichen werden, dass viele dieser Werkstoffe in der Vergangenheit nicht explizit für medizinische, sondern eher für technische Applikationen entwickelt wurden. Die Möglichkeit einer medizinischen Anwendung wurde

oftmals ad hoc ermittelt, indem Materialien mit einem bestimmten mechanisch-chemischen Eigenschaftsbild für eine spezifische Anwendung ausgewählt wurden (Lendlein 1999). Durch die vorherige Testung in vitro, dem in vivo Tierversuch und der nachfolgenden klinischen Erprobung konnten geeignete Biomaterialkandidaten ausgewählt werden. Es ist aber naheliegend, dass gerade wegen der Auswahl in Bezug auf physikalisch-chemische Eigenschaften Probleme mit der biologischen Verträglichkeit der Materialien bestehen. Diese können durch die lokale oder systemische Anwendung von Wirkstoffen, wie z.B. Heparin, abgeschwächt werden oder müssen in Abwägung zum therapeutischen Nutzen der Biomaterialanwendung toleriert werden.

Polymere Werkstoffe haben auf Grund ihrer guten Verarbeitbarkeit, ihrer meist guten chemisch-hydrolytischen Beständigkeit und vor allem wegen ihres breiten Eigenschaftsbildes bei einem i.A. relativ geringen Preis sehr vielfältige Anwendungen in der modernen Medizin gefunden. Nachteile von Polymeren bestehen in ihrer oft geringeren mechanischen Stabilität, die zur Deformation der daraus gefertigter Produkte führen kann, und bei längerer Anwendung im Organismus im unvermeidbaren Abbau durch Hydrolyse. Dennoch sind Polymere die am häufigsten verwendete Materialklasse in der Medizin.

1.2 Die Biokompatibilität von Polymeren und anderen Biomaterialien – eine Begriffsbestimmung

Während die physikalisch-chemischen Eigenschaften von Biomaterialien über weite Bereiche gezielt steuerbar sind (siehe auch Punkt 1.3), kann eine Vorhersage der Wechselwirkungen mit den verschiedenen Komponenten des Organismus, wie Proteinen aus Blut und anderen Körperflüssigkeiten, sowie den Zellen in Blut und Gewebe nicht gemacht werden. Diese werden überwiegend durch die Oberflächeneigenschaften der Materialien bestimmt, wobei weiterhin die Zeitdauer der Wechselwirkung, der Einsatzort, aber auch der physiologische Status des Patienten von Bedeutung sind (Klinkmann 1995). Die Verträglichkeit von Biomaterialien, die allgemein als Biokompatibilität bezeichnet wird, lässt sich dabei als die Reaktion des Empfängers auf den Kontakt mit dem körperfremden Material definieren. Biokompatibel bedeutet hierbei im weitesten Sinne, dass der Einsatz des Materials keine schädigenden Auswirkungen auf die Gesundheit des Empfängers haben darf (Williams 1986). Ein biokompatibles Material darf keinen negativen Einfluss auf die umgebenden biologischen Strukturen ausüben, so dass möglichst keine Veränderungen an Proteinen und Zellen nachgewiesen werden können, dass keine abnormale Entzündungsreaktion verursacht wird, dass allergische und immunologische Reaktionen ausbleiben und keine teratogene oder kanzerogene Wirkung auf den Organismus ausgeübt wird (Klinkmann et al. 1984). Dabei muss auch festgestellt werden, dass es keine

Biokompatibilität an sich gibt, sondern diese i.A. für eine bestimmte Anwendung definiert werden muss (Wolf et al. 1988). Das heißt zum Beispiel, dass Materialien, die für die Implantation im Knochen einen möglichst engen Kontakt mit Zellen haben sollen, auf der anderen Seite eher ungeeignet für den Blutkontakt sind, da sie die Adhäsion und Aktivierung von Blutzellen verursachen könnten. Umgekehrt sind Materialien, die für den Blutkontakt vorgesehen sind, so konzipiert, dass sie nur gering adsorptiv und adhäsiv für Blutkomponenten sind, was wiederum deren Anwendung für eine Implantation im Gewebe, bei der ein direkter Kontakt hergestellt werden soll, eher ungünstig erscheinen lässt. Andere Biokompatibilitätskriterien betreffen die Funktionalität der Biomaterialien bzw. daraus gefertigter Implantate, Vorrichtungen und Geräte (Park 1995). Dazu gehören der Anwendung genügende mechanische Eigenschaften, wie Elastizität, Steifheit, Stärke und Ermüdungsverhalten. Materialien für den Einsatz im Auge müssen brauchbare optische Eigenschaften aufweisen, Membranen für die Hämodialyse müssen bestimmte Permeabilitäten aufweisen, usw..

Die Testung der Biomaterialien folgt im Allgemeinen einem hierarchischen Prinzip, wobei zunächst deren physikalisch-chemische Eigenschaften bestimmt werden. Dazu gehören Eigenschaften, wie Zug- und Biegefestigkeiten, Korrosionsstabilität, Hydrolysebeständigkeit, etc. (Park 1995). Dann können in vitro Untersuchungen mit Zellkultursystemen erfolgen, die eine Aussage über die Biokompatibilität erlauben sollen. Dazu zählen eine Reihe von Parametern wie beispielsweise die Zellvitalität, Zelladhäsion, das Zellwachstum und der Zellstoffwechsel sowie die Stabilität spezifischer Zellfunktionen (Kirkpatrick und Mittermayer 1990). Biokompatibilitätsuntersuchungen von Materialien können in zwei Hauptrichtungen - Biosicherheit und Biofunktionalität -unterschieden werden (Kirkpatrick et al. 1998). Die Biosicherheit beinhaltet die Untersuchung von Zytotoxizität, Mutagenität und Kanzerogenität potentieller Biomaterialien. Diese können durch eine Reihe von in vitro Untersuchungen bestimmt werden, die solche schädigenden Effekte von Materialien auf den Organismus ausschließen sollen (Anon. ISO 10993, 1992, Groth et al. 1995). Die Biofunktionalität von Biomaterialien zielt dabei auf die spätere Anwendung hin, d.h. im Gegensatz zu eher unspezifischen standardisierten Testsystemen der Biosicherheit werden hier die für die Anwendung relevanten Zellen, Gewebe und Organe im Kontakt mit dem Biomaterial getestet. Das beinhaltet u.a. die Bestimmung von Zelladhäsion, Zellspreitung und nachfolgender Proliferation, wobei ein Schwerpunkt auf die Erfüllung der zellspezifischen Funktionen gerichtet sein sollte (Kirkpatrick et al. 1997, Kirkpatrick et al. 1998). So sind Untersuchungen an knochenkontaktierenden Biomaterialien darauf gerichtet, die Vitalität, das Wachstum und vor allem die Fähigkeit von Osteoblasten zur Neubildung von Knochen

nachzuweisen. Das kann zunächst in vitro geschehen, wird dann aber durch Implantation der Materialien im Tierversuch zu prüfen sein (Gross 1988).

In Analogie zu diesen Untersuchungen wird die Blutverträglichkeit von Biomaterialien zunächst ebenfalls wie oben beschrieben durch die Bewertung der Biosicherheit nachzuweisen sein. Nachfolgend können dann in vitro Untersuchungen mit Human-Blut durchgeführt werden, die die wesentlichen im Blut befindlichen Abwehr- bzw. Regulationssysteme humoraler und zellulärer Natur berücksichtigen (Anonymus, ISO 10993-4, 1992). Nachdem erfolgreiche in vitro Untersuchungen durchgeführt wurden, können bestimmte tierexperimentelle Untersuchungen und nachfolgend erste klinische Tests vorgenommen werden (ISO 10993 1992).

Trotz umfangreicher Untersuchungen muss man jedoch davon ausgehen, dass die Mehrzahl der gegenwärtig eingesetzten Materialien vom Organismus als fremd erkannt wird, was mit moderaten bis hin zu dramatischen Abwehrreaktionen, wie lokalen Entzündungsvorgängen, einer Thrombusbildungen und anderen Reaktionen, einher gehen kann. Ursache dafür ist die eher unphysiologische Wechselwirkung zwischen herkömmlichen Biomaterialien und dem biologischen System. Auf deren Ursachen und die Möglichkeiten, diese Wechselwirkungen zugunsten einer besseren Verträglichkeit durch die Anpassung von Volumenzusammensetzung und Oberflächeneigenschaften von Polymeren positiv zu beeinflussen, soll im Rahmen dieser Habilitationsschrift näher eingegangen werden.

2 Für die Biokompatibilität relevante Eigenschaften von Polymeren

Konventionelle Biomaterialien, wie sie gegenwärtig klinisch eingesetzt werden, sind im Vergleich zu körpereigenen Materialien weitgehend homogen aufgebaut. Das gilt nicht nur für anorganische, wie keramische und metallische Werkstoffe, sondern auch für Polymere. Ihnen fehlt damit die Komplexität biologischer Strukturen, die über spezifische Erkennungsmechanismen mit ihrer Umgebung kommunizieren und so die Struktur und Funktion von Zellen, Geweben und Organen gewährleisten. Das führt zu Problemen bei ihrer Anwendung, die sich im Wesentlichen aus dem Charakter der Grenzfläche Biomaterial-biologisches System ableiten lassen. Da der überwiegende Teil der in der Habilitationsschrift verwendeten Arbeiten sich mit der Wechselwirkung von polymeren Werkstoffen mit Proteinen und Zellen beschäftigt, soll an dieser Stelle nur kurz auf die Klassifizierung und Eigenschaften von polymeren Werkstoffen eingegangen werden.

2.1 Beziehung zwischen Polymerstruktur und Volumeneigenschaften

Organische Polymere sind langkettige Moleküle, welche durch kovalente Bindungen zwischen Grundbausteinen – den Monomeren - entlang einer Hauptkette gebildet werden. Eine wichtige Kenngröße für das Polymer stellt der Polymerisationsgrad dar. Er beschreibt die durchschnittliche Anzahl von Untereinheiten in einer Polymerkette. Dabei kann in einem Polymer die Anzahl von Untereinheiten je Kette variieren, was durch die Polymerisationsbedingungen bedingt ist. Das Molekulargewicht der Ketten kann rechnerisch aus dem Polymerisationsgrad und dem Molekulargewicht der Untereinheit ermittelt werden. Polymere, die aus identischen Untereinheiten, d.h. Monomeren, aufgebaut sind, werden als Homopolymere bezeichnet. Homopolymere sind beispielsweise das Polyvinylchlorid, Polyethylen und Polyacrylnitril. Bei der Polymerisation verschiedenartiger Monomere entstehen Copolymere wie die Polyurethane, Polyharnstoffe und Polyimide (Braun et al. 1999).

Polymere lassen sich durch ihre Kettenstruktur charakterisieren, die als lineare, verzweigte oder vernetzte Kette vorliegen kann. Lineare Makromoleküle werden als Isoketten bezeichnet, wenn sich in der Hauptkette nur Kohlenstoffatome befinden. Heteroketten enthalten dagegen noch weitere Elemente, wie z.B. Sauerstoff bei Polyacetalen oder Stickstoff bei Polyamiden. Polymere mit gleichen Grundbausteinen können sich dennoch durch Struktur- und Stereoisomerie unterscheiden. Von Strukturisomerie spricht man, wenn bei gleicher Monomereinheit lineare, verzweigte oder vernetzte Ketten gebildet werden. Die Stereoisomerie beinhaltet die räumliche Anordnung der Kette, wie beispielsweise die cis/trans-Isomerie bei Vorhandensein von Doppelbindungen in der Hauptkette. Bei linearen Ketten mit seitenständigen Substituenten existiert zudem die Möglichkeit der verschiedenen räumlichen Anordnungen von Seitengruppen, die als Taktizität bezeichnet wird. Sind alle Substituenten auf einer Seite der Ketten, bezeichnet man dies als isotaktisch, bei alternierender Anordnung (rechts-links) als syndiotaktisch, und bei dem Fehlen jeglicher Ordnung als ataktisch. Bei Copolymeren besteht zusätzlich noch die Möglichkeit der Strukturisomerie, die durch die Verteilung der verschiedenen Monomereinheiten gegeben ist. Bei regelmäßigem Wechsel der Monomereinheiten A und B (A-B-A-B-) spricht man von alternierenden Copolymeren. Sind die Monomere unregelmäßig verteilt, bezeichnet man dies als statistisches Copolymer (A-A-B-A-B-B-A). Die Eigenschaften solcher Polymere, die auf Basis von Acrylnitril mit verschiedenen Comonomeren synthetisiert wurden, werden in **Publikation 2, 17 und 18** beschrieben. Bei Vorhandensein von größeren Einheiten (Oligomeren), die aus einem Monomertyp bestehen, spricht man von Block-Copolymeren (A-A-A-A-B-B-B-B-). Dazu zählen auch die Polyurethane, auf deren Eigenschaften in **Publikation 9 und 10** eingegangen wird. Es ist auch möglich, nachträglich Seitenketten

kovalent zu koppeln, was als Pfropf-Copolymerisation bezeichnet wird. Diese Art von Polymeren wird in **Publikation 11 und 12** beschrieben, wo durch Photoimmobilisation Polyethylenglykol auf Polysulfon gepfropft wurde.

Die Eigenschaften von Polymeren werden durch die Konformation und Konfiguration der Polymerketten bestimmt. Im isolierten Zustand, d.h. in verdünnter Lösung nimmt die Polymerkette den Zustand größter Entropie ein, der als lockeres, statistisches Knäuel bezeichnet wird. Dabei hat die Kette nur mit sich und den Lösungsmittelmolekülen physikalische Wechselwirkungen. Im festen Zustand hingegen, treten die Wechselwirkungen der Ketten untereinander in den Vordergrund. Die Polymerketten werden dabei durch sekundäre Wechselwirkungskräfte, wie Wasserstoffbrückenbindungen, van der Waals-Kräfte, aber auch primäre kovalente Vernetzung zwischen den Ketten zusammengehalten. Behalten die Ketten eine Knäuelgestalt, die ähnlich der in Lösung ist, spricht man von amorphen Polymeren. Dabei führt die gegenseitige Durchdringung der Ketten zu Verschlaufungen und Verhakungen, die für die physikalischen Eigenschaften des Polymers von Bedeutung sind. Im sogenannten Glaszustand stellt das amorphe Polymer eine isotrope erstarrte Schmelze dar. Amorphe Polymere sind thermoplastisch, transparent und gut löslich bei Raumtemperatur. Beispiele für amorphe Polymere sind das Polyvinylchlorid, Polystyrol, Polymethylmethacrylat, Polysulfon, Polyethersulfon und Polyetherimid. Sind die Polymerketten genügend regelmäßig in ihrer Struktur, können sie beim Abkühlen aus einer Polymerschmelze kristallisieren. Unter diesen Umständen ordnen sich die Ketten in einem dreidimensionalen Gitter relativ regelmäßig an. Es ist jedoch relativ selten, dass sich ein vollständiges Gitter ausbildet. Eher finden sich kristalline Bereiche neben amorphen Regionen. Die kristallinen Bereiche haben typischerweise eine Ausdehnung von 10-40 nm, wobei sich die einzelnen Polymerketten sowohl durch kristalline als auch amorphe Bereiche hindurchziehen. Dadurch sind die kristallinen Bereiche miteinander verbunden, was für die mechanischen Eigenschaften des Polymers von Bedeutung ist. Die Fähigkeit zur Ausbildung von kristallinen Bereichen hängt von den Eigenschaften der Polymerketten, wie der Kettenstruktur (linear oder verzweigt), der Symmetrie entlang der Hauptkette, der Art und Anordnung der Seitengruppen, dem Vorhandensein polarer Gruppen, die beispielsweise die Ausbildung von Wasserstoffbrücken verursachen, u.a. Faktoren ab. Lineare Polymere kristallisieren relativ leicht unterhalb der Glasübergangstemperatur. Steigt die Kettenlänge jedoch auf über 50 Monomereinheiten (z.B. Polyethylen), können die Ketten nicht mehr vollständig auskristallisieren. Verzweigte Polymere können bedingt durch die sterische Hinderung der Seitengruppen nicht ohne weiteres kristalline Strukturen bilden. Diese nur teilweise kristallisierten Strukturen von Polymeren werden daher auch als semikristallin

bezeichnet. Kristalline Polymere sind opak und nur in wenigen Lösungsmitteln bei höheren Temperaturen löslich (Braun et al. 1999, Park 1995).

Die chemisch-physikalischen Eigenschaften von Polymeren können daher in vielfältiger Art und Weise beeinflusst werden. Dabei spielt die chemische Zusammensetzung eine besondere Rolle, um die Eigenschaften an eine bestimmte Nutzung anzupassen. Das Molekulargewicht eines Polymers und dessen Verteilung haben einen großen Einfluss auf die Polymereigenschaften, da die Rigidität eines Kunststoffes durch die Länge und Art der Ketten bestimmt wird. Die Molekulargewichtsverteilung ist von besonderer Bedeutung, da vorhandene kurzkettige Makromoleküle als Weichmacher fungieren. Auf diese Weise können auch sehr spröde Polymere durch den Zusatz von kurzkettigen Polymeren flexibler gemacht werden. Ein Beispiel dafür stellt PVC dar, das durch den Zusatz von Weichmachern flexibel wird und damit beispielsweise zu Blutschläuchen verarbeitet werden kann. Auch die chemische Zusammensetzung der Polymerhauptkette oder von Seitengruppen hat einen großen Einfluss auf die Polymereigenschaften. Beispielsweise erhöht der Ersatz von Kohlenstoff in der Polymerhauptkette durch Sauerstoff oder Schwefel die Rotationsfreiheitsgrade der Kette, was diese flexibler macht und sich in einer Erniedrigung des Schmelzpunktes und der Glasübergangstemperatur des Polymers äußert. Eine Vergrößerung der Seitenketten, wie beispielsweise bei Substitution von Wasserstoff durch Methyl, Ethyl verringert die Kristallinität, d.h. Packungsdichte der Ketten. Durch die verringerten intermolekularen Wechselwirkungen sinken der Schmelzpunkt und die Glasübergangstemperatur, während das Vorhandensein polarer Substituenten diese erhöht (Park 1995). Mit diesem Wissen lassen sich physikalisch-chemische Eigenschaften von Polymeren relativ gut einstellen. Die Volumenzusammensetzung des Polymers hat dabei auch einen großen Einfluss auf die Biokompatibilität, da sie die Eigenschaften der Polymeroberfläche bestimmt.

2.2 Zusammenhänge zwischen Polymerzusammensetzung und Oberflächeneigenschaften

Für die Biokompatibilität von polymeren und anderen Biomaterialien sind die Oberflächeneigenschaften von entscheidender Bedeutung. Diese bestimmen in enger Wechselwirkung mit dem umgebenden biologischen Milieu die nachfolgenden Reaktionen des Organismus. Die Oberflächeneigenschaften von Polymeren werden durch deren Volumenzusammensetzung determiniert. Wie im vorangegangenen Abschnitt 2.1 zusammengefasst, ist eine fast unüberschaubare Vielzahl von Polymeren bezüglich ihrer Zusammensetzung denkbar. Sie können jedoch grundlegend klassifiziert werden durch deren Morphologie, d.h. amorph, kristallin oder als phasenseparierte Block-Copolymer mit

amorphen und kristallinen oder hydrophilen und hydrophoben Domänen. Ein wichtiger Parameter ist daher auch der Gehalt an apolaren oder polaren bzw. geladenen Komponenten. Dieses kann die Polymerhauptkette betreffen, die apolar ist, wenn sie nur aus Kohlenstoffatomen besteht, und damit ein hydrophobes Polymer bildet. Beispiele für solch hydrophobe Homopolymere stellen die Polyolefine, wie das Polyethylen, dar. Auf der anderen Seite können in Heteroketten oder Comonomeren vorhandene polare Komponenten, wie z.B. Sauerstoff oder Stickstoff, die Hydrophilie des Polymers erhöhen. Beispiele hierfür sind die Polyamide, Polyester, Polyharnstoffe und Polyurethane, die wesentlich besser von Wasser benetzbar sind als beispielsweise Polyolefine. Der Gehalt von Seitengruppen trägt weiterhin wesentlich zu den Oberflächeneigenschaften von Polymeren bei. Apolare Seitengruppen, wie z.B. Methyl-, Ethyl-, Propyl-, aromatische u.a. Gruppen erhöhen die Hydrophobizität des Polymers, während die Präsenz von Sauerstoff, Stickstoff und Schwefel in Seitengruppen dessen Hydrophilie verbessert. Diese bis hier beschriebenen Eigenschaften der Polymere bestimmen auch die Mobilität der Ketten im Kontakt zu wässrigen Medien. So sind kristalline, hydrophobe Polymere eher immobil, während amorphe Polymere bzw. Domänen mit vorhandenen polaren oder geladenen Ketten bei Kontakt mit Wasser eine erhöhte Mobilität aufweisen. Diese kann beispielsweise zu einer Quellung des Polymeren bis hin zur Bildung von Hydrogelen führen. Neben den intrinsischen Volumeneigenschaften des Polymers spielt die durch die Verarbeitung bedingte Oberflächentopographie eine wichtige Rolle für die Proteinadsorption und Wechselwirkung mit Zellen. Dazu zählt die Oberflächenrauhigkeit oder auch das Vorhandensein von spezifischen (periodischen) Oberflächenstrukturen. Die wichtigsten Eigenschaften einer Grenzfläche zwischen Polymer und wässrigem (biologischem) System, die für die Wechselwirkung mit biologischen Komponenten relevant sind, bestehen in deren Benetzbarkeit und dem elektrochemischen Zustand der Polymeroberfläche (Norde und Lyklema, 1991).

Die Benetzbarkeit von Oberflächen kann durch die Bestimmung des Randwinkels von Wassertropfen ermittelt werden. Es sollte hierbei betont werden, dass die Wechselwirkung von Biomaterialien und damit auch Polymeren mit Wasser von fundamentaler Bedeutung ist. Wasser ist Hauptbestandteil aller komplexen biologischen Entitäten, wie Zellen, Blut, usw. Wasser bildet eine Hydrathülle um Ionen, Proteine und Zellen und spielt daher auch eine wichtige Rolle bei allen Arten von Grenzflächen von Biomaterialien mit biologischen Strukturen. Wassermoleküle haben eine starke Polarität, was zu den besonderen Eigenschaften des Wassers führt, insbesondere die Fähigkeit der Wassermoleküle zur Selbstassoziation durch die Ausbildung von Wasserstoffbrückenbindungen (Vogler 1998). Da hydrophobe Polymere an ihrer Oberfläche keine Fähigkeit zur Ausbildung von

Wasserstoffbrückenbindungen besitzen, kommt es an der Grenzfläche zwischen hydrophobem Biomaterial und Wasser zu einer sehr starken Assoziation der Wassermoleküle untereinander. Auf diese Weise erreichen die Wassermoleküle an der Grenzfläche einen wesentlich höheren Ordnungszustand und damit eine geringere Entropie als im angrenzenden Volumen (Norde und Lyklema 1991; Vogler 1998). Dieses hat Auswirkungen auf die nachfolgende Wechselwirkung mit Proteinen, wie im nächsten Abschnitt beschrieben wird.

In wässrigen Systemen besitzen zudem fast alle Grenzflächen von Polymeren und anderen Biomaterialien elektrisch geladene Gruppen. Diese Ladungen können durch die Assoziation oder Dissoziation von Oberflächengruppen entstehen. Dazu kommt es, wenn ionisierbare Gruppen an der Oberfläche existieren. Bei biologischen Materialien, wie z.B. Proteinen, sind dies Carboxyl-, Amino-, Imidazol- und Phosphatgruppen, die alle mit Protonen assoziiert sind. Bei Polymeren ist dies durch deren chemische Zusammensetzung bestimmt, wobei auch hier Carboxyl-, Amino-, Sulfon- und andere Gruppen einen Beitrag zur Oberflächenladung erbringen können. Eine weitere Möglichkeit der Präsenz von Ladungen auf Polymeren kann durch die spezifische Adsorption von Ionen aus der Lösung erreicht werden. Diese spezifische Adsorption setzt dabei voraus, dass die Adsorptionskraft nicht-elektrischer Natur ist (Norde und Lyklema, 1991). So lassen sich beispielsweise auch bei apolaren Polymeren Oberflächenladungen nachweisen, die durch Adsorption von Ionen verursacht werden (Werner et al. 1998). Unter Gleichgewichtsbedingungen muss die Grenzfläche zusammen mit der benachbarten Lösung elektroneutral sein. Dabei kommt es zur Ausbildung einer elektrischen Doppelschicht, die durch die Präsenz einer eher fixierten Schicht von Gegenionen nahe der Polymeroberfläche mit einer darauf folgenden diffusen Schicht von Gegenionen bestimmt wird und deren Konzentration mit zunehmender Entfernung exponentiell abnimmt. Modelle für solche elektrischen Doppelschichten, wie sie sich auch an Polymeroberflächen ausbilden, wurden von Guy und Stern zu Beginn des vergangenen Jahrhunderts entwickelt. Eine Übersicht über diese Modelle wurde von Lyklema 1985 veröffentlicht. Geladene Grenzflächen lassen sich durch das Zeta-Potential charakterisieren, welches das Potential an der hydrodynamischen Scherfläche der Phasengrenze darstellt. Diese werden üblicherweise durch Strömungspotentialmessungen ermittelt, bei denen durch den Fluss einer Elektrolytlösung über das Biomaterial in einem Strömungskanal eine Potentialdifferenz zwischen Eingang und Ausgang generiert wird, die gemessen werden kann und der Berechnung des Zeta-Potentials dient (van Wageningen und Andrade 1980, Werner et al. 1998).

3 Die Biokompatibilität von Polymeren – Oberflächeneigenschaften, Proteinadsorption und zelluläre Reaktionen

3.1 Die Adsorption von Proteinen an Biomaterialien

Treten Biomaterialien mit proteinhaltigen Medien und Körperflüssigkeiten in Kontakt, kommt es innerhalb kurzer Zeit zur Adsorption von Proteinen. Die treibenden Kräfte für diesen Prozess sind in den Oberflächeneigenschaften der Polymere bzw. anderer Biomaterialien einerseits und der Zusammensetzung des umgebenden Milieus andererseits zu suchen.

Proteine können als Copolymere aus 22 verschiedenen Aminosäuren angesehen werden, die über eine Peptidbindung verknüpft sind. Dabei unterscheiden sich die Aminosäuren durch ihre Seitengruppen. Einige Aminosäuren haben saure, andere basische Reste, so dass Polypeptide amphoter sind. Auch variieren die Seitengruppen in ihrer Hydrophobizität bzw. Polarität, was die Polypeptidkette zudem amphiphil werden lässt. Die Primärstruktur eines Proteins wird durch die Sequenz der Aminosäuren in der Polypeptidkette bestimmt. Mit dieser wird aber auch gleichzeitig die räumliche Anordnung des Proteins als Sekundärstruktur in Form von α-Helices, β-Faltblatt und statistischem Knäuel bestimmt. Die Tertiärstruktur des Proteins ergibt sich aus der Art und Weise, wie die einzelnen Segmente der Polypeptidkette im Raum angeordnet sind (Darnell et al. 1994). In Hinsicht auf ihre Raumstruktur können Proteine unterteilt werden in solche Polypeptide, die stark solvatisiert und flexibel sind und damit ein expandiertes Knäuel bilden, Polypeptide, die stark geordnete Strukturen wie α-Helices oder β-Faltblätter ausbilden, oder solche Moleküle, die sowohl α-Helices als auch β-Faltblätter und zufällig strukturierte Teile in einer kompakten Struktur enthalten. Die letztere Art sind die globulären Proteine, die eine Vielzahl enzymatischer, immunologischer und Transportfunktionen ausüben (Norde und Lyklema, 1991). Gerade bei der Wechselwirkung von Biomaterialien mit biologischen Komponenten spielt die Adsorption dieser Proteine eine herausragende Rolle für die Biokompatibilität.

Die Tertiärstruktur von Proteinen ist das Ergebnis einer Reihe von Wechselwirkungen sowohl innerhalb der Polypeptidkette als auch mit dem umgebenden wässrigen Milieu. Globuläre Proteine in wässrigen Medien haben eine Reihe von Strukturcharakteristika gemein (Norde und Lyklema, 1991):

- Sie sind annähernd sphärisch mit einem Durchmesser im Nanometerbereich.
- Hydrophobe Seitengruppen des Proteins befinden sich meist im Innern des Moleküls abgeschirmt vom Wasser. Beim Vorhandensein hydrophiler Aminsäuren in der Kette ist es damit auch wahrscheinlich, dass sich hydrophile Teile der Polypeptidkette im Innern befinden.

?? Geladene Gruppen werden vorzugsweise in dem Wasser zugewandeten Äußeren des Proteins gefunden. Geladene Gruppen im Innern des Proteins kommen stets paarweise vor.

?? Die Atome in einem Protein sind dicht gepackt, insbesondere in hydrophoben inneren Bereichen, wobei die Packungsdichte der in anorganischen Kristallen entsprechen kann.

Coulomb-Kräfte können zur Stabilisierung der kompakten Struktur globulärer Proteine beitragen. Um den isoelektrischen Punkt herum besitzt das Protein gleich viele positive und negative Ladungen, wobei die Netto-Coulomb-Kraft innerhalb des Proteins anziehend ist, was zu einer kompakten Struktur des Proteins führt. Außerhalb des isoelektrischen Punktes ist die Coulomb-Wechselwirkung repulsiv, was zu einer ausgedehnteren Struktur des Proteins führt (Norde, 1986). Die Hauptursache für die Faltung von Proteinen in eine kompakte Struktur stellt jedoch die Dehydratation hydrophober Seitengruppen dar, die auf den Entropiegewinn durch die Freisetzung von Wassermolekülen von den hydrophoben Komponenten zurückführbar ist. Andere Wechselwirkungskräfte, wie Wasserstoffbrückenbindungen, Dipol-Dipol-Wechselwirkungen und van der Waals-Wechselwirkungen, die hier zusammenfassend als Donor-Akzeptor-Wechselwirkungen bezeichnet werden, haben einen geringeren Einfluss auf die Stabilität der Proteinstruktur (Norde und Lyklema, 1991).

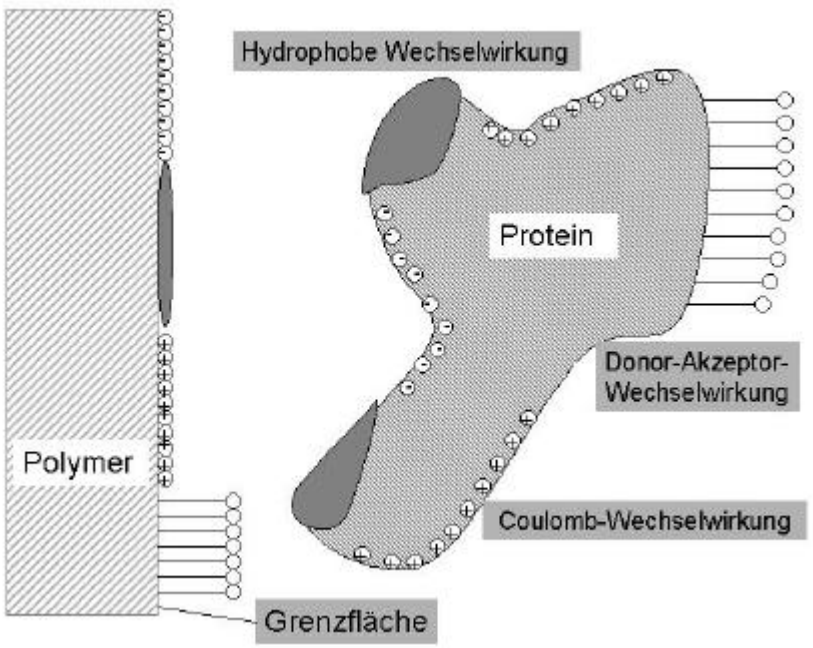

Abbildung 1: Schematische Darstellung der Hauptwechselwirkungskräfte zwischen Protein und Polymeroberfläche.

Die Adsorption von Proteinen ist demzufolge hauptsächlich durch die hydrophobe und die Coulomb als Hauptwechselwirkungen gekennzeichnet, wobei aber auch ein geringerer Beitrag durch Donor-Akzeptor-Wechselwirkungen erfolgen kann, was in Abbildung 1 schematisch dargestellt wurde (Sigal et al. 1998). Gerade viele Polymere als eher hydrophobe Werkstoffe führen zur Adsorption von Proteinen. Diese wird durch den Entropiegewinn bei der Dehydratation hydrophober Bereiche der Oberfläche und des Proteins energetisch bevorzugt. Es zeigt sich dabei auch, dass selbst bei vorhandener elektrostatischer Abstoßung gleichgeladener Areale der Oberfläche und des Proteins die hydrophobe Wechselwirkung einen größeren Zuwachs der freien Energie des Systems erlaubt und es deshalb immer zur Adsorption von Proteinen kommt (Norde und Lyklema, 1991). Ein weiterer Beitrag zur Adsorption von Proteinen erfolgt durch die Coulomb-Wechselwirkung geladener Areale der Oberfläche mit solchen Teilen des Proteins, die entgegengesetzt geladen sind. Diese sind zwar im Allgemeinen durch Gegenionen aus dem umgebenden Medium abgeschirmt. Jedoch kann durch die Umverteilung von Ladungen während der Adsorption ebenfalls eine Zunahme der freien Energie des Systems erfolgen, so dass die Adsorption von Proteinen begünstigt wird (Norde und Lyklema, 1991). Schließlich kann es während der Adsorption von Proteinen an Grenzflächen zu Konformationsänderungen kommen. Ursache hierfür ist, dass die in Lösung vorliegende Konformation von Proteinen nur eine von vielen möglichen energetisch bevorzugten Raumstrukturen darstellt. Der Transfer von Proteinen aus der Lösung an eine Grenzfläche beinhaltet eine Veränderung der Umgebungsbedingungen. Unter Einfluss der Oberflächen kann durch die Neuanordnung geladener Gruppen die freie Energie ebenfalls zunehmen. Bei Wechselwirkung mit hydrophoben Oberflächen bzw. Arealen können zudem hydrophobe Anteile des Proteins, die normalerweise im Innern versteckt sind, in direkten Kontakt mit der Oberfläche treten. Auch dieses führt durch den damit verbundenen Entropiegewinn zu einer Zunahme der freien Energie des Systems. Durch die erfolgenden Konformationsänderungen und damit verbundene Entropieerhöhung wird die Adsorption von Proteinen an Polymeroberflächen zu einem irreversibler Prozess, in dem Sinne, dass Proteine die an der Oberfläche haften, oder auch wieder von dort freigesetzt werden, eine vom Ausgangszustand veränderte Konformation und damit auch biologische Aktivität aufweisen (Feng und Andrade 1994).

In **Publikation 1** wird beschrieben, wie die mit der Veränderung der Oberflächenzusammensetzung von Polymerpartikeln verbundenen Änderungen der Oberflächeneigenschaften die Adsorption von Proteinen aus dem Blutplasma beeinflussen. Dabei war die Wahl der Liganden weniger darauf gerichtet, Grundlagen der Protein-Polymer-Wechselwirkung zu studieren, sondern es galt vielmehr Partikel für die Apherese, d.h. die

spezifische Bindung von Proteinen aus dem Blut für therapeutische oder präparative Zwecke, zu entwickeln. Dazu wurden zunächst aliphatische Diamine mit unterschiedlicher Kettenlänge (C-2 bis C-12) kovalent an mit Glycidylmethacrylat beschichteten Nanopartikel gekoppelt. Weiterhin wurden die Aminosäuren Tryptophan und Histidin und deren Amine über verschiedene Diaminspacer gekoppelt. Zur Charakterisierung der Partikel wurde deren Oberflächenladungsdichte sowie Hydrophobizität bestimmt. Blutplasma wurde an die Partikel adsorbiert. Zunächst wurden die Partikel gewaschen, um nicht gebundene Proteine zu entfernen. Danach wurden die Partikel in einer Lösung mit ionischen Detergentien auf 95°C erhitzt, um adsorbierte Proteine zu desorbieren. Auf diese Weise sollte eine möglichst vollständige Desorption der Proteine möglich sein, die anschließend mit Gelelektrophorese und Immunoblotting analysiert wurden. Im Ergebnis dieser Untersuchungen konnte festgestellt werden, dass i.A. die Adsorption von Proteinen mit der Hydrophobizität der Partikel zunahm, wie es nach Erkenntnissen anderer Autoren zu erwarten war (siehe weiter oben). Dabei wurde durch das Immunoblotting festgestellt, dass insbesondere Albumin dieses Verhalten bestimmt, was mit dessen hoher Konzentration im Blutplasma begründet werden kann. Aber auch für Fibrinogen konnte in Abhängigkeit von der Hydrophobie der gekoppelten Diamine eine Zunahme der Adsorption nachgewiesen werden, wie es auch für andere hydrophobe Materialien bestimmt wurde (Sigal et al. 1998). Insbesondere für die Bindung von Fibrinogen waren aliphatische Diamine größerer Kettenlänge gut geeignet, was deren Anwendung für die selektive Entfernung dieses Proteins aus dem Blutplasma denkbar erscheinen lässt. Andererseits konnte jedoch keine einfachen Korrelationen zwischen Oberflächenladungsdichte der Partikel und der Adsorption von Proteinen nachgewiesen werden. So sind qualitative Zusammenhänge erkennbar, die die Rolle hydrophober und der Coulomb-Wechselwirkungen für die Adsorption von Proteinen bestätigen. Jedoch zeigen die Ergebnisse auch den Einfluss der Art des Liganden, wobei klar wurde, dass aus der Kenntnis physikochemischer Oberflächenparameter allein keine Vorhersage der Proteinadsorption möglich ist. Diese muss deshalb bei Bedarf für ein bestimmtes Polymer immer spezifisch nachgewiesen werden.

Die Veränderungen der Proteinkonformation während des Adsorptionsprozesses implizieren, dass die Adsorption von Proteinen an Grenzflächen, wie der Polymeroberfläche im Kontakt zu biologischen Medien, ein dynamischer Prozess ist. Proteine werden an die Grenzfläche im Wesentlichen über vier Mechanismen transportiert: Diffusion, thermische Konvektion, Fluss-Konvektion und gekoppelte Konvektion-Diffusion (Andrade und Hlady 1986). Dabei kann davon ausgegangen werden, dass die externe Oberflächenchemie des Proteins bestimmt, ob die dabei erfolgenden Zusammenstöße der Proteine mit der Materialoberfläche zur Adsorption führen. Nur solche Zusammenstöße des Proteins mit der Oberfläche, bei

denen das Protein ein Areal präsentiert, das eine signifikante freie Adsorptionsenergie ergibt, werden zur Adsorption des Proteins führen. Nach dem initialen Kontakt mit der Oberfläche kann sich das Protein durch Konformationsänderungen an die neue Umgebung anpassen.

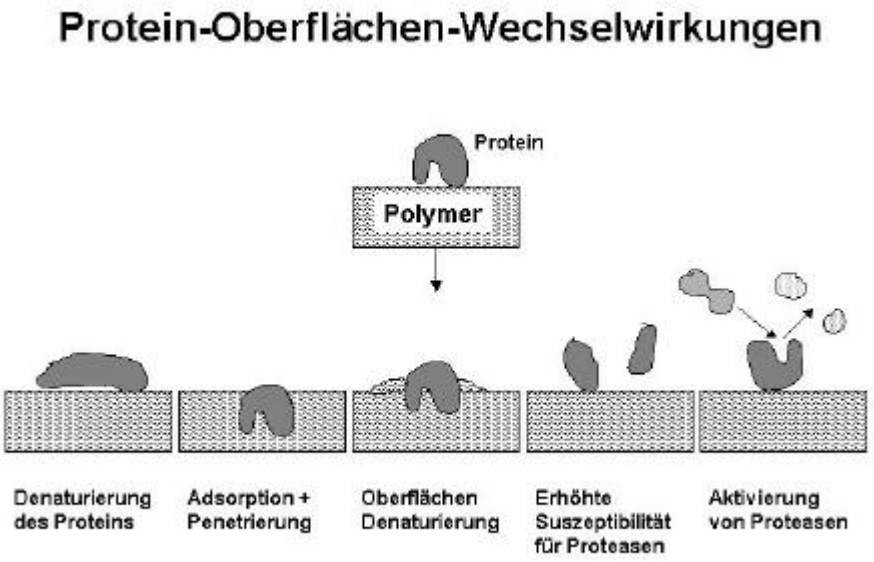

Abbildung 2: Darstellung der verschiedenen Möglichkeiten der Wechselwirkung von Proteinen mit Polymeroberflächen (Andrade 1992).

Proteine geringerer Konformationsstabilität werden größere Konformationsänderungen bis hin zu deren Denaturierung erleiden (Andrade und Hlady 1991). Dieser Prozess ist zeitabhängig, d.h. je länger die Verweilzeit eines Proteins an einer Grenzfläche ist, desto größer sind die erfahrenen Konformationsänderungen, was den Prozess der Proteinadsorption irreversibel macht (Andrade et al. 1987; Young et al. 1988). Die von Proteinen während der Adsorption erfahrenen Konformationsänderungen führen zu einer ganzen Reihe biologischer Konsequenzen. Dazu gehört die höhere Suszeptibilität adsorbierter Proteine gegenüber Proteasen. Eine Reihe von Untersuchungen konnten zeigen, dass die Adsorption von Blutproteinen an Biomaterialien zu deren erhöhter Proteolyse führt, was sich durch eine starke Zunahme proteolytischer Fragmente nach Elution von der Grenzfläche nachweisen lässt (Mulzer und Brash 1989; Parzer et al. 1993). In unmittelbarem Zusammenhang damit steht auch die Aktivierung proteolytischer Enzyme nach Adsorption an Biomaterialien. So ist beispielsweise bekannt, dass der Faktor XII des Blutgerinnungssystems an negativ geladenen Oberflächen eine Autoaktivierung erfährt, was zur Aktivierung des Kontaktsystems der plasmatischen Gerinnung führt (Tans und Rosing 1987; Vogler et al. 1995). Die Wechselwirkung von Polymeren mit Blutplasma kann auch zur Aktivierung des alternativen Weges des Komplementsystems führen. Dabei haben die Hydroxylgruppen der Cellulose eine außergewöhnlich starke Fähigkeit zur Aktivierung des

Komplementsystems (Chenoweth 1987; Klinkmann und Viencken 1995). Die Adsorption von Proteinen und die damit einhergehenden Konformationsänderungen sind auch Ursache dafür, dass Biomaterialien in vivo als fremd erkannt werden, was beispielsweise mit der Opsonisierung von Biomaterialien durch Komplementfaktoren und Immunglobuline erklärt werden kann. Nachfolgend kann es zur Anlagerung und Aktivierung weißer Blutzellen kommen, wie den neutrophilen Granulozyten oder Monozyten, was zur Freisetzung reaktiver Sauerstoffspezies und hydrolytischer Enzyme führen kann und sich klinisch als Entzündungsreaktion manifestiert (McNally und Anderson 1994; Falck 1994, Kao et al. 1999). In vergleichbarer Art und Weise kann die Adsorption von Adhäsivproteinen, wie Fibrinogen, Fibronektin, Thrombospondin, von-Willebrand-Faktor und Vitronektin, aus dem Blut oder der Gewebsflüssigkeit die Anlagerung und Aktivierung von Blutzellen verursachen (Brash 1990; Horbett 1993; Grunkemeier et al. 2000) und bei Implantaten die Anheftung, das Wachstum und die Funktion der adhäsionsabhängigen Zellen aus dem umgebenden Gewebe beeinflussen (Grinnell und Feld 1981; van Wachem et al. 1987; Underwood und Bennett 1993). Auf diese Aspekte wird im weiteren Verlauf der Habilitationsschrift näher einzugehen sein. Abbildung 2 fasst diese Erkenntnisse schematisch zusammen, wobei auch noch das bei Hydrogelen mögliche Eindringen von Proteinen, sowie die Veränderung der Polymeroberflächen durch adsorbierte Proteine einbezogen wurden.

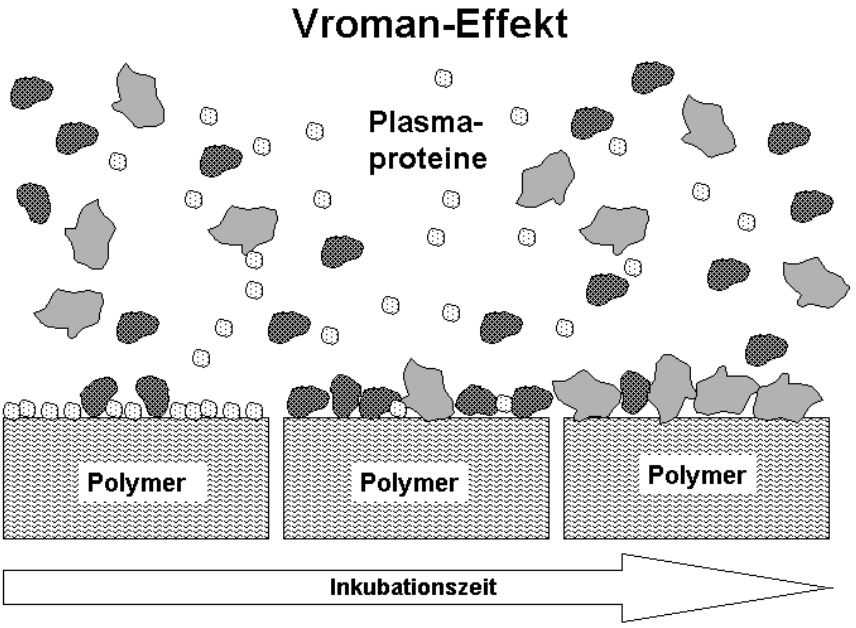

Abbildung 3: Schematische Darstellung des Vroman-Effektes mit Anreicherung größerer Plasmaproteine mit Zunahme der Adsorptionszeit.

Die Dynamik der Proteinadsorption beinhaltet jedoch nicht nur die nach Adsorption eines Proteins einsetzenden Konformationsänderungen. Die bei Wechselwirkung von

Biomaterialien mit dem Organismus vorhandene Umgebung im Blut oder Gewebe stellt ein äußerst komplexes Gemisch an Proteinen dar. Im Blutplasma wurden mehr als 100 verschiedene Proteine nachgewiesen (Fasman 1986). Schon vor längerer Zeit konnte durch Leo Vroman gezeigt werden, dass bei Kontakt von Blutplasma mit künstlichen Oberflächen eine hierarchische Abfolge von Zusammenstößen, Adsorption und Austauschprozessen der Proteine auf der Materialoberfläche stattfindet (Vroman und Adams, 1969 [a]; Vroman und Adams, 1969 [b]). Dieser Effekt konnte durch andere bestätigt werden, und wurde von ihnen als Vromaneffekt bezeichnet (Horbett 1984; Brash und Ten Hove 1985). Das so benannte Phänomen besteht darin, dass niedermolekulare Plasmaproteine wie das Albumin zuerst adsorbieren, dann jedoch durch Immunglobuline und nachfolgend durch Fibrinogen ersetzt werden, bis schließlich hochmolekulare Proteine, wie das hochmolekulare Kininogen (HMWK), auch das Fibrinogen verdrängen (siehe Abbildung 3). Die hier benannten Proteine stellen dabei etablierte Modellsysteme dar, die mit bestimmten Untersuchungssystemen experimentell erfassbar waren. Es ist sicher, dass weitere Proteine an diesem Prozess beteiligt sind. Die besondere Rolle des Kontaktsystems der plasmatischen Gerinnung, insbesondere von HMWK für den Vroman-Effekt, wurde jedoch nachgewiesen, da bei Abwesenheit dieses Proteins Fibrinogen an der Oberfläche verbleibt (Scott 1991).

3.2 Die Wechselwirkung von Blutbestandteilen mit Biomaterialien

3.2.1 Humorale Blutbestandteile in Kontakt mit Biomaterialien

Die Adsorption von Proteinen aus dem Blutplasma spielt eine Schlüsselrolle für die Blutverträglichkeit von Biomaterialien. Über die Rolle adsorbierter Adhäsivproteine wurde bereits im vorangegangenen Abschnitt berichtet. Unter Punkt 3.3 wird weiter darauf einzugehen sein. Die Adsorption spezifischer Plasmaproteine kann zur Aktivierung verschiedener Proteinsysteme im Plasma führen, die mit der Stillung von Blutungen, der unspezifischen Abwehr von Infektionen und der Auflösung von Thromben verbunden sind.

Das Gerinnungssystem

Die plasmatische Gerinnung wird normalerweise durch das extrinsische System aktiviert. Dies tritt bei Verletzungen der Gefäßwände ein, wenn aus beschädigtem Endothel Gewebsfaktor freigesetzt wird, der einen Kofaktor für die Bildung des Prothrombin-Komplexes darstellt. Auf diese Weise kommt es zur Generierung von Thrombin, welches die Blutgerinnung in Gang setzt, was in die Polymerisation von Fibrinogen zu Fibrin mündet (Lane und Bowry 1994). Thrombin ist gleichzeitig der stärkste Aktivator von Thrombozyten, die auf diese Weise zusätzlich in den Gerinnungsprozess einbezogen werden (Lindhout

1994). Eine vereinfachte Übersicht des Gerinnungssystems findet sich in Abbildung 4. Beim Kontakt von Biomaterialien mit Blut wird jedoch das intrinsische System der plasmatischen Gerinnung aktiviert. Dieses wird aus Faktor XI, Faktor XII (Hagemann-Faktor), Prekallikrein und HMWK gebildet. Während der Adsorption von Faktor XII, insbesondere an negativ geladenen hydrophilen Oberflächen, kann es zu dessen Autoaktivierung kommen. Prekallikrein und HMWK zirkulieren im Plasma als ein Komplex. Faktor XIIa spaltet Prekallikrein zu Kallikrein, welches seinerseits weiteren Faktor XII aktiviert. (Kaplan und Silverberg 1987). Adsorbiertes HMWK bildet dabei einen essentiellen Kofaktor für diesen Prozess, der in Abwesenheit einer negativ geladenen Oberfläche nicht ablaufen kann (Kaplan und Silverberg 1987; Lane und Bowry 1994).

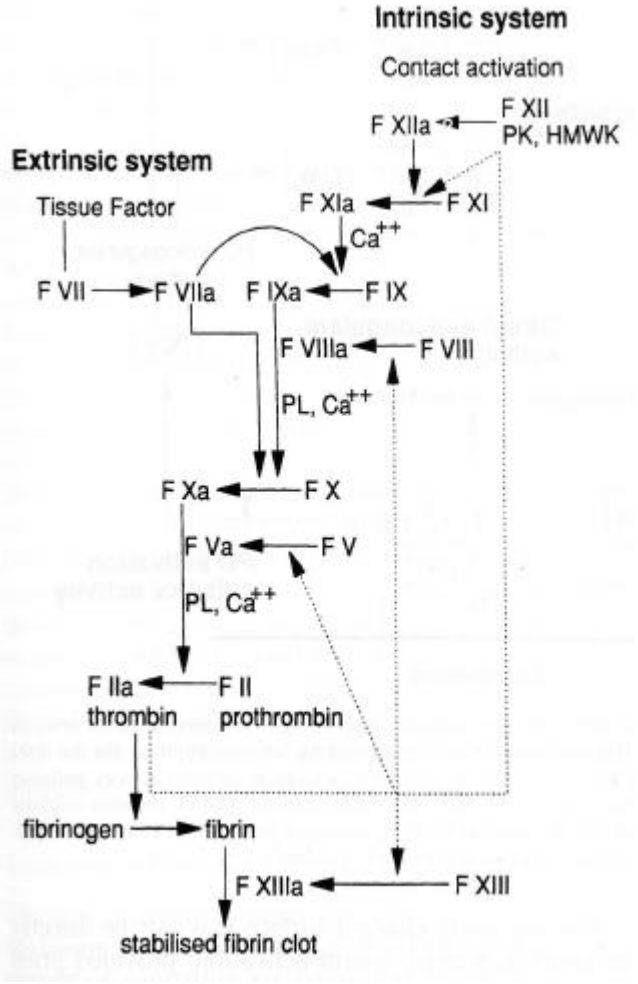

Abbildung 4:

Vereinfachte Darstellung des Gerinnungssystems mit intrinsischem und extrinsischem Weg der Blutgerinnung. Abkürzungen: F – Faktor; PK – Präkallikrein; HMWK – Hochmolekulares Kininogen; PL – Phospholipid. (Lane und Bowry 1993).

Gleichzeitig beginnt Kallikrein HMWK zu spalten, was zur Freisetzung von Bradykinin führt. Dieses Protein hat eine regulatorische Wirkung auf den Blutdruck. So wurden bei der Hämodialyse mit einer speziellen Polyacrylnitril-Natriumallylsulfonat-Membran (Handelsname AN 69S, Hospal, Frankreich), die als Copolymer einen geringen Anteil an sauren Sulfonatgruppen besitzt, bei gleichzeitiger Gabe von Inhibitoren des Angiotensin Converting Enzymes (ACE-Hemmer) klinische Probleme in Form von Hypotension bis hin zum anaphylaktischen Schock beobachtet (Tielemanns et al. 1990; Parnes und Shapiro 1991). Ursache für diesen Effekt ist die starke Aktivierung des Kontaktsystems der plasmatischen Gerinnung mit starker Freisetzung von Bradykinin an Oberflächen mit sauren Gruppen (Silverberg und Diehl 1987) bei gleichzeitiger Gabe von ACE-Hemmern, die den Abbau des Bradykinins hemmen (Veresen et al.1990). Auf der anderen Seite wurde gerade bei dieser Membran eine sehr geringe Komplementaktivierung und keine Leukopenie nachgewiesen, was ursprünglich zu ihrem klinischen Einsatz geführt hat (Chenoweth 1987). Aktivierter

Hagemann-Faktor spaltet Faktor XI in Faktor XIa, wobei wiederum HMWK einen notwenigen Kofaktor darstellt (Kaplan und Silverberg 1987). Schließlich generiert Faktor XIa den Faktor IXa, der in Kooperation mit aktivierten Thrombozyten den Prothrombinase-Komplex bildet, der ebenfalls zur Erzeugung von Thrombin führt (Lindhout 1994). Auf diese Weise sind Proteinkomponenten eng mit zellulären Systemen verzahnt, so dass bei der Entwicklung von Biomaterialien immer eine Reihe verschiedener Parameter berücksichtigt werden müssen. Eine vereinfachte Darstellung der Aktivierung des Kontaktsystems findet sich in Abbildung 5.

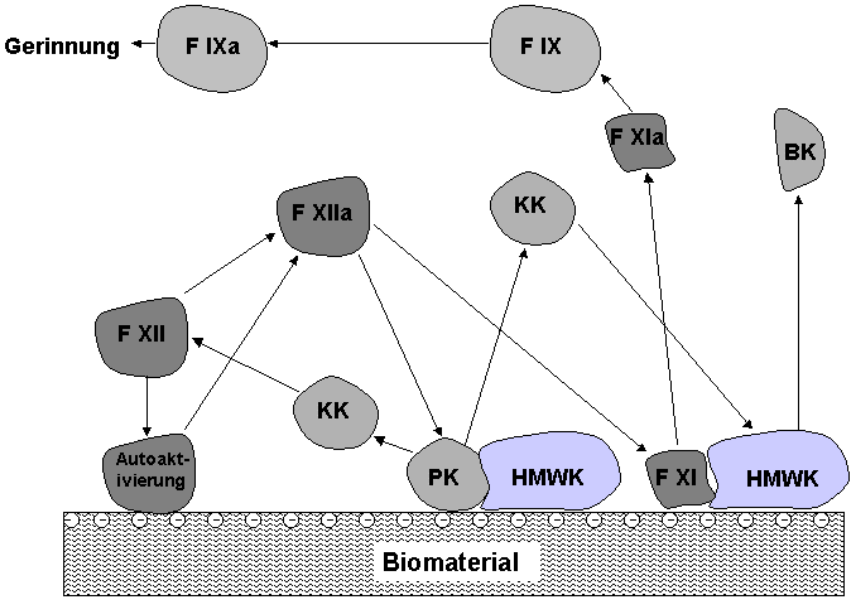

Abbildung 5: Darstellung der Aktivierung des Kontaktsystems der plasmatischen Gerinnung an negativ geladenen Biomaterialoberflächen mit Gerinnungsfaktoren (F), Präkallikrein (PK), Kallikrein (KK), Hochmolekularem Kininogen (HMWK) und Bradykinin (BK). Beginnend mit der Autoaktivierung von F XII zu F XIIa wird PK zu KK umgewandelt, das in einem positiven feed-back weiteren F XII aktiviert. Kallikrein spaltet auch HMWK und erzeugt daraus das vasoaktive Bradykinin. F XIIa aktiviert F XI zu F XIa, welcher seinerseits bei der Umwandlung von F IX in F IXa beteiligt ist, was zur Einleitung der Blutgerinnung führt.

Publikation 2 beschreibt den Effekt verschiedener Comonomere in Acrylnitril-Copolymeren auf die Generierung von Kallikrein als wichtiger Komponente des Kontaktsystems, welches folglich auch als Indikator der Kontaktaktivierung an Biomaterialien verwendet werden kann. Diese Publikation dokumentiert die Entwicklung eines Assays zur Detektierung von Kallikrein unter Verwendung chromogener Substrate. Gleichzeitig bestand Interesse daran, Copolymere des Acrylnitrils mit verbesserter Hydrophilie zu entwickeln, die das Kontaktsystem der plasmatischen Gerinnung nur wenig aktivieren. Hier wurde Acrylnitril mit verschiedenen Comonomeren, wie der Acrylsäure, Allylsulfonat und 2-Hydroxyethylacrylat polymerisiert. Dabei wurden für die Acrylsäure 6.1 mol%, für Allylsulfonat 0.8 und 1.6 mol%

und für 2-Hydroxyethylacrylat 0.6, 3.6 und 23.5 mol% Gehalt im Copolymer erreicht. Es zeigte sich in dieser Untersuchung, dass insbesondere durch die Verwendung der Acrylsäure als Comonomeren die größten Mengen an Kallikrein freigesetzt wurden. Betrachtet man den in der Literatur beschriebenen Zusammenhang von Carboxylfunktionen und der Kontaktaktivierung, wie sie von Vogler und Mitarbeitern (1995) beschrieben wurde, so sollten derartig hohe Gehalte von Acrylsäure bei der Copolymerisation vermieden werden. Im Vergleich dazu war die durch das Allylsulfonat als Comonomeres ausgelöste Kallikrein-Generierung nur moderat. Dies war unter Berücksichtigung der klinischen Probleme mit einem ähnlichen Copolymer (Handelsname AN 69S) bei vergleichbaren Gehalten eines sulfonathaltigen Comonomeren in bezug auf die Freisetzung von Bradykinin nicht erwartet worden (Tielemanns et al., 1990; Parnes und Shapiro, 1991). Im Rahmen der hier vorgestellten Untersuchung war jedoch der Gehalt an Sulfonat-Gruppen wesentlich geringer als jener der vorhandenen Carboxylgruppen, was die geringere Kallikrein-Generierung erklären könnte. Wenn hohe Anteile von 2-Hydroxylethylacrylat (23.5 mol%) im Copolymeren vorhanden waren, wurde ebenfalls eine starke Zunahme der Kallikreinerzeugung beobachtet. Wurden jedoch nur geringe Anteile diese Comonomers verwendet, blieb die Erzeugung von Kallikrein vernachlässigbar. Im Rahmen der hier beschriebenen Untersuchung kann deshalb die Verwendung diese Comonomeren bei geringeren Gehalten im Copolymyer gegenüber der Verwendung der Acrylsäure oder dem Allylsulfonat favorisiert werden. Wenn Kallikreinerzeugung, Wasserrandwinkel und Zetapotentiale miteinander verglichen wurden, konnte kein Bezug zwischen Benetzbarkeit und Kallikrein, jedoch ein qualitativer Zusammenhang mit den Oberflächenpotentialen gefunden werden. Dies steht in Übereinstimmung mit früheren Befunden, dass negativ geladene Oberflächen das Kontaktsystem aktivieren können (Kaplan und Silverberg 1987).

Das Komplementsystem

Ein weiteres wichtiges körpereigenes Abwehrsystem, das von Bedeutung für die Wechselwirkung mit Biomaterialien ist, wird als Komplementsystem bezeichnet. Dieses entwicklungsgeschichtlich alte Verteidigungssystem dient der unspezifischen Abwehr von Infektionen, ist ein wesentliches Element von akuten Entzündungsreaktionen und trägt zur unspezifischen Erkennung und Eliminierung von Fremdstoffen bei. Da im Rahmen der Habilitationsarbeit keine ausführlichen Untersuchungen zur Wechselwirkung von Komponenten des Komplementsystems mit Biomaterialien durchgeführt wurden, sollen die Aussagen an dieser Stelle auf wichtige Eigenschaften beschränkt werden. Die Aktivierung des Komplementsystems kann über den sogenannten klassischen Weg erfolgen, der durch Immunkomplexe initiiert wird, oder den alternativen Weg, der durch Fremdoberflächen getriggert wird. Insbesondere bei Wechselwirkung von Blut mit Biomaterialien kann es zu

einer Aktivierung des Komplementsystems über den alternativen Weg kommen. Dabei entsteht nach Bindung des Komplementfaktors C3 und verschiedener Kofaktoren aus dem Plasma an bestimmte Materialoberflächen ein aktivierter Komplex, der als C3-Konvertase bezeichnet wird und den Komplementfaktor C3b erzeugt. Dieser aktivierte Komplementfaktor

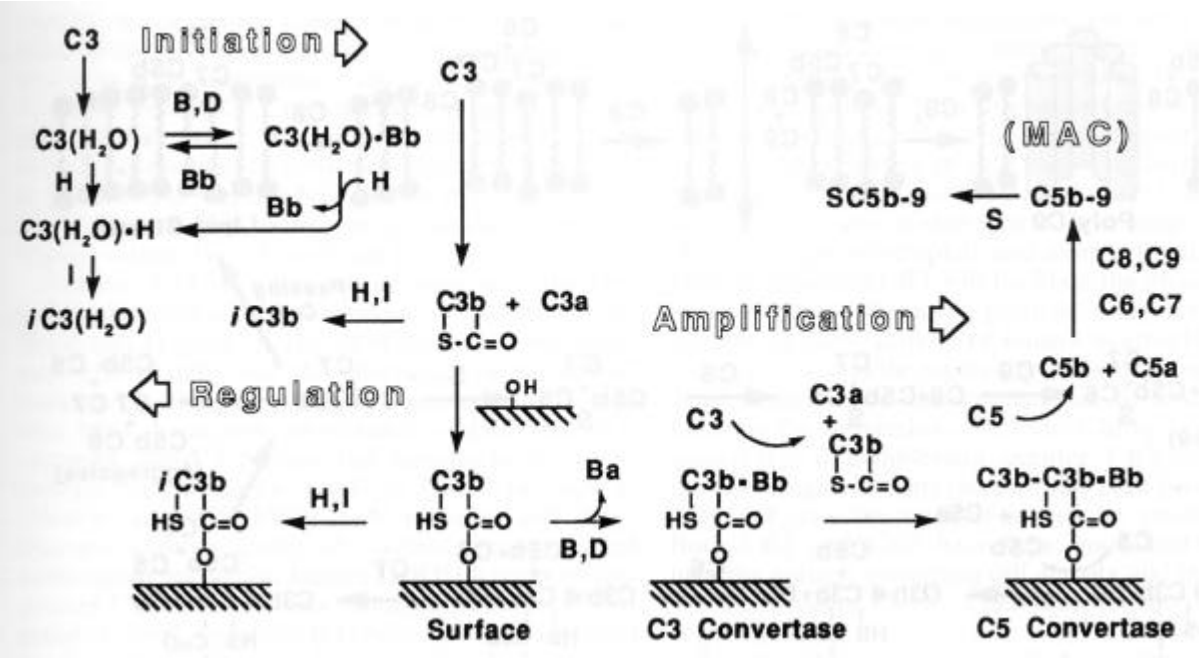

Abbildung 6: Vereinfachte Darstellung der Aktivierung des Komplementsystems über den alternativen Weg an Hydroxylgruppen von Fremdoberflächen bis zur Bildung des zytolytischen Komplexes (SC5b-9 oder MAC) (Johnson 1994).

kann in Gegenwart von Fremdoberflächen und spezifischen Kofaktoren die Fortsetzung der Komplementreaktion bewirken, die schließlich in die Bildung eines terminalen zytolytischen Komplexes mündet (Muller-Eberhard 1992). Dieser Komplex dient normalerweise der Lysis von Bakterien, kann aber auch bei der Anwendung von Biomaterialien die Zerstörung körpereigener Zellen verursachen (Salama et al. 1988). Gebundene Komplementfaktoren, wie C3 und C4 Fragmente dienen der Opsonisierung von Fremdoberflächen und können durch verschiedene Rezeptoren immunkompetenter Zellen, wie von Monozyten und Neutrophilen, erkannt werden, was die Phagozytose und Erzeugung reaktiver Sauerstoffspezies einleitet (Johnson 1994). Zudem werden während der Komplementreaktion kleine bioaktive Polypeptide C3a und C5a freigesetzt, die sekundäre Reaktionen nach sich ziehen, was mit lokalen oder auch systemischen Entzündungsreaktionen einhergehen kann (Chenoweth 1987). Diese Polypeptide werden auch Anaphylotoxine genannt, da sie Freisetzung von Histamin aus Mastzellen fördern und die Kontraktion glatter Muskelzellen mit Erhöhung der Gefäßpermeabilität verursachen und damit zum anaphylaktischen Schock führen können (Johnson 1994). Die Anaphylotoxine C3a und C5a bewirken auch die Chemotaxis und Aktivierung von Leukozyten mit

Freisetzung von Cytokinen, wie den Interleukinen und sind auf diese Weise eine Trigger für lokale und generalisierte Entzündungsreaktionen (Dinarello 1992; Johnson 1994). Insbesondere die Hämodialyse, bei der extrem große Fremdoberflächen in Form von Polymermembranen in Kontakt zum Blut treten, kann zur Aktivierung des alternativen Weges des Komplementsystems führen (Klinkmann und Viencken 1995, Cheung 1994). Dabei konnte gezeigt werden, dass die Hydroxylgruppen von Cellulose-Membranen starke Initiatoren des Komplementsystems sind, was in Zusammenhang zu der beobachteten Leukopenie und Hypoxämie gebracht werden konnte (Hoenich et al. 1995). Die Art der auf dem Polymer vorhandenen Oberflächengruppen spielt dabei eine wesentliche Rolle. Nukleophile Gruppen, wie z.B. Amin- und Hydroxylfunktionen fördern die Aktivierung des Komplementsystems, während negative Substituenten, wie beispielsweise Carboxyl- und Sulfonylgruppen, eine Hemmung der Komplementaktivierung verursachen können (Chenoweth 1987). Damit ist es möglich, mit der Veränderung der Oberflächenchemie von Polymeren, die Aktivierung des Komplementsystems zu verhindern. Entsprechende Ansätze wurden bei der Entwicklung von Dialysemembranen verfolgt (Klinkmann und Viencken 1994) und werden auch im Rahmen der hier vorgestellten Habilitationsschrift beschrieben. Eine Übersicht zum Ablauf der Komplementaktivierung durch Biomaterialoberflächen wird in Abbildung 6 gezeigt.

Das fibrinolytische System

Das System stellt den Gegenspieler des Gerinnungssystems dar und sorgt auf diese Weise für die Homöostase der Blutgerinnung. Bei der Fibrinolyse kommt es zur Auflösung von Fibringerinnseln, wobei diese durch Plasmin proteolytisch gespalten werden. Die Plasmingenerierung aus Plasminogen kann eng mit aktivierten Faktoren des Kontaktsystems, insbesondere mit Kallikrein (Coleman 1969) und Faktor XIa (Mandle und Kaplan 1977) verbunden sein. Dabei können diese Proteasen Plasmin direkt generieren oder über die Umwandlung von Prourokinase in Urokinase wirken, die einen noch stärkeren Aktivator von Plasminogen darstellt (Huisveld et al. 1985). Da es bei der Wechselwirkung von Blut mit Fremdoberflächen zur Aktivierung des Kontaktsystems der plasmatischen Gerinnung kommt, kann auch eine fibrinolytische Aktivität im Plasma entstehen. Insbesondere bei der Hämodialyse (Kurz et al. 1985) und dem kardiopulmonalen Bypass (Owen et al. 1985), wo sehr große Oberflächen in Wechselwirkung mit dem Blut treten, wurde eine Aktivierung der Fibrinolyse beschrieben.

3.2.2 Zelluläre Blutbestandteile in Kontakt mit Biomaterialien

Tritt Blut in Kontakt mit Biomaterialien, so kommt es innerhalb kurzer Zeit (Millisekunden bis Sekunden) zur Adsorption von Proteinen. Dies ist, wie oben ausführlich beschrieben wurde, ein dynamischer Prozess, der sowohl durch die Zusammensetzung des proteinhaltigen Mediums als auch den Eigenschaften der Oberfläche determiniert wird. Das heißt, dass Zellen aus dem Blut nicht direkt an die Materialoberfläche binden können, sondern dass diese durch adsorbierte Proteine abgeschirmt wird. Proteine vermitteln deshalb den Kontakt zwischen Zellen und Oberflächen. Dabei bestimmt die Zusammensetzung der Adsorbatschicht sowie die Konformation der darin befindlichen Proteine, welche Zellarten an der Oberfläche adhärieren und welche Folgeprozesse ablaufen. Die Zellen werden durch Diffusion, unter den Fließbedingungen des Blutes jedoch vor allem durch konvektiven Transport, zur Oberfläche befördert (Slack et al. 1993). Transportvorgänge sind gerade bei der Entwicklung von blutkontaktierenden biomedizinischen Geräten von großer Wichtigkeit, da auf der einen Seite im Falle sehr hoher Scherkräfte Aktivierungsprozesse bei Zellen, wie bei Thrombozyten, ausgelöst werden können, oder es im Falle sehr geringer Scherkräfte zu einer Akkumulation von Proteinen und Zellen am Substrat kommen kann, wie es bei der venösen Thrombose beispielsweise der Fall ist (Slack et al. 1993). Die direkte Interaktion der Zellen mit dem proteinbeschichteten Substrat wird zunächst über weitreichende physikalische Kräfte bewirkt, wie Coulomb-, aber auch van-der-Waals-Wechselwirkungskräfte. Eine ausführliche Beschreibung der Theorie der Wechselwirkung von Zellen mit Substraten findet sich bei Bongrand et al. (1982). Da jedoch die Materialoberfläche i.A. durch Proteine bedeckt ist, kommen nach Kontakt von Zellen mit dem Substrat spezifische Wechselwirkungen zum Tragen, die in der Regel vom Rezeptor-Ligand-Typ sind (Bell et al. 1984). Letztendlich werden auch diese über physikalische Kräfte stabilisiert, die bei der Wechselwirkung der Liganden mit den entsprechenden Bindungsstellen des Rezeptors ablaufen (Cozens-Roberts et al. 1990). Ein Beispiel für diesen Vorgang stellt die Bindung von zellulären Transmembranproteinen, den Integrinen, an RGD-haltige Sequenzen von Adhäsivproteinen, wie z.B. dem Fibronektin dar (Ruoslahti und Pierschbacher 1986). Darauf wird im Verlauf der Habilitationsschrift noch ausführlicher eingegangen. Auch die zelluläre Zusammensetzung des Blutes ist recht vielfältig, wenn auch bei weitem nicht so komplex wie die des Blutplasmas in Bezug auf die Vielzahl der dort vorhandenen Proteine.

Erythrozyten

Erythrozyten sind für den Transport von Sauerstoff zuständig und stellen zahlenmäßig die größte Fraktion dar. Sie spielen bei der Wechselwirkung von Blut mit Biomaterialien eine

eher passive Rolle, da sie im Wesentlichen, bedingt durch ihre innere und äußere Beschaffenheit, nur eine geringe Tendenz zur Interaktion mit Oberflächen besitzen. Erythrozyten können jedoch bei dem Auftreten hoher unphysiologischer Scherkräfte hämolysieren, wie sie z.T. bei der Anwendung von Biomaterialien (z.B. Blutpumpen) auftreten, wobei ADP freigesetzt wird, welches einen Aktivator für Thrombozyten darstellt (Schmid-Schönbein et al. 1981). Auf der anderen Seite können rote Blutzellen unter Bedingungen sehr geringen bzw. stagnierenden Blutflusses an künstlichen Oberflächen passiv beim Aufbau von Thromben durch Einbindung in das sich entwickelnde Fibringerinnsel einbezogen werden (Slack et al. 1993), was zum Wachstum des Thrombus beiträgt, wobei mit zunehmender Thrombusgröße dessen hydrodynamischer Widerstand im Blutfluss wächst, und damit die Gefahr einer Embolie vergrößert wird. Ein Beispiel für die Bildung eines roten Thrombus unter Bedingungen geringer Blutflussraten wird in Abbildung 7 gezeigt.

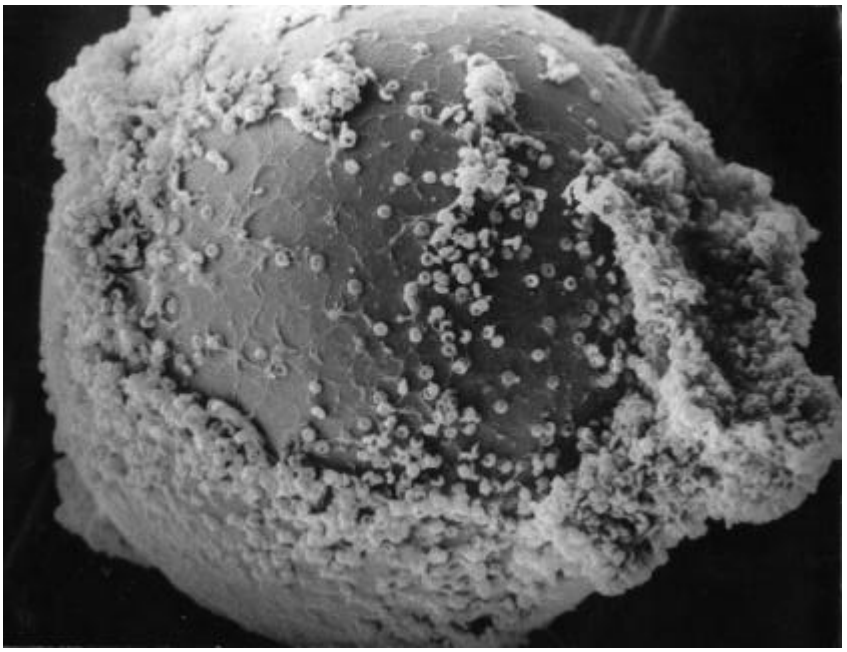

Abbildung 7: Darstellung eines Blutgerinnsels auf einem Polymerpartikel, welches überwiegend aus Erythrozyten besteht (Groth 1990).

Leukozyten

Leukozyten sind für die Immunabwehr des Organismus zuständig. Dabei handelt es sich um ein hochkomplexes System, das teilweise über lösliche Mediatoren, wie Immunglobulinen oder Cytokine und z.T. durch direkte Zellinteraktionen, die unspezifische und spezifische Immunantwort vermittelt (Darnell et al. 1994). Da die Wechselwirkung immunkompetenter

Zellen, d.h. insbesondere von Lymphozyten, mit Biomaterialien nicht Hauptgegenstand dieser Habilitationsschrift ist, kann hier nur eine kurze Zusammenfassung relevanter Fakten für die Wechselwirkung von Phagozyten mit Biomaterialien gegeben werden. Diese sind u.a. für die eher unspezifische Abwehr von Infektionen zuständig. Die geringere Spezifität ihrer Abwehrreaktion geht einher mit einer sehr schnellen Wirkung auf eindringende Mikroorganismen, was für eine erfolgreiche Verteidigung gegen Infektionen von eminenter Bedeutung ist.

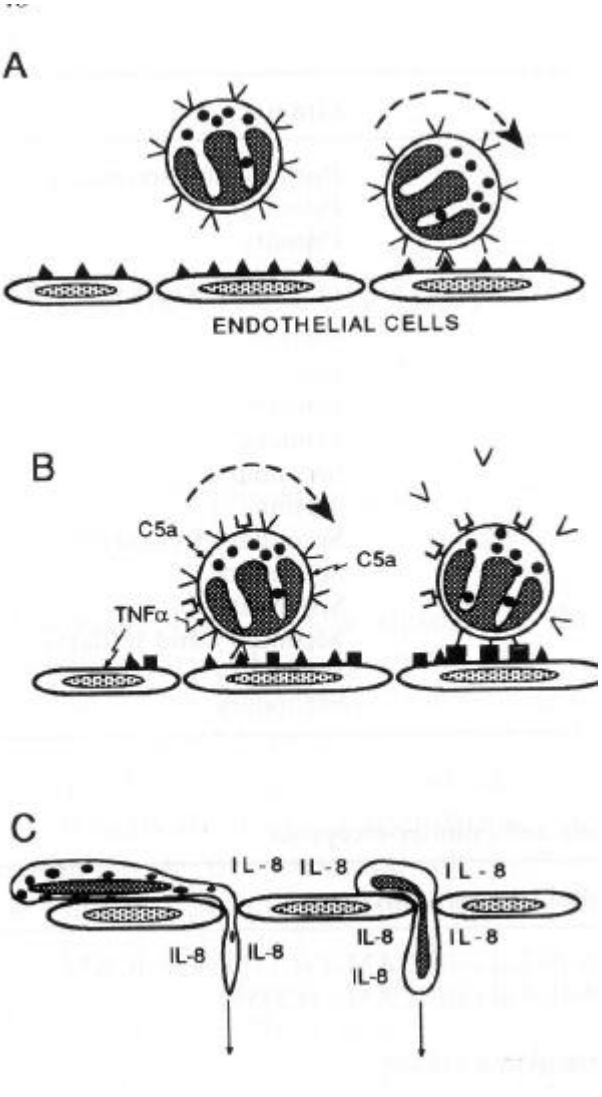

Abbildung 8:

Abfolge der Extravasation neutrophiler Granulozyten. (A) Anheftung an und Rollen auf Endothelzellen, vermittelt durch Selektine; (B) Entzündungsmediatoren wie der Komplementfaktor C5a und TNF führen zu einer verstärkten Expression des ß2-Integrins bei Neutrophilen und von ICAM-1 bei Endothelzellen; (C) Unter dem Einfluss von IL-8, das von Endothelzellen freigesetzt wird, machen Neutrophile eine Formänderung durch und migrieren durch das Endothel (Ward 1994).

Zirkulierende Phagozyten bestehen aus zwei unterschiedlichen Zelltypen, den neutrophilen Granulozyten und den Monozyten. Die Hauptfunktion dieser Zellen besteht in der Eliminierung eingedrungener Bakterien. Neutrophile eliminieren Bakterien im umliegenden Gewebe, indem sie zunächst an das vaskuläre Endothel adhärieren. Hierfür besitzen sie eine Reihe von Rezeptoren, wie dem LFA-1, Mac-1, LAM-1, die an entsprechenden

Liganden ICAM-1, ICAM-2 und E-Selektin binden, welche auf der Oberfläche der Zellmembran aktivierter Endothelzellen erscheinen (Carlos und Harlan 1994). Nach der Adhäsion folgt dann die Migration durch das Endothel zum Ort der Infektion, wo die Bakterien phagozytiert und durch die Erzeugung von reaktiven Sauerstoffspezies und verschiedener Hydrolasen vernichtet werden (Übersicht bei Ward 1994, siehe Abbildung 8). Die transvasale Migration wird dabei durch die Präsenz von Cytokinen induziert, wie dem Interleukin 8 (IL-8), das durch aktivierte Endothelzellen erzeugt wird (Huber et al. 1991). Die Komplementfaktoren C3a, C4a, und C5a, die auch während der Hämodialyse generiert werden können, üben dabei neben einer Reihe weiterer Mediatoren, die von Bakterien, Neutrophilen und Makrophagen freigesetzt werden, eine chemotaktische Wirkung auf diese Zellen aus (Snyderman and Goetzl 1981).

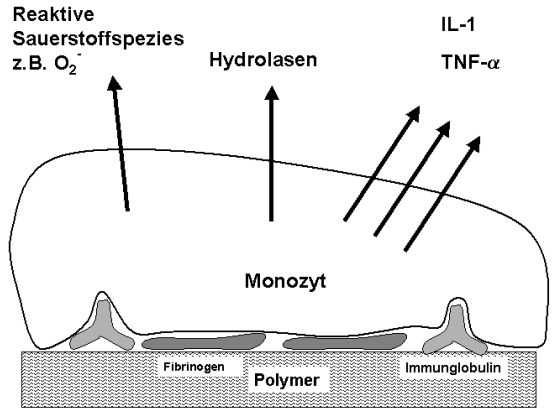

Abbildung 9:

Darstellung wichtiger Mediatoren für Entzündungsreaktionen des umliegenden Gewebes, die durch aktivierte Monozyten oder Makrophagen freigesetzt werden. Die Freisetzung kann durch an Polymere adsorbierte Proteine, wie dem Fibrinogen oder Immunglobuline getriggert werden.

Die Monozyten des Blutes sind sowohl für die unspezifische als auch für die spezifische Immunantwort von großer Bedeutung. Normalerweise erreichen sie den Ort einer Infektion später, aber auf vergleichbare Weise wie die Neutrophilen und nutzen die gleichen Stimuli (Faruqi und DiCorleto 1993). Monozyten besitzen jedoch andere Adhäsionsmoleküle, wie das β1-Integrin, VLA-4 (α4β1), die an induzierbaren Liganden, wie dem VCAM-1 auf Endothelzellen, adhärieren. Am Ort einer Infektion können sie Bakterien oder deren Fragmente phagozytieren und durch vergleichbare Mechanismen wie Neutrophile eliminieren (Faruqi und DiCorleto 1993). Sie spielen jedoch auch eine äußerst wichtige Rolle für die spezifische Immunität. Sie können verdaute Proteinsegmente phagozytierter Objekte zusammen mit zelleigenen HLA Klasse II Antigenen präsentieren, was für die Entwicklung einer spezifischen Immunantwort durch die B- und T-Lymphozyten von großer Bedeutung ist (Unanue und Allen 1987). Monozyten produzieren darüber hinaus eine Reihe bedeutender proinflammatorischer Cytokine, wie das IL-1β, und den Tumor-Nekrosis-Faktor (TNF-α) (Dinarello 1989). Eine Reihe von Untersuchungen konnte zeigen, dass während der

extrakorporalen Blutzirkulation die strenge Kontrolle der Funktion von Phagozyten gestört ist, was sowohl zur Stimulation als auch zur Hemmung ihrer Zellfunktionen führt. So wurde gezeigt, dass eine transiente Verringerung der Zahl von Leukozyten, durch deren Ansammlung in den Lungenkapillaren, mit der Aktivierung des Komplementsystems bei der Hämodialyse mit Cuprophan-Membranen verbunden war (Craddock et al. 1977). Andere Autoren konnten zeigen, dass Neutrophile während der Dialyse eine erhöhte Expression von Adhäsionsrezeptoren, wie dem β2-Integrin aufwiesen (Alvarez et al. 1991), welche die Ursache für die erhöhte Adhäsion der Neutrophilen an den Endothelzellen der Lungenkapillaren darstellt. Auch eine verringerte Fähigkeit zur Produktion reaktiver Sauerstoffspezies und zur Phagozytose nach Dialyse mit komplementaktivierenden Membranen wurde beschrieben (Himmelfarb et al. 1991; Jacobs et al. 1989). Andererseits können Fremdoberflächen Phagozyten auch durch Komplement-unabhängige Mechanismen stimulieren (Falck 1995). Dabei versuchen die Zellen das Fremdmaterial zu phagozytieren, was bei größeren Partikeln und Oberflächen zu der sogenannten frustrierten Phagozytose führt. Während dieses Vorganges kommt es zur Freisetzung reaktiver Sauerstoffspezies und Hydrolasen in die Umgebung, was lokale Entzündungsreaktionen zur Folge haben kann. Ursache hierfür sind die am Biomaterial adsorbierten Proteine. So wurde gezeigt, dass beispielsweise bei Vorhandensein von Fibrin(ogen) an Fremdoberflächen eine Erhöhung der Adhäsion und Aktivität von Phagozyten nachweisbar ist (Tang und Eaton 1993, Cobb und Molony 1996, Bhardwaj et al. 1997). Darüber hinaus stimulieren Fremdoberflächen die Freisetzung proinflammatorischer Cytokine aus Monozyten (Pereira und Dinarello 1994), die sowohl lokale als auch systemische Effekte wie Entzündungsreaktionen, Fieber, etc. induzieren (Dinarello 1991 und 1992). In Abbildung 9 wird eine Übersicht der Wechselwirkung von Monozyten mit Biomaterialoberflächen gezeigt.

Thrombozyten

Thrombozyten sind mit 1- 2 µm Durchmesser die kleinsten Blutzellen, haben jedoch durch ihre engen Wechselwirkungen mit dem Gerinnungssystem und durch die Freisetzung bzw. Präsentation einer Vielzahl von Mediatoren von Entzündungs- und Wundheilungsvorgängen eine sehr bedeutende Rolle für die Biokompatibilität von Biomaterialien (Missirlis und Wautier 1993). Thrombozyten sind kernlose Zellen, die im Ruhezustand eine diskoide Form besitzen (siehe Abbildung 10). Sie besitzen neben der äußeren Zellmembran ein mit der Oberfläche verbundenes Kanalsystem und verschieden Arten von Granula, deren Inhalt während der Aktivierung von Thrombozyten freigesetzt werden kann (White 1987). Sie haben normalerweise eine asymmetrische Verteilung von Lipiden in der Membran, wobei neutrale

und positive geladene in der Außenschicht und negativ geladene in der Innenschicht lokalisiert sind (Bevers et al. 1996).

Abbildung 10:

Rasterelektronenmikroskopische Aufnahme adhärenter Thrombozyten im Ruhezustand (diskoid) oder mit beginnender Aktivierung (Pseudopodienbildung).

Während der Thrombozytenaktivierung werden negativ geladene Phospholipide von der cytosolischen zur extrazellulären Seite der Membran befördert, wo sie an der Formierung des Prothrombinase-Komplexes beteiligt sind (Krishnaswamy et al. 1993). Dabei erfahren die Zellen einen Formwandel, der zunächst durch die Bildung von Pseudopodien eingeleitet wird und schließlich mit der völligen Ausbreitung der Zellen einhergeht, wie in Abbildung 11 gezeigt wird.

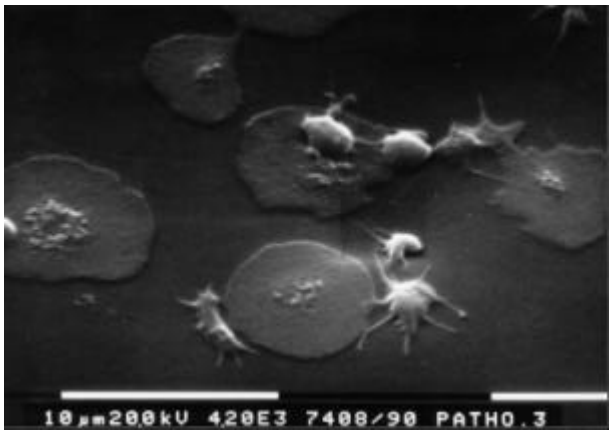

Abbildung 11:

Rasterelektronenmikroskopische Aufnahme aktivierter Thrombozyten mit Pseudopodienbildung und vollständigem Formwandel.

Abbildung 12 zeigt einen Überblick, über die wichtigsten während der Thrombozytenaktivierung ablaufenden Vorgänge. So werden durch die Aktivierung von Phospholipasen aus der Arachidonsäure der Thrombozytenmembran verschiedene Thromboxane und Prostaglandine, die sowohl weitere Thrombozyten aktivieren können als auch in Kooperation mit Leukozyten eine vasoaktive und chemotaktische Wirkung entfalten können (Harker and Fuster 1986, Marcus et al. 1987). Die Thrombozyten besitzen in ihrer Membran eine Vielzahl von Glykoproteinen (GP), die für die Adhäsion und Aktivierung notwendig sind (Kiefer 1993). Dazu gehört der zu den Sialoglykoproteinen zählende Ib-IX-

Komplex, der für die Adhäsion der Zellen an den vom Subendothel gebundenen von-Willebrand Faktor verantwortlich ist (George et al. 1984).

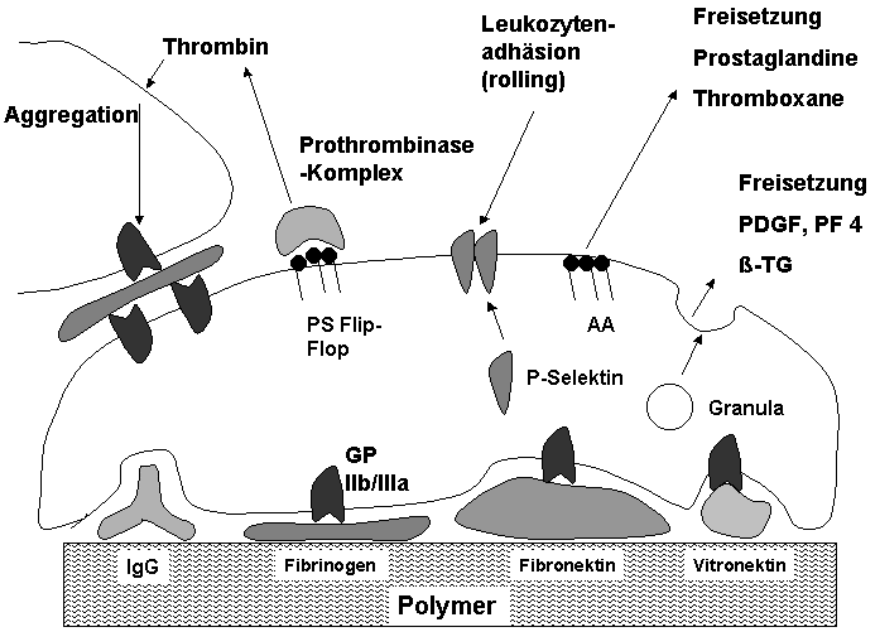

Abbildung 12: Zusammenfassung der wichtigsten Aktivierungsprozesse, welche durch die Adhäsion von Thrombozyten an adsorbierten Adhäsivproteinen induziert werden können, wobei insbesondere das Glykoprotein IIb/IIIa eine Schlüsselrolle spielt. Die Freisetzung des Plättchenwachstumsfaktor (PDGF), Plättchenfaktor 4 (PF 4), ß-Thromboglobulin erfolgt aus Granula durch Exocytose. Phospholipasen bewirken die Bildung von Prostaglandinen und Thromboxanen aus membranständiger Arachidonsäure (AA). Während der Thrombozytenaktivierung erscheint P-Selektin auf der äußeren Membran und dient der Anheftung von Leukozyten. Durch einen Transfer von negativ geladenem Phosphatidylserin (PS) von der Membraninnenseite zur Außenseite wird ein Kofaktor für die Bildung des Prothrombin-Komplexes als Bestandteil der Gerinnungskaskade gebildet. Entstehendes Thrombin aktiviert weitere Thrombozyten im Plasma, die dann an im Plasma befindlichem Fibrinogen über aktiviertes GP IIb/IIIa andocken und so die Aggregation von Thrombozyten einleiten.

Dieses Glykoprotein vermag nicht von-Willebrand-Faktor aus dem Plasma zu binden (Weiss et al. 1986). Thrombozyten exprimieren fünf verschiedene Integrine (Hynes 1987 und 1992). Dazu zählen das Glykoprotein IIb-IIIa (αIIBβ3), GP Ia-IIa (α2β1), GP Ic-IIa (α5β1), Ic´-IIa (α6β1) und der Vitronektin-Rezeptor (αvβ3). Die Thrombozyten-β1-Integrine sind ständig aktive Rezeptoren und verantwortlich für die spezifische Bindung an Fibronektin (α5β1), Kollagen (α2β1), und Laminin (α6β1). Im Gegensatz dazu sind die Thrombozyten-β3-Integrine αIIBβ3 und αvβ3 promiskuitive Rezeptoren, die eine Reihe verschiedener im Plasma gelöster Adhäsivproteine (Fibrinogen, Fibronektin, Vitronektin, von-Willebrand-Faktor und Thrombospondin) binden können. Dabei ist der Vitronektin-Rezeptor ständig aktiv, während GP IIb-IIIa sowohl einen aktivierungsabhängigen als -unabhängigen Rezeptor darstellt (Kieffer 1993). GP IIb-IIIa ist eng mit der Thrombozytenaggregation verbunden,

einem Vorgang der eminent wichtig für den Wundverschluss ist. In ruhenden Thrombozyten ist GP IIb-IIIa nicht in der Lage, im Plasma zirkulierende Liganden zu binden. Thrombozyten können aber durch eine Reihe von Agonisten aktiviert werden, wobei Thrombin neben ADP und Epinephrin stärkster Aktivator ist. Diese wirken über spezielle Membranrezeptoren, die über G-Proteine einen Signaltransfer zum GP IIb-IIIa auslösen (Übersicht in Manning und Brass 1991). Daraufhin erfolgt in diesem Glykoprotein eine Konformationsänderung, die zur Freilegung einer Bindungsstelle hoher Affinität für gelöstes Fibrinogen führt (Sims et al. 1991). Dieser Vorgang verursacht über die Bindung von Thrombozyten an das gleiche Fibrinogenmolekül die Aggregation der Zellen. Die Fähigkeit des GP IIb-IIIa zur Bindung verschiedener Adhäsivproteinen beruht auf der Bindung an die RDG-Sequenz in diesen Proteinen (Ruoslahti und Pierschbacher 1986, Hynes 1987 und 1992). Während nicht-aktiviertes GP IIb-IIIa nicht in der Lage ist, gelöstes Fibrinogen zu binden, kann es jedoch adsorbiertes Fibrinogen erkennen. Dafür ist jedoch nicht die RGD-Sequenz, sondern ein Dodecapeptid nahe dem Carboxylterminus der γ-Kette des Fibrinogens verantwortlich (Kloczewiak et al. 1989). Diese Sequenz wird dabei wahrscheinlich durch einen Konformationswandel des Moleküls während des Adsorptionsprozesses freigelegt und damit als Bindungsstelle für nicht-aktiviertes GP IIb-IIIa zugänglich. Die im Rahmen dieser Habilitationsschrift vorgestellte Untersuchung der Adhäsion und Aktivierung von Thrombozyten an Polyurethan-Harnstoffen (wird unter Punkt 4.2 eingehender besprochen) hat gezeigt, dass die Adhäsion und Aktivierung von Thrombozyten nicht einfach an die Quantität gebundenen Fibrinogens gekoppelt war, sondern mit der Bindungsfähigkeit eines monoklonalen Antikörpers korrelierte, der gegen die γ-Kette des Fibrinogens gerichtet war (**Publikation 10**). Dies steht in Übereinstimmung mit Ergebnissen anderer Untersuchungen, die gezeigt haben, dass die Aktivierung von Thrombozyten nicht einfach von der adsorbierten Menge Fibrinogens, sondern eher von dessen Konformation abhängig ist (Salzman et al. 1987). Ein weiteres Glykoprotein der Thrombozytenmembran ist das zu den Selektinen gehörende P-Selektin, welches in der Vergangenheit auch als GMP-140, PADGEM oder CD 62 bezeichnet wurde. Es ist ein 140 kDa schweres, integrales Membranprotein, welches auf der Oberfläche aktivierter Thrombozyten erscheint (McEver 1991). Die funktionelle Bedeutung dieses Zellrezeptors besteht in der Vermittlung heterotypischer Zelladhäsion. Insbesondere vermittelt dieses Glykoprotein die Anheftung von Neutrophilen und Monozyten an aktivierte Thrombozyten (Larsen et al. 1989, Hamburger und McEver 1990).

Da dieses Glykoprotein nur bei aktivierten Thrombozyten nachweisbar ist, wurde es von uns verwendet, um die Aktivität adhärierender Thrombozyten mittels eines Zell-Immunoassays nachzuweisen (**Publikation 3**). In dieser Publikation wird die Verwendung von Enzym-

Immunoassays für die Bestimmung der Adhäsion und Aktivierung von Thrombozyten beschrieben. Dabei wurde der Nachweis des Glykoproteins Ib für die Quantifizierung adhärierter Thrombozyten verwendet, da dieses Protein ständig auf der Membran der Zellen vorhanden ist. Auf der anderen Seite können aktivierungsabhängige Neoantigene wie das P-Selektin, die während der Thrombozytenaktivierung auf der Zellmembran erscheinen (Kieffer 1993), dazu genutzt werden, die Aktivierung dieser Zellen auf Biomaterialien nachzuweisen. Andere verwendeten diesen und andere Marker zur Charakterisierung des Aktivitätszustandes von Thrombozyten in Suspension (Gentry 1992). Zudem wurde in **Publikation 3** untersucht, ob vergleichbare Resultate in bezug auf Thrombozytenadhäsion und –aktivierung unter statischen und Fließbedingungen erhalten werden können. Für die Durchführung der Experimente unter statischen Bedingungen wurde thrombozytenreiches Plasma in Multiwell-Gefäßen inkubiert, an dessen Boden sich die zu untersuchenden Materialien befanden. Nach Ende der Inkubation wurde der Enzym-Immunoassay zur Erfassung der Adhäsion und Aktivierung von Thrombozyten durchgeführt. Die Untersuchungen unter Fließbedingungen hingegen, erfassten auch die Anzahl der Thrombozyten in Suspension mittels Zellzählgeräten und die Freisetzung von ?-Thromboglobulin vor und nach Kontakt mit den Oberflächen. Dabei konnte durch die Verwendung von Referenzpolymeren die Anwendbarkeit des beschriebenen Enzym-Immunoassays im Vergleich zu den anderen Methoden nachgewiesen werden. Es wurde jedoch auch sichtbar, dass die Adhäsion und Aktivierung der Thrombozyten stark von den Fließbedingungen abhängt, was durch die Anwendung verschiedener Schergeschwindigkeiten nachgewiesen werden konnte. Im Allgemeinen konnte eine bessere Übereinstimmung zwischen Enzym-Immunoassay-Messungen des P-Selektins und der Freisetzung von ?-Thromboglobulin beobachtet werden, als mit der quantitativen Bestimmung der Thrombozytenadhäsion durch Zellzählung im Blut. Dies sollte auf die Tatsache zurückgeführt werden können, dass es während des Kontaktes von Blut mit Biomaterialien nicht nur zur Adhäsion von Thrombozyten auf dem Substrat, sondern auch zur Bildung von Aggregaten auf der Materialoberfläche und im Plasma kommt. Alle drei Vorgänge führen zu einer Abnahme der Zellzahl im Blut. Da im Blut befindliche Agreggate nicht als Thrombozyten gezählt werden, kann die berechnete Thrombozytenadhäsion fehlerhaft sein. Es existieren jedoch Möglichkeiten einer Korrektur dieses Messfehlers (Bowry et al. 1984). Insgesamt konnte jedoch gezeigt werden, dass mit Hilfe der beschriebenen Enzym-Immunoassays eine zuverlässige Bewertung der Blutverträglichkeit von Polymeroberflächen bezüglich ihrer Wechselwirkung mit Thrombozyten möglich ist. Sie wurden deshalb auch bei der Entwicklung von blutverträglichen Polymeroberflächen, wie unter Punkt 4.2 und 4.3 beschrieben, eingesetzt.

3.3 Die Wechselwirkung adhäsionsabhängiger Zellen mit Biomaterialien

Werden polymere Biomaterialien bei Implantation in Kontakt mit dem Gewebe gebracht, kommt es zunächst zur Adsorption von Proteinen. Dies ist auf die durch den chirurgischen Eingriff entstehende Blutung zurückführbar, wobei neben Blutproteinen auch die verschiedenen Blutzellen auf dem Material adhärieren können. Mit diesem Vorgang wird eine akute Entzündungsreaktion eingeleitet, die bei erfolgreicher Anwendung nach kürzerer Zeit abklingt, aber bei ungenügender Biokompatibilität des Materials auch zu einer chronischen Entzündung führen kann (Clark 1997). Während der Wundheilung spielen Fibroblasten eine wichtige Rolle, wobei diese im ungünstigen Fall eine Verkapselung des Materials bewirken können. Es ist jedoch auch möglich und wünschenswert, dass Gewebezellen direkt auf der Materialoberfläche wachsen, wobei sie ihre normale Funktion ausüben sollten. Um den Zusammenhang zwischen den Eigenschaften von (polymeren) Biomaterialien und den nachfolgenden Wechselwirkungen mit Zellen besser zu verstehen, wurden zahlreiche Untersuchungen mit Fibroblasten durchgeführt (z.B. Webb et al. 1998, Tamada und Ikada 1994). Diese haben einen gewissen Modellcharakter, wobei festgestellt werden muss, dass Zellen bedingt durch ihren verschiedenen Ursprung, wie z.B. Bindegewebe, Epithelien, etc., auch unterschiedliche Reaktionen auf eine Materialoberfläche zeigen können (Webb et al. 2000). An dieser Stelle sollen die Aussagen im Wesentlichen auf Fibroblasten beschränkt werden.

Schon frühzeitig wurde bei der Beobachtung der Wechselwirkung von Zellen mit Biomaterialien beobachtet, dass auf hydrophoben Polymeren die Adhäsion, Ausbreitung und Vermehrung von Fibroblasten und anderen Zellen gehemmt wird (Grinnell et al. 1973, Tamada und Ikada 1994). Diese Aussage konnte dahingehend erweitert werden, dass auch sehr hydrophile Substrate einen solche Wirkung ausüben können (Tamada und Ikada 1994). Allerdings spielt hierbei die Art des Substrates eine große Rolle. Während anorganische hydrophile Oberflächen wie Glas oder Metalle die Wechselwirkung mit Zellen fördern, sind hydrophile Polymere durch eine höhere Wasseraufnahme und damit Mobilität der Ketten gekennzeichnet, was zur Verringerung der Proteinadsorption und Wechselwirkung mit Zellen führt (Leckband et al. 1999, Morra und Cassinelli 1999). Beispiele für solche Materialien sind Copolymere oder Oberflächen mit größeren Gehalten an Polyethylenglykol, Dextran, Hydroxyethylmethacrylat oder Polyvinylpyrrolidon (DeFife et al. 1999, Massia et al. 2000, Horbett und Schway 1988). Im Ergebnis dieser Untersuchungen wurde festgestellt, dass optimale Bedingungen für die Wechselwirkung mit Zellen an Materialien moderater Benetzbarkeit mit Wasser-Randwinkeln zwischen 50° bis maximal 80° gegeben sind (Tamada und Ikada 1994, Vogler 1998, Groth und Altankov 1998). Auch für die vorhandenen Zeta-Potentiale wurde versucht, ähnliche Zusammenhänge herzustellen (Seyfert et al.

1995). Doch sind hier viele widersprüchliche Resultate in der Literatur zu finden, was sicher auch auf die Art der Messung etc. zurückführbar ist. In jedem Fall lässt sich sowohl an Oberflächen mit starker negativer Oberflächenladung als auch positiver Oberflächenladung eine erhöhte Adhäsion und Proliferation von Zellen nachweisen (Kapur et al. 1993). Da solche Untersuchungen in Anwesenheit von Serumproteinen durchgeführt wurden, war es naheliegend, in der Adsorption von Proteinen die Ursache zu suchen. Insbesondere Adhäsivproteine, wie das Fibronektin, waren bereits vor längerer Zeit Gegenstand intensiver Untersuchungen. Dabei konnte festgestellt werden, dass die Adhäsion, die Ausbreitung und weitere Reaktionen, wie die Proliferation der Zellen, von der Menge und Konformation des Fibronektins abhängig waren (Grinnell und Feld 1981, Horbett und Schway 1988, Underwood und Bennet 1993). So zeigt sich, dass mit Zunahme der Hydrophobie von Materialien zwar eine Erhöhung der Quantität der Fibronektin-Adsorption einhergehen kann, das Protein jedoch Konformationsänderungen erleidet, welche seine Wechselwirkungen mit den Zellen behindern (Grinnell 1987, Juliano et al. 1993). Dies wurde vor allem an hydrophoben, aber auch an geladenen Oberflächen nachgewiesen. Fibronektin ist jedoch nicht das einzige Adhäsivprotein, das als lösliches Protein im Serum bzw. Plasma vorhanden ist. So kommt es auch zur Adsorption weiterer Proteine, wie dem Fibrinogen und dem Vitronektin (Fabricius-Homan und Cooper 1991). Wie der Charakter der Oberfläche die Adsorption solcher Proteine beeinflusst, wurde intensiv von verschiedenen Arbeitsgruppen untersucht. Dabei wurde beobachtet, dass moderat benetzbare Oberflächen mit stickstoffhaltigen funktionellen Gruppen die Adsorption von Fibronektin fördern, während sauerstoffhaltige Spezies an der Oberfläche die Adsorption von Vitronektin unterstützen (Steele et al. 1994). Beide Adhäsivproteine besitzen die Aminosäuresequenz RGD, für die Zellen spezifische Rezeptoren - die Integrine – besitzen (Ruoslahti und Pierschbacher 1986). Damit besteht ein enger Zusammenhang zwischen den physikalisch-chemischen Eigenschaften der Polymeroberfläche, der Adsorption von Proteinen und den nachfolgenden zellulären Reaktionen.

Seit Beginn der neunziger Jahre rückten die Integrine als Adhäsionsrezeptoren von Zellen in den Mittelpunkt zellbiologischer Untersuchungen. Wie bereits im Zusammenhang mit den Eigenschaften von Thrombozyten erwähnt, stellen Integrine heterodimere Membranproteine dar, die aus α und β Untereinheiten bestehen und sehr vielfältige Funktionen ausüben (Hynes 1987 und 1992). Sie vermitteln die Haftung von Zellen an der Unterlage und liefern in Kooperation mit dem Zellskelett die nötige mechanische Spannung für die Zellmigration (Webb et al. 2001). Zudem übermitteln sie Signale vom Substrat in die Zelle hinein (outside-in-signaling) und umgekehrt (inside-out-signaling) (Ruoslahti 1997). Integrine werden zellspezifisch und auch in Abhängigkeit vom Zustand der Zelle exprimiert. So besteht eine

wichtige Gruppe aktivitätsunabhängiger Integrine, die in einer Vielzahl von Zellen exprimiert werden, aus dem α5β1-, αvβ3- und dem αvβ6-Integrin. Andere sind nur in bestimmten Zelltypen vorhanden, wie z.B. das αIIBβ3-Integrin in Thrombozyten oder das α6β4-Integrin in Epithelzellen. Das αIIBβ3-Integrin stellt zudem ein Integrin dar, welches durch externe Stimuli, wie die Wechselwirkung von Thrombin mit Thrombozyten über intrazelluläre Signalprozesse aktiviert werden kann und damit erst die Fähigkeit zur Bindung ihres Liganden Fibrinogen erwirbt (siehe auch Punkt 3.2.2).

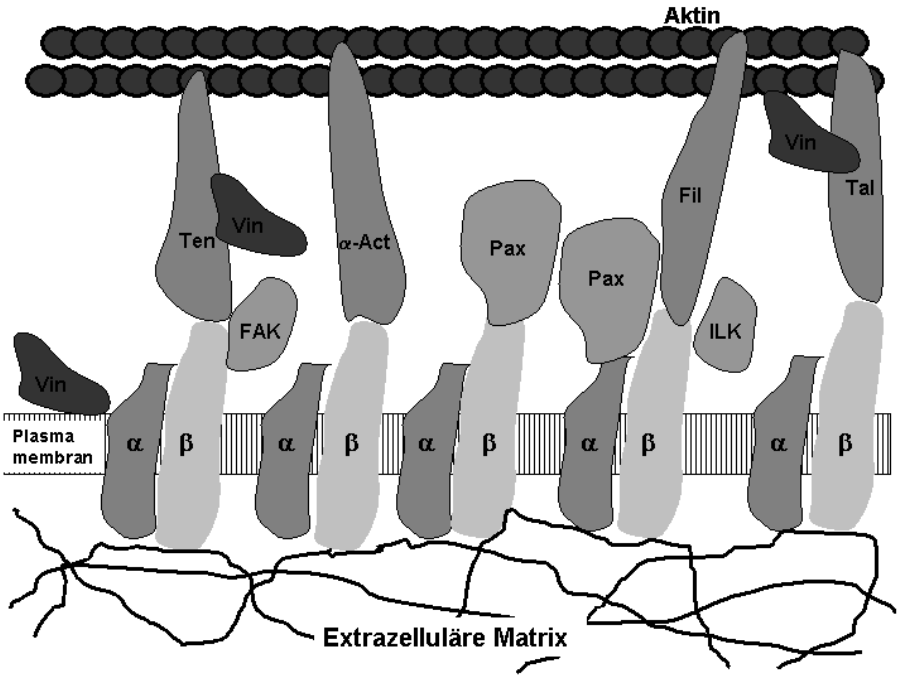

Abbildung 13: Vereinfachte Darstellung der Wechselwirkung von Zellen mit Matrixproteinen über Integrine in fokalen Adhäsionskomplexen. Die Integrine, die aus ?? und ??Untereinheiten bestehen, binden an Matrixproteine wie dem Fibronektin überwiegend über die RGD-Sequenz. Intrazellular sind die Integrine über ?-Actinin (?-Act), Filamin (Fil), Tensin (Ten) und Talin (Tal) direkt mit dem Aktin-Zellskelett verbunden. In den fokalen Adhäsionskomplexen befinden sich zudem verschiedene Kinasen, wie die fokale Adhäsionskinase (FAK), die Integrin-Linked-Kinase (ILK), die für den Signaltransfer verantwortlich sind, sowie Paxillin (Pax) und Vinculin (Vin).

Die Spezifität von Integrinen drückt sich jedoch vor allem in ihrer Binding an bestimmte Liganden aus. Viele der Integrine binden an die RGD-Zellbindungssequenz von Adhäsivproteinen (Ruoslahti und Pierschbacher 1986), wobei sie jedoch die Umgebung dieser Sequenz, die zwischen den verschieden Proteinen variiert, unterscheiden, so dass sie beispielsweise an Fibronektin oder an Vitronektin binden (Ruoslahti 1996). Integrine können dabei spezifisch für einen einzigen Liganden sein, wie beispielsweise für Fibronektin, oder aber eine ganze Reihe verschiedener Adhäsivproteine, wie Fibrinogen, Fibronektin, Vitronektin und von-Willebrand-Faktor erkennen. Das αIIBβ3-Integrin von Thrombozyten stellt ein Beispiel für einen solchen Rezeptor dar.

Während der Adhäsion von Zellen bilden die Integrine Cluster aus, die man als fokale Adhäsionskomplexe bezeichnet. Diese stellen flache ausgedehnte Strukturen dar, die vorwiegend in der Zellperipherie mit einer Größe von einigen µm² vorhanden sind. Sie vermitteln eine starke Adhäsion zum Substrat, wobei Bündel von Aktinfilamenten mit dem fokalen Adhäsionskomplex verbunden sind, der eine Vielzahl von Proteinen enthält. Dazu zählen α-Actinin, Filamin, Talin und Tensin, welche die Integrine mit dem Aktin-Zellskelett verbinden. Weiterhin sind fokale Adhäsionskomplexe reich an Vinculin, Paxillin und von Proteinen, die in Tyrosinresten phosphoryliert sind (Otey at al. 1990, Sharma et al. 1995, Zamir et al. 2000, Geiger et al. 2001). Die Ausbildung der fokalen Adhäsionskomplexe wird durch die Aktivität der kleinen GTPase Rho-A stimuliert und durch die Aktivität von Aktin/Myosin getrieben (Geiger et al. 2001). Ein Überblick zur Anordnung von Komponenten der fokalen Adhäsionskomplexe und deren Verbindung mit den Adhäsivproteinen und dem Zellskelett findet sich in Abbildung 13. Während in den fokalen Adhäsionskomplexen überwiegend das αvβ3-Integrin vorhanden ist, bilden Zellen auch fibrilläre Adhäsionen aus, die durch das α5β1-Integrin vermittelt werden (Pankov et al. 2000, Geiger et al. 2001). Diese stellen ausgedehnte fibrilläre Strukturen dar, die sich eher im Zentrum der Zelle befinden. Sie sind reich an Tensin, α5β1-Integrin und assoziieren mit Fibronektin-Fibrillen. Es wurde dabei beobachtet, dass die Rigidität oder Deformierbarkeit der extrazellulären Matrix die Ausbildung der fibrillären Adhäsionen beeinflusst. Wird Fibronektin kovalent an Substrate gebunden, ist die Ausbildung fibrillärer Adhäsionen verhindert. Stattdessen entstehen ausgedehnte fokale Adhäsionskomplexe, die sowohl αvβ3- als auch α5β1-Integrin sowie Tensin, Vinculin, Paxillin und tyrosinphosphorylierte Proteine enthalten (Katz et al. 2000).

Integrine sind mit dem Zellskelett im Zellinnern durch spezielle Proteinkomplexe verbunden, welche an der Übertragung von Signalen beteiligt und für das Wachstum, die Differenzierung und das Überleben von Zellen notwendig sind (Juliano und Haskill 1993, Ruoslahti 1997). Ein Signaltransfer kann durch die mechanische Verbindung mit dem Zellskelett vermittelt werden (Ingber 1998, Huang und Ingber 1999), ist jedoch vor allem chemischer Natur. So sind einige der Signalmoleküle, wie Paxillin und Cortactin, mit dem Zellskelett verbunden (Burridge and Turner 1992), und Signalereignisse durch Integrine kontrollieren die Polymerisation des Zellskelettes (Gilmore and Burridge 1996). Die wichtigsten Signalproteine sind dabei die fokale Adhäsionskinase FAK, Src, p130 – ein sogenanntes Docking-Protein und verschiedene mit dem Zellskelett verbundene Proteine, wie Paxillin und Tensin (Ruoslahti 1997). Während der Aggregation der Integrine und Signalmoleküle in den Adhäsionsplaques kommt es zur Aktivierung einer Reihe von Tyrosin-Kinasen einschließlich der FAK und Src (Juliano und Haskill 1993). Auf diese Weise werden Signale in das

Zellinnere übertragen, die das Wachstum, die Differenzierung und das Überleben von Zellen regulieren. Die Signalkaskaden kontrollieren die Adhäsionsabhängigkeit von Zellen, so dass nur adhärierende Zellen fähig sind zu wachsen. So stellen Fibroblasten in Suspension ihr Wachstum ein, während Epithel- und Endothelzellen in die Apoptose übergehen und absterben (Ruoslahti und Reed 1994). Es konnte dabei gezeigt werden, dass der kontrollierte Zelltod – Apoptosis genannt – durch die Aktivität von Integrinen reguliert wird. Die Expression des Integrins $\alpha v\beta 3$ in Endothelzellen wird durch die Anwesenheit von Tumoren stimuliert. Bei Hemmung dieses Integrins durch spezifische Antikörper gehen die Endothelzellen in die Apoptose über, wodurch die Neubildung von Blutgefäßen im Tumor verhindert werden kann (Brooks et al. 1994). Bei Bindung des $\alpha 5\beta 1$-Integrins an die extrazelluläre Matrix erhöht sich die Expression des Anti-Apoptose-Proteins bcl-2 (Ruoslahti 1997). Zudem wurde auch nachgewiesen, dass in Epithelzellen die Bindung der $\beta 1$-Untereinheit von Integrinen an die extrazelluläre Matrix die Aktivität des Interleukin-1-Converting Enzymes (ICE, caspase 1) hemmt und so die Zellen in beiden Fällen vor der Apoptose geschützt sind. Die Signaltransmission durch Integrine ist zudem mit den Signalwegen von Wachstumsfaktoren verknüpft, welche die Zellteilung regulieren. So konnte eine Verknüpfung zwischen Integrinen $\alpha v\beta 3$, sowie der $\beta 1$-Untereinheit mit sogenannten Mitogen-aktivierten Protein-Kinasen nachgewiesen werden (Wary et al. 1996). Paxillin scheint jedoch eine Schlüsselrolle für die Verknüpfung des Signaltransfers von Rezeptoren für Wachstumsfaktoren und Integrinen zu spielen, da es als Dockingprotein für eine Vielzahl von Signalproteinen dient (Turner 2000).

Der als inside-out-signaling bezeichnete Prozess des Signaltransfers hingegen dient der Regulation der Aktivität von Integrinen in Abhängigkeit von äußeren Stimuli. Wie bereits im Abschnitt 3.2.2 erwähnt, wird das $\alpha IIB\beta 3$-Integrin (GP IIb/IIIa) durch Agonisten wie Thrombin intrazellulär über einen G-Protein abhängigen Weg aktiviert, wodurch es extrazellulär zur Bindung von gelöstem Fibrinogen befähigt wird, was zur Aggregation von Thrombozyten führt (Ginsberg et al. 1993). Erst die Aktivierung von $\beta 2$-Integrinen in Leukozyten befähigt diese zur Bindung an Endothelzellen während einer Entzündung (Springer 1994). Die zugrunde liegenden Mechanismen können an dieser Stelle nicht ausführlich beschrieben werden. Es sei deshalb auf den Übersichtsartikel von Coppolino und Dedhar (2000) verwiesen. Eine stark vereinfachte Übersicht zu den während der Adhäsion von Zellen an die extrazelluläre Matrix verbundenen Signalereignissen findet sich in Abbildung 14.

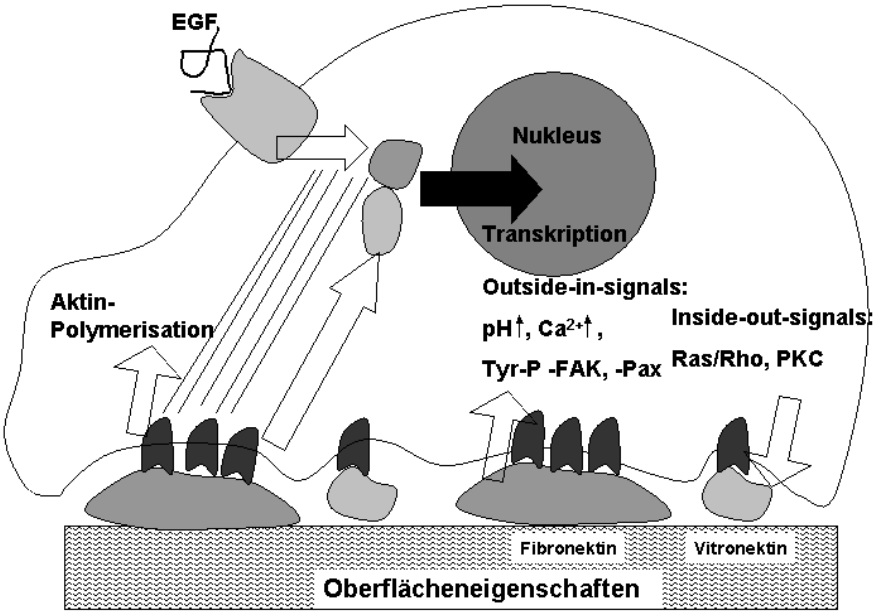

Abbildung 14: Darstellung der verschiedenen Signalwege und matrixbildender Aktivitäten von Fibroblasten auf Biomaterialien. Die Bindung von Integrinen an Fibronektin führt zu einer Signaltransmission in das Zellinnere (outside-in-signalling), die für die Einleitung der Aktinpolymerisation verantwortlich ist (links). Typische Signalereignisse bei Bindung von Integrinen an Fibronektin bestehen in einer Tyrosin-Phosphorylierung von Src, der fokalen Adhäsionskinase FAK, Paxillin und weiterer Kinasen. Dabei kommt es zu einem Anstieg des intrazellulären pH-Wertes und der Kalziumkonzentration (Mitte). Signale, die durch die Bindung von Integrinen an die extrazelluläre Matrix generiert werden, können mit Signalwegen von Wachstumsfaktoren kooperieren und so eine gemeinsame Regulation der Aktivität von Genen bewirken (links oben). Schließlich können Integrine durch intrazelluläre Ereignisse zur Bindung an einen spezifischen Liganden befähigt werden (inside-out-signalling, rechts).

Unter normalen Bedingungen synthetisieren die meisten adhäsionsabhängigen Zellen eine extrazelluläre Matrix. Diese Matrix besteht aus einer Reihe von Proteinen, wie verschiedenen Kollagenen, Fibronektin, Laminin, etc. (Darnell et al. 1994). Für diese Matrixproteine vermitteln die Integrine die Verankerung der Zellen auf dem Substrat (McDonalds 1988). Die extrazelluläre Matrix hat darüber hinaus vielfältige Funktionen. Sie liefert die für die Differenzierung, das Wachstum und Überleben von Zellen notwendigen Signale (McDonalds 1988, Ruoslahti 1996 und 1997). Zugleich stellt die extrazelluläre Matrix ein Reservoir für diffusible Wachstumsfaktoren dar. Sie ist zelluläres Produkt und zugleich Objekt von Veränderungen durch die Zellen mittels sogenannter Metallomatrixproteasen, die eine Proteolyse der Matrix bewirken, um die Migration von Zellen auf der bzw. durch die Matrix zu ermöglichen (Sato 1997, Koshikawa et al. 2000). Fibronektin stellt dabei den Prototyp eines solchen Proteins dar, das in den Matrices der meisten Zellarten vorkommt (Ruoslahti 1997). Die Fibrillogenese des Fibronektins während der Matrixsynthese ist ein zellabhängiger Prozess, der vor allem für die Embryogenese und weitere Entwicklung von Geweben, sowie

die Wundheilung von großer Bedeutung ist. Dabei spielt das $\alpha 5\beta 1$-Integrin, der Amino-Terminus des Fibronektins und dessen III-1- sowie III-10-Modul eine wichtige Rolle für den Prozess der Fibrillisierung (Hocking et al. 1996, Christopher et al. 1997). Auch für das $\alpha v\beta 3$-Integrin konnte eine Beteiligung am Prozess der Fibronektin-Matrix-Formierung nachgewiesen werden (Wennerberg et al. 1996). In einer kürzlich erschienen Publikation von Geiger und Mitarbeitern (Geiger et al. 2001) wurde der Prozess der Fibronektin-Fibrillisierung als Ergebnis der Wechselwirkung von Integrinen, und spezifischen Fibronektin-Epitopen dargestellt. Dabei spielt offensichtlich die Applizierung einer mechanischen Spannung auf das Fibronektin-Molekül durch die koordinierte Aktivität von Integrinen und Zellskelett eine besondere Rolle. Hierbei kommt es zu einer Freilegung versteckter Epitope des Fibronektins, die für die Polymerisation des Moleküls notwendig sind (siehe Abbildung 15).

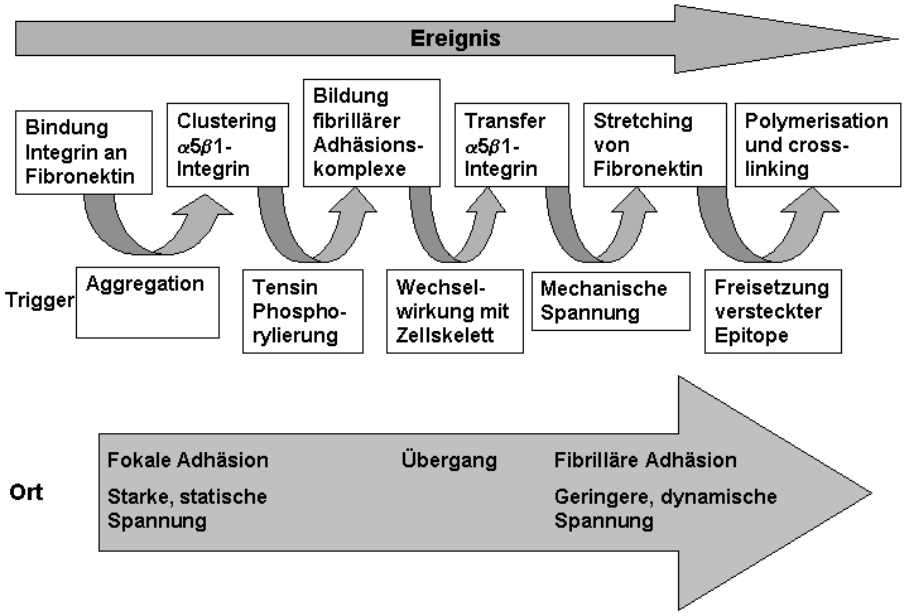

Abbildung 15: Schematischer Ablauf der Matrixsynthese durch das Zusammenspiel von Integrinen, Zellskelett und bestimmten Fibronektin-Modulen (Geiger et al. 2001).

Die bislang zu den zellbiologischen Grundlagen gemachten Ausführungen zeigen klar, dass Anheftung, Wachstum und Differenzierung von Zellen durch die Wechselwirkung zwischen zellulären Rezeptoren und dem Substrat, welches normalerweise die extrazelluläre Matrix darstellt, sowie von löslichen Faktoren (Wachstumsfaktoren) reguliert wird. Während unter den natürlichen Bedingungen Zellen mit einem strukturierten, inhomogenen Substrat über Rezeptor-Ligand-Wechselwirkungen kommunizieren, sind die Gegebenheiten bei der Wechselwirkung mit Biomaterialien völlig anderer Natur. Hier handelt es sich meist um homogene, unstrukturierte Oberflächen, an die Proteine aus der Umgebung stochastisch adsorbieren, wobei sie Konformationsänderungen erleiden können. Um die im ersten Absatz

des Abschnittes 3.3 erwähnten Befunde der Beeinträchtigung der Zelladhäsion, Proliferation und Funktion besser verstehen zu können, wurden deshalb von uns eine Reihe von Untersuchungen durchgeführt, welche die Rolle der Integrine, sowie den Prozess der Matrixsynthese von Fibroblasten auf Modellbiomaterialien zum Gegenstand hatten (**siehe Publikationen 4 – 8**). Dabei wurde ein von Grinnell 1986 entwickeltes Modell der frühen Bildung von Fibronektin-Matrixfibrillen, welches deren Aufbau aus fluoreszenzmarkiertem adsorbiertem Fibronektin darstellt, auf die Wechselwirkung von Fibroblasten mit polymeren Biomaterialien in Anwesenheit von Serumproteinen angewendet (**Publikation 4**). In dieser Untersuchung wurde nicht nur der Sachverhalt reproduziert, dass mit Abnahme der Benetzbarkeit von Biomaterialien die Ausbreitung und Vermehrung von Fibroblasten gehemmt wird (siehe weiter oben), sondern dass Zellen auf hydrophoben Materialien nur kurze oder keine fokalen Adhäsionsplaques und auch keine Aktin-Stressfasern ausbilden können. Darüber hinaus konnte jedoch erstmals nachgewiesen werden, dass die Fähigkeit von Fibroblasten zur Ausbildung von Fibronektin-Matrixfibrillen an hydrophoben Oberflächen stark bis vollständig gehemmt wird. Auf diese Weise konnte ein neues funktionelles Kriterium zur Bewertung der Gewebsverträglichkeit von Biomaterialien entwickelt werden. Da der Prozess der Fibronektin-Reorganisation normalerweise in Anwesenheit von Serum ablaufen sollte (Grinnell 1986), ergaben sich Hinweise darauf, dass die Wechselwirkung von Integrinen, insbesondere dem $\alpha 5\beta 1$-Integrin, mit dem adsorbierten Fibronektin gestört sein musste. Untersuchungen von Juliano et al. (1993) hatten ergeben, dass die Konformation von Fibronektin an hydrophoben Substraten die Wechselwirkung mit Zellen stark beeinträchtigt. Aus diesem Grunde war es interessant zu lernen, wie sich die Benetzbarkeit von Materialien auf den Prozess des „outside-in-signaling“ auswirkt, der über eine Tyrosin-Phosphorylierung nachweisbar war (**Publikation 5**). Dabei konnte ein Zusammenhang zwischen der Tyrosin-Phosphorylierung in Fibroblasten und der Benetzbarkeit der Oberflächen hergestellt werden. Mit Immunfluoreszenzmikroskopie konnte gezeigt werden, dass die Hauptaktivität der Tyrosin-Phosphorylierung an hydrophilen bis moderat benetzbaren Oberflächen in den fokalen Adhäsionsplaques konzentriert war, wo auch der Fibronektin-Rezeptor, das $\alpha 5\beta 1$-Integrin, nachgewiesen werden konnte. Hydrophobe Biomaterialien verursachten eine starke Hemmung der Phosphorylierung, wobei keine fokalen Adhäsionsplaques nachweisbar waren. Dieser Effekt wurde - wenn auch in abgeschwächter Form - nach Vorbeschichtung der Materialien mit Fibronektin beobachtet. Damit erfolgte erstmalig der Nachweis, dass der Prozess der Signalübertragung vom Substrat über die Integrine in die Zelle hinein auf hydrophoben Biomaterialien gestört ist. Untersuchungen anderer Gruppen haben den Zusammenhang zwischen an Biomaterialien gebundenen Fibronektin und der Tyrosin-Phosphorylierung bestätigen können (Garcia und Boettiger 1999). Die Funktion von Fibroblasten ist eng mit der Sekretion und Organisation

von extrazellulären Matrixkomponenten verbunden. Wie bereits in **Publikation 4** gezeigt wurde, ist die Fähigkeit von Fibroblasten gehemmt, adsorbiertes Fibronektin an hydrophoben Substraten zu strukturieren. Da die Zellen jedoch selbst Fibronektin synthetisieren und daraus Matrixstrukturen aufbauen, waren wir daran interessiert, wie dieser Prozess durch die Benetzbarkeit von Biomaterialien beeinflusst wird (**Publikation 6**). Im Ergebnis dieser Untersuchungen konnte festgestellt werden, dass sich die Menge synthetisierten Fibronektins mit Abnahme der Benetzbarkeit von Biomaterialien verringerte. Darüber hinaus konnte auch nachgewiesen werden, dass Fibronektin an hydrophilen bis moderat benetzbaren Oberflächen in eine extrazelluläre Matrix in Form von fibrillären Strukturen organisiert wird, während an hydrophoben Materialien nur punktförmige Ansammlungen von Fibronektin ohne erkennbare Bildung von Matrixfibrillen nachweisbar waren. Vergleichbare Untersuchungen auf Ebene der Transkription wurden von Nagahara und Matsuda (1996) mit der Quantifizierung von m-RNA für Aktin, Fibronektin und Laminin durchgeführt. Auch hier konnte gezeigt werden, dass an hydrophoben Materialien nicht nur die Zelladhäsion und das Wachstum abnimmt, sondern auch eine Verringerung der m-RNA Synthese für die betreffenden Proteine erfolgt. Mit diesen Befunden war klar, dass die schlechte Biokompatibilität von hydrophoben Biomaterialien nicht nur mit einem verringerten Wachstum von Zellen einhergeht, sondern vor allem die Funktion von Zellen – hier von Fibroblasten – stark beeinträchtigt. Ursache hierfür sollte in einer veränderten Konformation von Fibronektin an hydrophoben Materialien liegen, wie sie bereits von anderen Autoren festgestellt wurde (Grinnell 1987, Juliano et al. 1993). Die damit einhergehende Reduktion des Signaltransfers (outside-in-signaling) könnte als Ursache für eine verringerte Aktivität der entsprechenden Gene verantwortlich sein. Um die Rolle der Integrine bei diesen Vorgängen weiter aufzuklären, wurden Untersuchungen zur Fibronektin-Rezeptor-Funktion an Glas als hydrophiler und an silanisiertem Glas als hydrophober Modelloberfläche durchgeführt (**Publikation 7**). Dabei wurde von uns eine neuartige Technik angewendet, die von Altankov und Grinnell 1995 entwickelt wurde. Hierbei wird durch Inkubation lebender Zellen mit polyklonalen Antikörpern, die gegen die β1-Untereinheit des Fibronektin-Rezeptors gerichtet waren, eine Aktivierung des Integrins induziert, wie sie auch durch den eigentlichen Liganden – das Fibronektin – hervorgerufen wird. Während dieses Prozesses kommt es zu einer linearen Anordnung der Rezeptoren, die parallel zu Aktinfasern auf der Oberseite der Zellen (dorsal) erscheinen. Bei der Durchführung dieser Untersuchungen mit beiden Modelloberflächen zeigte sich, dass dieser Prozess an hydrophilen Substraten in der beschriebenen Form abläuft, während am hydrophoben Substrat keine solche Reorganisation der β1-Untereinheit beobachtet werden konnte. Um die Anfangsbedingungen der Kultivierung von Zellen mit beiden Substraten zu verbessern, wurde deshalb eine Vorbeschichtung mit Fibronektin vorgenommen. Dies ist eine verbreitete Methode, um die

initiale Wechselwirkung von Zellen mit inkompatiblen Substraten zu verbessern. Zwar konnte unter diesen Bedingungen am hydrophoben Substrat die Ausbildung von fokalen Adhäsionsplaques auf der ventralen Zelloberfläche beobachtet werden, jedoch war wiederum keine Organisation der β1-Untereinheit auf der dorsalen Seite nachweisbar. Wurde die Adsorption und Desorption von Fibronektin an beiden Modelloberflächen mit radioaktiv markiertem Protein bestimmt, zeigte sich, dass die Quantität adsorbierten Fibronektins am hydrophoben Substrat höher war. Gleichzeitig war jedoch die Möglichkeit, das Protein durch andere Proteine im Serum zu desorbieren, stark vermindert. Aus diesem Grunde wurde davon ausgegangen, dass die Kopplung von Integrinen an Fibronektin auf hydrophoben Substraten zu einem funktionellen und lokalen Arrest des Rezeptors führt. Als Beleg für einen funktionellen Arrest kann die verminderte Tyrosin-Phosphorylierung in den fokalen Adhäsionsplaques herangezogen werden (siehe weiter oben und **Publikation 5**). Ursache für den lokalen Arrest scheint die feste Bindung zwischen dem am Substrat adsorbierten Fibronektin und dem Rezeptor zu sein, die dessen Mobilität in der Zellmembran einschränkt. Aus diesem Grunde ist auch die Fähigkeit der Zellen zur Bildung von Fibronektin-Fibrillen begrenzt, da sich diese entlang des Fibronektin-Rezeptors auf der Zelloberfläche unter Beteiligung der spezifischen Fibronektin-Module und des α5β1-Integrins ausbilden. In einer kürzlich erschienenen Publikation aus der Gruppe von Kenneth Yamada (Pankov et al. 2000) wurde gezeigt, dass die Fibrillisierung von Fibronektin durch eine Translokation des α5β1-Integrins bewirkt wird, wobei der Fibronektin-Rezeptor aus den fokalen Adhäsionsplaques an der Zellunterseite zur dorsalen Zelloberfläche mit einer messbaren Geschwindigkeit wandert. Motor dieser Bewegung ist das Aktin-Zellskelett, das die für den Prozess der Fibronektin-Fibrillenbildung notwendige mechanische Spannung erzeugt. Diese Ergebnisse bestätigten unsere Vermutung, dass ein lokaler Arrest des Fibronektin-Rezeptors am hydrophoben Substrat die Ursache für das Fehlen einer normalen Matrixsynthese ist. Um diesen Effekt auch für weitere an der Fibronektin-Matrixbildung beteiligten Integrine nachzuweisen, wurden vergleichbare Untersuchungen mit den αv-Integrin durchgeführt (**Publikation 8**). In dieser Arbeit konnte der für den Fibronektin-Rezeptor gefundene Effekt bestätigt werden. Mit diesen Befunden kann die geringere Gewebsverträglichkeit hydrophober Biomaterialien und damit einer Vielzahl von Polymeren auf neue Weise interpretiert werden. Nicht nur die mit der Adsorption einhergehenden Konformationsänderungen der Adhäsivproteine sind dafür verantwortlich, sondern die starke adsorptive Bindung von Adhäsivproteinen wie dem Fibronektin u.a. an das Substrat verhindert eine Translokation von Protein und gekoppeltem Integrin, was den Aufbau einer extrazellulären Matrix beeinträchtigt bis verhindert. Da die Matrix ihrerseits wieder auf Zellwachstum und Funktion zurückwirkt, kommt es damit zu einer Schädigung der

Zellfunktion, die sich in einer geringeren Gewebsverträglichkeit solcher Materialien äußert. Die Vermutung, dass eine starke adsorptive Bindung von Fibronektin an Biomaterialien die Wechselwirkung mit Zellen beeinträchtigt, wurde von Petitt und Mitarbeitern (1994) schon vor längerer Zeit geäußert, ohne dass ein Wirkungsmechanismus vorgeschlagen wurde. Die hier beschriebenen Effekte gelten für hydrophobe Biomaterialien. Es ist aber durchaus denkbar, dass sehr polare Materialien, die ebenfalls eine geringere Biokompatibilität aufweisen, wegen ihrer starken Coulomb-Wechselwirkung mit adsorbierten Proteinen ähnliche Effekte bei Zellen bewirken.

4 Die Steuerung der Biokompatibilität polymerer Biomaterialien

Viele der in medizinischer Anwendung befindlichen Polymere stellen Homopolymere dar, die wegen ihres physikalisch-chemischen Eigenschaftsbildes ausgewählt wurden. Dazu gehören die für eine Applikation erforderliche mechanische Stabilität, wie z.B. der Einsatz von hochdichtem Polyethylen als Material für Hüftgelenkspfannen, oder eine sehr gute hydrolytische Beständigkeit wie bei Teflon, das als Material für den Langzeiteinsatz in Gefäßprothesen Anwendung findet. Dabei sind viele dieser Materialien nicht speziell für eine solche Nutzung entwickelt worden, werden aber für die Medizin in einer sehr hohen Reinheit hergestellt. Eine Vielzahl von Beispielen für die Anwendung solcher industriellen Standardpolymere lassen sich in verschiedenen Übersichtsartikeln finden (Griffith 2000, Helmus und Hubbel 1993, Lee 1995). Da die Materialien in der Mehrzahl der Fälle nicht explizit für medizinische Anwendungen konzipiert wurden, ist deren Biokompatibilität i.A. nicht befriedigend. Eine der Ursachen hierfür liegt in den physikalisch-chemischen Eigenschaften der meisten Polymere, wie ihrer relative schlechten Benetzbarkeit, die sich auf die Adsorption von Proteinen aus der Umgebung auswirkt und daher nachteilige Effekte bewirken kann, wie sie in den vorangegangenen Abschnitten beschrieben wurden. Bei blutkontaktierenden Biomaterialien werden deshalb bei ihrer Anwendung z.T. lebenslang (z.B. bei künstlichen Herzklappen) Gerinnungsinhibitoren, wie das Heparin appliziert (Ratner 1993[a]). Auf der anderen Seite wird eine geringere Biokompatibilität bei Implantaten, die sich in einer Verkapselung des Materials äußert, trotzdem als hinreichend für deren Einsatz betrachtet (Ratner 1993[b]). Neben diesen seit längerer Zeit in Anwendung befindlichen Standardpolymeren, die vor allem wegen ihres günstigen Preis-Leistungsverhältnisses für großvolumige Anwendungen als Schlauchsysteme, in Dialysatoren etc. eingesetzt werden, hat man in der Vergangenheit versucht, die Biokompatibilität von Polymeren durch eine Anpassung der Volumenzusammensetzung des Polymers zu verbessern, was im Abschnitt 4.2 näher erläutert werden soll. Die Biokompatibilität von Homopolymeren ist durch eine Veränderung ihrer Volumenzusammensetzung, die beispielsweise das Molekulargewicht,

Vernetzung, etc. betreffen, relativ schwierig einzustellen, da man hier vorrangig auf für die Anwendung ausreichenden physikalisch-chemischen Eigenschaften achten muss und damit deren biologische Verträglichkeit determiniert. Für diese Materialklassen sind jedoch Oberflächenmodifikationen eine Möglichkeit ihre Biokompatibilität zu steuern, was im Abschnitt 4.3 eingehender beschrieben wird.

4.1 Herangehensweisen zur Verbesserung der Biokompatibilität von Polymeren

Biokompatible Materialien können in bioinerte und bioaktive Typen klassifiziert werden. Ein bioinertes Material ist so gestaltet, dass es möglichst keine spezifischen Wechselwirkungen mit dem biologischen System eingeht. Das heißt, dass es nur in sehr begrenztem Ausmaß oder gar nicht zur Adsorption von Proteinen und der Adhäsion von Zellen kommt. Diese Art von Materialien ist hervorragend für blutkontaktierende Biomaterialien geeignet, jedoch weniger als Implantatmaterial, bei dem beispielsweise ein enger Verbund mit dem umliegenden Gewebe hergestellt werden soll. Solche Materialien können insbesondere durch die Oberflächenmodifikation von Polymeren hergestellt werden, wie unter Punkt 4.3 noch näher beschrieben wird. Ein bioaktives Material hingegen ist befähigt, Reaktionen des biologischen Systems zu erzeugen, die in der Adsorption (und Aktivierung) spezifischer Proteine bestehen können (siehe Abbildung 16). Dies kann beispielsweise eine bessere Blutverträglichkeit des Materials zur Folge haben, oder mit der verbesserten Wechselwirkung von bestimmten Zellen bzw. Zellrezeptoren verbunden sein, so dass diese am Material adhärieren, wachsen und funktionieren können. Gerade letzterer Ansatz wird zunehmend bei der Entwicklung von Implantatmaterialien im Rahmen des Tissue Engineerings verfolgt. Auf beide Ansätze wird noch im Abschnitt 4.2 und 4.3 näher einzugehen sein, wobei auch festgestellt werden muss, dass durch die Art der Materialmodifizierung höhere Kosten verursacht werden, die ihre Anwendung als Massenprodukte, wie beispielsweise für Schlauchsysteme, Dialysatoren, etc., erschweren.

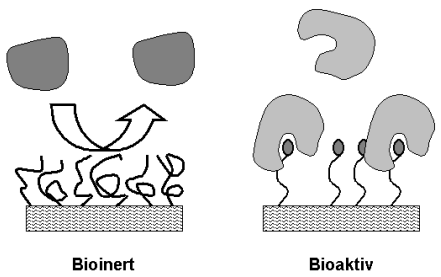

Abbildung 16:
Vergleich von bioinerten mit bioaktiven Polymeroberflächen. Beispielsweise kann durch die kovalente Kopplung von Polyethylenglykol die Adsorption von Proteinen verhindert werden, was das Polymer bioinert macht. Auf der anderen Seite kann durch die Immobilisierung von Signalpeptiden wie RGD eine spezifische Wechselwirkung mit Adhäsiv-proteinen, wie dem Fibronektin erzeugt und die Polymeroberfläche somit bioaktiv werden.

Aus diesem Grunde wurde auch versucht, relativ kostengünstige Polymere mit guter Biokompatibilität durch eine Anpassung der physikalisch-chemischen Oberflächen-Eigenschaften an entsprechende Anwendungen zu erzeugen. Auf diese Weise sollen bei Blutkontakt starke Aktivierungsprozesse der verschiedenen Komponenten vermieden oder eine gute Gewebsverträglichkeit bei Implantaten erzeugt werden. Dies kann durch eine Modifizierung der Materialoberfläche, wie sie beispielsweise an hydrophoben Polymeren durch die Behandlung mit Plasma zur Erzeugung polarer Gruppen vorgenommen wird (Yasuda und Gazicki 1982, Nydegger et al. 1996, Dewez et al. 1998), oder durch eine entsprechende Volumenzusammensetzung des Polymers erreicht werden. Besonders für die Entwicklung blutverträglicher Polymeroberflächen wurden in der Vergangenheit verschiedene Modelle entwickelt, die eine Vorhersage der Biokompatibilität anhand bestimmter Oberflächeneigenschaften erlauben sollte (Baier 1984, Baier 1999, Andrade und Hlady 1986). Diese haben ihre Berechtigung aufgrund von Erfahrungswerten, zielen jedoch eher in Richtung unspezifischer Wechselwirkungen zwischen dem biologischen System und der Materialoberfläche, wobei diese Gegenstand eines Optimierungsprozesses sein können. Ausgangspunkt solcher Überlegungen ist die Oberflächenenergie der Materialien oder besser die Grenzflächenenergie zwischen Oberfläche und biologischem System (Andrade und Hlady 1986, Baier 1984, Baier 1988). Diese ist auf die Zusammensetzung der Oberflächen, d.h. das Vorhandensein bestimmter Atome und funktioneller Gruppen zurückführbar, was bereits unter Abschnitt 2.2 diskutiert wurde. Dabei haben Materialien geringer Oberflächenenergie Werte unterhalb 30 dyn/cm. Diese apolaren oder auch hydrophob genannten Oberflächen (Hoffman 1986) beinhalten eine Reihe von Standardpolymeren, wie Fluorkohlenwasserstoffe, Silikone und Kohlenwasserstoffe. Sie sind durch Wasser nicht oder nur sehr schwer benetzbar. Materialien mittlerer Oberflächenenergie haben Werte zwischen 30 – 40 dyn/cm. Sie können als moderat benetzbar bezeichnet werden, was Wasserrandwinkeln um die 60° bis 70° entspricht. Dazu zählen beispielsweise Polyester, Polykarbonate, und Polyamide. Materialien hoher Oberflächenenergie, d.h. polare Biomaterialien, die auch hydrophil genannt werden können (Hoffman 1986), haben Werte oberhalb 40 dyn/cm bis ca. 70 dyn/cm. Das hat eine sehr gute bis komplette Benetzbarkeit mit Wasser zur Folge. Polymere, die diese Benetzbarkeit erreichen, sind z.B. Polyalkohole, Polysacharide, usw. (Andrade und Hlady 1986).

Trotz der Tatsache, dass extrem apolare Materialien mit Wasserrandwinkeln oberhalb 100° durch die hydrophobe Wechselwirkung (siehe Abschnitt 3.1) eine starke Adsorption und Denaturierung von Proteine bewirken können, werden solche Materialien sowohl im Blutkontakt, wie beispielsweise als Gefäßendoprothesen aus Polytetrafluorethylen (Hyde et al. 1999), als auch im Gewebekontakt, wie z.B. hochdichtes Polyethylen (HDPE), eingesetzt

(Sharkey et al. 2000). Vor allem bei blutkontaktierenden Materialien kommt es unter diesen Umständen zwar zur Auslösung der Proteinadsorption (Zardeneta et al. 1996), doch sind nachfolgende Wechselwirkungen mit anderen Blutkomponenten, wie mit Thrombozyten in Anwesenheit von Antikoagulantien, eher moderat. Als Ursache für dieses Phänomen wurde eine starke Denaturierung von Proteinen angesehen, die die Polymeroberflächen passivieren soll und so weitergehende Reaktionen, wie die Aktivierung des Gerinnungssystems und von Blutzellen, verhindert (Kaelble und Moacanin 1979, Matsuda et al. 1984). Auf diese Weise sollen die adsorbierten Proteine die Materialoberfläche abschirmen, so dass sie nicht mehr durch entsprechende Bindungspartner, wie z.B. Gerinnungsfaktoren, erkannt werden können. Solche Materialien im klinischen Einsatz stellen beispielsweise alle auf Teflon basierenden Biomaterialien dar, aber auch Silikone besitzen vergleichbare Eigenschaften. Tatsächlich lässt sich auf diesen Materialien eine starke Adsorption von Plasmaproteinen, wie von Fibrinogen, nachweisen (Rapoza und Horbett 1990). Auf der anderen Seite kann deren Anwendung auch zu chronischen Entzündungsreaktionen führen, die auf die vorhandenen adsorbierten Proteine zurückgeführt wurden (Zardeneta et al. 1996). Dies tritt verstärkt bei der Entstehung kleiner Polymerpartikel durch mechanischen Abrieb auf, welche die Aktivierung von Phagozyten bewirken können, wie es bei Hüftgelenkspfannen aus HDPE nachgewiesen wurde (Bauer und Schils 1999).

Eine Reihe von Autoren hat in der Vergangenheit die Nutzung moderat benetzbarer Polymere für biomedizinische Anwendungen favorisiert (Baier und Meier 1988, Tamada und Ikada 1994). Dies beruht auf der Erfahrung, dass Polymere, deren Wasser-Randwinkel zwischen 40 und 70° liegen, relativ gut biokompatibel sind. So besitzen beispielsweise die meisten der in Anwendung befindlichen Membranen für die Hämodialyse, wie z.B. Polyacrylnitril, Polyetherkarbonate, Polysulfon, u.a., eine Benetzbarkeit in diesem Bereich (Publikation 11, 12 und 17, Tzoneva et al. 2002). Auch für solche Polymere, die als Implantat genutzt werden oder in anderer Weise mit Gewebezellen in Kontakt treten, konnte von Tamada und Ikada (1994) gezeigt werden, dass die Adhäsion und Proliferation von Gewebezellen in diesem Bereich maximal ist, während sie an hydrophileren oder hydrophoben Oberflächen geringer waren. Dabei nimmt jedoch die Adhäsion und Proliferation nur bei polymeren, hydrophilen Oberflächen ab, was mit deren Wasseraufnahme und Hydrogelcharakter zusammenhängt (siehe weiter unten), während beispielsweise Glas ein gutes Kultursubstrat darstellt. Auch bei Vogler (1998) findet sich eine Zusammenfassung von Untersuchungen der Abhängigkeit von Zelladhäsion und Proliferation von Wasserrandwinkeln, die eine Bestätigung für diesen Bereich der Benetzbarkeit beinhaltet. Als eine Ursache für die bessere Biokompatibilität kann eine verminderte Tendenz zur Adsorption von Proteinen und geringere Triebkräfte für deren

Konformationsänderungen angesehen werden (Andrade und Hlady 1986). Neben den bereits oben erwähnten Homopolymeren können vor allem Copolymere durch eine Balance zwischen hydrophoberen und hydrophileren Komponenten, so gestaltet werden, dass ihre Benetzbarkeit in den als biokompatibel definierten Bereich fällt (Shalaby et al. 1986, Kumaki et al. 1985). Es ist jedoch zu beachten, dass auch eine der Anwendung entsprechende Nutzung von Monomeren mit bestimmten funktionellen Gruppen erfolgt. So führt die Verwendung eines hohen Anteils polarer Funktionalitäten zu einer verstärkten Coulomb-Interaktion zwischen Oberfläche und Proteinen (Norde und Lyklema 1991), was beispielsweise eine Aktivierung des Kontaktsystems der plasmatischen Gerinnung zur Folge haben kann (Vogler et al. 1995). Auf der anderen Seite führt ein höherer Gehalt hydrophober Komponenten zu einer stärkeren Adsorption von Proteinen durch hydrophobe Wechselwirkungen, was beispielsweise in einer Erhöhung der Adsorption von Fibrinogen mündet (Rapoza und Horbett 1990) und eine Zunahme der Adhäsion und Aktivierung von Thrombozyten bewirkt (Lee and Lee 1998).

Eine weitere Möglichkeit der Schaffung biokompatibler Materialien besteht darin, dass die Grenzflächenspannung zwischen Oberfläche und proteinhaltiger Lösung vernachlässigbar klein wird. Somit sollten keine treibenden Kräfte für die Adsorption von Proteinen und die Haftung von Zellen vorliegen (Andrade und Hlady 1986). In diesem Fall ist sowohl die Materialoberfläche vollständig solvatisiert, wie auch die der Proteine. Ein solcher Fall liegt bei Hydrogelen vor, die dadurch gekennzeichnet sind, dass mobile Polymerketten mit polaren oder geladenen Gruppen vorliegen. Das führt zu einer starken Wechselwirkung mit Wasser, das auch in das Polymer eindringen kann und dessen Quellung bewirkt (Hoffman 2001). Die Nachteile von Hydrogelen bestehen in ihrer geringen mechanischen Stabilität, die sie nur für ausgewählte Anwendungen als spezielle Formkörper für die klinische Anwendung brauchbar machen. Hier sind beispielsweise Kontaktlinsen auf Basis von Polymeren der Acrylsäure bzw. deren Derivaten zu nennen (Wheeler et al. 1996). Andererseits sind Hydrogele gut blutverträglich, was sie zu interessanten Materialien für die Anwendung als „drug carrier“ macht. Hier führen sie zu einer Verbesserung der Pharmakokinetik von Medikamenten, um beispielsweise eine verlangsamte Freisetzung im Blut zu erreichen (Duncan und Kopecek 1984). Zudem werden Hydrogele auch als biokompatibles Verkapselungsmaterial für die Immobilisierung von Langerhansschen Inselzellen genutzt (Prokop et al. 1998). Hydrogele werden zunehmend für die Herstellung von Substraten für das Tissue Engineering verwendet. Hierbei wird die Eigenschaft ausgenutzt, dass Hydrogele anti-adhäsiv sind, was die unerwünschte Anheftung von Zellen aus dem Blut oder Gewebe verhindert. Durch die Verbindung mit speziellen Signalsequenzen können jedoch Wechselwirkungen mit spezifischen Proteinen oder Zellkomponenten induziert werden (Hubbell 1998).

4.2 Verbesserung der Biokompatibilität von Polymeren durch Änderung der Volumenzusammensetzung

Die Änderung der Volumenzusammensetzung von polymeren Biomaterialien kommt als eine Möglichkeit zur Steuerung der Biokompatibilität in Betracht. Eine einfache Variante besteht in der Herstellung von Polymermischungen, die auch als Blends bezeichnet werden. Auf diese Weise können sehr rigide Polymere, wie das PVC, durch Zumischung eines hohen Volumenanteils (50% und mehr) einer niedermolekularen Komponente flexibler gemacht werden. So werden beispielsweise die meisten der in Anwendung befindlichen Blutschlauchsysteme aus Weich-PVC hergestellt. Ein Effekt solcher Zumischungen kann auch in einer verbesserten Benetzbarkeit des Materials bestehen, was die Adsorption von Proteinen verringert und damit auch einen positiven Einfluss auf die Biokompatibilität haben kann (Bots et al. 1986). Im Falle des PVC wurden eine Reihe verschiedener Weichmacher verwendet. Ein Problem der niedermolekularen Komponenten mit höherer Hydrophilie besteht jedoch in deren Tendenz zur Diffusion und Anreicherung in der Grenzschicht Material-Blut/Gewebe, von dem sie in die Umgebung abgegeben werden können (Tickner et al. 2001). Dabei sind die Auswirkungen der niedermolekularen Komponente auf die Biokompatibilität des resultierenden Gemisches wegen deren Diffusion in das Blut oder Gewebe negativ einzuschätzen (Tickner et al. 2001, Lamba et al. 2000). Auch bei anderen hydrophoben Homopolymeren kann durch Zugabe einer hydrophilen Komponente die Verarbeitbarkeit verbessert werden. Ein Beispiel für solche Blends ist die Mischung von Polysulfon mit Polyvinylpyrrolidon (PVP) zur Herstellung von Membranen für die Hämodialyse. Während dieses Verfahren in einer verbesserten Blutverträglichkeit des Materials resultiert (Klinkmann und Viencken 1995), verschlechtern sich beispielsweise die Bedingungen für eine Anheftung adhäsionsabhängiger Zellen, was durch die Präsenz einer hydrogelartigen Schicht von PVP und dessen Anreicherung an der Phasengrenze verursacht wird (Fey-Lamprecht et al. 2000).

Während bei der Herstellung von Blends verschiedene Polymere bzw. niedermolekulare Komponenten gemischt werden, kann der Charakter des Polymeren auch durch die Copolymerisation verschiedener Monomereinheiten gezielt beeinflusst werden. Wie unter Punkt 2.1 bereits beschrieben, kann die Copolymerisation auf verschiedene Weise durchgeführt werden. Dazu zählen die Herstellung statistischer oder alternierender Copolymere, sowie die Synthese sogenannter Block-Copolymere. Beispiele für die Synthese statistischer Copolymere sind auch Bestandteil der vorliegenden Habilitationsschrift. Dazu gehören die in **Publikation 2** vorgestellten Copolymere des Acrylnitrils. Diese bereits unter Punkt 3.2.1 beschriebene Publikation erläutert, wie die Verwendung von Comonomeren, die Blutverträglichkeit des resultierenden Copolymers beeinflusst. So zeigten die

Untersuchungen eine hohe Kallikrein-Generierung beim Vorhandensein von Acrylsäure als Comonomeren. Dies steht in Übereinstimmung mit Untersuchungen von Vogeler und Mitarbeitern (1995), die einen Anstieg der Faktor-XIIa-Generierung mit dem Gehalt von Carboxylgruppen an Oberflächen verbinden konnten, wobei den dort nachgewiesenen negativen Oberflächenpotentialen eine große Bedeutung zugemessen wurde. Auch an Oberflächen, die Sulfat- oder Sulfonatgruppen enthalten, ist normalerweise die Kontaktaktivierung hoch (Silverberg und Diehl 1987). Wegen des vergleichsweise geringen Gehaltes an Allylsulfonat im Copolymeren war offensichtlich die nachgewiesene Kontaktaktivierung recht gering. Wie bereits erwähnt, stimulieren aber sulfonathaltige Membranen die Generierung von Bradykinin, was bei deren klinischer Anwendung Probleme verursachen kann (Tielemanns et al., 1990; Parnes und Shapiro, 1991). Aus diesem Grunde sollte die Verwendung solcher Comonomere für die Herstellung von Membranen für die Hämodialyse vermieden werden. Als alternatives Copolymer konnte durch die Verwendung von Hydroxyethylacrylat bei vergleichbaren Volumengehalten eine wesentliche Erhöhung der Kallikreinerzeugung vermieden werden, was die bevorzugte Verwendung eines solches Copolymeren für die Synthese von membranbildenden Polymeren nahe legt. Wenn physikalisch-chemische Oberflächenparameter der Membranen, wie die Randwinkel und Zeta-Potentiale, mit der Kallikrein-Generierung verglichen wurden, konnten jedoch keine einfachen Korrelationen hergestellt werden konnten. Vielmehr müssen sowohl integrale Parameter, wie die Benetzbarkeit, als auch die Aktivität spezifischer Strukturen, wie beispielsweise die Aktivität der Carboxylfunktionen berücksichtigt werden.

Vergleichbare Copolymere auf der Basis von Acrylnitril und Comonomeren, wie dem Natriummethallylsulfonat (NaMAS) oder N-Vinylpyrrolidon (NVP) zur Erhöhung der Hydrophilie oder Aminoethylmethacrylat (AEMA) zur Einführung reaktiver Amingruppen, wurden für die Herstellung von Copolymeren und Membranen zur Anwendung in Biohybrid-Organen genutzt. Hier sollte die Biokompatibilität des Copolymeren sowohl für den Kontakt mit Blut als auch für die Ansiedlung von Gewebezellen durch Änderung der Hydrophilie und dem Vorhandensein bestimmter funktioneller Gruppen optimiert werden. Auf die letztere Anwendung wird noch im Rahmen der Habilitationsschrift unter Punkt 5 näher eingegangen. Die Verwendung eines Comonomeren mit stark saurer Funktionalität, wie dem NaMAS (ca. 2 Mol%), ergab eine erhöhte Benetzbarkeit der Membranoberfläche. Dies ist auf starke Wechselwirkung der sauren Sulfonatgruppe mit Wasser zurückführbar. Vergleichbare Volumenanteile von AEMA (ca. 5 Mol%) erhöhten die Wasserrandwinkel geringfügig im Vergleich zum PAN-Homopolymer. Dagegen wurden durch NVP trotz höherer Volumenanteile von bis zu 30 Mol% im Copolymer die Wasserrandwinkel nur in geringerem Maße verringert. Während die Auswirkungen der unterschiedlichen Comonomere auf die

Wasserrandwinkel eher gering waren, wurden beachtliche Unterschiede bei der Wechselwirkung mit Fibroblasten beobachtet. Diese haften und wachsen besser auf polaren Unterlagen, wie dem NaMAS, während höhere Gehalte von NVP eine Verringerung der Zellhaftung und Proliferation zur Folge hatten. Auf der anderen Seite konnte gezeigt werden, dass auch die Präsenz von aminfunktionalisierten Comonomeren einen fördernden Einfluss auf die Zelladhäsion und -wachstum haben. Diese Effekte sollten auf die Adsorption von Proteinen zurückführbar sein (Steele et al. 1994). Obschon solche Untersuchungen nicht Bestandteil der vom Habilitanden publizierten Artikel waren, kann davon ausgegangen werden, dass sowohl an sulfonathaltigen, als auch an aminfunktionalisierten Oberflächen eine stärkere Adsorption von Proteinen als an NVP-haltigen Copolymeren stattfindet, was durch die Arbeiten weiterer Autoren belegt ist (Lee et al. 1998, Mateo et al. 2000, Boffa et al. 1977). An den genannten Beispielen wird deutlich, dass sich durch die gezielte Copolymerisation die Biokompatibilität steuern lässt und so Materialien für bestimmte Anwendungen wie z.B. für die Immobilisierung von Zellen produziert werden können.

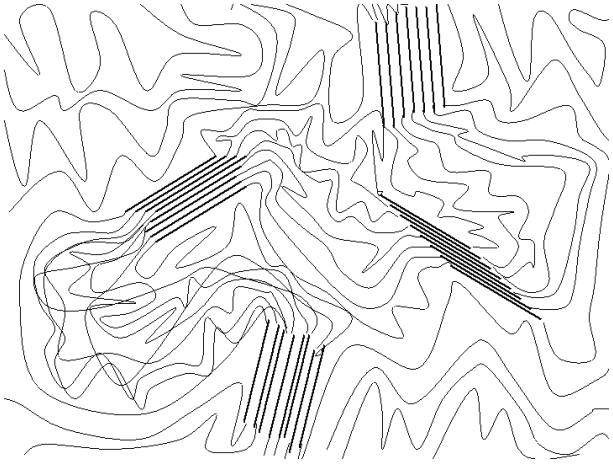

Abbildung 17:

Schematische Darstellung der Struktur von phasenseparierten Block-Copolymeren mit niedrigschmelzenden amorphen aufgelockerten Bereichen und hoch- schmelzenden kristallinen dichten Domänen.

Während Homopolymere, aber auch statistische und alternierende Copolymere relativ homogene Volumen- und Oberflächenphasen entfalten, können Block-Copolymere - wie in Abbildung 17 gezeigt - getrennte Phasen ausbilden, die zu einer mikroskopisch heterogen Strukturbildung führen (z.B. Rasmont et al. 2000). Diese Strukturbildung wird durch das Vorhandensein von Anteilen unterschiedlicher Eigenschaften in der Polymerkette verursacht. Dies können längere hydrophobe und hydrophile Segmente sein oder auch Abschnitte, die eine hohe Tendenz zur Kristallisation besitzen, im Gegensatz zu solchen, die amorphe Strukturen ausbilden (Matsuo und Sagaye 1971, Lyman et al. 1975). Unterhalb der Glasübergangstemperatur des Polymeren kommt es zur Segregation dieser Abschnitte, was die Ausbildung hydrophiler und hydrophober bzw. kristalliner und amorpher Domänen zur Folge hat (Dieterich 1987). Die Größe dieser Domänen hängt von den Eigenschaften der Ketten ab und kann bei einigen 10 bis 100 nm Durchmesser liegen. Eine Domänenstruktur

mit Bildung verschiedenartiger Blöcke im Polymervolumen wird mit Hilfe verschiedener Methoden nachgewiesen. Dazu zählen die dynamisch-mechanische Analyse (DMA) und die Differential-Scanning-Kalorimetrie (DSC).

Bei diesen Verfahren werden bei schrittweiser Temperaturerhöhung das Elastizitätsmodul bzw. die Energieaufnahme bestimmt. Da amorphe und kristalline Phasen bei unterschiedlichen Temperaturen aufschmelzen, kann dies in den entsprechenden Temperaturverläufen nachgewiesen werden (Billmeyer 1971). Eine Domänestruktur des Polymeren kann aber auch durch Kontrastierung des Polymers mit Osmiumtetroxid und Darstellung mit dem Transmissionselektronenmikroskop nachgewiesen werden. Da sich die Phasen in ihrer Bindung des Kontrastmittels unterscheiden, können die Domänen direkt dargestellt werden (Kumaki et al. 1985, Okano et al. 1986, Klosz 1993). Die Präsenz einer Domänenstruktur hat jedoch nicht nur Einfluss auf die Volumeneigenschaften, sondern wirkt sich auch auf die Oberflächeneigenschaften des Polymers aus. So kann beispielsweise durch dynamische Randwinkelmessungen eine Zunahme der Hysterese bei Vorhandensein von Domänen nachgewiesen werden, was auf deren unterschiedlichen Eigenschaften, wie z.B. hydrophil versus hydrophob hinweist (Takahara et al. 1989, Otsuka et al. 2000). Die Adsorption von Proteinen kann ebenfalls beeinflusst werden, so dass bestimmte Proteine wie Fibrinogen und Immunglobulin G an hydrophoben Arealen und Albumin an hydrophilen adsorbieren (Okano et al. 1978). Dies führt zu einer Mosaikstruktur an der Oberfläche, die für die beobachtete verbesserte Blutverträglichkeit von Block-Copolymeren verantwortlich sein soll (Merrill et al. 1982, Kumaki et al. 1985, Okano et al. 1986). So sind viele Blockcopolymere für eine relativ gute Blutverträglichkeit und eine geringe Adhäsion von (Blut)Zellen bekannt (Klosz 1993, Kumaki et al. 1985, Merrill et al. 1982, Okano et al. 1978, Okano et al. 1986, Otsuka et al. 2000, Takahara et al. 1989, Grasel and Cooper 1986, Okkema und Cooper 1991). Dabei wurden insbesondere Polyurethane beschrieben, die durch ihre hervorragenden physikalischen Eigenschaften und Biokompatibilität für viele biomedizinische Anwendungen geeignet sein können (Zdrahala und Zdrahala 1999).

Polyurethan-Blockcopolymere bestehen aus alternierenden Hart- und Weichsegmenten. Diese Segmente sind thermodynamisch unverträgliche Komponenten, die auf den Polaritätsunterschieden der Ausgangskomponenten beruhen. Wenig polare, tiefschmelzende Weichsegmente sind inkompatibel mit hochschmelzenden, polaren Hartsegmenten. Als Weichsegmentbildner werden Dihydroxypolyether und Dihydroxypolyester eingesetzt. Aromatische, aliphatische oder cycloaliphatische Diisocyanate bilden gemeinsam mit dem Kettenverlängerer das Hartsegment. Als Kettenverlängerer werden Diole oder Diamine und Wasser eingesetzt (Becker 1983, Dieterich 1989). Das Ausmaß der Phasenseparation ist abhängig von den Affinitäten der Hartsegmente untereinander und zu den Weichsegmenten.

Polyesterurethane weisen eine geringere Phasenseparation auf als Polyetherurethane. Das Ausmaß der Phasenseparation ist auch durch die Längenverteilung von Hart- und Weichsegmenten bestimmt. So können kurze Weichsegmente sich in Hartsegmenten lösen und umgekehrt können kurze Hartsegmente sich in der Weichsegmentmatrix lösen (Grasel und Cooper 1986). Die segmentierte Struktur von Polyurethanen und anderen Block-Copolymeren bestimmt neben deren Volumeneigenschaften, auf die hier nicht eingegangen werden kann, deren Oberflächeneigenschaften. Dabei wurde die chemische Natur der Oberfläche von Polyurethan-Blockcopolymeren auch kontrovers diskutiert. So wurde von einigen Autoren festgestellt, dass überwiegend das Weichsegment an der Oberfläche angereichert ist (Ratner 1985), während andere zeigen konnten, dass auch das Hartsegment an der Oberfläche zu finden ist (Lelah et al. 1986). Im Gegensatz zur Volumenphase, in der die polaren Gruppen der Hartsegmente durch intermolekulare Wechselwirkungen gebunden sind, treten an der Oberfläche diese Gruppen als Orte höheren chemischen Potentials und Träger partieller Ladungen auf (Andrade et al. 1973). Mit zunehmendem Hartsegmentgehalt nimmt die Zahl dieser Gruppen an der Oberfläche zu.

Eine Balance von polaren und unpolaren Oberflächendomänen kann einen günstigen Einfluss auf die Blutverträglichkeit haben (Ratner et al. 1979). In **Publikation 9** wurde der Versuch unternommen durch Verwendung eines apolaren Polyols die Blutverträglichkeit von Polyurethanen zu verändern. Sie beschreibt die Verwendung eines unpolaren Polyols – nämlich von Polyisobutylenglykol (PIBG) – zur Substitution von Polytetramethylenetherglykol (PTMEG) bei der Herstellung von Polyetherurethanen und dessen Einfluss auf die Thrombogenität des Polymers. Dazu wurden Polyetherurethane auf Basis von 4,4´-Methylenbisphenylisocyanate (MDI) als Hartsegmentbildner, sowie 1,4-Butandiol mit obigen Polyolen synthetisiert. Der Gehalt an Weichsegment wurde durch eine Variation des Verhältnisses von PTMEG zu PIBG variiert, wobei der Anteil von PIBG von 0 bis 100 Gewichtsprozent im Weichsegment eingestellt wurde. Zudem wurden zwei verschiedene Molekulargewichte von PTMEG 1000 und 2000 für die Synthese der Polyetherurethane verwendet. Die physikalisch-chemischen Eigenschaften dieser Materialien wurden mit verschiedenen Methoden bestimmt, worauf hier nur kurz eingegangen werden soll. Dabei zeigten alle Polymere eine Phasenseparation, wobei auch eine Tendenz zur Anreicherung des hydrophoben PIBG an der Oberfläche beobachtet wurde. Dieser Sachverhalt wurde insbesondere durch die Messung von Wasserrandwinkeln an Filmen der verschiedenen Copolymere deutlich. Danach führte die Erhöhung PIBG-Gehaltes zu einer Zunahme des statischen Wasserrandwinkel. Wenn dynamische Randwinkelmessungen mit Bestimmung des Vorwärts- und Rückzugswinkels vorgenommen wurden, zeigte sich, dass nur der Benetzungswinkel zunahm, während der Rückzugswinkel konstant blieb. Dieses Verhalten

deutet auf eine Heterogenität der Oberflächen hin, wie sie durch eine Zunahme der hydrophoben PIBG-Anteile im Vergleich zu besser benetzbaren Oberflächendomänen erklärt werden kann. Die biologische Verträglichkeit der erhaltenen Materialien wurde über die Wechselwirkung mit Thrombozyten ermittelt. Dabei diente Polypropylen als Vergleichsmaterial mit hoher Thrombogenität. Es zeigte sich, dass geringe Anteile von PIBG unter 25 Gewichtsprozent keine Zunahme der Thrombogenität bewirkten. Wenn man die durch die Verwendung von PIBG erzielten Änderungen mechanischer Eigenschaften des Polymeren berücksichtigt, sind solche Mengen in bezug auf die Blutverträglichkeit tolerierbar. Es zeigte sich jedoch insgesamt, dass die Zunahme des unpolaren PIBG eine Erhöhung der Thrombogenität zur Folge hatte. Dennoch kann im Vergleich zu Polypropylen und auch einem kommerziellen Polyetherurethane (Pellethan) davon ausgegangen werden, dass Polyetherurethane mit PIBG-Gehalten bis zu 25 Gewichtsprozent eine hervorragende Blutverträglichkeit besitzen.

In **Publikation 10** wurde ebenfalls die Blutverträglichkeit von Polyurethanen untersucht. Dabei handelte es sich um Polyurethan-Harnstoffe, bei denen durch die gezielte Einstellung des Verhältnisses von Urethan zu Harnstoff (i), des Gehaltes von Urethan (ii) und des Gehaltes von Harnstoff (iii) deren Einfluss auf die Blutverträglichkeit bewertet werden sollte. Dabei wurde zur Synthese ebenfalls MDI, sowie PTMG als Polyol verwendet. Durch die Nutzung von PTMG mit Molekulargewichten von 650, 1000, 1500 und 2000 und der Änderung des Verhältnisses von Diisocyanat, Polyol und Kettenverlängerer war es möglich, Polyurethan-Harnstoffe mit oben benannten Eigenschaften (i), (ii) und (iii) zu synthetisieren. Volumen- und Oberflächeneigenschaften wurden mittels DMA, Randwinkel- und Strömungspotentialmessungen erfasst. Wasserrandwinkelmessungen konnten keine signifikanten Effekte mit Änderungen der Volumenzusammensetzung nachweisen. Jedoch wurde bei Randwinkelmessungen mit verschiedenen Glykolen für Polyurethan-Harnstoffe mit konstantem Harnstoffgehalt eine Zunahme des polaren Anteils der freien Oberflächenenergie für die Zunahme des Hartsegmentgehaltes nachgewiesen. Für diese Materialreihe wurde auch eine Erhöhung der Oberflächenladungsdichte mit der Strömungspotentialmethode ermittelt. Wurde die Adhäsion gewaschener Lymphozyten an diesen Polymeren bestimmt, zeigte sich generell eine Erhöhung der Zelladhäsion mit Zunahme des Hartsegmentgehaltes, ohne jedoch durch die unterschiedliche Zusammensetzung beeinflusst zu werden. Auch die mittels polyklonaler Antikörper bestimmte Adsorption von Fibrinogen aus Plasma zeigte eine Zunahme mit steigendem Hartsegmentgehalt. Im Gegensatz dazu wurde bei Verwendung eines monoklonalen gegen die γ-Domäne des Fibrinogens gerichteten Antikörpers eine andere Beobachtung gemacht. Während mit der Zunahme des Harnstoffgehaltes für die Reihen (i) und (ii) auch eine

Erhöhung der Bindung des monoklonalen Antikörpers nachweisbar war, konnte bei konstantem Harnstoffgehalt (iii) eine solche Zunahme nicht festgestellt werden. Da in Übereinstimmung mit Arbeiten anderer Autoren eine Erhöhung der Adsorption von Fibrinogen mit zunehmenden Hartsegmentgehalt unabhängig von der Zusammensetzung der Polyurethan-Harnstoffe festgestellt wurde (Chen et al. 1998), sollten Konformations- oder Orientierungsänderungen des Fibrinogen für die verminderte Bindung des monoklonalen Antikörpers bei Reihe (iii) verantwortlich sein. Hinweise für die Richtigkeit dieser Vermutung ergaben sich aus der Bestimmung der Aktivierung von Thrombozyten. Während eine Zunahme der Adhäsion und Aktivierung von Thrombozyten mit Zunahme des Hartsegmentgehaltes für die Reihen (i) und (ii) in Analogie zur Bindung poly- und monoklonaler Antikörper gegen Fibrinogen beobachtet wurde, konnten bei Reihe (iii) keine signifikanten Veränderungen bei der Wechselwirkung mit Thrombozyten nachgewiesen werden. Wie bereits erwähnt, wird bei der Adsorption von Fibrinogen eine Dodecapeptidsequenz in der Gammakette des Proteins zum potentiellen Bindungsort der Thrombozyten (Kloszewiak et al. 1989). Die bei Reihe (iii) gemachte Beobachtung deutet darauf hin, dass dieses Epitop in seiner Konformation gestört wird, so dass die Interaktionen mit Thrombozyten vermindert sind. Ursache für dieses Effekt könnte eine stärkere polare Wechselwirkung der Polymeroberfläche mit Fibrinogen sein, die auf deren höheren Gehalt an Carbonylgruppen zurückführbar ist, was mit der höheren Polarität von Reihe (iii) in Übereinstimmung steht. Damit konnte gezeigt werden, dass der Gehalt an Harnstoff eine entscheidende Rolle für die Blutverträglichkeit von Polyurethan-Harnstoffen besitzt.

4.3 Verbesserung der Biokompatibilität von Polymeren durch Modifikation der Materialoberfläche

Um Polymere mit hervorragenden physikalisch-chemischen Eigenschaften, aber ungenügender Biokompatibilität trotzdem einer bestimmten Anwendung zuzuführen, bietet sich eine nachträgliche Oberflächenmodifikation des Materials an. Dies wird beispielsweise bei der Entwicklung von Kathetern genutzt, um Materialien blutkompatibel und anti-adhäsiv für Bakterien zu machen und gleichzeitig deren Gleitfähigkeit bei der Bewegung im Blutgefäß oder anderen Körperhohlräumen zu verbessern, was durch extrem hydrophile Oberflächenbeschichtungen erreicht werden soll (Kunz et al. 1998). Der Vorteil einer nachträglichen Oberflächenbehandlung besteht darin, dass es nicht zur Veränderung der mechanischen Eigenschaften des Polymers kommt, und man auf diese Weise ein Material an verschiedene Anwendungsgebiete anpassen kann. Für die Veränderung der Materialoberfläche bieten sich eine Reihe physikalisch-chemischer Methoden an, auf die hier nicht ausführlich eingegangen werden kann. Man kann sie jedoch unterteilen in Verfahren,

bei denen das Basismaterial chemisch unverändert bleibt und solchen, bei denen es chemisch modifiziert wird. Verfahren, die das Basismaterial chemisch unverändert lassen, bestehen in einer einfachen physischen Schichtabscheidung auf dem Material, die beispielsweise durch die Adsorption von Tensiden oder Proteinen aus einer Lösung erreicht werden kann. Zu den Verfahren, welche die Polymeroberfläche verändern, gehören die chemische Modifizierung, die beispielsweise zur Erzeugung bestimmter funktioneller Gruppen, der Kopplung von Molekülen bis hin zur Oberflächen-Copolymerisation genutzt wird. Das ist auch durch die plasmachemische Behandlung von Polymeren oder durch Strahlungseinwirkung, wie γ–Strahlung oder ultraviolettes Licht, möglich. Im letzteren Fall spricht man von einem photochemischen Prozess. Eine Übersicht der verschiedenen Möglichkeiten der Oberflächenmodifizierung findet sich in Tabelle 1. Wie bereits unter Punkt 4.1 beschrieben, kann durch solche Modifikationen die Polymeroberfläche bioinert oder bioaktiv gestaltet werden, worauf im Folgenden näher eingegangen werden soll.

Bioinerte Oberflächenmodifikationen versuchen, wie bereits für Hydrogele beschrieben, die Wechselwirkung des Materials mit der Umgebung zu minimieren. Während die unter Punkt 4.1 beschriebenen Konzepte der Biokompatibilität weitestgehend auf der Betrachtung einer phänomenologischen Größe – der Grenzflächenenergie zwischen Materialoberfläche und biologischen Milieu - beruhten, wurden auch andere Ansätze entwickelt, welche die molekularen Wechselwirkungen an der Grenzfläche berücksichtigen. Wie bereits im Kapitel 3.1 beschrieben, spielt die Wechselwirkung von Wasser mit Oberflächen und Proteinen eine wesentliche Rolle für die Proteinadsorption und damit die Biokompatibilität von Polymeren. So konnte die Gruppe um Whitesides zeigen, dass für eine Verhinderung von Proteinadsorption (und damit nachfolgender Zelladhäsion) eine Reihe von Minimalbedingungen erfüllt sein müssen, die nicht notwendigerweise mit einem Hydrogelcharakter der Oberfläche einhergehen, wie durch die Verwendung von „self assembling-monolayers“ (SAM) organischer Moleküle an Festkörperoberflächen gezeigt werden konnte (Ostuni et al. 2001). So lassen sich Oberflächen, welche die Adsorption von Proteinen verhindern, dadurch charakterisieren, dass sie hydrophil sind, Akzeptoren von Wasserstoff-Brückenbindungen darstellen, keine Donatoren für Wasserstoff-Brückenbindungen besitzen und ihre Gesamtladung elektrisch neutral ist. Diese Charakteristika treffen für eine Vielzahl der Hydrogele zu, wie zum Beispiel für solche aus Polyethylenglykol, Dextran, aber auch für eine Vielzahl anderer Molekülen, wie z.B. verschiedenen Phospholipiden etc.. Als Ursache für die geringe Adsorption von Proteinen an solchen Oberflächen, die damit inert werden, wird die Präsenz von Wasserstrukturen auf dem Protein und der Materialoberfläche angesehen, die eine repulsive Barriere für die Adsorption der Proteinen darstellen (Besseling 1997, Rau und Parsegian 1990).

Tabelle 1: Techniken der Oberflächenmodifizierung von Biomaterialien

Physikalische Abscheidung mittels ⁇ Adsorption ⁇ Adhäsion
Chemische Modifizierung
Oberflächen(Graft)-Copolymerisation mittels ⁇ Strahlung ⁇ Photochemisch ⁇ Chemisch
Plasma-Gasentladung ⁇ Ätzen ⁇ Abscheidung

Eine solche Minimierung von Wechselwirkungen mit Proteinen und Zellen ist durch die Immobilisierung von Lipiden auf Biomaterialien möglich, wobei die Lipidmembran von Erythrozyten als Modell für biokompatible Oberflächen nutzbar gemacht wurde (Hayward und Chapman 1984). Hauptbestandteil der Außenmembran dieser Zellen ist die Phosphatidylcholin-Kopfgruppe der Lipide (Zwaal und Hemker 1982). Ursache für die geringe Tendenz zur Adsorption an diesen Oberflächen ist die amphotere Natur der Kopfgruppe, die zu hoch geordneten Wasserstrukturen an der Oberfläche führt (Ishihara et al. 1998). Diese Wasserstrukturen verursachen dabei stark repulsive Kräfte, die eine Adsorption anderer Moleküle, wie von Proteinen oder gar Zellen verhindern (Vogler 1998). Auf diese Weise wurden bislang eine Reihe bioinerter Oberflächenbeschichtungen geschaffen, die eine verbesserte Blutverträglichkeit erzeugen (Harris und Chapman 1989, Iwasaki 1999, Ishihara 1992). Zusätzlich lassen sich die Eigenschaften dieser Oberflächenbeschichtung nutzen, um die Adhäsion von Zellen zu verhindern (Ishihara et al. 1999). Andere Möglichkeiten der Passivierung von Polymeroberflächen bestehen in der Immobilisierung stark hydrophiler (Makro)moleküle. Dazu zählt die Immobilisierung von Derivaten der Acrylsäure, die beispielsweise durch eine Pfropfung im Plasma erzielt werden kann (Nedelmann et al. 1999). Auf diese Weise entstehen gut benetzbare Oberflächen, die eine reduzierte Tendenz zur Adsorption von Proteinen aufweisen (Breuers et al. 1987). Zusätzlich zur Erhöhung der Hydrophilie kann die Präsenz von hoch mobilen Makromolekülen (mit Tentakeln) bei der Immobilisierung einen zusätzlichen stark repulsiven Effekt ausüben, der die Adsorption von Proteinen und damit auch weitere Reaktionen stark begrenzt. Dazu gehören die Kopplung von Poly(hydroxyethyl methacrylat) oder

Polyacrylsäure (Dvorankova et al. 1998, Ulbricht und Riedel 1998). Auch andere hydrophile Moleküle, wie das Poly(N-Vinylpyrrolidon) können durch eine Photoimmobilisation auf Polymeren eine Verringerung von Proteinadsorption und Verbesserung der Blutverträglichkeit bewirken (Wetzels und Koole 1999). Ebenfalls können hydrophile Polysaccharide, wie das Dextran genutzt werden, um Polymere proteinresistent, zellabweisend (Massia et al. 2000) und damit inert zu machen (Österberg et al. 1995). In der zuletzt zitierten Arbeit wird ein Vergleich mit Polyethylenglykol (PEG) vorgenommen, wobei sich zeigt, dass PEG schon bei geringeren Oberflächenkonzentrationen eine höhere Effektivität als Dextran besitzt. PEG ist wahrscheinlich eines der am häufigsten und am erfolgreichsten genutzten Makromoleküle, um die Adsorption von Proteinen und die Adhäsion von Zellen zu verhindern. Ursache hierfür ist die sehr gute Hydratation des Moleküls, gepaart mit seiner hohen Mobilität. Dabei kommt es bei Annäherung von größeren Proteinmolekülen an die gekoppelten PEG-Schicht zu einer sterischen Repulsion, was energetisch ungünstig ist, und damit zur Verhinderung der Adsorption führt. Eine ausführliche Beschreibung des Mechanismus findet sich bei Leckband und Mitarbeitern (1999). So wurde PEG verwendet um die Adsorption von Proteinen zu verringern (Alcantar et al. 2000) und die Adhäsion von Zellen zu verhindern (Defife et al. 1999). Dabei stellte sich heraus, dass die Fähigkeit immobilisierter PEG-Moleküle zur Verhinderung von Proteinadsorption von der Größe des PEG und dem Bedeckungsgrad der Oberfläche abhängig ist (Prime und Whiteside 1993). Eine ausführliche Beschreibung dieses Zusammenhangs findet sich bei Sofia und Mitarbeitern (1998). Damit bleibt eine gewisse Adsorption von Proteinen möglich, die auch von anderen Autoren beobachtet wurde (Benesch et al. 2001). Die biologischen Implikationen dieses Prozesses blieben bislang jedoch unbeachtet. Im Rahmen der vorliegenden Habilitationsschrift wird daher gezeigt, dass die kovalente Kopplung von PEG an hydrophoben Polymeren die Adsorption von Proteinen im gewissen Umfang erlaubt, wobei Hinweise darauf existieren, dass die Konformation und mithin die biologische Aktivität adsorbierter Proteine durch benachbarte PEG-Moleküle stabilisiert werden kann. Damit können Materialoberflächen mit PEG nicht nur bioinert gestaltet werden, sondern es ist möglich, durch Einstellung der Bedeckungsdichte mit PEG, ein bioaktives Substrat zu erzeugen.

Im Einzelnen wird in den **Publikationen 11 und 12** dargestellt, wie PEG durch Photoimmobilisation auf hydrophobes Polysulfon gepfropft werden kann. Dabei wird das photoreaktive α-4-Azidobenzoyl-β-Methoxy Polyethylenglykol (AMPEG) aus einer wässrigen Lösung an Polysulfon adsorbiert. In **Publikation 11** wird vorgestellt, wie durch Änderung der Volumenkonzentration des amphiphilen AMPEG während des Adsorptionsprozesses der Funktionalisierungsgrad der Oberfläche kontrolliert werden kann. Es wurden PEGs mit

unterschiedlichen Molekulargewichten von 2, 5 und 10 kDa verwendet. Wasserrandwinkelmessungen an Polysulfon modifiziert mit 10 kDa AMPEG zeigten, dass mit Zunahme der Volumenkonzentration von 0.001 g/l bis 100 g/l eine Abnahme des Vorwärts- und Rückzugswinkels verbunden sind. Dabei nimmt der Rückzugswinkel stärker ab als der Vorwärtswinkel, was eine Zunahme der Hysterese bedeutet. Vergleicht man den Gang der Hysterese für die verschiedenen Molekulargewichte, so ergibt sich eine Erhöhung für PEGs mit höherem Molekulargewicht. Dies deutet auf eine unvollständige Bedeckung der Polysulfonoberfläche mit PEG hin, die durch die zunehmende Größe und damit sterische Hinderung der benachbarten PEGs erklärt werden kann. Um zu prüfen, ob tatsächlich eine irreversible Kopplung des PEGs an Polysulfon erfolgte, wurde über Nacht mit Isopropanol gespült und vergleichende Randwinkelmessungen vorgenommen. Dabei bleiben die Randwinkel bis zu AMPEG-Konzentrationen von 10 g/l praktisch unverändert. Um die Wechselwirkung des modifizierten Polysulfons mit Proteinen näher zu charakterisieren, wurde die Adsorption von Fibronektin mit Ellipsometrie bestimmt. Dabei zeigte sich erwartungsgemäß, dass mit der Zunahme der AMPEG-Konzentration eine Abnahme der Proteinadsorption verbunden war. Die Zunahme der Proteinadsorption korrelierte mit den gemessenen Änderungen der Randwinkel, d.h. je hydrophober die Oberfläche desto höher die adsorbierte Menge Protein. In weiteren Versuchen wurde die Wechselwirkung so modifizierter Oberflächen mit Fibroblasten untersucht. Die Untersuchungen mit Zellen zeigten, dass Polysulfon als hydrophobes Material deren Anheftung und Spreitung nicht unterstützt. Auf der anderen Seite fördert auch PEG nicht die Adhäsion von Zellen, wenn hohe Bedeckungsgrade (10g/l Volumenkonzentration) vorliegen. Das bedeutsame Resultat dieser Untersuchung besteht jedoch in der Tatsache, dass bei geringeren Volumenkonzentrationen von AMPEG (0.001, 0.01, 0.1 g/l) eine Zunahme der Adhäsion und Spreitung von Zellen nachweisbar war. Dabei wurden besonders intensive Kontakte (fokale Adhäsionsplaques) zwischen Zellen und Substraten bei diesen Konzentrationen ausgebildet. Die adhäsionsfördernde Aktivität bei intermediären AMPEG-Konzentrationen wurde auf einen konformationsstabilisierenden Effekt benachbarter PEG-Moleküle hinsichtlich aus dem Serum adsorbierter oder von Zellen sezernierter Adhäsivproteine zurückgeführt. In Abbildung 18 wird der vorgeschlagene Mechanismus schematisch dargestellt.

Um diesen Sachverhalt weiter aufzuklären, wurden in **Publikation 12** Fibroblasten nach Vorbeschichtung der Substrate mit Fibronektin in Abwesenheit von Serumproteinen vorgenommen. Bei diesem Ansatz ist Fibronektin das einzige Adhäsivprotein, das in Wechselwirkung mit dem Substrat treten kann. In dieser Publikation konnte bestätigt werden,

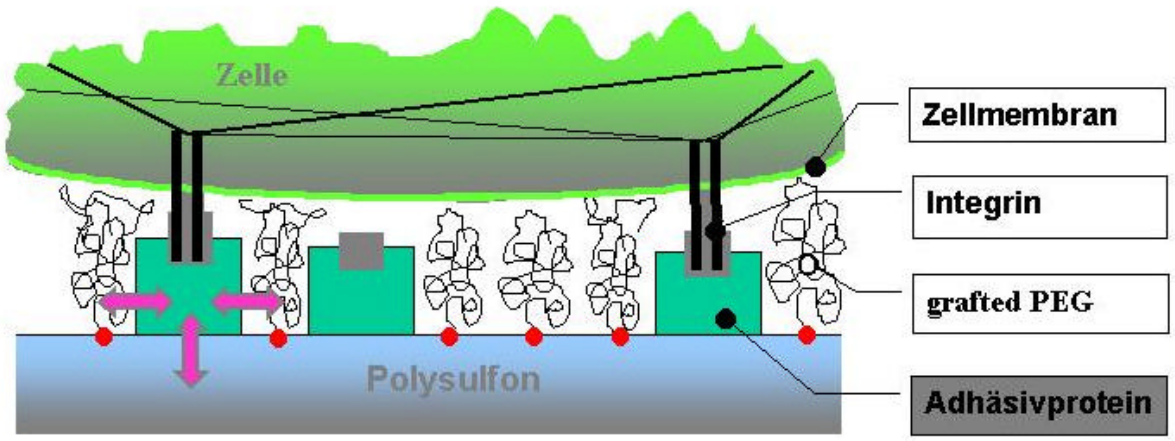

Abbildung 18: Bei der Immobilisierung von Polyethylenglykol auf hydrophoben Polymeren ist eine Stabilisierung der Konformation adsorbierter Proteine durch die Präsenz benachbarter hydrophiler Makromoleküle, wie Polyethylenglykol, denkbar.

dass intermediäre AMPEG-Konzentrationen eine Stabilisierung der biologischen Aktivität von Fibronektin bewirken, so dass bei geringeren Oberflächenkonzentrationen von Fibronektin eine erhöhte biologische Wirksamkeit gegeben ist, die durch eine maximale Zelladhäsion, Zellspreitung und Ausbildung fokaler Adhäsionskomplexe indiziert wurde. Wurden funktionelle Kriterien, wie das Wachstum von Fibroblasten, sowie ihre Fähigkeit zur Ausbildung einer Fibronektinmatrix hinzugezogen, so zeigte sich auch hier, dass Polysulfon modifiziert mit geringen Mengen PEG eine erhöhte biologische Aktivität besitzt. Berücksichtigt man zudem die Tatsache, dass die extrazelluläre Matrix durch die Aktivität von Proteasen und die Sezernierung weiterer Matrixproteine ständig erneuert wird, stellt die Verwendung solcher Oberflächen möglicherweise einen Vorteil gegenüber der herkömmlichen Praxis der kovalenten Kopplung dar. Die kovalente Kopplung von Peptiden und Proteinen verhindert in der Regel nicht deren Abbau durch Proteasen, so dass die bioaktiven Moleküle verloren gehen können. Bei der Immobilisierung an mit PEG modifizierten Oberflächen ist jedoch nach Verlust der Fragmente ein Einbau neuer Matrixproteine denkbar. Die Oberflächenmodifizierung mit PEG bietet sich folglich als einfache und zuverlässige Methode an, die Biokompatibilität von hydrophoben Polymeren maßgeschneidert an spezifische Anwendungen anzupassen.

Während in dem zuletzt beschriebenen Ansatz der Herstellung bioaktiver Oberflächen die Fähigkeit von Proteinen und Zellen zur Selbstorganisation erfolgreich genutzt werden konnte, sind andere Ansätze darauf gerichtet durch die Kopplung von Signalpeptiden, wie der Adhäsionssequenz RGD eine zielgerichtete Bindung von Zellen an Substrate zu erreichen. Die Zahl der zu dieser Thematik publizierten Arbeiten ist so groß, dass es nicht

möglich ist, hier einen vollständigen Überblick zu geben. Verwiesen sei zunächst auf Publikationen von Gruppen, die bald nach ihrer Entdeckung durch Ruoslahti und Pierschbacher (1986) diese Sequenz enthaltende Oligopeptide kovalent an Biomaterialien koppelten (Anderheiden et al. 1990, Massia und Hubbell 1990). Während die alleinige Kopplung von RGD adhäsive Substrate für eine Vielzahl verschiedener Zelltypen erzeugt, kann durch die gezielte Auswahl weiterer benachbarter Aminosäuren, eine Bindungssequenz für spezifische Integrine erzeugt werden (Hubbell 1998). Weitere Ansätze zielen darauf hin, Oberflächen vollständig selektiv zu gestalten. Das wird möglich, wenn bioinerte Materialien, wie sie beispielsweise durch die Immobilisierung von PEG oder Poly(methylmethacrylat)gelen erzeugt werden können, gleichzeitig mit Signalsequenzen für eine spezifische Zellart ausgestattet werden und damit für alle anderen Zellen anti-adhäsiv bleiben (Hern und Hubbell 1998). Vergleichbare Ansätze existieren, bei denen Wachstumsfaktoren kovalent über bestimmte Spacer an Substrate gekoppelt werden (z.B. Nimni 1997), wobei auch Kombinationen von Adhäsions- und Wachstumsfaktoren angestrebt werden, um die entsprechende Signalprozesse in den Zellen zu stimulieren (siehe Abschnitt 3.3), was die Apoptose verhindert und die Zellfunktion steigern kann (Li et al. 1997).

Während die bislang beschriebenen Ansätze genutzt wurden, um die Wechselwirkung von adhäsionsabhängigen Zellen mit Biomaterialien gezielt zu fördern und deren Funktion zu unterstützen, wird bei der Oberflächenmodifikation blutkontaktierender Biomaterialien versucht, einen hemmenden Einfluss auf verschiedene Blutkomponenten auszuüben. Insbesondere wurden Anstrengungen unternommen, die Thrombose auf Biomaterialien zu verhindern, die für kürzere (z.B. als intravenöse Katheter) oder längere Zeit (z.B. als intravaskuläre Stents, Herzklappen, künstliche Blutgefäße) im Kontakt mit Blut stehen. Versuche einer Reendothelisierung von Biomaterialien sind zahlreich und seit vielen Jahren unter Bearbeitung. Dabei wurden teilweise die im Abschnitt zuvor diskutierten Ansätze verfolgt. Es muss jedoch konstatiert werden, dass trotz langer und intensiver Arbeit auf diesem Gebiet endothelisierte Gefäßprothesen insbesondere für englumige Blutgefäße sich noch immer nicht in der klinischen Anwendung befinden. Auf der anderen Seite wurden für blutkontaktierende Biomaterialien eine Reihe von Strategien der Oberflächenmodifizierung verfolgt, die zu klinisch anwendbaren Systemen geführt haben. Insbesondere wurde versucht, die Aktivierung des Gerinnungssystems zu verhindern, wobei die Hemmung von Thrombin als Aktivator der Fibrinpolymerisation und Thrombozyten (siehe Abschnitt 3.2.1) am erfolgversprechendsten war. Heparin ist ein natürliches Glycosaminoglycan mit gerinnungshemmender Aktivität, welche auf eine Pentasaccharid-Sequenz mit N- und O-Sulfatgruppen zurückzuführen ist, die eine Bindungsstelle für Antithrombin III (AT III) ausbilden (Casu 1990). Dabei führt die Bindung von AT III an Heparin zu einem

Konformationswandel, der eine 1000-fache Zunahme der Affinität zu Thrombin bewirkt (Choay et al. 1983). Dabei verursacht Heparin nicht nur den notwendigen Konformationswandel von AT III, sondern bildet auch eine katalytische Oberfläche an die ATIII und Thrombin binden (Danielson et al. 1986). Die spezifische Wechselwirkung zwischen Heparin und AT III beruht auf der Coulomb-Wechselwirkung positiv geladener Aminosäuren in der Heparin-Bindungstasche von AT III mit den negativ geladenen Sulfatresten des Heparins (Hurst et al. 1979). Künstliche heparinoide Substanzen können auf Basis sulfatierter Polysaccharide synthetisiert werden (Josefonvicz und Jozefowicz 1990, Hurst et al. 1979).

Publikation 13 beschreibt wie die regioselektive Funktionalisierung von Cellulose dessen gerinnungshemmende Aktivität beeinflusst. Dafür wurden Sulfat- Phosphat- und quaternäre Ammoniumgruppen in C2-, C3- und C6-Position der Anhydroglucose-Einheit der Cellulose gekoppelt. Die gerinnungshemmende Aktivität der resultierenden Derivate wurde mit konventionellen Gerinnungsmessungen für die Bestimmung der Thrombinzeit und der partiellen Thromboplastinzeit bestimmt. Dabei zeigte sich, dass eine maximale gerinnungshemmende Aktivität bei der Derivatisierung mit Sulfat bei intermediären Derivatisierungsgraden erreicht werden konnte. Darüber hinaus war eine Sulfatierung in C2-Position besonders wirksam. Weiterhin wurden spezielle Assays für die Bestimmung der Anti-Thrombin und Anti-Faktor Xa-Aktivität entwickelt, mit denen gezeigt werden konnte, dass die gerinnungshemmende Wirkung der Cellulose-Sulfate hauptsächlich auf eine Anti-Thrombin-Aktivität zurückführbar war. Der Vergleich der Cellulose-Sulfate mit Phosphat- und quaternärer Ammonium-Cellulose zeigt, dass der Typ und die Ladung des Substituenten von entscheidender Bedeutung sind, da Cellulose-Phosphate nur schwach wirksam waren, während Cellulose-Ampholyte keine Wirksamkeit aufwiesen. Mit dieser Entwicklung wurde nicht nur die Möglichkeit aufgezeigt, gerinnungshemmende Cellulosederivate hoher Wirksamkeit zu synthetisieren, sondern es wurde auch der Mechanismus ihrer Aktivität aufgeklärt. Damit stehen blutkompatible Polymere zur Verfügung, die als Beimischung für die Herstellung von Blends von Cellulosemembranen für die Hämodialyse genutzt werden können (siehe Abschnitt 4.2) oder durch kovalente Kopplung im Sinne eines graftings an solchen und anderen Polymeren nutzbar gemacht werden.

Die Immobilisierung von Heparin und heparinoiden Substanzen auf Biomaterialien kann auf verschiedene Weise erfolgen. Eine Variante besteht in der ionischen Bindung zwischen negativ geladenen Heparinmolekülen und positiv geladener Materialoberfläche, wobei jedoch eine relativ rasche Abnahme der Oberflächenkonzentration durch die Migration des Heparins in das Blut nachweisbar ist (Eloy et al. 1987). Deshalb ist die kovalente Kopplung zu bevorzugen, da hier eine dauerhaftere Immobilisierung des Heparins erreicht werden kann

(Arnander et al. 1986). **Publikation 14** beschreibt den Effekt, den die Immobilisierung von Heparin auf die Blutverträglichkeit von Polylaktiden hat. Dieses Material wurde als Modell für die Beschichtung und Herstellung von intravaskulären Stents ausgewählt. Stents werden als Platzhalter nach der Ballondilatation englumiger Gefäße, wie von Koronararterien, verwendet, um ein Kollabieren des Gefäßes nach dem Eingriff zu verhindern. Dabei sind die meisten der im Einsatz befindlichen Stents aus Metall, das trotz systemischer Anwendung von Antikoagulantien Gerinnungsvorgänge und die Aggregation von Thrombozyten auslösen kann und so die Entstehung eines Thrombus auf der Oberfläche des Stents verursacht. Ein weiteres Problem besteht in der Induktion einer neointimalen Hyperplasie, die mit dem Wachstum glatter Muskelzellen verbunden ist (Palmaz 1993, Van Beusekom 1993). Damit kommt es im ungünstigsten Fall wieder zu einem erneuten Verschluss des Gefäßes. Ist das nicht der Fall, heilt der Stent innerhalb weniger Monate ein. In **Publikation 14** wurde Heparin durch die Herstellung einer Mischung mit dem Kopplungsagens Glutardialdehyd auf einem Polylaktid immobilisiert. Die Menge des an die Oberfläche gebundenen Heparins wurde quantitativ mit einem Farbstoffbindungsassay (Toluidinblau) bestimmt, wobei dessen biologische (gerinnungshemmende) Aktivität mit Hilfe eines spezifischen Anti-Faktor Xa Assays nachgewiesen wurde. Diese Heparinbeschichtung hatte eine anti-thrombogene Wirkung, die durch eine signifikante Abnahme der Adhäsion und Aktivierung von Thrombozyten im Vergleich zur unbehandelten Oberflächen bestimmt werden konnte. Bei Inkubation so funktionalisierter Oberflächen in wässrigen Medien konnte eine geringe Freisetzung gebundenen Heparins nachgewiesen werden. Die biologische Aktivität des oberflächengebundenen Heparins verbesserte sich jedoch noch weiter, was durch die Erhöhung der Anti-Faktor Xa Aktivität und die Verringerung der Aktivierung von Thrombozyten mit Zunahme der Inkubationszeit nachweisbar wurde. Schließlich wurden Stents mit Polylaktid beschichtet und in einem in vitro Modell mit Vollblut unter Fließbedingungen getestet. Dabei wurde eine geringere Thrombogenität von heparinisierten Stents beobachtet. Auf diese Weise wurde der Nachweis erbracht, dass sich die Blutverträglichkeit von Polylaktiden als potentielles Material für intravaskuläre Stents durch deren Heparinisierung verbessern lässt. Andere Autoren haben diesen Ansatz ebenfalls verfolgt und auf Stent-Beschichtungen angewendet (z.B. Christensen et al. 2001). Zusätzlich zur antikoagulierenden Wirkung besitzt das Heparin eine Hemmwirkung auf das Wachstum glatter Muskelzellen (Laemmel et al. 1998) und einen fördernden Effekt auf das Wachstum von Endothelzellen (Bos et al. 1999), was die Reendothelisierung des Gefäßabschnittes fördern und die neointimale Hyperplasie hemmen könnte. Aus diesen Gründen scheint insbesondere die Nutzung von Heparin für diese und andere Anwendungen von großem Interesse zu sein.

Neben Heparin wurde Hirudin als Gerinnungshemmer erprobt. Hirudin ist ein kleines Protein, bestehend aus 65 Aminosäuren und einem Molekulargewicht von 7 kDa, das von Blutegeln (Hirudo medicinalis) produziert wird. Hirudin wird auch gentechnisch hergestellt. Es ist ein spezifischer Inhibitor, der einen Komplex mit Thrombin bildet und dessen Aktivität total blockiert (Markwardt 1991). Durch die Hemmung von Thrombin wird nicht nur die Fibrinpolymerisation verhindert, sondern es wird auch die thrombinkatalysierte Aktivierung anderer Serinproteasen, wie Faktor V, VIII und XIII, und der Thrombozyten verhindert (Lindhout et al. 1990, Hoffman und Markwardt 1984). Daher sollte auch Hirudin geeignet sein, die Blutverträglichkeit von Polymeren zu verbessern. Um die prinzipielle Wirksamkeit von immobilisierten Hirudin für die Verhinderung der Thrombusbildung an Polymeroberflächen zu prüfen, wurde in **Publikation 15** eine vergleichbare Herangehensweise wie für die in Publikation 14 beschriebene Immobilisierung von Heparin gewählt. Allerdings wurde hier im ersten Schritt das Polylaktid mit Glutardialdehyd ohne Hirudin inkubiert, um dessen Vernetzung in der Lösung zu vermeiden. Nach Waschung mit Puffer wurde mit einem speziellen Assay die Präsenz freier Aldehydgruppen auf der Polymeroberfläche nachgewiesen. An diese wurde nachfolgend rekombinantes Hirudin immobilisiert, wobei versucht wurde die Bedingungen für dessen Bindung zu optimieren. Im Ergebnis konnte festgestellt werden, dass die Immobilisierung von Hirudin in einer verbesserten Blutverträglichkeit von Polylaktid-glykolid resultiert, die sich in einer im Vergleich zu unbeschichteten Polymer verlängerten Thrombinzeit, und geringeren Thrombusbildung ausdrückt. Zudem konnte auch eine Abnahme der Thrombozytenadhäsion und Aktivierung erreicht werden. Dieser Ansatz zur Nutzung von Hirudin zur Verbesserung der Blutverträglichkeit von Biomaterialien, insbesondere von Stents, wurde inzwischen von anderen Gruppen aufgegriffen, wie die Arbeit von Lahann und Mitarbeitern (2001) zeigt.

Neben der Beschichtung von Polymeren mit gerinnungshemmenden Substanzen wurden von anderen Autoren weitere Ansätze verfolgt, die Hämokompatibilität von Materialien durch eine Oberflächenmodifizierung zur Erzeugung spezifischer Wechselwirkungen zu verbessern. Dazu zählt die kovalente Kopplung von Alkylgruppen an Polymere, wodurch die Fähigkeit von Serum Albumin zur Bindung freier Fettsäuren zu dessen Adsorption an die Materialoberfläche ausgenutzt werden kann (Munro et al. 1981). Die Wirksamkeit einer Immobilisierung von C-16 und C-18 Alkylseitengruppen auf die Verringerung von Komplementaktivierung und Thrombogenität konnte in vitro und in vivo nachgewiesen werden (Eberhardt et al. 1987). In kürzlich vorgenommenen Untersuchungen zum Mechanismus der Albuminbindung konnte gezeigt werden, dass auch kürzere C4 und C8-Alkylseitengruppen eine erhöhte Bindung von Albumin bewirken und die Materialoberflächen eine verringerte Thrombogenität besitzen (Duncan et al. 1997). Vergleichbare Ergebnisse

wurden auch durch uns bei der Entwicklung von Adsorbentien für die Apherese erhalten. In **Publikation 1** wurden aliphatische Diamine zunehmender Kettenlänge an mit glycidylmethacrylatbeschichtete Polystyrenpartikel kovalent gekoppelt. Dabei konnte mit zunehmender Kettenlänge der Diamine eine Zunahme der Bindung von Albumin beobachtet werden, die den oben beschriebenen Resultaten entspricht. Eine bevorzugte Bindung von Albumin kann jedoch auch durch die Immobilsierung von (monoklonalen) Albumin-Antikörpern erfolgen, was die Fibrinogenbindung und Aktivierung von Thrombozyten an der Polymeroberfläche stark verringert (McFarland et al. 1998).

Neben den oben beschriebenen Ansätzen besteht auch die Möglichkeit, die Aktivierung von Thrombozyten spezifisch zu hemmen. Dieses hat zu einer Vielzahl von Versuchen mit Inhibitoren der Aktivierung von Thrombozyten, wie der Acetylsalizylsäure oder Dipyridamol geführt, auf die hier nicht weiter eingegangen werden soll. Jedoch wurde auch durch die Kopplung von Prostaglandinen, die mit Rezeptoren der Thrombozyten interagieren, eine Verringerung der Adhäsion und Aktivierung von Thrombozyten erreicht (Kim et al. 1987, Bamford and Al-Lamee 1992). Innovative neue Ansätze versuchen hingegen die Hemmung der Thrombozytenaktivierung durch Stickstoffmonoxid (Duan and Lewis 2002), durch dessen Freisetzung aus Polymeren zu nutzen und erhalten so Biomaterialien mit exzellenter Blutverträglichkeit.

5 Ausblick – Die Entwicklung von Membranen für Biohybrid-Organe

Beim Versagen von Niere und Leber stellt die Abtrennung von Toxinen aus dem Blut eine der wichtigsten Aufgaben der Organunterstützung dar. Dabei kann die Nierenfunktion zumindest teilweise durch das Verfahren der Hämodialyse ersetzt werden, bei dem Stoffwechselprodukte, überschüssige Salze und Wasser über eine Membran abgetrennt werden (von Sengbusch et al. 1993). Dieses Verfahren sichert das Überleben der Patienten, ist aber dennoch mit einer verringerten Lebensqualität sowie einer erhöhten Morbidität und Mortalität verbunden (Bonomini et al. 1995). Die bislang eingesetzten Methoden der Leberunterstützung, die in einer Sorption oder Filtration von Toxinen bestehen, haben leider nur geringen klinischen Erfolg, so dass die Sterblichkeit beim akuten Leberversagen sehr hoch ist (Hirasawa et al. 1997). Als Hauptursache für den unbefriedigenden klinischen Erfolg der herkömmlichen Systeme kann die Tatsache angesehen werden, dass mit Hilfe physikalischer Methoden, die in einer Filtration oder Sorption bestehen, nur Teile der komplexen Funktion von Leber und Niere ersetzt werden können. Die Organtransplantation stellt daher noch immer die beste Möglichkeit dar, die Gesundheit der betroffenen Patienten wiederherzustellen. Allerdings ist die Zahl der verfügbaren Spenderorgane geringer als die

Anzahl der Patienten, die auf eine Organtransplantation angewiesen sind. Zudem steht beim akuten Organversagen oftmals kein passendes Spenderorgan zur Verfügung. Aus diesem Grunde wird versucht, durch die Kombination von Membranverfahren mit immobilisierten Organzellen sogenannte Biohybrid-Organe zu schaffen, die einen adäquaten Ersatz der Funktion des natürlichen Organs ermöglichen sollen (Colton 1995). Damit soll einerseits die Zeit bis zum Erhalt eines passenden Spenderorgans überbrückt werden, andererseits kann vor allem beim akuten Versagen von Leber und Niere das Biohybrid-Organ die Regeneration des geschädigten Organs unterstützen (Gerlach 1996, Humes 2000). Nachteile der existierenden Systeme bestehen in ihrer relativ kurzen Nutzungsdauer, da die Funktion der immobilisierten Organzellen rasch verloren geht.

Eine wichtige Komponente dieser Art von Biohybrid-Organen stellen die verwendeten Membranen dar. Membranen dienen als Träger für die Zellen, die bislang xenogenen oder allogenen Ursprungs sind. Daher müssen sie vom Immunsystem des Empfängers getrennt werden, was durch die molekulare Ausschlussgrenze der Membran gewährleistet werden kann (Colton 1995). Um die Entgiftung des Blutes zu gewährleisten, muss auch ein enger Kontakt mit Blut hergestellt werden. Bislang wurden überwiegend kommerzielle Polymermembranen verwendet, die für die Hämodialyse oder biotechnologische Anwendungen entwickelt wurden (Legallais et al. 2000). Dabei sind Membranen für die Hämodialyse so optimiert, dass ihre Wechselwirkungen mit Blutkomponenten möglichst minimal sind (Klinkmann und Viencken 1995). Aus diesem Grunde sind sie jedoch weniger gut als adhäsives Substrat für Zellen geeignet. Materialien für biotechnologische Anwendungen hingegen sind so gestaltet, dass die adhäsionsabhängigen Zellen sehr gut auf ihnen haften.

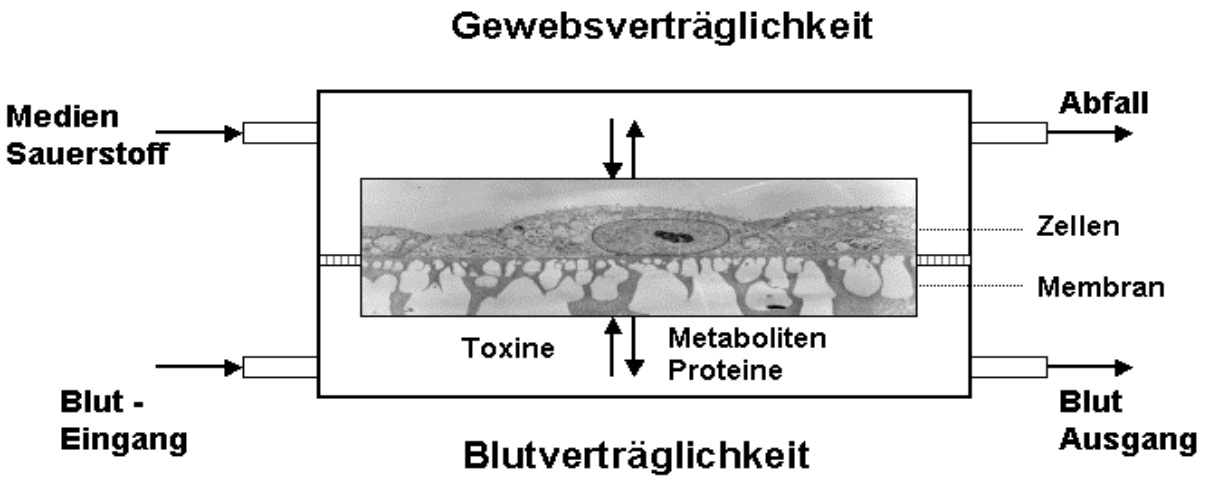

Abbildung 19: Prinzipschema eines Biohybrid-Organs

Das kann beim Kontakt mit Blutkomponenten zur Adhäsion und Aktivierung von Blutzellen führen. Daher müssen Membranen für Biohybrid-Organe, so optimiert werden, dass sowohl Blut- als auch Gewebekontakt möglich ist, wie aus Abbildung 19 ersichtlich ist. Um diese Anforderung zu erfüllen, bieten sich verschiedene Lösungswege an, auf die hier nur zum Teil eingegangen werden kann. Es ist aber denkbar, die Volumeneigenschaften von Polymeren so zu optimieren, dass sowohl blut - als auch gewebeverträgliche Polymere erhalten werden. Auf der anderen Seite ist es auch möglich, funktionalisierbare Polymere zu verwenden, wobei die blut- und gewebekontaktierende Seite durch eine entsprechende Oberflächen-modifizierung an die Umgebung angepasst werden.

Die Möglichkeit eines solchen Ansatzes wurde in **Publikation 16** mit der Entwicklung von Membranen für Biohybrid-Organe auf Basis von Polyetherimid (PEI) beschrieben. Diese Klasse von Polymeren wurde bislang kaum für medizinische Anwendungen eingesetzt, wobei sie jedoch aufgrund ihrer thermischen Eigenschaften, die eine Dampfsterilisation erlauben, einer guten mechanischen Stabilität und Verformbarkeit zu Membranen (Kawakami et al. 1997, Peinemann et al. 1998) interessant als Material für Biohybrid-Organe sind. Die Möglichkeit der Nutzung von PEI als Substrat für die Kultivierung adhäsionsabhängiger Zellen wurde beschrieben (Richardson et al. 1993). Auf der anderen Seite existieren kaum Untersuchungen über dessen Blutverträglichkeit. Aus diesem Grunde wurde in **Publikation 16** die Blutverträglichkeit von PEI in Abhängigkeit von bestimmten Oberflächenmodifizierungen getestet. Gleichzeitig wurde die Gewebsverträglichkeit mit der Kultivierung von Human-Fibroblasten geprüft. Da PEI ein eher hydrophobes Polymer mit Wasserrandwinkeln von 80° darstellt, wurde die Oberfläche durch die kovalente Kopplung verschiedener Liganden modifiziert, die einerseits eine verbesserte Blutverträglichkeit bewirken (Heparin) oder andererseits den Kontakt mit adhäsionsabhängigen Zellen durch die Einführung bestimmter funktioneller Gruppen wie Hydroxyl- und Amingruppen erleichtern sollten. Zu diesem Zwecke wurde PEI chemisch mit Tris-(Hydroxymethyl)-Aminomethan (Tris) zur Einführung von Hydroxylgruppen, mit Polyethylenimin zur Einführung von Aminfunktionen, und Heparin modifiziert. Die Bestimmung der Kontaktaktivierung der plasmatischen Gerinnung über die Generierung von Kallikrein zeigte, das unmodifiziertes PEI einen starken Aktivator für das Kontaktsystem darstellt. Alle Modifizierungen senkten das Niveau der Aktivierung des Kontaksystems signifikant, wobei die geringsten Werte durch Heparinisierung erreicht werden konnten. Andererseits wirkte sich die Einführung von Hydroxylgruppen am wenigsten günstig aus, da hier nicht nur die Werte für Kallikrein erhöht waren, sondern auch in weiteren Untersuchungen eine erhöhte Gerinnungsneigung des Plasmas im Vergleich zu PEI und allen anderen Modifikationen nachweisbar wurde. Die Generierung von aktiven Komplementfaktoren war ebenfalls hoch für unmodifiziertes PEI

und konnte durch die Oberflächenbehandlungen verringert werden. Hier wurde davon ausgegangen, dass die Imidgruppe als nukleophile Komponente für die starke Komplementaktivierung verantwortlich sein sollte. Die Kopplung von Amin- oder Hydroxylgruppen schwächte diesen Effekt nur geringfügig ab, was mit der unter Abschnitt 3.2.1 beschriebenen Wirkung nukleophiler Substituenten auf das Komplementsystem erklärbar ist (Chenoweth 1987). Die Adhäsion von Thrombozyten konnte lediglich durch die Kopplung von Heparin entscheidend verringert werden, während sich die Präsenz von Hydroxyl- und insbesondere von Aminfunktionen ungünstig darauf auswirkte. Auf der anderen Seite konnte nachgewiesen werden, dass nur die Immobilisierung von Tris eine signifikant verbesserte Gewebsverträglichkeit bewirkte, die durch eine Zunahme der metabolischen Aktivität der Fibroblasten und ein höheres Zellwachstum nachweisbar wurde. Auch die Funktionalisierung mit Heparin wirkte sich ungünstig auf die Gewebsverträglichkeit aus. Das Zellwachstum war auf diesen Oberflächen besonders gering, was mit der relativ ungünstigen Wirkung von Sulfonatgruppen auf die Wechselwirkung mit Zellen erklärt werden kann (Webb et al. 1998). Da Membranen für Biohybrid-Organe bifunktionell sein müssen, d.h. eine gewebs- und eine blutverträgliche Seite besitzen müssen, bietet sich deshalb im Ergebnis dieser Untersuchungen die heterogene Funktionalisierung von PEI mit Heparin für die blutkontaktierende und Tris für die gewebskontaktierende Seite der Membran an.

In **Publikation 17** wurde untersucht, wie sich die Veränderung der Volumenzusammensetzung von Polyacrylnitril-Copolymeren auf die Gewebsverträglichkeit daraus hergestellter Membranen auswirkt. Dabei wurde versucht, die Biokompatibilität der Membranen durch Veränderung der Hydrophilie und der Präsenz bestimmter funktioneller Gruppen zu modifizieren (siehe auch Abschnitt 3.2.2). Die Untersuchungen wurden mit Human-Fibroblasten durchgeführt, wobei neben deren Wachstum auch morphologisch-funktionelle Kriterien zur Beurteilung der Biokompatibilität herangezogen wurden. Die Copolymerisation wurde mit Acrylnitril und verschiedenen Comonomeren durchgeführt, wie N-Vinylpyrrolidon (NVP) zur Erhöhung der Hydrophilie, Natriummethallylsulfonat (NaMAS) zur Erzeugung saurer Gruppen oder Aminoethylmethacrylat (AEMA) für basische Gruppen. Erwartungsgemäß konnte die Hydrophilie des resultierenden Copolymeren durch erhöhte Gehalte von NVP verbessert werden. Das konnte auch durch die Copolymerisation mit NaMAS ereicht werden, während die Verwendung von AEMA keine wesentlichen Veränderung der gemessenen Wasserrandwinkel im Vergleich zum PAN ergab. Die Untersuchungen mit Fibroblasten zeigten eindrucksvoll, dass gute Wachstumsbedingungen für Fibroblasten am PAN-Homopolymer vorhanden waren. Diese konnten auch für die Copolymerisation mit AEMA nachgewiesen werden, was auf die Präsenz der Aminfunktion zurückgeführt werden kann (Steele et al. 1994). Im Gegensatz dazu führte ein zunehmender

Gehalt an NVP zu einer Verschlechterung der Gewebsverträglichkeit in bezug auf Fibroblasten, da deren Anheftung und Wachstum an Copolymeren mit einem Massegehalt von 30% NVP nur noch sehr gering war. Dies wird auf den zunehmenden Hydrogel-Charakter des Copolymers zurückgeführt, der mit einer Verringerung der Adsorption von Proteinen einhergehen sollte. Ein signifikant geringeres Wachstum von Zellen im Vergleich zu PAN und AEMA wurde auch auf Copolymeren mit NaMAS beobachtet, was mit dem bereits beschriebenen negativen Einfluss von Sulfonatgruppen auf die Zellanheftung, das Wachstum und die Funktion von Fibroblasten übereinstimmt (Webb et al. 1998, Groth und Altankov 2001). Auf der anderen Seite zeigt es sich beim Vergleich von Gewebezellen, dass mesenchymale Zellen, wie die des Bindegewebes (Fibroblasten), andere Ansprüche an Substrate stellen, als solche die epithelialen Ursprunges sind (Webb et al. 2000). Daher ist es prinzipiell möglich, dass Substrate, die suboptimal für Fibroblasten sind, hervorragend für die Immobilisierung von Zellen epithelialen Ursprunges geeignet sein können, wie weiter unten noch ausgeführt werden wird.

Die Untersuchung der Wechselwirkung von Epithelzellen, wie z.B. Hepatozyten ergab, dass stark adhäsive Substrate, welche die Anheftung und Spreitung der Zellen förderten, negative Auswirkungen auf die Funktion der Zellen haben (Sawamoto et al. 1997). Auf der anderen Seite kann die funktionelle Aktivität dieser Zellen durch einen Verbleib in Aggregaten gefördert werden (Gerlach et al. 1989). Unter diesen Umständen bleibt deren Funktion über längere Zeiträume erhalten als bei der Kultivierung auf stark adhäsiven Substraten. Um diesen Sachverhalt zu prüfen und gleichzeitig Membranen für die Immobilisierung von Hepatozyten in Biohybrid-Organen zu entwickeln, wurden Polymere verschiedener Benetzbarkeit zur Herstellung von Membranen verwendet (**Publikation 18**). PAN wurde genutzt, da es ein Standardpolymer zur Herstellung von Membranen für die Hämodialyse darstellt. Zudem existieren auch Berichte über die erfolgreiche Immobilisierung von Hepatozyten auf diesem Material (Quiang et al. 1997). Um die Wirkung einer erhöhten Hydrophilie des Polymers auf die Hepatozyten zu prüfen, wurde auch ein Acrylnitril-N-Vinylpyrrolidon-Copolymer mit 20% NVP eingesetzt. Weiterhin wurde PEI als hydrophober Membranträger verwendet. Außerdem wurde als ein Referenzmaterial eine kommerzielle mikroporöse Polyvinylidendifluorid-Membran (PVDF) genutzt. Die Untersuchungen wurden mit humanen C3A-Hepatoblastomazellen durchgeführt. Diese Zelllinie besitzt eine Vielzahl der Funktionen primärer Hepatozyten, hat aber dabei die Fähigkeit zur Zellproliferation und ist deshalb für Modelluntersuchungen gut geeignet. Zudem wird sie in einigen Modellen von Biohybrid-Organen zum Ersatz der Leberfunktion verwendet (Hughes und Williams 1996). Die Wechselwirkung der Zellen wurde durch Darstellung der Zellmorphologie, einschließlich der Ausbildung fokaler Adhäsionsplaques, der Strukturierung des Aktin-Zellskelettes sowie

der Zell-Zell-Wechselwirkung durch den Nachweis von E-Cadherin mittels Immunfluoreszenz-Mikroskopie charakterisiert. Die Funktion der Zellen wurde durch die Bestimmung ihrer metabolischen Aktivität, sowie der Sekretion von Human-Serum-Albumin bestimmt. Das Zellwachstum wurde ebenfalls ermittelt. Dabei zeigte sich, dass die Zelladhäsion und das Zellwachstum auf PAN als moderat benetzbarem Material am größten waren. Sehr ähnliche Ergebnisse wurden aber auch für das hydrophobe PEI erhalten. Dieses Ergebnis ist prinzipiell konträr zum Verhalten von Fibroblasten, die auf hydrophoben Substraten eine geringere Spreitung, vermindertes Wachstum und Funktionalität aufweisen (Grinnell et al. 1973, Tamada und Ikada 1994). Andererseits wurde in einer Untersuchung mit C3A-Zellen auf hydrophilen und hydrophoben Modellsubstraten ebenfalls beobachtet, dass sich Hepatoblastoma-Zellen auf solchen Substraten ähnlich verhalten (Krasteva et. al 2001). Die Untersuchungen der Kultivierung von C3A-Zellen auf P(AN-NVP) zeigten zwar, dass die Zellspreitung, -haftung und -proliferation am Substrat eingeschränkt war. Auf der anderen Seite konnte jedoch eine starke Zunahme der Funktionalität dieser Zellen nachgewiesen werden, die durch eine stark erhöhte metabolische Aktivität und Sekretion von Proteinen repräsentiert wurde. Damit scheinen gerade Copolymere mit größerer Hydrophilie eine interessante Alternative zu bislang genutzten Membranmaterialien darzustellen, wobei NVP-haltige Copolymere zudem auch eine sehr gute Blutverträglichkeit besitzen (Groth et al. 2002).

Weitere Untersuchungen mit verschiedenen Copolymeren wurden inzwischen durchgeführt. Neben der Bestimmung der Blutverträglichkeit, wurden experimentelle Arbeiten mit primären Hepatozyten und Nierenepithelzellen vorgenommen. Die Ergebnisse werden in zukünftigen Publikationen dargestellt.

6 Zusammenfassung

Es ist schon seit längerer Zeit bekannt, dass nach Kontakt des Biomaterials mit der biologischen Umgebung bei Implantation oder extrakorporaler Wechselwirkung zunächst Proteine aus dem umgebenden Milieu adsorbiert werden, wobei die Oberflächeneigenschaften des Materials die Zusammensetzung der Proteinschicht und die Konformation der darin enthaltenden Proteine determinieren. Die nachfolgende Wechselwirkung von Zellen mit dem Material wird deshalb i.d.R. von der Adsorbatschicht vermittelt. Der Einfluss der Oberflächen auf die Zusammensetzung und Konformation der Proteine und die nachfolgende Wechselwirkung mit Zellen ist von besonderem Interesse, da einerseits eine Aussage über die Anwendbarkeit ermöglicht wird, andererseits Erkenntnisse über diese Zusammenhänge für die Entwicklung neuer Materialien mit verbesserter Biokompatibilität genutzt werden können. In der vorliegenden Habilitationsschrift wurde deshalb der Einfluss der Zusammensetzung von Polymeren bzw. von deren Oberflächeneigenschaften auf die Adsorption von Proteinen, den Aktivitätszustand der plasmatischen Gerinnung und die Adhäsion von Zellen untersucht. Dabei wurden auch Möglichkeiten zur Beeinflussung dieser Vorgänge über eine Veränderung der Volumenzusammensetzung oder durch Oberflächenmodifikationen von Biomaterialien vorgestellt. Erkenntnisse aus diesen Arbeiten konnten für die Entwicklung von Membranen für Biohybrid-Organe genutzt werden.

7 Zusammenstellung der in der vorliegenden Habilitationsschrift angeführten Publikationen

Anmerkungen zur Relevanz der Publikationen für die Habilitation

Die in der vorliegenden Habilitationsschrift zusammengefassten Publikationen wurden, soweit es die biologischen Arbeiten betrifft, sämtlich im Labor des Habilitanden durchgeführt. Die beschriebenen chemischen Arbeiten und Teile der Oberflächencharakterisierung wurden durch die in den Publikationen genannten Kooperationspartner durchgeführt. Dabei wurden die Publikationen 1, 4 – 8, 11 – 13, 16 – 18 am GKSS Forschungszentrum erarbeitet. Die Durchführung der experimentellen Arbeiten in Publikation 1 erfolgte durch Mitarbeiter des Habilitanden, der diese wissenschaftlich betreute. Die experimentellen Arbeiten in Publikation 4 – 8 wurden vom Habilitanden, Herrn Prof. Altankov und anderen Mitarbeitern durchgeführt. Die Arbeiten in Publikation 11 und 12 wurden vom Habilitanden in Kooperation mit anderen Einrichtungen und von dessen Mitarbeitern durchgeführt. Der Habilitand war dabei originär an der Interpretation der Untersuchungsergebnisse, sowie an der Erarbeitung der Publikationen beteiligt. Die experimentellen Arbeiten in Publikation 13 wurden von technischen Mitarbeitern des Habilitanden durchgeführt, der diese Arbeiten anleitete und deren Ergebnisse auswertete. Publikation 16 – 18 entstanden in der Arbeitsgruppe des Habilitanden unter Kooperation mit anderen Abteilungen des Institutes. Publikation 2, 3, 9 und 10 wurden während der Arbeit des Habilitanden in der Abteilung Biomaterialforschung der Berliner Charité erstellt. Publikation 14 und 15 wurden experimentell von Frau Dr. B. Seifert im Rahmen einer Kooperation mit dem Institut für Röntgendiagnostik der Charité bearbeitet. Dabei wurde diese Kooperation durch den Habilitanden während seiner Tätigkeit an der Charité initiiert und nach seinem Wechsel an die GKSS wissenschaftlich weiter betreut.

Publikation 1

Mark Mullaney, Thomas Groth, Rita Darkow, Ruth Hesse, Wolfgang Albrecht, Dieter Paul, Günter von Sengbusch (1999).

Investigation of plasma protein adsorption on functionalized nanoparticles for application in apheresis.

Artificial Organs **23**, 87-97.

Artificial Organs
23(1):87–97, Blackwell Science, Inc.

Investigation of Plasma Protein Adsorption on Functionalized Nanoparticles for Application in Apheresis

Mark Mullaney, Thomas Groth, Rita Darkow, Ruth Hesse, Wolfgang Albrecht, Dieter Paul, and Günter von Sengbusch

GKSS Research Centre, Teltow, Germany

Abstract: Particles with specific ligands for the adsorption of plasma proteins can be used in therapeutic or preparative apheresis. The development of these particles may benefit from an improved knowledge of the relationship between protein adsorption and the structure of ligands. Nanoparticles were functionalized with aliphatic diamines of increasing chain length; with the amino acids lysine, tryptophan, histidine, and their corresponding amines; and with tryptophan and histidine spaced with diamines of different length. Suitable protocols were developed for the washing of particles and the subsequent desorption of proteins adsorbed from human plasma. The adsorption pattern, as well as the quantification of the overall adsorption of proteins on these modified particles, was investigated with gel electrophoresis. This was followed by immunoblotting which yielded specific assessments of bound human serum albumin and fibrinogen. The comparison of protein adsorption with surface charge density and measured hydrophobicities yielded no simple correlations although in general more hydrophobic ligands bound higher quantities of protein. The detection of human serum albumin yielded similar results because it was observed for overall protein adsorption while the adsorption of fibrinogen expressed a different pattern. In this case, particular nanoparticles functionalized with aliphatic diamines bound significantly higher amounts of fibrinogen than all other ligands. **Key Words:** Apheresis—Plasma proteins.

Small particles, and in particular nanoparticles, are playing an increasingly important role in modern healthcare. Innovations, more so in the fields of molecular biology and immunology based medical care, have been supported by an increased use of particles in diagnostic and therapeutic systems (1). These nanoparticles function by immobilizing biologically active molecules such as drugs, antibodies, or other ligands and can be administered intravenously or extracorporeally. By the use of micro- or nanoparticles in extracorporeal systems, harmful components such as specific toxins, immunoglobulins (2), low-density lipoproteins (LDL) (3–5), or other blood plasma proteins can be targeted and then removed from the system.

Apheresis is the process whereby a specific component of the blood is separated and removed with the remainder of the blood returned to the patient (6). Therapeutic apheresis, incorporating small particles, is used for the treatment of a variety of diseases and disorders characterized by the presence of abnormally high levels of blood proteins that are believed to play a major role in autoimmune, cardiovascular, or other diseases (2–6). These extracorporeal blood purification systems, which are based on adsorption technology, may also benefit from the use of nanoparticles (1). Conventionally adsorbents are used in columns perfused directly either by blood (hemoperfusion) or by plasma which has been filtered from the blood (plasma separation). The specifications of these extracorporeal methods, however, allow only microparticles of a certain and relatively large diameter, thereby excluding nanoparticles. Incorporation of nanoparticles would offer the following advantages among others: a higher external surface to volume ratio and shorter diffusion distances, in contrast to porous adsorbents. New advances such as the microsphere-based detoxification system (MDS) begin to offer such possibilities (1,7,8). Another sphere of interest for nanoparticles is use as drug carriers. Particulate polymeric colloidal carriers for intravenous injection are one approach to the

Received August 1998.
Address correspondence and reprint requests to Dr. Thomas Groth, GKSS Research Centre, Kantstrasse 55, Teltow, D 14513, Germany. E-mail: Thomas.Groth@gkss.de

site-specific delivery of drugs to reduce the side effects of certain medical treatments (9).

The interactions of biomaterials such as these nanoparticles with blood depend strongly on their physiochemical surface properties (9,10). When a foreign surface contacts blood, the initial response is the adsorption of plasma blood proteins (11). The subsequent cell interactions are most likely mediated by the character and composition of this initial protein layer (12). There are several important material properties and system factors which influence this biomaterial-blood interplay. Aspects of these surface characteristics to be taken into consideration include wettability, surface charge, charge distribution, and particular surface chemistry such as functional groups and the mobility of ligands (13).

Knowledge of the protein adsorption pattern on a nanoparticle with specific surface chemistry can be exploited for the development of adsorbents for specific blood proteins or for targeting to a specific population of cells (e.g., phagocytes) in the organism. In this paper, we present the results of our study of the dependence of protein adsorption (intensity and molecular weight distribution) on the type of ligands attached on nanoparticles, namely diamines with increasing chain length, amino acids and corresponding amines, and amino acids spaced with diamines. Immunoblotting was applied for the specific detection of adsorbed human serum albumin (HSA) and fibrinogen. While correlation was found for the structural features of ligands such as the chain length of diamines, the interplay observed between this protein adsorption pattern and physicochemical parameters was very complex. The results are presented in this report.

MATERIALS AND METHODS

Materials

Nanoparticles

Nanoparticles (of a mean diameter of 75 nm) consisting of a polystyrene core and a polyglycidyl methacrylate shell were prepared by a two-step emulsion polymerization. The size distribution and morphology were characterized by dynamic light scattering and scanning electron microscopy. These parent particles were modified by the covalent binding of a number of different ligands, namely, diamines of increasing chain length, amino acids, and finally, amino acids with diamine spacers. These groupings are represented in Table 1. Synthesis, modification, and characterization have been explained more thoroughly (14).

Surface charge density was determined by titration with a cationic (polydiallyldimethyl ammonium-chloride) or anionic (polyvinylsulphonate, potassium salt) polyelectrolyte standard, respectively, with a particle charge detector, PCD-03 Müteck, Herrsching, Germany).

Surface hydrophobicity was evaluated by adsorption of the hydrophobic dye Rose Bengal (Sigma-Aldrich, Deisenhofen, Germany) (9,15). A fixed amount of this dye (0.08 g/L) was added to suspensions of increasing nanoparticle concentration (0.025–0.5% wt/wt). This amount of dye was used because of the relatively large surface to volume ratio on these functionalized nanoparticles. The suspensions were incubated for 3 h at 37°C, the particles centrifuged (14,000 rpm for 30 min), and the amount of free Rose Bengal in the supernatant was determined spectrophometrically at 542 nm. Rose Bengal undergoes partitioning between the surface of the particle and the dispersion medium. At each nano particle concentration, the partitioning quotient (PQ) was calculated according to the following formula:

$$PQ = \frac{\textit{amount of Rose Bengal bound on surface}}{\textit{amount of Rose Bengal in the dispersion medium}} \quad (1)$$

From these calculations a plot of the PQ against the particle concentration yielded linear, straight line, relationships (not shown here). Increasing the nanoparticle concentration led to an increase in the sur-

TABLE 1. *Listing of ligands coated on parent polymer nanoparticles*

Group 1 Aliphatic diamines	Group 2 Amino acids and corresponding amines	Group 3 Amino acids spaced with diamines
OH (hydroxyl)	Lys (Lysine)	EDA-Trp
EDA (ethylene diamine)	Trp (Tryptophan)	HDA-Trp
HDA (hexamethylene diamine)	TrpA (Tryptamine)	DODA-Trp
ODA (octamethylene diamine)	His (Histidin)	EDA-His
DODA (Dodecyldiamine)	HisA (Histamine)	HDA-His
		DODA-His

face area, and as a consequence, the partition quotient increased linearly. The slope of such a plot can be taken as a measure of the hydrophobicity.

Human blood plasma (HBP)

Blood group O, anticoagulated with acid citrate dextrose (ACD), was used in the investigations.

Methods

Adsorption process

Five hundred microliters of the human blood plasma was added to 100 μl of the particle suspension (0.5% wt/wt concentration). Double estimates were used, and the process carried out twice for each particle suspension. The resulting solution was mixed thoroughly and incubated for 1 h at 37°C. These parameters were viewed as equilibrium conditions, as close to physiological conditions as possible (16). After incubation, the solution was mixed thoroughly again and the samples centrifuged (Hettrich Zentrifugen, Tuttlingen, Germany), (14,000 rpm, 30 min), and the supernatant pipetted off.

Washing process

Washing was carried out to remove all the free proteins between the polymer nanoparticles which had not been adsorbed on their surfaces. We were only interested in the blood plasma proteins which had been adsorbed on the surfaces of the nanoparticles. Washing was carried out with phosphate-buffered saline (PBS) (5.8 m*M* Na_2HPO_4, 5.8 m*M* NaH_2PO_4, 150 m*M* NaCl) pH 7.4 as described elsewhere (17). Three washings with 1 ml of PBS were undertaken, centrifugation was at 14,000 rpm for 30 min, and the supernatant was pipetted off and stored in cool conditions. To prevent aggregation of the particles, an ultrasonic emitter (UW 60, Brandelin Electronic, Berlin, Germany), the tip of which was coated with silicon, was used to assist with resuspension of particles between washings. The efficiency of the method was determined by UV spectrophometric analysis (adsorbance at 280 nm wavelength).

Desorption method

A number of procedures were tested to ascertain which was the most effective at desorbing the protein from the polymer microparticles. These basically consisted of 2 divisions (based on sodium dodecyl sulfate (SDS) concentration differences), Methods 1 and 2, with submodification to each one (based on temperature differences), Methods 3 and 4. An additional method was also considered, Method 5, a submodification of the aforementioned temperature differences with β-mercaptoethanol.

Methods 1 and 2. The elution of proteins was performed with 1 ml of SDS sample buffer (0.01 *M* phosphate, 1% SDS, pH 7.0) as described previously (18). This was added to the particles, and the resulting solution suspended by means of a shaker. The solution was then placed for 1 h at room temperature (RT) in an ultrasonic bath (Method 1). Alternatively, the solution was placed for 30 min at RT in an ultrasonic bath after which it was heated (100°C) for 10 min (Method 2).

Methods 3 and 4. The elution of proteins was carried out by the following method. One milliliter of sample buffer (10 m*M* Tris/HCL, 1 m*M* EDTA, SDS to 2.5%, pH 8.0) was added to the particles (remaining after 3 washes with PBS), and the resulting solution suspended (by means of shaker). This was then placed for 1 h at RT in an ultrasonic bath (Method 3). Alternatively, the solution was placed for 30 min at RT in an ultrasonic bath after which it was heated (100°C) for 10 min (Method 4).

Method 5. Method 5 is a submodification of Method 4. The elution of proteins was carried out by the following method. One milliliter of sample buffer (10 m*M* Tris/HCL, 1 m*M* EDTA, SDS to 2.5%, and β-mercaptoethanol to 5.0%, pH 8.0) was added to the particles (remaining after 3 washes with PBS), and the resulting solution suspended (by means of shaker). This was then placed for 30 min at RT in an ultrasonic bath after which it was heated (100°C) for 10 min.

To determine which of the desorption methods was best, the effectiveness of the methods was ascertained by UV spectrophotometer analysis at 280 nm. Preliminary experiments using modified particles, namely, hydroxyl (OH) (hydrophilic) and dodecyldiamine (DODA) (hydrophobic), were carried out to optimize the desorption procedure. First, experiments were performed with albumin (one of the most abundant blood plasma proteins) under conditions of 37°C for 1 h. After the choice had been narrowed to a couple of methods, human blood plasma (blood group O) was then utilized for a more representative result.

Sodium dodecyl sulfate polyacrylamide gel electrophoresis (SDS-PAGE)

SDS-PAGE was the electrophoretic method of choice for the separation of proteins. This was performed using the Pharmacia PhastSystem Separation and Development Units, (Pharmacia Biotech, Uppsala Sweden). The technique was that of Laemmli as employed by others (19–21). Bromphenol blue (0.01%) was added to the samples as a

tracking dye. PhastGel gradient 8–25 (Pharmacia Biotech) provided a molecular weight (MW) range of 6,000–300,000 daltons for SDS-denatured proteins. The Pharmacia standards employed were the high molecular weight (HMW) SDS (molecular weight range of 53,000–212,000 daltons) and the low molecular weight (LMW) (molecular weight range of 14,400–94,000 daltons) calibration kit. Development of the gels was performed afterwards using the PhastGel Silver Kit. The sensitivity limit for SDS-PAGE separations was then 0.05–0.1 ng protein per band.

Software analysis

The SDS-PAGE gels were scanned into a computer (ARTEC/// Scanner, Taipei, Taiwan, Viewstation AT6, at a resolution of 25,000 dpi), and the images processed by means of Kodak Digital Science 1D image analysis software (Eastman Kodak Co., Rochester, NY, U.S.A.). Briefly, the lanes on the gels were defined and labeled as either experimental (samples) or standard (LMW or HMW). The following parameters were measured.

Molecular weight. The MW was based on the relative mobility of each experimental band compared to one or more standard lanes. The 1D software uses the intensity information for each band to calculate the center of gravity of the band (second moment of intensity). This position is indicated graphically by a band marker on the image. The 1D software generates a MW curve from the band mobilities in the standard lane and the band sizes defined in the Standards File. The mobility of each experimental band is plotted against the standard curve to determine its MW.

Net intensity. The net intensity (NI) is the sum of the background subtracted pixel values in the band rectangle (The rectangle is used to delineate the limits or area of the protein band in the lane).

Net intensity ratio. The net intensity ratio (NIR) is the NI of the sample lane normalized by the NI of the plasma lane, that is, $NIR = I_{sample}/I_{plasma}$.

Immunoblotting

Specific detection of HSA and fibrinogen adsorption was performed with immunoblotting. For this reason, proteins were transferred, after SDS-PAGE, from a 12.5 homogeneous gel with a semidry blotting apparatus (PhastSystem, Pharmacia Biotech) to an Immobilon P membrane (Millipore, Bedford, MA, U.S.A.). Then, membranes were blocked with a 5% solution of nonfat dry milk solved in 50 m*M* Tris buffer (TBS with 150 m*M* NaCl, pH 7.0) for 1 h. These were then washed with TBS. Rabbit anti-HSA antibody (DAKO Diagnostica, Hamburg, Germany) or sheep anti-human fibrinogen antibody (Sigma Immunochemicals, St. Louis, MO, U.S.A.), solved in TBS with 0.5% nonfat dry milk, was added. After 1 h incubation at RT, the membranes were washed with TBS again, and polyclonal anti-rabbit (Kodak BioMax Kit, Eastman Kodak Company, U.S.A.) or anti-sheep antibodies developed in goat, labeled with peroxidase (Boehringer, Mannheim, Germany) were added. Polyclonal antibodies were dissolved in TBS in the presence of 0.5% nonfat dry milk. After a further incubation for 1 h, membranes were washed with TBS again. The detection of labeled albumin and fibrinogen was carried out by enhanced chemoluminescence (BioMax kit, Kodak, Inc.) using BioMax film (Kodak, Inc.) for the visualization of labeled proteins.

RESULTS

Physicochemical investigations of particle properties

Surface charge density and hydrophobicity measurements were undertaken to obtain more insight into the driving forces for the adsorption of plasma proteins on the nanoparticles. Table 2 provides a summary of the results of these measurements. It can be seen that the surface charge densities of particles functionalized with aliphatic diamines were positive

TABLE 2. *Functionalized polymeric nanoparticles (by means of ligands) and the corresponding surface charge density and hydrophobicity*

Ligands on parent nanoparticles	Surface charge density (σ) (μC/cm²)	Hydrophobicity (S)
Group 1		
OH[b]	−1.03	+[b]
EDA	5.5	2.2867
HDA	1.34	1.883
ODA	0.884	2.1484
DODA	3.3	3.4064
Group 2		
Lys	−0.4	0.2089
Trp	−2.04	0.6238
Trp A	−2.05	1.6455
His	2.2	0.0836
His A	2.0	4.9424
Group 3		
Trp-EDA	3.9	2.4745
Trp-HDA	5.8	1.923
Trp-DODA	[a]	[b]
His-EDA	4.4	1.7265
His-HDA	1.6	2.539
His-DODA	1.45	[b]

[a] The surface charge density was not determined.
[b] The hydrophobicity was not determined.

in contrast to hydroxylated nanoparticles with negative surface charge densities. Indeed, ethylene diamine (EDA) particles expressed the most positive surface charge followed by DODA, hexamethylene diamine (HDA), and octamethylene diamine (ODA). Hydrophobicity measurements with the Rose Bengal separation method yielded similar results with regard to the range of diamines although the binding of the dye to hydroxylated particles could not be determined. The particles derivatized with amino acids and corresponding amines displayed almost neutral surface charges for Lys, slightly negative surface charges for Trp and TrpA, and slightly positive surface changes for His and HisA. It is noteworthy that descarboxylation did not change the surface charge at all. In contrast, measured hydrophobicities increased in the corresponding amines while Lys and His were found to be rather hydrophilic indicated by the low slope of the function. If Trp and His were bound to the particles with increasing length of diamine spacers, it can be seen that the short length of the diamines (EDA and HDA) is related to a more positive surface charge. Measurements of hydrophobicity were not carried out for all types of amino acids spaced with diamines. Thus, it was not possible to obtain any recognizable trend in hydrophobicity for the change in diamine spacer length for Trp and His.

Establishment of washing and desorption procedure

To remove plasma protein that was not bound on the functionalized nanoparticle surface, a number of washings were undertaken. A typical example of the result is shown in Fig. 1 for Group 3 amino acids spaced with diamines. The figure demonstrates that there was no soluble protein in the supernatant solution after the third wash and subsequent centrifugation of the particles. This supernatant solution was then discarded, and the adsorbed protein on the surface of the nanoparticles assessed.

For the desorption of proteins, a number of different methods were applied. These were undertaken to optimize the amount of desorbed proteins, given the high binding energy between protein and substratum. Figure 2 shows the result of these measurements. It can be seen that it was possible by means of a rise in SDS concentration, temperature, and duration of the desorption process, to increase the amount of the desorbed protein. The best results were obtained with the additional reduction of disulfide bonds necessary for the SDS gel electrophoresis. For a comparison, OH particles and particles functionalized with DODA were initially analyzed after

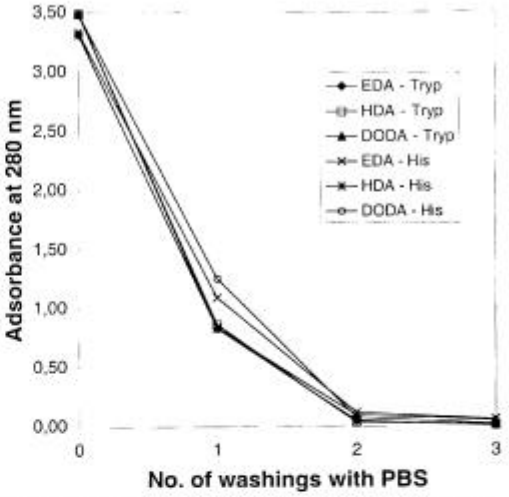

FIG. 1. Shown is the efficacy of the washing steps with phosphate buffered saline for Group 3 nanoparticles, i.e., amino acids spaced with diamines. The absorbance of the supernatant solution was measured after the centrifugation of the nanoparticles at a wavelength of 280 nm.

desorption of the most abundant protein in plasma, namely HSA. As is evident from Fig. 2, higher amounts of protein could be desorbed from DODA particles than hydroxyl particles. This result was confirmed using plasma for both types of particles (not shown here).

Electrophoretical analysis of desorbed plasma proteins

First, the MW distribution of the bound proteins on the polymeric nanoparticles was investigated. The most prominent protein bands, analyzed by densitometry are based on their intensity, were noted and plotted as shown in Fig. 3. Human blood plasma was taken as a standard in each case. Observations from the respective groupings are listed subsequently. It is noteworthy that these results dealt with the MW distribution and not with the intensities of the respective bands. All MW values are expressed in daltons.

For Group 1 (Fig. 3A), a broad MW distribution for ODA and to some extent for OH was found. A narrower distribution was observed for HDA and DODA with a few single bands. Analysis of protein desorbed from EDA functionalized nanoparticles revealed the presence of 3 bands still detectable. Defined band ranges were found on all nanoparticles between 50,000 and 65,000 and between 70,000 and 85,000. Further, it was noticed that there was a defined band range between 20,000 and 30,000 for OH, HDA, and ODA.

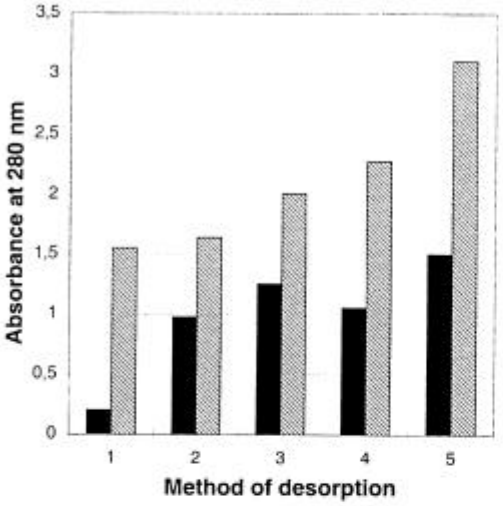

FIG. 2. The comparison is of desorption methods 1–5 for OH (black columns) and DODA (shaded columns) functionalized nanoparticles after previous adsorption of HSA. The absorbance of the supernatant solution after the desorption procedure was measured at a wavelength of 280 nm. For a more detailed description of desorption methods 1–5, see the materials and methods section.

For Group 2 (Fig. 3B), the broadest MW distribution was seen for Trp and the least for HisA. Further a defined band range was found on all nanoparticles between 50,000 and 70,000. In the range between 25,000 and 35,000, bands were found for Lys, Trp, Trp A, and His and in the range between 80,000 and 100,000, for Lys, Trp, Trp A, and His. Also visible was a reduction in the band range in the corresponding amines, TrpA and HisA, compared to the amino acids.

For Group 3 (Figure 3C), it was perceived that the increasing length of the diamine spacer produced a rising MW distribution for Trp and a decreasing one for His. Again, defined band ranges were detected on all nanoparticles between 50,000 and 65,000 and between 70,000 and 80,000 while band ranges between 15,000 and 30,000 were not found for EDA-Trp.

The prominent protein distribution of adsorbed proteins on polymer nanoparticles is therefore complex and unique. Overall though, one notices that the protein distribution range, 50,000–70,000 (daltons) predominates for all functionalized nanoparticles.

The amount of protein adsorbed on the functionalized nanoparticle surfaces is expressed as the net intensity ratio (NIR) as shown in Fig. 4 and represents the cumulative intensities of the single bands still detectable, normalized for the intensity of the bands in the corresponding plasma sample. Taking each group sequentially, one notices an increase in overall protein adsorption for increasing chain lengths of diamines with maximum adsorption for ODA and DODA as demonstrated in Fig. 4A. It is also visible that more hydrophilic ligands such as OH or short length diamine EDA adsorbed less protein than long chain diamines such as ODA, which are per se more hydrophobic. The comparison of amino acids and corresponding amines (Fig. 4B) shows a decrease in protein adsorption after descarboxylation for both TrpA and HisA. Further, Lys and Trp demonstrated considerably higher protein adsorption than His. With respect to the amino acids spaced with diamines shown in Fig. 4C, Trp spacers EDA, HDA, and DODA witness a gradual increase in protein adsorption. An increase between EDA-His and HDA-His is countered by a decrease from HDA-His to DODA-His.

Major plasma proteins that may play a role in therapeutic apheresis are fibrinogen, in the case of hyperfibrinogenemia (22), and albumin, which is known to bind many blood born toxins (23). The main bands for both proteins appear in SDS-PAGE under reducing conditions in the MW range of 50,000–80,000 daltons (24). When the net intensity ratio for this MW range was plotted for the different groups, a quite similar picture was obtained. This pattern is summarized in Fig. 5 with the only exception that protein adsorption dropped for the diamine spaced His from EDA to DODA.

To obtain more insight into the extent to which the aforementioned proteins are bound to the different particles, immunoblotting for HSA and fibrinogen was carried out. Figures 6 and 7 give a qualitative overview as to how these proteins have been absorbed on the different types of particles. It can be seen in Fig. 6 that in general albumin binding was lower in Group 3 with spaced amino acids than in Groups 1 and 2. Short length diamines like EDA bound considerably less albumin than long chain diamines such as HDA, ODA, and DODA. It was also visible that amino acids Lys and Trp and its corresponding amine TrpA bound high amounts of albumin while His expressed low binding. Indeed, descarboxylation of His was followed by increasing albumin adsorption as observed for HisA. Increasing the spacer length of diamines for Trp resulted in increased binding of albumin although binding was quite low in comparison to that of diamines or Trp itself. Increasing the spacer length of His again produced a peak adsorption for HDA-His, as was observed for the overall protein adsorption.

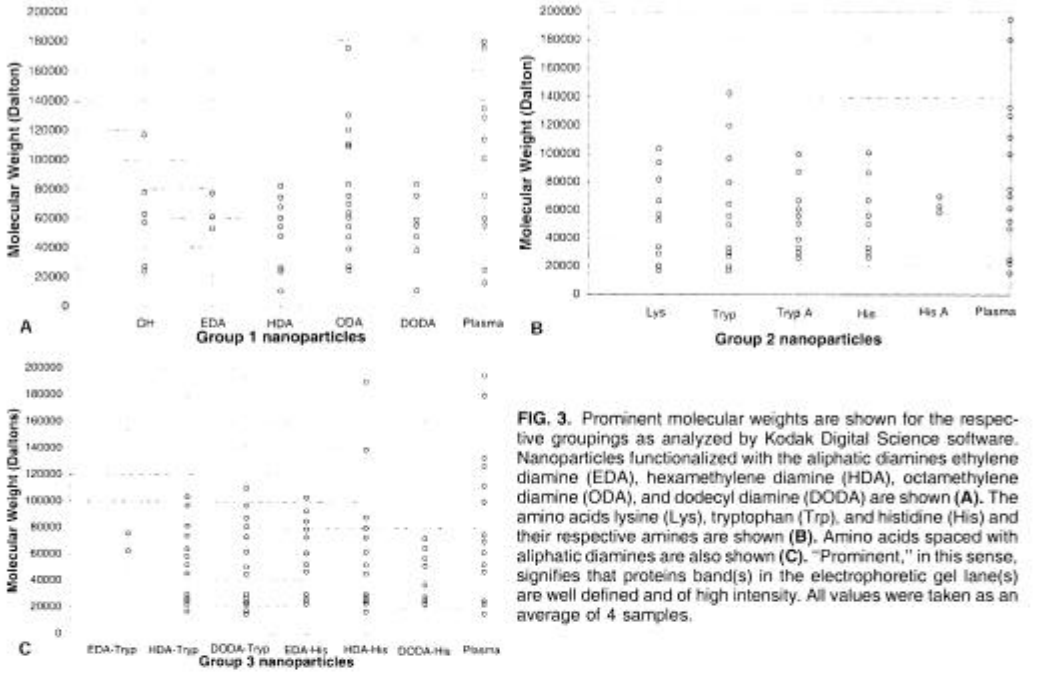

FIG. 3. Prominent molecular weights are shown for the respective groupings as analyzed by Kodak Digital Science software. Nanoparticles functionalized with the aliphatic diamines ethylene diamine (EDA), hexamethylene diamine (HDA), octamethylene diamine (ODA), and dodecyl diamine (DODA) are shown **(A).** The amino acids lysine (Lys), tryptophan (Trp), and histidine (His) and their respective amines are shown **(B).** Amino acids spaced with aliphatic diamines are also shown **(C).** "Prominent," in this sense, signifies that proteins band(s) in the electrophoretic gel lane(s) are well defined and of high intensity. All values were taken as an average of 4 samples.

When immunoblotting was carried out for fibrinogen, enhanced adsorption on aliphatic diamines was evident as demonstrated in Fig. 7. In this case, a different trend for fibrinogen adsorption was observed with decreased binding of the protein with the increasing chain length of the diamines. Lys, Trp, and TrpA bound similar quantities of fibrinogen while His and HisA adsorbed considerably less of this protein. Indeed, it was obvious that HisA expressed strongly one of the main bands which indicates some enrichment of this fibrinogen subunit. Spaced amino acids did express much lower fibrinogen binding as was observed in Groups 1 and 2. There was also no change of adsorption detectable with the increase in the length of diamine spacers.

DISCUSSION

In this paper, we have presented a suitable method for the detection of proteins previously adsorbed from human plasma onto polymeric nanoparticles. The novelty of the study consists of the controlled change of surface structure by the covalent binding of aliphatic diamines with increasing chain length; amino acids with increasing hydrophobicity from Lys, His, and Trp and their corresponding amines; and the use of the respective diamines as spacers for the binding of Trp and His. Washing and desorption procedures were optimized to ensure that no residual nonadsorbed plasma proteins were present in the particle sediment before desorption was started. Increases in SDS concentration and the temperature of treatment and the addition of disulfide-bond breaking β-mercaptoethanol could maximize the desorption of proteins. Determination of the protein adsorption pattern and total amount of protein adsorbed, as well as the detection of specific proteins, was accomplished by the use of electrophoresis and immunoblotting.

The investigation of the protein adsorption pattern and derived total protein adsorption revealed generally a broad distribution of detectable molecular weight bands, as well as increasing adsorption with the increasing chain length of diamines. This result was to have been expected because the increase in the length of the carbohydrate chain should provoke an increased hydrophobicity of the particles, which is one of the driving forces for protein adsorption (13). However, DODA, in possession of the longest carbohydrate chain, adsorbed slightly less protein than ODA. Nevertheless, the measured hydrophobicity was maximal as well. Because protein adsorption is not only dependent on hydrophobicity but also on surface charges and the presence of

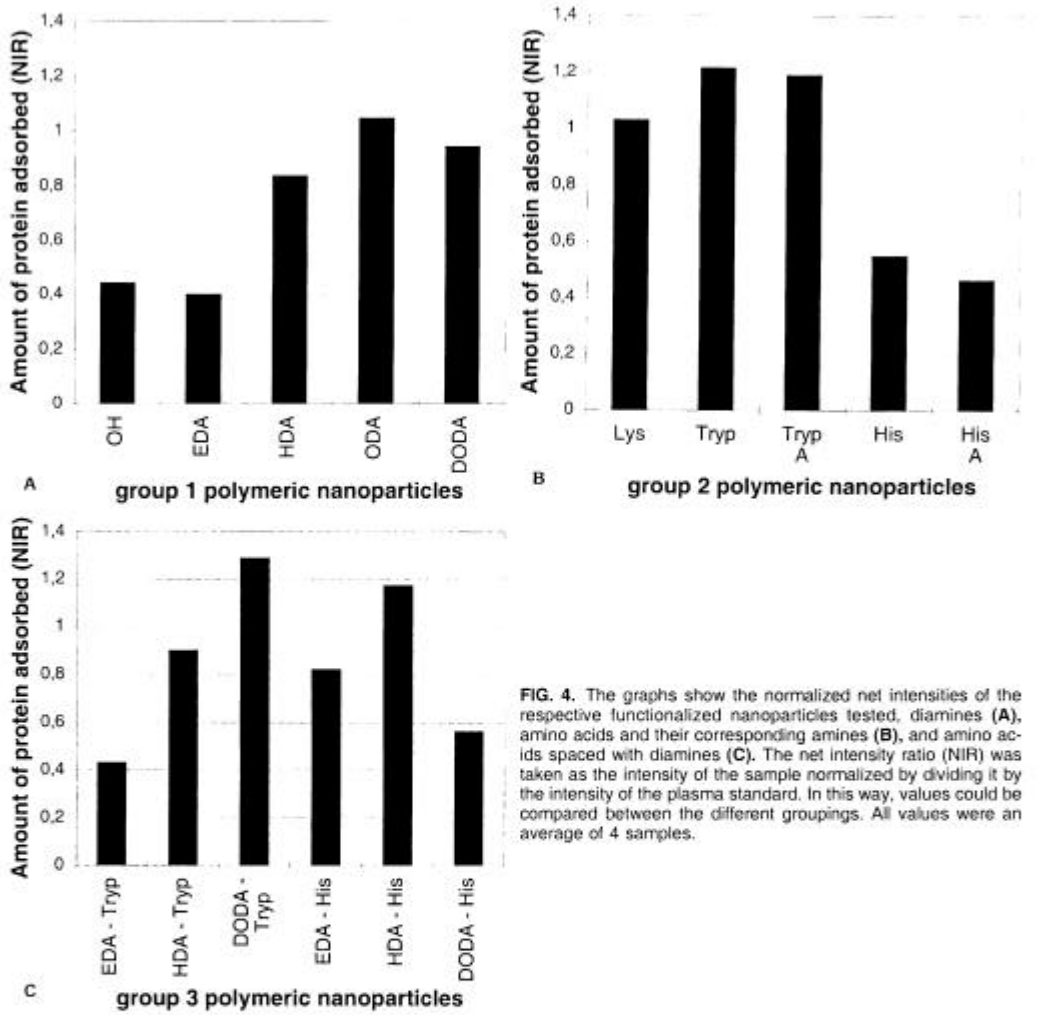

FIG. 4. The graphs show the normalized net intensities of the respective functionalized nanoparticles tested, diamines **(A)**, amino acids and their corresponding amines **(B)**, and amino acids spaced with diamines **(C)**. The net intensity ratio (NIR) was taken as the intensity of the sample normalized by dividing it by the intensity of the plasma standard. In this way, values could be compared between the different groupings. All values were an average of 4 samples.

specific functional groups, etc. (13), adsorption from complex mixtures such as blood plasma may follow a more complicated pattern (9,11–13,17) and is not simply related to the physicochemical surface parameters measured in this study. A further reason for the deviation of the protein adsorption pattern from expected results may be the different degree of functionalization of nanoparticles with the various ligands used in this study. Functionalization may have been affected as a result of the different reactivity and stereo chemistry of the used substances such as diamines or amino acids.

Correspondingly, amino acids bound to nanoparticles did not display simple correlations between physicochemical features and protein adsorption. According to Eisenberg et al. (25), the hydrophobicity of amino acids increases from Lys to His to Trp. However, this observation was not the result of the measurement of protein adsorption and hydrophobicity. In the present study, it was observed that Trp expressed the broadest distribution range and highest overall adsorption, followed by Lys and not by His. The high affinity of Trp for a variety of proteins cannot be explained simply by the physicochemical data, but may be explained by the presence of a large heterocyclic aromatic system which might be particularly suited for the adsorption of proteins. In this context, a number of adsorbents on the market cur-

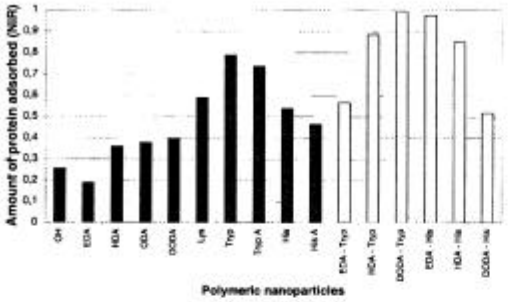

FIG. 5. The graph shows the normalized net intensity, in the molecular weight range of 50,000 to 77,000 daltons, of the respective functionalized nanoparticles tested. The net intensity ratio (NIR) was taken as the intensity of the sample normalized by dividing it by the intensity of the plasma standard. In this way values could be compared between the different groupings. All values were an average of 4 samples.

rently apply tryptophan or other amino acids with heterocyclic side groups as ligands (2,26,27). In addition the low protein adsorption of His functionalized nanoparticles indicates less immobilization of His in comparison to the other amino acids. Interestingly, the descarboxylation of Trp to TrpA and His to HisA increased the measured hydrophobicities tremendously in part while the surface charge density remained unchanged. The decrease in overall protein adsorption, as well as in the MW distribution of proteins observed for the corresponding amines (particularly for HisA), indicates an important role of the carboxylic function in the immobilization and adsorption process.

When Trp was spaced with diamines, a great reduction in protein adsorption was achieved compared to Trp alone for short diamine spacers such as

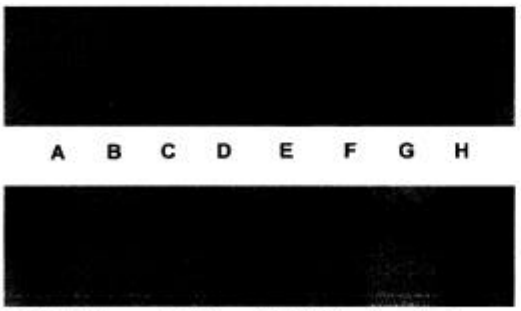

FIG. 6. The immunoblot is from SDS-PAGE under reducing conditions for human serum albumin performed with enhanced chemoluminescence. (**Upper panel:** lane **A:** EDA, lane **B:** HDA, lane **C:** ODA, lane **D:** DODA, lane **E:** Lys, lane **F:** Trp, lane **E:** TrpA, lane **F:** His; **Lower panel:** lane **A:** HisA, lane **B:** EDA-Trp, lane **C:** HDA-Trp, lane **D:** DODA-Trp, lane **E:** EDA-His, lane **F:** HDA-His, lane **E:** DODA-Trp, lane **F:** plasma).

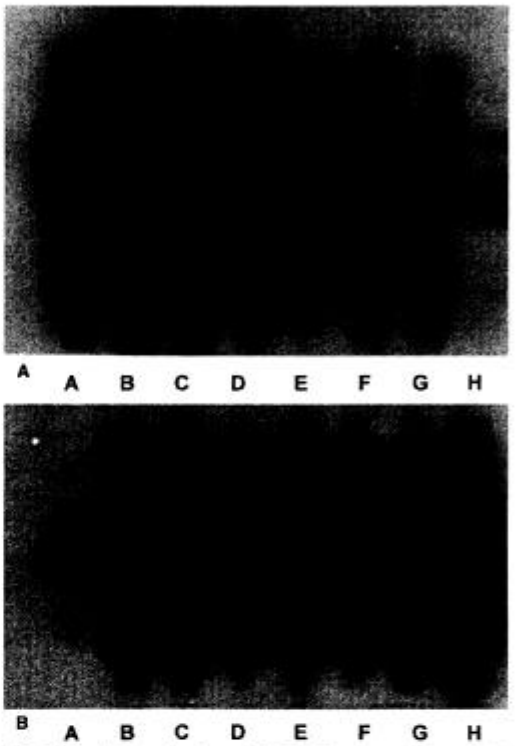

FIG. 7. The immunoblot form SDS-PAGE under reducing conditions for fibrinogen was performed with enhanced chemoluminescence. (**Panel A:** lane **A:** EDA, lane **B:** HDA, lane **C:** ODA, lane **D:** DODA, lane **E:** Lys, lane **F;** Trp, lane **G:** TrpA, lane **H:** (His); **Panel B:** Lane **A:** HisA, lane **B:** EDA-Trp, lane **C:** HDA-Trp, lane **D:** DODA-Trp, lane **E:** EDA-His, lane **F:** HDA-His, lane **G:** DODA-Trp, lane **H:** plasma).

EDA and HDA. In contrast, higher binding was observed on DODA-Trp. This result shows that the quantities of Trp immobilized via the diamine spacer are reduced in comparison to Trp alone. It is interesting to note that increasing the length of the diamine spacer resulted in an increase molecular weight distribution and general protein binding which might be related to improved mobility of the Trp ligand. The use of the diamine spacers EDA and HDA for the immobilization of His provoked a considerably higher adsorption capacity of the particles. In this case, the overall protein adsorption and the protein MW distribution were enhanced in comparison to His alone. It can be postulated that the interplay of change in density and mobility of ligands contributes to this phenomenon.

As was shown previously, a multitude of plasma proteins adsorbed onto the particles which cannot be analyzed in detail. We selected the MW range be-

tween 50,000 and 70,000 daltons for a further analysis of protein adsorption. Both HSA with a MW of 69,000 daltons and fibrinogen subunits under reducing conditions with MWs of 47,000 daltons (γ), 56,000 daltons (β), and 67,000 daltons (α) appear in this range. HSA plays an important role in the passivation of material surfaces, minimizing reactions with the different defense systems of the organism (28). More important in this study was albumin being known to bind a variety of blood-born toxins. The selective removal or exchange of HSA can be applied for blood detoxification in hepatic failure (23). The removal of fibrinogen can be used for the reduction of thromboembolic complications in hyperfibrinogenemia (22). When the adsorption of proteins was assessed quantitatively by the calculation of the net intensity ratios, a quite similar pattern was obtained in comparison to the overall net intensity ratio. Because serum albumin is the most abundant protein in plasma (24), one could expect that this protein accounts most for the observed protein adsorption. Immunoblotting could confirm this assumption in general by a quite similar adsorption pattern of HSA with low detection of HSA on EDA, His, EDA-Trp, and DODA-His while binding was high on longer chain diamines, amino acids, and specific spaced amino acids. In comparison, the binding of fibrinogen was quite different from HSA adsorption. Immunoblots showed a number of different bands derived from fibrinogen subunits, but most probably also from fibrinogen degradation products as described previously by others (19). When the 3 different groups were compared, it was evident that aliphatic diamines bound the highest quantities of fibrinogen. Studies on fibrinogen adsorption of biomaterials have discovered a transient binding of fibrinogen on hydrophilic, charged surfaces known as the Vroman effect (16) while hydrophobic materials bind irreversibly high quantities of fibrinogen (17). Because aliphatic diamines can be considered per se as more hydrophobic than amino acids, which was also supported partially by the measured hydrophobicities, the higher binding of fibrinogen on nanoparticles functionalized with diamines can be explained. Spaced amino acid, as well as Lys, Trp, and TrpA, bound obviously similar quantities of fibrinogen. One exception was His and HisA with one prominent band of a fibrinogen subunit, which cannot be justified on the basis of the physicochemical measurements done in this study.

CONCLUSION

In summary of this and other studies, it can be stated that there are no simple relationships between the structure/physicochemical surface properties of functionalized particles and their adsorption of specific plasma proteins. This is primarily due to the complex interplay between proteins and surfaces, but to some extent also to the different extent of immobilization of various ligands on a specific type of particle. Because ligands with high specificity such as monoclonal antibodies are too costly for many applications, simple ligands as investigated in this study may be a good alternative if the proteins of interest are adsorbed in sufficient quantities. Therefore, it is concluded that the developed techniques may be useful for the development of tailor-made surfaces for the adsorption of specific blood proteins in therapeutic and preparative apheresis.

REFERENCES

1. Falkenhagen D. Small particles in medicine. *Artif Organs* 1995;19:792–4.
2. Fadul JEM, Danielson BG, Wilkström B. Reduction of plasma fibrinogen, immunoglobulin G, and immunogloblin M concentrations by immunoadsorption therapy with tryptophan and phenylalanine adsorbents. *Artif Organs* 1996;20: 986–90.
3. Stefanutti C, Vivenzio A, Di Giacomo AS, Colombo C, Alessandri C, Ricci G. In: Agishi T, ed. *Therapeutic plasmapheresis (XII)*. Utrecht: VPS, 1993:463–70.
4. Olbricht CJ. Extracorporeal removal of lipids by dextran sulfate cellulose adsorption. *Artif Organs* 1996;20:332–5.
5. Bosch T. State of the art of lipid apheresis. *Artif Organs* 1996; 20:292–5.
6. Zydney AL. Therapeutic apheresis and blood fractionation. In: Bronzino JD, ed. *The biomedical engineering handbook*. Boca Raton, FL: CRC and IEEE Press, 1997:1936–51.
7. Weber C, Ragnoch C, Loth F, Schima H, Falkenhagen D. The microsphere based detoxification system (MDS)—A new extracorporeal blood purification technology based on recirculated microspherical adsorbent particles. *Int J Artif Organs* 1994;17:595–602.
8. von Appen K, Weber C, Losert U, Schima H, Gurland HJ, Falkenhagen D. Microsphere based detoxification system: A new method in convective blood purification. *Artif Organs* 1996;20:420–5.
9. Lück M, Paulke B-R, Schröder W, Blunk T, Müller RH. Analysis of plasma protein adsorption on polymeric nanoparticles with different surface characteristics. *Journal of Biomater Res* 1997;39:478–85.
10. Lee HB, Kim SS, Khang G. Polymeric biomaterials. In: Bronzino JD, ed. *The biomedical engineering handbook*. Boca Raton, FL: RC and IEEE Press, 1997:581–97.
11. Courtney JM, Lamba NMK, Sundaram S, Forbes CD. Biomaterials for blood-contacting applications. *Biomaterials* 1994;15:737–44.
12. Groth T, Klosz K, Campbell EJ, New RRC, Hall B, Goering H. Protein adsorption, lymphocyte adhesion and platelet adhesion/activation on polyurethane ureas is related to hard segment content and composition. *J Biomater Sci Polym Ed* 1994; 6:497–510.
13. Norde W, Lyklema J. Why proteins prefer interfaces. *J Biomater Sci Polym Ed* 1991;2:183–202.
14. Darkow R, Groth T, Albrecht W, Paulke BR, Paul D. Synthetic microparticles with pseudobiological ligands for endotoxin removal. *Proceedings of polymers in medicine and surgery PIMS '96*. Glasgow: University of Strathclyde, 1996: 113–20.

15. Lukowski G, Müller RH, Müller BW, Dittgen M. Acrylic acid copolymer nanoparticles for drug delivery: 1. Characterization of the surface properties relevant for in vivo organ distribution. *Int J Pharm* 1992;84:23–31.
16. Slack SM, Horbett TA. The effects of temperature and buffer on fibrinogen adsorption from blood plasma to glass. *J Biomater Sci Polym Ed* 1991;2:227–37.
17. Absolom DR, Zingg W, Neumann AW. Protein adsorption to polymer particles: Role of surface properties. *J Biomed Mater Res* 1987;21:161–71.
18. Bohnert JL, Horbett TA. Changes in adsorbed fibrinogen and albumin interactions with polymers indicated by decreases in detergent elutability. *J Colloid Interface Sci* 1986;111:363–77.
19. Brash JL, Thibodeau JA. Identification of proteins from human plasma to glass bead columns: Plasmin-induced degradation of adsorbed fibrinogen. *J Biomed Mater Res* 1986;20:1263–75.
20. Parzer S, Balcke P, Mannhalter C. Plasma protein adsorption to haemodialysis membranes: Studies in an in vitro model. *J Biomed Mater Res* 1993;27:455–63.
21. Mulzer SR, Brash JL. Identification of plasma proteins adsorbed to haemodialyzers during clinical use. *J Biomed Mater Res* 1989;23:1483–504.
22. Seidel D. Risikofaktoren der Arteriosklerose. Unterschiedliche Profile—Unterschiedliche Mechanismen? *Z Kardiol* 1993;82:33–7.
23. Stange J, Mitzner S. A carrier-mediated transport of toxins in a hybrid membrane. Safety barriers between a patient's blood and a bioartificial liver. *Int J Artif Organs* 1996;19:677–91.
24. Stryer L. *Biochemistry, 3rd Edition.* New York: W.H. Freeman and Company, 1988.
25. Eisenberg D, Schwarz E, Komaromy M, Wall R. Analysis of membrane and surface protein sequences with the hydrophobic moment plot. *J Mol Biol* 1984;179:125.
26. Sueoka A. Present status of apheresis technology, Part 3: Adsorbent. *Thera Apheresis* 1997;1:271–83.
27. Bueno SMA, Legallais C, Haupt K, Vijayalakshmi MA. Experimental kinetic aspects of hollow fiber membrane-based pseudoaffinity filtration: Process for IgG separation from human plasma. *J Membr Sci* 1996;117:45–56.
28. Eberhardt RC, Munro MS, Frautschi JR, Lubin M, Clubb FJ, Miller CW, Sevastianov VI. Influence of endogenous albumin binding on blood-material interactions. *Ann NY Acad Sci* 1987;516:78–95.

Publikation 2

Thomas Groth, Judith Synowitz, Günter Malsch, Klaus Richau, Wolfgang Albrecht, Klaus-Peter Lange, Dieter Paul (1997).

Contact activation of plasmatic coagulation on polymeric membranes measured by the activity of kallikrein in heparinized plasma.

Journal of Biomaterials Science - Polymer Edition **8**, 797-808.

J. Biomater. Sci. Polymer Edn, Vol. 8, No. 10, pp. 797–807 (1997)

Contact activation of plasmatic coagulation on polymeric membranes measured by the activity of kallikrein in heparinized plasma

TH. GROTH,[1,*] J. SYNOWITZ,[2] G. MALSCH,[1] K. RICHAU,[1] W. ALBRECHT,[1] K.-P. LANGE[2] and D. PAUL[1]

[1]*GKSS Research Center, Institute of Chemistry, Department of Membrane Research, Kantstrasse 55, 14513 Telow-Seehof, Germany*

[2]*Humboldt University, School of Medicine (Charité), Dental School, Department of Prosthetics, Schumannstrasse 21-22, 10098 Berlin, Germany*

Received 29 January 1997; accepted 1 April 1997

Abstract—Kallikrein is involved in the generation of bradykinin during extracorporal circulation, that is believed to play an important role in cases of anaphylactic shock during hemodialysis. Therefore, a method for the assessment of kallikrein generation was developed, based on the chromogenic substrate S-2302. Comparison of kallikrein-like activity on glass using citrate or heparinized plasma demonstrated enhanced activity in the presence of heparin. The applicability of the assay, and the time course of kallikrein generation was demonstrated with glass and cuprophan. Membranes based on pure polyacrylonitrile, or its copolymers differing in their content of acrylic acid, 2-hydroxyethyl acrylate, and allylsulphonate were investigated with respect to kallikrein-like activity, and physicochemical surface properties. It was found that high content in 2-hydroxyethyl acrylate, and acrylic acid caused a substantial activation of the contact system while low content in allylsulphonate (less than 2 mol%) did not result in enhanced kallikrein-like activity. The activating materials were characterized to be highly wettable, and had the most negative zeta potentials.

Key words: Membranes; polyacrylonitrile; copolymers; contact phase activation; kallikrein; heparin.

INTRODUCTION

The clinical application of biomedical devices in contact with blood may be limited by the activation of the coagulation system. The molecular mechanism by which negatively charged surfaces promote kallikrein-dependent factor XII activation is not completely understood [1–5]. The autoactivation of factor XII (Hageman factor) occurs presumably on hydrophilic, negatively charged surfaces [6–8]. Factor XIIa is able to cleave prekallikrein into kallikrein [3, 4, 9, 10]. Kallikrein is the most potent

*To whom correspondence should be addressed. E-mail: Thomas.Groth@gkss.de

activator of factor XII enhancing the formation of factor XIIa in a positive feedback reaction [2–5, 10, 11]. Factor XIIa cleaves also factor XI leading to the activation of the intrinsic system which may finally result in fibrin polymerization and formation of a hemostatic plug [4, 5, 9]. The activation of the contact system is also connected with other systems of the hemostasis; such as the complement, the fibrinolytic, and the kallikrein–kinin system [9, 12–14]. The latter involves the cleavage of absorbed high molecular weight kininogen (HMWK) by kallikrein resulting in the release of the vasoactive nonapeptide bradykinin [9, 14].

Anaphylactic reactions associated with hemodialysis have been reported for patients on angiotensin-converting enzyme (ACE) inhibitors undergoing dialysis with a specific high-flux membrane, Hospal AN69 [15, 16], that has been applied because of low activation of the complement system [17, 18]. One of the possible pathological mechanisms has been associated with the activation of factor XII by the dialysis membrane, which increases bradykinin as a mediator of anaphylaxis leading to hypotension through action on vascular smooth muscle [15, 16, 19]. ACE is believed to be the major metabolic pathway of bradykinin degradation [20]. Therefore, the inhibition of ACE may cause high concentrations of bradykinin. Membranes with negative surface charges have found to be activating purified factor XII in an *in vitro* system [21]. Apart from the negative surface charge the high surface to volume ratio in hollow fiber dialysis may contribute to the release of significant amounts of bradykinin during hemodialysis [22]. The formation of bradykinin could be a relevant parameter for the evaluation of hemocompatibility of dialysis membranes.

Because bradykinin assays have limited availability, other types of assays measuring the activation of contact system may be applied. Kallikrein is the enzyme generating bradykinin by the cleavage of HMWK [9, 11, 23]. Therefore, the measurement of kallikrein formation might be a useful assay for the estimation of contact activation on biomaterials. Assays for kallikrein have been described before, though all these measurements were carried out with citrate plasma [24–26]. Since heparin is used during hemodialysis, results of the above mentioned studies may have limited relevance to the application of membranes. The activity of kallikrein generation is measured by use of a chromogenic substrate for kallikrein (S-2302) [27]. In this study we have worked with heparinized blood to approach the *in vivo* conditions of hemodialysis, and to obtain more insight into the role of heparin during contact activation on membranes. We have measured the kallikrein activation induced by two reference materials (glass and cuprophan), and different membranes based on polyacrylonitrile, including selected copolymers. Further, we have estimated prekallikrein in separate experiments to validate the results of kallikrein measurements. In addition, results of specific contact activation (kallikrein formation) were compared with a common whole blood clotting test for measuring non-activated partial thromboplastin time.

MATERIALS AND METHODS

Materials

Glass surfaces were used as the activating reference material. Glass slides (Menzel, Germany) were cleaned with cold chromium sulfuric acid, and rinsed with distilled water. Flat sheet membrane cuprophan was used as a second reference material.

Selected acrylic polymers of polyacrylonitrile (PAN), i.e. pure PAN, and its copolymers with differing kind and concentration of functionality attributed to 2-hydroxyethyl acrylate (HEA), acrylic acid (AA), and sodium allylsulphonate (NaAS) were investigated. The content of the introduced functionality in the different copolymers was 0.6, 3.6, and 23.5 mol% for HEA; 0.8 and 1.6 mol% for NaAS; and 6.1 mol% for AA. The copolymers are characterized by a random arrangement of the functionality along the backbone. The polymers were prepared in dimethylformamide (DME) solution by free radical initiation using ammonium peroxidisulphate as an efficient catalyst, precipitated from their solutions by acidified methanol, and dried under vacuum to constant weight. Polymerization was carried out at balanced monomer/initiator concentration ratios ($[M]/[I] > 10^3$) and low temperatures ($T \leqslant 50°C$). This preparation resulted in high molecular weight products ($M_{\eta.\mathrm{DMF}} \geqslant 70$ kD) with film forming properties.

Blood collection and preparation

Fresh blood was obtained from healthy volunteers who had no medication for at least 10 days. Blood was anticoagulated either with sodium citrate (3.19×10^{-2} g ml^{-1}) at a blood/citrate ratio of 9 : 1, or with sodium heparin (10 IU ml^{-1}). The blood was centrifuged at 2000 g for 10 min immediately after collection. The supernatant platelet poor plasma (PPP) was separated and pooled from ten donors. Aliquots were snap frozen and stored until use at −70°C. Blood and plasma were collected and stored in polypropylene tubes.

Plasma/material contact

Glass slides or polymer foils were fixed on silicone rubber sandwiched by two Teflon® plates, the upper plate with holes of 22 mm diameter. Pooled PPP was thawed and 1 ml added to each hole of the measuring chamber. The chamber was moved on an orbital shaker for the times indicated. All experiments were carried out at 37°C. The measuring chambers were prewarmed and the whole equipment placed in an incubation hood type ITS (Infors, Switzerland).

Measurement of kallikrein-like activity

Kallikrein-like activity was measured with the chromogenic substrate S-2302 (Chromogenix, Sweden) using the end-point method. 400 μl PPP was mixed with 200 μl S-2302 (2 mM), and incubated at 37°C. The reaction was stopped by the addition of 200 μl acetic acid (20%). Plasma without material contact was used as a control. Optimization of the assay was carried out as previously [26, 28], and has been described in detail elsewhere [28]. There, it was found out that a five-fold dilution of

plasma with Tris–HCl enhances the kallikrein-like activity considerably. Consequently, plasma dilution was applied throughout this study. The optical density (OD) was measured either in a microplate reader or with a photometer Spekol 21 (Carl Zeiss Jena, Germany) set at 405 nm.

Measurement of prekallikrein

A commercial assay for prekallikrein measurement (PK-COA-Set) was obtained from Chromogenix, Sweden. Briefly, factor XII in plasma samples is converted by the addition of an activator in factor XIIa, which activates the prekallikrein still present in the plasma.

Samples of PPP were taken after incubation with different materials. According to the instructions of the producer, 50 μl samples were then diluted with 3 ml sample buffer (Chromogenix). 200 μl plasma prekallikrein activator was incubated at 37°C for 4 min and mixed with 200 μl diluted PPP. After 2 min incubation 200 μl S-2302 was added, followed by a further 2-min incubation. Then 200 μl acetic acid (20%) was added and the OD measured at 405 nm. The measured OD is related to the amount of prekallikrein not consumed by the foreign surface.

Measurement of partial thromboplastin time

According to the valid standards for blood contacting devices, partial thromboplastin times were assessed without kaolin as an activator [29]. The non-activated partial thromboplastin time (NAPTT) was estimated with a commercial test kit (Behring Werke, Germany). The NAPTT was measured after contact of 1 ml citrate PPP with the polymer surface at 37°C for 30 and 60 min, respectively. 100 μl PPP was taken and added to a prewarmed test tube followed by the addition of phospholipid (cephalin) and calcium chloride solution. The time after addition of the activator solution until the clotting of plasma was measured with a coagulometer KC 4a (Amelung, Germany) at 37°C. Measurements were taken in relation to a negative control, i.e. plasma without material contact. The results are presented as a ratio between NAPTT of control to NAPTT of samples and called relative NAPTT.

Measurement of contact angles and streaming potentials

Advancing and receding contact angles were measured by the sessile drop method using water as the test liquid. Streaming potential measurements were carried out as described previously [30] with an EKA Electro Kinetic Analyzer manufactured by Anton Paar KG (Austria). A flat plate measuring cell similar to that described by van Wagenen *et al.* [31] was used. An electrolyte channel between sample surfaces of an effective area of 2×1100 mm^2 and an effective height in the order of 0.3 mm was established. Measurements were performed at 25.0 ± 0.5°C using aqueous KCl solution ($I = 10^{-3}$ mol^{-1}), the pH was adjusted with equimolar KOH and HCl solutions, respectively. The zeta-potential was calculated according to Stern [32], while surface conductivity was not taken into account.

RESULTS

Since heparin is used as anticoagulant during extracorporal circulation, its influence on the kallikrein formation during contact with foreign surfaces was investigated. Table 1 shows the comparison of kallikrein-like activity on glass for either citrate, or heparinized plasma. Since it was apparent that kallikrein-like activity for short term contact up to 9 min was significantly enhanced for heparinized plasma in comparison to citrate plasma ($p \leqslant 0.05$, t-test). Therefore, further experimental work with the kallikrein assay was carried out with heparinized plasma.

The applicability of the kallikrein assay, and the time course of kallikrein-like activity was then tested using two reference materials, i.e. glass and cuprophan. The results shown in Fig. 1 demonstrate increasing kallikrein-like activity over a period up to 120 min for both materials. It is apparent that the kallikrein-like activity on glass was significantly higher than on cuprophan ($p \leqslant 0.05$, t-test). Next, it was investigated how the kallikrein-like activity was related to the presence of prekallikrein in plasma after contact with the materials. Figure 2 shows that the concentration of prekallikrein in plasma dropped for both materials with increasing contact time. The steeper decrease found for glass was related to the higher increase in kallikrein-like

Table 1.
Comparison of kallikrein formation on glass depending on the anticoagulation

Contact time glass/plasma (min)	Citrate plasma (OD[a] at 405 nm, mean ± S.D.)	Heparinized plasma (OD[a] at 405 nm, mean ± S.D.)
0	0.01 ± 0.02	0.01 ± 0.02
3	0.402 ± 0.13	0.499 ± 0.23
6	0.526 ± 0.18	0.703 ± 0.12*
9	0.524 ± 0.17	0.730 ± 0.21*

[a]OD was measured with a micro plate reader.
*Values are significantly higher ($p \leqslant 0.05$, t-test, $n = 6$).

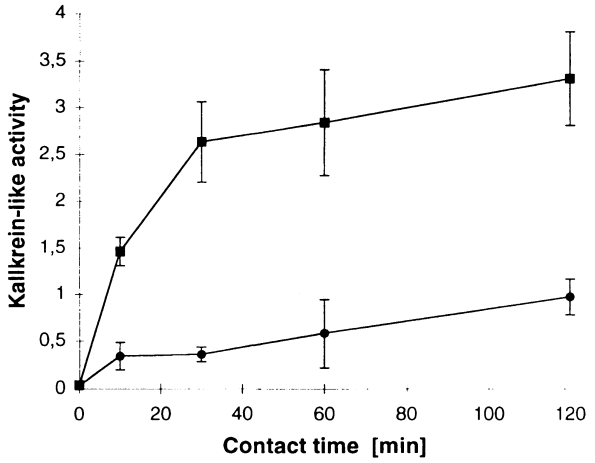

Figure 1. Kallikrein-like activity (OD, mean ± S.D.) for glass (■), and cuprophan (●) plotted vs contact time.

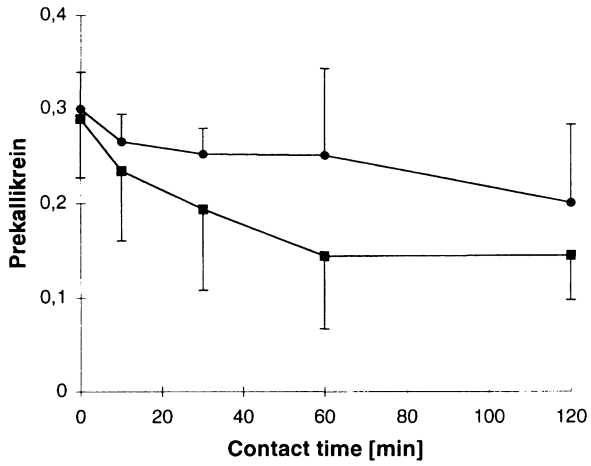

Figure 2. Amount of prekallikrein (OD, mean ± S.D.) for glass (■), and cuprophan (●) plotted vs contact time.

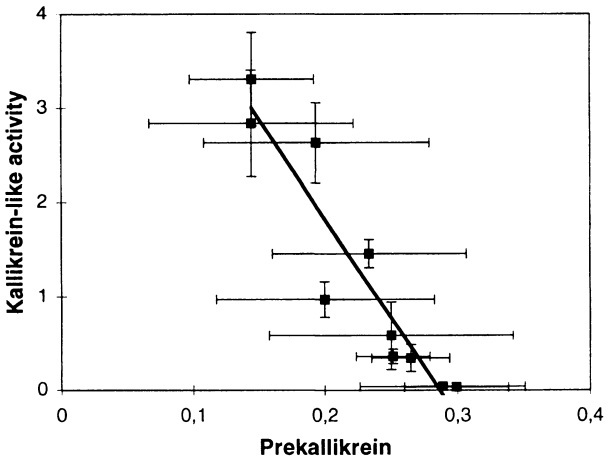

Figure 3. Plot of kallikrein-like activity (OD, mean ± S.D.) vs amount of prekallikrein (OD, mean ± S.D.) with the following linear regression curve $y = -21.1x + 6.05$, and a correlation coefficient $R = 0.935$.

activity. Figure 3 shows a plot of kallikrein-like activity vs the amount of prekallikrein still present in plasma after contact with glass or cuprophan. Both parameters were negatively correlated with a correlation coefficient of $R = 0.935$.

The results shown in Fig. 4 allow a comparison of contact activation for polyacrylonitrile and the different copolymers. PAN and copolymers with small HEA content (0.6 and 3.6 mol%, respectively) exhibited low levels of kallikrein-like activity, whereas 23.5 mol% HEA increased the kallikrein generation significantly ($p \leqslant 0.05$, t-test). Increasing molar content of NaAS up to 1.6 mol% did not change significantly kallikrein formation in comparison to pure PAN (results not shown). In contrast, it was observed that 6.1 mol% AA resulted in very high kallikrein-like activity which was even significantly enhanced in comparison to 23.5 mol% HEA ($p \leqslant 0.05$, t-test).

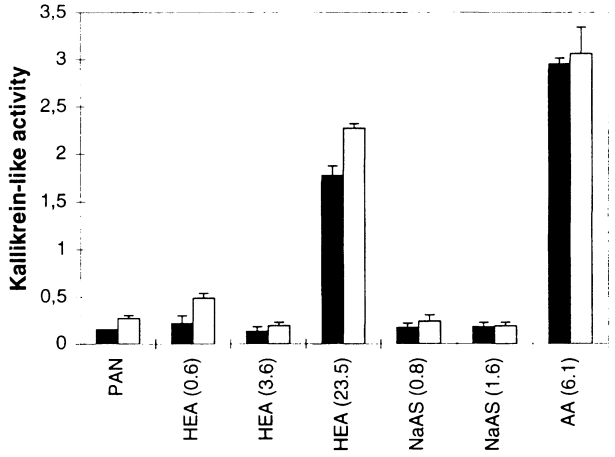

Figure 4. Kallikrein-like activity (OD, mean ± S.D.) measured after 30 min (black bars), and 60 min (white bars) for polyacrylonitrile (PAN), and acrylonitrile copolymers with 2-hydroxyethyl acrylate (HEA), allylsulphonate (NaAS), and acrylic acid (AA) differing in their functionality content in mol%.

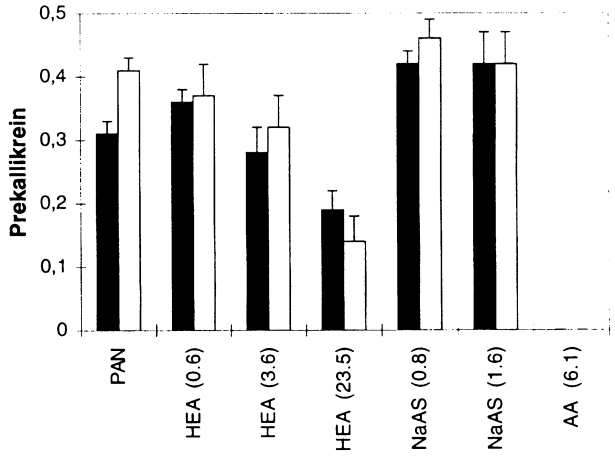

Figure 5. Prekallikrein (OD, mean ± S.D.) measured after 30 min (black bars), and 60 min (white bars) for polyacrylonitrile (PAN), and acrylonitrile copolymers with 2-hydroxyethyl acrylate (HEA), allylsulphonate (NaAS), and acrylic acid (AA), differing in their functionality content in mol%.

The prolongation of the incubation time of plasma from 30 to 60 min produced a slight increase in kallikrein-like activity for all materials. The presence of prekallikrein in plasma samples after contact with the different PAN polymers was measured to find out if there are differences between kallikrein-like activity and kallikrein consumption due to adsorption on the membrane surfaces. Figure 5 shows a gradually decrease of prekallikrein for the HEA copolymers and a complete consumption of prekallikrein for the AA (6.1). Slight changes in prekallikrein were observed with increasing incubation time from 30 to 60 min.

A NAPTT assay for measuring the activation of the coagulation system on biomaterials was performed with citrate plasma. The results are shown in Fig. 6. Obviously,

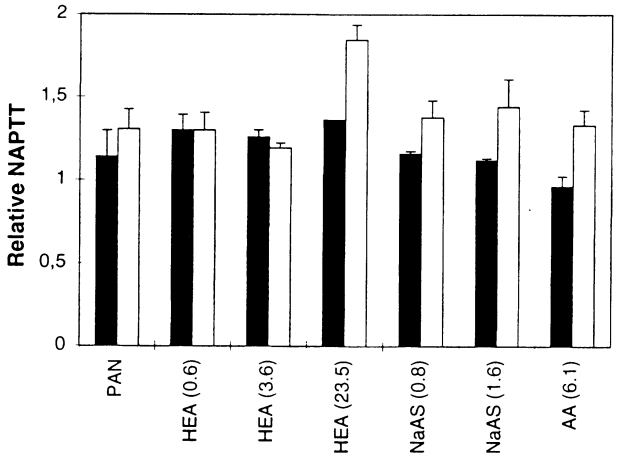

Figure 6. Relative nonactivated partial thromboplastin time (NAPTT) measured after contact of citrate plasma for 30 min (black bars), and 60 min (white bars) for polyacrylonitrile (PAN), and the acrylonitrile copolymers with 2-hydroxyethyl acrylate (HEA), allylsulphonate (NaAS), and acrylic acid (AA), differing in their functionality content in mol%.

Table 2.
Water contact angles and zeta potentials of polyacrylonitrile polymers

Material (mol% copolymer)	Water contact angle θ (deg)		Zeta potential (mV) at pH 7.1
	θ_{adv}	θ_{rec}	
PAN	57	29	−6
HEA (0.6)	60	26	Not estimated
HEA (3.6)	49	23	−4
HEA (23.5)	64	18	−14.5
NaAS (0.8)	41	15	−6
NaAS (1.6)	15	14	−5
AA (6.1)	50	17	−9

no huge differences between the various materials were observed. One exception was HEA (23.5 mol%) with a significantly increased NAPTT at 60 min, which is in agreement with the observed high kallikrein-like activity. In contrast, AA (6.1 mol%), the most activating material in the kallikrein assay, did not change at 30 min, and prolonged the clotting time at 60 min. In general, it was observed that all materials provoked a prolongation of clotting times from 30 to 60 min.

Physicochemical investigations were carried out to learn more about the dependence of contact phase activation on surface wettability, and the zeta potential of the different polymers. Table 2 shows a decrease of receding contact angles for increasing content of HEA that was not observed for advancing contact angles. Low receding contact angles were found for NaAS and AA that was not observed for advancing contact angles. Zeta potentials did not vary considerably between the different polymers, although it was found that zeta potential at pH 7.1 was most negative for HEA (23 mol%) and AA (6.1 mol%).

DISCUSSION

One of the findings of this paper was the enhancement of kallikrein-like activity in plasma with heparin as anticoagulant. Since heparin is used during hemodialysis and other applications of blood contacting devices, its stimulating effect on contact activation has to be taken into account. Similar results have been described previously and were attributed to the adsorption of negatively charged heparin molecules onto the materials surfaces with subsequent increase in autoactivation of factor XII [7, 21]. In addition, it seems that the inhibition of kallikrein, as observed in investigations with citrate blood [25, 26], is smaller or less important in heparinized blood because kallikrein-like activity remained high over periods of up to 2 h. Normally, fast inactivation of kallikrein occurs due to the presence of inhibitors in plasma, such as C1-esterase inhibitor and $\alpha 2$ macroglobulin [33]. Possible reasons for the observed effect might be the observed high kallikrein generation, and/or plasma dilution. Plasma dilution favors the adsorption of HMWK and factor XII [34, 35] and decreases the concentration of inhibitors in plasma, making less probable the formation of the kallikrein inhibitor complex [36].

The comparison of glass with cuprophan demonstrated significantly higher kallikrein formation on the negatively charged glass surface. These experiments clearly demonstrated the applicability of the assay to differentiate high from low activating surfaces. Moreover the results revealed that kallikrein formation was continuing over a period of 2 h. While the kallikrein-like activity increased for both materials with time, the concentration of prekallikrein in plasma decreased continuously. The comparison of both parameters resulted in a negative correlation, i.e. the consumption of prekallikrein was related to the activity of kallikrein in plasma, and not on the surface.

Further experimental work dealt with the contact activation on different polyacrylonitrile polymers. Derivatives of polyacrylonitrile are in current use as dialysis membranes, such as AN69S (Hospal) and SPAN (Akzo). Kallikrein-like activity of PAN, and NaAS was observed to be fairly low. In contrast, high content in AA or HEA produced considerable amounts of kallikrein. It could also be shown that high kallikrein-like activities were corroborated by very low amounts of prekallikrein in plasma, indicating prekallikrein consumption. If we consider the chemical composition of the copolymers it becomes clear that high contents in acrylate and 2-hydroxyethyl acrylate comonomers have a high impact on contact activation. Other polar groups, like the sulphonate group in NaAS seemed to have less influence on contact activation in this study, may be because of the low molar content of this compound (less than 2 mol%). The physicochemical investigations support the conclusion that a higher content either in electronegative or hydrophilic groups play a major role for the observed results. Receding water contact angles were lower than 20 deg for the high activating membranes based on HEA (23.5 mol%) and AA (6.1 mol%). In contrast, advancing contact angles did not allow any conclusion, most probably because they are reflecting apolar components of surface energy and heterogeneity of the materials [37]. However, although very small receding water contact angles were also found for NaAS copolymers, kallikrein generation was insignificant. Similarly, low *in vitro* factor XIIa activity in plasma was observed for AN69S which contains sodium methallyl sulphonate as copolymer [21], although this membrane has shown to be

generating high quantities of bradykinin during hemodialysis [15, 16, 19]. Streaming potential measurements and calculation of zeta-potentials revealed that the high activating polymers HEA (23.5 mol%) and AA (6.1 mol%) also possessed the most negative zeta-potentials. The electronegativity/hydrophilicity of these polymers should be due to the high content in either potential alcoholate groups (HEA) or carboxyl groups (AA). Autoactivation of factor XII, as well as adsorption of proteins of the contact system, like HMWK, is strongly enhanced on electronegative, hydrophilic substrata [4–9, 21, 38]. Moreover, carboxyl groups have shown to have a high procoagulant activity [7].

A further result of this study was that specific testing of contact phase activation expressed considerable advantages over common coagulation tests like the NAPTT test. It is well accepted that the estimation of PTT is sensitive to changes in the contact system of the plasmatic coagulation cascade [39]. Moreover, the PTT assay is recommended for testing the hemocompatibility of blood-contacting devices [29]. However, the results obtained in our study revealed a higher sensitivity of the method for kallikrein formation, while the NAPTT assay could not be used to differentiate the materials with respect to contact activation. Notable material-induced changes in contact activation were only found for HEA (23.5 mol%) and AA (6.1 mol%). Both are either electronegatively charged (AA) or very hydrophilic (HEA). The general prolongation of clotting times in comparison to the control blood for most of the materials indicated a consumption of clotting factors due to the long interaction time between plasma and surfaces. In general, the NAPTT assay was not found to be very useful for the estimation of contact activation on the various materials in this study, a fact that was also addressed by others recently [10].

CONCLUSION

The estimation of hemocompatibility of dialysis membranes has to include the assessment of a possible contact activation of plasmatic coagulation, considering the central part of clot formation, complement activation, fibrinolysis, and bradykinin release [40]. The *in vitro* assessment of kallikrein-like activity as a parameter of contact activation seems to be reasonable because of the crucial role of kallikrein for the generation of bradykinin. Problems with the release of bradykinin and anaphylactic shock have been reported for patients on ACE inhibitors undergoing dialysis with negatively charged membranes. The applicability of the kallikrein assay was demonstrated for high and low activating substrata (glass and cuprophan), and it was obvious that kallikrein is released in the supernatant plasma. Indeed, surface associated kallikrein was not detectable, as found in our previous studies [28]. The use of heparin as an anticoagulant seems to increase the reactivity of materials with respect to contact activation, a fact that has to be taken into account because of the use of heparin during extracorporal circulation. It was also shown that derivatives of polyacrylonitrile (HEA and AA) have a high reactivity vs the contact system.

REFERENCES

1. S. D. Revak, C. G. Cochrane, A. R. Johnson and T. H. Hugli, *J. Clin. Invest.* **54**, 151 (1974).
2. J. Rosing, G. Tans and J. H. Griffin, *Eur. J. Biochem.* **151**, 53 (1985).
3. G. Tans and J. Rosing, *Seminars Thrombosis Hemostasis* **13**, 131 (1987).
4. R. W. Colman, C. F. Scott, A. H. Schmaier, Y. T. Wachtfogel, R. A. Pixley and L. H. Edmunds, Jr., *Ann. NY Acad. Sci.* **516**, 253 (1987).
5. G. Fuhrer, M. J. Gallimore, W. Heller and H. E. Hoffmeister, *Blut* **61**, 258 (1990).
6. M. Silverberg and S. Diehl, *Ann. NY Acad. Sci.* **516**, 268 (1987).
7. E. A. Volger, J. C. Graper, G. R. Harper, H. W. Sugg, L. M. Lander and W. J. Brittain, *J. Biomed. Mater. Res.* **29**, 1005 (1995).
8. C. F. Scott, *J. Biomater. Sci. Polymer Edn* **2**, 173 (1991).
9. A. P. Kaplan and M. Silverberg, *Blood* **70**, 1 (1987).
10. K. W. H. J. van der Kamp and W. Oeveren, *J. Biomed. Mater. Res.* **28**, 349 (1994).
11. F. van der Graf, G. Tans, J. H. Griffin and B. N. Bouma, *J. Biol. Chem.* **257**, 14 300 (1982).
12. B. Ghebrehewit, B. P. Randazzo, J. T. Dunn, M. Silverberg and A. P. Kaplan, *J. Clin. Invest.* **71**, 1450 (1983).
13. G. Goldsmith, H. Saito and O. D. Ratnoff, *J. Clin. Invest.* **62**, 54 (1978).
14. D. Regoli and J. Barabe, *Pharmacol. Rev.* **32**, 1 (1980).
15. L. Verresen, M. Waer, Y. Vantrenterghein and P. Michielsen, *Lancet* **336**, 1360 (1990).
16. E. L. Parnes and W. B. Shapiro, *Kidney Int.* **40**, 1148 (1991).
17. L. C. Smeby, T. E. Wideroe, T. Balstad and S. Jorstad, *Blood Purif.* **4**, 93 (1986).
18. K. E. Burhop, R. J. Johnson, J. Simpson, D. E. Chenoweth and J. Borgia, *J. Lab. Clin. Med.* **121**, 276 (1993).
19. C. Tielemans, P. Madhoun, M. Lenaers, L. Schandene, M. Goldman and J.-L. Vanherweghem, *Kidney Int.* **38**, 982 (1990).
20. M. Ehlers and J. F. Riordan, *Biochemistry* **28**, 5311 (1989).
21. B. M. Matata, J. M. Courtney, S. Sundaram, S. Wark, S. K. Bowry, J. Vienken and G. D. O. Lowe, *J. Biomed. Mater. Res.* **31**, 63 (1996).
22. G. von Sengbusch, S. Bowry and J. Vienken, *Artificial Organs* **17**, 244 (1993).
23. T. Nakayasha and S. Nagasaw, *J. Biochem.* **85**, 249 (1979).
24. M. J. Gallimore and P. Friberger, *Thromb. Res.* **25**, 293 (1982).
25. P. Giusti, G. D. Guerra, M. Palla, G. Soldani, S. Bonanni and G. Mazzanti, *Polymers Med.* **3**, 51 (1988).
26. G. D. Guerra, N. Barbani, L. Lazzeri, L. Lelli, M. Palla and C. Rizzo, *J. Biomater. Sci. Polymer Edn* **4**, 643 (1993).
27. C. Kluft, *J. Lab. Clin. Med.* **91**, 83 (1978).
28. J. Synowitz, Thesis, Humboldt University, Berlin (1996).
29. Anon., ISO 10993-4, International Organisation for Standardisation, London (1992).
30. K. Richau, Ch. Eisold, V. Kudela, H.-H. Schwarz and D. Paul, *Desalination* **104**, 19 (1996).
31. R. A. van Wagenen and J. D. Andrade, *J. Colloid Interface Sci.* **76**, 305 (1980).
32. O. Stern, *Z. Elektrochemie* **30**, 508 (1924).
33. M. Schapira, C. F. Scott and R. W. Coleman, *Biochemistry* **20**, 2738 (1981).
34. L. Vroman and A. L. Adams, *J. Colloid Interf. Sci.* **111**, 391 (1986).
35. H. Elwing, P. Tengvall, A. Askendal and I. Lundström, *J. Biomater. Sci. Polymer Edn* **3**, 7 (1991).
36. G. Motta, E. Fink, M. U. Sampaio and C. A. M. Sampaio, *AAS* **381**, 265 (1992).
37. K. L. Mittal, *Contact Angle, Wettability and Adhesion*. VSP, Utrecht, The Netherlands (1993).
38. H. N. Randriamahazaka and J. M. Nigretto, *Blood Coagul. Fibrinolysis* **5**, 567 (1994).
39. T. Lindhout, *Nephrol. Dial. Transplant.* **9** (suppl. 2), 83 (1994).
40. J. M. Courtney, N. M. K. Lamba, S. Sundaram and C. D. Forbes, *Biomaterials* **15**, 737 (1994).

Publikation 3

Thomas Groth, Andreas Podias, Yiannis Missirlis (1994).

Platelet adhesion and activation under static and flow conditions.

Colloids and Surfaces B: Biointerfaces **3,** 241-249.

ELSEVIER

Colloids and Surfaces B: Biointerfaces 3 (1994) 241–249

COLLOIDS AND SURFACES B

Platelet adhesion and activation under static and flow conditions ☆

Th. Groth [a,*], A. Podias [b], Y. Missirlis [b]

[a] *Biomaterials Research Unit, School of Medicine (Charité), Humboldt University, Tucholskystraße 2, 10098 Berlin, Germany*

[b] *Biomedical Engineering Laboratory, Department of Mechanical Engineering, University of Patras, 26110-Patras, Greece*

Received 24 November 1993; accepted 21 February 1994

Abstract

An investigation of platelet deposition and activation was carried out using E.C. reference materials (EUROBIOMAT program), applying static and flow test systems. The following materials were investigated: polyethylene (PE), polypropylene (PP), poly(vinyl chloride with di(ethylhexyl) phthalate as plasticizer (PVC-D) and pellethane (PEL). Platelet adhesion and activation were studied under non-flow conditions, applying a recently developed enzyme immunoassay (EIA) for the detection of the platelet proteins GP Ib and GMP 140, also known as PADGEM, after a 30 min incubation. Furthermore, how platelets adhere under laminar flow conditions was examined. These experiments were carried out with use of a capillary perfusion model in order to estimate the adhesion and activation of platelets in open and closed loop systems at a shear rate of 2000 s^{-1}. The contact times between anti-coagulated whole blood and the test materials were from about 2 min for the open loop system to 20 min for the closed loop system. As parameters, the retention of platelets and the release of β-thromboglobulin were measured. A modified EIA for GMP 140 was applied to obtain more insight into the distribution of platelets over the length of the tubes. It was shown that testing under non-flow conditions yielded comparable data to results obtained under flow conditions in the closed loop system. PE and PP exhibited low haemocompatibility compared with PVC-D and PEL, as indicated by the measurement of GP Ib and GMP 140 under static conditions. The investigation under flow conditions demonstrated generally the same sequence concerning platelet attachment and activation. However, it was shown that platelet retention and activation increased with contact time.

Keywords: Laminar flow conditions; Platelet activation; Platelet adhesion; Polymers; Static conditions

1. Introduction

The adhesion and activation of platelets during the contact of blood with foreign surfaces pose a serious problem in the application of biomaterials for implant devices and for extracorporeal circulation systems. Platelets contribute to thrombus formation by a positive feedback mechanism due to the release of attachment proteins such as fibrinogen, of platelet aggregating substances such as ADP, and thromboxane A_2, and the exposure of a procoagulant surface [1,2].

The physicochemical properties of biomaterials in contact with blood are believed to govern the following reactions, such as plasma protein adsorption and blood cell adhesion [3,4]. The composition and the conformational state of the adsorbed protein layer is considered to be of particular importance in the reaction of platelets with the

☆ Presented at the VIIth Colloquium on Biomaterials, held at the Technical University of Aachen, Germany, September 23–24, 1993.

* Corresponding author.

SSDI 0927-7765(94)01131-N

biomaterial surface [3,5]. The adsorption of attachment proteins such as fibrinogen, fibronectin, von Willebrandt factor and vitronectin seems to be a prerequisite for platelet adhesion and the following activation [6,7]. Platelet activation via the thrombin-dependent pathway leads to the rapid translocation of platelet α-granules to the cell membrane followed by membrane fusion [8]. This causes the release of several platelet constituents such as β-thromboglobulin (β-TG), platelet factor 4 and others [1,2,9]. During the same process, GMP 140, also known as P-selectin, contained in the membrane of the α-granules is translocated and accessible at the outer cell membrane [10]. Both β-TG and GMP 140 can be used as markers of platelet activation during blood/biomaterial contact [11,12].

Further aspects of blood/biomaterial interactions to be considered are the flow conditions. These concern the transport of platelets from the bulk to the surface in laminar or turbulent flow, including the haematocrit [13,14] and shear-stress-dependent activation of the platelets [15]. Furthermore, the flow conditions determine the distribution of released platelet constituents important for the activation of the platelets and the coagulation system [16]. Flow methods for haemocompatibility testing may be expensive, and labour- and time-consuming. Therefore, simple static test systems may be used for the screening of materials haemocompatibility if the results obtained under static conditions are comparable with those obtained under flow conditions.

The aim of this study was to compare the adhesion and activation of platelets on reference materials under non-flow and flow conditions. Therefore, testing of platelet adhesion and activation as indicated by the presence of the platelet membrane proteins GP Ib and GMP 140 was performed under static conditions using polymer films. These results were compared with platelet retention, release of β-TG and the distribution of activated platelets as indicated by the presence of GMP 140 under flow conditions. Flow experiments were carried out with a capillary perfusion model in an open and closed loop system applying a shear rate of 2000 s^{-1}.

2. Experimental

2.1. Biomedical polymers tested

The reference materials used were kindly provided by Dr. W. Lemm (Free University Berlin, Klinikum Charlottenburg), the coordinator of the EUROBIOMAT research program of the European Communities. Since all materials were medical grade they were used without any further cleaning procedure. The materials consisted of polymer films and tubes (i.d., 0.6 mm; length, 100 cm) composed of polyethylene (PE), polypropylene (PP), pellethane (PEL) 2363-80AE (polyetherurethane) and poly(vinyl chloride with di(ethylhexyl) phthalate as plasticizer (PVC-D).

The compositions of and manufacturing procedures for the polymers are given by Lemm [17].

2.2. Collection and handling of blood

Blood was collected from healthy donors who had not taken any medication for at least 10 days. The blood was collected in sodium citrate (3.19 g per 100 ml) at a blood/citrate ratio of 9:1.

Platelet-rich plasma (PRP) was prepared by centrifuging the blood at 200*g* for 10 min. The supernatant PRP was collected and the blood was centrifuged at 2000*g* for 20 min to prepare platelet-poor plasma (PPP). The platelet count in the PRP was adjusted to 200 000 μl^{-1} by mixing PRP and PPP.

2.3. Platelet adhesion and activation assays under static conditions

Films of each test material were placed in a Teflon measuring chamber with 24 wells, 10 mm in diameter, as described by Poot et al. [18].

The estimation of platelet adhesion and activation was performed according to Groth et al. [19] based on the method proposed by Campbell et al. [12]. PRP (150 μl) was added to four sample wells, and PPP (150 μl) to two sample wells as a control. The plate was sealed and placed in an incubation hood (IHT, Infors AG Basel, Switzerland) at 37 °C for 30 min. The samples were then washed four times with phosphate-buffered

saline (PBS) of the following composition: 150 mM NaCl, 5.8 mM Na_2HPO_4, pH 7.4. For the estimation of platelet adhesion the monoclonal antibody CD 42b anti-GP Ib (Immunotech S.A., France) was prepared at a dilution of 1:1000 in 1% bovine serum albumin (BSA) dissolved in PBS. The monoclonal antibody CD 62 anti-P-selectin (Immunotech S.A., France) was prepared at a dilution of 1:100 in 1% BSA in PBS, and was used for the platelet activation assay. Antibody solution (150 μl) was added to all sample wells and the plate was agitated at room temperature for 60 min. Thereafter the samples were washed four times with PBS. Sheep anti-mouse IgG peroxidase conjugated antibody (Sigma) was prepared at a 1:200 dilution in 1% BSA in PBS. A portion (150 μl) of the second antibody solution was added to each sample well. The plates were incubated for 60 min. The solution was then discarded and the samples were washed four times with PBS. *o*-Phenylenediamine solution (OPD; 1 mg ml^{-1}) was prepared in 0.1 M citrate buffer with hydrogen peroxide (0.03%). Chromogen (150 μl) was added to each sample well and the plates were incubated for 10 min to generate the chromophore. The reaction was halted by adding 150 μl of 2 M sulphuric acid in 0.1 M sodium sulphide. A portion (100 μl) of the solution was transferred to a microtitre plate and the optical densities (OD) were read in a microplate reader (Anthos 2001, Austria) set at a wavelength of 492 nm.

2.4. Platelet adhesion and activation studies under flow conditions

For the open loop method, a syringe pump (Precidor, Infors AG Basel, Switzerland) was used to pump the blood through the polymer tubes. The tubes were prefilled with PBS to avoid an air/blood interface during the experiment. The whole device was thermostatted at 37°C in the incubation hood. The flow rate was adjusted to obtain a wall shear rate of 2000 s^{-1}. An amount (4.5 ml) of the outflowing blood was collected into Diatube H (Diagnostica Stago, France) at a ratio 9:1. The platelet counts in the influent and effluent blood were then assessed using a Coulter Counter S Plus IV (Coulter Electronics, U.S.A.). For the quantification of platelet attachment on the polymer surface, the platelet retention index was calculated as the dimensionless quantity

$$\text{Platelet retention index} = \frac{PLT_{INFLUENT} - PLT_{EFFLUENT}}{PLT_{INFLUENT}} \quad (1)$$

where $PLT_{INFLUENT}$ is the platelet count in the blood before contact with the whole circuit (control) and $PLT_{EFFLUENT}$ is the platelet count in the fractions. The platelet retention index was selected because platelets are retained both by adhesion and aggregation of platelets on the surface.

The remaining blood was immediately cooled at 0°C and kept for β-thromboglobulin estimation. The collected blood samples were centrifuged for 30 min at 2000*g*, after which 80 μl of the PPP are removed and used for β-TG measurement using a commercial test kit supplied from Diagnostica Stago, France.

The polymer tube was then flushed with paraformaldehyde (PFA) solution (1% (vol/vol)) in PBS, applying the same shear rate to fix the adhering platelets. The tubes filled with PFA were used for measurements of the expression of P-selectin on the adhering platelets. To stop the fixation the tubes were flushed with 1% BSA and 1% glycine in PBS for 15 min. The estimation of GMP 140 was performed inside the polymer tubes, as described previously. For this purpose the antibody solutions were injected into the tubes, followed by an incubation period of 60 min. The tubes were then flushed four times with PBS. Finally, OPD solution was introduced. Fractionated collection of the OPD solution was carried out after 10 min incubation into 50 μl of stopping buffer. Thus, each fraction was assigned to a tube segment 10 cm in length.

For the closed loop method (see Fig. 1), a peristaltic pump (Watson Marlow 505 Di, Verder Deutschland GmbH, Germany) was used to pump the blood through the circuit. The circuit itself was constructed from a silicone tube, with an i.d. of 2 mm, and from fittings and three-way valves made of Teflon. This part of the circuit was first filled with human serum albumin solution (10 mg ml^{-1}) dissolved in PBS, and then stored overnight in a

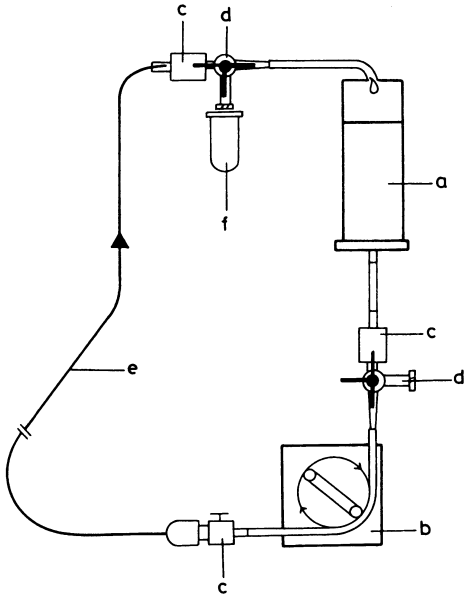

Fig. 1. Experimental equipment for the closed loop system: a, blood reservoir; b, peristaltic pump; c, fittings; d, three-way valve; e, test tube; f, blood sample.

refrigerator to minimise the interaction of blood with materials other than the test tube. Before use, the albumin solution was washed out with PBS. The circuit was connected to the test tube and the entire system filled with PBS. Blood was then introduced into the system, displacing the PBS solution. The experiments were performed under a shear rate of 2000 s^{-1}. The perfusion time was 20 min. The entire system was maintained at 37°C in a thermostatted hood.

In each experiment, 1 ml of blood was collected from the circuit into polypropylene tubes at four different times (1.3, 5, 10, and 20 min). Each blood sample was divided in two fractions for analysis: 450 μl of blood were mixed with 50 μl of Diatube H (Diagnostic Stago, France) for β-TG estimation and were kept at 37°C until the end of the experiment. The remaining blood was used for cell counting using the Coulter Counter S Plus IV. The test tubes were treated in a similar manner to that described for the open loop system, and were used for GMP 140 estimates. However, in contrast to the procedure for the open loop system, the test tubes were cut into 20 cm segments after 10 min incubation with OPD. A portion (50 μl) of OPD solution from each segment was mixed with 50 μl of stopping buffer, and the OD were measured at 492 nm.

3. Results

The results of platelet adhesion and activation under static conditions are shown in Fig. 2. It is shown that the platelet adhesion after a 30 min contact time, as measured by the OD of GP Ib, decreased in the order PP > PE ⩾ PVC-D ⩾ PEL (⩾, not significant; >, significant with $p \leqslant 0.05$ t-test). The activation of platelets as indicated by the OD of GMP 140 confirmed this trend. Fig. 2 shows that the OD decreased significantly in the order PP > PE > PVC-D > PEL ($p \leqslant 0.05$).

The results of platelet adhesion and activation under flow conditions for the open loop system are shown in Figs. 3–5. Fig. 3 shows that the platelet retention was not significantly different for PE, PP and PVC-D. PEL caused a significantly lower retention of platelets in comparison to all

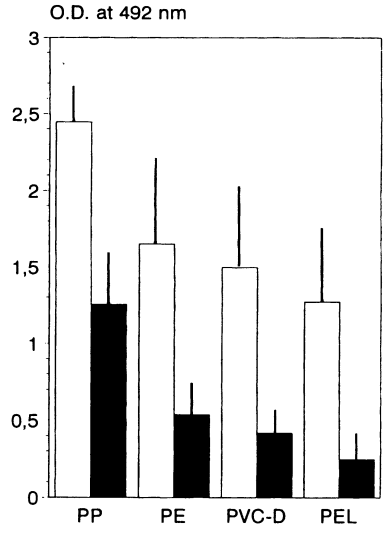

Fig. 2. Platelet adhesion and activation under non-flow conditions indicated by the OD (mean ± standard deviation (SD); $n = 20$), related to the presence of GP Ib (□) and GMP 140 (■) after 30 min contact of PRP with PP, PE, PVC-D and PEL.

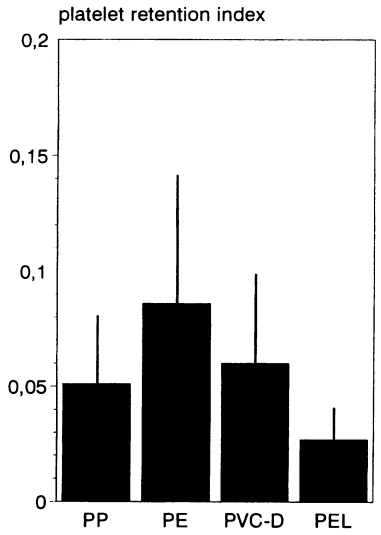

Fig. 3. Platelet retention index (mean ± SD; $n=6$) after 2 min perfusion with anti-coagulated whole blood with PP, PE, PVC-D and PEL at a shear rate of 2000 s^{-1}. Open loop system; tube i.d., 0.6 mm.

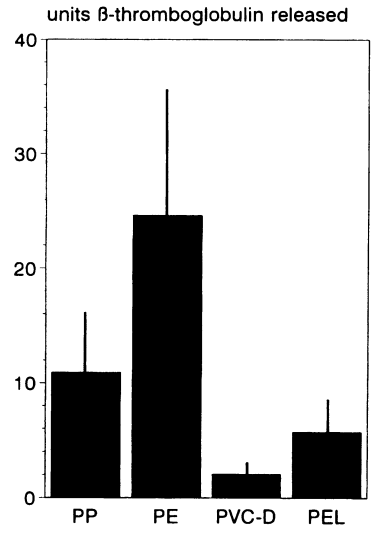

Fig. 4. Release of β-thromboglobulin (mean ± SD; $n=6$) after 2 min perfusion with anti-coagulated whole blood with PP, PE, PVC-D and PEL at a shear rate of 2000 s^{-1}. Open loop system; tube i.d., 0.6 mm.

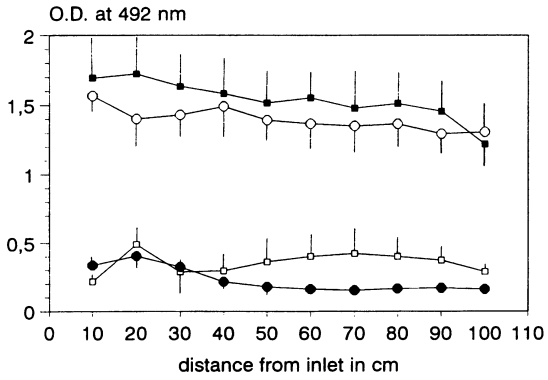

Fig. 5. Distribution of activated platelets over the length of the tube as indicated by the OD, related to the presence of GMP 140 (mean ± standard error of the mean (SEM); $n=6$), with the open loop system and with 2 min perfusion with anti-coagulated whole blood at a shear rate of 2000 s^{-1}. ○, PP; ■, PE, ●, PVC-D; □, PEL.

other materials ($p \leqslant 0.05$). Fig. 4 shows that the release of β-TG decreased significantly in the order PE > PP > PEL > PVC-D ($p \leqslant 0.05$). The measurement of the expression of GMP 140 shows that PE and PP exhibited a comparable distribution and level of platelet activation over the length of the tube, as seen in Fig. 5. It is shown for both materials that the density of platelets decreased from the entrance to the exit, as indicated by the lowering of the OD. On the other hand, PEL and PVC-D exhibited significantly lower platelet activation ($p \leqslant 0.05$). The OD for PVC-D again decreased slightly from the entrance to the exit. However, PEL showed a different behaviour, with first a decreasing and then an increasing OD. The range of the materials was the same as observed for the β-TG release.

Figs. 6–8 show the results of platelet adhesion and activation for the closed loop system. The retention of platelets, shown in Fig. 6, decreased in the order PP ⩾ PE > PVC-D > PEL (⩾, not significant; >, significant with $p \leqslant 0.05$). However, PE showed first decreasing and then increasing retention whereas PP, exhibited increasing platelet retention with time. PVC-D and PEL showed decreasing or stable retention of platelets at a lower level. If the measurements were extended to 60 min the platelet retention of both materials

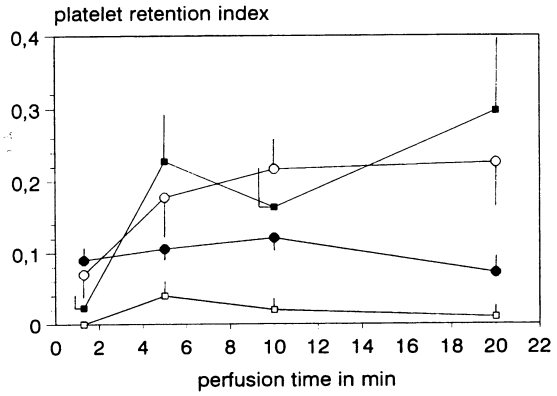

Fig. 6. Platelet retention index (mean ± SEM; $n=3$) at various perfusion times with anti-coagulated whole blood at a shear rate of 2000 s^{-1} in the closed loop system. ○, PP; ■, PE; ●, PVC-D; □, PEL.

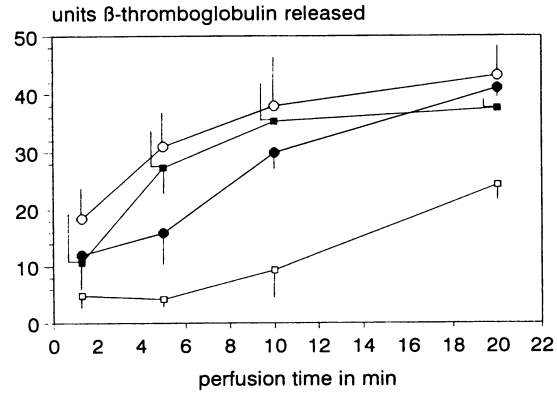

Fig. 7. Release of β-thromboglobulin (mean ± SEM; $n=3$) at various perfusion times with anti-coagulated whole blood at a shear rate of 2000 s^{-1} in the closed loop system. ○, PP, ■, PE; ●, PVC-D; □, PEL.

equaled zero, whereas PE continued with oscillating retention values and PP still accumulated platelets (data not shown). The release of β-TG shown in Fig. 7 increased with time for all materials. PE and PP released the highest amounts of β-TG and could not be differentiated. PVC-D exhibited intermediate retention values with a significant lower release of β-TG in comparison to PE and PP at 5 and 10 min ($p \leqslant 0.05$). PEL caused the lowest release of β-TG at all times measured, with significantly lower values ($p \leqslant 0.05$). The

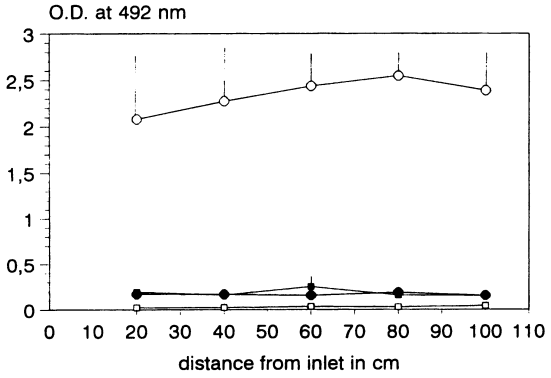

Fig. 8. Distribution of activated platelets over the length of the tube as indicated by the OD related to the presence of GMP 140 (mean ± SEM; $n=3$), with 60 min perfusion with anti-coagulated whole blood at a shear rate of 2000 s^{-1} in the closed loop system. ○, PP; ■, PE; ●, PVC-D; □, PEL.

measurement of the translocation of GMP 140 is shown in Fig. 8. PP exhibits the highest OD. PE and PVC-D showed intermediate values which were significantly lower than for PP ($p \leqslant 0.05$). The lowest OD was observed for PEL.

4. Discussion and conclusions

It was shown in this investigation that PP and PE exhibited lower haemocompatibility than PVC-D and PEL, as shown by platelet adhesion and activation. This result is in agreement with other studies using the same reference materials [20,21]. From the results of this study, the adhesion and activation of platelets as measured under non-flow conditions seem to be qualitatively comparable to the results obtained under flow conditions with the closed loop method.

The measurement of platelet adhesion and activation under non-flow conditions using monoclonal antibodies versus GP Ib and GMP 140 can be considered as particularly suited to the screening of biomaterials. In contrast to the flow experiments, PRP instead of whole blood was used to increase the reproducibility of the experimental system by adjusting the constant platelet count. Moreover, in static test systems, red blood cells may have a minor influence on the final result, because platelets

are transported to the surface by diffusion/sedimentation and not by diffusion/convection as in flow systems. The results obtained under static conditions coincided well with the results from the closed loop investigations. GP Ib, the receptor for von Willebrandt factor [22], was selected to assess solely platelet adhesion because this protein is present on resting and activated platelets. Moreover, the use of GP Ib and GMP 140 as markers of platelet adhesion and activation, respectively, might be suitable for characterising the relationship between platelet adhesion and activation. Since the degree of activation of adhering platelets on a surface may be different, a small ratio of GP Ib to GMP 140 may indicate high thrombogenicity of a surface, as is the case for PP, and vice versa, a high ratio would indicate a rather haemocompatible surface (e.g. PEL). The results obtained with the closed loop technique seem to support this assumption. However, it is planned to confirm this hypothesis in further studies using scanning electron microscopy for morphological evidence.

A capillary perfusion model was established as an open and closed loop system in order to obtain data of platelet adhesion and activation under flow conditions. The short-term testing of biomaterials in the range of a few minutes is considered to predict poorly the long-term in vivo applicability of biomaterials [23]. Although open loop systems are usually short-term interacting test methods, they are frequently used [18,20,21,24]. The results of this study indicate some differences in the evaluation of blood compatibility with respect to the results from the open and the closed loop systems. If the retention of platelets was compared after about 2 min of perfusion, then PE, PP, and PVC-D were not differentiated. Only PEL exhibited significantly lower platelet retention with both the open and the closed loop systems. In contrast to this finding, PVC-D demonstrated rather low retention compared with PE and PP after a longer blood–material contact. This underlines the necessity of longer contact times for haemocompatibility testing. The magnitude of β-TG release was comparable for both methods at time 2 min. However, the pattern of β-TG release was different. An influence of the flow regime could not be ruled out. In contrast to the situation in the open loop system, a peristaltic flow profile is established in the test section of the closed loop system. The calculated shear rate of 2000 s^{-1} is a mean value with respect to the steady-state flow. For such systems, a characteristic Reynolds number termed the Womersley number a is introduced [25]. If a^2 is less than 0.66, inertial effects are predicted to be small compared with the viscous effects, and Poiseuille's law should be valid. The calculated Womersley number for the closed loop system used in this study is $a^2 = 0.044$ [26]. Therefore a pseudo-steady Poiseuille flow profile is established in the case of the closed loop system.

Finally, a new technique was developed to investigate the distribution of activated platelets over the length of the tube by applying the enzyme immunoassay (EIA) for GMP 140 inside the tubes. It was shown for the open loop system that again PE and PP can be considered as highly activating surfaces in comparison to PVC-D and PEL. Furthermore, PE, PP and PVC-D demonstrated a slight decrease in OD from the entrance of the tube downstream, indicating a slight decrease in the number of adhered activated platelets along the tube. In general, platelet deposition decreases rather significantly along the tube [27], especially with activating surfaces [28]. However, this trend is opposed by the reaction (binding)-limited step of the overall reaction and transport process, because of the high shear rate of 2000 s^{-1} [29] which by itself would result in a position-independent adhesion/activation of the platelets. Therefore the two opposing actions result in the observed slight decrease of the OD along the tube. If the mean values of the OD are compared with the release of β-TG the same range of materials is observed. This is not surprising, because both markers of platelet activation stem from the same storage pool, the platelet α-granule, underlining the value of the developed method. If these results of the GMP 140 expression are compared with the OD values obtained after 60 min of perfusion in the closed loop system, striking differences are observed. All materials exhibited a rather constant OD over the length of the tube, indicating that surface saturation with platelets was reached. However, only PP demonstrated a further increase

of the OD, in contrast to the other materials, with respect to the results obtained for the open loop method. There are at least two possible reasons for the decrease of the OD after prolonged perfusion. The expression of GMP 140 is known to be transient and decreases to the background level within 1 h [30]. On the other hand, aggregate formation of platelets on the surface might deteriorate the labelling of the GMP 140, thus masking the present antigens for the antibodies. Such an effect was discussed in connection with the labelling of the GP IIb/IIIa complex [31]. As a result, it seems that the high level of GMP 140 expression as observed for PP indicates a continuous deposition of platelets on this surface, whereas all other materials reached a state of surface saturation at shorter perfusion times. This assumption is supported by the results of retention measurements for perfusion times up to 60 min.

In conclusion, the screening of biomaterials may be performed using static adhesion tests. The developed technique using different surface antigens of platelets might give more insight into the ratio between adhering resting and activated platelets. The open loop technique, as a short-term method, has limitations concerning the interpretation of the results for long-term applications because of the observed differences from the static and closed loop system with contact times up to 30 min. The developed method for the evaluation of platelet distribution over the length of the tube can give more insight into the process of platelet binding and activation for a given material. An advantage of such a technique is that no prior labelling of platelets nor the use of radioactive isotopes are necessary. The closed loop technique finally supplies information on the haemocompatibility of biomaterials in the longer term. However, prolongation of perfusion to over 20 min led to haemolysis, which interferes with the surface reactions. Thus, perfusion experiments longer than 20 min seem not to be reasonable.

Acknowledgements

This work was in part supported by the Bundesministerium für Forschung und Technologie, Germany, and the Hellenic General Secretariat of Science and Technology in the framework of bilateral cooperation between Greece and Germany. The work of Mr. Kuhn in constructing the measuring chamber for the enzyme immunoassay is gratefully acknowledged. We thank Mrs. R. Hesse for her excellent technical assistance.

References

[1] B.S. Coller, Ann. N.Y. Acad. Sci., 516 (1987) 362.
[2] P.A. Gentry, J. Comp. Pathol., 107 (1992) 243.
[3] J.D. Andrade and V. Hlady, Prog. Surf. Sci., 79 (1986) 1.
[4] B.D. Ratner, A. Chilkoti and D.G. Castner, Clin. Mater., 11 (1992) 25.
[5] J.J. Sixma, G. Hindriks, H. Van Breugel, R. Hantgan and P.G. de Groot, J. Biomater. Sci. Polym. Ed., 3 (1991) 17.
[6] E.W. Salzman, J. Lindon, G. McManama and J.A. Ware, Ann. N.Y. Acad. Sci., 516 (1987) 184.
[7] R.O. Hynes, Thromb. Haemostasis, 66(1), (1991) 40.
[8] R.P. McEver and M.N. Martin, J. Biol. Chem., 259 (1984) 9799.
[9] K.L. Kaplan, M.J. Broekman, A. Chernoff, G.R. Lesnik and M. Drillings, Blood, 53 (1979) 604.
[10] S.C. Hsu-lin, C.L. Berman, B.C. Furle, D. August and B. Furie, J. Biol. Chem., 259 (1984) 9121.
[11] M.-C. Rissoan, R. Eloy and J. Baguet, in S. Dawids (Ed.), Test Procedures for the Blood Compatibility of Biomaterials, Kluwer Academic Publishers, Dordrecht, 1993.
[12] E.J. Campbell, R.R.C. New and S.A. Charles, in L.G. Cima and E.S. Ron (Eds.), MRS Symp. Proc., Tissue-Inducing Biomaterials, Vol. 252, Material Research Society, Pittsburgh, 1992, p. 229.
[13] V.T. Turitto, Prog. Hemostasis Thromb., 6 (1982) 139.
[14] V.T. Turitto and H.J. Weiss, Ann. N.Y. Acad. Sci., 416 (1983) 363.
[15] L.J. Wurzinger, P. Blasberg and G.W. Schmid-Schönbein, Biorheology, 22 (1985) 437.
[16] J.A. Hubbell and L.V. McIntire, Biomaterials, 7 (1986) 354.
[17] W. Lemm, The Reference Materials of the European Communities, Kluwer, Dordrecht, 1992.
[18] A.A. Poot and T. Beugeling, in Y. Missirlis and W. Lemm (Eds.), Modern Aspects of Protein Adsorption on Biomaterials, Kluwer, Dordrecht, 1991, p. 29.
[19] Th. Groth, A. Gronert, S. Ziemer and R. Hesse, in W. Lemm (Ed.), The Reference Materials of the European Communities, Kluwer, Dordrecht, 1992, p. 183.
[20] Y. Missirlis and G. Mihanetzis, in W. Lemm (Ed.), The Reference Materials of the European Communities, Kluwer, Dordrecht, 1992, p. 157.
[21] J.N. Mulvihill and J.P. Cazenave, in W. Lemm (Ed.), The

Reference Materials of the European Communities, Kluwer, Dordrecht, 1992, p. 165.
[22] N.O. Solum, Semin. Hematol., 4 (1985) 289.
[23] P. Didisheim, M.K. Dewanjee, M.P. Kaye, C.S. Frisk, D.N. Fass, M.V. Tirrell and P.E. Zollman, Trans. Am. Soc. Artif. Intern. Organs, 30 (1984) 370.
[24] Th. Groth, Ch. Vassilieff, H. Wolf, G. Richter and F. Förster, J. Biomater. Sci. Polym. Ed., 3 (1992) 285.
[25] E.N. Lightfoot, Jr., Transport Phenomena and Living Systems, John Wiley, New York, 1974, p. 113.
[26] A. Podias, Th. Groth and Y. Missirlis, J. Biomater. Sci. Polym. Ed., 6 (1994) 399.
[27] A.A. Poot, Ph.D. Thesis, Twente University, Enschede, The Netherlands, 1989.
[28] I.A. Feuerstein and B.D. Ratner, Biomaterials, 11 (1990) 127.
[29] E.F. Leonhardt, E.F. Grabowski and V.T. Turitto, Ann. N.Y. Acad. Sci., 201 (1972) 392.
[30] N. Kieffer, in Y. Missirlis and J.L. Wautier (Eds.), The Role of Platelets in Blood/Biomaterial Interactions, Kluwer, Dordrecht, 1993, p. 15.
[31] J.N. Mulhivill, H.G. Huisman, J.-P. Cazenave, J.A. van Mourik and W.G. van Aken, Thromb. Haemostasis, 58 (1987) 724.

Publikation 4

Georgi Altankov, Frederic Grinnell, Thomas Groth (1996).

Studies on the biocompatibility of materials: Fibroblast reorganization of substratum-bound fibronectin on surfaces varying in wettability.

Journal of Biomedical Materials Research **30**, 385-391.

Studies on the biocompatibility of materials: Fibroblast reorganization of substratum-bound fibronectin on surfaces varying in wettability

Georgi Altankov,[1,*] Frederick Grinnell,[2] and Thomas Groth[3]
[1]*Institute of Biophysics, Bulgarian Academy of Sciences, Acad. G. Bonchev Str. bl. 21, 1113 Sofia, Bulgaria;*
[2]*Department of Cell Biology and Neurosciences, UT Southwestern Medical Center, Dallas, Texas 75235;* [3]*GKSS Research Center Geesthacht, Institute of Chemistry, Department of Membrane Research, Kantstrasse 55, 14513 Teltow, Germany*

The ability of human fibroblasts to remove and reorganize fibronectin (FN) bound on material surfaces was studied as a novel feature of material surface biocompatibility. Other traditional parameters of biocompatibility analyzed included cell spreading, clustering of fibronectin receptors into focal adhesions, development of stress fibers, and cell growth. Five different materials with surface wettability ranging from hydrophilic (underwater contact angle 25°) to hydrophobic (underwater contact angle 111°) were used, i.e., clean glass (GLASS), aminopropylsilane (APS), octadecylsilane (ODS), polylactate (PL), and silicone (SI). When cells were cultured on these materials in serum-containing medium, formation of FN receptor-rich focal adhesions and actin stress fibers were more evident on the hydrophilic surfaces (GLASS and APS) compared to the hydrophobic ones (PL, ODS, and SI). Cell growth showed a similar pattern, that is, increased cell proliferation with increasing material surface wettability. Preadsorption of FN on the material surfaces increased subsequent cell spreading and cytoskeletal reorganization on hydrophobic surfaces except SI. Removal and reorganization of FN from the material surfaces into extracellular matrixlike structures occurred on GLASS but not on less wettable surfaces, suggesting that this removal/reorganization process may be more sensitive to changes in surface wettability than other parameters of biocompatibility.

INTRODUCTION

Initial interaction of foreign materials with the living tissues begins with adsorption of proteins onto their surfaces.[1–3] Therefore the surface properties of the materials such as wettability, surface charge, surface structure, and others might be critical for biocompatibility and have to be considered in the selection of materials suitable for surgical implantation. Some time ago, we reported that mammalian fibroblasts interact better with wettable surfaces in comparison to nonwettable (hydrophobic) ones.[4,5] The basis for this difference is still poorly understood, but may be explained in part by variations in the amount or conformation of adhesion proteins, such as fibronectin (FN) and vitronectin, when they are adsorbed on hydrophilic compared to hydrophobic surfaces.[6–16]

*To whom correspondence should be addressed. E-mail: biophys@bgearn.bitnet

Recently much has been learned about the cell receptors that mediate cell adhesion to proteins like FN. These receptors belong to the integrin superfamily and have been identified on many types of cells.[17,18] Integrins form a critical linkage between extracellular matrix (ECM) proteins and the internal structural elements of the cell.[17–22] Relatively little is known, however, about how surface chemistry influences integrin–FN interactions.

One of the less well-studied consequences of integrin binding to material surface-adsorbed FN is removal of the FN followed by reorganization of this adhesion protein into extracellular matrix fibrils.[23–25] The goal of the present study was to learn how removal and reorganization of material surface-adsorbed FN varied with surface wettability. In a preliminary study, we found that unlike glass, fibroblasts were unable to reorganize FN adsorbed on a 2% silane-coated surface (underwater contact angle 95.1°).[24] In this study we investigated a series of graded surfaces with water contact angles ranging

Journal of Biomedical Materials Research, Vol. 30, 385–391 (1996)

CCC 0021-9304/96/030385-07

from 25° to 111°. On the more hydrophobic surfaces we observed markedly decreased ability of cells to remove and reorganize material surface-adsorbed FN. Details are reported herein.

MATERIALS AND METHODS

Cells

Human foreskin fibroblasts were obtained from fresh biopsies and used up to the ninth passage. The cells were grown in Dulbecco's minimal essential medium (DMEM) containing 10% fetal bovine serum (FBS) (Sigma Chemicals Co., St. Louis, MO) in a humidified incubator with 5% CO_2. Fibroblasts from preconfluent cultures were harvested with 0.05% trypsin/0.6 m*M* EDTA (Sigma), and trypsin was neutralized with FBS.

FN and fluorescent FN preparation

Human plasma FN was prepared by affinity chromatography on gelatin-Sepharose 4B according to Engvall and Ruoslahti[27] and further purified on heparin-Sepharose 4B. FN was eluted with 0.5*M* NaCl in 50 m*M* Tris pH 7.3 and lyophilized. FN was conjugated to FITC (Sigma) as described previously.[22,23] Fluorescent FN (FFN) retained complete biological activity based on a cell spreading assay (data not shown).

Preparation of surfaces with different wettabilities

Glass coverslips (18 × 18 mm, Menzel, Germany) were cleaned with cold chromium sulfuric acid. The clean glass slides (GLASS) were stored in double distilled water until use to keep the surface hydrophilic. To obtain surfaces with gradually increasing hydrophobicity, clean dry glass slides were coated with the following materials: aminopropyltriethoxysilane (APS), octadecyldimethylchlorosilane (ODS), poly-(D,L)lactide (PL), and silicone (SI). GLASS, APS, and ODS surfaces are composed of monomolecular layers, whereas PL and SI form complex polymeric films.

For coating with APS, the slides were put in 95% ethanol containing 5% APS (Fluka, Germany) and sonicated for 5 min, then baked at 120°C for 25 min and washed with ethanol. For coating with ODS the slides were incubated in a 2% (vol/vol) solution of ODS (Sigma) in chloroform for 24 h, then rinsed with chloroform, and finally washed with distilled water. PL-coated slides were prepared by evaporation of 200 mL of 1% solution of PL R 203 (Boehringer Ingelheim, Germany) in chloroform dispersed on the surface by centrifugation at 2000 rpm. Siliconized slides were prepared by incubation for 2 h in a 5% aqueous emulsion of silicone oil (Serva Biochemistry, Germany), washing with distilled water, and then baking the slides for 4 h at 200°C. Remaining unbound silicone oil was removed by rinsing the slides in acetone. Static contact angles were measured by the sessile drop method on three different slides for each material.

Cell attachment and morphology

Approximately 5×10^5 cells in 3 mL of medium containing 10% FBS were incubated for 2 h on 6-well tissue culture plates (Falcon, Becton Dickinson & Company, New Jersey) containing the slides. For experiments with FN-coated material surfaces, slides were preincubated with 20 μg/mL FN or 40 μg/mL FFN in PBS for 30 min at 37°C as previously described.[22,23] Although 20 μg/μL FN is sufficient for complete material surface coverage,[6,7] a slightly higher concentration of FFN is useful for increasing the intensity of the fluorescence signal.[24] At the end of the incubations the samples were fixed with 3% paraformaldehyde in PBS and viewed and photographed under phase contrast on a Zeiss Universal Microscope (Carl Zeiss Jena, Germany).

Measurement of cell growth

Cells (1×10^5) in 3 mL of medium containing 10% FBS were cultured in a humidified CO_2 incubator for 3 days in 6-well tissue culture plates (Falcon) containing the slides. A MTT Cell Proliferation Kit I (Boehringer Mannheim Biochemica, Germany) was used to measure cell proliferation according to the manufacturer's instructions. The data presented are given as proliferative index, i.e., the cell count at 72 h divided by the initial cell count.

Distribution of FN receptor, FFN, and actin

Attached cells to be processed for fluorescence microscopy were permeabilized with 0.2% Triton X-100 for 5 min. To detect actin, samples were incubated for 30 min at 37°C with 5 U/mL FITC-conjugated phalloidin (Sigma). To detect FN receptors, cells were incu-

bated for 30 min at 37°C with rabbit anti-FN receptor (mostly against the β1 integrin subunit; a gift from Dr. Kenneth Yamada, National Institutes of Health, Bethesda, MD) diluted in PBS (with Ca^{2+} and Mg^{2+}) containing 1% BSA, and then for 30 min at 37°C with rhodamine-conjugated goat anti-rabbit IgG (Dianova, Germany) containing 10% normal goat serum. At the end of the incubations, samples were washed, mounted with Mowiol, and observed and photographed with a Jenamed Fluorescence Microscope (Carl Zeiss Jena). In some experiments FFN reorganization by fibroblasts was observed by both phase contrast and fluorescence microscopy (directly on the plates) using a Zeiss Universal Inverted Microscope (Carl Zeiss Jena). Photographs were made on fixed preparations.

RESULTS

Wettability of different material surfaces

Underwater contact angles for the material surfaces studied are shown in Table I. We chose these five material surfaces because of their gradually increased surface hydrophobicity (from 25.1° to 110.5°). Based on trypan blue exclusion, none of the surfaces showed cytotoxic activity during the experiments (data not shown).

Morphology of fibroblasts attached to different material surfaces

Figure 1 shows the results when human fibroblasts were incubated on the various surfaces for 2 h in medium containing 10% FBS. The morphological features of the cells indicated a clear dependence between initial cell spreading and material surface wettability. Many of the cells attached on GLASS and APS were spread (a, d) and contained prominent linear arrays of actin bundles (i.e., stress fibers) (b, e).

TABLE I
Wettability of Different Material Surfaces

Material	Contact Angle
GLASS	25.1 ± 2.7
APS	57.0 ± 3.9
PL	70.0 ± 2.3
ODS	91.5 ± 1.7
SI	110.5 ± 3.8

Static contact angles were measured by the sessile drop method on three different slides for each material. Data shown are mean ± SD.

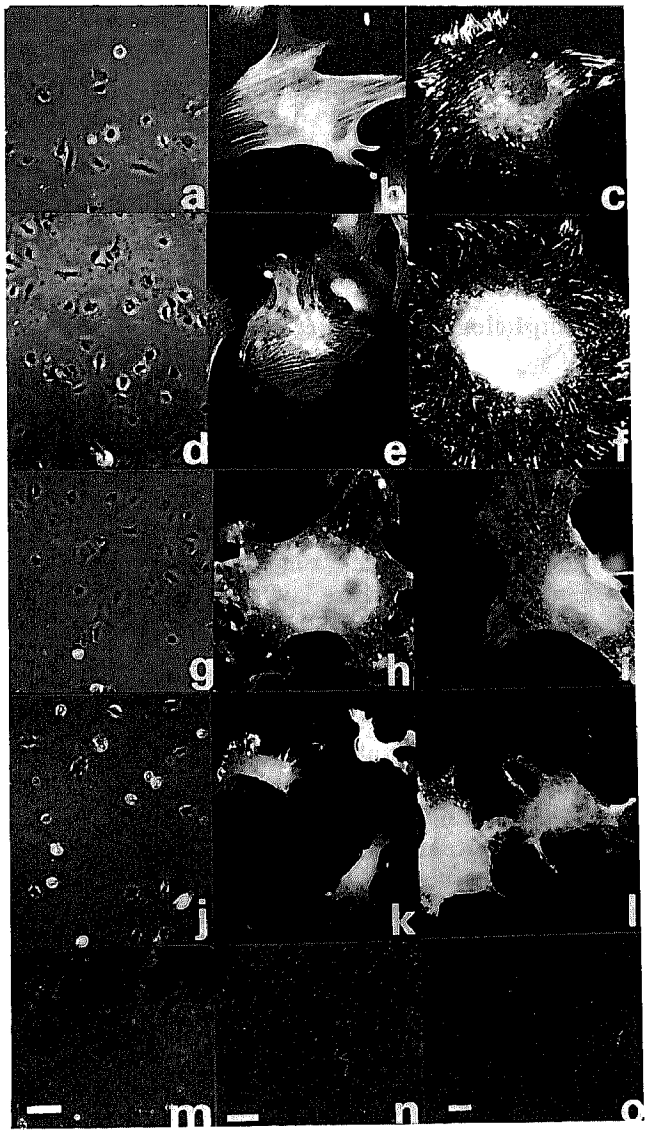

Figure 1. Morphology of fibroblasts attached to different material surfaces. Human fibroblasts in medium containing 10% FBS were attached for 2 h on the following surfaces: (a–c) GLASS, (d–f) APS, (g, k, l) PL, (j, k, l) ODS, and (m, n, o) SI. Samples were examined by (a, d, g, j, m) phase contrast microscopy or fluorescence microscopy to detect (b, e, h, k, n) actin or (c, f, i, l, o) fibronectin receptors. Bar = 100 μm: (a, d, j, i, m); bar = 50 μm: (b, e, h, k, n); bar = 10 μm: (c, f, i, l, o).

We also observed numerous FN receptor-rich streaks of focal adhesions along the cell margins (c, f). On more hydrophobic PL, the cells were spread (g) but stress fibers and focal adhesion were less evident (h, i). On ODS, there was diminished cell attachment and spreading (j) and an absence of stress fibers or focal adhesions (k, l). Finally, few attached cells were observed on SI (m).

To quantify cytoskeletal reorganization on the different substrata we counted the percentage of cells possessing longitudinal stress fibers (complete

spreading), versus cells with circumferentially organized or only aggregated actin (incomplete spreading). The results are shown on Table II. Approximately 60% of the cells on GLASS and APS (left column) showed complete cytoskeletal reorganization compared to only about 10% of the cells on PL or ODS.

Cell morphology on material surfaces precoated with FN

Figure 2 shows the morphology of cells attached to material surfaces coated with FN (20 μg/mL) before the surfaces were incubated with cells in 10% FBS-containing medium. Cell spreading was increased on all of the material surfaces (a, d, g, j, m) compared to the results shown in Figure 1. On GLASS, APS, and PL, the cells developed a pronounced elongated shape (a, d, g). Stress fibers and focal adhesion streaks were evident for cells on PL (h, i) and ODS (k, l). For cells spread on SI, these structures were not as apparent (n, o). As shown in Table II (right column), approximately 90% of the cells adhering on FN-coated GLASS, APS, PL, or ODS had a completely reorganized cytoskeleton compared to ~60% of the cells on SI. It also should be noted that the cells attached to SI (although flattened) tended to detach from the substratum.

Reorganization of FN precoated on different material surfaces

Fibroblasts not only attach to FN adsorbed on material surfaces, but the cells also can remove FN from the material surface and reorganize the adhesion protein into fibrillar ECM-like structures.[23–25] This phenomenon was tested with different material surfaces by precoating the surfaces with FITC-conjugated FN,

TABLE II
Percentage of Fibroblasts Attached to Different Material Surfaces That Developed Stress Fibers

Material	Fibronectin Precoating	
	No	Yes
GLASS	59.6 ± 13.6	91.9 ± 5.8
APS	56.5 ± 17.4	95.3 ± 3.6
PL	9.7 ± 10.0	90.5 ± 5.3
ODS	10.2 ± 7.3	93.3 ± 4.8
SI	No cells found	63.9 ± 14

Quantification of results from Figures 1 and 2. Data shown are mean ± SD for 10 separate fields.

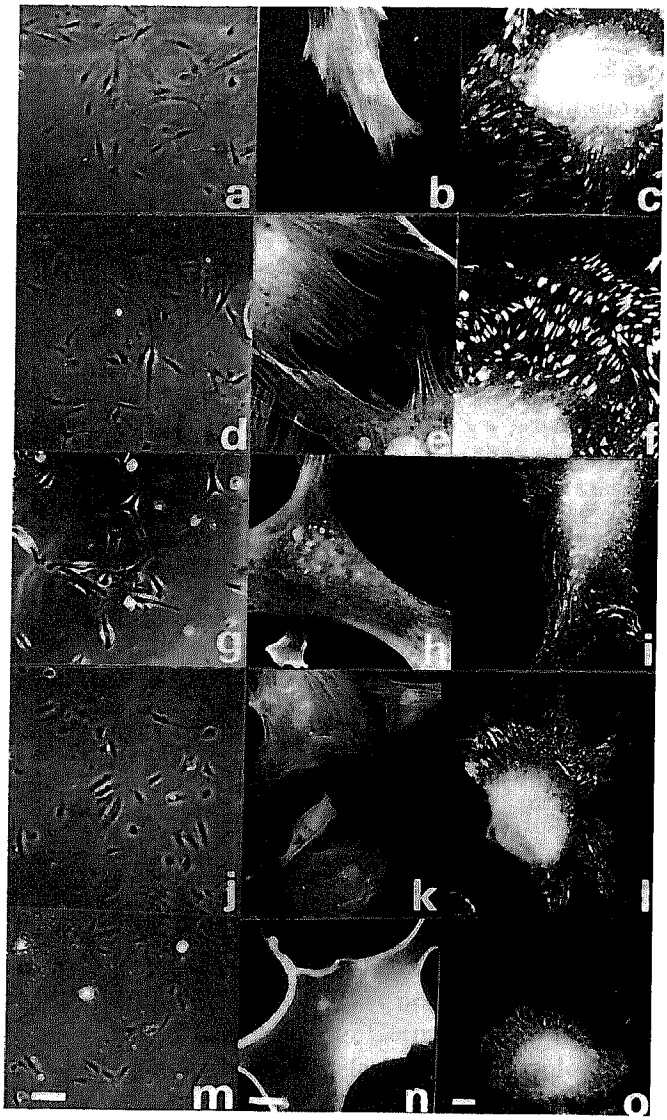

Figure 2. Morphology of fibroblasts adhered to different material surfaces precoated with FN. Same as Figure 1 except that the surfaces were coated with 20 μg/mL FN for 30 min at 37°C.

and then culturing the surfaces with fibroblasts for 4 h in 10% FBS-containing medium. As shown in Figure 3(a), the cells removed significant amounts of FFN from the hydrophilic GLASS surface, which resulted in dark patches and streaks in an otherwise bright fluorescent background. Moreover, the removed FFN accumulated in fibrillar structures that were along the margins and above the attached cells. In the fluorescent images shown in Figure 3, the cells are difficult to see directly; but when fluorescence and phase contrast images were compared, it appeared that more than 90% of the cells on GLASS were associated with the reorganized FFN (data not shown).

In marked contrast to the results with FFN-coated

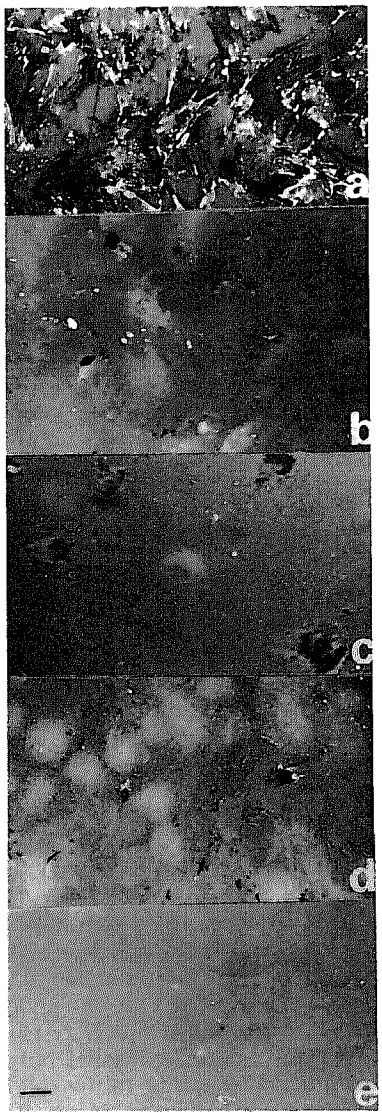

Figure 3. Removal and reorganization of FFN from different material surfaces. FITC-conjugated FN was adsorbed to (a) GLASS, (b) APS, (c) PL, (d) ODS, and (e) SI. The surfaces were incubated for 4 h with human fibroblasts in medium containing 10% FBS. At the end of incubation the cells were fixed, mounted, and processed for fluorescence microscopy.

GLASS, little FFN removal and reorganization occurred when fibroblasts were cultured on more hydrophobic surfaces, despite the fact that the cells attached and underwent cytoskeletal reorganization on these surfaces (Fig. 2, Table II, right). As shown in Figure 3, small dark patches in the background were visible for APS, PL, and ODS surfaces (b, c, d) indicating some removal of FFN, but no fibrillar structures developed such as seen for GLASS (a). On SI (e) the background was uniformly bright indicating that the cells were essentially unable to remove FFN.

Cell growth on different surfaces

As one additional measure of biocompatibility, fibroblasts were cultured for 3 days on the different surfaces. Figure 4 shows that cell growth decreased with decreasing wettability of the materials, and there was little proliferation on SI.

DISCUSSION

A variety of factors affect protein adsorption on material surfaces and material surface biocompatibility. Previously, surface wettability has been implicated as an important feature that regulates biocompatibility.[4–16] We measured several parameters of human fibroblast interactions on a series of surfaces with underwater contact angles ranging from 25° to 111°. As discussed below, our results suggest that the ability of cells to remove and reorganize FN adsorbed to the material surface is more sensitive to surface wettability than other parameters such as cell spreading and cell growth.

Spreading of fibroblasts is one indicator of stable adhesion and is usually accompanied by clustering of integrin receptors and reorganization of the cytoskeleton.[17–20,28–30] Previously, we used the formation of actin stress fibers as an indicator of cell polarization.[28] In serum-containing medium without FN precoating of the material surfaces, increasing the hydrophobicity of the material surface (underwater contact angle above 50°–60°) resulted in decreased formation of actin stress fibers and focal adhesions, which indicated

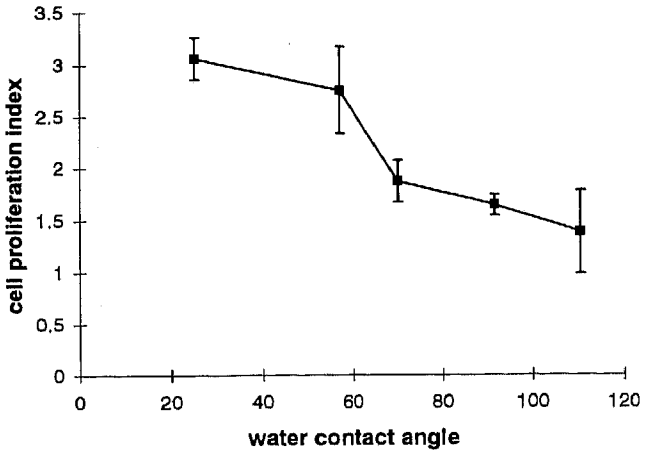

Figure 4. Cell proliferation on different material surfaces. Human fibroblasts were cultured for 3 days on surfaces varying in wettability as indicated after which cell proliferation was measured using the MTT assay. Data shown are averages ± SD from triplicate experiments. Proliferation index corresponded to the ratio between 12 and 72 h time points.

impaired interaction of fibroblasts with the surfaces. Precoating surfaces with FN tended to restore cell spreading regardless of surface wettability, although not completely. Even with FN precoating, however, there was decreased stress fiber and focal adhesion formation by cells attached to SI.

As a novel parameter of material surface biocompatibility, we investigated the removal and reorganization of FN precoated on the material surfaces. In a preliminary study, we found that fibroblasts were unable to remove FFN from a silane surface (underwater contact angle 95.1°). Our current findings confirm and extend the previous results. Fibroblasts efficiently removed FFN from GLASS but not from APS, PL, ODS, or SI, although the cells were able to attach and spread on all of these surfaces. Therefore, removal of FN from the material surface appeared to be more sensitive to surface wettability than the other parameters measured. As FN removal depends on the exchange of plasma proteins on the substratum,[24] it seems reasonable that stronger FN adsorption of hydrophobic surfaces[6,7] might be responsible for decreased FN reorganization by the cells. Therefore, our results suggest that there may be a critical value in the strength of FN adsorption determined by surface wettability, which will influence the ability of cells to remove material surface-adsorbed FN. This possibility should be investigated further in the future.

This research was supported by a Bulgarian National Science Fund Grant L 404/94 (to G.A.), Deutsche Forschungsgemenschaft Grant Gr 1290/4-1 (to T.G. and G.A.), and NIH Grant GM31321 (to F.G.).

References

1. F. Grinnell, "Cellular adhesiveness and extracellular substrata," *Int. Rev. Cytol.*, **53**, 65–144 (1978).
2. G. K. Imamoto, L. C. Winterton, R. S. Stoker, R. A. Van Wagenen, J. D. Andrade, and D. F. Moser, "Fibronectin adsorption detected by interfacial fluorescence," *J. Colloid Interface Sci.*, **106**, 459–464 (1985).
3. L. Vroman and A. L. Adams, "Adsorption of proteins out of plasma and solutions is narrow spaces," *J. Colloid Interface Sci.*, **111**, 391–402 (1986).
4. F. Grinnell, M. Milam, and P. Srere, "Studies on cell adhesion. II. Adhesion of cells to surfaces of diverse chemical composition and inhibition of adhesion by sulfhydryl binding reagents," *Arch. Biochem. Biophys.*, **153**, 193–198 (1972).
5. F. Grinnell, M. Milam, and P. Srere, "Attachment of normal and transformed hamster kidney cells to substrata varying in chemical composition," *Biochem. Med.*, **7**, 87–90 (1973).
6. F. Grinnell and M. Feld, "Adsorption properties of fibronectin in relationship to biological activity," *J. Biomed. Mater. Res.*, **15**, 363–381 (1981).
7. F. Grinnell and M. Feld, "Fibronectin adsorption on hydrophilic and hydrophobic surfaces detected by antibody binding and analyzed during cell adhesion in serum-containing medium," *J. Biol. Chem.*, **257**, 4888–4893 (1982).
8. U. Jonsson, B. Ivarsson, I. Lundstrom, and L. Berghem, "Adsorption behavior of fibronectin on well characterized silica surfaces," *J. Colloid Interface Sci.*, **90**, 148–163 (1982).
9. P. B. van Wachem, T. Beugeling, J. Feijen, A. Bantjes, J. P. Detmers, and W. G. van Aken, "Interaction of cultured endothelial cells with polymeric surfaces of different wettabilities," *Biomaterials*, **6**, 403–408 (1985).
10. T. A. Horbett and M. B. Schway, "Correlations between mouse 3T3 spreading and serum fibronectin adsorption on glass and hydroxyethylmethacrylate-ethylmethacrylate copolymers," *J. Biomed. Mater. Res.*, **22**, 763–793 (1988).
11. H. Wolf, R. Karwath, and Th. Groth, "Interaction of blood with biomedical polymers—Some basic aspects," in *Advances in Biomedical Measurements*, E. R. Carson, P. Kneppo, and I. Krekule (eds.), Plenum Press, New York/London, 1988, pp. 133–142.
12. P. A. Underwood and F. A. Bennett, "A comparison of the biological activities of the cell-adhesive proteins vitronectin and fibronectin," *J. Cell Sci.*, **93**, 641–649 (1989).
13. M. D. Bale, L. A. Wohlfarth, D. F. Mosher, B. Tomasini, and R. C. Sutton, "Identification of vitronectin as a major plasma protein adsorbed on polymer surfaces of different copolymer composition," *Blood*, **74**, 2698–2706 (1989).
14. T. G. van Koten, J. M. Schakenraad, H. C. Van der Mei, and H. J. Buscher, "Influence of substratum wettability on the strength of adhesion of human fibroblasts," *Biomaterials*, **13**, 897–904 (1992).
15. D. J. Iuliano, S. S. Saavedra, and G. A. Truskey, "Effect of the conformation and orientation of adsorbed fibronectin on endothelial cell spreading and the strength of adhesion," *J. Biomed. Mater. Res.*, **27**, 1103–1113 (1993).
16. D. K. Pettit, A. S. Hoffman, and T. A. Horbett, "Correlation between corneal epithelial outgrowth and monoclonal antibody binding to the cell binding domain of fibronectin," *J. Biomed. Mater. Res.*, **28**, 685–691 (1994).
17. R. O. Hynes, "Integrins: A family of cell surface receptors," *Cell*, **48**, 549–554 (1987).
18. E. Ruoslahti and M. D. Pierschbacher, "New perspectives in cell adhesion: RGD and integrins," *Science*, **238**, 491–497 (1987).
19. S. K. Akiyama, K. Nagata, and K. M. Yamada, "Cell surface receptors for extracellular matrix components," *Biochim. Biophys. Acta*, **1031**, 91–110 (1990).
20. S. M. Albelda and C. A. Buck, "Integrins and other cell adhesion molecules," *FASEB J.*, **4**, 2868–2880 (1990).
21. M. E. Hemler, "VLA proteins in the integrin family: Structures, functions, and their role on leukocytes," *Annu. Rev. Immunol.*, **8**, 365–400 (1990).
22. T. A. Springer, "Adhesion receptors of the immune system," *Nature*, **346**, 425–434 (1990).
23. A. Avnur and B. Geiger, "The removal of extracellular fibronectin from areas of cell-substratum contact," *Cell*, **25**, 121–132 (1981).
24. F. Grinnell, "Focal adhesion sites and removal of substratum-bound fibronectin," *J. Cell. Biol.*, **103**, 2697–2706 (1986).
25. G. Altankov and F. Grinnell, "Fibronectin receptor internalization and AP-2 complex reorganization in po-

tassium-depleted fibroblasts," *Exp. Cell Res.*, **216**, 299–309 (1995).

26. G. Altankov and Th. Groth, "Reorganization of substratum-bound fibronectin on hydrophilic and hydrophobic materials is related to biocompatibility," *J. Mater. Sci. Mater. Med.*, to appear.
27. E. Engvall and E. Ruoslahti, "Binding of soluble form of fibroblasts surface protein fibronectin to collagen," *Int. J. Cancer*, **20**, 1 (1977).
28. G. Altankov and F. Grinnell, "Depletion of intracellular potassium disrupts coated pits and reversibly inhibits cell polarization during fibroblast spreading," *J. Cell Biol.*, **120**, 1449–1459 (1993).
29. M. H. Heggeness, J. F. Ash, and S. J. Singer, "Transmembrane linkage of fibronectin to intracellular actin-containing filaments in cultured human fibroblasts," *Ann. NY Acad. Sci.*, **312**, 414–417 (1978).
30. W. Chen, E. Hasegawa, T. Hesegawa, C. Wenstock, and K. Yamada, "Development of cell surface linkage complexes in cultured fibroblasts," *J. Cell. Biol.*, **100**, 1003–1114 (1985).

Received January 19, 1995
Accepted July 25, 1995

Publikation 5

Thomas Groth, Georgi Altankov (1996).

Studies on the cell-biomaterial interaction: Role of tyrosine phosphorylation during fibroblasts spreading on surfaces varying in wettability.

Biomaterials **17**, 1227-1234

ELSEVIER

Biomaterials **17** (1996) 1227–1234

0142-9612/96/$15.00

Studies on cell–biomaterial interaction: role of tyrosine phosphorylation during fibroblast spreading on surfaces varying in wettability

Thomas Groth* and George Altankov†

GKSS Research Center Geesthacht, Institute of Chemistry, Department of Membrane Research Teltow, Kanstraße 55, 14513 Teltow-Seehof, Germany; †Institute of Biophysics, Bulgarian Academy of Sciences, Strasse Academic G. Bonchev block 21, 1113 Sofia, Bulgaria

In a previous study we observed that protein tyrosine phosphorylation was significantly diminished in the focal adhesions of human fibroblasts attached on a hydrophobic surface in comparison with hydrophilic glass. This result raises the possibility that the tyrosine phosphorylation pathway may be involved in the regulation of cell–biomaterial interaction. To learn more about the interaction of anchorage-dependent cells with biomaterials, four different materials with wettability ranging from hydrophilic (water contact angle 25°) to hydrophobic (water contact angle 111°) were investigated, i.e. clean glass (glass), aminopropylsilane (APS), octadecylsilane (ODS) and silicone (SI). Immunofluorescence microscopy revealed increased stress formation and fibronectin (FN) receptor-rich focal adhesions for fibroblasts attached on more hydrophilic surfaces (glass and APS) in comparison to the relatively hydrophobic materials (ODS and SI). Phosphorylation of tyrosine residues, also studied by immunofluorescence microscopy, was considerably higher on glass and APS, lower for ODS, negligible for SI, and was found to colocalize with FN receptor-rich focal adhesions. Preadsorption of FN tended to restore cell adhesion and spreading on the hydrophobic ODS and SI. Quantitative data on cell proliferation and tyrosine phosphorylation showed moderate wettable material maximum values for APS, followed by glass, ODS and SI, demonstrating a non-linearity of these parameters with the wettability of materials. Interestingly, the preadsorption of FN increased both parameters, particularly for the hydrophobic materials ODS and SI. Phosphorylation of tyrosine on FN-coated substrata was corroborated by the accessibility of binding sites estimated by ELISA using polyclonal and monoclonal FN antibodies. Our results suggest that measurement of the phosphotyrosine activity of cells may be a sensitive parameter for the ability of biomaterials to support the attachment and proliferation of cells. Copyright © 1996 Elsevier Science Limited

Keywords: Wettability, fibroblasts, tissue compatibility, fibronectin, integrins, tyrosine phosphorylation, signalling

Received 4 April 1995; accepted 20 July 1995

It has been known for a long time that the attachment and growth of anchorage-dependent cells is inhibited on non-wettable biomaterials[1–3], a fact that has been attributed to the possible conformational changes of adsorbed proteins[4,5]. While cells interact in their natural environment with proteins of the extracellular matrix (ECM), including fibronectin (FN) and vitronectin (VN), these proteins are adsorbed from plasma or serum on to biomaterials as a prerequisite for successful cell adhesion and spreading[6–8]. In particular, FN seems to be sensitive to conformational changes upon adsorption on hydrophobic materials, as demonstrated by FTIR and fluorescence spectroscopy[9,10], and binding of polyclonal or monoclonal antibodies[11,12]. Adsorption of FN on hydrophobic biomaterials is followed by a decrease in cell adhesion and adhesion strength, and diminished cell spreading[10,13,14].

Recently, much has been learned about FN-dependent cell adhesion and integrins[15–17]. The FN receptor has been identified as an $\alpha 5\beta 1$ integrin present on fibroblasts and many other cells, and it functions as a transmembrane link between the substratum and the cell cytoskeleton[16,17]. It is known

Correspondence to Dr T. Groth.

that the FN receptor is rich in focal contacts — where the closest approach of cells to the substratum occurs, and where the actin filaments insert to the cell surface[18–20]. Integrins are also thought to be responsible for the transfer of signals from the substratum to the cell interior, also called 'outside-in-signalling'[21,22]. Recently, it was shown that the adhesion of fibroblasts on FN as well as antibody-induced $\beta 1$ integrin clustering stimulates tyrosine phosphorylation of proteins, as well as an up-regulation of genes controlling the cell cycle and synthesis of metalloproteases[22,23]. The FN receptor, like other integrins, has no intrinsic tyrosine kinase activity. However, it was shown that FN receptor occupancy in fibroblasts induces the tyrosine phosphorylation of a 120000 molecular weight protein, and this protein, called pp 125^{FAK} (or focal adhesion kinase), seems to be involved in the regulation of cell adhesion[22–24].

In a previous study we reported on a diminished phosphotyrosine activity in focal contacts of fibroblasts adhering on a hydrophobic surface in comparison to a hydrophilic substrate[25]. In the current investigation we chose four different surfaces with gradually decreasing wettability to extend our knowledge on the adverse effects of hydrophobic substrata on cells. The cell behaviour was estimated by morphological and functional criteria. The overall cell shape, the organization of FN receptor and actin filaments were investigated for cell morphology. Functionally, signalling via integrins through tyrosine phosphorylation was characterized by both immunofluorescence and enzyme immunoassay methods, and was correlated with the subsequent cell growth. In particular, the effect of FN preadsorption was studied, and it was finally concluded that tyrosine phosphorylation could be a sensitive measure for the tissue compatibility of biomaterials. Details are reported herein.

MATERIALS AND METHODS

Cells

Human foreskin fibroblasts were obtained from fresh skin biopsy and used up to the 12th passage. The cells were maintained in Dulbecco's minimal essential medium (DMEM) containing 10% fetal bovine serum (FBS; Sigma Chemical Co., St. Louis, MO, USA) in a humidified incubator with 5% CO_2. Fibroblasts from pre-confluent cultures were harvested with 0.05% typsin/0.6 mM EDTA (Sigma). Trypsin was neutralized with FBS.

Fibronectin preparation

Human plasma FN was produced by affinity chromatography on gelatine-Sepharose 4B according to Engvall and Ruoslahty[26], and further purified on heparin-Sepharose 4B, from where FN was eluted with 0.5 M NaCl in 50 mM Tris, pH 7.3. The prepared FN was lyophilized from a solution equivalent to approx. 1 mg protein per 1 ml buffer containing 50 mM Tris, 10 mM glycine, 150 mM NaCl, pH 7.3. For the experiments FN was dissolved in distilled water.

Substrata with different wettability

Glass coverslips (18 × 18 mm^2; Menzel, Germany) were cleaned with cold chromium sulphuric acid for 24h and rinsed thoroughly with distilled water. The clean glass slides (glass) were stored in distilled water to keep the surface hydrophilic. For the preparation of surfaces with decreasing wettability, clean dry glass slides were coated with the following materials: aminopropyltriethoxysilane (APS), octadecyldimethylchlorosilane (ODS) and silicone (SI). APS slides were prepared by the incubation of glass slides in 95% ethanol containing 5% APS (Fluka, Germany) and sonication for 5 min. The slides were baked at 120°C for 25 min and washed with ethanol. ODS slides were prepared by the incubation of glass slides in 2% solution of ODS (Sigma) in chloroform for 24 h, then rinsed three times with chloroform and finally washed with distilled water. SI slides were prepared using a 5% aqueous emulsion of silicone oil (polydimethylsiloxane, Serva Biochemistry, Germany). The slides were stored in the emulsion for 2 h and washed with distilled water. The slides were baked for 4 h at 200°C. Remaining silicone oil was finally removed by washing the slides in acetone. The water contact angles were measured by the sessile drop method on three different slides for each material. Water contact angles were 25° for glass, 57° for APS, 91° for ODS and 111° for SI. In some experiments the substrata were coated with 20 $\mu g\,ml^{-1}$ FN in phosphate-buffered saline (PBS) for 60 min at 37°C.

Distribution of actin, fibronectin receptor and phosphotyrosine

Adhesion of fibroblasts was carried out in six-well tissue culture plates containing the slides. Fibroblasts (10^5 cells suspended in 3 ml DMEM, 10% FBS) were pipetted into each well and incubated in a CO_2 incubator for 2 h. Attached cells to be processed for fluorescence microscopy were fixed with paraformaldehyde (3%) for 10 min, washed with PBS, permeabilized with 0.2% Triton X-100 for 5 min and saturated with 1% glycine, 1% bovine serum albumin (BSA) in PBS.

To detect actin, samples were incubated for 30 min at 37°C with 5 $U\,ml^{-1}$ (fluorescein isothiocyanate (FITC)-conjugated phalloidin (Sigma).

For the visualization of $\beta 1$ integrin (FN receptor), cells were incubated for 30 min at 37°C with rabbit anti-$\beta 1$ antibody (a kind gift from Dr Kenneth Yamada, National Institutes of Health, Bethesda, USA), diluted in PBS (with Ca^{2+} and Mg^{2+}) containing 1% BSA followed by FITC-conjugated goat anti-rabbit IgG (Jackson Immuno Research, USA) containing 10% normal goat serum (Sigma), for 30 min at 37°C.

Proteins phosphorylated on tyrosine residues were labelled using a monoclonal mouse anti-phosphotyrosine antibody (Upstate Biotechnology, NY, USA) diluted in PBS with 1% BSA followed by an incubation with rhodamine-conjugated goat anti-mouse IgG (Jackson Immuno Research, USA) containing 10% goat serum for 30 min at 37°C. The fixation and permeabilization were carried out in the presence of 0.2 mM sodium orthovanadate (Sigma) to stabilize the phosphotyrosine.

At the end of the incubation samples were washed, mounted with Mowiol[27], observed and photographed with a fluorescence microscope (Carl Zeiss, Germany).

Measurement of cell growth

A total of 10^5 cells in 3 ml medium containing 10% FBS was cultured in a humidified CO_2 thermostat for 3 days in six-well tissue culture plates (Falcon) containing the slides. At the end of the incubation the slides were rinsed with PBS and transferred to new plates. An MTT Cell Proliferation Kit I (Boehringer Mannheim Biochemica, Germany) was used to measure cell proliferation, according to Mossman[28].

Enzyme immunoassay for cellular phosphotyrosine activity

The quantification of the cellular phosphotyrosine activity of adhering fibroblasts was carried out by an ELISA using a measuring chamber with a surface area of 100 mm^2, as described elsewhere[29]. Fibroblasts (10^5 cells ml^{-1}) were incubated for 2 h, fixed and permeabilized as described above, but in the presence of 0.2 mM sodium orthovanadate. After saturation with 1% BSA, 1% glycine for 15 min and a further washing with PBS, monoclonal mouse anti-phosphotyrosine (Upstate Biotechnology, USA) was added at a suitable working dilution for 30 min followed by an incubation with goat anti-mouse IgG labelled with peroxidase (POD, Jackson Immuno Research, USA). *o*-Phenylene diamine (OPD, 1 mg ml^{-1}, Sigma) was prepared in 0.1 M citrate buffer with hydrogen peroxide (0.03%). OPD solution was added to the chambers and incubated for 10 min. The reaction was stopped by adding 2 M sulphuric acid in 0.1 M sodium sulphite. Then the chromophore was transferred to a microtitre plate and read in a plate reader set at a wavelength of 492 nm. To normalize the measured phosphotyrosine activity cell count was estimated under identical conditions with the MTT assay. The normalized phosphotyrosine activity was calculated by the ratios of optical density of phosphotyrosine activity to cell count.

Enzyme immunoassay for FN adsorption

The amount of adsorbed FN from 20 μg ml^{-1} solution on the materials was investigated with an ELISA after an incubation at 37°C for 1 h. Then the surfaces were rinsed three times with PBS and incubated with the following antibody solutions: polyclonal rabbit IgG anti-human FN at a working dilution of 1:50 000, monoclonal mouse IgG anti-human FN directed versus the cell binding domain at a working dilution of 1:10 000, or a mouse IgG anti-human FN directed versus the heparin-binding domain (all antibodies from Biomol GmbH, Germany). The secondary antibodies used were polyclonal goat anti-rabbit IgG conjugated with POD at a working dilution of 1:10 000 or goat anti-mouse IgG conjugated with POD (both antibodies from Jackson Immuno Research, USA). OPD (1 mg ml^{-1}) was used as chromogenic substrate, as described above. The results are given as optical densities (OD) and allow a semiquantitative measure of the protein adsorption and the presence of binding sites on the surface.

RESULTS

Cell morphology upon adhesion

The overall cell morphology of fibroblasts adhering on the different surfaces visualized by actin staining is shown in *Figure 1*. The left column (*Figure 1a, c, e, g*) represents the morphology of fibroblasts adhering in the absence of preadsorbed FN. It is obvious that normal cell spreading occurred only on glass and APS (*Figure 1a, c*), while on ODS and SI fibroblasts did not spread sufficiently (*Figure 1e, g*), where only a diffuse presence of actin was observed. Moreover, only a few adhering fibroblasts were detected on ODS and SI, most probably because of the several washing steps during the staining procedure. The preadsorption of FN on the materials not only restored the normal fibroblast morphology but tended to improve spreading of cells and the formation of pronounced actin stress fibres, as shown in *Figure 1b, d, f, h*. Indeed, it was obvious that wettable and moderately

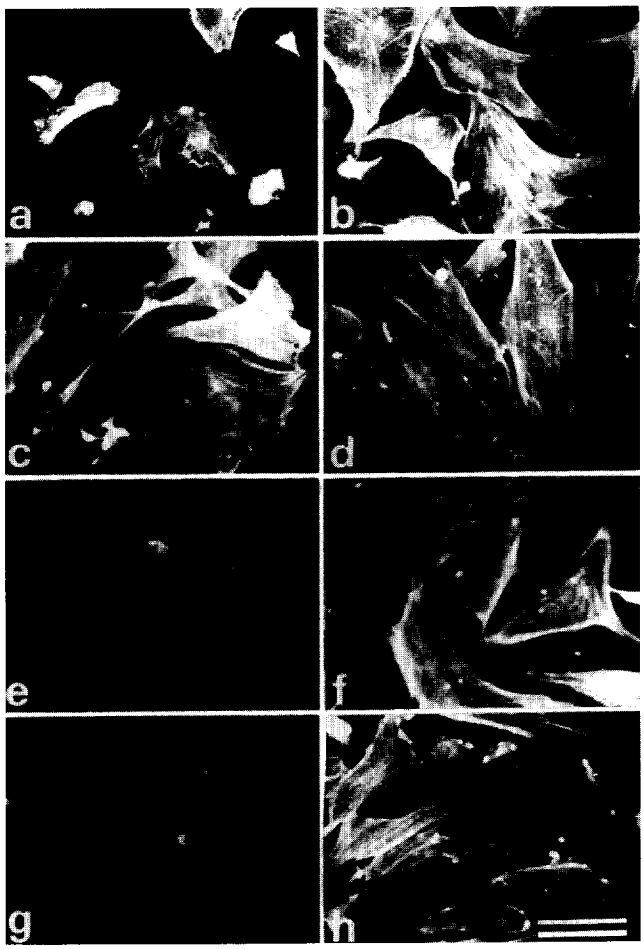

Figure 1 Morphology of fibroblasts adhering on plain substrata (left lane) or after preadsorption of FN (20 μg ml^{-1}, right lane) visualized by the staining of actin cytoskeleton with FITC–phalloidin. The following materials were investigated: **a**, **b**, glass; **c**, **d**, APS; **e**, **f**, ODS; **g**, **h**, SI. Bar: 100 μm.

wettable surfaces such as glass and APS stimulated the formation of pronounced actin stress fibres (*Figure 1b, d*), whereas on more hydrophobic ODS and SI spreading was less pronounced and stress fibres appeared to be more diffuse (*Figure 1f, g*).

FN receptor organization and colocalization with phosphorylated tyrosine residues in focal contacts

Figure 2 shows the organization of the $\beta 1$ integrin (*Figure 2a, c, e, g*) and phosphotyrosine (*Figure 2b, d, f, h*) in fibroblasts adhering on the plain substrata in the presence of 10% serum. It is shown that cells developed $\beta 1$ integrin in clusters and streaks corresponding to the focal adhesion plaques on glass and APS (*Figure 2a, c*). In contrast, on hydrophobic ODS and SI only a diffuse presence of the $\beta 1$ integrin was observed, and there was no distinct formation of focal contacts (*Figure 2e, g*). In parallel with the $\beta 1$ integrin organization phosphotyrosine activity was higher on APS and somewhat lower on glass (*Figure 2b, d*). Only a weak activity of phosphotyrosine was observed on ODS and SI (*Figure 2f, h*). It is obvious from *Figure 2* that the phosphotyrosine activity declined with decreasing wettability of the materials. It is also evident from *Figure 2* that the phosphotyrosine activity was colocalized with the $\beta 1$ integrin, presumably in the focal adhesion plaques (see *Figure 2a, b* and *c, d*).

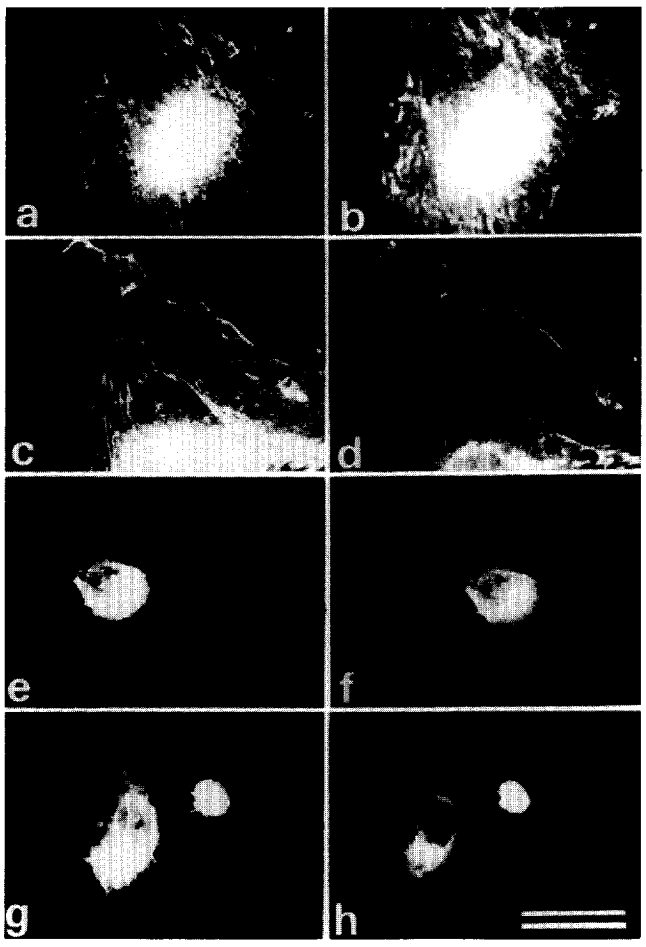

Figure 2 FN receptor organization and phosphorylation of tyrosine of fibroblasts adhering on plain substrata visualized by double-staining with monoclonal antibodies versus $\beta 1$ integrin (left lane) and phosphotyrosine (right lane). Note the colocalization between $\beta 1$ integrin and phosphotyrosine in focal adhesions. The following materials were investigated: **a**, **b**, glass; **c**, **d**, APS; **e**, **f**, ODS; **g**, **h**, SI. Bar: 30 μm.

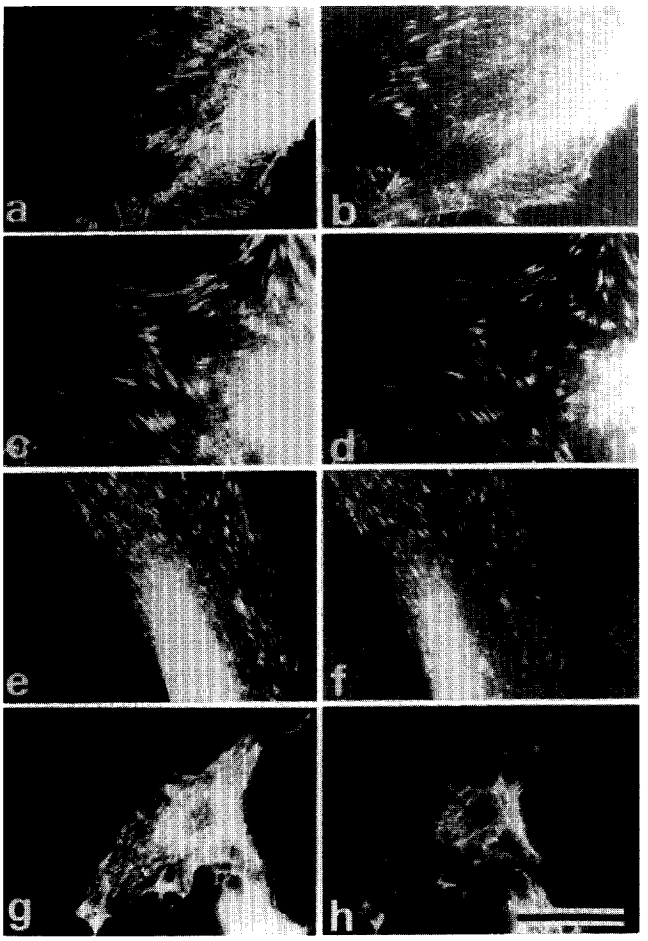

Figure 3 FN receptor organization and phosphorylation of tyrosine of fibroblasts adhering on substrata preadsorbed with FN ($20\,\mu g\,ml^{-1}$) visualized by double-staining with monoclonal antibodies versus $\beta 1$ integrin (left lane) and phosphotyrosine (right lane). Note the colocalization between $\beta 1$ integrin and phosphotyrosine in focal adhesions. The following materials were investigated: **a**, **b**, glass; **c**, **d**, APS; **e**, **f**, ODS; **g**, **h**, SI. Bar: 30 μm.

Precoating of the materials with FN ($20\,\mu g\,ml^{-1}$) improved the interaction with fibroblasts, but not completely. This is illustrated in *Figure 3*, where spreading of cells and organization of focal contacts ($\beta 1$ integrin) was improved, especially on the hydrophobic substrata, although spreading of cells, organization of focal contacts and tyrosine phosphorylation were less pronounced on ODS (*Figure 3e, f*) and SI (*Figure 3g, h*) than on glass (*Figure 3a, b*) and APS (*Figure 3c, d*).

Enzyme immunoassay for phosphotyrosine

The results of the ELISA for phosphotyrosine activity of fibroblasts after 2 h adhesion on the substrata are shown in *Figure 4*. Phosphotyrosine activity was significantly

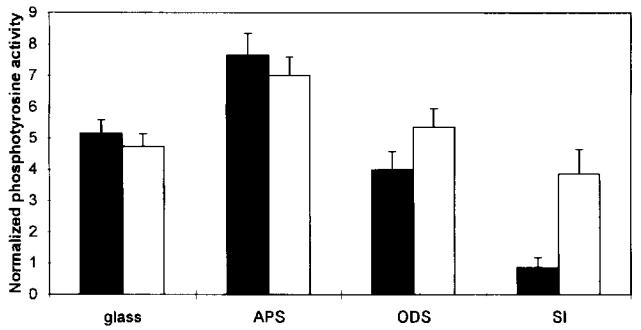

Figure 4 Semiquantitative estimation of tyrosine phosphorylation on the different surfaces in the absence (black bars) or presence (white bars) of preadsorbed FN (20 μg ml^{-1}). The phosphotyrosine activity was normalized for the number of attached cells (means ± s.d., $n = 6$) estimated with the MTT test[28] in parallel experiments under identical conditions.

higher on APS and glass than on ODS and SI ($P \leqslant 0.05$, *t*-test). Moreover, there was a significant drop in the activity from APS with moderate wettability to the hydrophobic substrata ODS and SI ($P \leqslant 0.05$, *t*-test). The preadsorption of FN on to the surfaces enhanced the phosphotyrosine activity significantly only on the hydrophobic ODS and SI ($P \leqslant 0.05$), but not on glass and APS.

Adsorption of FN from single solution on the materials measured with polyclonal and monoclonal anti-FN antibodies

The results of the ELISA for FN adsorption are shown in *Figure 5*. FN adsorption was detected with a polyclonal antibody, while the monoclonal antibodies have been used to detect the presence of binding sites for the cell binding and heparin binding domains of adsorbed FN. In general, it was observed that the binding of all antibodies declined in the following order: APS > ODS > SI > glass. This result holds for all antibodies, although there were some indications that exposure of cell and heparin binding domains was increased on APS, as evidenced by the higher ratio between monoclonal and polyclonal antibody binding.

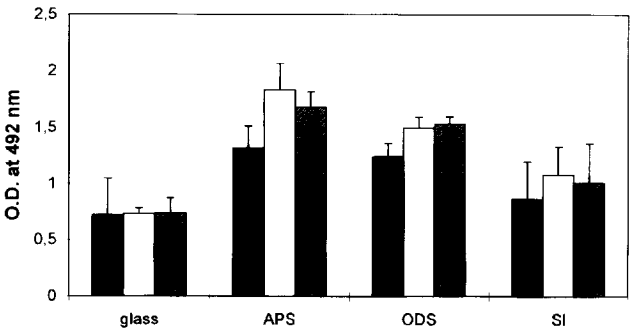

Figure 5 Adsorption of FN from single solution (20 μg ml^{-1}) with the ELISA technique. FN adsorption was estimated as OD (means ± s.d., $n = 6$) with polyclonal antibody (black bars), monoclonal antibody directed versus the cell binding domain (white bars) and monoclonal antibody directed versus the heparin binding domain (shaded bars).

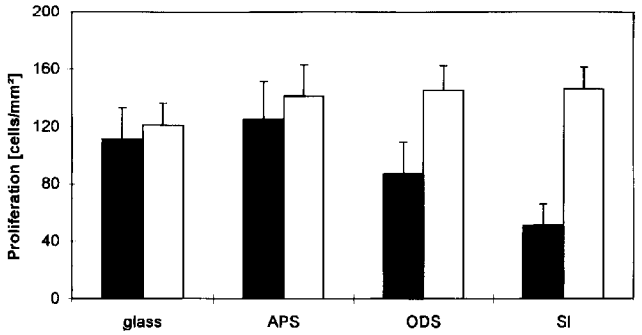

Figure 6 Proliferation of fibroblasts (means ± s.d., $n = 6$) on the plain substrata (black bars) or after preadsorption of FN (20 μg ml^{-1}, white bars). Fibroblasts were cultivated in the presence of 10% FBS for 72 h. The number of cells was estimated with the MTT test.

Proliferation of fibroblasts on the materials in the presence or absence of preadsorbed FN

The proliferation of fibroblasts in the presence of 10% serum was estimated after 72 h incubation. The results shown in *Figure 6* demonstrate that the best growth of cells was obtained on the moderately wettable surface APS, followed by glass. In contrast, cell proliferation was significantly reduced on hydrophobic ODS and was nearly absent on SI ($P \leqslant 0.05$, *t*-test). Precoating of surfaces with FN not only restored the cell growth but also significantly increased the growth on hydrophobic ODS and SI ($P \leqslant 0.05$, *t*-test) and made the growth indistinguishable between the hydrophobic substrata.

DISCUSSION

Reversible phosphorylation of proteins on tyrosine residues has long been recognized to regulate various metabolic pathways[21,30], and more recently it has been connected with the transfer of signals from the ECM to the cell interior, and gene expression responsible for the adhesion and proliferation of cells[31]. Surface wettability has been shown to be one of the main features of cell–biomaterial interaction responsible for different ways of protein adsorption[4–6,9–11]. However, how those differences in the adsorption properties reflect the biological reactivity of materials, especially on a cellular level, is not well understood. In a previous study we demonstrated that tyrosine phosphorylation in focal contacts of adhering fibroblasts was diminished on a hydrophobic surface in comparison to hydrophilic glass[25]. Assuming a possible direct effect of the hydrophobic environment on the signalling through the FN receptor we continued this investigation studying the phosphotyrosine activity of human fibroblasts with a series of surfaces with water contact angles ranging from 25° to 111°. We have demonstrated that most of the phosphotyrosine activity, visualized by specific antibodies, was colocalized with the β1 integrin in the focal adhesions. Moreover, this activity was related to other parameters of cell–biomaterial interaction, developed in our previous investigations[25,32,33], such as the overall cell shape of adhering fibroblasts, the ability of cells to develop actin stress fibres, the

organization of FN receptor and subsequent cell proliferation.

The observed decrease in cell spreading, as well as the diminished proliferation of cells with decreasing wettability of substrata, has long been studied and was also confirmed by us previously[1,2,25,32,34]. However, here we found that not the most wettable surface, glass, but APS, which represents a moderate wettable surface, expressed the best environment for cell spreading, as well as subsequent cell proliferation. This corresponded to the better cell signalling on APS, judged by the phosphotyrosine activity in focal contacts and quantitatively the total phosphotyrosine activity measured by the ELISA. The absence of cell spreading and the impaired proliferation of cells on ODS and SI as more hydrophobic materials was accompanied by a weak or nearly absent phosphorylation of tyrosine. In contrast to other studies demonstrating a decline in cell spreading and proliferation with decreasing wettability[1,34], our results are in agreement with the observations obtained by others who found that adhesion of fibroblasts and their biosynthetic activity have an optimum at about 60° water contact angle[35–37].

It is of particular interest from our study that the preadsorption of FN on more hydrophobic substrata improved the interaction of fibroblasts indicated by partly restored cell spreading and proliferation. However, the tyrosine phosphorylation was still significantly lowered on ODS and SI, indicating an impaired signalling, possibly by the FN receptor, on more hydrophobic substrata. The involvement of FN receptor in the transfer of signals from the substratum was demonstrated after antibody-induced clustering of $\beta 1$ integrins[22], or during adhesion of cells on FN or VN, but not on polylysine, where cells adhered but did not spread[23]. Indications for a regulation of cell–material interaction by signal transfer from the substratum to the cell interior are given by the concentration of phosphotyrosine activity in the focal contacts. The focal adhesion kinase (FAK) has been shown to be involved in the reorganization of the actin cytoskeleton and the formation of focal adhesions, thus influencing the maintenance and propagation of cell adhesion[38–40]. Moreover, it is suggested that FAK may be a part of the general transcription pathways leading to downstream events, such as cell proliferation[21,22,31]. The results of our study strongly support the assumption that surface properties of biomaterials, such as wettability, may directly affect signalling via integrins.

The measurement of FN adsorption was correlated in a qualitative manner with the observed changes in cell morphology and signalling after FN preadsorption, but not with the subsequent cell proliferation, which was surprisingly higher for the hydrophobic materials ODS and SI. This points to the possibility that adhesion to the material and signalling is only a prerequisite and must be followed by other stimuli, for example via the growth receptor pathway, keeping in mind that all experiments were carried out in the presence of serum[31]. Polyclonal antibodies were used to get a measure of FN adsorption, since it is known that they are not very sensitive to conformational changes of the adsorbed protein[41,42], while monoclonal antibodies have been applied to investigate the availability of cell and heparin binding domains. The optimum FN adsorption determined on moderately wettable APS is in agreement with the fact that protein adsorption not only increases with decreasing wettability, but may also be decreased by conformational changes of the adsorbed proteins, reducing the available space for protein adsorption[4,6,11,12]. However, Pettit *et al.* have reported[43] that an increasing presence of adsorbed FN is accompanied by a decreasing recognition of the cell-binding domain. In light of this fact it may be concluded that, although surprisingly low amounts of FN were bound on glass, its conformation and orientation were suitable for interaction with cells. Moreover, we have shown previously that cells are able to reorganize and rearrange adsorbed FN on glass but not on hydrophobic substrata, thus enhancing the surface concentration of FN under the cell surface[32,33]. Our results demonstrate the relationship between FN adsorption and initial cellular response, since the phosphotyrosine activity was related to the FN adsorption. For example, on APS with the highest phosphotyrosine activity most quantities of cell and heparin binding domains were found. The importance of both cell and heparin binding domains for $\alpha 5\beta 1$ integrin binding and tyrosine phosphorylation on glass was demonstrated recently[23].

In summary, it may be concluded that the adverse effect of hydrophobic substrata on cells with respect to adhesion and proliferation is due to an impaired transfer of signals via integrins from the substratum to the cell interior. The reason for this effect may be the mode of adsorption of attachment proteins such as FN, resulting in an impaired interaction with the corresponding integrin receptor, as well as the lack of a possible rearrangement of FN into ECM-like structures, as we found recently[32,33]. Indeed, the preadsorption of FN on hydrophobic substrata may provide better starting conditions, thus improving the tissue compatibility of the material.

ACKNOWLEDGEMENTS

This work was supported by the Deutsche Forschungsgemeinschaft grant GR 1294/1-4 and 436 BUL 113/80/2. We wish to thank Dr Fred Grinnell for his helpful advice.

REFERENCES

1 van Wachem PB, Vreriks CM, Beugeling T *et al.* The influence of protein adsorption on interactions of cultured human endothelial cells with polymers. *J Biomed Mater Res* 1987; **21**: 701–718.

2 Grinnell F, Milam M, Spree P. Attachment of normal and transformed hamster kidney cells to substrata varying in chemical composition. *Biochem Med* 1973; **7**: 87–90.

3 van Kooten TG, Schakenraad JM, van der Mei HC,

Busscher HJ. Influence of substratum wettability on the strength of adhesion of human fibroblasts. *Biomaterials* 1993; **13:** 897–904.
4 Andrade JD, Hlady V. Protein adsorption and materials biocompatibility. A tutorial review and suggested hypothesis. *Prog Surface Sci* 1986; **79:** 1–64.
5 Norde W, Lyklema J. Why proteins prefer interfaces. *J Biomater Sci Polymer Edn* 1991; **2:** 183–202.
6 Grinnell F, Feld MK. Adsorption characteristics of plasma fibronectin in relationship to biological activity. *J Biomed Mater Res* 1981; **15:** 363–381.
7 Steele JG, McFarland C, Dalton BA *et al.* Attachment of human bone cells to tissue culture polystyrene: the effect of surface chemistry upon initial cell attachment. *J Biomater Sci Polymer Edn* 1993; **5:** 245–257.
8 Howlett CR, Evans MDM, Walsh WR, Johnson G, Steele JG. Mechanism of initial attachment of cells derived from human bone to commonly used prosthetic materials during cell culture. *Biomaterials* 1994; **15:** 213–222.
9 Pitt WG, Spiegelberg SH, Cooper SL. Adsorption of fibronectin to polyurethane surfaces: Fourier transformed infrared spectroscopic studies. In: Brash JL, Horbett TA, eds. *ACS Symposium Series 343, Proteins at Interfaces: Physicochemical and Biochemical Studies*, 1987: 324–338.
10 Juliano DJ, Saavedra SS, Truskey GA. Effect of the conformation and orientation of adsorbed fibronectin on endothelial cell spreading and the strength of adhesion. *J Biomed Mater Res* 1993; **27:** 1103–1113.
11 Grinnell F, Feld M. Fibronectin adsorption on hydrophilic and hydrophobic surfaces detected by antibody binding and analyzed during cell adhesion in serum containing medium. *J Biol Chem* 1982; **257:** 4888–4893.
12 Grinnell F. Fibronectin adsorption on material surfaces. In: Blood in Contact with Natural and Artificial Surfaces. *Ann NY Acad Sci* 1987; **516:** 280–290.
13 Groth Th, Zlatanov I, Altankov G. Adhesion of human peripheral lymphocytes on biomaterials preadsorbed with fibronectin and vitronectin. *J Biomater Sci Polymer Edn* 1994; **6:** 729–739.
14 Truskey GA, Proulx TL. Relationship between 3T3 cell spreading and the strength of adhesion on glass and silane surfaces. *Biomaterials* 1993; **14:** 243–254.
15 Ruoslahty E, Pierschbacher MD. New perspectives in cell adhesion: RGD and integrins. *Science* 1987; **238:** 491–497.
16 Hynes RO. Integrins: a family of cell surface receptors. *Cell* 1987; **48:** 549–554.
17 Springer TA. Adhesion receptors of the immune system. *Nature* 1990; **346:** 425–433.
18 Buck CA, Horwitz AF. Cell surface receptors for extracellular matrix molecules. *Ann Rev Cell Biol* 1987; **3:** 179–205.
19 Grinnell F. Focal adhesion sites and the removal of substratum-bound fibronectin. *J Cell Biol* 1986; **103:** 2697–2706.
20 Geiger B, Avnur A, Kreis TE, Schlesinger J. The dynamics of cytoskeletal organization in areas of cell contact. *Cell Muscle Motility* 1989; **5:** 195–234.
21 Hynes RO. Integrins: versatility, modulation and signaling. *Cell* 1992; **69:** 11–25.
22 Kornberg LJ, Earp HS, Turner CE, Prockop C, Juliano RL. Signal transduction by integrins: increased protein tyrosine phosphorylation caused by clustering of $\beta 1$ integrins. *Proc Natl Acad Sci USA* 1991; **88:** 8392–8396.
23 Guan J-L, Trevithick JE, Hynes RO. Fibronectin/integrin interaction induces tyrosine phosphorylation of a 120-kDa protein. *Cell Regul* 1991; **2:** 951–964.
24 Schaller MD, Borgman CA, Cobb BS, Vines RR, Reynolds AB, Parsons JT. pp125fak, a structurally distinctive protein-tyrosine kinase associated with focal adhesions. *Proc Natl Acad Sci USA* 1992; **89:** 5192–5196.
25 Groth Th, Altankov G. Fibroblast spreading and proliferation on hydrophilic and hydrophobic surfaces is related to tyrosine phosphorylation in focal contacts. *J Biomater Sci Polymer Edn* 1995; **7:** 297–305.
26 Engvall E, Ruoslahty E. Binding of soluble form of fibroblasts surface protein fibronectin to collagen. *Int J Cancer* 1977; **20:** 1–7.
27 Rodriguez J, Deinhardt F. Preparation of a semipermanent mounting medium for fluorescent antibody studies. *Virology* 1960; **12:** 316–317.
28 Mossman T. Rapid colorimetric assay for cellular growth and survival: application to proliferation and cytotoxicity assays. *J Immunol Meth* 1983; **65:** 55–63.
29 Groth Th, Derdau K, Strietzel F, Förster F, Wolf H. The haemocompatibility of biomaterials *in vitro*—investigations on the mechanism of the whole blood clot formation test. *Alternatives to Lab Anim* 1992; **20:** 390–395.
30 Shattil SJ. Regulation of platelet anchorage and signaling by integrin aIIbβ3. *Thromb Haemost* 1993; **70:** 224–228.
31 Juliano RL, Haskill S. Signal transduction from the extracellular matrix. *J Cell Biol* 1993; **120:** 577–585.
32 Altankov G, Groth Th. Reorganization of substratum-bound fibronectin on hydrophilic and hydrophobic materials is related to biocompatibility. *J Mater Sci: Mater Med* 1994; **5:** 732–737.
33 Altankov G, Grinnell F, Groth Th. Studies on the biocompatibility of materials: fibroblast reorganization of substratum-bound fibronectin on surfaces varying in wettability. *J Biomed Mater Res*, in press.
34 van Wachem PB, Beugeling T, Feijen J, Bantjes A, Detmers JP, van Aken WG. Interaction of cultured human endothelial cells with polymeric surfaces of different wettabilities. *Biomaterials* 1985; **6:** 403–408.
35 Tamada Y, Ikada Y. Fibroblasts growth on polymer surfaces and biosynthesis of collagen. *J Biomed Mater Res* 1994; **28:** 783–789.
36 Baier RE, DePalma VA, Goupil DW, Cohen E. Human platelet spreading on substrata of known surface chemistry. *J Biomed Mater Res* 1985; **19:** 1157–1167.
37 Horbett TA, Schway MB. Correlations between mouse 3T3 cell spreading and serum fibronectin adsorption on glass and hydroxyethylmethacrylate–ethylmethacrylate copolymers. *J Biomed Mater Res* 1988; **22:** 763–793.
38 Chrzanowska-Wodnicka M, Burridge K. Tyrosine phosphorylation is involved in reorganization of the actin cytoskeleton in response to serum or LPA stimulation. *J Cell Sci* 1994; **107:** 3643–3654.
39 Chen H-C, Guan J-L. Association of focal adhesion kinase with its potential substrate phopshatidylinositol 3-kinase. *Proc Natl Acad Sci USA* 1994; **91:** 10148–10152.
40 Burridge K, Turner CE, Romer LH. Tyrosine phosphory-

lation of paxillin and pp125FAK accompanies cell adhesion to extracellular matrix: a role in cytoskeletal assembly. *J Cell Biol* 1992; **119:** 893–903.

41 Slack SM, Posso SE, Horbett TA. Measurement of fibrinogen adsorption from blood plasma using ^{125}I-fibrinogen and a direct ELISA technique. *J Biomater Sci Polymer Edn* 1991; **3:** 49–68.

42 Groth Th, Campbell EW, Herrmann K, Seifert B. Enzyme immuno assays for testing the haemocompatibility of biomedical polymers. *Biomaterials* 1994; **16:** 1009–1015.

43 Pettit DK, Hoffman AS, Horbett TA. Correlation between corneal epithelial cell outgrowth and monoclonal antibody binding to the cell binding domain of adsorbed fibronectin. *J Biomed Mater Res* 1994; **28:** 685–691.

Publikation 6

Georgi Altankov, Thomas Groth (1997).

Fibronectin matrix formation by fibroblasts on surfaces varying in wettability.

Journal of Biomaterials Science - Polymer Edition **8**, 299-310.

J. Biomater. Sci. Polymer Edn, Vol. 8, No. 4, pp. 299–310 (1997)

Fibronectin matrix formation by human fibroblasts on surfaces varying in wettability

GEORGI ALTANKOV[1,*] and THOMAS GROTH[2,*]

[1] *Institute of Biophysics, Bulgarian Academy of Sciences, Str. Acad. G. Bonchev, Bl. 21, 1113 Sofia, Bulgaria*

[2] *GKSS Research Centre, Institute of Chemistry, Department of Membrane Research, Kantstrasse 55, 14513 Teltow, Germany*

Received 6 May 1996; accepted 5 September 1996

Abstract—The spatial organization of extracellular fibronectin on biomaterial surfaces might be important for interaction with tissue cells. In previous investigations we have demonstrated that hydrophilic materials bind preadsorbed fibronectin that can easily be reorganized by fibroblasts in a specific matrix-like structure, while on less wettable materials (possessing water contact angles above 60 deg) the cells were unable to do this. As the cells continuously produce their fibronectin matrix, we tried in this study to answer the question of how the surface wettability of biomaterials influences the endogenous fibronectin matrix formation and its subsequent organization on the substrate. We cultured fibroblasts for 72 h on five different wettable surfaces: glass, aminopropyltriethoxysilane, pellethane, polyvinylchloride, and silicone, with water-contact angles gradually ranging from 25 to 105 deg. We demonstrated that the decreasing wettability of the materials significantly reduced endogenous fibronectin deposition on the substratum. Moreover, fibrillar organization of fibronectin appeared only on relatively hydrophilic glass and APS substrate, while on more hydrophobic materials like PVC and SI, cells secreted some fibronectin but were not able to organize it into a fibronectin matrix. These results were correlated with an altered cell morphology and spreading on these materials. In addition, an ELISA method has been implemented to quantify fibronectin matrix formation as a possible measure of the biocompatibility of materials, where a clear relation has been found between fibroblast growth and fibronectin matrix formation.

Key words: Biomaterials; wettability; fibroblasts; fibronectin; extracellular matrix.

INTRODUCTION

The need to implant foreign materials to substitute some of the body's structures and functions has long been recognized and implemented in medicine. However, the complex of molecular and cellular events which occur in response to the implantation of biomaterials, although extensively studied, is still poorly understood. According to current knowledge, the interaction between foreign materials and living tissues

*Correspondence should be sent to either Georgi Altankov or Thomas Groth.

begins with the adsorption of proteins from the surrounding medium, followed by cell–biomaterial interactions [1–3]. Among the adsorbed proteins, fibronectin (FN) seems to play a critical role as it can increase the initial cell attachment [3] and induce subsequent cell growth and differentiation [3, 4] by means of a specific cell surface integrin receptor ($\alpha_5\beta_1$ integrin) occupation [5, 6], and signaling to the cell interior [7, 8]. One example for such an anchorage-dependent cell growth is the behavior of fibroblasts in contact with foreign materials. Once they attach to a substratum they rapidly begin to proliferate and start to cover the foreign material surface [9]. Thus, fibroblasts are among the first cells which contact biomaterials, and hence, can be considered as a useful cellular system for studying cell–biomaterial interactions.

On the other hand, it is well known that many types of cells interact better with wettable surfaces in comparison to non-wettable (hydrophobic) substrata [10–13]. In our previous investigations we have demonstrated that the mode of FN binding on hydrophilic materials allows an easy removal and reorganization by cells [14, 15] in a specific matrix-like structure [16, 17]. As we have shown, fibroblasts adhering on hydrophilic substrata begin to reorganize preadsorbed FN within the first 3–4 h of cultivation. In contrast, on less wettable materials these cells are unable to rearrange FN, presumably because the binding of FN to the substrate is much stronger [14, 15].

In vivo, however, cells continuously synthesize their own FN matrix which they deposit and slowly organize as a three-dimensional matrix network [18]. The interesting question rises: how does the surface wettability of the implanted biomaterials influence the FN matrix formation during interaction with tissue cells?

In the present investigation we have studied the influence of the surface wettability of biomaterials on FN matrix deposition and organization on the substratum by human fibroblasts *in vitro*. The cells were cultured for 72 h on five different wettable materials, with water-contact angles gradually ranging from 25 to 105 deg. We could demonstrate with immunofluorescence microscopy that decreasing the wettability of materials significantly decreased endogenous FN matrix formation, which was correlated with an altered cell morphology, but also reduced cell growth on these surfaces. In addition, an ELISA method has been implemented to quantify FN matrix formation as a possible criterion for the biocompatibility of materials. A clear correlation between cell growth and FN matrix formation in simultaneously measured samples has been found.

MATERIAL AND METHODS

Cells

Human skin fibroblasts were obtained from fresh skin biopsy and used up to the 9th passage. The cells were grown in Dulbecco's Modified Eagle Medium (DMEM) containing 10% fetal bovine serum (FBS, Sigma Chemicals Co., St. Louis, MO, USA) in an humidified incubator with 5% CO_2. Fibroblasts from preconfluent cultures were harvested with 0.05% trypsin/0.6 mM EDTA (Sigma), and trypsin was neutralized with FBS.

Substrata with different wettability

Glass slides (Menzel, Germany) were cleaned with chromium sulphuric acid (c trated H_2SO_4 saturated with $K_2Cr_2O_7$) for 24 h and rinsed thoroughly with d water. Surfaces with decreasing wettability were prepared by coating clean dr with the following materials: aminopropyltriethoxysilane (APS), pellethane polyvinylchloride (PVC), and silicone (SI).

For coating with APS, glass slides were immersed in 95% ethanol containi APS (purchased from Fluka, Germany) and sonicated for 5 min. Thereafter th was baked at 120°C for 25 min and washed with ethanol. For coating with PI polymer was dissolved in tetrahydrofurane (2% w/v), the slides were covere the polymer solution and spin coated with a Convac 1001 device (Convac (Germany) at 2000 rpm for 5 min. The same procedure was applied for the ration of PVC surfaces, but with a 2.5% w/v solution of PVC (Sigma) disso tetrahydrofuran.

Polydimethylsiloxane coated slides (SI) were prepared using a 5% aqueous en of silicone oil (Serva Biochemistry, Germany). The slides were stored in the en for 2 h, and washed with distilled water. Thereafter the slides were baked for 200°C. The remaining silicone oil was finally removed by washing the surf acetone.

The static water contact angles were estimated by under-water contact angl surements on three different slides for each material. Water contact angles material surfaces studied are shown in Table 1.

Fibronectin matrix formation and cell morphology

Approximately 5×10^5 cells in 3 ml medium containing 10% FBS were in for 72 h in six-well tissue culture plates (Falcon, Becton Dickenson & Co NJ, USA) containing clean or surface coated glass slides. At the end of th bation cells were fixed with 3% paraformaldehyde in PBS. Fixed preparatio non-permeabilized cells were used for visualization and quantification of FN deposition.

Table 1.
Wettability of material surfaces

Material	Water-contact angle
Glass	25.1 ± 2.7
APS	62.9 ± 0.5
PEL	72.4 ± 0.4
PVC	82.8 ± 1.0
SI	103.1 ± 0.3

Static contact angles were measured by under-water technique on three different slides for each material. Data shown are means ± SD ($n = 3$).

FN matrix deposited on the different wettable surfaces was visualized by immunofluorescence using a specific anti human FN matrix mouse monoclonal antibody (Immunotech SA, France, lot No. 0326), followed by Cy^3-conjugated goat anti-mouse secondary IgG_1 antibody (Jackson Immuno Research, Inc., West Growe, PA, USA). The samples were then mounted. Further investigations and microphotography was carried out by both phase contrast and immunofluorescence microscopy with an inverted fluorescence microscope type Axiovert 100 (Carl Zeiss, Germany).

Quantification of cell proliferation and fibronectin matrix formation

Cell proliferation and fibronectin synthesis were quantified simultaneously using the same sample surface. The different surfaces were covered by a reusable tissue culture vessel made of silicone (Flexiperm Slide, Hereaus Instruments, Germany), forming eight small chambers for cell culture per slide. 2.5×10^4 cells ml^{-1} suspended in DMEM with 10% FBS were added and cultivated for 72 h.

Cell proliferation was measured by XTT assay (Boehringer Mannheim, Germany); a spectrophotometrical method for the quantification of cell growth and viability using a water soluble reaction product [19]. Briefly, cells were incubated in DMEM with 10% FBS without phenolred, and mixed with sodium 3′-[1-(phenylaminocarbonyl)-3,4-tetrazolium]-bis(4-methoxy-6-nitro) benzene sulfonic acid hydrate (XTT) reagent in the ratio 2 : 1. After 4 h incubation the supernatant containing the formazan dye was removed, and the OD measured at 450 nm.

FN matrix deposition by human fibroblasts was quantified by ELISA using the same anti human FN matrix antibody as for the immunofluorescence investigations (see above), followed by peroxidase conjugated goat anti-mouse (Jackson Immuno Research, Inc., West Growe, PA, USA) as a secondary antibody. Appropriate working dilutions for primary and secondary antibodies were found in previous experiments.

FN adsorption/desorption

Human plasma FN was produced by affinity chromatography on gelatin-Sepharose 4B according to Engvall and Ruoslahti [20], and further purified on heparin-Sepharose 4B. Labelling of FN with ^{125}I was carried out with chloramine T method [21]. Briefly, FN (500 $\mu g\,ml^{-1}$) was dissolved in PBS (150 mM NaCl, 1 mM K_2HPO_4, 5 mM NaH_2PO_4), and 50 μl $Na^{125}I$ (IZOTOP, Budapest, Hungary) with an activity of 0.5 mCi was added. The iodination was initiated by the addition of chloramine T (4 mg ml^{-1} PBS), and the reaction was stopped by adding sodium metabisulfite (8 mg ml^{-1} PBS) after 45 s. ^{125}I-FN was separated from unreacted ^{125}I by filtration over a Sephadex G-25 column. Specific activity of ^{125}I-FN was measured with a gamma counter (LKB).

Protein adsorption was carried out with a diluted solution containing a mixture of ^{125}I-FN and native FN at a concentration of 20 $\mu g\,ml^{-1}$. This solution was added to six well multiplates containing the different materials. After 60 min incubation at ambient temperature the materials were washed extensively with PBS, and activity was measured in the gamma counter. For desorption measurements, materials were

incubated for 60 min with FN (20 $\mu g\,ml^{-1}$), washed with PBS, followed by a further incubation with FBS (10%) for 4 h. After washing with PBS, the activity was measured again.

RESULTS

Fibronectin matrix formation on different wettable surfaces

Figure 1 (left panel, A, C, E, G, I) shows the phase contrast morphology of fibroplasts adhering on different wettable surfaces after 72 h incubation in medium containing 10% FBS. Significant alterations in the overall cell shape were found with decreasing wettability of materials. On hydrophilic glass (Fig. 1A) and APS (Fig. 1C) the cell attachment was higher, and well spread fibroblasts represented typical elongated cell shapes. On the less wettable PEL (Fig. 1E) and PVC (Fig. 1G), however, significantly less cells were found, and cell morphology was partly shrunk because of uncompleted cell spreading. Finally, on the most hydrophobic material SI (Fig. 1I) many of the fibroblasts were round or possessed an irregular cell shape with many extensions.

On the right panel of Fig. 1 (B, D, F, H, and K), the same cells were viewed with fluorescence microscopy to visualize the deposited FN matrix (see chapter Material and methods). The immunofluorescence features indicated a clear dependence between the FN matrix formation and the material's surface wettability. On glass (Fig. 1B) and APS (Fig. 1D) FN was deposited as bright fibrillar-like structure, which follows (but not exactly) the direction of cell polarization (compare with Fig. 1A and C on the left lane). The further decrease of the wettability lead to significantly less FN deposition, following the order PEL (Fig. 1F), PVC (Fig. 1H), and SI (Fig. 1K).

Organization of fibronectin matrix on different wettable surfaces

The high magnification micrographs in Fig. 2 show that fibrillar organization of the FN matrix appears only on relatively hydrophilic materials, such as glass (Fig. 2A) and APS (Fig. 2B), and only partially on PEL (Fig. 2C). It seems that the development on FN fibrils runs in parallel with the elongation of the cell body. On the less wettable materials, however, possessing a water-contact angle above 70 deg, as measured for PVC (Figs 1H and 2D), and SI (Figs 1K and 2E), a complete absence of extracellular FN organization has been found although some FN was secreted from the cells and stained diffusely along the cell body, or on the substratum beneath the cells.

Enzyme immunoassay for fibronectin matrix formation

The quantification of extracellular FN deposited on the different surfaces by human fibroblasts cultured for 72 h, was carried out with an ELISA. The results are presented in Table 2 (right column). The colorimetric signal (OD at 450 nm), which reflects the FN matrix deposition, was significantly higher on glass and APS, and diminished according to the decrease in surface wettability: APS $\geqslant$ glass > PEL > PVC > SI, up to about a seven-times lower OD for SI.

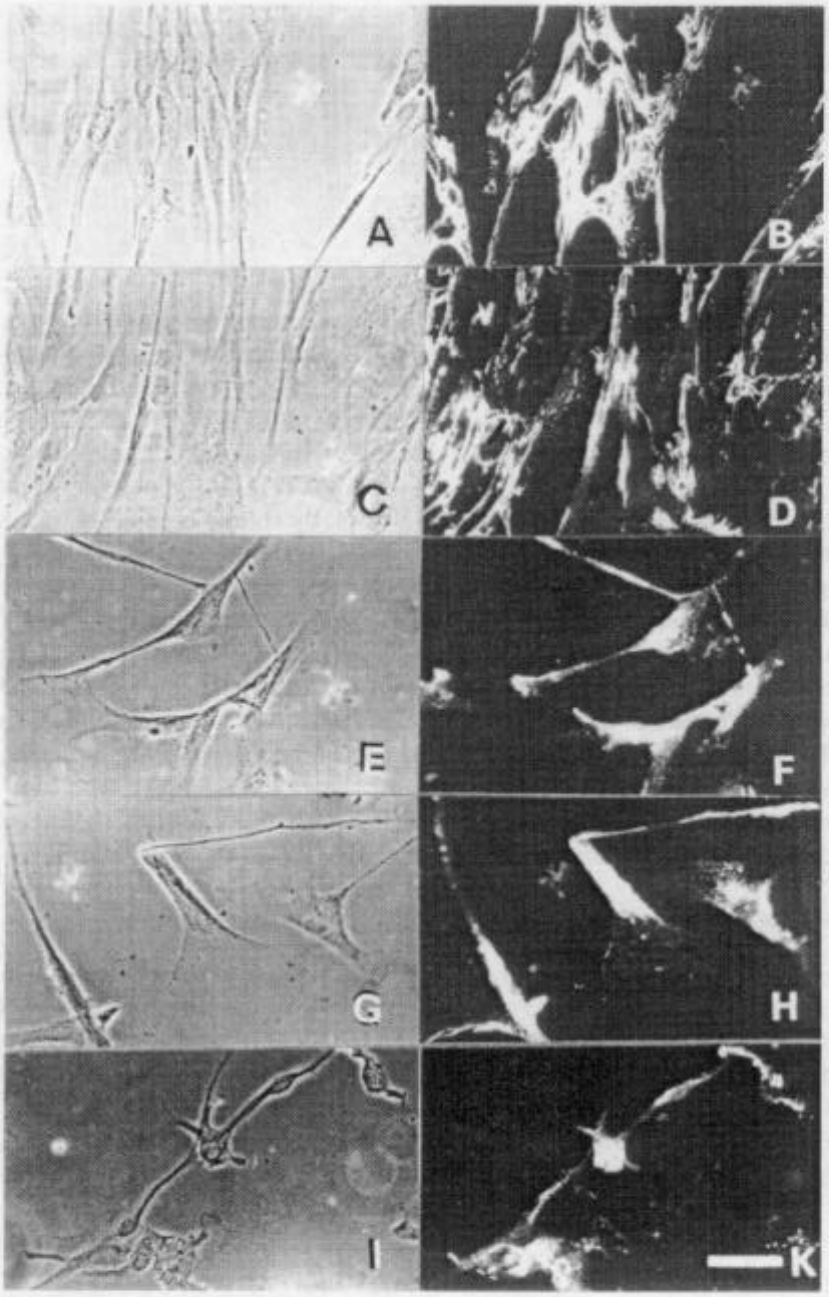

Figure 1. Fibronectin matrix formation and overall morphology of fibroblasts cultured on different material surfaces. Human fibroblasts in medium containing 10% FBS were cultured for 72 h on the following surfaces: A and B (glass), C and D (APS), E and F (PEL), G and H (PVC), I and K (SI). Samples were examined by phase contrast (A, C, E, G, I) or fluorescence (B, D, F, H, K) microscopy to detect cell morphology and endogenous fibronectin matrix formation, respectively (bar = 20 μm).

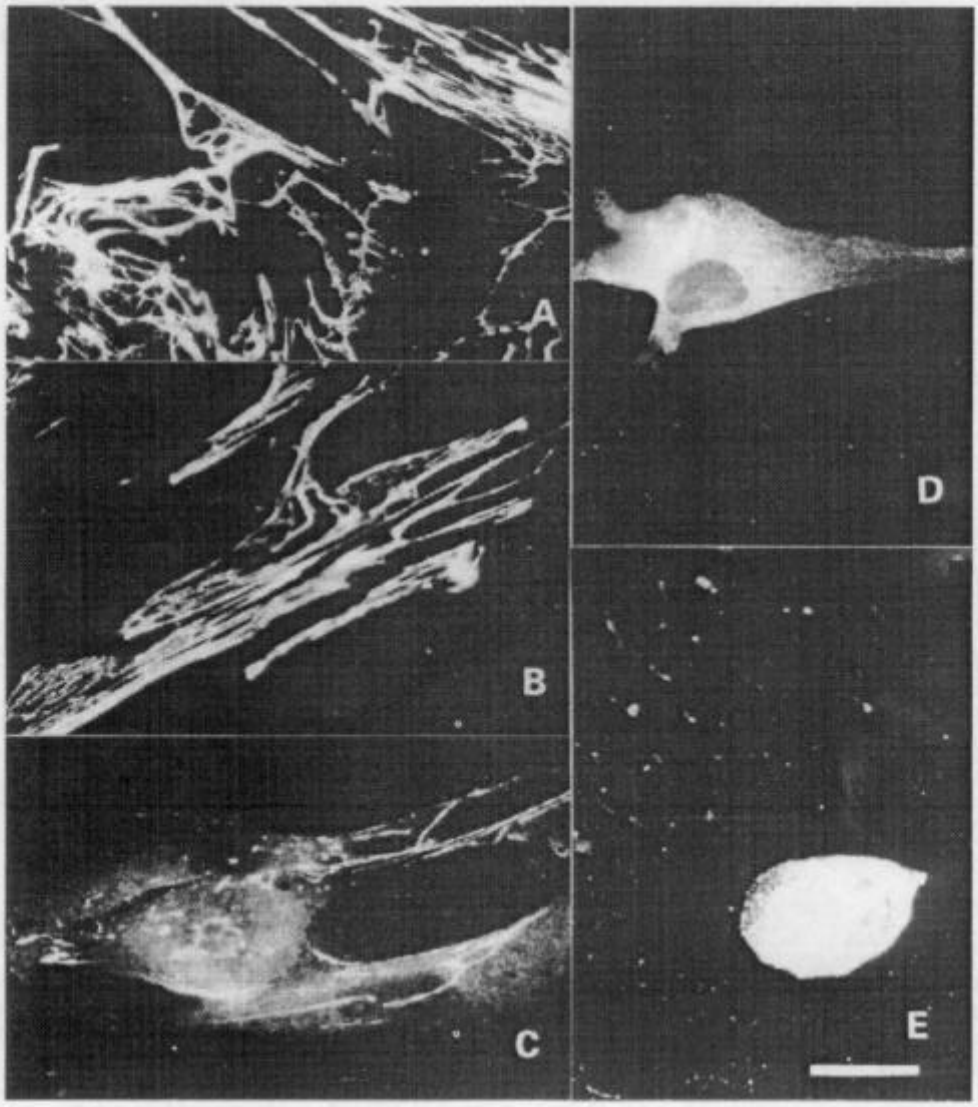

Figure 2. Organization of fibronectin matrix by human fibroblasts on different wettable material surfaces. Experimental were the same as described for Fig. 1, except that the samples A (glass), B (APS), C (PEL), D (PVC), and E (SI) were examined and photographed at a higher magnification (100×) of the fluorescence microscope (bar = 10 μm).

Cell proliferation

Cell proliferation was estimated by XTT assay after 72 h of cultivation onto different wettable surfaces in the presence of 10% FBS. The results shown in Table 2 (left column) represent the OD at 492 nm, which is comparable to the number of viable cells. It is demonstrated that the best growth of fibroblasts was observed on glass and APS. Overall, cell proliferation decreased significantly from glass and APS > PEL > PVC > SI.

Table 2.
Cell proliferation and FN matrix synthesis

Material	Cell proliferation (OD at 492 nm)	FN matrix synthesis (OD at 450 nm)
Glass	2.58 ± 0.2	2.11 ± 0.1
APS	2.44 ± 0.2	2.2 ± 0.1
PEL	1.74 ± 0.3	1.03 ± 0.2
PVC	0.91 ± 0.2	0.47 ± 0.3
SI	0.75 ± 0.2	0.29 ± 0.2

Cell proliferation was measured with XTT assay and FN matrix synthesis was quantified by ELISA for FN after 72 h cultivation of human fibroblasts on the different substrata. Quantities are given as OD and represent means ± SD ($n = 8$).

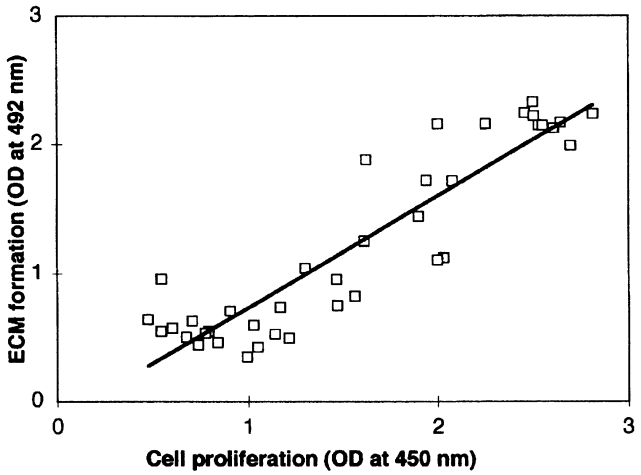

Figure 3. Plotting of FN matrix deposition vs cell proliferation. Human fibroblasts were cultivated on the different materials in Flexiperm Slide^{TM} culture chambers for 72 h. First, cell proliferation was measured with XTT assay. After washing with culture medium and fixation, FN matrix deposition was quantified in the same sample wells with an ELISA for FN.

For a comparison of the ability of cells to proliferate with their production of FN matrix, the results of cell growth were plotted vs data from ELISA for quantification of FN matrix deposition. As shown in Fig. 3, a linear correlation between FN matrix deposition and cell proliferation exists. The equation for the relationship between both parameters was $y = 0.887x - 0.137$ with a correlation coefficient $R = 0.913$. As a result it can be assumed that FN matrix synthesis and cell proliferation are strongly related to each other.

Fibronectin adsorption/desorption

Adsorption properties of biomaterial surfaces are critical for interaction with cells. A variety of factors may affect FN adsorption, such as surface wettability [10–13], the

Table 3.
Adsorption/desorption of ^{125}I-FN

Material	FN adsorbed ($\mu g\,cm^{-2}$)	Desorption (%)
Glass	0.153	86
APS	0.201	28
PEL	0.215	36
PVC	0.282	42
SI	0.301	43

concentration of bulk proteins in the medium [2–4], the existence of a competitive removal of proteins [2, 3], and activity of some proteolytic enzymes [3]. To learn more about the interaction of FN with the different material surfaces tested under present experimental conditions, FN adsorption was studied after 60 min incubation at ambient temperature from a single solution containing ^{125}I-FN. Desorption of ^{125}I-FN was measured after 4 h incubation of the same surfaces in the presence of 10% FBS. The results from these experiments are calculated as surface concentration of FN in $\mu g\,cm^{-2}$ (see Table 3). A clear tendency for higher FN adsorption with decreasing surface wettability of the materials has been found. The adsorption of FN was 0.15 $\mu g\,cm^{-2}$ for glass, and increased gradually in the following order: glass < APS < PEL < PVC < SI, to about 0.3 $\mu g\,cm^{-2}$ for SI.

The results for ^{125}I-FN desorption measured after 4 h of incubation in the presence of 10% FBS are also shown in Table 3. It was found that glass expressed almost complete desorption of FN, because only 14% of adsorbed FN was retained on the surface after 4 h. The other substrata, however, represented a slight increase of desorption for the high adsorbing substrata, such as PVC and SI. It was observed that the moderate wettable APS expressed the lowest desorption of FN, which was only about 30%.

DISCUSSION

It is generally accepted that the physicochemical properties of a biomaterial are key determinants for the adsorption of proteins influencing the quantities and conformation of adsorbed cell adhesion proteins [2–4, 10–13, 22] which, in turn, mediate cell attachment to the material surface [3, 10, 13]. Previously, surface wettability has been implicated to be an important feature that may affect biocompatibility through different adsorption of FN [10–13]. However, the role of cells with respect to their ability to synthesize and secrete adhesive proteins, such as FN, and to organize them in a specific matrix structure [18], remains unclear. Recently, we have shown that removal and reorganization of adsorbed FN varied significantly with the wettability of material surfaces [14, 15]. For example, unlike glass, fibroblasts were unable to reorganize FN adsorbed on a hydrophobic octadecylsilane-coated surface (water-contact angle 95 deg) [14], as well as on other less wettable surfaces possessing water-contact angles above 50–60 deg [15]. As FN removal depends on the exchange of plasma

proteins on the substratum [17] it seemed reasonable that stronger FN adsorption on hydrophobic surfaces might be responsible for decreased FN reorganization [13, 14].

In the present study we have investigated the endogenous FN matrix formation by human fibroblast cultured for 72 h onto a series of surfaces; their water contact angles ranging from 25 to 105 deg. These experiments were carried out to answer the question of how the surface wettability affects FN deposition and matrix assembly on biomaterials. Our current findings show that FN was easily secreted and deposited on hydrophilic glass and moderate wettable APS, as demonstrated by the immunofluorescence microscopy studies. However, with decreasing wettability of the materials, deposition of FN was significantly diminished. These differences were confirmed quantitatively by ELISA for secreted FN, where the values showed the same reduction in the FN deposition with the decrease in wettability. It is noteworthy, that the cellular FN matrix deposition was inverse to the FN adsorption from solutions obtained by ^{125}I-labeled FN. It was then observed that less wettable substrata bound substantially higher amounts of FN from single solutions than more hydrophilic surfaces. This fact leads to the first conclusion; that there is a distinct difference between the passive FN adsorption from solutions and the active process of FN matrix formation by the cells.

The second important finding was the different organization of the FN matrix in dependence on the surface wettability. From the high magnification micrographs in Fig. 2, it is evident that fibrillar organization of FN matrix appears on relatively wettable materials such as glass and APS, and only partly on PEL. However, on more hydrophobic materials like PVC and SI, cells can secrete small quantities of FN but are not able to organize a FN matrix. In accordance with our previous findings for the reorganization of adsorbed FN [14, 15], one can assume that stronger binding of FN on relatively hydrophobic substrata [10, 11, 15, 22] may be one reason why cells can not remove newly secreted FN from the substratum and organize it into a matrix. However, our quantitative data concerning FN desorption in medium containing 10% FBS used for culturing fibroblasts did not support this possibility. For example, as shown in Table 3, there was a significant higher desorption of ^{125}I-FN from glass than from APS, while FN matrix formation on both surfaces was almost identical. In contrast, the higher desorption of FN from more hydrophobic materials, like PVC and SI was accompanied by a complete absence of FN matrix organization. High desorption of FN from hydrophobic materials like PVC was shown previously, and was found to be due to multilayer adsorption of the protein [23] which desorbs more easily. It seems reasonable that such FN cannot be involved in the process of FN matrix formation. Another reason for the lack of FN matrix formation on hydrophobic materials may be that adsorption of FN on hydrophobic substrata leads to significant changes in protein conformation, which may diminish the interaction with cells [10–12]. We have shown recently that fibroblast adhering on hydrophobic materials express an impaired signaling via integrins [24, 25]. Since signaling via integrins is involved in the upregulation of genes controlling protein synthesis [7, 26], decreased secretion of FN by cells adhering on hydrophobic substrata may be a further consequence. Likewise, we have demonstrated with monoclonal antibodies, that cell and heparin binding domains are less well recognized in FN preadsorbed

on hydrophobic surfaces [25]. Hence, adsorption of secreted FN on hydrophobic substrata seems diminish its interaction with $\alpha_5\beta_1$ integrin, which is important for the arrangement of FN into a matrix structure [27, 28].

In the present study we have also observed that decreasing wettability of the substratum may alter not only FN matrix formation, but also normal cell morphology and spreading, which is in accordance with literature data [10, 29], and our previous investigations [14, 15]. Also in agreement with these studies we have found a diminished cell growth on less wettable materials in the present investigation. We have measured simultaneously both cell proliferation (XTT assay) and FN matrix deposition (ELISA assay). As we could demonstrate, there is a clear relationship between fibroblast proliferation and the amount of FN matrix deposited on the substratum (see Fig. 3), suggesting that the ability of cells to organize an extracellular matrix is a prerequisite for successful cell–biomaterial interaction. Moreover, it was found that there is a steep decrease of matrix synthesis and cell proliferation around 70 deg water-contact angle (see Tables 1 and 2). Comparable results were discovered for fibroblasts cultured on wettability gradient surfaces, where a profound decrease in cell adhesion, spreading, and proliferation was detected for water-contact angles greater than 60 deg [29, 30]. Similar studies dealing with gradient surfaces and adsorption of FN found that FN antibody adsorption was maximal between 50 and 60 deg, though adhesion of cells in this experimental model was almost absent [31]. Increasing adsorption of FN was detected to run in parallel with decreasing FN antibody binding and cellular outgrowth [32]. In light of these facts we may conclude that a water-contact angle of about 70 deg is some threshold, above adsorption of FN (plasmatic or cellular) may lead to severe conformational changes that diminish the interaction with the cellular FN receptor. Necessary interactions for FN fibrillization between the $\alpha_5\beta_1$ integrin and specific sequences of FN [33, 34] might be inhibited resulting in a diminished matrix formation which in turn is a prerequisite for successful function of anchorage dependent cells [18].

Indeed we have to consider that not only the wettability of materials has been different in this study, but the materials may vary in other physicochemical surface properties such as surface charges, too. This can be illustrated by the peculiar behavior of glass regarding the high FN desorption that may be related to the negative surface charge of glass while the other materials are positively or non-charged. Therefore, future research will be devoted to the interplay between wettability, surface charges, and biological responses. Overall this study has shown that the quantification of FN deposition and the investigation of its structural organization on biomaterials might be a sensitive measure for the biocompatibility of materials.

Acknowledgements

This research was supported by Deutsche Forschungsgemeinschaft grants Gr 1290/4-1 and 436 BUL 113/80/2, and by Bulgarian National Science Fund grants L-404/94 and K-523/95. The authors are thankful to Mrs. Götz for measuring the contact angles.

REFERENCES

1. H. Wolf, R. Karwath and Th. Groth, in: *Advances in Biomedical Measurements*, E. R. Carson, P. Kneppo and I. Krekule (Eds), p. 133. Plenum Press, New York, London (1988).
2. J. D. Andrade and V. Hlady, *Prog. Surface Sci.* **79**, 1 (1986).
3. F. Grinnell, *Int. Rev. Cytol.* **53**, 65 (1978).
4. G. K. Imamoto, L. C. Winterton, R. S. Stoker, R. A. Van Wagenen, J. D. Andrade and D. F. Mosher, *J. Colloid Interface Sci.* **106**, 459 (1985).
5. S. K. Akiyama, K. Nagata and K. M. Yamada, *Biochim. Biophys. Acta* **1031**, 91 (1990).
6. S. M. Albelda and C. A. Buck, *FASEB J.* **4**, 2868 (1990).
7. R. O. Hynes, *Cell* **69**, 11 (1992).
8. L. J. Kornberg, H. S. Earp, C. E. Turner, C. Proskop and R. L. Juliano, *Proc. Natl. Acad. Sci. USA* **88**, 8392 (1991).
9. Y. Ikada, in: *Polymers of Biological and Biomedical Significance*, W. Shalaby, Y. Ikada, R. Langer and J. Williams (Eds), p. 35. ACS Symposium Series 540, Washington, DC (1994).
10. F. Grinnell and M. Feld, *J. Biomed. Mater. Res.* **15**, 363 (1981).
11. F. Grinnell and M. Feld, *J. Biol. Chem.* **257**, 4888 (1982).
12. U. Jonsson, B. Ivarsson, I. Lundstrom and L. Berghem, *J. Colloid Interface Sci.* **90**, 148 (1982).
13. D. J. Iuliano, S. S. Saavedra and G. A. Truskey, *J. Biomed. Mater. Res.* **27**, 1103 (1993).
14. G. Altankov and Th. Groth, *J. Mater. Sci. Mater. Med.* **5**, 732 (1994).
15. G. Altankov, F. Grinnell and Th. Groth, *J. Biomed. Mater. Res.* **30**, 385 (1996).
16. A. Avnur and B. Geiger, *Cell* **25**, 121 (1981).
17. F. Grinnell, *J. Cell. Biol.* **103**, 2697 (1986).
18. J. A. McDonald, *Ann. Rev. Cell Biol.* **4**, 183 (1988).
19. W. Henkes, C. Doppler, R. Eckert, H.-P. Halbritter, E. Russmann and B. Stier, *BioTec 2*, p. 1. Vogel Verlag und Druck KG, Würzburg, Germany (1993).
20. E. Engvall and E. Ruoslahti, *Int. J. Cancer* **20**, 1 (1977).
21. D. J. Yamashita, B. Tycko, S. R. Fluss and F. R. Maxfield, *Cell* **37**, 789 (1984).
22. W. Norde and J. Lyklema, *J. Biomater. Sci. Polymer Edn* **2**, 183 (1991).
23. L. C. Winterton, J. D. Andrade, J. Feijen and S. W. Kim, *J. Colloid Interface Sci.* **111**, 314 (1986).
24. Th. Groth and G. Altankov, *J. Biomater. Sci. Polymer Edn* **7**, 297 (1995).
25. Th. Groth and G. Altankov, *Biomaterials* **17**, 1227 (1996).
26. R. L. Juliano and S. Haskill, *J. Cell Biol.* **120**, 577 (1993).
27. K. Wennerberg, L. Lohinkangas, D. Gullberg, M. Pfaff and S. Johansson, *J. Cell Biol.* **132**, 227 (1996).
28. C. Wu, V. M. Keivens, T. E. O'Toole, J. A. McDonald and M. H. Ginsberg, *Cell* **83**, 715 (1996).
29. J. H. Lee and H. B. Lee, *J. Biomater. Sci. Polymer Edn* **4**, 467 (1993).
30. T. G. Ruardy, J. M. Schakenrad, H. C. van der Mei and H. J. Busscher, *J. Biomed. Mater. Res.* **29**, 1415 (1995).
31. R. L. Williams, J. A. Hunt and P. Tengvall, *J. Biomed. Mater. Res.* **29**, 1545 (1995).
32. D. K. Pettit, A. S. Hoffman and T. A. Horbett, *J. Biomed. Mater. Res.* **28**, 685 (1994).
33. D. C. Hocking, R. K. Smith and P. J. McKeown-Longo, *J. Cell Biol.* **133**, 431 (1996).
34. J. L. Sechler, Y. Takada and J. E. Schwarzbauer, *J. Cell Biol.* **134**, 573 (1996).

Publikation 7

Georgi Altankov, Thomas Groth, Natalia Krasteva, Wolfgang Albrecht, Dieter Paul (1997).

Morphological evidence for a different fibronectin receptor organization and function during fibroblast adhesion on hydrophilic and hydrophobic glass substrata.

Journal of Biomaterials Science – Polymer Edition **8**, 721-740.

J. Biomater. Sci. Polymer Edn, Vol. 8, No. 9, pp. 721–740 (1997)

Morphological evidence for a different fibronectin receptor organization and function during fibroblast adhesion on hydrophilic and hydrophobic glass substrata

GEORGI ALTANKOV,[1,*] THOMAS GROTH,[2,*] NATALIA KRASTEVA,[1] WOLFGANG ALBRECHT[2] and DIETER PAUL[2]

[1] *Institute of Biophysics, Bulgarian Academy of Sciences, Str. Acad. G. Bonchev, Bl. 21, 1113 Sofia, Bulgaria*
[2] *GKSS Forschungszentrum, Institut für Chemie, Abteilung Membranforschung, Kantstrasse 55, 14513 Teltow, Germany*

Received 27 January 1997; accepted 7 March 1997

Abstract—A polyclonal antibody against the $\beta 1$ subunit of the fibronectin (FN) receptor was used to mimic the early events of integrin receptor functioning to study the initial cellular processes during the organization of FN matrix on biomaterials. Hydrophilic glass and hydrophobic octadecylsilane (ODS) surfaces have been applied as models for different biocompatible materials. By immunofluorescence we could demonstrate that FN receptors organize on the dorsal cell surface of adhering fibroblasts in a specific linear pattern along with actin filaments, but only if the cells were attached to hydrophilic glass. In contrast, FN receptors were not reorganized on hydrophobic octadecylsilane (ODS). In parallel experiments, FN matrix formation after 72 h of incubation on the same substrata has been analyzed microscopically, and quantified by cell ELISA, in order to be further correlated with the integrin receptor functioning in contact with the biomaterials. It was found that FN structuring and the amount of FN matrix have been significantly diminished on ODS that was related to the observed changes in integrin receptor functioning. To learn more about the mechanism of this phenomenon, desorption of ^{125}I-FN from these substrata was studied and found to be significantly decreased on hydrophobic ODS. As a consequence, FN receptor (function) might be arrested on the ventral cell surface, thus the important role of $\beta 1$ integrins in the positional organization of the FN matrix may be disturbed. In light of these facts, antibody-induced clustering of FN receptor can be considered as a useful model for studying the early steps of FN matrix formation on biomaterials.

Key words: Fibronectin; $\beta 1$ integrin; matrix deposition; biomaterials; wettability.

*To whom correspondence should be addressed:
Georgi Altankov at E-mail: altankov@obzor.bio21.acad.bg
Thomas Groth at E-mail: Thomas.Groth@gkss.de

INTRODUCTION

Attachment, spreading, and function of cells on foreign surfaces is critical for the compatibility of biomaterials when they are considered for implantation as cardiovascular prosthesis, bone implants, skin substitutes, etc. According to current knowledge, initial interaction of cells with foreign materials begins with the adsorption of proteins [1], and among them it seems that fibronectin (FN) plays a crucial role [2, 3]. Many types of cells can attach, spread, and migrate to a different extent on a variety of extracellular glycoproteins adsorbed on the substratum including FN, laminin, vitronectin, and collagen [4]. These interactions occur through specific cell-surface receptors belonging to the integrin superfamily of cell adhesion molecules [4, 5]. Integrins are transmembrane heterodimeric glycoproteins composed of an α- and β-subunit present in almost all cells [4–6]. Cell adhesion is controlled by binding affinity and interaction kinetics between adhesive ligands and both integrin subunits. Subsequent events, however, such as lateral diffusion and organization of receptors [7], and interaction with the cytoskeleton [8] strengthens cell adhesion, inducing changes in cell morphology and behavior [4–6]. While the effects of different adhesive glycoproteins, especially FN on cell–biomaterial interaction [2, 3, 9, 10] have been extensively studied during the last decade, relatively little is known about the corresponding integrin receptor functioning in contact with the material surfaces.

Fibronectin is a major cell-adhesive glycoprotein secreted in soluble form by many normal and tumorigenic cells [11], that is involved in cell–biomaterial interactions [2, 3]. Beside its role in cell adhesion and migration, FN is able to polymerize into a disulfide-linked pericellular network in a multistep process that is under cellular control [12]. Recent investigations suggest that the FN matrix is imprinted with positional information that contributes to the direction of cell migration, most importantly, for the colonization and organization of tissues, for example in mesoderm formation [13, 14], or during the wound-healing process [15]. Cell migration along FN matrices may be important for the preservation of the left–right asymmetry of the embryo [16]. Furthermore, loss of capacity to form FN matrix, is a feature of the transformed phenotype [17], and restoration of FN matrix assembly correlates with reduced malignant behavior [18]. Thus, the generation of FN matrices is vital in vertebrate organisms [11]. We anticipate that such positional information of FN matrices might be important during cell–biomaterial interaction.

In a previous study we used a polyclonal antibody against $\beta 1$ subunits of the FN receptor to mimic the early events of integrin receptor clustering and organization on the membrane plane [19]. By immunofluorescence studies we could demonstrate that clusters of the FN receptor, initially distributed in discrete patches on the dorsal cell surface, quickly organized in a specific linear pattern presumably matching the future organization of the FN matrix [19]. Other investigations have shown that signal transfer (outside-in-signaling) can be induced by antibody-induced clustering of integrins leading to the phosphorylation of the pp130 protein [20], and FAK [21], or by interaction with the substratum adsorbed ligand [22, 23], thus reflecting the real biochemical signal transduction process transmitted by integrins.

On the other hand, it is long known that attachment and growth of anchorage-dependent cells are altered on hydrophobic surfaces [24–26], a fact that has been

recently attributed to the conformational changes of adsorbed FN [2, 3]. Although the mechanism of this phenomenon is still poorly understood [27], it was frequently used as a model for studying the biocompatibility of materials [22, 24, 26–28]. Previously, in a series of investigations with this model, we could demonstrate that FN matrix formation on the biomaterials surface is an important feature for their biocompatibility [29–32]. For example, FN matrix deposited on the substratum by adhering fibroblasts, utilizing the newly synthesized pool of FN [33], or those removed from the substratum (preadsorbed FN) [29, 30] was significantly altered on hydrophobic materials [29–32].

Here we describe the effect of substratum wettability on earlier cellular events, matching the initial positional organization of the FN matrix by integrins, using the above model of antibody-induced FN receptor clustering and organization on the dorsal cell surface of adhering fibroblasts. The receptor pattern was visualized by immunofluorescence as described previously [19]. In parallel experiments FN adsorption/desorption and FN matrix formation on hydrophobic and hydrophilic substrata has been analyzed, and quantified by ELISA [32], to be further correlated with the integrin receptor functioning in contact with biomaterials.

MATERIAL AND METHODS

Hydrophilic and hydrophobic substrata

To obtain hydrophilic surfaces glass slides (Menzel, Germany) were cleaned in a 9 : 1 mixture of 96% sulfuric acid, and 25% hydrogen peroxide for 15 min. After washing extensively with distilled water, glass slides were dried until use. To render the surface hydrophobic, cleaned dry glass slides were treated with octadecyldimethylchlorosilane (ODS). For that purpose, the slides were incubated in 5% (v/v) solution of ODS (purchased from Sigma) in hexane for 1 h, then rinsed with ethanol, washed with distilled water, and air-dried. The wettability of the materials was assessed by the sessile drop method with advancing and receding water contact angles.

FN adsorption/desorption

Human plasma FN was prepared by affinity chromatography on gelatin-Sepharose 4B according to Engvall and Ruoslahti [33], and further purified on heparin-Sepharose 4B.

Labeling of FN with ^{125}I was performed with the chloramine-T method [34]. Briefly, FN (500 $\mu g\,ml^{-1}$) was dissolved in PBS (150 mM NaCl, 1 mM K_2HPO_4, 5 mM NaH_2PO_4, pH 7.4), and 50 μl ^{125}I (IZOTOP, Budapest, Hungary) with an activity of 0.5 mCi were added. Iodination started by the addition of chloramine T (4 $mg\,ml^{-1}$ PBS) was stopped by adding sodium metabisulfite (8 $mg\,ml^{-1}$ PBS) after 45 s. ^{125}I-FN was separated from unreacted ^{125}I by filtration over a Sephadex G-25 column. The specific activity of ^{125}I-FN was measured with a gamma counter (LKB).

Protein adsorption was carried out with a diluted solution containing a mixture of ^{125}I-FN and native FN at a concentration of 20 $\mu g\,ml^{-1}$. This solution was added to six-well multiplates containing the different materials. After 60 min incubation at

ambient temperature, the materials were washed extensively with PBS, and activity was measured in the gamma counter. For desorption measurements, materials were incubated for 60 min with FN (20 $\mu g\,ml^{-1}$), washed with PBS, followed by a further incubation with fetal bovine serum FBS (10%) for the time indicated. After washing with PBS, the activity was measured with a gamma counter.

Cells

Human fibroblasts were obtained from fresh skin biopsy and used up to the ninth passage. The cells were grown in Dulbecco's Modified Eagle Medium (DMEM) containing 10% FBS (Sigma Chemicals Co., St. Louis, MO, USA) in a humidified incubator with 5% CO_2. Fibroblasts from nearly confluent cultures were harvested with 0.05% trypsin/0.6 mM EDTA (Sigma), and trypsin was neutralized with FBS.

Cell morphology, fibronectin receptor, and actin on fixed cells

Adhesion of fibroblasts was carried out in six-well tissue culture plates containing the slides. Fibroblasts (10^5 cells suspended in 3 ml DMEM, 10% FBS) were pipetted into each well and incubated in a CO_2 incubator for 2 h. Cell morphology was assessed directly from living cells with a Telaval 31 inverted phase contrast microscope (Carl Zeiss, Germany).

Attached cells to be processed for fluorescence microscopy were fixed with paraformaldehyde (3%) for 10 min, washed with PBS, permeabilized with 0.2% Triton X-100 for 5 min (if necessary), and saturated with 1% glycine, 1% bovine serum albumin (BSA) in PBS.

To detect actin, samples were incubated for 30 min at 37°C with 5 $U\,ml^{-1}$ fluorescein-conjugated phalloidin (Sigma), and washed with PBS.

For the visualization of $\beta 1$ integrin (FN receptor), cells were incubated for 30 min at 37°C with rabbit anti-$\beta 1$ antiserum (lot No. 3847, a generous gift from Dr. K. Yamada, National Institute of Health, USA), diluted in PBS (with Ca^{2+} and Mg^{2+}) containing 1% BSA followed by fluorescein-conjugated goat anti-rabbit IgG (Jackson Immuno Research, West Grove, USA) containing 10% normal goat serum (Sigma), for 30 min at 37°C.

At the end of the incubation samples were washed, mounted with Mowiol [35], and photographed with an Axiovert 100 inverted fluorescence microscope (Carl, Zeiss, Germany).

Fibronectin receptor clustering and visualization on living cells

Cells attached on surfaces for 1 h were incubated for another hour at 37°C with 10 $\mu g\,ml^{-1}$ polyclonal anti-$\beta 1$ receptor IgG in DMEM containing 1% BSA. The IgG was purified from a rabbit antiserum (see above) on protein A Sepharose according to Harlow and Lane [35]. The samples were washed three times with PBS, then fixed in 3% paraformaldehyde for 5 min, and stained with rhodamine conjugated goat anti-rabbit IgG (Jackson Immuno Research, USA) for 30 min at 37°C. Finally, the samples were mounted in Mowiol [35] and investigated with an Axiovert 100 fluorescence microscope (Carl Zeiss, Germany).

Fibronectin matrix formation

Approximately 5×10^5 cells in 3 ml medium containing 10% FBS were incubated for 72 h in 6-well tissue culture plates (Falcon, Becton Dickenson & Company, NJ, USA) containing glass or ODS slides. At the end of the incubation, cells were fixed with 3% paraformaldehyde in PBS. Fixed preparations with non-permeabilized cells were used for visualization and quantification of FN matrix deposition.

Fibronectin matrix deposited on the different wettable surfaces was detected by immunofluorescence using a specific anti-human FN matrix mouse monoclonal antibody (Immunotech SA, France, lot No. 0326), followed by Cy^3-conjugated goat anti-mouse secondary IgG_1 antibody (Jackson Immuno Research, USA). The samples were then mounted. Further investigations and microphotography was carried out by both phase contrast and immunofluorescence microscopy with an Axiovert 100 inverted fluorescence microscope (Carl Zeiss, Germany).

Quantification of FN matrix formation

Fibronectin matrix deposition by human fibroblasts was quantified by ELISA as described previously [32]. Briefly, glass and ODS surfaces were covered by a reusable tissue culture vessel made of silicone (Flexiperm Slide, Hereaus Instruments, Germany), forming eight small chambers for cell culture per slide. 2.5×10^4 cells ml^{-1} suspended in DMEM with 10% FBS were added and cultivated for 72 h, then the cells were fixed with 3% paraformaldehyde, saturated with 1% BSA and 1% glycine for 15 min, and stained using the same anti-human FN matrix antibody as for the immunofluorescence investigations (see above), followed by peroxidase conjugated goat anti-mouse (Jackson Immuno Research, USA) as a secondary antibody. Appropriate working dilution for primary and secondary antibodies were found in previous experiments. *o*-Phenylene diamine (OPD, 1 mg ml^{-1}) was used as chromogenic substrate and solved in 0.1 M citrate buffer with hydrogen peroxide (0.03%). OPD solution was added to the chambers and incubated for 10 min. The reaction was stopped by the addition of 2 M sulfuric acid in 0.1 M sodium sulfite. The solution was transferred to a microtitre plate and the optical density (OD) was measured at a wavelength of 492 nm with an Anthos reader (Anthos, Austria).

RESULTS

Contact angle measurements

The results of contact angle measurements are shown in Table 1. The glass surface has low advancing and receding contact angles demonstrating the hydrophilic nature of the substratum. In contrast, silanization rendered the glass hydrophobic which is indicated by the high advancing and receding contact angles. Differences between advancing and receding contact angles observed on both surfaces point to slight surface heterogeneity.

Table 1.
Wettability of material surfaces

Material	Water contact angle (deg)	
	Advancing	Receding
Glass	33.2	25.6
ODS	99.5	90.7

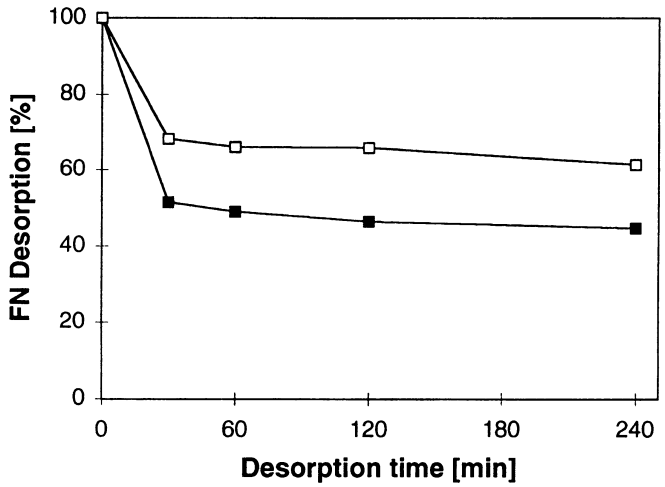

Figure 1. Desorption of ^{125}I-labeled FN from glass (■) and ODS (□). For measuring desorption of FN, surfaces were first incubated for 60 min at 37°C with FN dissolved in PBS (20 $\mu g\,ml^{-1}$). Desorption was measured after incubation of precoated surfaces in PBS with 10% FBS for the times indicated.

Fibronectin adsorption and desorption

Glass and ODS slides were incubated with ^{125}I-FN solution for 60 min at 37°C. The adsorption of ^{125}I-FN was found to be 0.13 $\mu g\,cm^{-2}$ on glass, and 0.24 $\mu g\,cm^{-2}$ on ODS. The slides were then washed with PBS and incubated up to 4 h in PBS containing 10% serum to study FN desorption. Figure 1 shows that FN was desorbed more easily from glass than from ODS, thus reflecting the stronger adsorption of this protein on the hydrophobic material.

Overall cell morphology

Figure 2 shows the overall phase contrast morphology of fibroblasts adhering for 2 h on plain glass (Fig. 2A) and ODS (Fig. 2B) substrata, as well as the effect of FN preadsorbed on glass (Fig. 2C) and ODS (Fig. 2D) substrata. On plain glass we found almost normal cell spreading and morphology, while on hydrophobic ODS the cells appeared rounder and much smaller in their main diameter because of the uncompleted cell spreading. Preadsorption of FN completely restored normal cell morphology on ODS reflected by the development of a more extended cell shape, and morphology. It

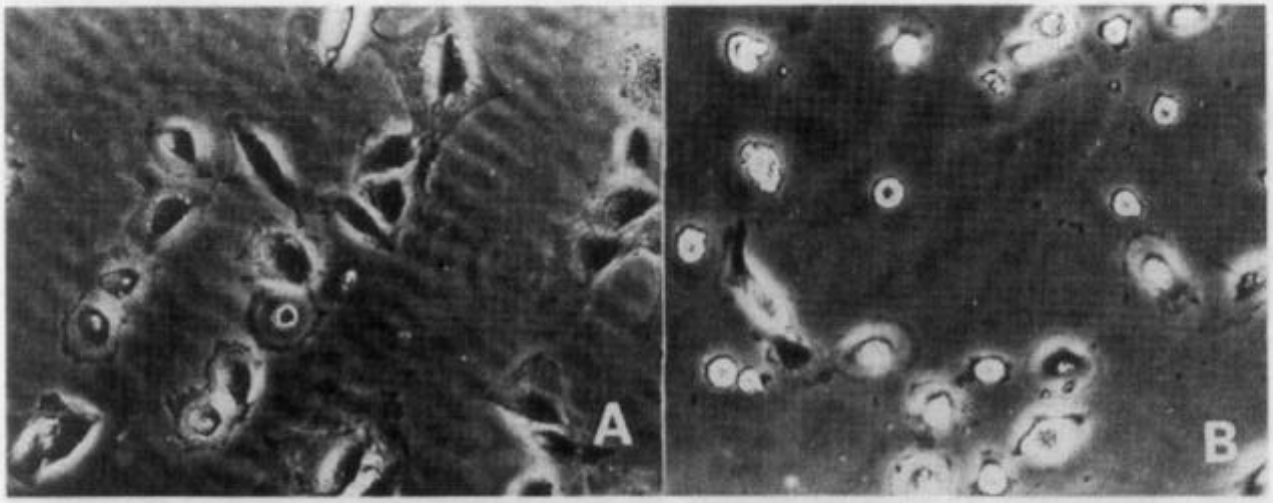

Figure 2. Overall cell morphology of fibroblasts adhering on plain glass (A) or FN coated glass (C) and on plain ODS (B), or FN-coated ODS (D) surfaces. Cells were incubated for 2 h at 37 °C in six-well plates containing glass or ODS coated slides some of which were pre-incubated with 20 $\mu g\,ml^{-1}$ FN for 30 min at 37 °C. At the end of incubations the cells were examined and photographed through phase contrast microscopy.

Figure 2. (Continued).

also improved cell spreading on glass almost unifying the cell morphology on these two different surfaces.

Organization of FN receptor on the ventral and dorsal cell surface

Figures 3 and 4, left panels, represent the organization of FN receptor on the ventral cells surface of fibroblasts adhering on plain glass and ODS, as well as on the same surfaces preadsorbed with FN. In these experiments the cells were incubated for 2 h, then fixed, permeabilized and stained with rabbit polyclonal anti-FN receptor antibody followed by rhodamine-conjugated goat anti-rabbit secondary antibody. On plain glass the cells possessed a typical distribution of the FN receptor in focal adhesions (Fig. 3A) while on ODS (Fig. 4A) such organization can not be seen. Only aggregates of FN receptor were found, that were dispersed irregularly; predominantly in the cell periphery. Preadsorption with FN increased the quantity and length of focal adhesions on glass (Fig. 3C), and restored the organization of the FN receptor on ODS comparable to glass (Fig. 4C). Fibroblasts were more spread and elongated, and pronounced clusters of local adhesions were concentrated in the directions of cell polarization, on both glass, and ODS.

The organization of the FN receptor on the dorsal cell surface was studied by specific antibody binding to living cells, as described earlier [19]. Cells were attached to the surfaces, either coated with FN, or not, for 1 h at 37°C, then anti-FN receptor polyclonal antibody was added at a final concentration of 10 $\mu g\,ml^{-1}$. Figures 3 and 4, right panels, show the distribution of FN receptor under these conditions. Only cells adhering on glass were able to organize antibody-tagged FN receptor in a typical fibrilar pattern (Fig. 3B) as elucidated before [19]. This effect was even more pronounced when glass was precoated with FN (Fig. 3D). In contrast, on ODS fibroblasts were not able organize the FN receptor (Fig. 4C). Even after precoating with FN more than 70% of the estimated 1000 cells failed to organize the FN receptor (Fig. 4D) (data not shown). In this case only single streaks of FN receptors were found predominantly at the cell periphery, representing the place of focal adhesion, that was co-localized with the FN fibrils accumulated (see below).

Co-localization of FN receptor and actin filaments on the dorsal cell surface

Double staining experiments were carried out to analyze the patterns of antibody-tagged FN receptor and arrangement of actin filaments of fibroblasts adhered on glass and ODS. Figure 5 shows the pattern of antibody induced FN receptor organization (right panel) and actin filaments (left panel) of cells attached on glass (Fig. 5A and B) and ODS (Fig. 5C and D) precoated with FN. The pattern of FN receptor organization on glass–FN ran in parallel with many of the longitudinal actin stress fibers (compare Fig. 5A and B), but not with circumferential organized fibers. On FN coated ODS, however, such a co-extensive pattern of FN receptor and actin filaments was generally absent (compare Fig. 5C and D).

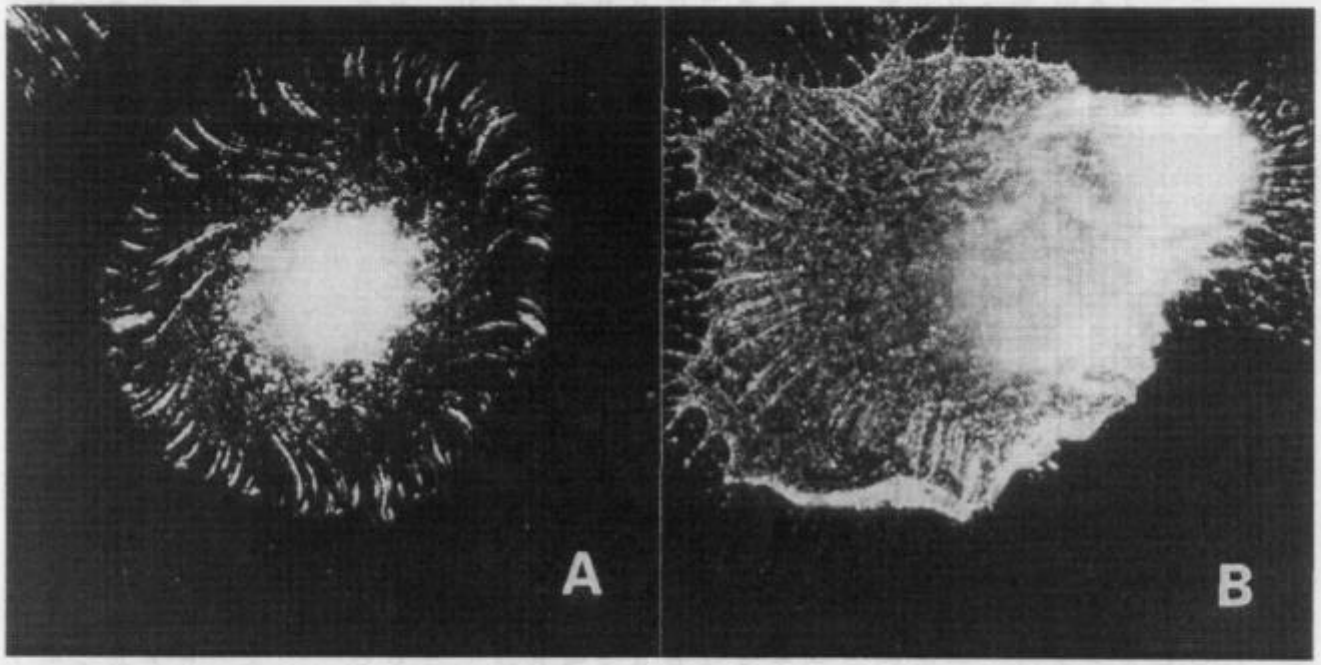

Figure 3. Organization of FN receptor on the dorsal (B, D) and ventral (A, C) cell surface of fibroblasts adhering on plain glass surface (A, B) or glass coated with FN (C, D). In (A) and (C), cells were cultured for 2 h at 37 °C, then fixed, permeabilized, and stained for FN receptor with polyclonal anti-β1 antibody followed by rhodamin-conjugated goat anti-mouse secondary antibody for 30 min at 37 °C each. In (B) and (D), cells were allowed to adhere on the glass surface for 1 h, and then anti-β1 polyclonal antibody was added in medium containing 1% BSA. The samples were incubated for 1 h more, then washed, fixed, and stained with secondary antibody as described above (bar length is 10 μm).

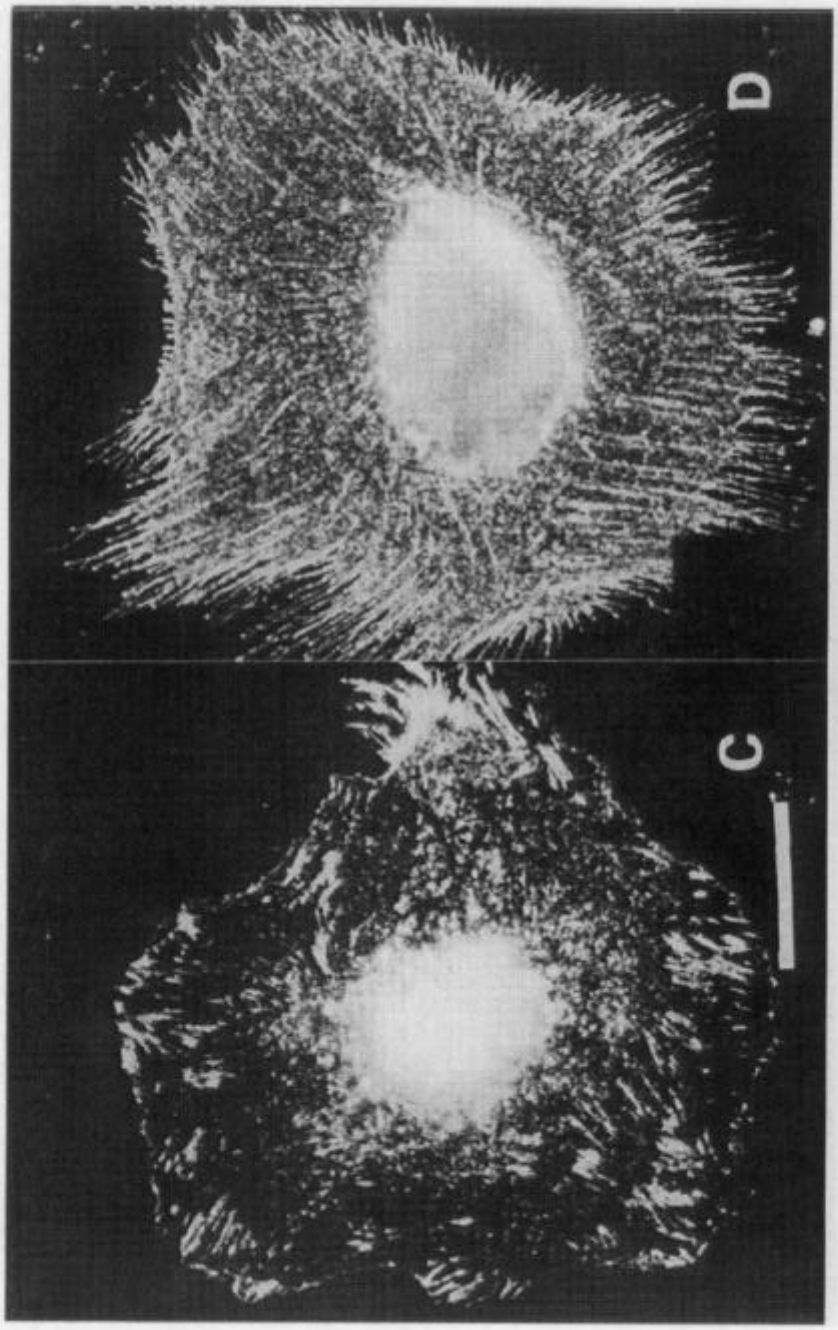

Figure 3. (Continued).

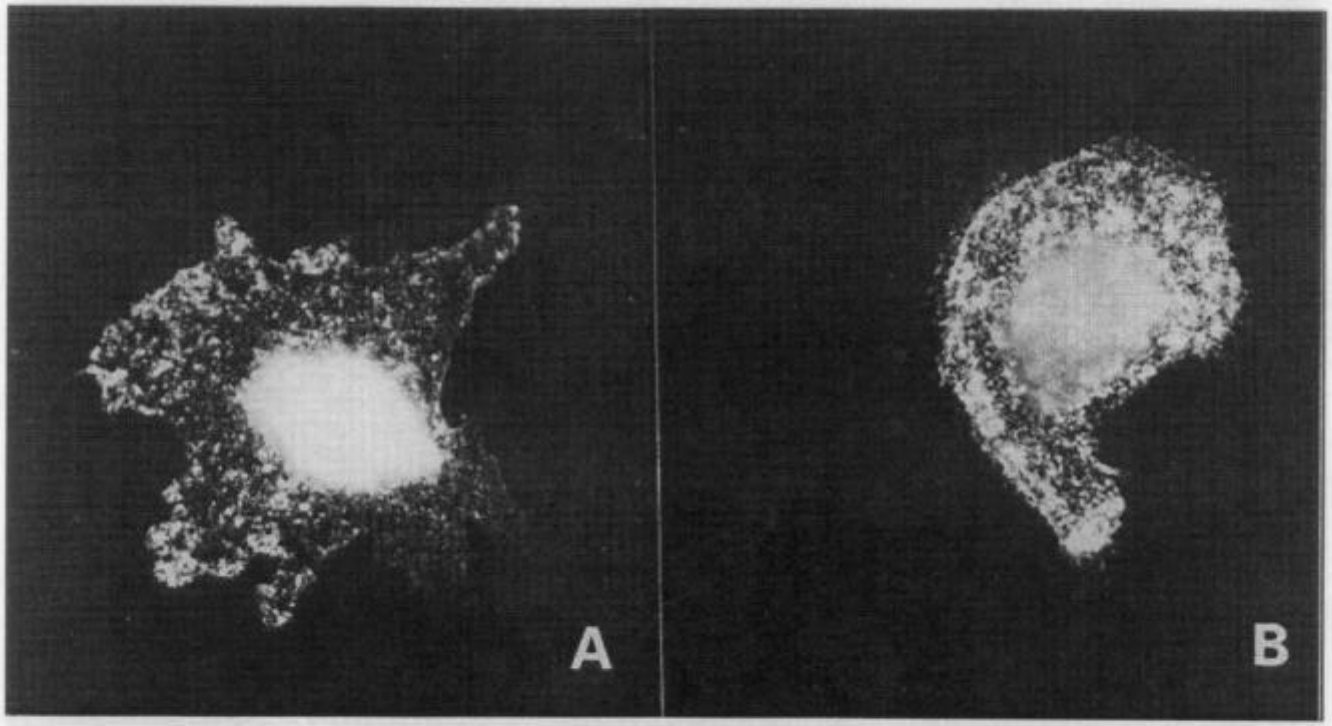

Figure 4. Organization of FN receptor on the dorsal (B, D) and ventral (A, C) cell surface of fibroblasts adhering on plain ODS (A, B) or ODS coated with FN (C, D). The samples were processed as described in Fig. 3.

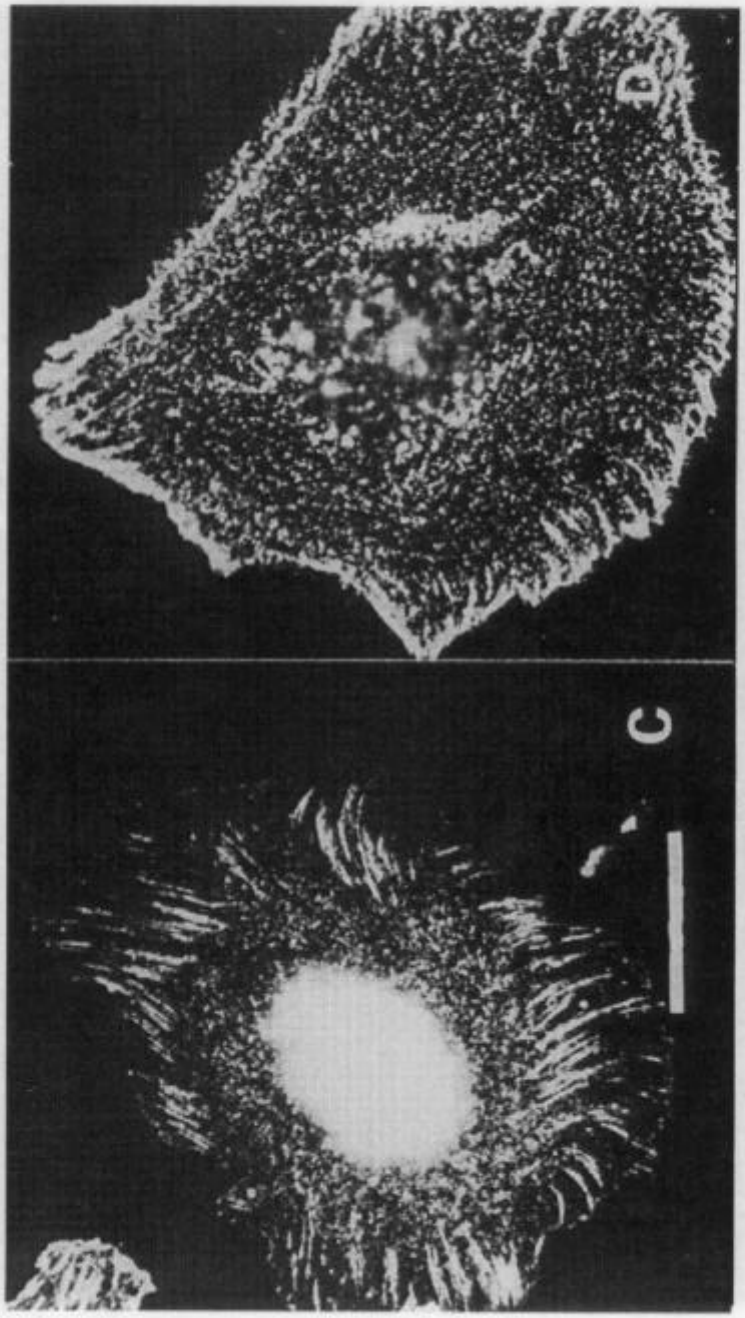

Figure 4. (Continued).

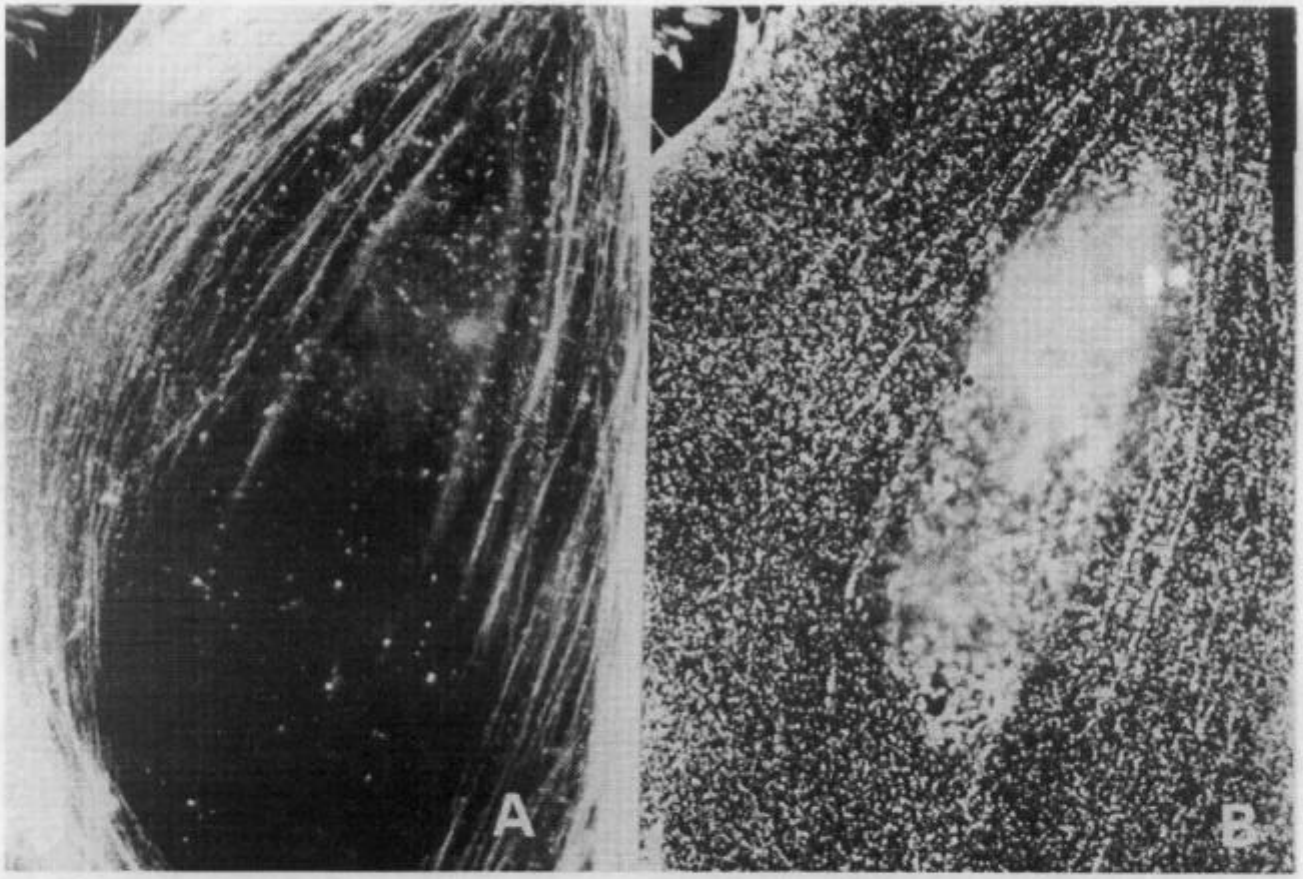

Figure 5. Co-localization of FN receptor (B, D) and actin cytoskeleton (A, C). Cells were incubated as described in Fig. 2B and D, on FN-coated glass (A, B), or FN-coated ODS (C, D). When the FN receptor was visualized the cells were further permeabilized and stained with fluorescein-labeled phalloidin for 30 min at 37 °C. The same cells were investigated and photographed through the red and green channel of the fluorescent microscope consequently (bar length 10 μm).

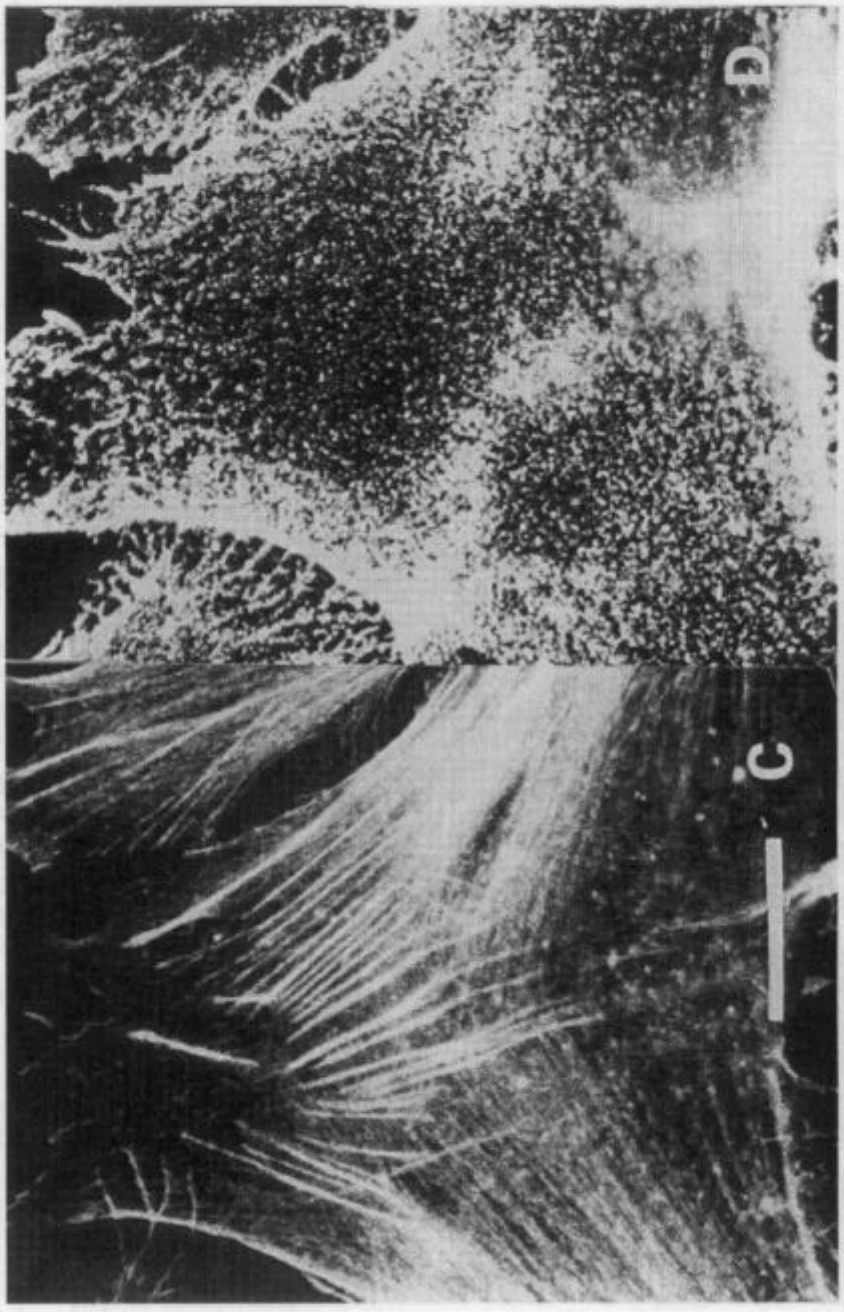

Figure 5. (Continued).

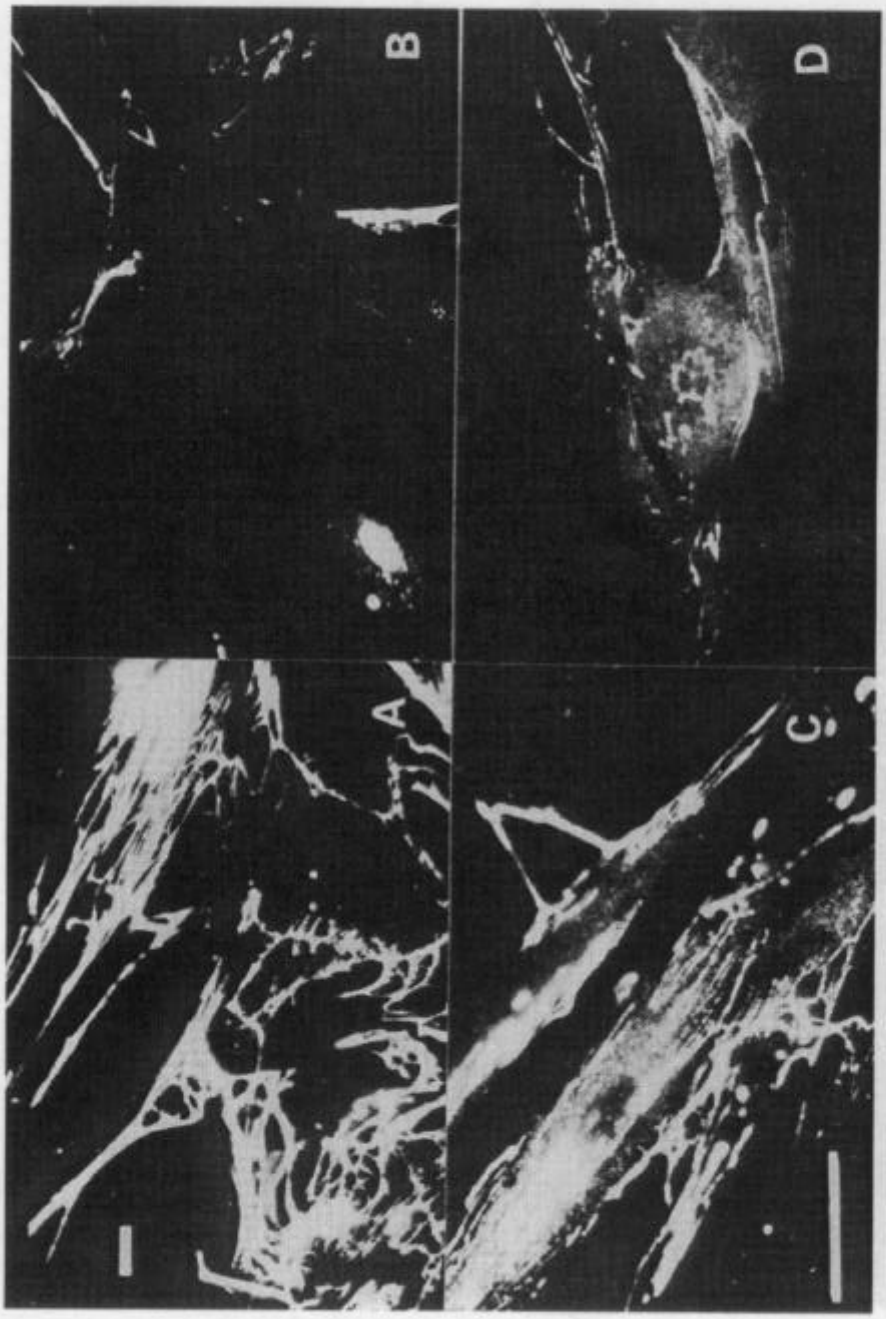

Figure 6. Fibronectin matrix formation on glass (A, C) and ODS (B, D). Human fibroblasts were cultured in DMEM containing 10% FBS for 72 h, fixed with paraformaldehyde, and stained for FN with monoclonal anti-ECM-FN antibody followed by rhodamin-conjugated goat anti-mouse secondary antibody for 30 min at 37°C each. Observation was carried out with fluorescence microscopy with low (A, B) and high magnification (C, D) (bar length 10μm).

Table 2.
Fibronectin matrix synthesis

Material	FN matrix synthesis (OD at 492 nm)
Glass	1.76 ± 0.26
ODS	1.32 ± 0.53

FN matrix synthesis was quantified by ELISA for FN after 72 h cultivation of fibroblasts on glass or ODS. Quantities are given as OD and were significantly higher for glass ($p \leqslant 0.01$, t-test). Values represent means $\pm$ SD ($n = 12$).

Fibronectin matrix formation

Under normal conditions cells continuously synthesize FN that is deposited on the substratum in a polymerized form by the involvement of a specific $\alpha 5\beta 1$ integrin function. In this respect studies on the FN matrix formation might be a sensitive measure for FN receptor functioning. In these experiments we did not study the effect of FN preadsorption because of the competitive effect of serum proteins on cell attachment on FN (data not shown). Alternatively, the plain surfaces could not be investigated in the absence of any dissolved proteins because fibroblasts can not grow under serum-free conditions.

Figure 6 shows the FN matrix formation after 72 h incubation of cells on glass and ODS in the presence of 10% FBS in the medium. The FN matrix was visualized by specific anti-human FN antibody. The immunofluorescence micrographs indicate a clear difference in FN matrix formation between hydrophilic and hydrophobic surfaces. As it is demonstrative on low magnification micrographs FN was deposited on glass as bright fibrilar structures that follow (but not exactly) the direction of cell polarization (see Fig. 6A). Conversely, on hydrophobic ODS significant smaller amounts of FN were deposited (Fig. 6B). Moreover, the FN was less organized in these preparations, as could be seen in high magnification micrographs (Fig. 6D) in comparison to glass (see Fig. 6C). Moreover, some of the deposited FN on ODS substrata displayed a dot-like pattern (Fig. 6D).

Cell ELISA for FN matrix

In order to get a quantitative measure for FN receptor functioning on different materials we used a cell ELISA method previously described [32]. Using this method we found significant differences between the quantities of FN matrix deposited on glass and ODS. As shown in Table 2, the OD from glass was significantly higher than that from ODS indicating a substantial increased matrix production on the hydrophilic glass surface.

DISCUSION

Several integrins have been reported to interact with FN (e.g. $\alpha 3\beta 1$, $\alpha 4\beta 1$, $\alpha 5\beta 1$, $\alpha_v\beta 1$, $\alpha_v\beta 3$, and $\alpha_v\beta 6$) [4–6, 36]. Among these, the $\alpha 5\beta 1$ has been shown to promote

FN polymerization [37]. $\alpha 5\beta 1$ binds FN to the cell surface, and possibly induces the conformational changes that seem to be required for FN polymerization [38]. In a previous study [19] we could demonstrate that antibody-induced clusters of $\beta 1$ integrin might organize in a specific linear pattern on the dorsal cell surface of adhering fibroblasts, presumably matching the initial positional organization of FN matrix. In this investigation the same approach has been used to study the early cellular events involved in FN matrix formation on biomaterial surfaces. After 1 h of antibody tag a typical linear pattern of $\beta 1$ integrin clusters has been found in fibroblasts adhering on glass, as previously described [19], but not on ODS. It was also observed that the FN receptor may colocalize, although not exactly, with the longitudinal stress fibers (see Fig. 5), suggesting the role of actin cytoskeleton for the initial linear arrangement of the FN receptor. Presumably, this transmembrane association with the cytoskeleton is realized through a reversible phosphorylation of the proteins involved in integrin–cytoskeleton link [39]. A significant tyrosine phosphorylation within the same period of time has been found in our previous investigations with fibroblasts adhering on glass, that was considerably diminished on ODS [22, 23]. Therefore, we conclude that antibody-induced FN receptor organization may reflect the early cellular events involved in FN matrix formation on biomaterials.

On ODS–FN the cells formed normal focal adhesions, very similar to those on FN-coated glass, but did not develop a linear organization of the FN receptor. This fact suggests that the adhesive interaction with the substratum is only the initial step in cell–biomaterial interaction, and must be followed by secondary events that are important to maintain normal cell functioning. This is supported by our previous findings that signaling via integrins [22, 23], as well as other parameters reflecting the tissue compatibility of materials, is impaired on ODS [22, 23, 28–31]. On the other hand, it is known that cells remove FN from focal adhesions [40], most probably as an attempt to organize it into a three-dimensional matrix meshwork. Immunoelectron microscopic studies also revealed that FN is absent from focal adhesions [41] and might be moved along with the actin filaments [8]. Therefore, it seems reasonable that the different adsorption, as well as the different conformation of adsorbed FN might be responsible for the observed differences in the biological properties of glass and ODS. Pettit *et al.* (1994) have suggested that the decreased outgrowth of cells on less wettable substrata might be connected with the lower desorption of proteins from those surfaces [42]. In the present study we show that ^{125}I labeled FN adsorbed much better on ODS in comparison to glass. As a consequence, the stronger adsorption of FN on ODS might arrest the FN receptors on the ventral cell surface, thus preventing their movement and organization in the plane of the membrane (along with longitudinal stress fibers). Indeed, we consider that about 50% of the total FN receptors face the ventral cell surface, and are, thus, relatively immobilized on ODS. Moreover, as mentioned above signal transduction via integrins including tyrosine phosphorylation of proteins involved in the integrin–cytoskeleton link is decreased on ODS. Therefore, the lack of organization of FN receptor along the actin filaments on the dorsal cell surface might be a direct consequence of the cellular contact with the hydrophobic substratum. This assumption is also supported by our previous investigation where we

have shown that hydrophobic materials bind FN that can not be reorganized in matrix-like structures, including on ODS [29, 30]. A similar effect of significantly diminished FN matrix formation from secreted FN (after 72 h) on ODS was demonstrated in the present study, in accordance with our previous investigations on other hydrophobic materials [31, 32].

These data suggest that cells not only passively bind to FN adsorbed secreted on biomaterials, but also need to remove and reorganize this protein on the substratum, presumably as an attempt to form their normal FN matrix. The antibody induced clustering of the FN receptor ($\beta 1$ integrin) can be considered as a useful model for studying integrin function during early steps of the extracellular matrix formation on biomaterials. Further investigations should be devoted to a better understanding of the mechanisms of integrin receptors function during cell–biomaterial interaction, and to learn how the surface properties of biomaterials might be improved to support normal cellular functions.

Acknowledgements

This work was partly supported by the Bulgarian Academy of Sciences, the Deutsche Forschungsgemeinschaft, and the GKSS Forschungszentrum. We are thankful to Ms. I. Stimming for measuring contact angles.

REFERENCES

1. J. D. Andrade and V. Hlady, *Prog. Surface Sci.* **79**, 1 (1986).
2. F. Grinnell and M. Feld, *J. Biol. Chem.* **257**, 4888 (1982).
3. F. Grinnell, *Ann. NY Acad. Sci.* **516**, 280 (1987).
4. R. O. Hynes, *Cell* **48**, 549 (1987).
5. T. A. Springer, *Nature* **346**, 425 (1990).
4. R. O. Hynes, *Cell* **69**, 11 (1992).
7. B. Geiger, *Cold Spring Harbor Symp. Quant. Biol.* **46**, 671 (1982).
8. K. Burridge, G. Nuckolls, C. Otey, F. Pavalko, K. Simon and C. Turner, *Cell Differ. Dev.* **32**, 337 (1990).
9. J. G. Steele, C. McFarland, B. A. Dalton, G. Johnson, M. D. M. Evans, C. R. Howlett and P. A. Underwood, *Biomater. Sci. Polymer Edn* **5**, 245 (1993).
10. P. B. van Wachem, C. M. Vreriks, T. Beugeling, J. Feijen, A. Bantjes, J. P. Detmers and W. G. van Aken, *J. Biomed. Mater. Res.* **21**, 701 (1987).
11. R. O. Hynes, *Fibronectins*. Springer-Verlag, New York (1990).
12. D. F. Mosher, I. Sottile, C. Wu and J. A. McDonald, *Curr. Opin. Cell Biol.* **4**, 810 (1992).
13. J. C. Boucaut, K. E. Johnson, T. Darribere, D. L. Shi, J. F. Riou, H. B. Bache and M. Delarue, *J. Dev. Biol.* **34**, 139 (1990).
14. R. Winkelbauer and M. Nagel, *Dev. Biol.* **148**, 573 (1991).
15. R. A. F. Clark and R. B. Colvin, in: *Plasma Fibronectin Structure and Function*, J. A. McDonald (Ed.), p. 197. Marcel Dekker, New York (1985).
16. H. J. Yost, *Nature* **357**, 158 (1992).
17. R. O. Hynes, I. U. Ali, A. T. Destree, A. T. Mautner, M. E. Perkins, D. R. Singer, D. D. Wagner and K. K. Smith, *Ann. NY Acad. Sci.* **312**, 317 (1978).

18. F. G. Giancotti and E. Ruoslahti, *Cell* **60**, 849 (1990).
19. G. Altankov and F. Grinnell, *Exp. Cell Res.* **216**, 299 (1995).
20. G. Kornberg, H. S. Earp, C. E. Turner, C. Prockop and R. L. Juliano, *Proc. Natl Acad. Sci. USA* **88**, 8392 (1991).
21. M. D. Schaller, C. A. Borgman, B. S. Cobb, R. R. Vines, A. B. Reynolds and J. T. Parsons, *Proc. Natl Acad. Sci. USA* **89**, 5192 (1992).
22. Th. Groth and G. Altankov, *J. Biomater. Sci. Polymer Edn* **7**, 297 (1995).
23. Th. Groth and G. Altankov, *Biomaterials* **17**, 1227 (1996).
24. F. Grinnell, M. Milam and P. Spree, *Biochem. Med.* **7**, 87 (1973).
25. E. T. den Braber, J. E. de Ruijter, H. T. J. Smits, L. A. Ginsel, A. F. von Recum and J. A. Jansen, *J. Biomed. Mater. Res.* **29**, 511 (1995).
26. D. J. Juliano, S. S. Saavedra and G. A. Truskey, *J. Biomed. Mater. Res.* **27**, 1103 (1993).
27. F. Grinnell and M. K. Feld, *J. Biomed. Mater. Res.* **15**, 363 (1981).
28. Th. Groth, I. Zlatanov and G. Altankov, *J. Biomater. Sci. Polymer Edn* **6**, 729 (1994).
29. G. Altankov and Th. Groth, *J. Mater. Sci. Mater. Med.* **5**, 732 (1994).
30. G. Altankov, F. Grinnell and Th. Groth, *J. Biomed. Mater. Res.* **30**, 385 (1996).
31. G. Altankov and Th. Groth, *J. Mater. Sci. Mater. Med.* **7**, 425 (1996).
32. G. Altankov and Th. Groth, *J. Biomater. Sci. Polymer Edn* **8**, 299 (1997).
33. E. Engvall and E. Ruoslahti, *Int. J. Cancer* **20**, 1 (1997).
34. D. J. Yamashita, B. Tycko, S. R. Fluss and F. R. Maxfield, *Cell* **37**, 789 (1984).
35. E. Harlow and D. Lane, in: *Antibodies. A Laboratory Manual*, p. 726. Cold Spring Harbor (1988).
36. M. Buck, R. Pytela and D. Sheppard, *J. Biol. Chem.* **267**, 5790 (1992).
37. C. Wu, J. S. Bauer, R. L. Juliano and J. A. McDonald, *J. Biol. Chem.* **268**, 21 883 (1993).
38. A. Molra, Z. Zhang and E. Ruoslahti, *Nature* **367**, 193 (1994).
39. M. A. Schwartz, *Trends Cell Biol.* **2**, 304 (1992).
40. A. Woods, J. R. Couchman, S. Johansson and M. Hook, *EMBO* **5**, 665 (1985).
41. W.-T. Chen and S. J. Singer, *J. Cell Biol.* **95**, 205 (1982).
42. D. K. Pettit, A. S. Hoffman and T. Horbett, *J. Biomed. Mater. Res.* **28**, 685 (1994).

Publikation 8

Thomas Groth, Georgi Altankov, Anelia Kostadinova, Natalia Krasteva, Wolfgang Albrecht, Dieter Paul (1999).

Altered vitronectin receptor (alpha v integrin) function in fibroblasts adhering on hydrophobic glass.

Journal of Biomedical Materials Research **44**, 341-351.

Altered vitronectin receptor (α_v integrin) function in fibroblasts adhering on hydrophobic glass

Thomas Groth,[1] Georgi Altankov,[2] Anelia Kostadinova,[2] Natalia Krasteva,[2] Wolfgang Albrecht,[1] Dieter Paul[1]

[1]*GKSS Research Center, Institute of Chemistry, Department Membrane Research, Kantstrasse 55, D-14513 Teltow, Germany*

[2]*Institute of Biophysics, Bulgarian Academy of Sciences, Acad. G. Bonchev Str. bl. 21, BG-1113 Sofia, Bulgaria*

Received 4 November 1997; accepted 4 September 1998

Abstract: Function of integrins is crucial for adhesion, movement, proliferation, and survival of cells. In a recent study we found impaired fibronectin receptor function on hydrophobic substrata (G. Altankov et al. J Biomater Sci Polym Edn 1997;8:712–740). Here, we have studied the distribution and function of the vitronectin receptor (α_v integrin) in fibroblasts adhering on hydrophilic glass and hydrophobic octadecyl glass (ODS). The morphology of fibroblasts and the organization of actin cytoskeleton were studied and found to be altered on ODS, where the cells did not spread and possessed condensed actin. Pretreatment of the surfaces with serum or pure vitronectin improved cell morphology on both substrata, resulting in the development of longitudinal actin stress fibers. It was found with biotinylated vitronectin that comparable quantities of vitronectin were adsorbed from single vitronectin solutions or serum on glass and on hydrophobic ODS. The organization of the vitronectin receptors on the ventral cell surface was investigated in permeabilized cells showing normal focal adhesions in fibroblasts plated on glass but none of these structures on ODS. The distribution of α_v integrin on the dorsal cell surface was studied on nonpermeabilized living cells after antibody tagging. While fibroblasts adhering on plain or serum-treated glass developed a linear organization of α_v integrin, cells on plain and serum-treated ODS were not able to reorganize the vitronectin receptor. Studies on signal transduction with antiphosphotyrosine antibodies revealed co-localization of α_v integrin and phosphotyrosine in focal adhesions on glass and serum-treated glass. However, signaling was almost absent on plain ODS and weak on serum-treated ODS. It was concluded that alterations in vitronectin receptor function on the ventral cell surface caused by the hydrophobic material surface inhibit signal transfer and subsequent intracellular events that are important for the organization and function of integrins. © 1999 John Wiley & Sons, Inc. J Biomed Mater Res, 44, 341–351, 1999.

Key words: vitronectin; α_v integrin; actin; biomaterials; tissue compatibility

INTRODUCTION

Foreign materials do not interact directly with tissue cells when they are implanted in the body. Adsorption of proteins, such as fibronectin (FN) and vitronectin (VN), from surrounding fluids is the first step of cell–biomaterial interaction,[1,2] followed by cell attachment and spreading.[3] Subsequently, cell growth and differentiation may be important for adoption of the implant.[4,5] It is well known that mammalian cells attach, spread, and grow better on wettable surfaces compared to hydrophobic materials.[6,7] In the past the different behaviors of cells were explained by conformational changes of adhesive proteins on hydrophobic substrata, resulting in altered biological properties.[8–10] However, how the cells can recognize changed biological properties of the adsorbed proteins still is under investigation.

Most cells are able to attach and migrate on a variety of extracellular matrix (ECM) glycoproteins, including FN, VN, laminin, and collagens.[11–13] These interactions occur mainly through specific cell surface receptors belonging to the integrin superfamily of cell adhesion molecules.[13–15] Integrins are heterodimeric glycoproteins consisting of noncovalently bound α and β subunits.[14–16] In general, cell–substratum interaction is controlled by the binding affinity of integrins and their clustering on the cell surface.[5,14–16] However ad-

Correspondence to: T. Groth; e-mail: Thomas.Groth@gkss.de; or G. Altankov; e-mail: altankov@obzor.bio21.acad.bg

Contract grant sponsor: Deutsch Forschungsgemeinschaft; contract grant number: GR 1290/4-2
Contract grant sponsor: Bulgarian National Science Fund
Contract grant sponsor: GKSS Forschungszentrum

 CCC 0021-9304/99/030341-11

ditional events, such as activation of specific signaling pathways[15,17,18] and interaction with the cytoskeleton, strengthen cell adhesion and induce changes in cell morphology and function.[19] Insights into the role of integrins in cellular adhesion may be obtained by localizing them, using immunofluorescence microscopy, on the surface of cultured cells.[20] To learn more about the initial stages of integrin function during cell–biomaterial interactions, we recently have been using antibodies that bind specifically to β_1 integrins and visualize them clustered in focal adhesion plaques where cell–surface contacts occur.[21] In these experiments we have demonstrated that less efficient spreading of fibroblasts on hydrophobic materials is accompanied by an altered clustering of integrins[21,22] as well as by lowered outside–in signaling, indicated by tyrosine phosphorylation, which adsorbed fibronectin provides to the corresponding β1 integrins and to the cell interior.[23] Recently, in a model study we showed that antibody tagging of β_1 integrin on the dorsal cell surface in living fibroblasts can induce a specific linear organization of this antibody receptor complex, presumably matching the initial cellular events of fibronectin matrix assembly.[24] Using this approach we demonstrated that hydrophobic biomaterials inhibit this FN receptor arrangement into a fibrillar pattern[25] as well as intracellular signaling[23] and subsequent extracellular matrix formation.[26]

Evidence from the literature suggests that VN adsorption on some biomaterial surfaces may play a greater role compared to FN with respect to attachment and spreading of anchorage dependent cells.[3,27] However, relatively little is known about the particular function and organization of the VN receptor on biomaterial surfaces. VN, together with FN, is the major cell adhesion and spreading factor existing in the plasma and in the extracellular matrix.[28,29] VN is recognized by a number of integrin heterodimers containing the common α_v subunit and distinct β subunits.[15,29] The main receptor for VN is $\alpha_v\ \beta_3$, but $\alpha_{IIB}\beta_3$, $\alpha_v\beta_1$, $\alpha_v\beta_5$, and $\alpha_v\beta_6$ heterodimers also have been described as recognizing this ligand.[15,29] Despite extensive investigations in this field, there are no data available on how the VN receptor is organized on different biomaterials and whether or not this receptor may become reorganized upon specific antibody tagging. Finally, it would be interesting to know if the VN receptor transmits the signals properly when living cells interact with hydrophobic materials.

Here we describe the functional organization of α_v integrin during fibroblast spreading on octadecylsylan (ODS) and glass as general models for hydrophobic and hydrophilic surfaces. Using a specific monoclonal antibody against α_v integrin, we demonstrated significant differences in the organization of this integrin in the plane of the membrane on both dorsal and ventral cell surfaces. We also showed that a decreased signaling via tyrosine phosphorylation in response to the hydrophobic surface correlates with less VN receptor clustering. Furthermore, we observed that this antibody can induce a linear organization of αv integrin on the dorsal cell surface of living cells adhering on glass but not on hydrophobic ODS. The possible implications of these phenomena in understanding the material surface biocompatibility are discussed herein.

MATERIALS AND METHODS

Hydrophilic and hydrophobic glass surfaces

Hydrophilic glass was prepared as previously prescribed[30] by immersion of glass slides (Menzel, Germany) in a 9:1 mixture of 96% sulfuric acid and 25% hydrogen peroxide for 15 min. After washing extensively with distilled water, the glass slides were dried until use. Hydrophobic silane surfaces were prepared by treatment of clean dry glass slides with octadecyldimethylchlorosilane (ODS).[31] For that purpose the slides were incubated in a 5% (vol/vol) solution of ODS (Sigma Chemicals Co., St. Louis, Missouri) in hexane for 1 h, then rinsed with ethanol, washed with distilled water, and air dried.

For some experiments glass and ODS slides were pretreated with pure fetal bovine serum (FBS, Sigma Chemicals Co., St. Louis, Missouri), VN, and FN dissolved in phosphate-buffered saline, pH 7.4 (PBS: 150 m*M* of NaCl and 5.8 m*M* of phosphate) for 1 h and washed afterwards with PBS.

Measurement of VN adsorption

The relative quantities of VN adsorbed from single VN solutions or from serum on glass and ODS were estimated with labeled VN by way of a technique that uses biotinylated VN. Biotinylation of VN was performed with a kit provided by Boehringer Mannheim, Germany. The surfaces were incubated with serum to which biotinylated VN (50 μg/mL serum) previously had been added (1, 10, or 100% serum) or with biotinylated VN dissolved in PBS (0.1, 1.0, or 10 μg/mL) at 37°C for 60 min. Then the surfaces were rinsed three times with PBS and streptavidin conjugated with peroxidase (Boehringer Mannheim, Germany) dissolved in PBS containing 1% bovine serum albumin (which was added to prevent nonspecific binding) and incubated for 60 min at room temperature (RT). Then surfaces were washed with PBS. o-Phenylene diamine (OPD; 1 mg/mL) dissolved in 0.1*M* of citrate buffer with 0.03% hydrogen peroxide was used as a chromogenic substrate. The chromogen solution was added to the samples, incubated at room temperature for 10 min, and then the reaction was stopped by the addition of 2*M* of sulfuric acid in 0.1*M* of sodium sulfide. The results are given as optical densities (OD) read at 492 nm and allow a semi-quantitative measure of the VN adsorption on glass and ODS. Plain glass and ODS slides have been used as controls showing that binding of streptavidin in the

absence of biotinylated VN was very low under these conditions.

Contact angle measurements

Water contact angle measurements were performed using a goniometer (Krüss, Germany) with the sessile drop method. Advancing and receding water contact angles were estimated on the plain surfaces or surfaces that were precoated with different concentrations of pure VN or serum. Surfaces were pre-adsorbed with vitronectin or serum for 60 min, then washed three times with PBS, and, finally, washed with distilled water to remove any remaining salts from the PBS. Surfaces were air dried and then contact angle measurements were carried out.

Cells

Human skin fibroblasts were obtained from fresh skin biopsies and used up to the 9th passage. The cells were grown in Dulbecco's modified Eagle medium (DMEM) containing 10% FBS in an humidified incubator with 5% CO_2. Fibroblasts from nearly confluent cultures were harvested with 0.05% trypsin/0.6 m*M* of EDTA (Sigma), and the trypsin was neutralized with FBS. The cells were washed three times with culture medium without FBS to remove any contaminating proteins.

If not otherwise indicated, the fibroblasts were seeded on glass or ODS and incubated in DMEM in the absence of FBS at 37°C for 2 h. The cells were incubated on plain surfaces, on surfaces precoated with VN (10 μg/mL), or on pure serum surfaces for 60 min.

Cell morphology and staining of actin

Approximately 5×10^5 cells in 3 mL of medium were incubated for 2 h in 6-well tissue culture plates (Falcon, Becton Dickenson & Company, New Jersey) containing glass or ODS slides. At the end of the incubation cells were fixed with 3% paraformaldehyde in PBS and observed with phase contrast microscopy. Staining of actin was performed with FITC–phalloidin (Sigma Chemicals Co., St. Louis, Missouri). Cell were permeabilized with 0.2% Triton X-100 for 5 min, washed with PBS, and incubated with 0.5 U/mL of FITC–phalloidin for 30 min. After washing with PBS, the slides were mounted with Mowiol.[32] Samples were viewed with immunofluorescence microscopy using an inverted fluorescence microscope, type Axiovert 100 (Carl Zeiss Jena, Germany).

Vitronectin receptor clustering and visualization

Visualization of the VN receptor on the ventral cell surface was achieved by incubation of fibroblasts for 2 h on glass or ODS. Then cells were fixed with 3% paraformaldehyde for 15 min, washed with PBS, permeabilized with 0.2% Triton X-100 for 5 min, and saturated with 1% glycine and 1% albumin in PBS for 15 min. After washing with PBS, monoclonal mouse anti-α_v or, in some instances, anti β_3 antibody (Cymbus Biotechnology Ltd., UK) diluted in PBS with 1% albumin was added and incubated for 30 min. Thereafter, polyclonal goat anti-mouse IgG conjugated with rhodamine (Jackson Immuno Research, West Grove, PA) diluted in PBS with 10% goat serum was added. After 30 min samples were washed, mounted with Mowiol, and viewed with fluorescence microscopy.

Organization of the VN receptor on the dorsal cell surface was studied in fibroblasts attached on glass or ODS for 60 min. These cells were washed with DMEM and incubated with monoclonal mouse anti-α_v receptor antibody (10 μg/mL in DMEM containing 1% albumin) for 60 min at 37°C. The samples were washed three times with PBS, fixed in 3% paraformaldehyde for 10 min, and stained with rhodamine-conjugated goat anti-mouse IgG for 30 min at 37°C. Finally the samples were mounted with Mowiol and investigated with fluorescence microscopy.

Double staining of VN receptor and phosphotyrosine or actin

The signal transfer from the substratum was visualized by staining proteins phosphorylated in tyrosine residues and co-localized with the α_v integrin on the ventral cell surface, as shown previously.[23] Fibroblasts were cultivated and processed, as described above, for staining of the VN receptor on the ventral cell surface. Then polyclonal rabbit antiphosphotyrosine antibody (Upstate Biotechnology, Lake Placid, NY) diluted in PBS with 1% albumin was added (30 min incubation), followed by incubation with FITC-labeled goat anti-rabbit IgG (Jackson Immuno Research, West Grove, PA) with 10% goat serum for 30 min. After being washed with PBS, the samples were mounted with Mowiol and studied with fluorescence microscopy.

To study the distribution of the vitronectin receptor on the dorsal cell surface and the co-localization with actin filaments, fibroblasts were processed, as described above, for staining of the vitronectin receptor. Then the cells were permeabilized with Triton X-100 for 5 min, washed with PBS, and incubated with 5 U/mL of FITC–phalloidin. Thereafter, the samples were mounted with Mowiol and viewed by fluorescence microscopy.

RESULTS

Vitronectin adsorption

The results of VN adsorption measurements by biotinylated VN, shown in Figure 1 (A,B), demonstrate that slightly more VN was adsorbed from single VN solutions or serum on ODS than from glass. The de-

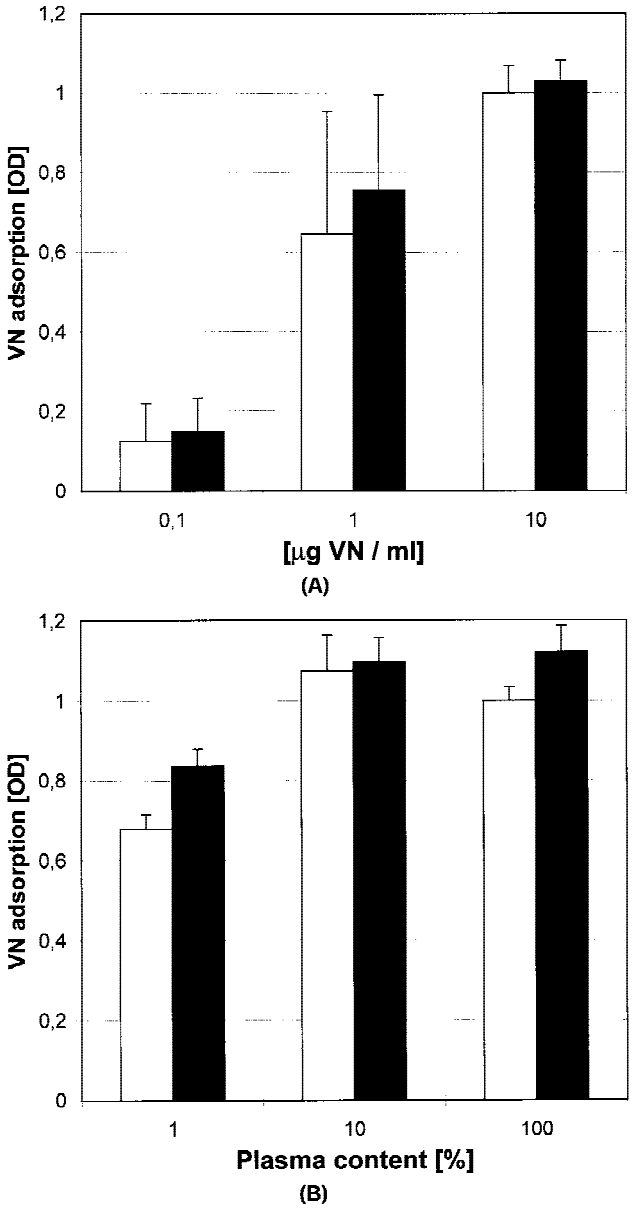

Figure 1. Adsorption of vitronectin. Glass (empty columns) and ODS (black columns) slides were incubated for 1 h with pure vitronectin solutions (A) or serum (B) diluted with PBS. Biotinylated vitronectin was used in the pure vitronectin solutions or was added to serum (50 µg VN/mL). Detection was carried out with streptavidin labeled with peroxidase using OPD as a substrate. Results represent means with standard deviations (n = 12) and are given as optical density (OD) measured at 492 nm.

crease of VN concentration during adsorption from 10 µg/mL to 1.0 and 0.1 µg/mL caused a reduction in the quantities of adsorbed VN, as indicated by the decreasing OD. In comparison, serum dilution to 10% yielded no detectable decrease in VN adsorption, which was observed when 1% serum was applied. Overall it can be stated that glass and ODS adsorbed comparable amounts of VN from single VN solutions and serum.

Contact angle measurements

Advancing and receding water contact angles were measured on plain glass and ODS or on surfaces that were precoated with increasing concentrations of vitronectin or serum. Figure 2 (A) shows that plain ODS had an advancing water contact angle of about 90° while the receding angle was about 85°. Plain glass had an advancing water contact angle of about 25° and a receding angle of about 15°. The observed hysteresis

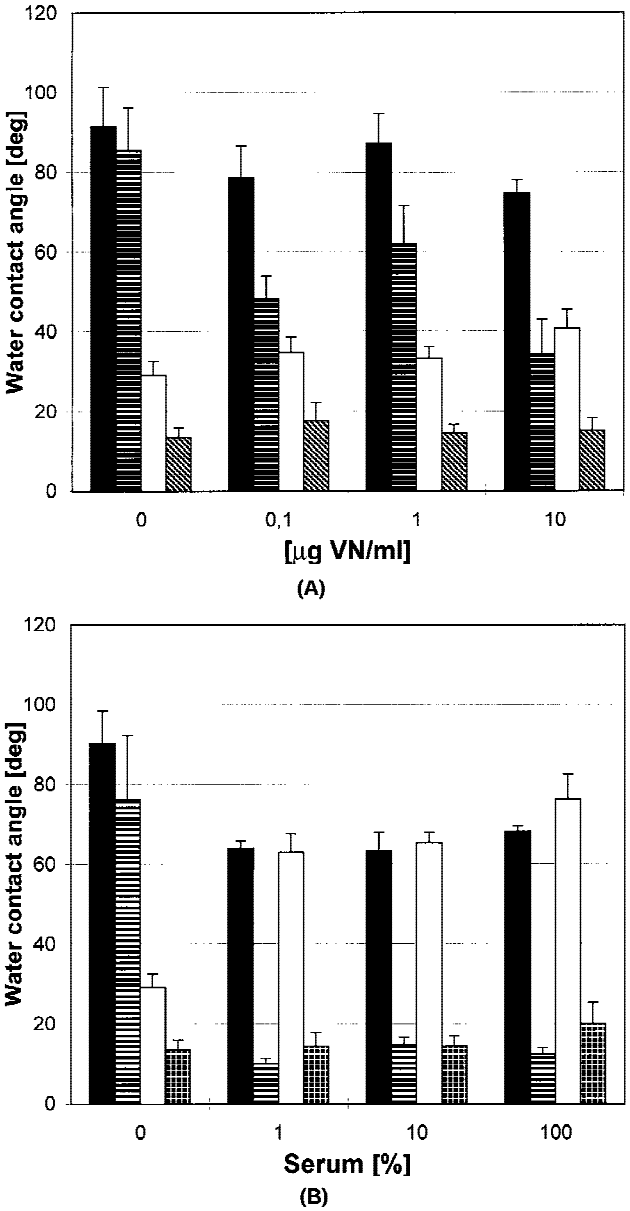

Figure 2. Water contact angle measurements. Water contact angles were measured on plain ODS and glass or after preadsorption of VN (A) or serum (B). Black bars = ODS advancing contact angle; black bars with horizontal lines = ODS receding contact angle; empty bars = glass advancing contact angle; shaded bars = glass receding contact angle. Results are given as means with standard deviations ($n \geq 10$).

on both surfaces indicates surface heterogeneity, which may be due to surface roughness or uneven distribution of the attached silane in the case of ODS. It was found that by pretreatment of surfaces with vitronectin, ODS became more hydrophilic, indicated by the decrease in advancing and receding angles, while glass became more hydrophobic, indicated by the increased advancing contact angles. The hysteresis was increased for both surfaces. Interestingly, the pretreatment of glass and ODS with serum, as shown in Figure 2(B), caused for an already very low serum content of 1% a uniformity of advancing and receding contact angles for both substrata. A steep increase in advancing contact angles was observed for glass, which tended then to rise slightly with increasing serum concentration. The precoating of ODS with increasing serum concentration caused a reduction of advancing and a dramatic drop in receding contact angles. Receding contact angles were similar for glass and ODS and changed little with increasing serum concentration.

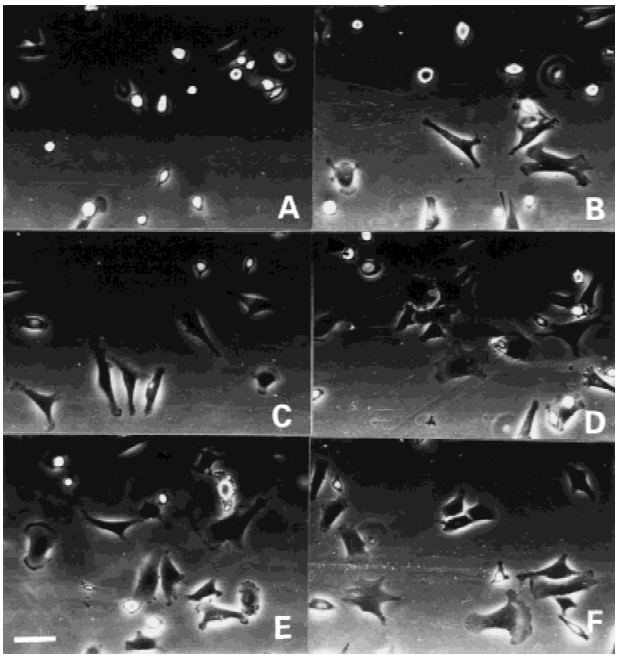

Figure 3. Overall cell morphology. Human fibroblasts were cultured under serum-free conditions on ODS (A,C,E) and glass (B,D,F) slides for 2 h. Some of the preparations were precoated with FBS (C,D) or pure vitronectin (E,F). At the end of incubation the fixed cells were observed and photographed under phase contrast microscopy. Bar = 50 μm.

Overall cell morphology and distribution of actin

Human skin fibroblasts were incubated for 2 h in serum-free medium on ODS and glass as well as on the same surfaces precoated with serum or with pure VN. Figure 3 demonstrates the overall cell morphology on these substrata. On plain glass almost normal cell spreading and morphology were found [Fig. 3 (B)] as compared with hydrophobic ODS where the cells appeared smaller and round because of insufficient cell spreading [Fig. 3 (A)]. Preadsorption with serum restored the normal cell morphology on ODS [Fig. 3(C)] and increased slightly the cell spreading on glass [Fig. 3 (D)]. It was assumed that this effect is related in part to the adsorption of VN from the serum because approximately the same cell number and morphology were found when both surfaces were coated with pure VN [Fig. 3 (E,F)], and it differed from cells attached to fibronectin-coated surfaces (not shown here). Moreover, in separate experiments (shown in Fig. 4) we could demonstrate that cells attached on VN [Fig. 4 (A)] and on serum [Fig. 4 (B)] but not on fibronectin [Fig. 4 (C)] expressed the β_3 integrin, a subunit of the main VN receptor, organized in focal adhesion contacts. Therefore, in further experiments serum-coated surfaces were used as a substratum for VN receptor studies.

A clear difference in the initial cell spreading also was observed when adhering fibroblasts were stained for actin (see Fig. 5). While on plain glass many of the cells expressed prominent stress fibers [Fig. 5 (B)], on ODS actin was present as much less organized clusters and aggregates [Fig. 5 (A)]. Coating the slides with serum could increase the stress fiber formation on ODS [Fig. 5 (C)]. Differences in the structuring of the cell cytoskeleton still could be observed. Longitudinal stress fibers were well pronounced on glass precoated with serum [Fig. 5 (D)], better than on glass, while on ODS–serum the predominant circumferential organization of actin filaments was obvious.

Organization of vitronectin receptor (α_v integrin) on the ventral and dorsal cell surface

Figure 6 represents the organization of VN receptor (α_v integrin) of fibroblasts adhering onto serum-coated glass, depending on the antibody treatment. If the a_v integrin antibody was added to living cells, during the second hour of incubation the α_v integrin was found to be linearly organized on the dorsal cell surface [Fig. 6 (A)], an effect very similar to one we previously have shown for the β_1 integrin.[24,25] To visualize the distribution of α_v integrin on the dorsal cell surface without antibody activation, fibroblasts were fixed and stained for α_v integrin without permeabilization, resulting in the appearance of a much less organized and almost diffuse distribution of small VN receptor aggregates [Fig. 6 (B)]. When fixed cells were permeabilized and stained with α_v integrin antibody, a typical pattern of VN receptor-rich clusters in focal

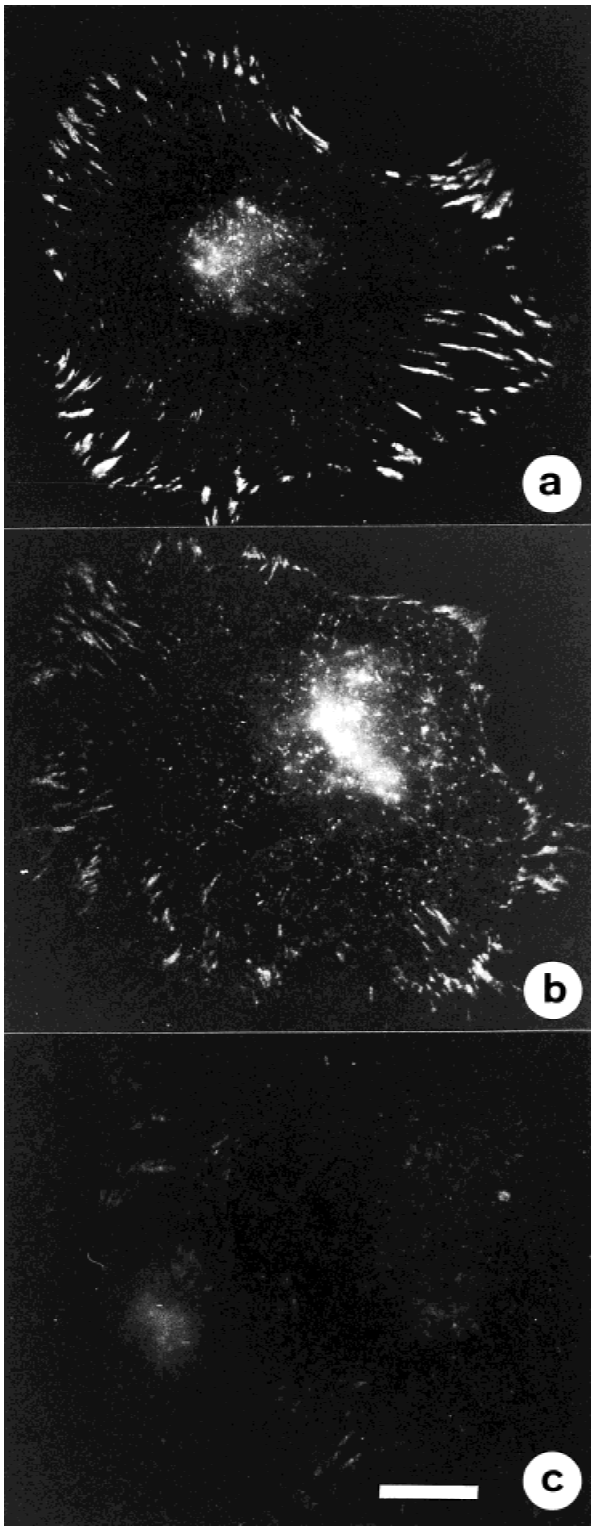

Figure 4. Comparison of β_3 integrin expression. Fibroblasts were plated for 2 h in the absence of serum on glass slides precoated with VN (A), serum (B), or FN (C), then fixed, permeabilized, and stained for β_3 integrin. Note that focal adhesions positive for β_3 integrin could be detected on VN- and serum-coated glass but not on FN. Bar = 10 μm.

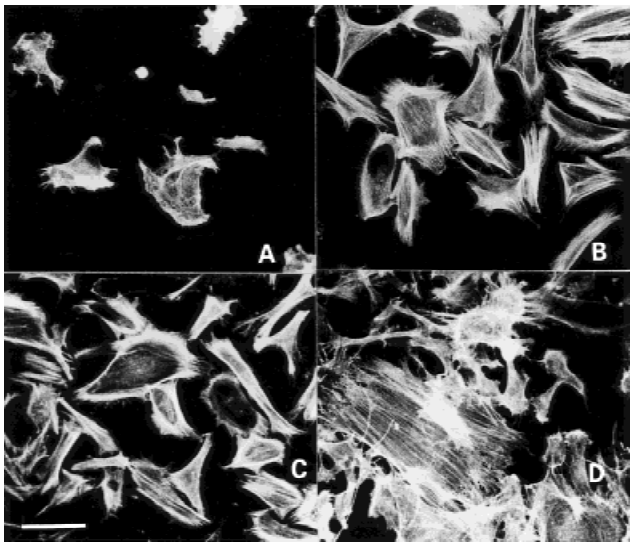

Figure 5. Visualization of actin cytoskeleton. Human fibroblasts were cultured, as described in Reference 32, on ODS (A,C) or glass (B,D) slides. Some of the preparations were studied alone, as plain surfaces (A,B); the others were precoated with FBS (C,D). At the end of the incubation, the cells were fixed and stained with FITC–phalloidin, then viewed and photographed with fluorescence microscopy. Bar = 50 μm.

adhesions was found [Fig 6 (C)]. These clusters were located on the ventral cell surface (faced toward the substratum) and their organization was completely different from those on the dorsal cell surface.

Co-distribution of α_v integrin on the ventral cell surface and phosphotyrosine activity

Double staining experiments were carried out to analyze both the organization of α_v integrins on the ventral cell surface and the cellular phosphotyrosine activity of fibroblasts adhering on ODS and glass. On hydrophobic ODS neither extended clusters of α_v integrin nor significant cellular phosphotyrosine activity in the cell periphery was detected [Fig. 7 (A,B)]. In contrast, some clusters of VN receptor in the area of cell–surface contacts were observed on glass with co-localized cellular phosphotyrosine activity [Fig. 7(C,D)].

When glass slides were precoated with serum, the cells became more spread and the main phosphotyrosine activity was co-localized with α_v integrins clustered in a well pronounced way with the focal adhesion plaques, as shown in Figure 8. However, it was apparent that on ODS both αv integrins and cellular phosphotyrosine [see Fig. 8 (A,B)] were less expressed compared to glass [Fig. 8 (C,D)].

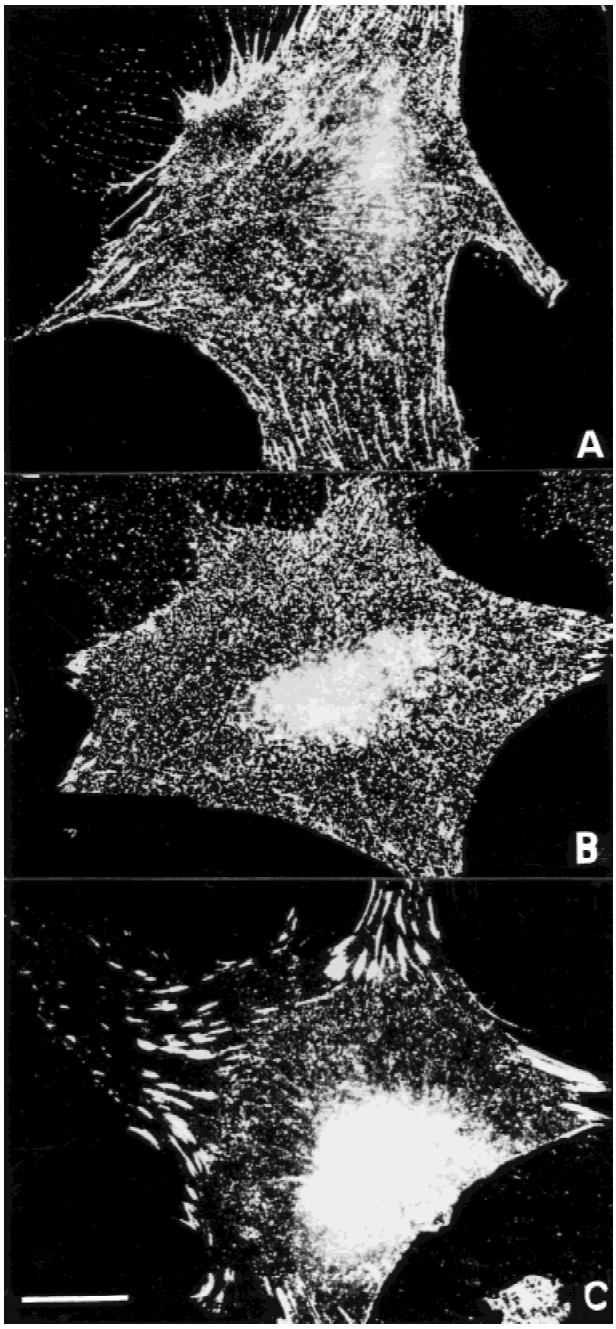

Figure 6. Cellular distribution of vitronectin receptor (α_v integrin). On (B) and (C) human fibroblasts were cultured, as described in Reference 32, on serum-coated glass slides for 2 h, then fixed and stained for α_v integrin without permeabilization (B), to visualize the normal vitronectin receptor distribution on the dorsal cell surface, or with permeabilization (C), to study the distribution of vitronectin receptors on the ventral cell surface. Sample (A) represents antibody-induced reorganization of vitronectin receptors on the dorsal cell surface when an antibody was added to the medium for 1 h and cells were fixed and stained with a secondary antibody afterwards. Bar = 10 μm.

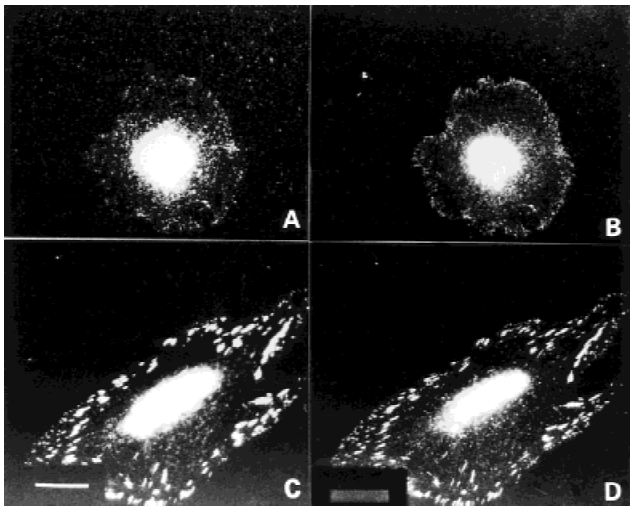

Figure 7. Co-distribution of α_v integrin and cellular phosphotyrosine activity on plain ODS and glass. Cells were cultured on plain ODS (A,B) and glass (C,D) as described, then fixed, permeabilized, and double stained for α_v integrin and cellular phosphotyrosine activity (see Methods section). α_v integrin (A,C) was viewed in the same cells by a rhodamine-conjugated secondary antibody while an FITC-labeled secondary antibody has been used to visualize phosphotyrosine activity. Bar = 10 μm.

Organization of α_v integrin on the dorsal cell surface of living cell. Association with actin filaments

Double staining experiments also were carried out to determine the pattern of antibody-tagged α_v integrin and arrangement of actin filaments in fibroblasts adhering on ODS and glass. Figure 9 demonstrates the typical pattern of actin (left panel) and antibody-induced VN receptor reorganization (right panel) in fibroblasts attached on glass [Fig. 9 (A,B)] and glass precoated with serum [Fig. 9 (C,D)]. It was detected that the linear organization of α_v integrin was weakly expressed on plain glass [Fig. 9 (B)] and more pronounced on serum-coated glass [Fig. 9 (D)]. The linearly organized VN receptor clusters were arranged in parallel with longitudinal stress fibers rather than with circumferentially organized actin on glass [compare Fig. 9 (A) and (B)] and on serum-coated glass [compare Fig. 9 (C) and (D)].

As demonstrated in Figure 10, on hydrophobic ODS substrata, such a co-alignment of α_v integrin and actin filaments generally was absent. On plain ODS, insufficient cell spreading was related to the inability of fibroblasts to organize the actin cytoskeleton into stress fibers and into the punctuate structuring of α_v integrin [Fig. 10 (A,B)]. Figure 10 (C,D) shows that despite well pronounced cell spreading and formation of longitudinal actin filaments on serum-coated ODS,

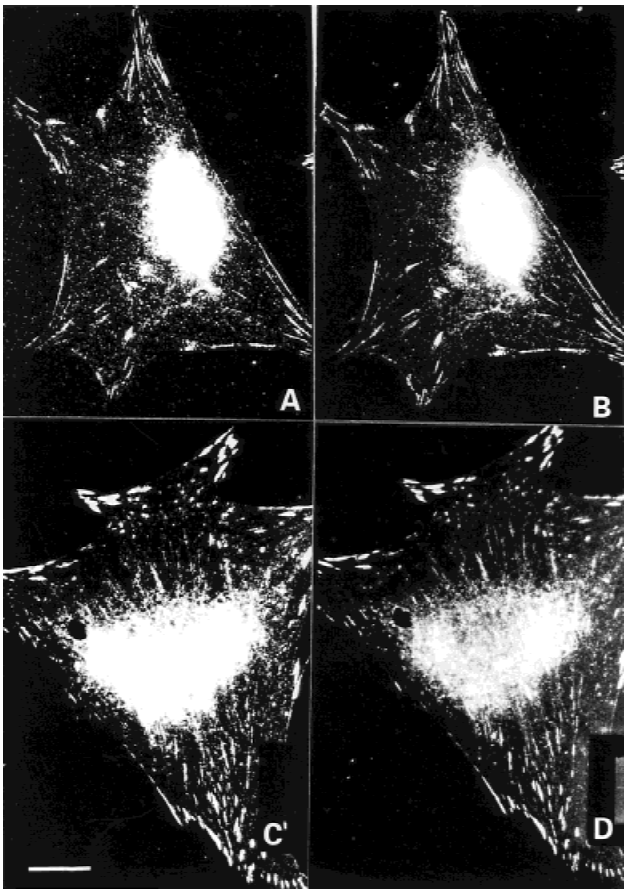

Figure 8. Co-distribution of α_v integrin and cellular phosphotyrosine activity on serum-coated ODS (A, B) and glass (C, D). Cells were treated exactly as described in Figure 7 except that slides were pretreated with serum. Bar = 10 μm.

no linear structuring of the VN receptor could be detected.

DISCUSSION

Vitronectin, together with fibronectin, adsorbs readily from plasma onto biomaterials and is important for successful adhesion and spreading of cells. Although its plasma concentration is similar to that of fibronectin, the extent of vitronectin adsorption is much greater.[33] On the other hand, the amount of fibronectin in serum is considerably less than in plasma because it forms cold-insoluble complexes with fibrinogen.[4] Therefore it is conceivable that VN is the main attachment factor adsorbing from the serum onto biomaterials.[2,3,27,33,34] Moreover, experiments with adsorption of vitronectin under denaturating conditions have shown that this protein is less sensitive (than fibronectin) to conformational changes with regard to its ability to promote cell attachment and spreading[34,35] and, in addition, it has a low tendency to desorb.[2,33] Our comparative measurements in this study performed with biotinylated VN show that comparable quantities of VN were adsorbed on hydrophobic ODS and glass from single VN solutions or serum to which labeled VN had been added. The results of contact angle measurements underline that VN adsorbed readily on both substrata. Low amounts of VN in the PBS caused a change in the advancing and receding water contact angles. However, it seems that the quantities adsorbed were too low for a complete surface coverage because ODS had still higher advancing and receding water contact angles than glass treated the same way. In contrast, the preadsorption of serum produced at relatively low concentrations (1% serum) similar advancing and receding water contact angles, indicating a coverage of the surfaces by the adsorbed serum proteins.

Vitronectin interacts with cells through a number of integrin receptors containing the α_v subunit, mainly $\alpha_v\beta_3$.[15,16,18] In this study we could demonstrate that a hydrophobic surface significantly alters the organization of α_v integrins on both the ventral (facing the substratum) and dorsal cell surface. The morphologi-

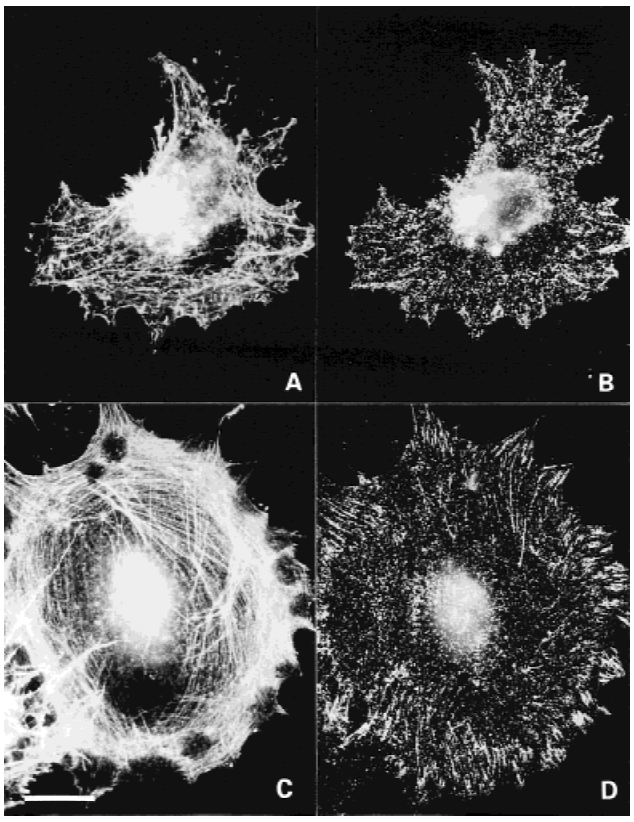

Figure 9. Functional organization of α_v integrin along with actin filaments in cells adhering on glass. Cells were cultured in the presence of antibody, as explained in Figure 6(A). α_v integrin (B,D) was visualized on the dorsal cell surface of fibroblasts adhering on plain glass (A,B) and on serum-coated glass (C,D); then the samples were stained for actin (A,C). Bar = 10 μm.

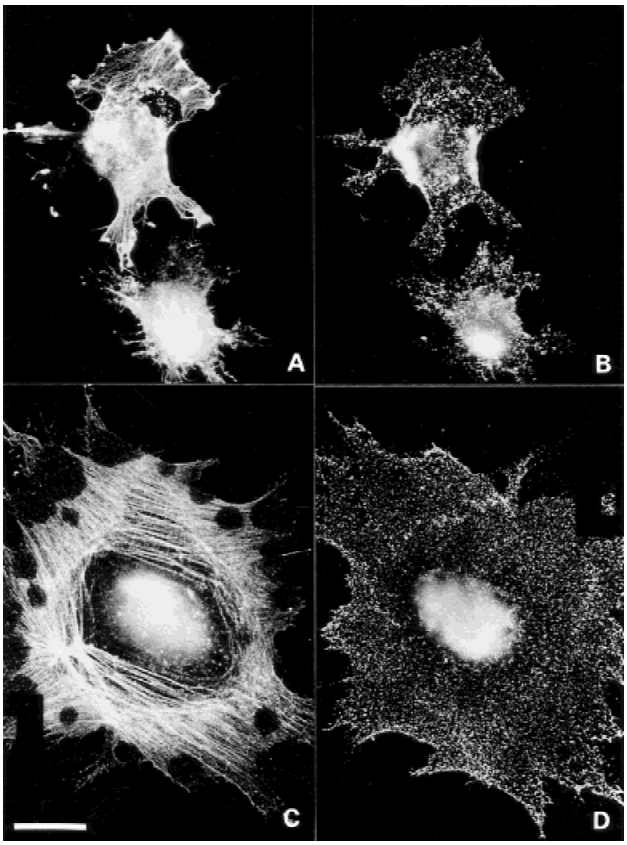

Figure 10. Lack of α_v integrin linear organization along the actin filaments in cells cultured on hydrophobic ODS. Cells were cultured in the presence of antibody as explained in Figure 6(A). α_v integrin (B,D) was visualized on the dorsal cell surface of fibroblasts adhering on plain ODS (A,B) and serum-coated ODS (C,D); then the samples were stained for actin (A,C). Bar = 10 μm.

cal studies with permeabilized cells have shown that fibroblasts were not able to form focal adhesions on hydrophobic ODS while pronounced α_v integrin positive focal contacts could be detected on glass. In the absence of serum, the hydrophobic nature of the substratum also resulted in an altered spreading of fibroblasts. Precoating with serum did considerably improve cell adhesion and spreading on ODS and also on glass. Likewise the cellular organization of the actin cytoskeleton was improved for both substrata. From predominantly aggregated actin on ODS and mainly circumferentially oriented microfilaments on glass, this protein became (longitudinally) organized when cells adhered on serum-precoated materials. If serum pretreatment was substituted with pure VN, the same improvement in cell morphology was observed for both hydrophilic and hydrophobic substrata. We have studied comparatively the expression and organization of the integrin subsets of FN and VN receptors in fibroblasts plated on serum, VN- and FN-coated glass. We have demonstrated clustered focal adhesions of α_v and β_3 integrin predominantly on serum- or VN-coated glass and to some extent on FN-coated glass. There was less α_5 and β_1 integrin on serum- or VN-coated glass compared to FN-coated glass. In this study we have shown the expression of β_3 integrin as an example (see Fig. 4). These results are consistent with the findings of McKeown-Longo et al. that the FN receptor does not organize into focal adhesions on VN-coated glass.[36] Therefore, in this study we considered that serum pretreatment was a sufficient approach for studying the VN receptor organization on biomaterials.

The observed low cellular phosphotyrosine activity of fibroblasts adhering on ODS is consistent with our previous investigations where altered outside-in signaling on hydrophobic substrata has been demonstrated.[23] It is known that integrins cluster in focal adhesion plaques where they link the surface-adsorbed attachment proteins with the actin cytoskeleton.[14–20] Various signaling molecules assemble in the focal adhesions as well, resulting in the activation of tyrosine kinases.[15–18] Therefore it is not surprising that the focal adhesions were co-localized with the main cellular phosphotyrosine activity as VN receptor has been shown to be associated with a 190 kDa phosphoprotein after adherence of 3T3 fibroblasts to vitronectin.[37] However, while in our previous investigations signaling from the biomaterial surface into the cell was attributed solely to the action of FN receptors, particularly β_1 integrin,[23] here we could demonstrate an additional involvement of the VN receptor as well. The pretreatment with serum did enhance the formation of focal adhesions and the corresponding signaling on both ODS and glass, but not to the same extent. Despite the relatively high amounts of VN on ODS, the smaller number and extension of focal adhesions, as well as the lower phosphotyrosine activity, compared to glass was apparent. These results suggest an impaired interaction between the adsorbed VN and the corresponding α_v integrin on the cell surface due to the hydrophobic environment.

Cells may organize ECM proteins like fibronectin in a specific pericellular network[11,38] through a distinct function of integrins, reflecting the inside-out signaling process[15,18] that is promoted mainly by β_1 integrins.[38–40] Recently it was found that despite its role in cell adhesion and spreading, α_v integrin may be involved in the cellular matrix assembly as well.[18,41] In our recent investigations we have shown that the organization of β_1 integrins may be induced by specific antibody binding to this integrin on the dorsal cell surface of living fibroblasts.[24,25] During this process the FN receptor, possibly in cooperation with the actin cytoskeleton, begins to organize into a linear pattern that resembles the structure of newly organized FN matrix fibrils.[25] Furthermore, we have found that hydrophobic substrata, such as ODS, may inhibit this process.[25] Currently there are no morphological data

on the organization of VN receptors on the dorsal surface of substratum attached fibroblasts. Our results revealed that the VN receptor is randomly distributed over the entire dorsal cell surface in fixed fibroblasts. Further, we anticipated that under appropriate conditions anti-α_v antibodies may induce receptor activation similar to the physiological signaling events that take place after VN receptor occupation. Indeed, in this study, using the same approach as described before,[24,25] we could study the functioning of α_v integrins on the dorsal cell surface of living fibroblasts adhering onto ODS and glass. Our results show that a similar effect of altered α_v organization, as we have previously found for the β_1 integrin, can be observed. A weak VN receptor organization on the plain surface and notable structuring along with actin filaments after preadsorption of serum have been found for glass. In contrast, on hydrophobic ODS, even after precoating with serum, no linear organization of the VN receptor could be detected although pronounced longitudinal actin stress fibers were observed. In accordance with our previous investigations[25,42] and from the results obtained here, we may conclude that binding of extracellular matrix proteins to hydrophobic biomaterials may lead to a local functional arrest of α_v integrins on the substratum. This arrest of α_v integrins on the ventral cell surface may impair the signal transfer via the tyrosine phosphorylation pathway, thus altering the organization of integrins over the entire cell surface. As the later processes are necessary prerequisites for cell motility and matrix formation, it may be important for the impaired interaction of cells with such biomaterials.

CONCLUSIONS

From the study presented here, we can conclude that alteration in the integrin functioning of cells adhering on hydrophobic materials prevents their reorganization on the cell surface that is necessary for both signaling processes and extracellular matrix formation. Indeed, these processes may play a crucial role in the tissue compatibility of biomaterials. Hence the techniques we have introduced in this and our other recent papers[21–25] seem to be suitable for investigations of the tissue compatibility of prospective materials and might be helpful in the development of tailor-made biomaterials.

The technical assistance of Ruth Hesse is gratefully acknowledged.

References

1. Andrade JD, Hlady V. Protein adsorption and materials biocompatibility. A tutorial review and suggested hypothesis. Prog Surf Sci 1986;79:1–64.
2. Fabricius-Homan DJ, Cooper SL. A comparison of the adsorption of three adhesive proteins to biomaterial surfaces. J Biomater Sci Polym Edn 1991;3:27–47.
3. Underwood PA, Bennet FA. The effect of extracellular matrix molecules on the in vitro behavior of bovine endothelial cells. Exp Cell Res 1993;205:311–319.
4. Grinnell F. Cellular adhesiveness and extracellular substrata. Int Rev Cytol 1977;53:65–144.
5. Gumbiner BM. Cell adhesion: The molecular basis of tissue architecture and morphogenesis. Cell 1996;84:345–357.
6. van Wachem PB, Beugeling T, Feijen J, Bantjes A, Detmers JP, van Aken WG. Interaction of cultured human endothelial cells with polymeric surfaces of different wettabilities. Biomaterials 1985;6:403–408.
7. Groth T, Zlatanov I, Altankov G. Adhesion of human peripheral lymphocytes on biomaterials preadsorbed with fibronectin and vitronectin. J Biomater Sci Polym Edn 1994;6:729–739.
8. Grinnell F. Fibronectin adsorption on material surfaces. Ann NY Acad Sci 1987;516:280–290.
9. Juliano DJ, Saavedra SS, Truskey GA. Effect of the conformation and orientation of adsorbed fibronectin on endothelial cell spreading and the strength of adhesion. J Biomed Mater Res 1993;27:1103–1113.
10. Pitt DK, Hoffman AS, Horbett TA. Correlation between corneal epithelial outgrowth and monoclonal antibody binding to the cell-binding domain of adsorbed fibronectin. J Biomed Mater Res 1994;28:685–691.
11. McDonald JA. Extracellular matrix assembly. Ann Rev Cell Biol 1988;4:183–207.
12. Zhang K, Kramer RH. Laminin 5 deposition promotes keratinocyte motility. Exp Cell Res 1996;227:309–322.
13. Huttenlocher A, Ginsberg MH, Horwitz AF. Modulation of cell migration by integrin-mediated cytoskeletal linkages and ligand-binding affinity. J Cell Biol 1996;134:1551–1562.
14. Buck CA, Horwitz AF. Integrin, a transmembrane glycoprotein complex mediating cell–substratum adhesion. J Cell Sci 1987; 8:231–250.
15. Hynes RO. Integrins: Versatility, modulation, and signalling in cell adhesion. Cell 1992;69:11–25.
16. Springer TA. Adhesion receptors of the immune system. Nature 1990;46:425–433.
17. Juliano RL, Haskill S. Signal transduction from the extracellular matrix. J Cell Biol 1993;120:577–585.
18. Ruoslahti E. Integrin signaling and matrix assembly. Tumor Biol 1996;17:117–124.
19. Otey CA, Burridge K. Patterning of the membrane cytoskeleton by the extracellular matrix. Sem Cell Biol 1990;1:391–399.
20. Singer II, Scott S, Kawka DW, Kazazis DM, Gailit J, Ruoslahti E. Cell surface distribution of fibronectin and vitronectin receptors depend on substrate composition and extracellular matrix accumulation. J Cell Biol 1988;106:2171–2182.
21. Altankov G, Groth T. Reorganization of substratum-bound fibronectin on hydrophilic and hydrophobic materials is related to biocompatibility. J Mater Sci Mater Med 1994;5:732–737.
22. Altankov G, Grinnell F, Groth T. Studies on the biocompatibility of materials: Fibroblast reorganization of substratum-bound fibronectin on surfaces varying in wettability. J Biomed Mater Res 1996;30:385–391.
23. Groth T, Altankov G. Studies on cell–biomaterial interaction: Role of tyrosine phosphorylation during fibroblast spreading on surfaces varying in wettability. Biomaterials 1996;17:1227–1234.
24. Altankov G, Grinnell F. Fibronectin receptor internalization and AP-2 complex reorganization in potassium-depleted fibroblasts. Exp Cell Res 1995;216:299–307.
25. Altankov G, Groth T, Krasteva N, Albrecht W, Paul D. Morphological evidence for a different fibronectin receptor organization and function during fibroblast adhesion on hydro-

philic and hydrophobic glass substrata. J Biomater Sci Polym Edn 1997;8:712–740.
26. Altankov G, Groth T. Fibronectin matrix formation by human fibroblasts on surfaces varying in wettability. J Biomater Sci Polym Edn 1997;8:299–310.
27. Steele JG, Johnson G, McFarland C, Dalton BA, Gengenbach TR, Chatelier RC, Underwood PA, Griesser HJ. Roles of serum vitronectin and fibronectin in initial attachment of human vein endothelial cells and dermal fibroblasts on oxygen- and nitrogen-containing surfaces made by radiofrequency plasmas. J Biomater Sci Polym Edn 1994;6:511–532.
28. Preissner KT. Structure and biological role of vitronectin. Ann Rev Cell Biol 1991;7:275–310.
29. Felding-Habermann B, Cheresh DA. Vitronectin and its receptors. Curr Opin Cell Biol 1993;5:864–868.
30. Tremsina YS, Sevastianov VI, Petrash S, Dando W, Foster MD. Competitive adsorption of human serum albumin and gamma globulin from a binary mixture onto hexadecyltrichlorosilane-coated glass. J Biomater Sci Polym Edn 1998;9:151–161.
31. Healy KE, Lom B, Hockberger PE. Spatial distribution of mammalian cells dictated by material surface chemistry. Biotech Bioeng 1994;43:1–10.
32. Rodriguez J, Deinhardt F. Preparation of a semipermanent mounting medium for fluorescent antibody studies. Virology 1960;12:316–317.
33. Bale MD, Wohlfahrt LA, Mosher DF, Tomasini B, Sutton RC. Identification of vitronectin as a major plasma protein adsorbed on polymer surfaces of different copolymer composition. Blood 1989;74:2698–2706.
34. Underwood PA, Steele JG, Dalton BA. Effects of polystyrene surface chemistry on the biological activity of solid phase fibronectin and vitronectin, analysed with monoclonal antibodies. J Cell Sci 1993;104:793–803.
35. Miyamoto CY, Izumi M, Ishizaka S, Hayashi M. Adsorption of vitronectin in human serum onto plastics is augmented by sodium dodecyl sulfate. Cell Struc Func 1989;14:151–162.
36. Christopher RA, Kowalczyk AP, McKeown-Longo PJ. Localization of fibronectin matrix assembly sites on fibroblasts and endothelial cells. J Cell Biol 1997;110:569–581.
37. Bartfeld NS, Pasquale EB, Geltosky JE, and Languino LR. The alpha v beta 3 integrin associates with a 190 kDa protein that is phosphorylated on tyrosine in response to platelet-derived growth factor. J Biol Chem 1993;268:17270–17276.
38. Wu C, Bauer JS, Juliano RL, McDonald JA. The alpha 5 beta 1 integrin fibronectin receptor, but not the alpha 5 cytoplasmic domain, functions in an early and essential step in fibronectin matrix assembly. J Biol Chem 1993;268:21883–21888.
39. Wu C, Fields AJ, Kapteijn BAE, McDonald JA. The role of $\alpha_4\beta_1$ integrin in cell motility and fibronectin matrix assembly. J Cell Sci 1995;108:821–829.
40. Wu C, Keivens VM, O'Toole TE, McDonald JA, Ginsberg MH. Integrin activation and cytoskeletal interaction are essential for the assembly of a fibronectin matrix. Cell 1995;83:715–724.
41. Wennerberg K, Lohikangas L, Gullberg D, Pfaff M, Johansson S, Fässler R. β_1 Integrin-dependent and -independent polymerization of fibronectin. J Cell Biol 1996;132:227–238.
42. Groth T, Altankov G. Cell–surface interactions and the tissue compatibility of biomaterials. In: Harris PI, Chapman D, editors. New biomedical materials—Applied and basic studies. Amsterdam: IOS Press; 1998. p 12–23.

Publikation 9

Elke Mitzner, Thomas Groth Th (1996).

Modification of poly(ether urethane)elastomers by incorporation of poly/isobutylene)glycol. Relation between polymer properties and thrombogenicity.

Journal of Biomaterials Science - Polymer Edition **7**, 1105-1118.

J. Biomater. Sci. Polymer Edn, Vol. 7, No. 12, pp. 1105–1118 (1996)

Modification of poly(ether urethane)elastomers by incorporation of poly(isobutylene)glycol. Relation between polymer properties and thrombogenicity*

E. MITZNER[1†] and TH. GROTH[2]

[1] *Technische Fachhochschule Wildau – WIP-Gruppen Adlershof, Rudower Chaussee 5/Haus 12.5, D-12484 Berlin, Germany*

[2] *GKSS Research Centre, Institute of Chemistry, Department of Membrane Research, Kantstrasse 55, D-14513 Teltow, Germany*

Received 23 December 1995; accepted 10 January 1996

Abstract—Non-polar hydrophobic poly(isobutylene)glycol (PIBG) was substituted for poly(tetramethylene ether)glycol (PTMEG) in poly(ether urethanes) based on 4,4'-methylenebis-(phenylisocyanate) (MDI) and 1,4-butanediol (BD) as chain extender. Two series of polyurethanes differing in their soft segment length, polymer composition, and hard segment content were studied by dynamic mechanical analysis (DMA) and static, as well as dynamic, contact angle measurements. The thrombogenicity of these polymers was characterized by studying the adhesion and activation of platelets using ELISA for GMP 140 and fluorescence microscopy. It was found by DMA that in PIBG-containing polyurethanes (PUE) exist soft domains containing hard segments, strictly separated hard segment domains, and hard segments partially mixed with soft segments. Contact angle measurements revealed that 25% PIBG or even less, are sufficient for a remarkable enrichment of these non-polar soft segments on the polymer surface. The platelet adhesion/activation on these materials was demonstrated to increase with the rise in hard segment content, as well as with an enhancement of the PIBG content. However, comparison of PIBG-containing PUE with medical applied polypropylene and pellethane expressed that PUE with PIBG content equal or less 25% have excellent haemocompatibility.

Key words: Polyurethane elastomers; bulk properties; surface wettability; thrombogenicity.

INTRODUCTION

Polyurethane elastomers (PUE) are widely used in biomedical applications because of their ease of handling, high tensile strength, lubricity, good abrasion resistance, and good haemocompatibility [1]. It has been proposed that both good mechanical properties and improved haemocompatibility are caused by the separation of hard and soft segments [2]. In the last few years several techniques have been investigated in order to improve the haemocompatibility of PUE, many of them according to the hypothesis that a balance of polar (hydrophilic) and non-polar (hydrophobic) sites at the polymer surface may be important for their blood compatibility [3]. Those techniques with a subsequent modification of the PUE are for example: grafting the surface by highly hydrophobic perfluoralkyl chains [4], modification of the PUE by incorporation of sulfonate groups [5], grafting by poly(ethylene oxide) (PEO), and further sulfonate group incorporation [6]. On

---

* Dedicated to Prof. Dr. Robert Becker on the occasion of his 65th birthday.

† To whom correspondence should be addressed.

the other hand, it is possible to influence the properties of PUE, including their surface properties, by the choice of starting materials and their composition. Recently, it was shown that hard segment content, as well as composition are related to the haemocompatibility of poly(ether urethane)ureas [7]. Although, the rise in the hard segment content in general was shown to decrease the haemocompatibility, increasing amounts of urethane bonds alone did not deteriorate the blood-contacting properties of polyurethane ureas. A modification of the surface of PUE by incorporation of hydrophilic PEO in the soft segment [2] demonstrated an enhanced surface hydrophilicity with increasing PEO content. However, the thrombogenicity of these PUEs was not improved. This unexpected result was attributed to the high hard segment content of the PUE. In contrast, the use of different hydrophobic chain extenders was reported to enhance the antithrombogenicity of hydrophobic PUE surfaces [8, 9]. The synthesis of PU/polystyrene interpenetrating polymer networks (IPN) that exhibit phase-separated structures on the polymer surface [10], as well as hydrophobic polydimethylsiloxane polyureaurethanes have been shown to have good blood-contacting properties [11].

The haemocompatibility of biomaterials can be characterized by the interaction of platelets with the material surface. Platelets can adhere on a surface and may become activated that is visible by the formation of pseudopodia, cell spreading and release reaction [12]. The activation process is initiated by the presence of surface-bound proteins such as fibrinogen, or other adhesive proteins, as well as by the presence of soluble agonist such as ADP or thrombin [12–15]. The platelet activation on a surface leads to the recruitment of further platelets from the blood stream and the development of platelet aggregates [12, 15]. Moreover, activated platelets have a procoagulant activity that is the involvement in the formation of the prothrombinase complex [12, 16]. The assessment of platelet adhesion/activation in contact with biomaterials is usually performed under flow conditions and estimated by cell counting and the measurement of released products [17–19]. On the other hand, it was found that the measurement of platelet adhesion/activation under flow conditions is in a qualitative agreement with that under static conditions [20]. Despite the existence of common parameters like platelet count, release of β-thromboglobulin and others, recently the detection of platelet antigens on the cell membrane with immunological means has shown to be an useful tool for the assessment of platelet interactions with biomaterials [7, 21–23].

OH-functionalized polyisobutylene is a very non-polar hydrophobic polyol. Since it has become possible to synthesize this polymer with a well-defined functionality it has become interesting as a starting material for PU. Recently we have demonstrated that PUE based on mixtures of poly(tetramethylene ether)glycol (PTMEG) and poly(isobutylene)glycol (PIBG) as soft segments exhibit reasonable mechanical properties up to a PIBG content of 25% [24]. In this paper we report on the characterization of two series of those PUE incorporating different amounts of PIBG based on PTMEG / 1,4-butanediol (BD) / 4,4'-methylenebis-(phenylisocyanate) (MDI) by dynamic mechanical analysis (DMA) and contact angle measurements. The haemocompatibility of these PUE was studied by the assessment of the adhesion and activation of platelets.

MATERIALS AND METHODS

Polymer synthesis

The synthesis of narrow molecular weight distribution PIBG (PIBG 2200: M_n = 2200; M_w/M_n = 1.08; F_n = 2.0±0.05. PIBG 1200: M_n = 1200; M_w/M_n = 1.15; F_n = 2.0±0.1).

was performed according to Kennedy *et al.* [25–27]. BD and PTMEGs TERATHANE 1000 and 2000 were obtained from Aldrich and MDI from Pfaltz and Bauer. The PUEs (see Fig. 1) were synthesized using a two-step technique. NCO-terminated prepolymers were prepared by refluxing the polyol, or the polyol mixture and MDI in a solvent mixture of tetrahydrofurane (THF) and dimethyl formamide (9:1; v/v) for 1.5 h. After adding the chain extender BD this mixture was allowed to reflux for another 6 h. After this time no NCO-groups were detectable by end group titration. The high viscous PUE solution (25%) was cast in an open Teflon mould and the solvent evaporated in a hood overnight. Subsequently, the PUE films were stored in a vacuum oven for 1 day at room temperature and then for 2–3 days at 50°C. The polymers were named according the molecular weight of PTMEG, such as PUE1000 or PUE2000, and the content of PIBG, such as PIB0 up to PIB100.

Polymer characterization

Molecular weights were determined by gel permeation chromatography in THF (conc.: 0.5 wt%; injection volume 100 μl; flow rate 1.0 ml min^{-1}) at room temperature relative to polystyrene standards. Two PLmix PS-DVB columns (10 μm) by KNAUER were used with a refractive index detector. Dynamic mechanical data were obtained using a Rheovibron viscoelastometer DDV-IIb. Data were taken from −90°C until sample failure at a test frequency of 3.5 Hz and a temperature rise rate of 5 K min^{-1}. Strips of 5 mm width and 30 mm length were used. The dielectric behavior of polyols, characterized by the complex dielectric permittivity, was measured in the −110–50°C range at 1 kHz by a four-probe impedance analyzer HP 4284A. Dynamic contact angles were measured on dry samples using a Cahn DCA-312 instrument and both advancing and receding angles were obtained at a platform speed of 0.15 mm s^{-1}. The averages of ten measurements (two cycles for each five test specimen per sample) using double-distilled water as test liquid are reported. Static contact angles were taken with a Kruess G 40, equipped with video system and automatic analysis. Five drops (0.4 ml) of double-distilled water were measured thirty times every 1.5 s on dry samples. The standard deviation of the dynamic method was ±1 deg and that of the static ±2 deg.

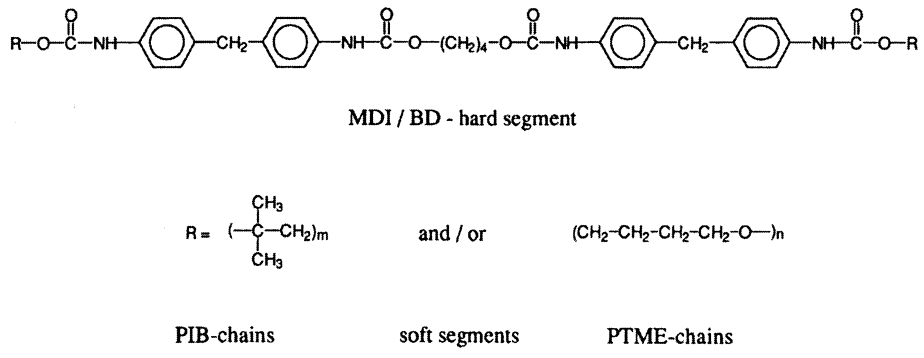

Figure 1. Structural formula of synthesized PEUs.

Blood collection and preparation

Blood was withdrawn from anticubital vein of healthy volunteers who had no medication at least for 10 days. The blood was collected in sodium citrate (3.19 per 100 ml) at a blood/citrate ratio of 9:1. The fresh blood was used for the preparation of platelet-rich plasma (PRP). For this purpose, the blood was spun at 200 *g* for 10 min. The supernatant PRP was collected and the remaining blood was centrifuged at 2000 *g* for 20 min. The obtained platelet-poor plasma (PPP) was used to prepare PRP with 200000 platelets per μl by the appropriate dilution of PRP with PPP.

Measurement of platelet activation by ELISA for GMP 140

The quantification of platelet adhesion/activation on the different polyurethanes was performed by a recently developed ELISA which recognizes the platelet glycoprotein P-Selectin or GMP 140 as marker of platelet activation [7, 20, 22, 23]. The procedure is described briefly. The polymer foils were cut in stripes and mounted in a measuring chamber with holes of 100 mm^2 area. PRP was filled in three sample wells with PPP in one sample well used as a control. After 30 min incubation at 37°C the chambers were washed with PBS and incubated with monoclonal mouse anti-GMP 140 (Immunotech S.A., France) for 60 min. After further washing with PBS, the samples were incubated with a sheep anti-mouse IgG labelled with peroxidase (Sigma Immunochemicals, USA) for 60 min. Then, samples were washed and incubated with *o*-phenylenediamine (Sigma) as substrate. The conversion of the substrate was stopped with sulfuric acid. The OD was measured at 492 nm and used as a quantitative measure for the presence of activated platelets on the material surface.

Fluorescence microscopy of adhering platelets

The polymers were incubated with PRP for 30 min as described above, followed by a fixation with 1% paraformaldhehyde for 10 min. The samples were washed with PBS and saturated with 1% bovine serum albumin and 1% glycin in PBS for 15 min. After a further washing step, monoclonal mouse anti-GP IIa/IIIb antibody in 1% BSA (Immunotech S.A., France) was added and incubated for 30 min. Then followed a washing step and the incubation with goat anti-mouse IgG labelled with FITC (Jackson Immuno Research, USA) in the presence of 10% goat serum. The polymer foils were then placed on glass slides and covered with mounting medium and a microscopic cover slip. The platelets were visualized and photographed with a fluorescent microscope Jenamed Fluorescence (Carl Zeiss Jena, Germany).

Reference materials for investigations with platelets

Polypropylene and Pellethane 2363-80AE films were used as reference materials for the investigations of haemocompatibility. These materials are considered as reference materials and were a kind gift of Dr. W. Lemm (Free University Berlin).

RESULTS AND DISCUSSION

Bulk properties

The composition and weight-average (M_w) and number-average (M_n) molecular weights determined by gel permeation chromatography, as well as the dispersity (M_w/M_n) of

Table 1.
PUE of Series A and B

Sample	PIBG in soft phase (wt%)	Hard Segment Content (wt%)	M_w	M_n	M_w/M_n
PUE1000-PIB0	0	48	69400	18300	3.8
PUE1000-PIB28	28	44	61700	18400	3.4
PUE1000-PIB51	51	39	52900	16000	3.3
PUE1000-PIB72	72	34	55700	16400	3.4
PUE1000-PIB100	100	30	23700	9500	2.5
PUE2000-PIB0	0	32	50700	18200	2.7
PUE2000-PIB5	5	32	46500	21300	2.2
PUE2000-PIB10	10	32	53300	13600	3.9
PUE2000-PIB15	15	32	54900	17400	3.2
PUE2000-PIB20	20	32	36500	14500	2.5
PUE2000-PIB25	25	32	39800	13000	3.1
PUE2000-PIB100	100	30	17100	7500	2.3

Series A: Polyol/BD/MDI = 1/2/3; Polyols: PTMEG 1000; PIBG 2200
Series B: Polyol/BD/MDI = 1/2/3; Polyols: PTMEG 2000; PIBG 2200

samples of series A and B are shown in Table 1.

The morphology of the PUE was studied by dynamic mechanical analysis (DMA). These measurements give detailed information about the compatibility between PIBG and PTMEG soft segments and between both types of soft segments as well as the hard segments within the PUE chains. Figures 2 and 3 display the moduli E' and the mechanical loss factors tan δ of the PUE of series A and B depending on the temperature at fixed frequency. Table 2 contains the glass transition temperatures (T_g) of the polymers determined by DMA (E'') and these of the basic polyols determined by dielectrical measurements. The relaxation spectra of samples PUE1000-PIB0 of series A (Fig. 2) and PUE2000-PIB0 of series B (Fig. 3) show remarkable differences. For PUE1000-PIB0 the T_g of the soft segments that is indicated by the temperature positions of the maxima of the loss modulus E'' (see Table 2), as well as of the loss factor tan δ (Fig. 2) is found at –25°C. As expected, T_g of this pure PTMEG sample is dramatically

Table 2.
Glass transition temperatures of PUE determined by DMA (E'') and polyols determined by dielectric measurements

Series A	T_g (°C)	Series B	T_g (°C)
PUE1000-PIB0	–25	PUE2000-PIB0	–64
PUE1000-PIB28	-27	PUE2000-PIB5	–62
PUE1000-PIB51	-28	PUE2000-PIB10	–59
PUE1000-PIB72	-31	PUE2000-PIB15	–60
PUE1000-PIB100	-33	PUE2000-PIB20	–58
		PUE2000-PIB25	–56
		PUE2000-PIB100	–30
PTMEG 1000	-53	PTMEG 2000	–60
PIBG 2200	-37	PIBG 2200	–37

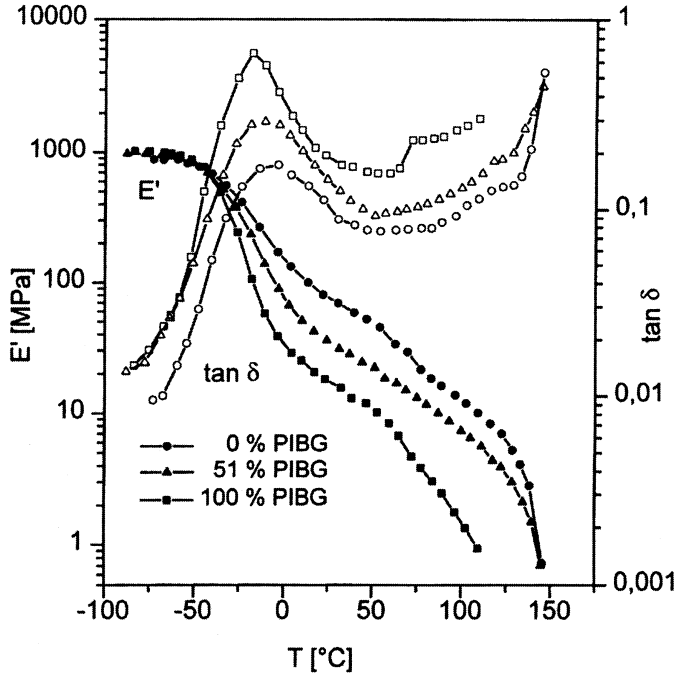

Figure 2. Storage modulus E' and mechanical loss factor tan δ of selected PUE of series A vs temperature.

higher than that of the equivalent PUE2000-PIB0 (−64°C; see Table 2 and Fig. 3). This is caused by the forced soft and hard segment mixing in case of shorter soft segments. Therefore, the detected T_g represents a soft phase that is partially mixed with hard segments. The glass transition is accompanied by a drop in modulus E'. The different shape of the modulus curves of both pure PTMEG-PUE is caused by the different soft segment lengths, too. The reason for the modulus decrease at −15–10°C in case of PUE2000-PIB0 is the melting of crystalline parts of the PTMEG segments. PUE1000-PIB0 of series A does not show this behaviour because the lower PTMEG molecular weight prevents soft segment crystallization. PUE1000-PIB0 has a significant higher hard segment content in comparison to PUE2000-PIB0. According to this circumstance the former shows higher modulus values above T_g. For both pure PTMEG polyurethanes chain mobility takes place above 145°C and the PUE lose their dimensional stability ($E' < 1$ MPa). Before melting in the temperature range 60–90°C, the modulus drops slightly indicating a transition region that is influenced by a mixed phase of hard and soft segments.

All Series A and B samples show well defined single glass transitions of the mixed soft phases regardless of the polarity difference between PTMEG and PIBG. The decrease of T_g of PUE of series A with increasing PIBG content (Fig. 2, Table 2) is a result of substitution longer soft segments (PIBG 2200) for shorter ones (PTMEG 1000). The remarkable differences in the modulus values above T_g are caused by different hard segment contents as explained above. With increasing PIBG content samples of series B show T_g shifting to higher temperatures (Fig. 3). As can be seen in Table 2 this shifting

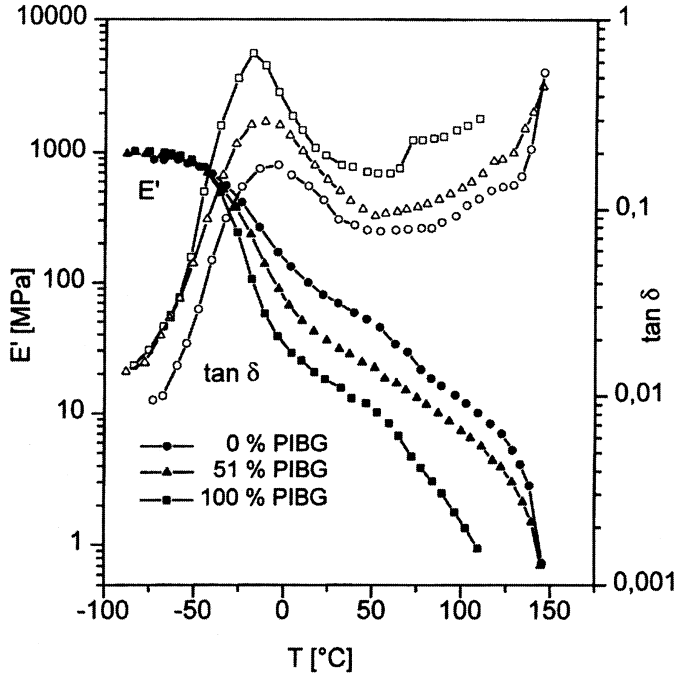

Figure 2. Storage modulus E' and mechanical loss factor tan δ of selected PUE of series A vs temperature.

higher than that of the equivalent PUE2000-PIB0 (−64°C; see Table 2 and Fig. 3). This is caused by the forced soft and hard segment mixing in case of shorter soft segments. Therefore, the detected T_g represents a soft phase that is partially mixed with hard segments. The glass transition is accompanied by a drop in modulus E'. The different shape of the modulus curves of both pure PTMEG-PUE is caused by the different soft segment lengths, too. The reason for the modulus decrease at −15–10°C in case of PUE2000-PIB0 is the melting of crystalline parts of the PTMEG segments. PUE1000-PIB0 of series A does not show this behaviour because the lower PTMEG molecular weight prevents soft segment crystallization. PUE1000-PIB0 has a significant higher hard segment content in comparison to PUE2000-PIB0. According to this circumstance the former shows higher modulus values above T_g. For both pure PTMEG polyurethanes chain mobility takes place above 145°C and the PUE lose their dimensional stability ($E' < 1$ MPa). Before melting in the temperature range 60–90°C, the modulus drops slightly indicating a transition region that is influenced by a mixed phase of hard and soft segments.

All Series A and B samples show well defined single glass transitions of the mixed soft phases regardless of the polarity difference between PTMEG and PIBG. The decrease of T_g of PUE of series A with increasing PIBG content (Fig. 2, Table 2) is a result of substitution longer soft segments (PIBG 2200) for shorter ones (PTMEG 1000). The remarkable differences in the modulus values above T_g are caused by different hard segment contents as explained above. With increasing PIBG content samples of series B show T_g shifting to higher temperatures (Fig. 3). As can be seen in Table 2 this shifting

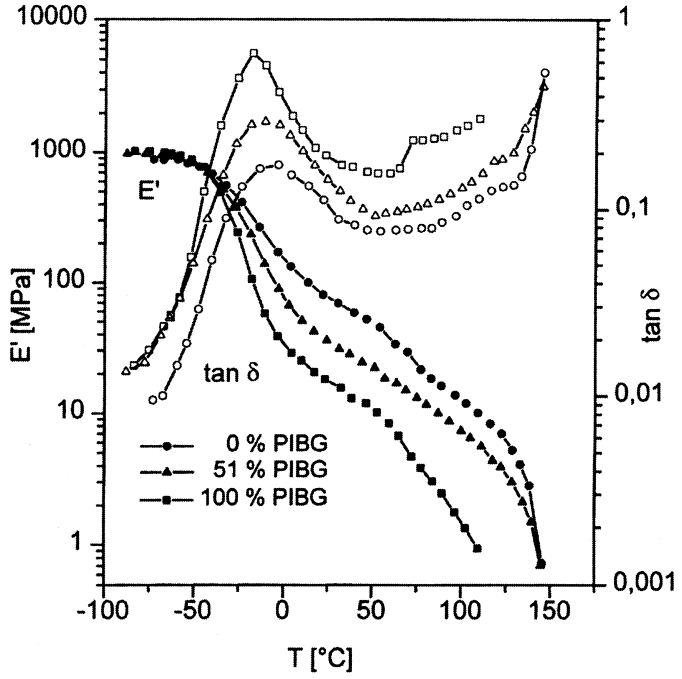

Figure 2. Storage modulus E' and mechanical loss factor tan δ of selected PUE of series A vs temperature.

higher than that of the equivalent PUE2000-PIB0 (−64°C; see Table 2 and Fig. 3). This is caused by the forced soft and hard segment mixing in case of shorter soft segments. Therefore, the detected T_g represents a soft phase that is partially mixed with hard segments. The glass transition is accompanied by a drop in modulus E'. The different shape of the modulus curves of both pure PTMEG-PUE is caused by the different soft segment lengths, too. The reason for the modulus decrease at −15–10°C in case of PUE2000-PIB0 is the melting of crystalline parts of the PTMEG segments. PUE1000-PIB0 of series A does not show this behaviour because the lower PTMEG molecular weight prevents soft segment crystallization. PUE1000-PIB0 has a significant higher hard segment content in comparison to PUE2000-PIB0. According to this circumstance the former shows higher modulus values above T_g. For both pure PTMEG polyurethanes chain mobility takes place above 145°C and the PUE lose their dimensional stability ($E' < 1$ MPa). Before melting in the temperature range 60–90°C, the modulus drops slightly indicating a transition region that is influenced by a mixed phase of hard and soft segments.

All Series A and B samples show well defined single glass transitions of the mixed soft phases regardless of the polarity difference between PTMEG and PIBG. The decrease of T_g of PUE of series A with increasing PIBG content (Fig. 2, Table 2) is a result of substitution longer soft segments (PIBG 2200) for shorter ones (PTMEG 1000). The remarkable differences in the modulus values above T_g are caused by different hard segment contents as explained above. With increasing PIBG content samples of series B show T_g shifting to higher temperatures (Fig. 3). As can be seen in Table 2 this shifting

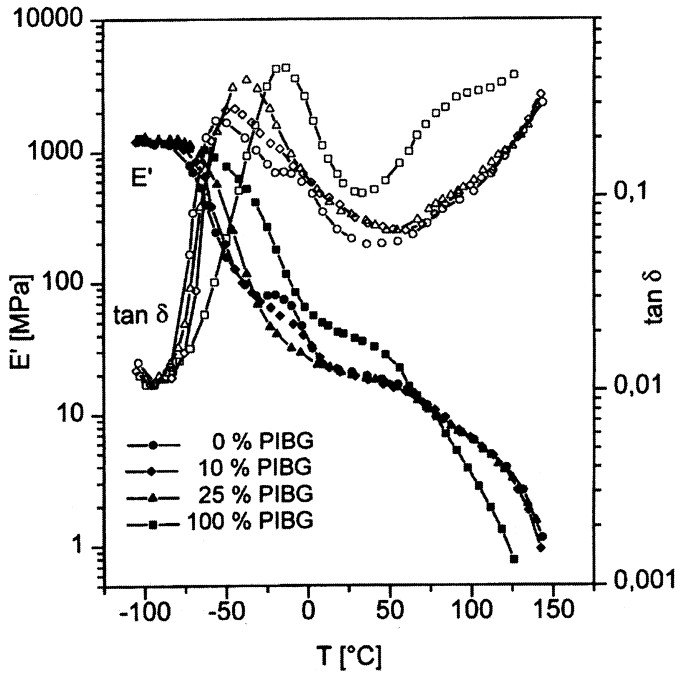

Figure 3. Storage modulus E' and mechanical loss factor tan δ of selected PUE of series B vs temperature.

is of the same order of magnitude like the difference between the T_gs of the polyols PTMEG 2000 and PIBG 2200 measured by dielectric relaxation spectroscopy. In contrast to Yoon *et al.* [28] who was working with the assumption that the T_gs of both polyols are similar, a significant difference in the T_g of PTMEG 2000 and PIBG 2200 used for the synthesis of the PUE was found in this investigation (see Table 2). The T_g of the PUE is the result of the molecular mobility of the mixed two types of soft segments. The value for the pure PIBG-PUE sample is higher than expected from the T_g of PIBG, i.e. partial mixing of soft and hard segments is more pronounced than in the case of PTMEG-PUE. The shape of the modulus curves of samples of series B is changing in dependence on the PIBG content. With increasing PIBG content the formation of crystalline parts of PTMEG is decreasing and the melting peak disappears. The mechanical indicated melting points (E' = 1 MPa) of samples with mixed soft phase of both series do not differ from that of the pure PTMEG-PUE. By contrast, the 100% PIBG-samples lose their dimensional stability at significant lower temperatures.

Regardless of the polarity difference between PIBG soft segments and hard segments not only PTMEG soft segments are partially mixed with hard segments but also the former. This result was also found in the literature [28]. The results give evidence for side by side existence of strictly phase separated hard segments and such that are mixed with soft segments to a certain degree.

Surface properties

Regarding the surface composition of PUE the opinion got through that there is an

enrichment of soft segments on the surface of dry samples because of their less polarity in comparison to hard segments. Recently, this assumption was again confirmed by ESCA measurements [28]. In these investigations the soft phase was hydrophobized by the incorporation of totally non-polar PIBG. Therefore it was investigated by static and dynamic contact angle measurements [29, 30] how the hydrophobicity of the PUE surface is related to the PIBG content.

The static contact angles of materials of both series obtained with water as test fluid are shown in Fig. 4. They exhibit the same tendency for series A and series B. The significant smaller contact angles of materials containing only PTMEG soft segments in comparison to all other materials indicate that the former are the most hydrophilic within a series. In series A, the substitution of 28% PIBG for PTMEG leads to a jump of the contact angle. However, the further increase of the PIBG content causes only a slight enhancement of the contact angles. Therefore, it was concluded that the enrichment of the non-polar PIBG on the surface within the soft phase is only possible to a certain degree. Using the model of Takahara [31] this phenomenon might be explained by the enrichment of the less polar soft segments in comparison to hard segments on the dry surface. In case of a mixed soft phase there is a preferred enrichment of totally non-polar PIBG soft segments. From the contact angle measurements, it was assumed that the maximum enrichment of PIBG is reached when 25% of these soft segments are substituted for PTMEG or even less. Therefore, a further increase of the PIBG content did not significantly increase the contact angles. In series B the soft phase composition was varied in smaller steps. As shown in Fig. 4 there is a small jump for 5% PIBG content. In the range 5–25% PIBG (PUE2000-PIB5–PUE2000-PIB25) the contact angle increases about 10 deg. In contrast to series A there is a higher increase of the contact angle from PUE with mixed soft segments (PUE2000-PIB25) to PUE with only PIBG soft segments (PUE2000-PIB100). The different behaviour of series A and B is probably due to their differences in morphology, especially in phase separation. The slightly

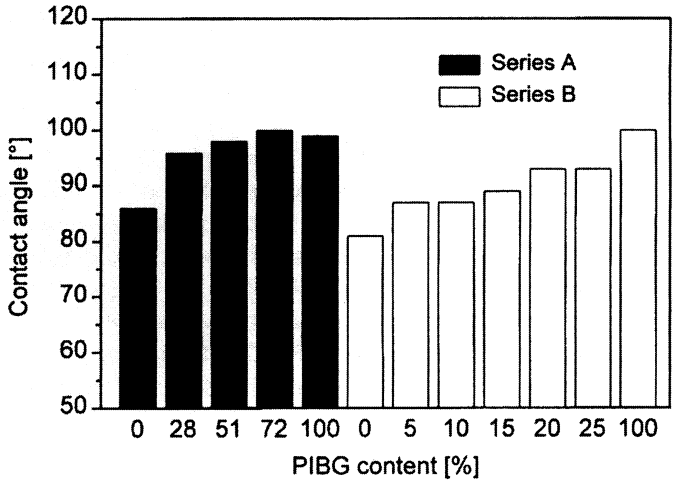

Figure 4. Static contact angles of PUE of series A and B in dependence on the PIBG content (test liquid: water).

different results of the static contact angle measurements indicate a reflection of these differences in the surface properties. Nevertheless, the main result for both series is that hydrophobizing of the surface occurs mainly in the range between 0 and 25% PIBG in the soft phase.

To find out the influence of the PIBG content on surface wettability, heterogeneity and chain mobility Wilhelmy plate technique [30] was applied to series B because of the constant hard segment content. The PIBG content was the only parameter varied. The data presented in Fig. 5 are results of two cycles that were run for each sample. Overall the dynamic measurements confirm the results of the static contact angle measurements. The advancing angles (Θ_A) that are characteristic of the non-polar component at the polymer surface [5] show that there is a remarkable jump between samples PUE2000-PIB0 and PUE2000-PIB5 that contains only 5% PIBG soft segments. The advancing angles of the samples PUE2000-PIB10–PUE2000-PIB25 are almost constant. The sample PUE1000-PIB100 with 100% PIBG shows a little higher Θ_A. In contrast to the advancing angle the receding one (Θ_R) is characteristic of the polar component at the surface upon contact with water [5]. The receding angles within series B are almost constant. That means that there is a hysteresis jump like the jump of the advancing angles caused by substitution of PIBG for PTMEG. Hysteresis could be caused by surface roughness. However, atomic force micrographs of the samples of series B demonstrate that the surfaces are relatively smooth (data not shown). According to the theory of Holly and Refojo [32] hysteresis can be due to polymer surface reorientation. In the very hydrophobic medium air non-polar groups (PIBG and/or PTMEG chains) may orient toward the outer surface, minimizing the surface free energy. In the hydrated state molecular movement takes place. Thus, it is possible that PTMEG blocks with their oxygen bridges and perhaps even the most polar hard segments are enriched at the surface. It was also found that cycles 1 and 2 were almost identical. This indicates that surface restructuring is not permanent, but occurs fast enough to respond to environmental changes during the time scale of the measurement [31]. Both static and dynamic contact angle measurements

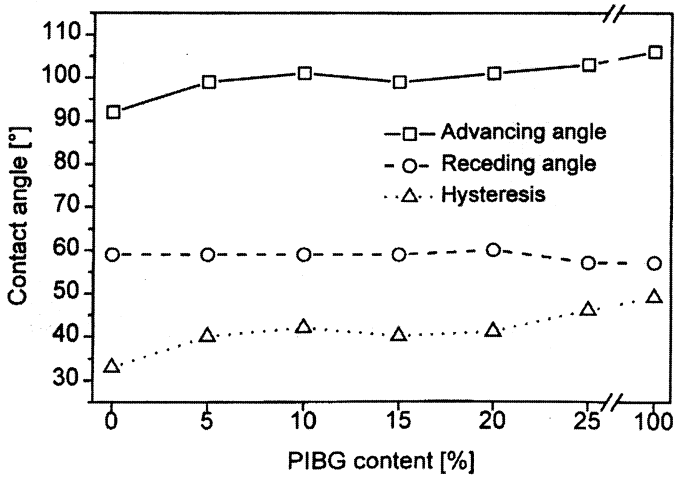

Figure 5. Dynamic contact angles of PUE of series B in dependence on the PIBG content (test liquid: water).

lead to the conclusion that the surface of PUE is maximally enriched by PIBG soft segments substituting 25% PIBG for PTMEG or even less.

Platelet adhesion and activation

The results of platelet activation studies for series A and B are shown in Fig. 6a and b, respectively. In Fig. 6a it is demonstrated that series A expressed a minimal thrombogenicity for a PIBG content of 28%. The appearance of this minimum might be due to the change of two parameters at the same time, namely the decreasing hard segment content with the rise in the PIBG content, that means the hydrophobicity of the polymer. The microscopic investigations of platelet interaction with the materials support these

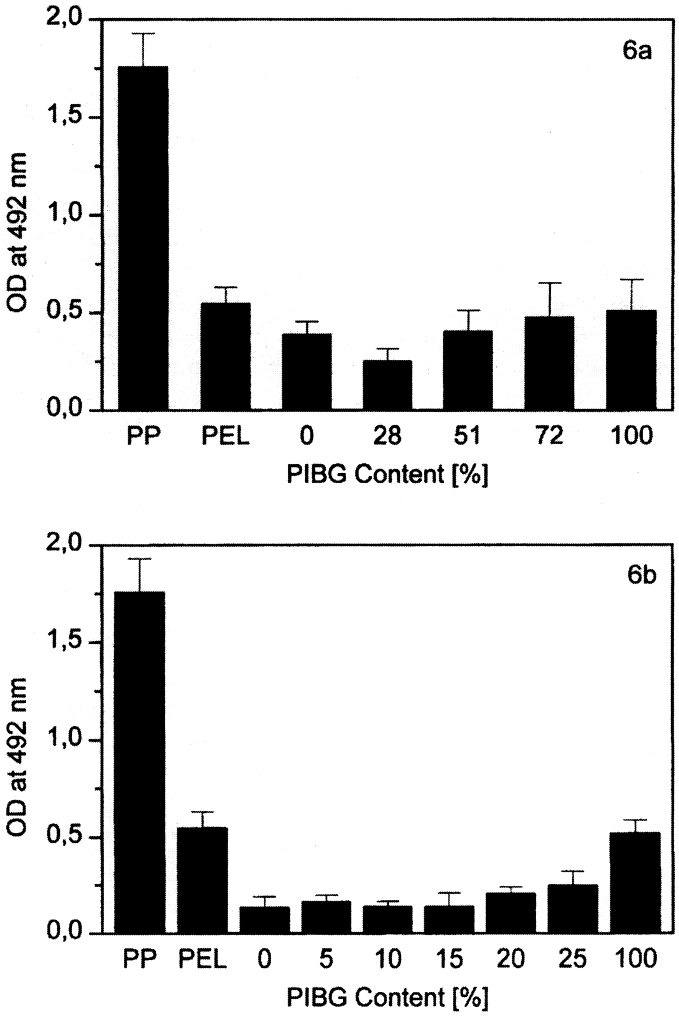

Figure 6. Quantification of platelet adhesion/activation on PUE of series A (a) and series B (b) in dependence on the PIBG content and on reference materials polypropylene and pellethane by enzyme immuno assay for GMP 140.

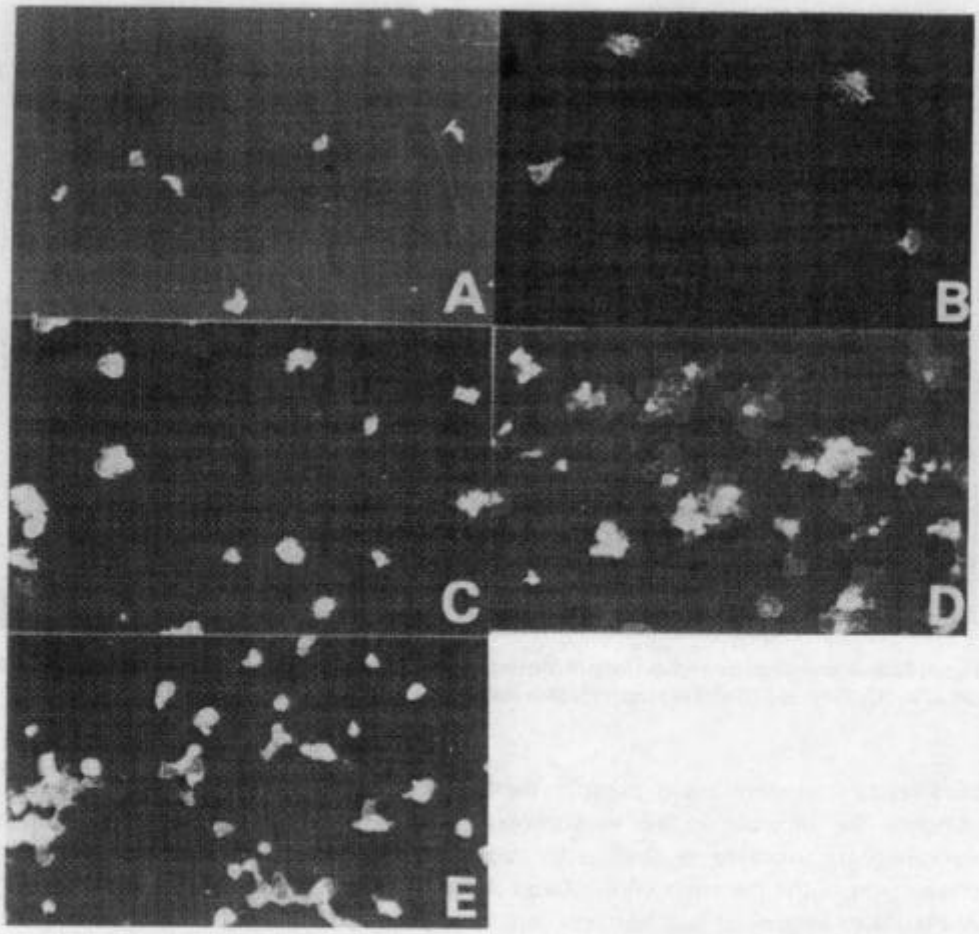

Figure 7. Immunofluorescence microscopy of platelets adhering on PUE of series A (PIBG content: (A) 0%; (B) 28%; (C) 51%; (D) 72%; and (E) 100%) (magnification 600×).

results as shown in Fig. 7. There it is demonstrated that for PIBG contents of 0% (Fig. 7A) and 28% (Fig. 7B) minimal adhesion of platelets was observed. Further, only limited spreading of platelets was visible indicated by beginning pseudopodia formation. If the PIBG content was increased from 51 to 100% an increase in platelet adhesion/activation was detected. This was obvious by the increasing number of adhering platelets, as well as the spreading of platelets which became more prominent as shown in Fig. 7D for PUE1000-PIB72 and Fig. 7E for PUE1000-PIB100. In comparison to series A, in general decreased thrombogenicity was obtained for series B as demonstrated in Fig. 6b and Fig. 8. In contrast to series A the hard segment contents of PUE of series B were smaller and approximately constant. PUE with PIBG contents up to 15% expressed a comparable haemocompatibility like the pure PTMEG-PUE as indicated by the measurement of platelet activation (see Fig. 6b) and the microscopical investigations (see Fig. 8A and B for PUE2000-PIB0 and PUE2000-PIB10, respectively). It is obvious that the further increase of the PIBG content provoked an increase in the thrombogenicity as indicated by increasing platelet adhesion and activation (see Fig. 8C and D). While the decreasing

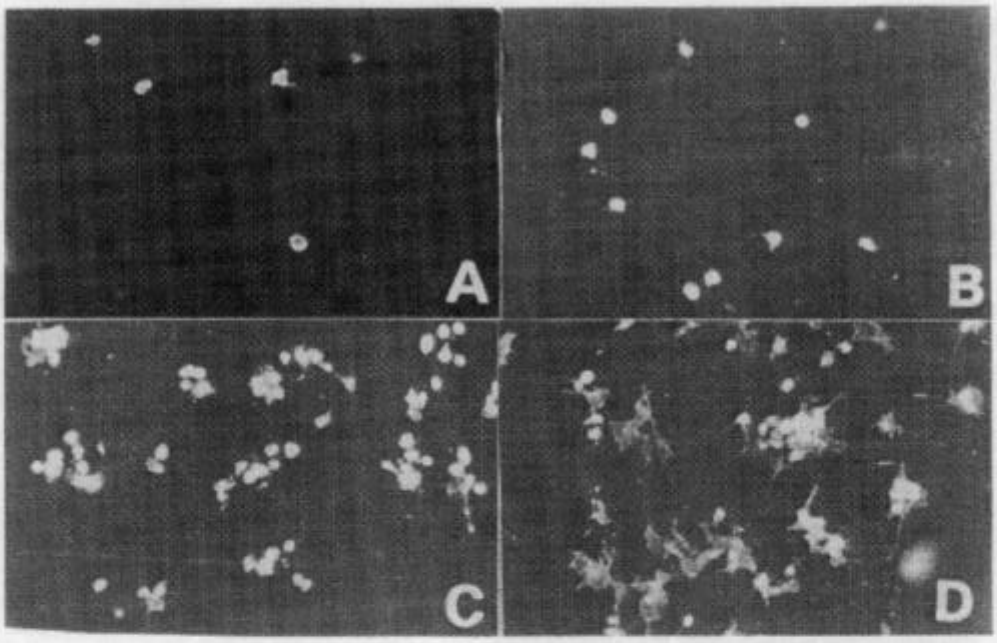

Figure 8. Immunofluorescence microscopy of platelets adhering on PUE of series B (PIBG content: (A) 0%; (B) 10%; (C) 25%; and (D) 100%) (magnification 600×).

hard segment content could improve the blood contacting properties with respect to platelets, the increase in the hydrophobicity at the same time resulted in a more thrombogenic substrate as obvious by comparison of series A and B, as well as by comparison of the materials within series A and B. An increase in the thrombogenicity of PUE with increasing hard segment content of polyurethanes is also known from other studies [7, 31, 33]. For a comparison of these newly developed materials with currently applied blood-contacting polymers polypropylene and pellethane foils were investigated. The platelet adhesion/activation indicated by the OD was higher for PP and PEL than for the investigated PUE (see Fig. 6a and b). The fluorescence microscopy revealed that PP caused massive adhesion and spreading of platelets (see Fig. 9B), while PEL caused a moderate thrombogenic reaction (see Fig. 9A) comparable to PUE with higher PIBG content.

It was concluded that the incorporation of small amounts of hydrophobic polyols like PIBG may improve the haemocompatibility of PUE as found by the comparison with medical applied PP and PEL. Moreover, it is suspected that PIBG containing polyurethanes may show an enhanced hydrolytic stability which is to be tested in future investigations. Therefore, it is assumed that the rather good haemocompatibility and the reasonable mechanical properties of PIBG containing PUE [24] make the materials suitable for medical applications.

Acknowledgements

E. M. is grateful to the Deutsche Forschungsgemeinschaft for fellowship support and to Prof. J. P. Kennedy for the possibility to work in his lab and helpful discussions. The

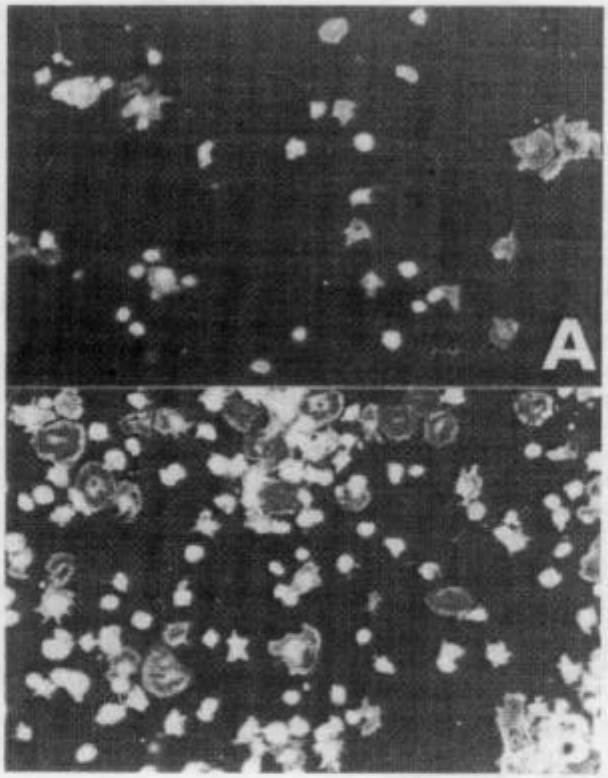

Figure 9. Immunofluorescence microscopy of platelets adhering on reference materials pellethane (A) and polypropylene (B) (magnification 600×).

investigation of PUEs morphology by Dr. H. Goering and the determination of polyol T_gs by Dr. A. Schoenhals is gratefully acknowledged. We are thankful to Mrs. I. Geike for technical assistance.

REFERENCES

1. L. Pinchuk, *J. Biomater. Sci. Polymer Edn* **6,** 225 (1994).
2. A. Z. Okkema, T. G. Grasel, R. J. Zdrahala, D. D. Solomon and S. L. Cooper, *J. Biomater. Sci. Polymer Edn* **1,** 43 (1989).
3. B. D. Ratner, A. S. Hoffman, S. R. Hanson, L. A. Harker and J. D. Whiffen, *J. Polymer Sci. Polymer Symp.* **66,** 363 (1979).
4. D. K. Han, S. Y. Jeong, Y. H. Kim and B. G. Min, *J. Biomater. Sci. Polymer Edn,* **3,** 229 (1992).
5. H. D. Wabers, T. J. McCoy, A. T. Okkema, R. W. Hergenrother, M. F. Wolf and S. L. Cooper, *J. Biomater. Sci. Polymer Edn* **4,** 107 (1992).
6. D. K. Han, S. Y. Jeong, K.-D. Ahn, Y. H. Kim and B. G. Min, *J. Biomater. Sci. Polymer Edn* **4,** 579 (1993).
7. Th. Groth, K. Klosz, E. J. Campbell, R. R. C. New, B. Hall and H. Goering, *J. Biomater. Sci. Polymer Edn* **6,** 497 (1994).
8. K. Kashiwagi, Y. Ito and Y. Imanishi, *J. Biomater. Sci. Polymer Edn.* **5,** 157 (1993).
9. W. Marconi, A. Martinelli, A. Piozzi and D. Zane, *Macromol. Chem. Phys.* **195,** 875 (1994).
10. Y. C. Shin, D. K. Han, Y. H. Kim and S. C. Kim, *J. Biomater. Sci. Polymer Edn* **6,** 281 (1994).
11. R. W. Hergenrother, X.-H. Yu and S. L. Cooper, *Biomaterials* **15,** 635 (1994).
12. P. A. Gentry, *J. Comp. Path.* **107,** 243 (1992).

13. E. W. Salzman, J. Lindon, G. McManama and A. Ware, *Ann. NY Acad. Sci.* **516,** 184 (1987).
14. N. Kiefer, in: *The Role of Platelets in Blood–Biomaterial Interactions,* p. 15, Y. F. Missirlis and J.-L. Wautier (Eds). Kluwer Academic Publishers, Dordrecht (1993).
15. E. W. Salzman and E. W. Merrill, in: *Hemostasis and Thrombosis. Basic Principles and Clinical Practice,* p. 1335, R. W. Coleman, J. Hirch, V. J. Marder and E. W. Salzman (Eds). J. B. Lippindorf Company, Philadelphia, PA (1987).
16. T. Lindhout, R. Blezer, C. Maassen and C. Reutlingsperger, *Nephrol. Dial. Transplant.* **9 (suppl. 2),** 83 (1994).
17. R. Eloy, J. Belleville, J. Paul, C. Pusineri, J. Baguet, M.-C. Rissoan, D. Cathignol, P. Ffrench, D. Ville and M. Tartullier, *Thromb. Res.* **47,** 223 (1987).
18. C. L. Haycox and B. D. Ratner, *J. Biomed. Mater. Res.* **27,** 1181 (1993).
19. A. Podias, Th. Groth and Y. Missirlis, *J. Biomater. Sci. Polymer Edn* **6,** 399 (1994).
20. Th. Groth, A. Podias and Y. Missirlis, *Colloids and Surfaces B: Biointerfaces* **3,** 241 (1994).
21. A. H. Goodall, *Blood Coagulation Fibrinolysis* **2,** 377 (1991).
22. Th. Groth, A. Gronert, S. Ziemer and R. Hesse, in: *The Reference Materials of the European Communities — Results of hemocompatibility Tests,* p. 183, W. Lemm (Ed.). Kluwer Academic Publishers, Dordrecht (1992).
23. Th. Groth, E. J. Campbell, K. Herrmann and B. Seifert, *Biomaterials* **16,** 1009 (1995).
24. E. Mitzner, H. Goering, R. Becker and J. P. Kennedy, *J. Macromol. Sci. Pure Appl. Chem.*, submitted.
25. J. Si and J. P. Kennedy, *J. Polym. Sci.: Part A* **32,** 2011 (1994).
26. J. P. Kennedy, V. S. C. Chang, R. A. Smith and B. Iván, *Polym. Bull.* **1,** 575 (1979).
27. J. P. Kennedy, L. R. Ross, J. E. Lackey and O. Nuyken, *Polym. Bull.* **4,** 67 (1981).
28. S. C. Yoon, B. D. Ratner, B. Iván and J. P. Kennedy, *Macromolecules* **27,** 1548 (1994)
29. M. D. Lelah and S. L. Cooper, *Polyurethanes in Medicine,* Ch. 7. CRC Press, Boca Raton, FL (1986).
30. J. D. Andrade, L. M. Smith and D. E. Gregonis, in: *Surface and Interfacial Aspects of Biomedical Polymers. Vol. 1: Surface Chemistry and Physics,* p. 249, J. D. Andrade (Ed.). Plenum Press, New York and London (1985).
31. A. Takahara, N. J. Jo and T. Kajiyama, *J. Biomater. Sci. Polymer Edn* **1,** 17 (1989).
32. F. J. Holly and F. R. Refojo, *J. Biomed. Mater. Res* **9,** 315 (1975).
33. K. Srinivasan, *Clin. Mater.* **7,** 27 (1991).

Publikation 10

Thomas Groth, Kerstin Herrmann, Ewan J. Campbell, Ryan R.C. New, Brenda Hall, Ruth Hesse, Hans Goering (1994).

Protein adsorption, lymphocyte adhesion and platelet adhesion/activation on polyurethane ureas is related to hard segment content and composition.

Journal of Biomaterials Science – Polymer Edition **6**, 497-510.

J. Biomater. Sci. Polymer Edn, Vol. 6, No. 6, pp. 497–510 (1994)

Protein adsorption, lymphocyte adhesion and platelet adhesion/activation on polyurethane ureas is related to hard segment content and composition

TH. GROTH[1]*, K. KLOSZ[2], E. J. CAMPBELL[3], R. R. C. NEW[3], B. HALL[3] and H. GOERING[4]

[1]*Biomaterials Research Unit, School of Medicine (Charité), Humboldt University, Tucholskystrasse 2, 10098 Berlin, Germany*
[2]*WIP,* [4]*ZMC (KAI e. V.), Geb. 12.5, Rudower Chaussee 5, 12489 Berlin, Germany*
[3]*Biocompatibles Limited, Brunel Science Park, Kingston Lane, Uxbridge UB8 3PQ, UK*

Received 6 October 1993; accepted 25 November 1993

Abstract—Segmented polyurethane ureas with different hard segment content and composition were synthesized using 4,4′-diphenylmethane diisocyanate and polytetramethylene glycols. Using polyols with different molecular weights, it was possible to synthesize polyurethane ureas with either: (i) a constant ratio of urethane to urea bonds; (ii) a constant urethane content; or (iii) a constant urea content. Bulk properties were assessed by dynamic mechanical analysis. Surface properties were estimated by contact angle measurements and streaming potential measurements. Haemocompatibility was evaluated *in vitro* by measuring the adsorption of human serum albumin (HSA) and fibrinogen (Fg), the adhesion of human peripheral blood lymphocytes (PBL), and the presence of activated platelets on the biomaterial surfaces. Enzyme immuno assays (EIA) have been specially developed for this purpose for the detection of antibody-recognizable plasma proteins and platelet surface membrane proteins. No simple correlation between chemical structure of the polymers and surface properties was found. Parameters of haemocompatibility correlated more closely with hard segment content and chemical composition than with the surface characteristics of the polymers. Adsorption of plasma proteins, adhesion of lymphocytes and the adhesion/activation of platelets were found to increase with increasing hard segment content of the polyurethane ureas. However, the monoclonal-antibody recognisable fibrinogen and the platelet activation were nearly constant with increasing hard segment content, if the urea content was kept constant.

Key words: Polyurethane ureas; physiochemical properties; blood cell adhesion; enzyme immuno assays; protein adsorption; platelet activation.

INTRODUCTION

The haemocompatibility of polymers can be considered as a multiparameter function of physicochemical surface properties such as surface hydrophilicity/hydrophobicity, surface charge density, hydrogen bonding properties, chain mobility on the surface, and others [1, 2]. These properties determine the adsorption profile of plasma proteins and subsequent cell adhesion and activation processes [3]. Central to the haemocompatibility of biomaterials is whether there is adsorption of cellular matrix proteins such as fibrinogen. These proteins are prerequisites for the adhesion and activation of platelets [4, 5] and subsequent thrombus formation.

Polyurethanes are one of the most widely used biomaterials because of their ease of synthesis, good mechanical properties, and a relatively good haemocompatibility.

* To whom correspondence should be addressed.

It has been proposed that both good mechanical properties and improved haemocompatibility are caused by the separation of a hard segment and a soft phase [6].

There have been several attempts to understand the mechanism of blood interaction with polyurethane ureas. Studies on the physicochemical and biological properties of polyurethane ureas were carried out using different types of polyols changing the hard segment content and the amount of urethane and urea at the same time [7–9]. Other investigations were concerned with the coupling of polyethylene oxide [6, 10] or ionic side groups such as sulfonate [11] and tertiary amino groups [12] to polyurethanes. Physicochemical properties of the synthesized materials were estimated in a comprehensive manner delivering an understanding of the relationship between polymer composition and the respective bulk and surface properties. However, the estimation of the haemocompatibility covered only limited aspects of the blood–polymer interaction.

To date relatively few investigations have been carried out to assess physicochemical properties of polyurethane ureas with increasing hard segment content and defined ratios/amounts of urethane and urea and relating it to parameters of haemocompatibility such as plasma protein adsorption/conformation, blood cell adhesion and platelet adhesion/activation. The objective of this study was therefore, to synthesise polyurethane ureas with increasing hard segment content having: (i) a constant ratio of urethane to urea; (ii) a constant urethane content; and (iii) a constant urea content. The physicochemical polymer properties were estimated by dynamic mechanical analysis, contact angle and streaming potential measurements and compared with the haemocompatibility as defined by the adsorption of HSA and Fg. The measurement of the adhesion of PBL was carried out to monitor changes of the adhesivity of the polymer with changing chemical structure. Finally, the adhesion and activation of platelets was estimated and compared with the adsorption of plasma proteins to give information on the relative haemocompatibility of the synthesized polyurethane ureas.

MATERIALS AND METHODS

Polymer synthesis

Segmented polyurethane ureas (PUU) with different hard segment content and hard segment composition were synthesized using 4,4′-diphenylmethane diisocyanate (MDI) and polytetramethylene glycols (PTMG). The expression 'hard segment content' includes all urethane and urea bonds. Using polyols with molecular weights 650, 1000, 1500, and 2000 and changing the ratio between diisocyanate, polyol and chain extender, it was possible to synthesise polyurethane ureas with either a constant ratio of urethane to urea bonds (UR/U), a constant urethane content (UR) or a constant urea content (U). Because there was no PTMG with a molecular weight of 1500 commercially available a mixture of PTMG 1000 and PTMG 2000 in a molar ratio of 1:1 was used. Figure 1 shows all synthesized PUUs with respect to their content of urethane and urea. Neopentyl glycol (NPG) and butanediol (BD) were used to increase the dispersity between hard and soft segment in the ratio PTMG : NPG : BD = 2 : 2 : 1.

The polyurethane ureas were synthesized by a prepolymerisation technique followed by chain extension. The prepolymer was formed from a mixture of the diisocyanate and glycol by heating at 80°C for 4 h. Chain extending was carried out

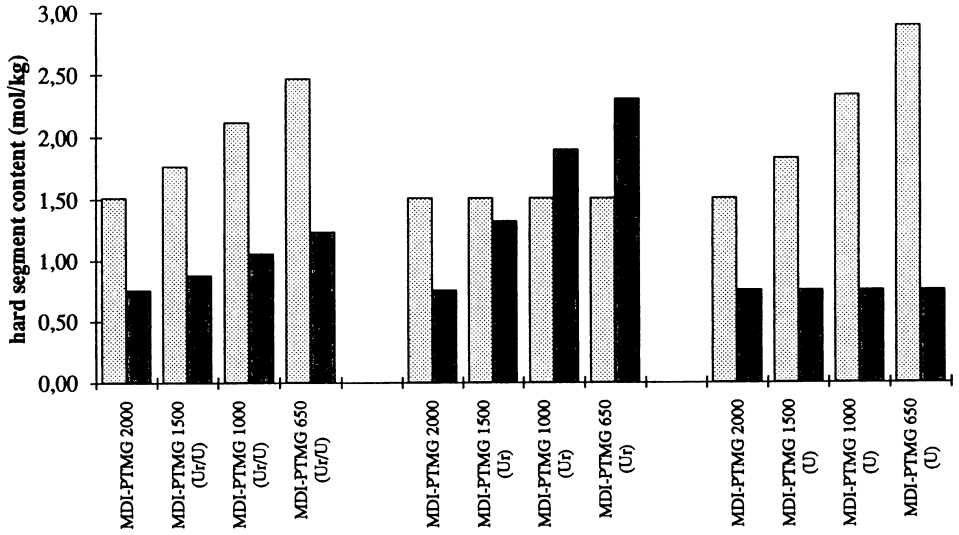

Figure 1. Scheme of synthesized polyurethane ureas based on 4,4′-diphenylmethane diisocyanate (MDI) and polyetramethylene glycoles (PTMG) with different molecular weights with: constant ratio of urethane (shaded columns) to urea (black columns) PUU-(UR/U); constant urethane content PUU-(UR); and constant urea content PUU-(U).

in solution (DMF) using water as chain extender. Cast sheets were prepared from the polymer solutions using glass plates. The polymer sheets were separated from the glass plates after evaporation of the solvent.

Bulk characterization

Dynamic mechanical analysis (DMA) of the polymers was performed for the estimation of polymer microphase morphology and mechanical behaviour using a Rheovibron DDV-II-B. Samples (size: 50 × 5 × 0.1 mm) were cooled to −120°C and a test frequency of 3.5 Hz was used. The temperature was then increased at $3°C\,min^{-1}$. The modulus E' and the $\tan\delta$ were estimated with respect to temperature. The maximum in the $\tan\delta$ curve was used for the estimation of the glass transition temperature (T_g).

Surface characterization

The estimation of the streaming potentials was carried out using a method developed by van Wagenen and Andrade [13]. The measured surface potentials were used for the calculation of zeta-potentials according to Eq. (1):

$$\zeta = \frac{\eta \times K_B \times E}{\varepsilon \times \varepsilon_0 \times \Delta P} \tag{1}$$

where E is the potential difference, ε is the dielectric constant of the solution, ε_0 is the dielectric constant of the vacuum, η is the viscosity of the solution, ΔP is the pressure drop along the measuring chamber, and K_B is the conductivity of the solution. The surface charge density σ of the polyurethane samples was calculated

from the zeta-potentials according to Eq. (2):

$$\sigma = \frac{\zeta \times \varepsilon \times \varepsilon_0}{\kappa^{-1}} \tag{2}$$

where κ^{-1} is the Debye-Hückel length. The surface potential measurements were carried out in 1 mM sodium chloride solution at pH 7.0.

The wettability of the polymers was estimated to assess the hydrophilicity of the polymer surfaces. The measurements were performed with contact angle measurements using sessile drops of water.

The surface free energy of the polyurethane ureas was estimated by contact angle measurements according to the method proposed by Rabel [14]. For this purpose various glycols (glycerol, ethylene glycol, polypropylene glycol, and diethylene glycol) were used as liquids *i*. The contact angle was measured using sessile drops of the various liquids. The surface free energy with dispersive and polar components was calculated according to Eq. (3):

$$\left[\frac{\cos\Theta + 1}{2} \times \frac{\gamma_L}{\sqrt{\gamma_L^d}} = \sqrt{\gamma_S^d} + \sqrt{\gamma_S^p} \times \sqrt{\frac{\gamma_L - \gamma_L^d}{\gamma_L^d}}\right]_i \tag{3}$$

with γ_L the surface tension of the liquid, γ_L^d and γ_L^p as the dispersive and polar parts of the surface tension, respectively. Equation (3) can also be considered as linear function $y = n + mx$. The polar and dispersive parts of the surface free energy of the polymer surface were then estimated from the slope and the intercept of the function (3).

Collection and handling of blood

Blood was collected from healthy donors who had not taken any medication for at least 10 days. The blood was collected in sodium citrate (3.19 g 100 ml^{-1}) at a blood/citrate ratio of 9 : 1.

Platelet rich plasma (PRP) was prepared by centrifuging the blood at 200*g* for 10 min. The supernatant PRP was collected and the blood was centrifuged at 2000*g* for 20 min to prepare platelet poor plasma (PPP). The platelet count in PRP was adjusted to 200 000 per μl by mixing PRP and PPP.

PBL were prepared by diluting citrated blood with PBS 2 : 1 and then centrifuging with Lymphoprep (TM, Nyegaard & Co., Oslo, Norway) at 400*g*, according to the method of Boyum [15]. The PBL were washed three times with phosphate buffered saline (PBS) containing 9 g l^{-1} sodium chloride, 10 mM sodium hydrogen phosphate, pH 7.4, and resuspended in Eagle-MEM to a final concentration of 2.5×10^6 cells ml^{-1}. The viability of lymphocytes was determined by trypan blue exclusion test and was higher than 95%.

Adhesion measurements

Measurement of PBL adhesion was determined under static conditions using the method of Altankov *et al.* [16, 17]. The polymer sheets were fixed on the bottom of a measuring chamber with an inner diameter of 10 mm. The PBL suspension (0.5 ml, 2.5×10^6 cells ml^{-1}) was pipetted into each measuring chamber. The chambers were then incubated at 37°C in a humidified CO_2-incubator for 60 min.

At the end of incubation non-adherent cells were removed by washing the surfaces three times with PBS. The adherent fraction of PBL was fixed by adding 1% glutaraldehyde solution. After 15 min fixation the surfaces were washed with PBS again and the cells were stained with 1% methylene blue for 1 h. The staining procedure was finished by removing the supernatant and washing the surfaces several times with tap water.

The degree of adherence was assayed photometrically by adding 1 ml 70% ethanol to each chamber to extract the dye from the cells. The supernatant was removed and the absorbance was measured at $\lambda = 627$ nm. The measured absorbances were compared with the number of cells counted microscopically in control experiments. A correlation has been shown between the number of cells and absorbances obtained at 627 nm [16]. Therefore, the measured absorbances were used to calculate the number of cells during the experiments.

Protein adsorption and platelet activation assays

Six-millimeter discs (six per sample) were cut from each test material and placed into wells of a microtitre plate. All following procedures were performed at ambient temperature.

Protein adsorption experiments were performed by adding 300 μl fresh frozen plasma (FFP) to each sample well. The samples were incubated for 10 min on a rotary plate shaker, then washed three times in PBS. For the estimation of HSA adsorption a solution of rabbit anti-HSA (Sigma) diluted 1:500 with 1% bovine serum albumin (BSA) in PBS was prepared. The Fg adsorption was investigated employing a solution of goat anti-human Fg (Sigma) diluted 1:1000 with 1% BSA in PBS. 300 μl of the appropriate antibody solutions were pipetted in four sample wells and 300 μl goat IgG fraction at the same concentration was added to two sample wells as a control for non antigen-antibody binding. The microtitre plates were incubated for 30 min on the rotary plate shaker. The samples were then washed four times with PBS. To all sample wells, 300 μl rabbit anti-goat IgG (Sigma) diluted 1:500 with 1% BSA was added and the plates incubated for 30 min on the rotary plate shaker. The samples were washed as described above.

The adsorption of Fg was further monitored using a monoclonal mouse anti-human Fg (Sigma) diluted 1:1000 with 1% BSA in PBS. Three hundred microlitres were added to four sample wells. A solution of mouse IgG at the same concentration was given to two sample wells as nonspecific control. The incubation and washing procedure was the same as described above. Then 300 μl of sheep anti-mouse IgG conjugated with peroxidase (Sigma) in a 1:400 dilution was added to all sample wells and the plates agitated for 30 min. The samples were washed with PBS. The samples were then transferred to a second plate and 300 μl *o*-phenylenediamine (OPD, Sigma) 0.4 mg ml^{-1} in 0.05 M phosphate citrate buffer with hydrogen peroxide (0.014%) was added and incubated for 10 min. At the end of the reaction 200 μl chromophore was then transferred to a third plate and the optical density read at 450 nm using a Techgen microplate reader giving a semiquantitative measure on the amount of proteins adsorbed onto the surface.

The estimation of platelet activation was performed according to the method proposed by Campbell *et al.* [18]. It was shown in previous studies that the degree of P-selectin translocation during platelet-biomaterial contact reflects the extent of

platelet adhesion and activation on a polymer surface [18, 19]. One hundred microlitres of PRP was added to four sample wells and 100 μl PPP to two sample wells as a control. The plate was put on the rotary shaker at room temperature of 30 min. Then the samples were washed four times with PBS. The monoclonal antibody CD 62 anti-P-selectin (Immunotech S. A., France) was prepared at a dilution of 1:100 in 1% BSA in PBS. One hundred microlitres of the antibody solution was added to all sample wells and the plate was agitated at room temperature for 60 min. Thereafter, the samples were washed four times with PBS. Sheep anti-mouse IgG peroxidase conjugated antibody (Sigma) was prepared at a 1:200 dilution in 1% BSA to prevent nonspecific adsorption. One hundred microlitres of the second antibody solution was added to each sample well. The plates were incubated for 60 min. Then the solution was discarded and the samples were washed four times with PBS. The samples were transferred to a second clean micro titre plate. OPD solution (1 mg ml^{-1}) was prepared in 0.1 M citrate buffer with hydrogen peroxide (0.03%). One hundred microlitres of chromogen was added to each sample well and the plates were incubated for 10 min to generate the chromophore. The reaction was stopped by adding 100 μl of 2 M sulphuric acid in 0.1 M sodium sulphide and the absorbances were read in a microplate reader set at a wavelength of 492 nm.

RESULTS

Bulk characterization

The bulk phase behaviour was characterized by the estimation of the modulus (E') shown in Fig. 2 and for tan δ in Fig. 3 in DMA measurement. As a result of the large number of samples, data are presented for the materials with the lowest hard segment content MDI-PTMG 2000 and the highest hard segment content MDI-PTMG 650 (UR/U), MDI-PTMG 650 (UR), and MDI-PTMG 650 (U). Generally, the measurements show that all materials have only one phase transition. However, the transitions vary in temperature and magnitude. Only the sample MDI-PTMG 2000 shows a tendency of phase separation in two wide phases with respect to

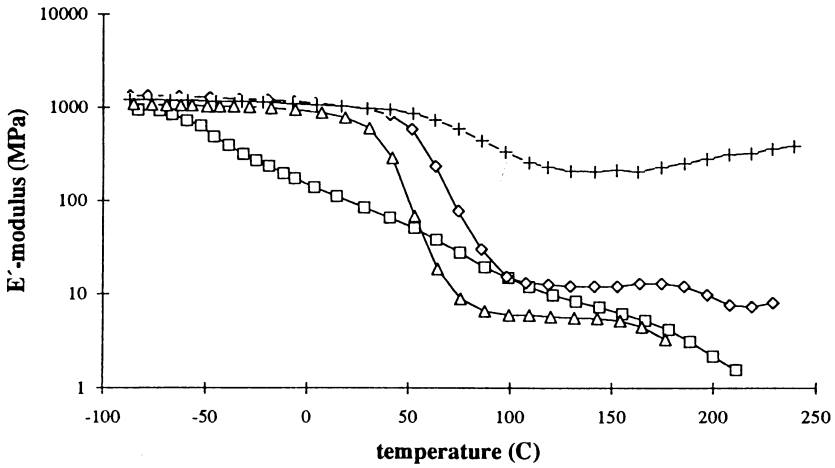

Figure 2. Results of dynamic mechanical analysis with E' plotted vs temperature T for: □ MDI-PTMG 2000; ◇ MDI-PTMG 650 (UR/U); + MDI-PTMG 650 (UR); and △ MDI-PTMG 650 (U).

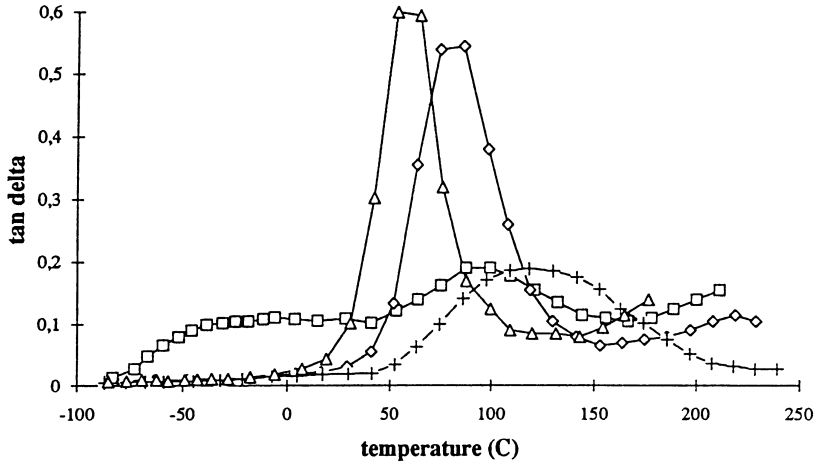

Figure 3. Results of dynamic mechanical analysis with tan δ plotted vs temperature T for: □ MDI-PTMG 2000; ◇ MDI-PTMG 650 (UR/U); + MDI-PTMG 650 (UR); and △ MDI-PTMG 650 (U).

temperature. Furthermore, with increasing hard segment content the glass transition temperature increases, but independently of the hard segment composition (not shown here).

Since the biological environment interacts at a temperature of 37°C with the polymers, E' at 37°C was plotted versus the hard segment content of the PUUs. It is shown in Fig. 4 that the E' of the PUU-(UR/U) and PUU-(UR) rises with increasing hard segment content from about 100 to about 1000 MPa. In comparison to this result the increase in E' of PUU-(U) is much less and remains below 300 MPa, even for the highest hard segment content polymer.

Surface measurements

The calculated surface charge densities were plotted vs the hard segment content as shown in Fig. 5. All the materials investigated possessed a negatively charged

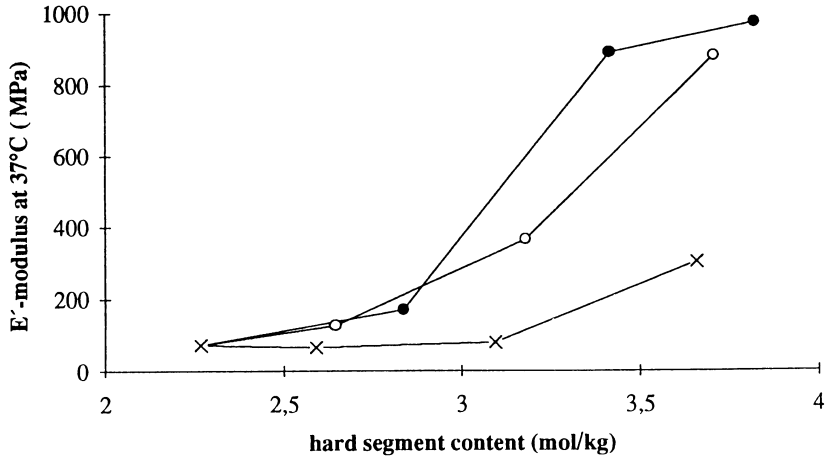

Figure 4. E' plotted vs the hard segment content of the different PUUs with: ○ PUU-(UR/U); ● PUU-(UR); and × PUU-(U).

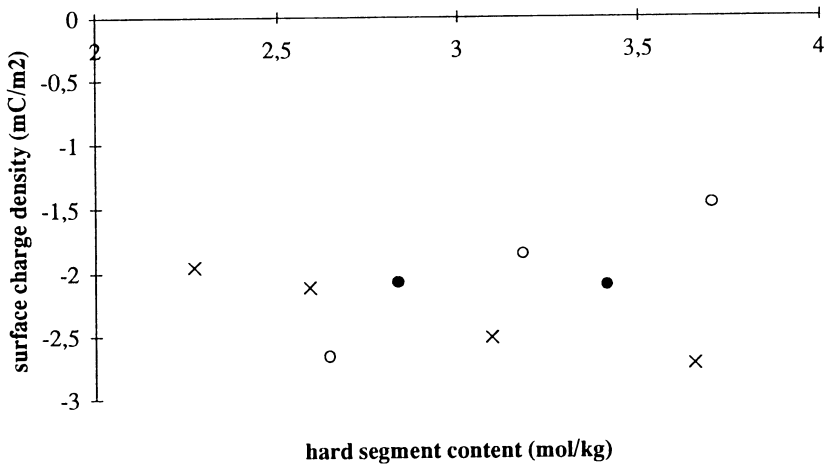

Figure 5. Results of streaming potential measurements with the calculated surface charge densities plotted vs the hard segment content of the different PUUs with: ○ PUU-(UR/U); ● PUU-(UR); and × PUU-(U).

surface. Excepting the material MDI-PTMG 1500 (UR/U) the surface charge density decreased with increasing hard segment content if the ratio of urethane to urea was constant (PUU-(UR/U)). If the urea content was increased (PUU-(UR)) then the surface charge density was constant. Whereas the surface charge density rose for increasing urethane content (PUU-(U)).

Figure 6 shows the results of wettability studied. The contact angle of water was plotted versus the hard segment content of the PUU. As can be seen in the figure the different types of PUU as well as the different hard segment contents did not cause any significant differences in the wettability of the polymers. Thus, all investigated PUU have similar properties concerning their wettability.

The results of contact angle measurements are demonstrated in Table 1. The table shows the contact angles for the different liquids and the calculated surface free

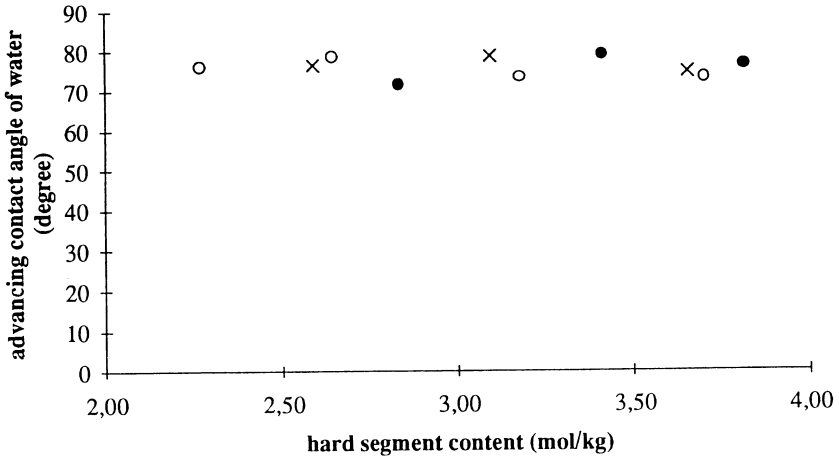

Figure 6. Results of wettability studies with the water contact angles plotted vs the hard segment content of the PUUs with: ○ PUU-(UR/U); ● PUU-(UR); and × PUU-(U).

Table 1.
Contact angles of PUUs measured with different glycols: Glyc—glycerol, EG—ethylene glycol, PG—propylene glycol, DEG—diethylene glycol. The surface free energy γ_S with polar part γ_S^p and dispersive part γ_S^d were calculated according to the method proposed by Rabel [14].

Material	θ_{Glyc}	θ_{EG}	θ_{PG}	θ_{DEG}	$\gamma_{s'}$ (mNm^{-1})	$\gamma_{s'}^d$ (mNm^{-1})	$\gamma_{s'}^p$ (mNm^{-1})
Series I							
MDI-PTMG 2000	78	61	51	53	26.8	22.9	3.9
MDI-PTMG 1500 (UR/U)	77	62	45	49	26.2	21.0	5.2
MDI-PTMG 1000 (UR/U)	74	60	43	51	27.3	20.4	6.9
MDI-PTMG 650 (UR/U)	79	65	43	—	27.5	25.0	2.5
Series II							
MDI-PTMG 2000	78	61	51	53	26.8	22.9	3.9
MDI-PTMG 1500 (UR)	75	60	33	52	28.6	24.1	4.5
MDI-PTMG 1000 (UR)	73	56	34	54	27.0	22.8	4.2
MDI-PTMG 650 (UR)	76	56	38	46	30.1	26.2	3.9
Series III							
MDI-PTMG 2000	78	61	51	53	26.8	22.9	3.9
MDI-PTMG 1500 (U)	76	62	44	51	27.4	22.9	4.5
MDI-PTMG 1000 (U)	75	61	47	55	26.8	21.1	5.7
MDI-PTMG 650 (U)	75	60	46	52	27.4	21.7	5.7

energy for the dispersive and polar components, respectively. Considering the deviation of the measurements the differences between the surface free energy were not significant. However, if only the polar part of the surface free energy was considered, differences between the three types of PUU could be observed. The PUU-(UR/U) caused an increase in the polar part with a final drop for MDI-PTMG 650 (UR/U). The anomalous behaviour of MDI-PTMG 650 (UR/U) was caused because it was not possible to obtain a round sessile drop of diethylene glycol. Therefore the contact angle for this liquid was not estimated. The dispersive part of surface free energy rose slightly for the PUU-(UR) with increasing hard segment content whereas the polar part was constant. The polar part of the surface free energy increased with increasing hard segment content if the amount of urea was kept constant (PUU-(U)).

PBL adhesion

Figure 7 shows the adhesion of PBL on the different PUU. It is shown in the figure that the adhesion of lymphocytes increased with increasing hard segment content of the polymers. Furthermore, no significant differences in PBL adhesion were observed in dependence on the type of PUU.

Protein adsorption studies

Figure 8 shows the amount of adsorbed HSA plotted versus the hard segment content of the polymers. As can be seen in the figure the amount of adsorbed HSA increased with increasing hard segment content of the PUU. Indeed the quantities of HSA adsorbed seemed to depend on the chemical composition of the polymers. However, the differences between the types of PUU were not significant.

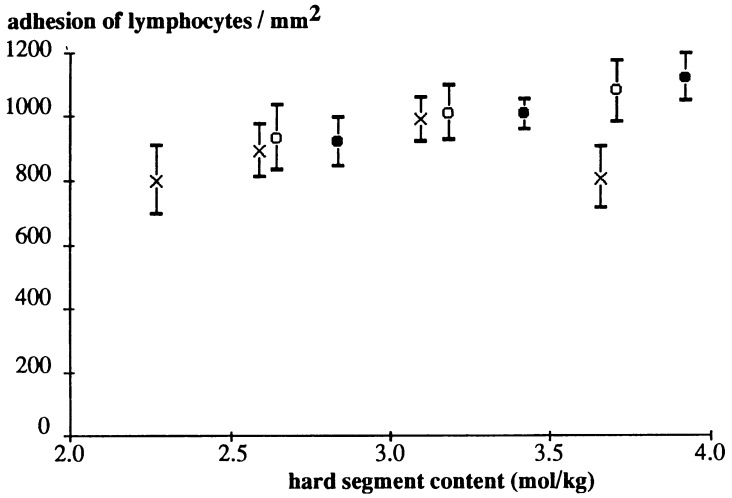

Figure 7. Adhesion of PBL under static conditions plotted vs the hard segment content of the PUUs with: ○ PUU-(UR/U); ● PUU-(UR); and × PUU-(U).

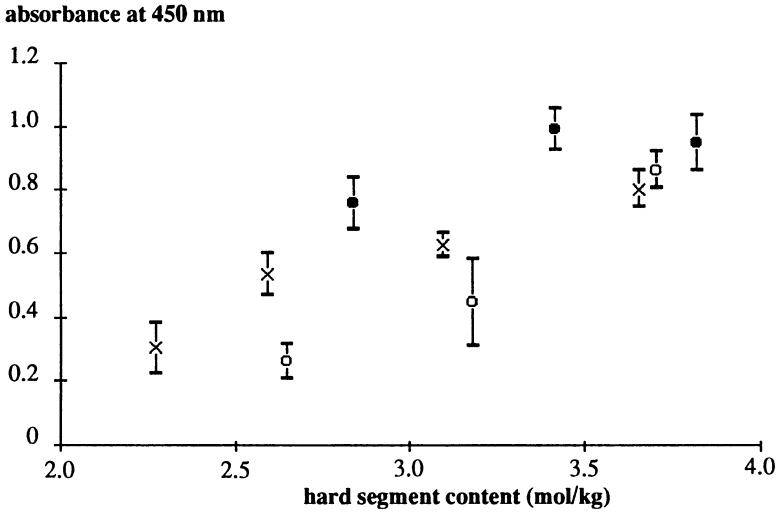

Figure 8. Adsorption of serum albumin after contact of citrated plasma with the PUUs measured with enzyme immuno assay using polyclonal anti-hsa with: ○ PUU-(UR/U); ● PUU-(UR); and × PUU-(U).

The adsorption of Fg was measured with polyclonal and monoclonal antibodies. Figure 9 shows that the amount of adsorbed Fg estimated with polyclonal antibodies was increasing with increasing hard segment content of the PUU independent on the chemical variations. If the amount of adsorbed Fg was measured with monoclonal antibodies a different adsorption pattern was observed. Figure 10 shows that the Fg adsorption increased with increasing hard segment content for PUU-(UR/U) and PUU-(UR). However, the amount of antibody-recognisable Fg decreased slightly with constant urea content (PUU-(U)).

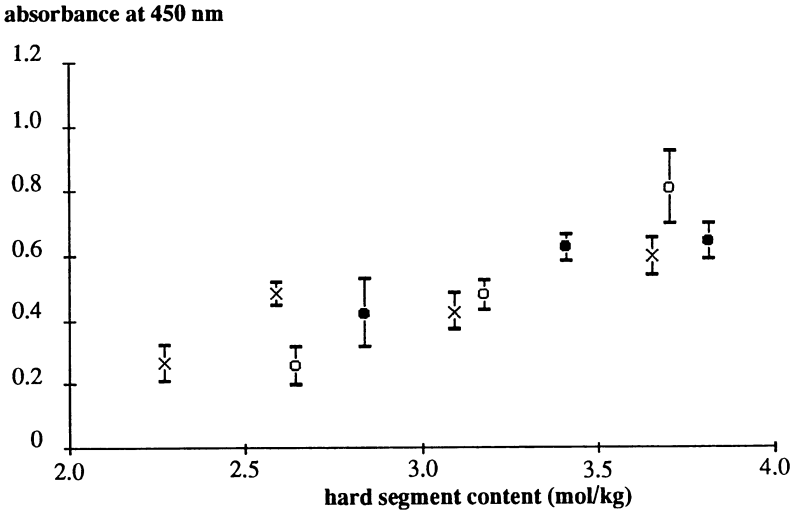

Figure 9. Adsorption of fibrinogen after contact of citrated plasma with the PUUs measured with enzyme immuno assay using polyclonal anti-human fibrinogen with: ○ PUU-(UR/U); ● PUU-(UR); and × PUU-(U).

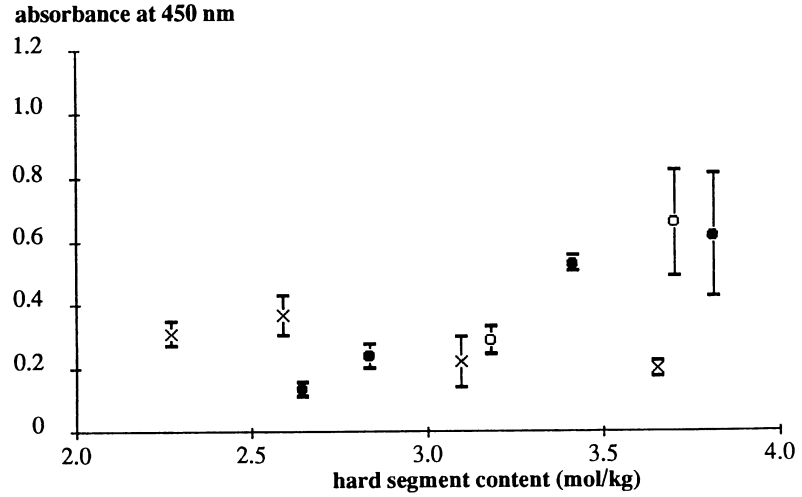

Figure 10. Adsorption of fibrinogen after contact of citrated plasma with the PUUs measured with enzyme immuno assay using monoclonal mouse anti-human fibrinogen with: ○ PUU-(UR/U); ● PUU-(UR); and × PUU-(U).

Platelet activation studies

The platelet activation measured with the monoclonal antibody for P-selectin expressed a rise with increasing hard segment content for PUU with constant ratio of urethane/urea (PUU-(UR/U)) and constant amount of urethane (PUU-(UR)) as shown in Fig. 11. In the same figure it was shown that the platelet activation was constant if the urea content was kept constant (PUU-(U)).

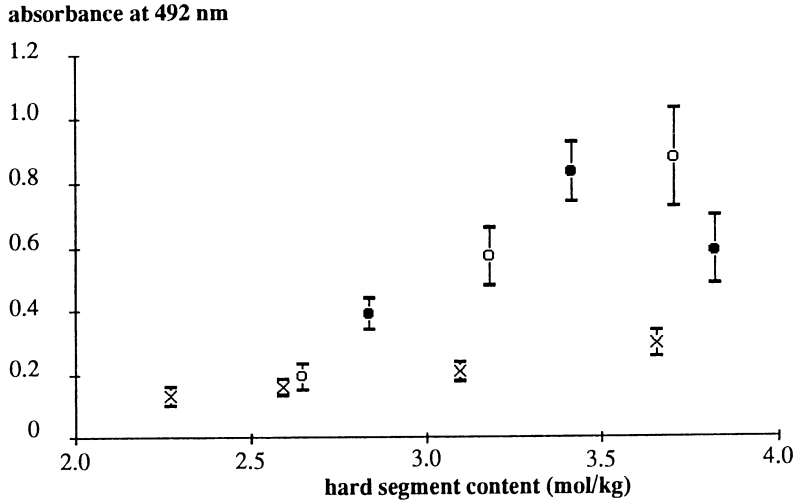

Figure 11. Measurement of platelet activation by an enzyme immuno assay for platelet P-selectin as marker of platelet activation. The estimated adsorbances were plotted vs the hard segement content of: ○ PUU-(UR/U); ● PUU-(UR); and × PUU-(U).

DISCUSSION AND CONCLUSIONS

It was shown in this study that the gradual increase of hard segment content significantly influences physicochemical material properties and the biological behaviour of polyurethane ureas. Furthermore, it was demonstrated that the quantities of functional groups contained might play a major role with respect to the haemocompatibility of polyurethane ureas. Interestingly, all three types of PUU expressed similarities in dependence on the hard segment content with respect to their physicochemical properties and differences concerning the final biological response e.g., platelet activation. Moreover, the newly developed EIA allow a semi-quantitative estimation of the adsorption of several plasma proteins as well as the monitoring of platelet activation processes.

The DMA showed a broad range of the transition temperature in the E' and tan δ measurements with only one phase transition for all synthesized materials. Since the width of the transition temperature is a measure of the phase microheterogeneity it indicates that all materials are highly amorphous. Because of the amorphous phase behaviour E' may also be considered as a measure of chain stiffness or otherwise the mobility of the polymer chain. When E' was plotted vs the hard segment content of the three types of PUUs at 37°C it was obvious that PUU-(U) had a lower E'. This result indicates that the mobility of the polymer chain with increasing urethane content does not change dramatically whereas the chain mobility decreases with increasing hard segment content for PUU-(UR/U) and PUU-(UR). It is known from other investigations that the state of hydrogen-bonding of urea is increased if the urea content itself increases and that non-bonded urea is rarely observed [9, 20]. The reason for this phenomenon is that urea shows a tendency to interact preferably with other urea groups [21]. It was further shown that the ratio of bonded to non-bonded carbonyl oxygen increases with increasing hard segment content [9, 20]. This may explain why E' at 37°C is increased with a rise in urea content shown for PUU-(UR) and PUU-(UR/U). However, in the studies mentioned above the ratio

of urethane to urea decreased creating a higher probability for hydrogen-bonding between urea groups and carbonyl oxygen. Since the urea content was kept constant for PUU-(U) the increased urethane content could be followed by a rise in non-bonded carbonyl oxygen allowing a higher chain mobility and thus possible structural rearrangement in contact with aqueous media.

If the surface free energy of all PUU was considered then obviously no significant differences could be observed. This was evident by the calculated surface free energy and the estimation of the wettability of polymers. Similar results have been obtained for other polyurethane ureas [9] showing that despite structural changes the measured surface free energies were similar. However, with increasing hard segment content it seemed that the content of urethane has an influence on the surface charge density and the polar part of surface free energy. It was shown that both parameters rise when the urethane content increases (PUU-(U)). In contrast both quantities were approximately constant for the other polymers (PUU-(UR/U) and (PUU-(UR)). This result could support the assumption of a higher amount of free carbonyl oxygen on the polymer surface available for polar interactions.

The results of biological investigations demonstrate generally decreasing haemocompatibility of PUUs with increasing hard segment content as described in many other studies [7, 8, 22]. However, as a result of our study a differentiation of PUUs concerning the composition of hard segment was possible. If completely non-specific interactions are considered than there is a general trend for all three types of PUUs of increasing cell adhesion and protein adsorption as shown for PBL, HSA and Fg. Non-specific means here interactions we define as those not dependent on receptor-ligand binding as required for the adhesion of cells and is therefore simply governed by physical forces such as electrostatic, dispersive, hydrophobic-hydrophilic interactions.

If specific interactions e.g., receptor-ligand interactions were considered then it was possible to differentiate the PUUs with respect to the their hard segment composition. It was shown that the adhesion and activation of platelets was nearly constant with increasing hard segment content of PUU-(U) in contrast to enhanced platelet activation for the other PUUs. Platelets interact via their GP IIb/IIIa receptor with Fg whereby the conformation of Fg is important for adhesion and activation [23, 24]. The investigation of Fg adsorption with a monoclonal antibody demonstrated decreasing antibody-binding with increasing hard segment content for PUU-(U) although the binding of polyclonal antibody was increased. Since the decrease of monoclonal antibody binding runs in parallel with the constant activation of platelets it was concluded that conformational changes diminish the binding of platelets to fibrinogen via GP IIb/IIIa receptor. Indeed also conformational changes of other attachment proteins may contribute to the smaller extent of platelet adhesion. The reason for the qualitatively different behaviour of PUU-(U) in this study may be explained by a higher amount of non-bonded carbonyl oxygen in comparison to the other series of PUU as indicated by physicochemical measurements. Since polyurethanes show a tendency to increase their state of hydrogen-bonded carbonyl oxygen at the interface upon hydration with water as proton donor [25], water molecules may be replaced by proteins. Hydrogen bonding is one major element of protein tertiary structure. Therefore, the interaction with such hydrogen acceptors on the surface of the polyurethane ureas might lead to conformational changes of Fg as indicated by the studies with monoclonal anti-fibrinogen antibodies.

The importance of the hydrogen bonding properties of PUU for protein denaturation was also clarified in other studies [12, 20].

In summary of this study it was shown that the haemocompatibility of polyurethane ureas is not simply a function of hard segment content but also dependent on hard segment composition. The applied EIA offer a more comprehensive view on the haemocompatibility of polymers since the comparison of whole fibrinogen binding as measured with polyclonal antibodies with the recognizability of fibrinogen measured with monoclonal antibodies is useful to detect conformational changes of proteins upon adsorption. Further, the estimation of platelet adhesion/activation gives information if any detected conformational changes of the protein are important for interaction of platelets with the biomaterial surface. Since the physicochemical measurements of surface properties in this study only indicated a different surface structure of PUU-(U) surface spectroscopy such as ESCA and AT-FTIR are planned in future investigations.

Acknowledgements

This work was supported in part by the School of Medicine (Charité) at Humboldt University Berlin and the programme WIP, grant 018484/M of the Ministry of Research and Technology (BMFT), Germany. The excellent technical assistance of Mrs Ruth Hesse is gratefully acknowledged.

REFERENCES

1. E. W. Merrill, *Ann. NY Acad. Sci.* **516**, 196 (1987).
2. H. Wolf, R. Karwath and Th. Groth, *Advances of Biomedical Measurements*, 411 (1988).
3. J. D. Andrade and V. Hlady, *Prog. Surface Sci.* **79**, 1 (1986).
4. D. M. Haverstick, J. F. Cowan, K. M. Yamada and S. A. Santoro, *Blood* **86**, 946 (1985).
5. E. W. Salzman, J. Lindon, G. McManama and J. A. Ware, *Ann. NY Acad. Sci.* **516**, 184 (1987).
6. A. Z. Okkema, T. G. Grasel, R. J. Zdrahala, D. D. Solomon and S. L. Cooper, *J. Biomater. Sci. Polymer Edn.* **1**, 43 (1989).
7. V. Sa Da Costa, D. Brier-Russell, G. Trudel III, D. F. Waugh, E. W. Salzman and E. W. Merrill, *J. Colloid Interface Sci.* **76**, 594 (1980).
8. V. Sa Da Costa, D. Brier-Russell, E. W. Salzman and E. W. Merrill, *J. Colloid Interface Sci.* **80**, 445 (1981).
9. T. G. Grasel and S. L. Cooper, *Biomaterials* **7**, 315 (1986).
10. S. Q. Liu, Y. Ito and Y. Imanishi, *J. Biomat. Sci. Polymer Edn* **1**, 111 (1989).
11. T. G. Grasel and S. L. Cooper, *J. Biomed. Mater. Res.* **23**, 311 (1989).
12. Y. Ito, M. Sisido and Y. Imanishi, *J. Biomed. Mater. Res.* **20**, 1139 (1986).
13. R. A. van Wagenen and R. A. Andrade, *J. Colloid Interface Sci.* **76**, 305 (1980).
14. W. Rabel, *Farbe Lack* **77**, 997 (1971).
15. A. Boyum, *Scand. J. Clin. Invest.* **21(suppl. 97)**, 77 (1968).
16. G. Altankov, Th. Groth, A. Kostadinov, F. Förster, H. Wolf, N. Nikolaeva and L. Marinova-Mutachiena, *C. r. Acad. bulg. Sci.* **43(7)**, 107 (1990).
17. G. Altankov and L. Smilenov, *Haematologia* **22**, 115 (1989).
18. E. J. Campbell, R. R. C. News and S. A. Charles, in: *MRS Symp. Proc.—Tissue-Inducing Biomaterials*, Vol. 252, p. 229, L. G. Cima and E. S. Ron (Eds) (1992).
19. Th. Groth, A. Gronert, S. Ziemer and R. Hesse, in: *The Reference Materials of the European Communities, Results of Hemocompatibility Tests*, W. Lemm (Ed.) (1992).
20. T. Sanada, Y. Ito, M. Sisido and Y. Imanishi, *J. Biomed. Mater. Res.* **20**, 1179 (1986).
21. D. Dieterich, *Polyurethane—Methoden der Organischen Chemie* **E20**, 1561 (1987).
22. K. Srinivasan, *Clin. Mater.* **7**, 27 (1991).
23. R. O. Hynes, *Thromb. Haemost.* **66**, 40 (1991).
24. J. N. Lindon, G. McManama, L. Kushner, E. W. Merrill and E. W. Salzman, *Blood* **6**, 355 (1986).
25. R. Barbucci, M. Casolaro and A. Magnani, *Clin. Mater.* **11**, 37 (1992).

Publikation 11

Volkmar Thom, Georgi Altankov, Thomas Groth, Katja Jankova, Gunnar Jonsson, Mathias Ulbricht (2000)

Optimizing Cell-Surface Interactions by Photo-Grafting of Poly(Ethylene Gylcol) (PEG).

Langmuir **16**, 2756-2765.

Optimizing Cell−Surface Interactions by Photografting of Poly(ethylene glycol)

V. H. Thom,[†] G. Altankov,[‡] Th. Groth,[§] K. Jankova,[†] G. Jonsson,[†] and M. Ulbricht*[,§]

Department of Chemical Engineering, Technical University of Denmark, DK-2800 Lyngby, Denmark, Institute of Biophysics, Bulgarian Academy of Sciences, Str. Acad. G. Bonchev, BG-1113 Sofia, Bulgaria, and Institute of Chemistry, GKSS Research Centre, Kantstrasse 55, D-14513 Teltow, Germany

Received March 30, 1999. In Final Form: November 5, 1999

A new general approach for improving polymer substratum biocompatibility is proposed. In a first example, polysulfone (PSf) film was modified by covalent end-on grafting of poly(ethylene glycol) (PEG) (2, 5, and 10 kDa) using well-defined, photoreactive α-4-azidobenzoyl *β*-methoxy PEG conjugates (ABMPEG). After adsorption from aqueous solution, ABMPEG was photografted under wet conditions onto PSf, where the degree of surface functionalization could be controlled through the applied ABMPEG concentration during adsorption. Attained surface characteristics, after changing systematically ABMPEG concentration, molecular weight, and the ratio of binary ABMPEG mixtures, were monitored by air−water contact angles (CA, captive bubble method) and partially also by X-ray photon spectroscopy (XPS). For ABMPEG 10 kDa adsorption kinetics and grafting efficiency as a function of applied concentration were evaluated by both CAs and fibronectin (FN) adsorption (in situ ellipsometry) to surfaces modified at different degrees of functionalization. CAs attained equilibrium values only after about 1−2 h, suggesting that surface organization processes retard ABMPEG adsorption. FN adsorption decreased monotonically as the degree of surface functionalization increased. Human skin fibroblast interaction with ABMPEG 10 kDa functionalized PSf films was studied, and a clear optimum of fibroblast−material interaction on mildly modified surfaces could be found based on the number of adhering cells, but also on morphological criteria including overall cell morphology, cell spreading, and formation of focal adhesion contacts, visualized by fluorescent staining of vinculin. The results suggest that adhesive proteins such as FN are adsorbed in a biologically active state yielding enhanced cell−substratum interaction when a hydrophobic substratum is surface modified at an intermediate degree with hydrophilic, flexible, sterically demanding, and possibly "self-assembled" macromolecules, e.g., PEG. Presumably, those macromolecules exert a lateral pressure upon neighboring adsorbed adhesive proteins, yielding surface bound but in their active conformation stabilized proteins with high biological activity.

Introduction

Unique properties make poly(ethylene oxide) (PEO) (We use PEG in place of PEO when referring to molecular weights below 25 kDa.) a polymer of considerable commercial and fundamental interest.[1] Surfaces modified by tethered, water-soluble, and nonionic polymer can create a "bioinert" interphase and are used in a host of biomedical applications.[1,2] Surface-induced thrombosis is one of the major problems in clinical applications of blood-contacting devices.[2] In this respect, PEG is gaining particularly extensive recognition due to its resistance to protein adsorption and cell adhesion. In contrast, however, to facilitate and control the cellular interaction is one of the main goals for designing biomaterial surfaces, especially when considered for advanced applications in bioengineered tissues and biohybrid organs.[3]

The protein-repellent character of PEG-coated (pegylated) surfaces is accredited to a combination of several molecular mechanisms.[4] Today, consensus seems to be that steric stabilization forces between tethered PEG and solvated proteins represent the dominant mechanism.[5,6] The functionality of PEG coatings is dependent on the molecular weight,[7] the interfacial chain density,[5,8] the structural properties (e.g., linear versus branched/cross-linked),[9] and the way of attachment (e.g., adsorption versus covalent grafting) of the coat-forming PEG molecules. However, one observes that a dominant correlation between repellent character and PEG interfacial density exists: the higher the latter, the lower the adsorption of proteins.

On the other hand, adsorption of proteins on biomaterials plays an important role in mediating cell attachment and cell−surface interactions. Cell attachment corresponds in many cases with the presence of adsorbed adhesive proteins, such as fibronectin (FN), vitronectin (VN), fibrinogen (FG), and others.[10−13] Several studies show that the functionality or biological activity of adhesive proteins depends on the substratum on which

* Address correspondence to this author at ELIPSA GmbH, Innovationspark Wuhlheide, Köpenicker Strasse 325, D-12555 Berlin, Germany. Fax: x 49-30-65762941. E-mail: ELIPSA@t-online.de.

[†] Technical University of Denmark.

[‡] Bulgarian Academy of Sciences.

[§] GKSS Research Centre.

(1) Harris, J. M. In *Poly(ethylene glycol) chemistry. Biotechnical and biomedical applications*; Harris, J. M., Ed.; Plenum Press: New York, 1992; p 1.

(2) Lee, J. H.; Lee, H. B.; Andrade, J. D. *Prog. Polym. Sci.* **1995**, *20*, 1043.

(3) Lanzer, R. P.; Langer, R.; Chick, W. L. In *Principles of tissue engineering*; Academic Press: Austin, TX, 1997; p 808.

(4) Andrade, J. D.; Hlady, V. *Adv. Polym. Sci.* **1986**, *79*, 1.

(5) Sofia, S. J.; Premnath, V.; Merrill, E. W. *Macromolecules* **1998**, *31*, 5059.

(6) Szleifer, I. *Curr. Opin. Solid State Mater. Sci.* **1997**, *2*, 337.

(7) Prime, K. L.; Whitesides, G. M. *J. Am. Chem. Soc.* **1993**, *115*, 10714.

(8) Schröen, C. G. P. H.; Cohen Stuart, M. A.; Voort Maarschalk van der, K.; Padt van der, A.; Riet van't, K. *Langmuir* **1995**, *11*, 3068.

(9) Elbert, D. L.; Hubbell, J. A. *Annu. Rev. Mater. Sci.* **1996**, *26*, 365.

(10) Grinnell, F. *Int. Rev. Cytol.* **1978**, *53*, 65.

10.1021/la990303a CCC: $19.00
Published on Web 01/27/2000

they are adsorbed.[11,13,14] It is well-known that proteins adsorbed onto solid surfaces may undergo conformational changes because of their relatively low structural stability and their tendency to unfold in order to realize further bond formation with the surface.[15,16] Thus, whether cells attach, grow, or become activated appears to depend on how the adsorbed protein layer is formed. Adsorption of FN for example to solid surfaces can induce conformational changes in the protein which have been monitored by (1) changes in the IR spectra of adsorbed FN over time,[17] (2) changes in the total internal reflection of intrinsic trytophan fluorescence of adsorbed FN,[18] (3) directly observed changes in physical shape (unfolding into an "extended" conformation),[19] (4) changes in antibody binding,[20] and (5) changes in solvent accessibility of the free sulfhydryl group as examined by a spin-label study.[21] Similar observations exist for FG and VN.[17,22,23] Few attempts to correlate the observed physical changes of adsorbed adhesive proteins with their biological activity have been undertaken, and the results are not unambiguous. Pettit et al.[14] could not find a strong correlation between the extent of antibody binding to the integrin recognizable RGD containing domain of FN adsorbed on a variety of surfaces and outgrowth of corneal epithelial cell on the same surfaces. (The tripeptide arginine−glycine−aspartic acid, RGD, is the minimal cell-recognizable sequence in many adhesive plasma and extracellular matrix proteins.) However, Lewandowska et al.[24,25] demonstrated that attachment and spreading of murine fibroblasts (3T3) and human neuroblasts (Platt) on self-assembled monolayers terminated with different specific end groups correlated well with the conformational properties of adsorbed FN monitored by FTIR/ATR techniques.

In this paper we present experimental results which counteract the general appreciation of PEG coatings in relation to cellular adhesion. Our study shows that the pegylation of surfaces at intermediate interfacial densities, noneffective for complete reduction of protein adsorption, can in fact enhance cellular adhesion. We explain the results through the stabilizing effect of neighboring PEG moieties on adsorbed adhesive proteins yielding tightly bound but in their active conformation stabilized adhesive proteins resulting in high biological activity. This was obtained by modifying polymer surfaces with well-defined PEGs using UV initiated grafting of photoreactive PEG aryl azide conjugates (ABMPEG) of different molecular weights,[26] a technique earlier introduced by Guire et al.[27] and Tseng and Park.[28] As a model substratum, polysulfone (PSf) spin-coating films applied either on glass or on silicon wafers were used. The attained interfacial density of the ABMPEG layer depends on the first adsorption step in this procedure and thus on substratum−ABMPEG interactions which are directly related to the amphiphilic character of the PEG conjugate, its structure (e.g. chain length), substratum characteristics, and the solution conditions (concentration, salt, temperature). Keeping all other parameters constant, layer density can be controlled by changing ABMPEG concentration.

We present contact angle data characterizing ABMPEG adsorption and photografting to PSf substratum, where advancing and receding contact angles at the air−water interface were measured using the captive bubble method. X-ray photon spectroscopy (XPS) was applied to reveal the elemental composition of the outer surface of unmodified and modified PSf films. FN adsorption to differently modified PSf surfaces was monitored by in situ ellipsometry. Cell−material interaction was characterized using human fibroblasts in a short-term culture model where cell adhesion to the different surfaces was quantified and further characterized by studying the overall cell morphology and the extent of focal adhesions formation of the adhering cells. All surfaces were studied either plain or after precoating with serum in order to simulate surfaces that are covered with adhesive proteins.

Methods and Materials

1. Preparation and Characterization of PSf Substrata. Glass coverslips (15 mm × 15 mm; Menzel, Germany) are first cleaned with detergent, rinsed with Milli-Q water, and etched for 15 min at approximately 40 ± 5 °C in a freshly mixed 3:1 (v:v) sulfuric acid (96%):hydrogen peroxide (30%) solution, then thoroughly rinsed, stabilized for 2 h, and rinsed again in Milli-Q water, and finally dried free of dust for 2 h at 120 °C. Polished silicon wafers (Topsil, Denmark; for ellipsometry measurements) are thermally oxidized in pure oxygen followed by annealing and cooling under argon flow to yield an oxide layer of about 30 nm. Wafers are cut into rectangular slides (10−14 mm × 20−30 mm). To attain a hydrophobic surface for enhanced PSf film adhesion on the supports, *n*-octadecyldimethylchlorosilane (ODMS; Sigma) is grafted by immersing them in a 2% (w:w) ODMS in *n*-hexane solution for 1 h at room temperature. Supports are consecutively rinsed twice with *n*-hexane and three times with ethanol and air-dried at room temperature. Then ODMS-treated supports are spin-coated with a 3% (w:w) solution of polysulfone (PSf; Udel 3500, Amoco; received from Danish Separation Systems ApS, Denmark) in 1,2-dichlorobenzene (10 s at 500 rpm and consecutively for 50 s at 5.000 rpm) and dried for at least 4 h in vacuum at 60 °C. This yields a PSf film thickness of approximately 40 nm as ellipsometrically verified by Koehler et al.,[29] who used an identical polymer solution and a similar spinning regime. The roughness of the PSf films is determined with a scanning force microscope (SFM; Nanoscope III, Digital Instruments, USA) using the height mode under ambient conditions.

2. PSf Surface Modification with ABMPEG. Synthesis of ABMPEG by quantitative esterification of monomethoxypoly(ethylene glycol) (MPEG) having a molecular weight (MW) of about 5 kDa (i.e., 5000 g/mol) (Shearwater Polymers, Netherlands) with 4-azidobenzoyl chloride is described in detail in a previous paper.[26] In this study ABMPEGs in three different MWs

(11) Grinnell, F. In *Blood in contact with natural and artificial surfaces*; Leonard, E. F., Turitto, V. T., Vroman, L., Eds.; Ann. N.Y. Acad. Sci.; New York, 1987; p 280.
(12) Groth, T.; Zlatanov, I.; Altankov, G. *J. Biomater. Sci. Polym. Ed.* **1994**, *6*, 729.
(13) Groth, T.; Herrmann, K.; Campell, E. J.; New, R. R. C.; Hall, B.; Hesse, R.; Goering, H. *J. Biomater. Sci. Polym. Ed.* **1994**, *6*, 497.
(14) Pettit, D. K.; Hoffman, A. S.; Horbett, T. A. *J. Biomed. Mater. Res.* **1994**, *28*, 685.
(15) Norde, W.; Lyklema, J. *J. Biomater. Sci. Polym. Ed.* **1991**, *2*, 183.
(16) Andrade, J. D.; Hlady, V.; Feng, L.; Tingey, K. In *Interfacial phenomena and bioproducts*; Brash, J. L., Wojciechowski, P. W., Eds.; Marcel Dekker: New York, 1996; p 19.
(17) Pitt, W. G.; Spiegelberg, S. H.; Cooper, S. L. In *Proteins at interfaces*; Horbett, T. A., Brash, J. L. Eds. ACS Symposium Series 343; American Chemical Society: Washington, DC, 1987; p 992.
(18) Iwamoto, G. K.; Winterton, L. C.; Stoker, R. S.; Wagenen van, R. A.; Andrade, J. D.; Mosher, D. F. *J. Colloid Interface Sci.* **1985**, *106*, 459.
(19) Erickson, H. P.; Carrel, N. *J. Biol. Chem.* **1983**, *258*, 14539.
(20) Ugarova, T. P.; Zamarron, C.; Veklich, Y.; Bowditch, R. D.; Ginsberg, M. H.; Weisel, J. W.; Plow, E. F. *Biochemistry* **1995**, *34*, 4457.
(21) Narasimhan, C.; Lai, C. S. *Biochemistry* **1989**, *28*, 5041.
(22) Fabrizius-Homan, D. J.; Cooper, S. L. *J. Biomater. Sci. Polym. Ed.* **1991**, *3*, 27.
(23) Lenk, T. J.; Horbett, T. A.; Ratner, B. D.; Chittur, K. K. *Langmuir* **1991**, *7*, 1755.
(24) Lewandowska, K.; Pergament, E.; Sukenik, C. N.; Culp, L. A. *J. Biomed. Mater. Res.* **1992**, *26*, 1343.
(25) Cheng, S.-S.; Chittur, K. K.; Sukenik, C. N.; Culp, L. A.; Lewandowska, K. *J. Colloid Interface Sci.* **1994**, *162*, 135.
(26) Thom, V.; Jankova, K.; Ulbricht, M.; Kops, J.; Jonsson, G. *Macromol. Chem. Phys.* **1998**, *199*, 2723.
(27) Guire, P. E.; Dunkirk, S. G.; Josephson, M. W.; Swanson, M. J. US Patent 5002582, 1991.
(28) Tseng, Y. C.; Park, K. D. *J. Biomed. Mater. Res.* **1992**, *26*, 373.
(29) Koehler, J. A.; Ulbricht, M.; Belfort, G. *Langmuir* **1997**, *13*, 4162.

Scheme 1. Polymer Surface Functionalization Procedure

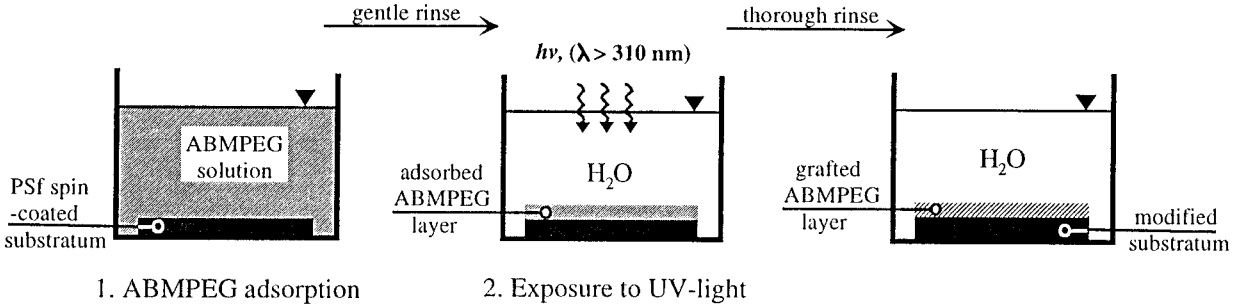

are prepared accordingly: ABMPEG 2 kDa, ABMPEG 5 kDa, and ABMPEG 10 kDa. ABMPEGs are additionally diafiltrated using a 500 Da MW cutoff membrane in order to remove low-MW impurities. The number-average molecular mass ($\bar{M}_n$) and weight-average molecular mass ($\bar{M}_w$) of MPEGs and ABMPEGs are determined by size exclusion chromatography (SEC), using a Shimadsu LC-10AD pump, two consecutive cross-linked polystyrene columns (Mixed-D, Polymer Laboratories), and a differential refractometer (Model 200, Viscotek). Measurements are performed in THF solvent at room temperature with a 1 mL/min flow. The calibration is based on PEG standards having $\bar{M}_w/\bar{M}_n < 1.1$. UV absorbance of aqueous solution of ABMPEGs is determined with a Perkin-Elmer UV/vis spectrophotometer Model 320.

ABMPEG grafting onto PSf surfaces includes the following two consecutive steps as illustrated in Scheme 1: first, aqueous ABMPEG solution of different concentrations, is placed on the PSf-coated surface, covered, and kept in the dark for 12−18 h. Thereafter samples are gently rinsed in Milli-Q water, covered by water, and immediately exposed to UV light for 1 min. UV irradiation is generated by a 50 W high-pressure mercury lamp (L.O.T.−ORIEL, Germany) equipped with a condenser and a high-pass glass filter with a cutoff at 320 nm yielding an intensity of 30 mW/cm^2. After exposure surfaces are thoroughly rinsed with Milli-Q water. Additionally, one set of samples is shaken during adsorption using a rocker table, while the other set of samples remains static. Adsorption kinetics of ABMPEG onto PSf is monitored by interrupting the adsorption step after different time periods, varying from 15 min to 16 h. Certain indicated reference surfaces are either not exposed to UV light or modified with either unfunctionalized MPEG or binary mixtures of ABMPEGs of different MW or, to remove nongrafted moieties, flushed overnight with an 2-propanol/water (1:1, v:v) mixture.

3. Contact Angle Measurement. Contact angles (CAs) are measured using the captive bubble method, where an air bubble is injected from a syringe with a stainless steel needle onto the inverted sample surfaces immersed into ultrapure Milli-Q water. The diameter of the contact area between surface and bubble is always greater than 3 mm. While the needle remains inside the bubble, advancing and receding angle measurements are realized with a goniometer fitted with a tilting stage (Carl Zeiss, Germany) by stepwise withdrawing/adding air from/to the captured bubble. At least 10 measurements of different bubbles on at least three different locations are averaged to yield one CA value. The standard deviation is indicated as error bars.

4. X-ray Photon Spectroscopy (XPS). XPS experiments are performed with a SpecsLab Sage 100 instrument. The spectra are acquired at a pressure of under 10^{-4} Pa and an operating power of 100 W, from 1×2 mm^2 sample regions illuminated by a Mg Kα X-ray source at an angle of 90° between sample surface and electron analyzer. Survey scans were performed on each sample to ensure no foreign elements were present. High-resolution scans of the C_{1s}, O_{1s}, N_{1s}, and S_{2p} regions were aquired with a pass energy of 23 eV. Elemental surface compositions were determined after including the appropriate elemental sensitivity factors.

5. Fibronectin Adsorption Measured by *in Situ* Ellipsometry. 5.1. Procedure. FN (human plasma, lyophilized, MW 440 kDa; Boehringer Mannheim, Germany) is reconstituted in phosphate-buffered saline (PBS; 5.8 mM Na_2HPO_4/NaH_2PO_4, 150 mM NaCl, pH 7.4) containing 0.02% (w/v) sodium azide giving a concentration of about 0.12 g/L. An automated Rudolph Thin Film ellipsometer, Type 43603-200E, equipped with a thermostated quartz cuvette and a stirring device is used. The light source is a helium−neon laser having a beam wavelength of 632.8 nm and an angle of incidence 68°. Differently modified PSf films on silicon wafers are placed in the quartz cuvette and stabilized in 2.5 mL of PBS buffer for at least 15 min or until constant polarizer and analyzer signals are obtained. A volume of 0.5 mL of the concentrated FN solution is added, yielding 3 mL with a defined concentration of 0.02 g/L. The magnetic stirrer is activated for 2−3 s upon addition of the protein concentrate in order to homogenize the solution. After 30 min the cuvette is flushed for 10 min with PBS buffer using preinstalled tubings and a flow rate of 20 mL/min. The polarizer and analyzer data is automatically collected during the whole period.

5.2. Calculation of the Adsorbed Amount. There are detailed descriptions of the physical principles of the method[30] and the instrumental setup.[31] From the measured ellipsometric angles, Ψ and Δ, it is possible to calculate the thickness and refractive index of an adsorbed layer on a surface, as done by McCrackin et al.[32] The determined thickness and refractive index of the adsorbed film is converted to a value of adsorbed mass using the Lorentz−Lorenz relationship for the refractive index of a mixture of substances as developed and experimentally verified by Cuypers et al.[33] As shown by these authors, a higher accuracy will be obtained in the determination of the adsorbed mass than in the determination of the refractive index and the thickness, especially at low surface coverage.

In the calculations of the amount of protein adsorbed, the different layers, silicon support, silicon oxide, ODMS-layer, PSf film, and tethered ABMPEG, are treated as one optical unit with an effective refractive index (cf. Results and Discussion). The molar refractivity of FN is calculated as the sum of the individual molar refractivities of all amino acids in FN using tabulated data from Pethig[34] yielding a value of 3.99 g/mL. For the partial specific volume of FN the value 0.75 mL/g is used.

6. Cell Studies. 6.1. Cell Culture. Human fibroblasts are obtained from fresh skin biopsy and used up to the ninth passage. The cells are grown in Dulbecco's Modified Eagle Medium (DMEM) containing 10% fetal bovine serum (FBS; Sigma) in a humidified incubator with 5% CO_2. Fibroblasts from nearly confluent cultures are harvested with 0.05% trypsin/0.6 mM EDTA (Sigma), and trypsin is neutralized with FBS.

6.2. Cell Morphology and Number of Adherent Cells. Adhesion of fibroblasts is carried out in six-well tissue culture plates containing the unmodified and modified PSf-coated glass coverslips. Experiments are performed without or with precoating of the surfaces with FBS (Sigma) for 30 min at 37 °C. Approximately 10^5 cells in DMEM are pipetted into each well and incubated for 2 h at 37 °C in a humidified CO_2 incubator. Cell morphology is studied and photographed directly in the wells with an inverted phase contrast microscope Telaval 31 (Carl

(30) Azzam, R. M. A.; Bashara, N. M. *Ellipsometry and polarized light*, 3rd ed.; Elsevier Science: Amsterdam, 1987.
(31) Arnebrant, T. Thesis, Lund University, Lund, Sweden, 1987.
(32) McCrackin, F. L.; Passaglia, E.; Stromberg, R. R.; Steinberg, H. L. *Natl. Bur. Stand. U.S.A.: Phys. Chem.* **1963**, *67A*, 363.
(33) Cuypers, P. A.; Corsel, J. W.; Janssen, M. P.; Kop, J. M. M.; Hermens, W. T.; Hemker, H. C. *J. Biol. Chem.* **1983**, *258*, 2426.
(34) Pethig, R. *Dielectric and electronic properties of biological materials*; Wiley: New York, 1979.

Table 1. Molecular Weight Characteristics and Absorbance Coefficients of MPEGs and Their 4-Azidobenzoyl Conjugates

sample	$\bar{M}_n$(theor) (g mol^{-1})	SEC results $\bar{M}_n$ (g mol^{-1})	SEC results $\bar{M}_n/\bar{M}_w$	UV absorb. coeff[a] (L mol^{-1} cm^{-1})
MPEG 2 kDa	2000	1860	1.07	0
ABMPEG 2 kDa	2150	2030	1.04	15 500
MPEG 5 kDa	5000	4920	1.01	0
ABMPEG 5 kDa	5150	5150	1.06	16 030
MPEG 10 kDa	10 000	8940	1.02	0
ABMPEG 10 kDa	10 150	9230	1.02	17 040

[a] At wavelength λ = 275 nm, assuming $\bar{M}_n$(theor) and a stoichiometry of (aryl azide/PEG) = (1/1).

Table 2. Contact Angles and Surface Roughness (from Scanning Force Microscopy) for PSf Spin-Coating Films

PSf spin-coated on	advancing CA (deg)	receding CA (deg)	CA hysteresis (deg)	RMS (nm)
silicon wafer	90.5 ± 0.7	78.6 ± 2.0	11.9	0.44
cover glass	92.0 ± 1.5	77.0 ± 1.9	14.4	2.48

Zeiss, Germany). The mean number of adherent cells is determined by evaluating at least 30 different randomly chosen microscopic fields on each surface. Cell counts are normalized to the number of cells per square millimeter, and the standard deviation is determined for each set of fields on a surface.

6.3. Focal Adhesion Formation. Focal adhesions are visualized by immunofluorescence of vinculin. Samples are processed as follows: Attached cells are fixed with paraformaldehyde (3%) for 10 min and permeabilized with 0.2% Triton X-100 for 5 min. To detect focal adhesions, samples are incubated for 30 min at 37 °C with monoclonal anti vinculin antibody (Sigma), followed by Cy3 conjugated goat anti mouse secondary antibody (Jackson Immuno Research, USA). Samples are mounted with Mowiol and viewed and photographed with an inverted fluorescent microscope Axiovert 100 (Carl Zeiss, Germany).

Results and Discussion

1. Characterization of MPEG and ABMPEG. Table 1 lists characteristics of the MPEGs and their photoreactive conjugates as studied by SEC and UV spectroscopy. Symmetrical SEC curves and low polydispersities $\bar{M}_n/\bar{M}_w$ for both MPEG and ABMPEG indicate that conjugate synthesis involved no chain scission (cf. Thom et al.[26]). All photoreactive conjugates exhibit similar molar UV absorbance. Thus, through the use of well-defined, monofunctional MPEGs as educts, and their successful quantitative functionalization, well-defined, monofunctional ABMPEGs are obtained.

2. Pegylation of PSf Substrata. 2.1. Characterization of PSf Substrata. The modification of PSf substrata with ABMPEG (see Scheme 1) was characterized with CA data. Table 2 compares surface roughness as determined by SFM and CA for PSf films spin-coated on either glass or silicon wafers. The films on glass were rougher due to the elevated roughness of this support in relation to a polished silicon wafer. CAs were essentially identical for both films, but show slightly smaller hysteresis for the less rough film. Possible reasons for the hystereses are surface roughness and morphological heterogeneities. However, the quality of both films is considered sufficient for the intended studies.

It is important to note that modified substrata, independent of whether exposed to UV irradiation or not after the first adsorptive step, exhibited unchanged CAs for at least 2 weeks when kept in aqueous environment. Only by flushing with a 2-propanol/water-mixture was it possible to remove nongrafted moieties (see section 2.5).

2.2. Variation of the Time of Adsorption. Figure 1 shows advancing and receding CAs for PSf films which

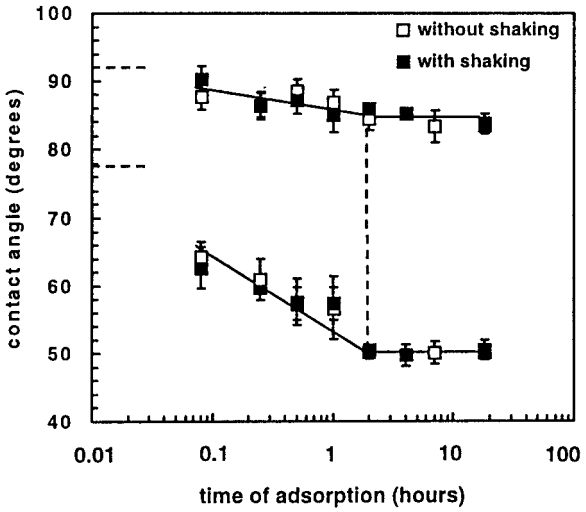

Figure 1. Adsorption kinetics of ABMPEG 10 kDa on PSf spin-coating films monitored by contact angle measurements. Adsorption was carried out with or without shaking. Error bars indicate standard deviations.

were exposed for different periods of time to an ABMPEG 10 kDa solution of 1 g/L, either with shaking or under static conditions. Both data sets, falling CAs and rising CA hystereses over a period of approximately 1−2 h followed by constant values, are essentially identical. Both the period of time necessary to reach an apparent equilibrium situation at the interface and the fact that shaking had no influence indicate an adsorption mechanism which is not diffusion controlled. Note that at a concentration of 1 g/L, assuming purely diffusive mass transport ($D_{(ABMPEG)} = 9.9 \times 10^{-7}$ cm^2/s)[35] and a perfect adsorber, 67 μg/cm^2 ABMPEG should have reached the interface in 1 h. This is an unrealistically high value, exceeding reported values for PEG amphiphiles by 1−2 orders of magnitude.[8,36]

The results suggest that an ordering mechanism takes place, where surface-active and head group anchored ABMPEG 10 kDa molecules seek an interfacial organization which minimizes lateral interaction between sterically demanding PEG tails resulting in a "self-assembled" ABMPEG monolayer. Various experimental and theoretical studies are in qualitative agreement with this proposed mechanism.[37]

2.3. Variation in Concentration. In Figure 2 it can be seen that with rising ABMPEG 10 kDa solution concentrations the modified PSf films showed decreasing advancing and receding CAs and increasing CA hystereses. This is a typical result for a surface of a material with low surface energy (PSf) which is gradually covered by a material exhibiting a higher surface energy (PEG). As the receding angle tends to characterize the material of higher surface energy, and the advancing angle the material of lower surface energy, an initial rise in CA hystereses is expected for increasing surface coverage.[38] XPS characterization of the same range of surfaces showed the expected trends of elemental composition, i.e., rising atom percentage for oxygen and nitrogen and falling atom percentage for carbon and sulfur. However, a total shielding of the underlying PSf was not observed (the atom percentage of sulfur was reduced only by 25% for the

(35) Devanand, K.; Selser, J. C. *Macromolecules* **1991**, *24*, 5943.
(36) Alstine van, J. M.; Malmsten, M. *Langmuir* **1997**, *13*, 4044.
(37) Amiel, C.; Sikka, M.; Schneider, J. W.; Tsao, Y.-H.; Tirrell, D. A.; Mays, J. W. *Macromolecules* **1995**, *28*, 3125.
(38) Dettre, R. H.; Johnson, R. E. *J. Phys. Chem.* **1965**, *69*, 1507.

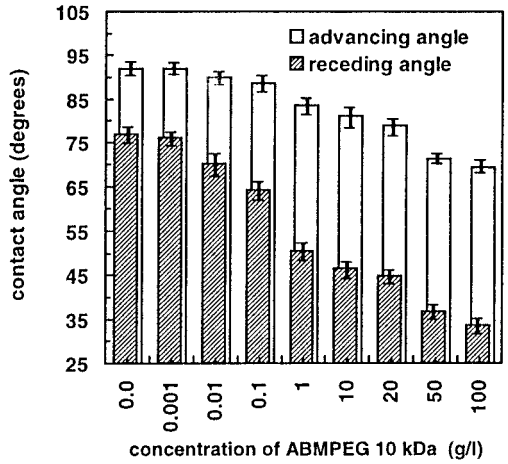

Figure 2. Advancing and receding contact angles of PSf spin-coating films modified with different ABMPEG 10 kDa solution concentrations. Error bars indicate standard deviations.

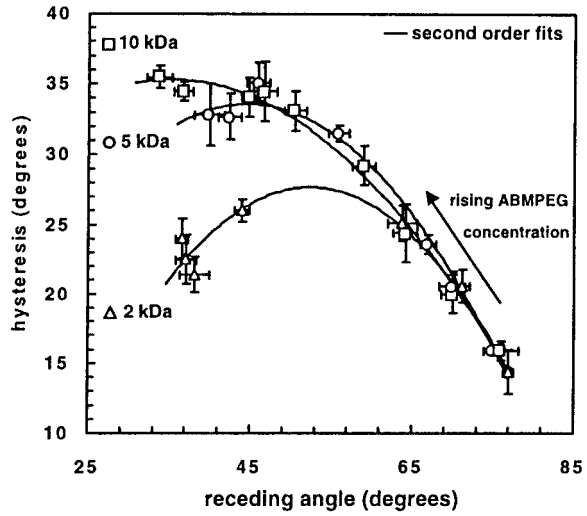

Figure 3. Receding contact angles and their hysteresis of PSf spin-coating films modified with different solution concentrations of ABMPEG with a molecular weight of 10, 5, and 2 kDa (data from Table 3). Error bars indicate standard deviations. Trend lines (second-order least-squares fits) are introduced for clarity. The arrow indicates rising ABMPEG concentrations.

highest ABMPEG concentration). For PSf modified with ABMPEG solution concentrations under 1 g/L, no changes in elemental composition were detected.

The observed CAs and XPS data indicate a significant but incomplete PEG coating of the underlying PSf for the highest solution concentration of ABMPEG. Surfaces saturated (brush regime) with PEG moieties of MW = 10 kDa would effectively shield the underlying PSf with respect to XPS analysis and typically show advancing/receding CAs of 30 ± 5/20 ± 5 deg, respectively.[7,39] The attained degree of surface coverage will depend on the first step in the modifying procedure (cf. Scheme 1) and thus on substratum−ABMPEG interactions which are directly related to the amphiphilic character of the PEG conjugate, its structure (e.g., chain length), substratum characteristics (e.g., hydrophobicity, swelling), and the solution conditions (concentration, salt, temperature).

2.4. Variation in MW. Figure 3 shows the data of Figure 2, supplemented by data for PSf modified at the same range of concentrations with ABMPEG 5 kDa and ABMPEG 2 kDa, visualized as CA hystereses as a function of receding CAs (see also Table 3). Receding CAs decrease for all applied ABMPEGs as their concentration in the modifying solution is increased. Data points superimpose for low ABMPEG concentrations irrespective of the applied molecular weight. The attained minimum values for receding CAs at maximum applied ABMPEG concentrations show no clear trend. However, for the higher ABMPEG concentrations decreasing hystereses values were observed for decreasing MW. Data for ABMPEG 5 kDa and ABMPEG 2 kDa exhibit a maximum in the studied range which is more pronounced and observed for lower receding angles as the MW of ABMPEG decreases. Furthermore, the surface characteristics for ABMPEG 2 kDa are essentially identical for the three highest applied concentrations, i.e., for 20, 50, and 100 g/L.

Figure 4 shows advancing and receding CAs for PSf substrata modified with binary mixtures of ABMPEG 10 kDa and ABMPEG 2 kDa, prepared by varying the relative weight content while keeping the total ABMPEG conjugate concentration constant at 10 g/L. A smooth transition of CA characteristics is observed for changing ratios.

These observations can be explained by a changed intramolecular polarity balance for ABMPEG as PEG MWs change. Rising ABMPEG surface activity, as expected for decreasing PEG MWs, leads to higher surface coverages and surface saturation already at lower solution concentrations. The latter is observed for ABMPEG 2 kDa, and MW-dependent surface coverage would explain the observed MW-dependent hysteresis values. Furthermore, the molar concentrations in the experiments were higher for ABMPEG 2 kDa, also increasing the adsorption tendency as compared with ABMPEG 10 kDa; nevertheless, receding CAs remain essentially unchanged. This may indicate that the end-on surface-bound PEGs are in a coiled conformation, yielding similar hydrophilization with a 10 kDa and a 2 kDa PEG, irrespective of the lower PSf surface coverage achieved with the ABMPEG 10 kDa.

2.5. Photografting Efficiency. Figure 5 shows receding CAs of substrata, modified with ABMPEG 10 kDa, before and after overnight flushing with an 2-propanol/water (1:1, v:v) mixture. CAs remain essentially unchanged for applied ABMPEG concentrations of up to 10 g/L, but increase again after flushing for higher concentrations. High photografting efficiency from the adsorbed layer is thus only achieved for ABMPEG 10 kDa concentrations up to 10 g/L, and is remarkably reduced for higher applied concentrations. Note that, according to CAs before flushing, the adsorbed amounts of ABMPEG increased monotonically with increasing solution concentrations.

The reduction in grafting efficiency may be related to a differently ordered/oriented ABMPEG layer. A multilayer structure cannot be expected when CA values and XPS data are considered. However, the formation of micelles or the appearance of microphase separation in the interphase might deteriorate the intimate contact between aryl-azide head groups and PSf necessary for successful grafting. Correlating very well with these results, Tseng and Park[28] observed a similar optimum in photografting efficiency for 2-azido-2-nitrophenyl PEG (MW = 3.4 kDa) onto methylated glass substrata at a solution concentration of 10 g/L.

2.6. Other Observations. When MPEG is used as modifying agent, CAs exhibit a similar trend toward lower values for higher applied concentrations (data not shown), but the data are within the standard deviation interval for unmodified PSf. Thus, CAs remain essentially unchanged for MPEG even at high solution concentrations. This indicates the elevated surface activity of ABMPEG

(39) Lin, Y. S.; Hlady, V.; Gölander, C. G. *Colloids Surf. B: Biointerfaces* **1993**, *3*, 49.

Table 3. Contact Angles and Their Respective Hystereses of PSf Spin-Coating Films Modified with Different Solution Concentrations of ABMPEG with Molecular Weight of 10, 5, and 2 kDa (cf. Figure 3)

	ABMPEG 2 kDa			ABMPEG 5 kDa			ABMPEG 10 kDa		
ABMPEG concn (g/L)	adv[a] (deg)	rec (deg)	hys (deg)	adv (deg)	rec (deg)	hys (deg)	adv (deg)	rec (deg)	hys (deg)
0	92.0	77.6	14.4	92.0	77.6	14.4	92.0	77.6	14.4
0.001	nd[b]	nd	nd	91.0	75.2	15.8	92.0	76.1	15.9
0.01	91.8	71.2	20.6	90.6	67.0	23.6	90.1	70.1	20.0
0.1	90.6	70.0	20.6	88.2	59.0	29.2	88.7	64.2	24.4
1	88.9	63.8	25.1	87.3	55.9	31.4	83.7	50.5	33.1
10	70.0	44.0	26.0	81.0	45.9	35.1	81.2	46.7	34.5
20	59.6	37.1	22.5	n.d.	n.d.	n.d.	78.9	44.8	34.1
50	59.4	38.1	21.3	72.7	39.9	32.8	71.2	36.7	34.5
100	60.6	36.6	24.0	75.1	42.4	32.7	69.2	33.7	35.5

[a] Average and maximal standard deviations of all values are 1.2 and 2.2, respectively. [b] nd = no data available.

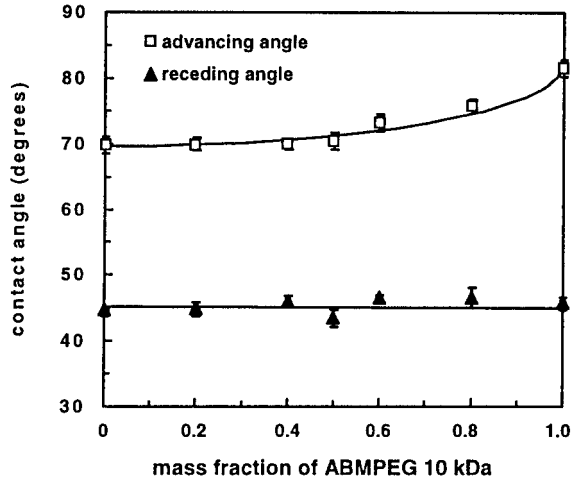

Figure 4. Advancing and receding contact angles of PSf spin-coating films modified with different blends of ABMPEG 2 kDa and ABMPEG 10 kDa. The total solution concentration is kept constant at 10 g/L. Error bars indicate standard deviations.

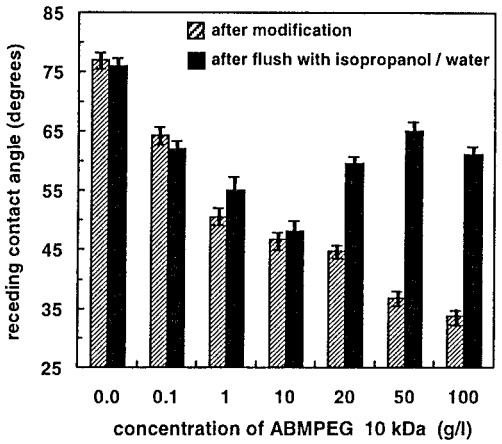

Figure 5. Receding contact angles of PSf spin-coating films modified at different ABMPEG 10 kDa solution concentrations, before and after a consecutive overnight 2-propanol/water (1:1, v:v) flush. Error bars indicate standard deviations.

in comparison to MPEG based on attractive interactions between PSf and the head group of ABMPEG. Two mechanisms could contribute: (1) Both PSf and the aryl-azide group are hydrophobic and aromatic in their character leading to attractive interactions;[40] (2) PSf swells in aqueous environments,[41] and therefore may enhance the penetration of the aryl-azide group into the PSf film. Hence, the effective photografting of ABMPEG after adsorption from solution concentrations up to 10 g/L seems to be caused by a close spatial configuration between the photoreactive aryl-azide group and the PSf interphase. Quantitative data for surface coverage from other methods could not be obtained. Alkaline hydrolysis of grafted ABMPEGs and the consecutive detection of carboxylic groups with fluorescent dyes was not sensitive enough. However, this is in agreement with the estimated maximum (dense packing) density on the flat and smooth PSf (approximately 8×10^{-12} mol/cm^2). With SFM, sufficient resolution to identify ABMPEG molecules could be achieved on rigid substrata such as hydrophobized silicon wafers (data not shown), but not with the ABMPEG-grafted PSf films. Quantitative information regarding PEG surface concentrations could not be retrieved from the XPS data; a main reason is seen in possible interphase restructuring during drying the samples. Nevertheless, the PEG functionalization could be verified qualitatively with an independent method.

However, Figures 1−5 unambiguously illustrate that PSf substratum characteristics, in regard to CA and CA hysteresis, are easily modulated by ABMPEG grafting, either by changing solution concentrations or by mixing different ABMPEG moieties at appropriate ratios, but that total coverage is not reached. To be able to control such characteristics can be useful especially in the field of material biocompatibility, as the quality and extent of interactions between biological matter and synthetic substrata is known to depend, at least partly, on these characteristics.[42]

3. FN Adsorption to Pegylated PSf Substrata. FN, as a well-described and studied protein, was chosen to represent, at least qualitatively, the interactions between adhesive proteins in general and the pegylated PSf substrata.

The assumption that a multilayer system can be treated as one optical unit, holds, e.g., for impermeable and incompressible PSf films on silicon wafers, as verified previously by Wahlgren et al.[43] A very different interfacial situation is attained for ellipsometric measurements of FN adsorption on ABMPEG-modified PSf film. This highly hydrated and flexible ABMPEG layer is most likely permeable and also compressible. Proteins are thus thought to penetrate this grafted ABMPEG layer, forming a two-component (FN/ABMPEG) system. For the calculation of the amount of adsorbed protein, a constant refraction of the ABMPEG layer per underlying surface

(40) Israelachvili, J. N. *Intermolecular and Surface Forces*, Academic Press: London, 1991.

(41) Lencki, R. W.; Williams, S. *J. Membr. Sci.* **1995**, *101*, 43.

(42) Ratner, B. D. *Surface modification of polymeric biomaterials*, 1st ed.; Plenum Press: New York, 1997.

(43) Wahlgren, M.; Arnebrant, T. *J. Colloid Interface Sci.* **1990**, *136*, 259.

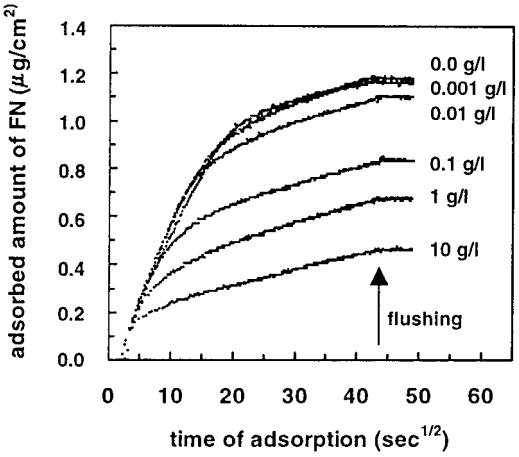

Figure 6. FN adsorption onto PSf spin-coating films on silicon wafers modified at different ABMPEG 10 kDa concentrations as indicated at the data curves. Arrow indicates the start of the flushing with buffer.

area is assumed, whether the layer is compressed or not. This assumption should be fulfilled when the ABMPEG mass in the layer is conserved and when the refractive index increment is constant for the range of attained ABMPEG densities in the grafted layer. A change in the total mass of the ABMPEG is not expected, as ABMPEGs are effectively grafted to the PSf film in the studied range of degrees of functionalization as shown in Figure 5. The constancy of the refractive index increment of surface bound PEG conjugates was employed in several studies where the thus calculated adsorbed amounts correlated well with other employed experimental techniques.[8,36]

Figure 6 shows the kinetic adsorption data for FN adsorbing onto substrata pegylated with different concentrations of ABMPEG 10 kDa. Adsorption was interrupted after 30 min, and the cuvette was immediately flushed with buffer for 10 min. This procedure is chosen in order to simulate a FN-preadsorption step applied in a parallel detailed cell-adhesion study (publication in preparation). Even if plateau values are typically observed after 1−2 h (or much longer), it is possible to describe qualitatively protein−substratum interactions. All data curves follow the expected monotonic rise; FN desorption upon flushing is not observed. The adsorbed amount of FN decreases with higher degrees of ABMPEG surface functionalization and thus correlates qualitatively with the CA decrease shown in Figure 2. Maximum adsorption of almost 1.2 μg/cm^2 is attained for both unmodified PSf and PSf modified with the lowest ABMPEG concentration, i.e., 0.001 g/L. Similar amounts of FN were found to adsorb to polymer substrata of intermediate to pronounced hydrophobicity in other studies.[44] The adsorbed FN amount decreases by more than 60% to 0.45 μg/cm^2 for an ABMPEG concentration of 10 g/L. Previously,[26] albumin adsorption to PSf ultrafiltration membrane surfaces photografted with ABMPEG 5 kDa was quantified by total hydrolysis and consecutive amino acid analysis of the adsorbed protein: The relative reduction depending on the degree of functionalization correlates very well with the results presented here for FN.

Several studies reported similar results for protein adsorption to PEG-modified surfaces.[8,45] Recently, Sofia et al.[5] characterized protein (FN, cytochrome *c*, and albumin) adsorption on PEG-grafted (MW 3.4, 10, 20 kDa) silicon surfaces over a range of grafting densities. Additionally, the grafted amount of PEG moieties could be measured with XPS. Protein adsorption decreases for all proteins with rising PEG grafting density and is reduced by more than 95% for the highest PEG grafting density when compared to the unmodified silicon substrate. From measurements of the thickness of the adsorbed protein layer, it was deduced that FN, having a rodlike shape, adsorbs for all PEG grafting densities "lying down" with its long axis parallel and in close contact to the surface. Thus, proteins are able to penetrate the PEG layer to effectively adsorb to the underlying surface between grafted chains. A compromise between conformational entropy of the grafted PEG chains, PEG chain−protein repulsions, and attraction of the protein to the underlying surface is attained. Depending on the grafting density of the PEG chains, the adsorbed protein will deform the surrounding grafted chains to some degree. As such, the greater the grafting density, the greater the deformation and the less favorable the overall interaction resulting in lower protein adsorption. Following this line of argument, adsorbed protein molecules experience a lateral pressure originating from surrounding and deformed PEG chains. From protein adsorption isotherms onto differently dense pegylated surfaces, Szleifer[6] deduces that the structure of the resulting mixed layer of adsorbed proteins and tethered polymers (PEG) is rather different from that of the tethered polymer layer without adsorbed protein. In support of this hypothesis, Sofia et al.[5] calculated that protein adsorption started to decrease for grafting densities where grafted PEG chains began to overlap, and that protein adsorption became negligible when PEG chains were, due to the grafting density, confined to approximately half their relaxed volume. This correlation between protein adsorption and PEG chain overlap was found for all investigated PEG molecular weights, and the calculations were based on the assumption that grafted PEG chains exert the same radius of gyration or spatial dimension as in their solvated state.

4. Fibroblast Interactions with Pegylated PSf Substrata. Preliminary cell adhesion studies showed more pronounced effects for PSf substrata modified with ABMPEG 10 kDa compared with ABMPEG 2 kDa. In an attempt to rationalize this qualitative result, it might be noted that often more heterogeneous surfaces (cf. Figure 3) show a more pronounced interaction with biological matter.[46,47] Thus to assess the biocompatibility of the novel materials, PSf films modified with ABMPEG 10 kDa were chosen.

Attachment, spreading, and morphology of cells can be used as a first indicator for the quality and strength of cell−material interaction.[10] In general, extensive cell spreading is a hint for good cell-contacting properties of a material while rounding up of cells on a substratum characterizes weak cell−material interaction which may be followed by cell death due to apoptosis.[10,49] In particular hydrophobic substrata have been found to be nonadhesive for a variety of anchorage-dependent cells.[11,12,14,50] This effect can also be seen in Figure 7a for plain PSf showing

(44) Pettit, D. K.; Horbett, T. A.; Hoffman, A. S. *J. Biomed. Mater. Res.* **1992**, *26*, 1259.
(45) Malmsten, M.; Emoto, K.; Alstine van, J. M. *J. Colloid Interface Sci.* **1998**, *202*, 507.
(46) Sadana, A. *Chem. Rev.* **1992**, *92*, 1799.
(47) Curtis, A.; Wilkinson, C. *Biomaterials* **1997**, *18*, 1573.
(48) Bongrand, P.; Claesson, P. M.; Curtis, A. In *Studying cell adhesion*; Bongrand, P., Claeeson, P. M., Curtis, A. Eds.; Springer-Verlag: Berlin, 1994.
(49) Burridge, K.; Fath, K.; Kelly, T.; Nuckolls, G.; Turner, C. *Annu. Rev. Cell. Biol.* **1988**, *4*, 487.
(50) Altankov, G.; Grinnell, F.; Groth, T. *J. Biomed. Mater. Res.* **1996**, *30*, 385.

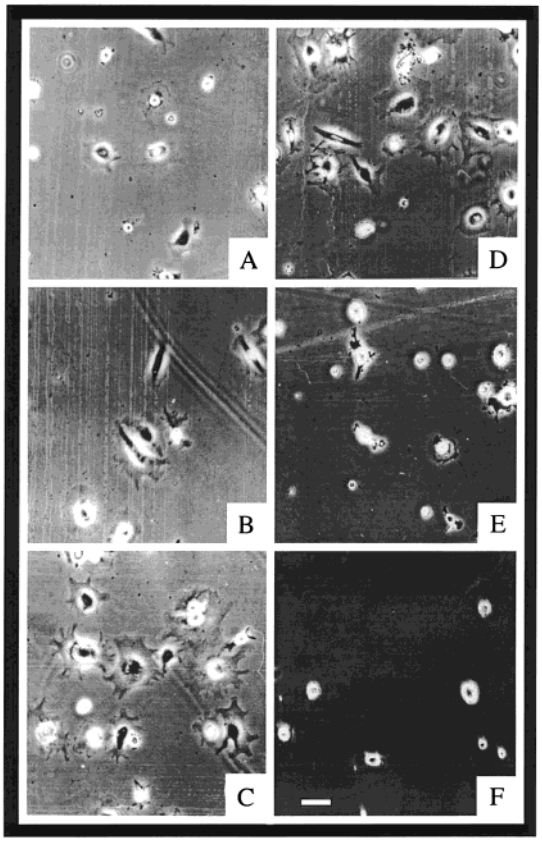

Figure 7. Overall cell morphology of fibroblasts adhering on different PSf spin-coating films modified with different solution concentrations of ABMPEG 10 kDa. Effect of ABMPEG concentration. Fibroblasts were plated for 2 h on unmodified PSf (a), or PSf grafted with ABMPEG at concentrations (in g/L) as follows: (b) 0.001, (c) 0.01, (d) 0.1, (e) 1, (f) 10. At the end of incubation, samples were investigated and photographed under phase contrast at low magnification (20×).

Table 4. Mean Number of Fibroblasts per Microscopic Field Adhering on PSf Spin-Coating Films Modified with Different Solution Concentrations of ABMPEG 10 kDa

ABMPEG 10 kDa concn (g/L)	no. of adherent cells ± std (no. of cells/microscopic field)
0	5.8 ± 3.1
0.001	6.7 ± 2.0
0.01	18.2 ± 9.8
0.1	13.1 ± 5.1
1	12.4 ± 5.7
10	5.3 ± 2.3
20	3.2 ± 1.4

only few adherent fibroblasts of which some are still round and only some spread.

Pegylation has been used in recent years extensively for the prevention of protein adsorption and blood cell adhesion,[1,9,51] and the repellent character of PEG-coated surfaces is apparent in Figure 7e,f, where high degrees of surface modification (attained at solution concentrations of 1 and 10 g/L) lead to poor attachment or spreading of cells. The striking finding of this paper, however, is that, at intermediate degrees of surface modification the adhesion of fibroblasts is considerably improved as indicated by the increase in cell number and development of cell spreading morphology (see Figure 7c,d). Data in Table 4 demonstrate a clear dependence of cell adhesion on the degree of surface pegylation. Optimal adhesion for

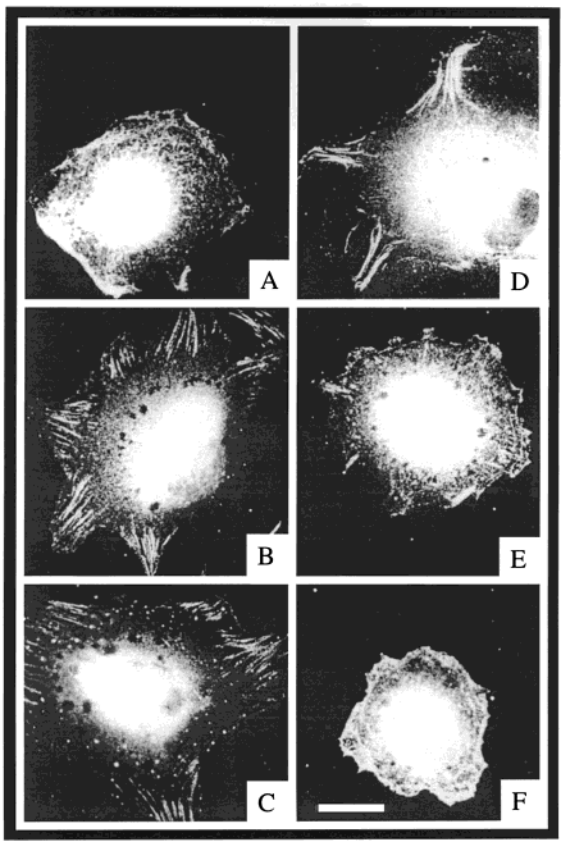

Figure 8. Focal adhesion formation of fibroblasts adhering on different PSf spin-coating films modified with different solution concentrations of ABMPEG 10 kDa. Effect of ABMPEG concentration. Cells were plated for 2 h on unmodified PSf (a), or PSF modified with ABMPEG at concentrations (in g/L) as follows: (b) 0.001, (c) 0.01, (d) 0.1, (e) 1, (f) 10. At the end of incubation, the cells were fixed, permeabilized, and stained for vinculin. Samples were visualized by immunofluorescence and photographed at high magnification (100×).

plain surfaces was found at applied ABMPEG concentrations ranging between 0.001 and 0.1 g/L. The same trend was found for cells adhering on serum coated surface (data not shown).

Attachment of cells on artificial and natural substrata occurs through specific transmembrane proteins, such as integrins which link the adsorbed or secreted matrix proteins with the cytoskeleton.[52,53] In this way, a cell can build up the necessary traction needed for its tight attachment or movement on the substratum.[53] Furthermore, integrins are responsible for transmembrane signaling between the extracellular matrix and the cytoskeleton necessary for the regulation of important cellular functions deciding on life or death of a cell.[52,54] Integrins assemble in so-called focal adhesions and are linked to vinculin bridging focal adhesion complexes with the cytoskeleton.[53] Number and extension of focal adhesions are good indicators for the intensity of cell−material interaction.[50] Therefore, to further characterize cellular interaction with PEG surfaces, we studied the organization of focal adhesions by immunofluorescence of vinculin.

Figure 8 shows the distribution of vinculin in fibroblasts adhering for 2 h on the different substrata. It is evident that neither PSf alone (see Figure 8a) nor "highly" pegylated PSf (see Figure 8f, and to some extent Figure

(51) Jeon, S. I.; Andrade, J. D. *J. Colloid Interface Sci.* **1990**, *142*, 159.
(52) Hynes, R. O. *Cell* **1992**, *69*, 11.
(53) Buck, C. A.; Horwitz, A. F. *Annu. Rev. Cell Biol.* **1987**, *3*, 179.
(54) Ruoslahti, E. *Tumor Biol.* **1996**, *17*, 117.

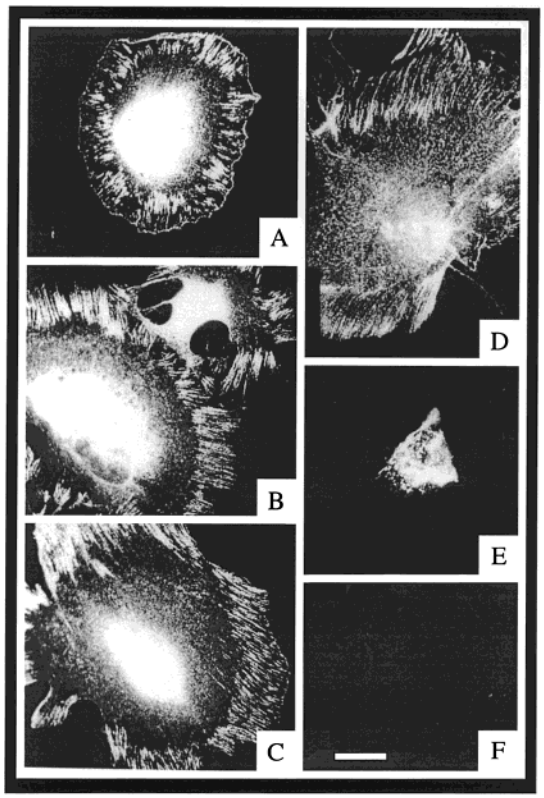

Figure 9. Focal adhesion formation of fibroblasts adhering on different PSf spin-coating films modified with different solution concentrations of ABMPEG 10 kDa. Effect of serum precoating. Cells were plated for 2 h on serum-coated unmodified PSf (a), or on serum-coated PSf prior modified with ABMPEG 10 kDa at concentrations (in g/L) as follows: (b) 0.001, (c) 0.01, (d) 0.1, (e) 1, (f) 10. At the end of incubation, the samples were fixed, permeabilized, and stained for vinculin. Samples were visualized by immunofluorescence and photographed at high magnification (100×).

8e) permits the formation of focal adhesion complexes. Intermediate degrees of surface modification at ABMPEG concentrations between 0.001 and 0.1 g/L, however, enable fibroblasts to build up the focal adhesion complexes as indicated by the bright streaks in the cell periphery (Figure 8b–d). According to comprehensive experience from previous investigations, spreading of cells and extensive formation of focal adhesions indicate good tissue compatibility of materials as shown by cell proliferation and functional activity of fibroblasts.[50,55] It must be noted here that the exposure of surfaces to UV light during modification cannot be held responsible for the change of surface properties since PSf, exposed as a control to UV light only, exhibited the same cell-adhesion properties as unmodified PSf.

Precoating of material surfaces with serum can result in the adsorption of soluble adhesive proteins, such as FN and VN.[11,56,57] To simulate in vivo conditions, surfaces were precoated with serum, fibroblasts were added, and focal adhesion formation was investigated. Contrary to findings in the absence of preadsorbed serum proteins (Figure 8a), focal adhesion formation was possible even on unmodified PSf as shown in Figure 9a. Although following the same trend, the formation of focal adhesion for serum precoated surfaces was much more pronounced. Moreover, the repelling character at high degrees of surface modification (at 1 and 10 g/L) seems to be more prominent leading to the complete absence of cells (Figure 9e).

The differently pronounced formation of focal adhesions at intermediate degrees of surface functionalization in the absence (Figures 7 and 8) or presence (Figure 9) of preadsorbed serum proteins suggests distinct strengths of adhesive cell–substratum interaction. One can support that, in the absence of preadsorbed serum, only FN, which is synthesized very soon after cell–material contact, should be present on the surfaces.[58] The fate of the secreted protein, however, depends on the nature of the underlying substratum. The ellipsometry results show that the amount of adsorbed FN decreases gradually with increasing degree of surface modification (cf. Figure 6). On the other hand, it is well-known that hydrophobic substrata decrease the functionality of adsorbed FN with regard to cell adhesion and cell function,[11,14,55,56] evident from the incomplete cell spreading (Figure 7a) and the absence of focal adhesions (Figure 8a) on PSf. A decreased activity of the FN receptor in fibroblasts adhering on hydrophobic surfaces was recently described by Altankov et al.[59] The repelling character of densely pegylated surfaces is well-known and does not need to be discussed here in detail. More interesting, however, is the completely new finding that lower PEG concentrations can lead to improved cell contacting properties of a material with low tissue compatibility. The model developed by Sofia et al.[5] can be extended to a sterically stabilizing effect of end-on grafted PEG molecules on intercalated (adhesive) proteins, such as FN (see Scheme 2). By this means, these proteins could be protected from undergoing conformational changes which would occur in the absence of this surface layer. Evidence for such a model can be taken from other investigations performed by Grinnell and co-workers on the adsorption of FN on hydrophobic polystyrene.[11,56] FN adsorption on polystyrene led to very weak adhesion and spreading of fibroblasts accompanied by low binding of FN antibodies. In contrast, when FN was adsorbed out of a mixture of FN and human serum albumin, enhanced cell adhesion and an increase of binding sites was observed. This effect was attributed to a stabilizing effect of coadsorbed FN-neighboring albumin (a protein actually preventing adhesion of cells) on the orientation and conformation of FN.[11,60] Employing this model, we can deduce a similar effect when tethered, sterically demanding PEG moieties neighbor adsorbed adhesive proteins.

After precoating the substrata with serum, a more complex pattern of protein adsorption is expected. Vitronectin, as another important adhesive protein, is known to be adsorbed from serum in relative higher amounts than FN,[22] but a variety of other proteins can adsorb under these conditions as well. Since VN is less sensitive to conformational changes than FN,[61] the existence of focal adhesion on serum-coated PSf (Figure 9a) could be explained and was also observed on other hydrophobic materials in our previous studies.[57,59] Indeed, the improvement of surface properties by lower quantities of

(55) Groth, T.; Altankov, G. In *New Biomedical Materials—Applied and Basic Studies*; Harris, P., Chapman, D., Eds.; ID Press: Amsterdam, 1998; p 225.
(56) Grinnell, F.; Feld, M. K. *J. Biol. Chem.* **1982**, *257*, 4888.
(57) Groth, T.; Altankov, G.; Kostadinova, A.; Krasteva, N.; Albrecht, W.; Paul, D. *J. Biomed. Mater. Res.* **1998**, *44*, 341.
(58) Hynes, R. O. *Fibronectins*; Springer-Verlag: New York, 1990.
(59) Altankov, G.; Groth, T.; Krasteva, N.; Albrecht, W.; Paul, D. *J. Biomater. Sci. Polym. Ed.* **1997**, *8*, 721.
(60) Gordon, J. L. In *Blood-surface interactions: Biological principles underlying haemocompatibility with artificial materials*; Cazenave J. P., Davies, J. A., Kazatchchkine, M. D., Aken van, W. G., Eds.; Elsevier Science: New York, 1998; p 5.
(61) Underwood, P. A.; Steele, J. G.; Dalton, B. A. *J. Cell Sci.* **1993**, *104*, 739.

Scheme 2. Descriptive Model for Cell−Adhesive Protein−ABMPEG−Substratum Interactions

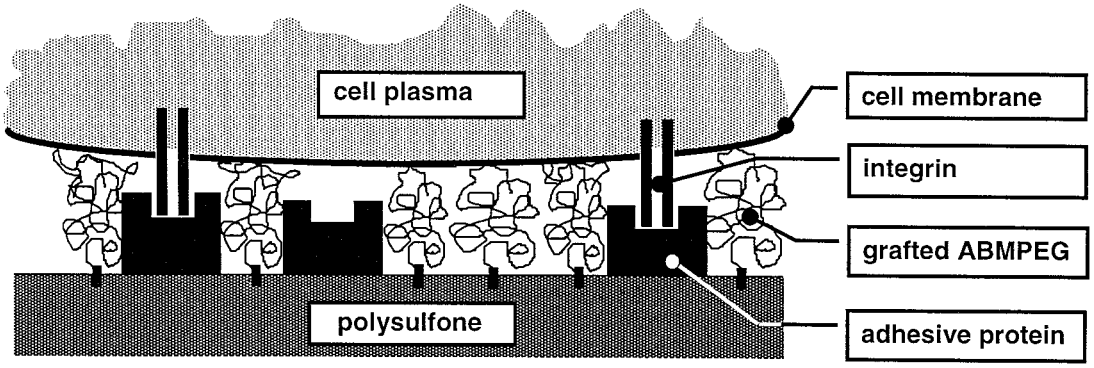

immobilized PEG, compared to serum-free conditions (cf. Figure 8), is also clearly visible in Figure 9b−d (0.001, 0.01, and 0.1 g/L) by the improved spreading of cells and higher number and length of focal adhesions. Since cell adhesion was almost absent on serum-coated surfaces, pegylated at 1 and 10 g/L, the improvement of cell contacting properties of nontissue compatible surfaces is even more evident. Finally, it can be assumed that an at least very similar mechanism as described for secreted FN is responsible for the improved tissue compatibility of the PSf surface. We will explore the details of the underlying mechanism in more detail in future investigations.

Conclusions

In this paper a new approach for controlling biocompatibility of polymer surfaces is described, based on structuring a hydrophobic polymer surface with a "self-assembled" and then covalently bound layer of hydrophilic, flexible macromolecules. A patterned monolayer of macromolecules exhibiting a pronounced exclusion volume in a controlled lateral density on the substratum surface can lead to controlled cellular interaction. A descriptive model (cf. Scheme 2) is proposed which includes the adsorption and preservation of active conformation of adhesive proteins, either secreted by the cells and/or from serum, in this monolayer. These active proteins trigger the adhesion, spreading, and, eventually, proliferation of cells.

With the described system, a novel, improved application of the widely used PEGs is introduced. The relatively hydrophobic character of the photoreactive aryl-azide head group renders the adsorption behavior compared with the unfunctionalized MPEG; an amphiphilic character of the PEG conjugates ABMPEG can be discussed. These properties have direct impact on the efficiencies of both adsorption and photografting steps, and thus on adjusting grafting density (patterning) on the substratum. On the other hand, the interface properties of the substratum (hydrophobicity and morphology) have also influence on grafting effectiveness. Therefore, variations in PEG conjugate head group and linker chemistry, as well as solution conditions during the adsorption step, are means extending the scope of the surface modification process. Even if CA measurements have been proven to give versatile biomaterial surface characteristics, additional attempts will be made in developing/using refined analytical methods and equipment for the direct quantification of PEG grafting densities.

The photochemical coupling process is relatively independent of the chemical composition of the support and therefore permits the modification of many different materials. The UV-light energy for initiating aryl-azide photolysis can be selected so that it is nondestructive for an underlying polymer. Hence, sophisticated morphologies (e.g., microporous membranes) can be functionalized without destroying their valuable properties (e.g., sieving characteristics).[26] Furthermore, the simple generic process (cf. Scheme 1) permits covalent attachment of a wide variety of other macromolecules via their photoreactive head group conjugates, making it a versatile process for the development of advanced biomaterials. Photostructuring in the micrometer scale using the described system provides an additional dimension for surface "patterning" of biomaterials.

The studied combination of PSf and PEG has significant practical relevance, especially because PSf is a material for high-performance dialysis and ultrafiltration membranes which will be increasingly applied in tissue and artificial organ engineering. In a next paper the FN matrix formation and the organization of β-1-integrin (FN receptor) of human fibroblasts adhering on different PSf−ABMPEG surfaces will be reported. Ongoing investigations focus on the role of other adhesive proteins (e.g., VN) and their mutual interactions. These will, step by step, add more information to the proposed general model for controlling cell−surface interactions. Furthermore, the applicability of the approach for surface design of other polymeric biomaterials and of applications with other cells is currently being explored.

Acknowledgment. This study has been financed by The Danish Materials Development Program MUP-II and carried out within the framework of the Danish Polymer Center. Parts of this study have been supported by the Deutsche Forschungsgemeinschaft, Grant Gr1290/4-2. Dr. Helmut Kamusewitz, Yvonne Fritsche, and Manuela Keller, from the GKSS Research Center, Institute of Chemistry, Teltow (Germany), are acknowledged for their advice and technical support for CA and SFM measurements. Ellipsometry was performed at the Institute for Food Technology, Lund University, Lund (Sweden), financially supported by the Nordic Research Council, and Ulla Eloffson is accredited for her technical and organizational support. Walter Bathsberg, Lotte Nielsen, and Lene Hubert, Risø National Laboratories, Roskilde (Denmark), are acknowledged for SEC and XPS measurements.

LA990303A

Publikation 12

Volkmar Thom, Georgi Altankov, Thomas Groth, Katja Jankova, Gunnar Jonsson, Mathias Ulbricht (2000).

Modulating the biocompatibility of polymer surfaces with Poly(Ethylene Gylcol) (PEG) – Effects of fibronectin.

Journal of Biomedical Materials Research **52**, 219-230.

Modulating the biocompatibility of polymer surfaces with poly(ethylene glycol): Effect of fibronectin

G. Altankov,[1] V. Thom,[2] T. Groth,[3] K. Jankova,[4] G. Jonsson,[4] M. Ulbricht[5]
[1]*Bulgarian Academy of Sciences, Institute of Biophysics , Str. Acad. G. Bonchev, Bl. 21, BG-1113 Sofia, Bulgaria*
[2]*Condensed Matter Physics and Chemistry Department, Risø National Laboratory, Building 108, P.O. Box 49, DK-4000 Roskilde, Denmark*
[3]*GKSS Research Center, Institute of Chemistry, Kantstr. 55, D-14513 Teltow, Germany*
[4]*Technical University of Denmark, Department of Chemical Engineering, DK-2800 Lyngby, Denmark*
[5]*ELIPSA GmbH, Innovationspark Wuhlheide, Köpenicker Str. 325, D-12555 Berlin, Germany*

Received 28 July 1999; revised 19 January 2000; accepted 16 February 2000

Abstract: A novel approach described earlier for improving polymer substratum biocompatibility[1] is further elucidated. Polysulfone (PSf) spin-coating films were modified by covalent end-on grafting of hydrophilic and sterically demanding photo-reactive poly(ethylene glycol) (PEG) conjugates (ABMPEG; 10 kDa). The degree of grafting density was varied systematically, yielding a wide spectrum of attained surface characteristics monitored by air–water contact angles (captive bubble method). Fibronectin (FN) adsorption was studied by *in situ* ellipsometry and found to decrease monotonically as ABMPEG grafting density increased. The adhesive interaction of human skin fibroblasts with these substrata and, in particular, the effect of FN precoating were investigated in detail. A clear optimum of cell–substratum interactions was found for mildly modified substrata, employing well established microscopic and immunofluorescence techniques, namely the monitoring of cell adhesion and spreading, overall cell morphology, organization of FN receptors, and focal adhesions as well as FN matrix formation. The results suggest that cell interactions with hydrophobic polymer substrata are enhanced considerably when modified with hydrophilic and sterically demanding PEG moieties at a low surface coverage due to enhanced biologic activity of adsorbed and intercalated adhesive proteins such as FN. © 2000 John Wiley & Sons, Inc. J Biomed Mater Res, 52, 219–230, 2000.

Key words: surface modification; polymer biocompatibility; poly(ethylene glycol); cell adhesion; fibronectin

INTRODUCTION

Cell–biomaterial interaction is dependent on the initial adsorption of fibronectin (FN) or other attachment factors from surrounding body fluids and serum-containing media.[2,3] The quality of interaction is greatly influenced by the surface properties of the biomaterials.[4,5] For instance, it is well known that mammalian cells adhere better to hydrophilic than to hydrophobic material surfaces.[6,7] This phenomenon appears to be attributable to conformational changes of adsorbed adhesive proteins (as, e.g., FN) when they are in contact with such hydrophobic surfaces.[2,3,8,9] Hydrophobic surfaces adsorb comparatively more FN[8–11]; however, this seems to be accompanied with the loss of some of its biologic activity, resulting in poor cell adhesion and spreading. Recent investigations further indicate that strong hydrophobic interactions with substrata may inhibit the necessary rearrangement of FN during the process of extracellular matrix formation.[10,11] Hence, different approaches for materials surface functionalization have been developed,[12,13] particularly for when those materials are to be adopted for contact with cells.

Attachment is important for normal development of the shape and morphology of cells.[14,15] Recently it became clear that cell adhesion influences such diverse biologic processes as, for example, cell migration, differentiation, growth, and apoptosis, and also is connected to their malignant transformation and metastasis.[14–16] Cell adhesion to FN and to other adhesive

No benefit of any kind will be received either directly or indirectly by the authors.

Correspondence to: G. Altankov or T. Groth; e-mail: Thomas.Groth@gkss.de

Contract grant sponsor: The Danish Materials Development Program MUP-II, carried out within the framework of the Danish Polymer Center

Contract grant sponsor: Deutsche Forschungsgemeinschaft; contract grant number: Gr1290/4-2

proteins is dependent on the protein's interaction with distinct cell-surface receptors belonging to the integrin superfamily.[17] Integrins are transmembrane heterodimeric glycoproteins consisting of α and β subunits,[17,18] which are functional when making a "bridge" between the adhesive protein-ligand and the cytoskeleton.[15–17] A major FN receptor, present on most cells is the $\alpha_5\beta_1$ integrin,[16,17,19] which interacts with the RGD containing cell-adhesion sites of FN. Other β_1 integrins also may recognize FN.[17] When integrins are occupied by the respective ligand, they tend to cluster in focal adhesion plaques, which are located where the closest adhesion to the substratum occurs and where specific signaling pathways start.[15–19] Hence, focal adhesion formation seems to be characteristic for the quality of cell–material interaction.[11,20] Well developed cell–biomaterial interaction usually is a desired property when those materials are designed for implantation as biohybrid tissues and organs.[21] For other biomedical devices, however, in particular those considered for contact with blood, materials with a low potential for protein adsorption and low cellular interactions are required[22] because surface-induced thrombosis is a major problem in clinical applications of such devices.[23] In this respect, poly(ethylene glycol; PEG) is gaining wide recognition as a hemocompatible material due to its noninteraction with proteins and cells.[24,25]

Recently we developed a novel approach to the "design" of material surfaces. It is an approach based on the structuring of a hydrophobic polymer surface with a "self-assembled" and covalently bound monomolecular layer of hydrophilic, flexible macromolecules.[1] In a two-step process, amphiphilic, photo-reactive poly(ethylene glycol) conjugates (ABMPEG) were grafted to polysulfone (PSf) film substrata, yielding different grafting (pegylation) densities. The term "pegylation" is used as a synonym for interfacial grafting of poly(ethylene glycol). Surprisingly, we found an optimum of cellular interactions at intermediate pegylation densities. Facilitated adhesion and improved spreading of fibroblasts in comparison to surfaces exhibiting either low or high pegylation densities indicated a favorable balance between the impact of the hydrophobic polymer surface and the protein-repelling nature of the PEG layer. Thus the biologic activity of adsorbed attachment proteins might be stabilized by both, the remaining hydrophobic interactions of PSf from beneath and the lateral forces stemming from hydrophilic PEG domains.[26]

Here we describe, in particular, the effect of precoated FN on the interaction of human fibroblasts with PSf surfaces pegylated at different densities. For a more comprehensive characterization of the biologic properties of these novel surfaces, we studied initial cell adhesion and spreading, overall cell morphology, organization of FN receptors, and focal adhesions as well as FN matrix formation.

MATERIALS AND METHODS

Preparation of polysulfone (PSf) surfaces

Glass coverslips were cleaned with detergent, rinsed with ultrapure water, and etched for 15 min at approx. 40° ± 5°C in a freshly mixed 3:1 (v/v) sulfuric acid (96%):hydrogen peroxide (30%) (Piranha) solution. Coverslips were thoroughly rinsed, stabilized for 2 h, rinsed again with/in ultrapure H_2O, and dried free of dust for 2 h at 120°C. Polished silicon wafers (Topsil Semiconductor Materials A/S, Frederikssund, Denmark; for ellipsometry measurements) were oxidized thermally in pure oxygen, followed by annealing and cooling under argon flow to yield an oxide layer of about 30 nm. Wafers were cut into rectangular slides (10–14 mm × 20–30 mm). To attain a hydrophobic surface for enhanced spin-coating film adhesion, n-octadecyldimethylchlorosilane (ODMS; Sigma-Aldrich Co., St. Louis, Missouri) was grafted to cleaned coverslips by immersing them into a 2% (w/w) ODMS in n-hexane solution for 1 h at room temperature. The ODMS-treated coverslips were rinsed twice with n-hexane and three times with ethanol and air dried at room temperature (RT), and thereafter they were spin-coated with a 3% (w/w) PSf in 1,2-dichlorbenzene solution. Complete wetting by the polymer solution, then spinning for 10 s at 500 rpm and consecutively for 50 s at 5000 rpm gave a smooth PSf film.[1] Those PSf substrata were dried for at least 4 h in vacuum at 60°C.

Functionalization with α-4-azidobenzoyl ω-methoxy (polyethylene glycol), (ABMPEG)

Synthesis and characterization of ABMPEG is described in detail in a previous paper.[27] Briefly, 4-aminobenzoic acid was converted into 4-azido benzoyl chloride and used for quantitative esterfication of monomethoxy poly(ethylene glycol) with a molecular weight of about 10,000 g/mol (Shearwater Polymers, Huntsville, AL, USA), yielding ABMPEG, which was purified by consecutive precipitation from CH_2Cl_2/diethylether and aqueous-phase diafiltration. ABMPEG grafting onto the PSf surfaces included the two steps illustrated in Scheme 1: First, an aqueous ABMPEG solution of varied concentration was placed on the PSf substrata, covered, and kept in the dark for 12 to 18 h at RT. Thereafter, the substrata were rinsed gently in ultrapure water, covered by water, and immediately exposed to UV light for 1 min (50 W high pressure mercury lamp, Oriel, and glass filter with a cut-off at 320 nm, yielding an intensity of 30 mW/cm^2). PEG-modified PSf substrata will be abbreviated consecutively by PSf/PEG appended by the ABMPEG bulk concentration used in the adsorption step of the modification procedure (e.g., PSf/PEG-0.01).

Surface characterization

Contact angles (CAs) of unmodified and pegylated PSf substrata were measured using captive air bubbles in the

SCHEME 1
PSf Substrata Functionalization Procedure

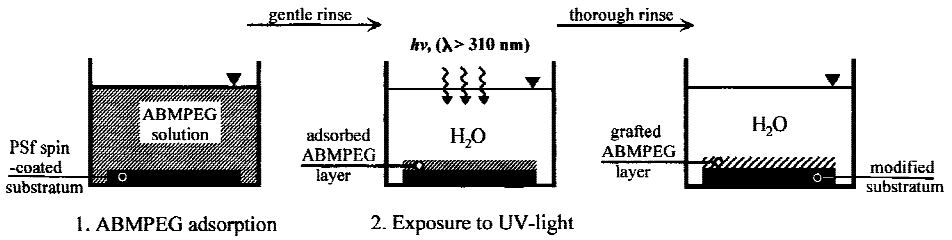

Scheme 1.

aqueous phase, the method being described elsewhere in detail.[1] At least ten measurements of different bubbles on at least three different locations were averaged to yield one CA value. The respective standard deviations are indicated as error bars.

FN adsorption measured by *in situ* ellipsometry

The experimental procedure and calculation of the adsorbed amount of FN is described in detail in a previous paper.[1] An in-depth description of the physical principles of the method[28] and the instrumental setup[29] are available. Briefly, FN (from human plasma, lyophilized, MW 440 kD; Boehringer Mannheim, Mannheim, Germany) was reconstituted in phosphate-buffered saline (PBS) containing 0.02% (w/v) sodium azide, giving a final FN concentration of about 0.12 g/L. An automated Rudolph thin-film ellipsometer, type 43603-200E, equipped with a thermostatic quartz cuvette and a stirring device, was used. The light source was a helium-neon laser having a beam wavelength of 632.8 nm and an angle of incidence of 68. Differently modified PSf spin-coating films on silicon wafers were placed in the quartz cuvette and stabilized in 2.5 mL of PBS buffer for at least 15 min or until constant polarizer and analyzer signals were obtained. The concentrated FN solution (0.5 mL) was added, yielding 3 mL with a defined concentration of 0.02 g/L. The magnetic stirrer was activated for 2–3 s upon addition of the protein concentrate in order to homogenize the solution. After 30 min the cuvette was flushed for 10 min with PBS buffer and the amount of adsorbed FN determined from the continuously measured ellipsometric angles, Ψ and Δ.

Purification of fibronectin (FN), conjugation with fluorescein isothiocyanate (FITC), and precoating

Human plasma FN was prepared by affinity chromatography on gelatin-Sepharose 4B and further purified on heparin-Sepharose 4B, as previously described.[30] FN was eluted with 0.5*M* of NaCl, 50 m*M* of Tris (pH 7.3), and lyophilized.

Fluorescent fibronectin (FFN) was prepared by conjugation with FITC (Sigma), as described by Grinnell.[31] Briefly, 10 μg of FITC in DMSO were added to 2 mg of FN dissolved in 0.1*M* of carbonate buffer (pH 9) to obtain a final concentration of 10 μg/mL. The reaction mixture was incubated at RT for 2 h, and nonreacted dye was separated by Sephadex G-25 column (Pharmacia, Upsalla, Sweden) equilibrated with PBS. The obtained FFN completely retained its biologic activity, as verified by fibroblast spreading assays. For cell experiments, pegylated and control PSf substrata sometimes were precoated with FN by contacting them with 20 μg/mL of FN or 40 μg/mL of FN in PBS solution for 30 min at 37°C. Thereafter, samples were washed three times with PBS and used immediately.

Cells

Human fibroblasts were obtained from fresh skin biopsy and used up to the 9th passage. The cells were grown in Dulbecco's modified Eagle's medium (DMEM) containing 10% fetal bovine serum (FBS; Sigma Chemical Co., St. Louis, Missouri) in a humidified incubator with 5% CO_2. Fibroblasts from nearly confluent cultures were harvested with 0.05% trypsin/0.6 m*M* of EDTA (Sigma), and trypsin was neutralized with FBS.

Cell adhesion

Approximately 10^5 cells per well were incubated in the absence of serum for 2 h in six-well polystyrene plates (Falcon, Becton Dickenson & Company, Franklin Lakes, New Jersey). The wells contained PSf substrata that either were unmodified or modified at different pegylation densities, and sometimes they were precoated with FN or FFN. At the end of the incubations the samples were washed with PBS and fixed with 3% paraformaldehyde. Cell adhesion was quantified microscopically by counting 30 different randomly chosen microscopic fields, determining an arithmetic mean and standard deviation of the number of cells per field.

Reorganization of substratum-bound fluorescent fibronectin

Approximately 10^5 cells, in serum-containing medium, were incubated for 2 h in six-well polystyrene plates con-

taining the FFN-precoated slides prepared as described above. After incubation, the cells were fixed with 3% paraformaldehyde in PBS at pH 7.4 and mounted with Mowiol. Further investigations and photography were carried out with an inverted fluorescence microscope, type Axiovert 100 (Carl Zeiss, Jena, Germany).

Fibronectin-matrix formation

Approximately 10^5 cells per well in 3 mL of serum-containing medium were cultured for 5 days in six-well tissue culture plates containing plain and differently pegylated PSf substrata. At the end of the incubation, cells were fixed with 3% paraformaldehyde and FN-matrix deposition was visualized by immunofluorescence using anti-human FN-matrix mouse monoclonal antibody (Immunotech SA, Marseille, France, lot No 0326), followed by Cy^3-conjugated goat anti-mouse secondary antibody (Jackson Immuno Research, Inc. West Grove, Pennsylvania). Thereafter, samples were mounted and investigated as described above.

Overall cell morphology and distribution of fibronectin receptor

Overall cell morphology was studied and photographed under phase contrast on freshly fixed fibroblasts cultured with or without FN precoating on the described substrata for 2 h in serum-free medium. Subsequently, substrata were washed and adherent cells permeabilized with 0.5% Triton X-100 for 5 min and saturated with 1% albumin for 15 min. In order to detect β_1-integrin (FN receptor), substrata were incubated for 30 min at 37°C with mouse anti-β_1 monoclonal antibody (Dianova, Hamburg, Germany) in PBS, followed by FITC-conjugated goat anti-mouse IgG (Jackson Immuno Research, Inc., West Grove, Pennsylvania) in the presence of 1% normal goat serum. At the end of incubation, substrata were mounted and investigated for fluorescence, as described above.

RESULTS

The pegylation density resulting from the here applied surface modification step (cf. Scheme 1) is determined by ABMPEG—substratum and ABMPEG—ABMPEG interactions, that is, through the dynamic interfacial equilibrium attained in the adsorption step. For a given hydrophobic head-group and underlying substratum, the molecular weight of the PEG chain, and thus the size of ABMPEG, determine the attained pegylation density. Variation of ABMPEG concentration exclusively allows for the adjustment of pegylation density. By this means a more or less loose regular pattern of end-on-grafted hydrophilic, flexible, PEG entities, with less or more space allowing access to the hydrophobic PSf surface, is created. In Figure 1 it can be seen that with rising ABMPEG solution concentrations, the modified PSf films show decreasing advancing and receding CAs and increasing CA hystereses. This is a typical result for a surface of a material with low surface energy (PSf) that gradually is covered by a material exhibiting a higher surface energy (ABMPEG).

The observed CA data indicate a significant but incomplete PEG coating of the underlying PSf for the highest solution concentration of ABMPEG (cf. Thom et al.[1]). Furthermore, it should be noted that at least the lower limit of the here-achieved range of pegylation densities, to our knowledge, has not been subject to further investigations relating substratum-surface properties to cell–substratum interactions. Most investigations have dealt with rather densely pegylated substratum surfaces where the grafted PEG chains are not far or in a brush regime, thus representing rather effectively nonadhesive interfaces.

Since the adsorption of adhesive proteins plays a crucial role for cell–substratum interactions, FN adsorption to the different surfaces was quantified. In accordance with the substratum preparations (FN precoating) employed for some of the cell experiments, relatively short adsorption times of 30 min were selected, and the adsorption was monitored by *in situ* ellipsometry. With increasing ABMPEG bulk concentration employed in the grafting procedure, adsorption of FN decreased gradually from expectedly high values for plain PSf to substantially lower values for PSf/PEG-10 (see Fig. 2). No FN desorption was observed upon flushing with PBS for 10 min.

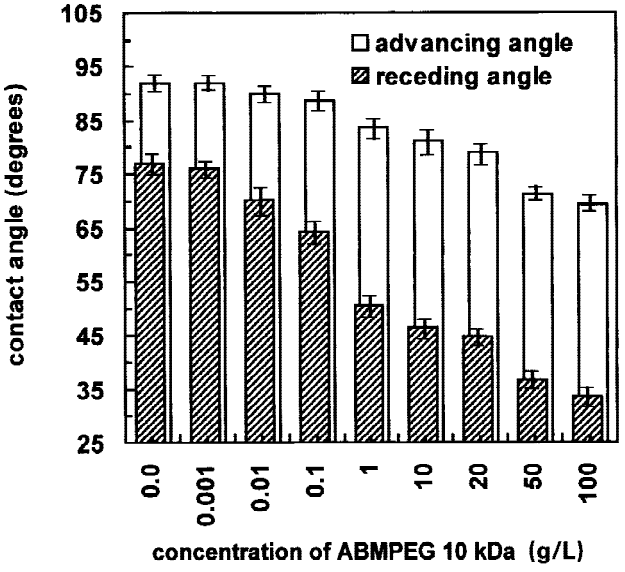

Figure 1. Advancing and receding contact angles of modified PSf spin-coating films being modified at different ABMPEG bulk concentrations. Error bars indicate standard deviations (number of measurements per data point = 30).

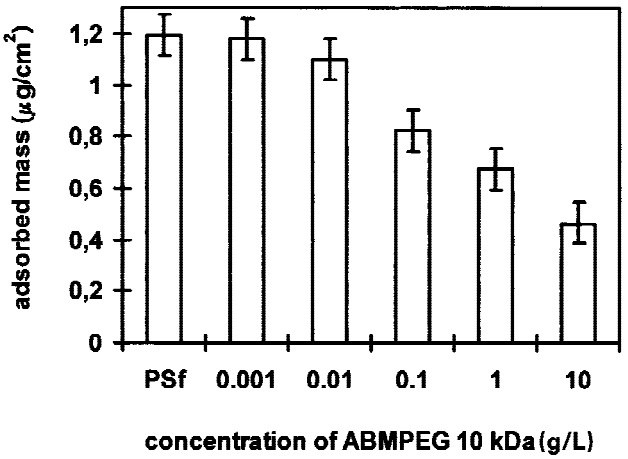

Figure 2. Ellipsometrically determined amount of FN adsorbed to different PSf spin-coating films modified with different solution concentrations of ABMPEG. Substrata were contacted for 30 min by a solution of 0.02 g/L of FN in PBS and consecutively flushed for 10 min with PBS. Error bars indicate estimated errors.

The effect of FN precoating on the adhesive interactions of human fibroblast was studied, assuming that different pegylation densities not only result in different amounts of adsorbed FN but also may influence the biological activity of FN. The data for cell adhesion after 2 h of incubation are presented in Table I. Attachment to plain and pegylated PSf surfaces in the absence of precoated FN, studied as a control, demonstrated a phenomenon already found previously.[1] The stepwise increase in the surface density of PEGs enhanced cell adhesion with a maximum effect for PSf/PEG-0.01 and PSf/PEG-1. Further increase in pegylation density, however, gradually diminished fibroblast adhesion. In these experiments, precoating with FN tended to increase cell adhesion, especially to plain PSf or to only mildly pegylated surfaces (PSf/PEG-0.001) as well as to relatively densely pegylated surfaces (PSf/PEG-10 and -20). However, for moderately pegylated surfaces (PSf/PEG-0.1 and -1), initial cell adhesion was somewhat lower. Nevertheless, the data followed the same trend as described above, with the optimum of fibroblast adhesion at moderate pegylation density (see Table I); however, differences were less pronounced as compared to surfaces not precoated with FN.

TABLE I
Effect of FN Coating

Concentration of ABMPEG (g/L)	PSf/PEG (Cells/Field)	PSF/PEG Precoated with FN (Cells/Field)
0	5.8 (± 3.1)	9.4 (± 2.1)
0.001	6.7 (± 2)	8.3 (± 2.7)
0.01	18.2 (± 9.8)	14.6 (± 5)
0.1	13.1 (± 5.1)	no data available
1	12.4 (± 5.7)	12.1 (± 5.1)
10	5.3 (± 2.3)	8.9 (± 3.7)
20	3.2 (± 1.4)	7.8 (± 3.3)

Mean number of human fibroblasts per microscopic field adhering on PSf spin-coating films modified with different solution concentrations of ABMPEG with or without FN precoating. The respective standard deviations are indicated in parentheses following each value.

To characterize the effect of FN precoating on the interaction of human fibroblasts, overall cell morphology and formation of focal adhesions was studied. The same range of substrata as listed in Table I was investigated, but only characteristic differences are presented (see Fig. 3). On plain PSf most of the cells were not completely spread and often exhibited an irregular morphology [Fig. 3(a)], as described previously. If PSf was precoated with FN, cell spreading improved but cells still exhibited irregular shapes [Fig. 3(b)], many of them still being round. In contrast, on FN-precoated PSf/PEG-0.1, maximum cell spreading occurred [Fig. 3(c)]. In these preparations fibroblasts resembled those cultured on tissue culture plastic, exhibiting typical morphologies, represented by extended cell bodies and polarized shapes. Some of them also possessed characteristic motile morphologies, with distinct leading and trailing cell edges. At higher pegylation densities, however, as shown for FN-precoated PSf/PEG-10, cell adhesion and spreading diminished again [Fig. 3(d)].

Formation of focal adhesion complexes was studied by immunofluorescence of vinculin, a main constituent of the integrin–cytoskeleton complex.[17,18] Almost no focal adhesions were expressed on cells adhering on plain PSf [see Fig. 4(a)]. After precoating PSf with FN, vinculin-positive focal adhesions appeared; however, they were rather short and localized at the cell borders only [Fig. 4(b)]. In contrast, on FN-precoated PSf/PEG-0.01 well-expressed focal adhesions were observed, oriented along the cell polarization [Fig. 4(c)]. On FN-precoated PSf/PEG-10, many of the fibroblasts could not develop focal adhesions although some cells still expressed vinculin, organized predominantly in the cell periphery [Fig. 4(d)].

To characterize cell adhesion in further detail, we also studied the distribution of β_1-integrin, the main constituent subunit of the FN receptor.[16,17] Figure 5 shows typical results from these immunofluorescence studies. Striking dependencies of the organization of FN receptor of fibroblasts adhering to differently pegylated substrata were found. Diffuse staining and no clusters of FN receptors were detected for fibroblasts adhering to PSf [Fig. 5(a)], and very tiny fibril-like β_1-integrin structures were found on FN-precoated PSf [Fig. 5(b)]. However, much more pronounced organization of β_1-integrin into focal adhesions was detected on FN-precoated PSf/PEG-0.01 [Fig. 5(c)] and, again, diffusely distributed integrins and the absence of focal adhesions on FN-precoated PEG 10 [Fig. 5(d)].

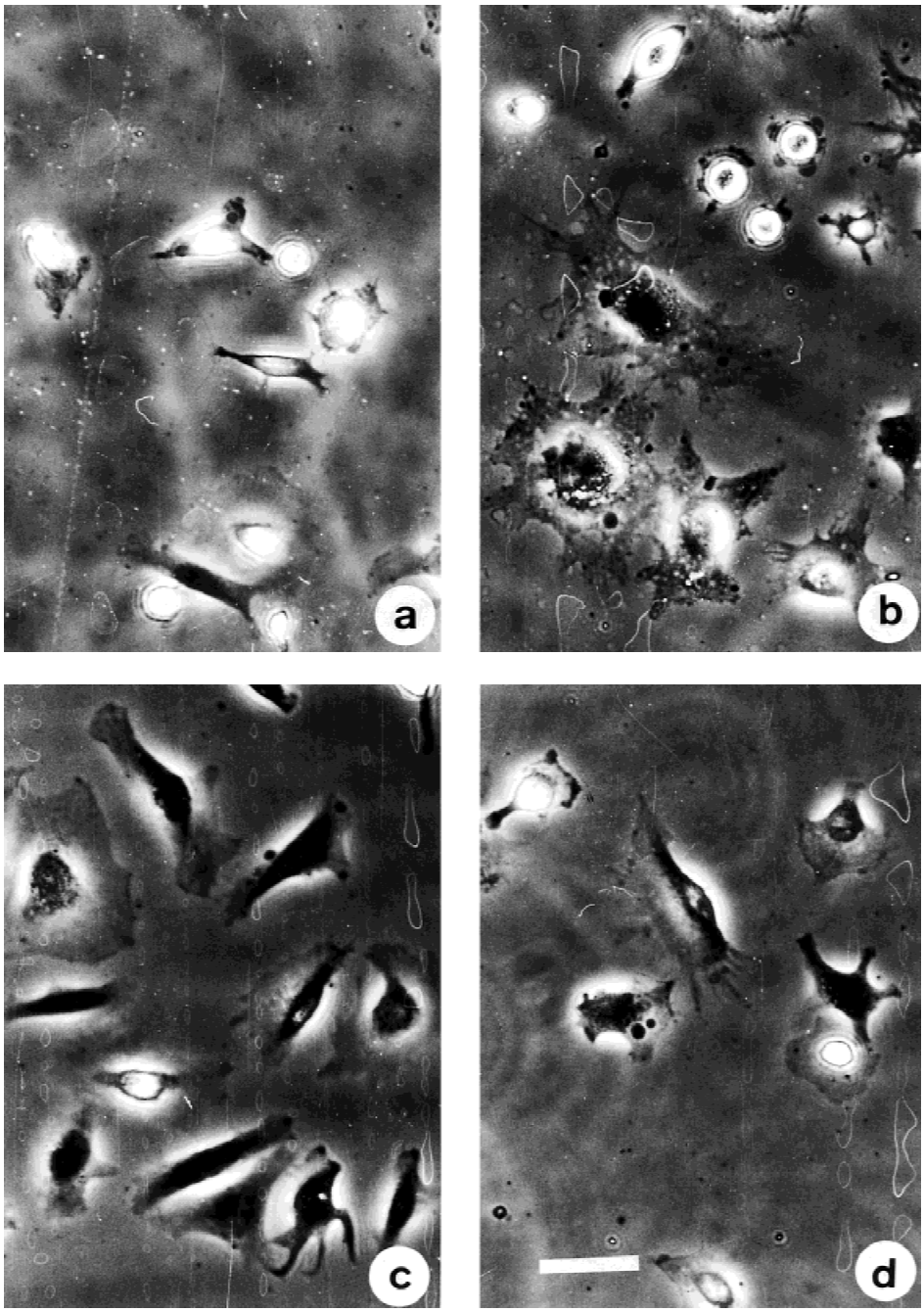

Figure 3. Overall cell morphology of fibroblasts adhering on different PSf spin-coating films modified with different solution concentrations of ABMPEG and effect of ABMPEG concentration and FN precoating. Fibroblasts were plated for 2 h on (a) unmodified plain PSf or on FN-precoated substrata: (b) unmodified PSf, (c) PSf/PEG-0.01, (d) PSf/PEG-10. At the end of incubation, substrata were investigated and photographed under phase contrast at low magnification (original magnification ×20; bar: 20 μm).

Figure 6 demonstrates the reorganization of preadsorbed FFN is dependent on pegylation density. No reorganization of FFN was found on plain PSf, demonstrated by the homogeneous fluorescence of the substratum [Fig. 6(a)] while FFN reorganization started to appear on PSf/PEG-0.001 [Fig. 6(b)]. The most pronounced FFN reorganization was found on PSf/PEG-1.0 [Fig. 6(c)], as indicated by many dark FFN-depleted and concomitant FFN-rich zones (visible as bright streaks) where reorganization into fibrillike structures occurred. It is noteworthy that at higher pegylating densities, FFN removal and reorganization still were observed [Fig. 6(d)]; however, they were much less pronounced, presumably due to reduced amounts of adsorbed FFN on these densely pegylated surfaces (cf. Fig. 2).

Further evidence for improved surface properties of PSf when pegylated at intermediate degrees stems

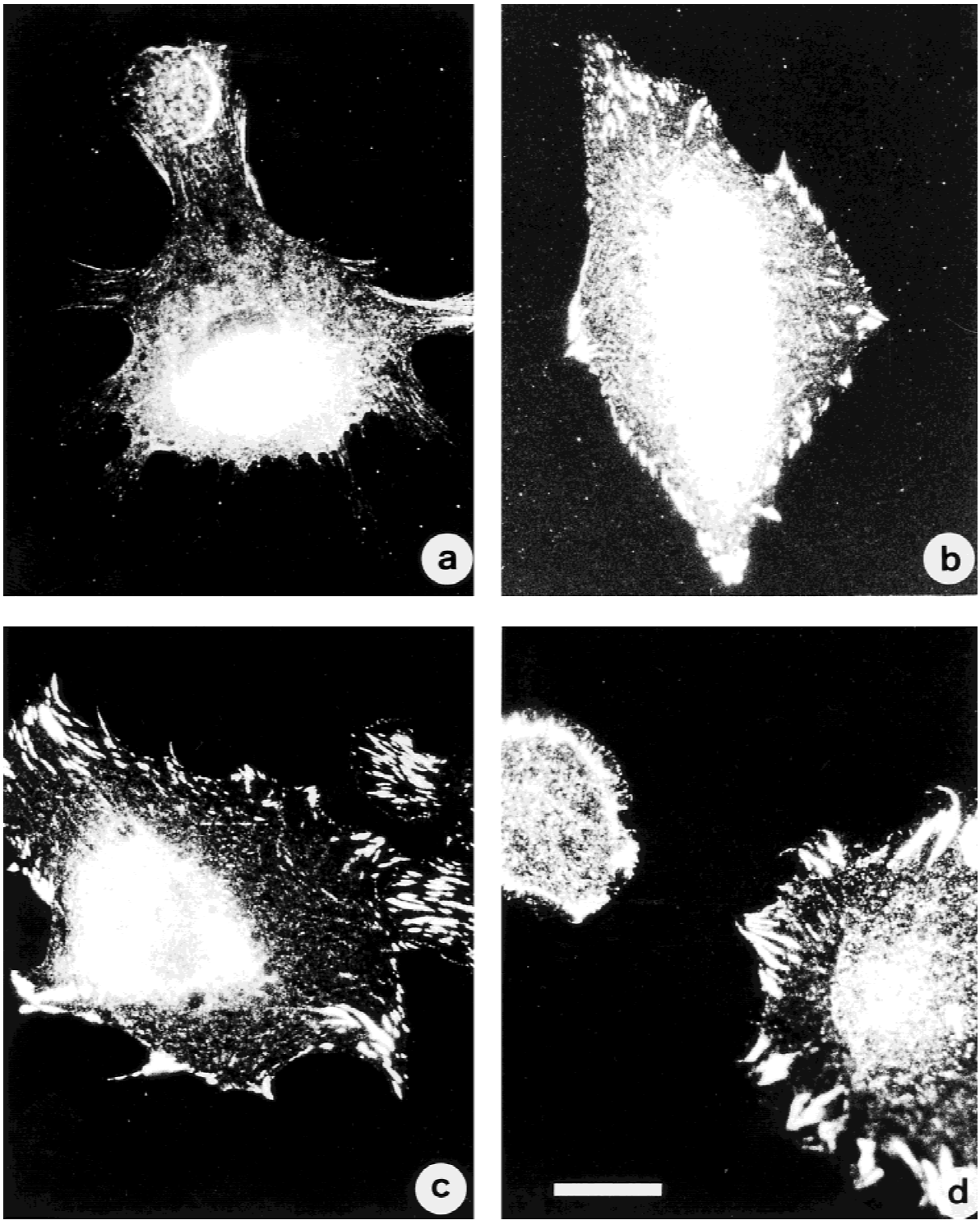

Figure 4. Focal adhesion formation of fibroblasts adhering on different PSf spin-coating films modified with different solution concentrations of ABMPEG and effect of ABMPEG concentration and FN precoating. Fibroblasts were plated for 2 h on (a) unmodified, plain PSf or on FN-precoated substrata: (b) unmodified PSf, (c) PSf/PEG-0.01, (d) PSf/PEG-10. At the end of incubation, substrata were fixed, permeabilized, and stained for vinculin. Substrata were visualized by immunofluorescence and photographed at high magnification (original magnification ×100; bar: 10 μm).

from experiments monitoring FN-matrix formation, where human fibroblasts were cultured for 5 days on different ABMPEG-modified PSf surfaces. Due to the extended period of cultivation, cells could deposit auto-synthesized FN, which was visualized with fluorescent monoclonal anti-FN antibody (see Fig. 7). Almost no FN synthesis and deposition was found on unmodified PSf except for some small single streaks

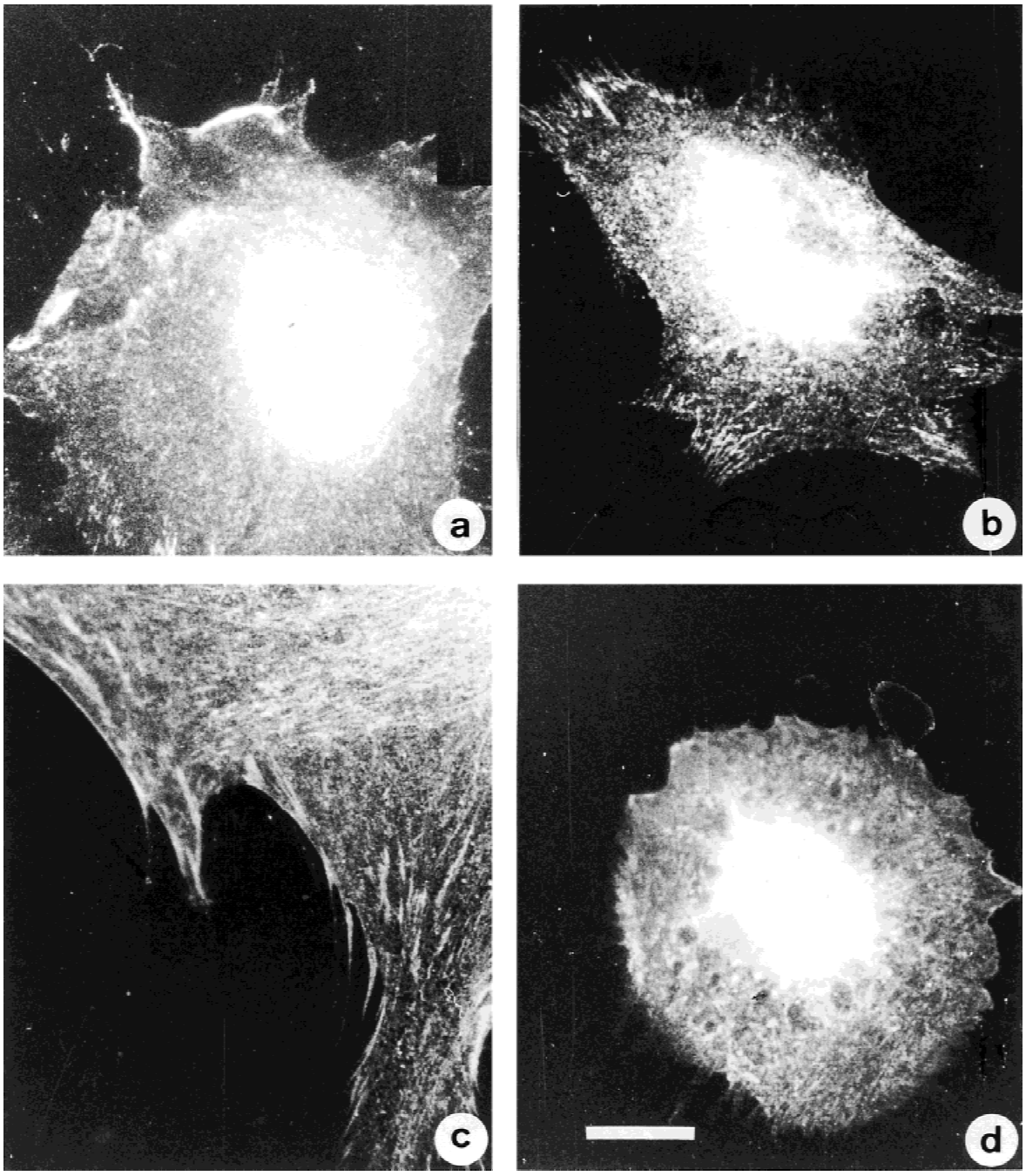

Figure 5. Organization of β_1-integrins in fibroblasts adhering on different PSf spin-coating films modified with different solution concentrations of ABMPEG and effect of ABMPEG concentration and FN precoating. Fibroblasts were plated for 2 h on (a) unmodified, plain PSf or on FN-precoated substrata: (b) unmodified PSf, (c) PSf/PEG-0.01, (d) PSf/PEG-10. At the end of incubation, substrata were fixed, permeabilized, and stained for β_1-integrins by immunofluorescence. Substrata were investigated with the fluorescence microscope and photographed at high magnification (original magnification ×100; bar: 10 μm).

[Fig. 7(a)]. Increasing pegylation density, however, significantly increased FN-matrix deposition, in the following order: PSf/PEG-0.001, PSf/PEG-0.01, PSf/PEG-0.1. In support of the trend observed in already described experiments (see above), the further increase in pegylation density caused a considerable decrease of matrix synthesis, as visible for PSf/PEG-1.0 [Fig. 7(e)] and PSf/PEG-10 [Fig. 7(g)].

DISCUSSION

Our results show that cell adhesive properties and cell–substratum interactions are considerably improved through substratum pegylation with ABMPEG when intermediate concentrations of ABMPEG are applied during the adsorption step of the photografting procedure (cf. Scheme 1). Particularly, we could show

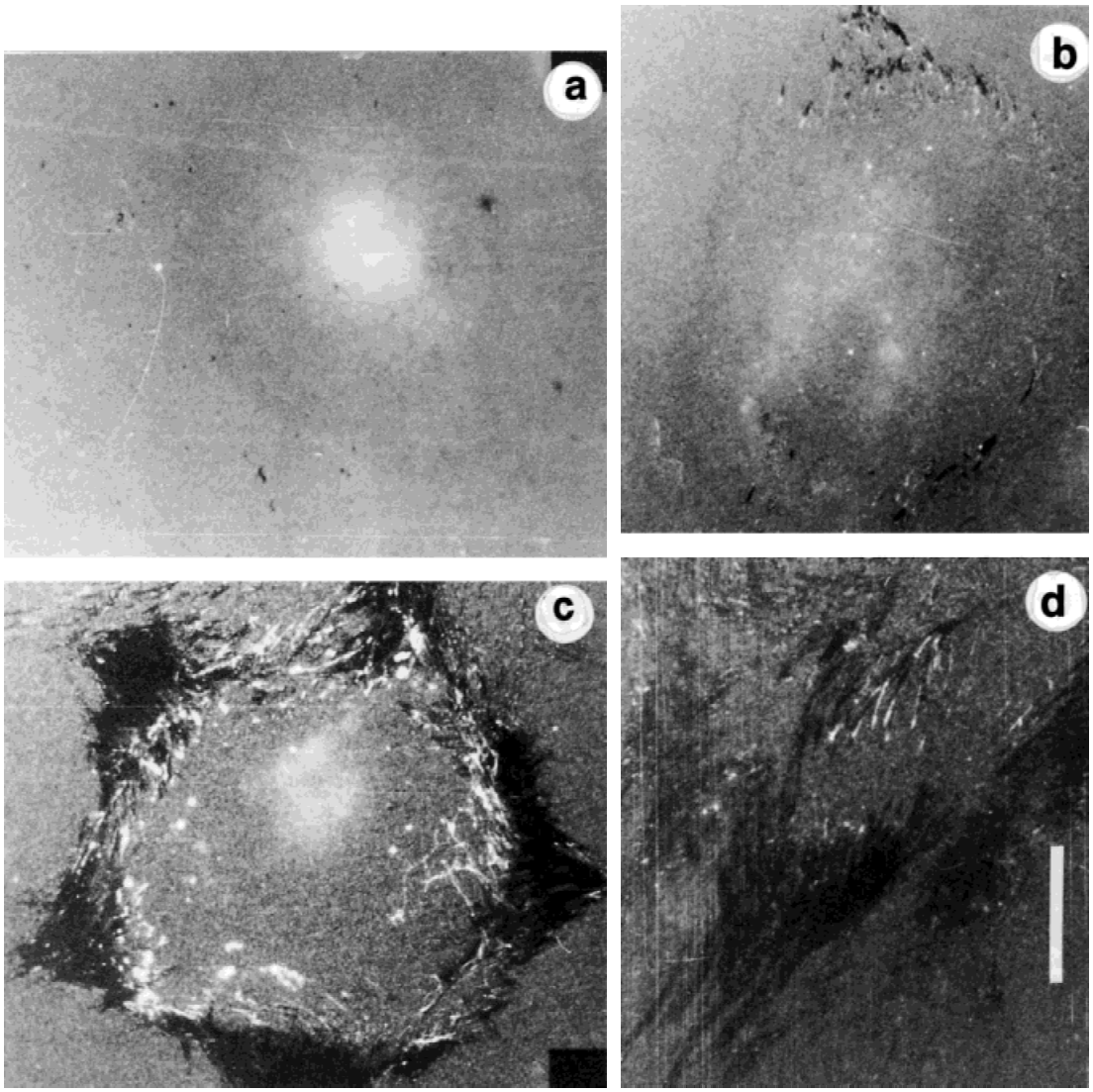

Figure 6. Reorganization of fluorescent FN (FFN). Fibroblasts were plated for 2 h on different PSf spin-coating films modified with different solution concentrations of ABMPEG and precoated with FFN: (a) unmodified PSf, (b) PSf/PEG-0.001, (c) PSf/PEG-1, (d) PSf/PEG-10. At the end of incubation, substrata were fixed and investigated with the fluorescence microscope at high magnification (original magnification ×100; bar: 10 μm).

that FN is directly involved in the process of cell–substratum interactions. This was evidenced by significantly enhanced cell adhesion and spreading as well as by FN-matrix formation on PSf/PEG-0.01 and PSf/PEG-0.1 after FN precoating. When cultured on plain hydrophobic PSf, fibroblasts exhibited round shapes and irregular morphology even after precoating with FN. This behavior of cells when cultured on hydrophobic substrata is well known and has been related to conformational changes of FN upon adsorption.[7–9] The observed inability of cells to rearrange adhesive proteins such as FN into extracellular matrix-specific structures indicates the poor cell–substratum interactions on plain PSf, a phenomenon that we observed recently for other hydrophobic materials as well.[11] Round cells also were observed on rather densely pegylated surfaces, in accordance with the expected protein- and cell-repelling effect of these rather nonadhesive interfaces.[24,25,32] Cell attachment and spreading was optimal at intermediate degrees of pegylation, indicating well developed cell–substratum interactions. More insight into adhesive interactions was obtained by studying focal adhesion formation by vinculin. Focal adhesions are the connections between cell and substratum where closest cell–substratum contact occurs.[31] Again, focal adhesions were particularly well expressed for cells adhering to PSf pegylated at intermediate degrees [cf. Fig. 4(c)]. A similar expression and organization was found for β_1-integrin clusters [cf. Fig. 5(c)]. Since β_1-integrin is the main part of the cell membrane receptor for FN, it can be speculated that FN is responsible for the interaction with cells at intermediate PEG densities. Support for this hypothesis can be drawn from studies of Grinnell

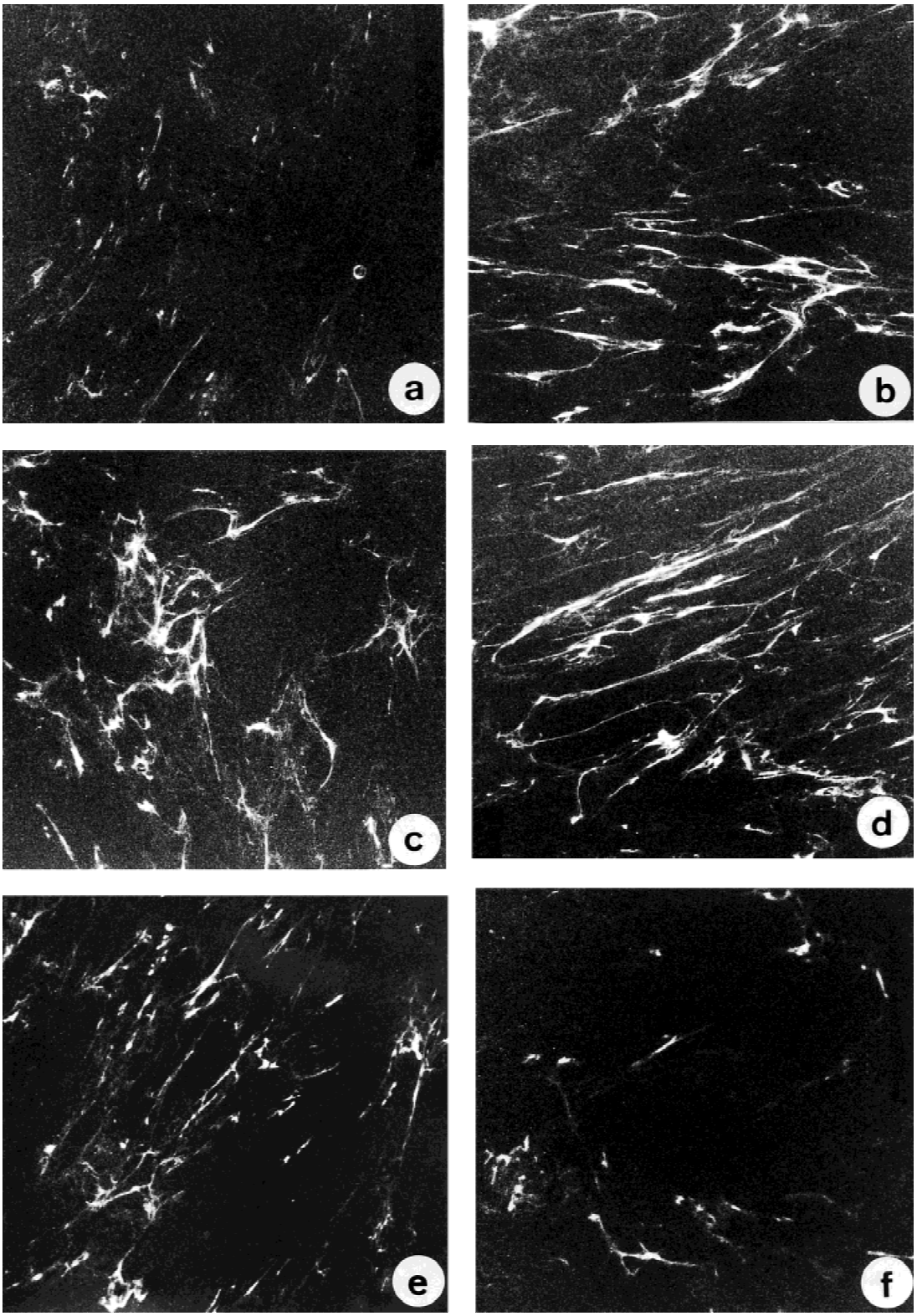

Figure 7. Fibronectin matrix formation by fibroblasts cultured on different PSf spin-coating films modified with different solution concentrations of ABMPEG and effect of ABMPEG concentration. Cells were cultured for 5 days in DMEM containing 10% FBS on different substrata: (a) unmodified PSf, (b) PSf/PEG-0.001, (c) PSf/PEG-0.010, (d) PSf/PEG-0.1, (e) PSf/PEG-1, (f) PSf/PEG-10. At the end of incubation, substrata were fixed and stained for fibronectin by immunofluorescence. Substrata were viewed and photographed at low magnification (original magnification ×20).

and co-workers, who found that competitively adsorbed albumin molecules could enhance the biologic activity of FN on hydrophobic polystyrene.[33] They assumed that adsorbed FN molecules are stabilized laterally in a biologically active conformation when surrounded by tightly adsorbed albumin molecules. Covalently grafted and sterically demanding macromolecules such as PEG could have a similar effect on intercalated FN. In both cases, adsorbed FN has a tight connection to the underlying hydrophobic polymer, but FN's unfolding and concomitant increase in occupied surface area is inhibited by surrounding and sterically demanding entities, namely albumin or PEG molecules. Further evidence for such a model comes also from the recent investigations of Sofia and Merrill on the influence of the molecular weight and grafting density of PEG entities on the adsorption of FN.[26] They convincingly showed that FN will occupy any surface area not densely covered by PEG molecules and, more important, that the protein indeed will be in close contact with the underlying surface. However, these authors did not consider the possible implications of their findings for the biologic activity of proteins intercalated into a grafted PEG layer.

The observed reorganization of fluorescent FN highlights again the important influence of surface properties on cell behavior (cf. Fig. 6). Our results suggest that upon adsorption to hydrophobic PSf, FN undergoes conformational changes accompanied by a rise in the strength of adsorption, counteracting its removal and reorganization by cells, as we have shown for other hydrophobic substrata in previous investigations.[7,11] Considering the reorganization of adhesive proteins as an attempt of fibroblasts to render their matrix *in vitro,* a great disturbance in their functional activity could be expected. However, increasing PEG grafting density increases the possibility for reorganization although the total amount of adsorbed FN decreases, as shown by ellipsometry measurements. Indeed, reorganization also is observed at higher PEG concentrations [cf. Fig. 6(d)], indicating more loosely bound fibronectin.

Assays for cell functionality play an important role in the evaluation of the biocompatibility of materials.[7,20] Surfaces that provide the appropriate signals via common cellular signaling pathways[7,34,35] may stimulate the physiologic activity of cells. A main function of fibroblasts is to secrete and organize extracellular matrix proteins, such as FN and collagens. We recently have shown that this ability of fibroblasts is greatly inhibited on hydrophobic surfaces.[7,11] The involved signaling pathways include attachment, activation of integrins, such as β_1-integrin, and the integrin-linked phosphorylation of tyrosine residues of some functional cytoskeletal proteins,[15–19] corresponding to the observed suppression of these interactions on relatively bioincompatible surfaces.[7,11,34,36] Considering these facts, it becomes understandable why fibroblasts adhering to either plain hydrophobic or highly pegylated PSf exhibit diminished functionality. In contrast, on PSf pegylated at intermediate densities, a well organized FN matrix is observed [cf. Fig. 7(b–d)], corresponding to the assumption that secreted FN is adsorbed in a biologically active conformation that is capable of delivering appropriate signals to the cell's interior, which leads to further FN secretion and matrix assembly.

Future studies are in progress that further will elucidate conformational properties, and thus the biologic activity of attachment proteins adsorbed to these novel surface architectures, as well as the cell–substratum interactions of other relevant primary cells.

CONCLUSIONS

The novelty in this and in our previous study[1] is the finding that end-on-grafting of PEGs on hydrophobic biomaterials can be used to modulate the biocompatibility of polymeric material surfaces. One popular strategy for achieving biocompatible material surfaces has been to render them bioinert, that is, noninteracting with biologic entities. Densely pegylated surfaces were particularly successful in this respect.[22,24,25,32] Biocompatible material surfaces, in turn, also can be achieved by rendering material surfaces bioactive, that is, actively interacting with biologic entities.[13,37] Bioactivity of surfaces has been achieved through the immobilization of extracellular matrix constituents, such as fibronectin, or oligopeptides resembling binding sites for cellular receptors, such as RGD,[38] cytokines,[39] etc. However, the latter strategy does raise two concerns, namely the durability of these surfaces and their ability to be in a dynamic exchange with the surrounding body fluids. Proteins and other oligopeptides permanently are attacked in a biologic environment by the activity of proteases, enzymes, reactive oxygen species, etc., deteriorating the long-term stability of their surfaces. Furthermore, the dynamic exchange of biologic matter at a "living" interface, such as a tissue surface, involves permanent regeneration and restructuring of living matter. To combine durability and flexibility therefore could be advantageous and perhaps a fruitful approach. In this work we described a first step in this direction, namely that pegylation of biomaterial surfaces may be used to modulate the biologic activity of adsorbed adhesive proteins, leading to improved biocompatibility of normally incompatible (hydrophobic) material surfaces.

Dr. Helmut Kamusewitz and Yvonne Fritsche, from the GKSS Research Center, Institute of Chemistry, Teltow, Germany, are acknowledged for their advice and technical sup-

port for CA measurements. Ulla Elofsson is credited for her technical and organizational support for ellipsometry measurements performed at the Institute for Food Technology, Lund University, Sweden, and financed by the Nordic Research Council.

References

1. Thom V, Altankov G, Groth T, Jankova K, Jonsson G, Ulbricht M. Optimizing cell–surface interactions by photo-grafting of poly(ethylene glycol) (PEG). Langmuir 2000;16:2756–2765.
2. Grinnell F, Milam M, Spree PA. Attachment of normal and transformed hamster kidney cells to substrata varying in chemical composition. Biochem Med 1973;7:87–90.
3. Steele JG, McFarland C, Dalton BA, Johnson G, Evans MD, Howlett CR, Underwood PA. Attachment of human bone cells to tissue culture polystyrene and to unmodified polystyrene: The effect of surface chemistry upon initial cell attachment. J Biomater Sci, Polym Edn 1993;5:245–257.
4. van Wachem PB, Beugling T, Feijen J, Detmers JP, van Aken WG. Interaction of cultured human endothelial cells with polymeric surfaces of different wettabilities. Biomaterials 1985;6: 403–408.
5. den Braber ET, de Ruijter JE, Smits HTJ, Ginsel LA, Recum AF, Jansen JA. Effect of parallel surface microgrooves and surface energy on cell growth. J Biomed Mater Res 1995;29:511–518.
6. Webb K, Hlady V, Tresco PA. Relative importance of surface wettability and charged functional groups on NIH 3T3 fibroblast attachment, spreading, and cytoskeletal organization. J Biomed Mater Res 1998;41:422–430.
7. Groth T, Altankov G. Cell–surface interactions and the tissue compatibility of biomaterials. In: Harris PI, Chapman D, editors. New biomedical materials—Basic and applied studies, biomedical and health research. Vol. XVI. Amsterdam, The Netherlands: IOS Press; 1998. p 12–23.
8. Juliano DJ, Saavedra SS, Truskey GA. Effect of the conformation and orientation of adsorbed fibronectin on endothelial cell spreading and the strength of adhesion. J Biomed Mater Res 1993;27:1103–1113.
9. Grinnell F, Feld MK. Adsorption characteristics of plasma fibronectin in relationship to biological activity. J Biomed Mater Res 1981;15:363–381.
10. Pettit DK, Horbett TA, Hoffman AS. Influence of the substrate binding characteristics of fibronectin on corneal epithelial cell outgrowth. J Biomed Mater Res 1992;26:1259–1275.
11. Altankov G, Grinnell F, Groth T. Studies on the biocompatibility of materials: Fibroblast reorganization of substratum-bound fibronectin on surfaces varying in wettability. J Biomed Mater Res 1996;30:385–391.
12. Elbert D, Hubbell JA. Surface treatments of polymers for biocompatibility. Ann Rev Mater Sci 1996;26:365–394.
13. Griffith LG, Lopina SY. Microdistribution of substratum-bound ligands affects cell function: Hepatocyte spreading on PEO-tethered galactose. Biomaterials 1998;19:979–986.
14. Gumbiner BM. Cell adhesion: The molecular basis of tissue architecture and morphogenesis. Cell 1996;84:345–357.
15. Ruoslahti E, Reed JC. Anchorage dependence, integrins, and apoptosis. Cell 1994;77:477–478.
16. Ruoslahti E. Integrin signaling and matrix assembly. Tumor Biol 1996;17:117.
17. Hynes RO. Integrins: Versatility, modulation, and signaling in cell adhesion. Cell 1992;69:11–25.
18. Albelda SM, Buck CA. Integrins and other cell adhesion molecules. FASEB J 1990;4:2868–2880.
19. Juliano RL, Haskill S. Signal transduction from the extracellular matrix. J Cell Biol 1993;120:577–585.
20. Kirkpatrick CJ, Bittinger F, Wagner M, Kohler H, van Kooten TG, Klein CL, Otto M. Current trends in biocompatibility testing. Proc Inst Mech Engrs 1998;212:75–84.
21. Saltzman WM. Cell interactions with polymers. In: Lanza R, Langer R, Chick W, editors. Principles of tissue engineering. Austin, TX: R.G. Landes Company; 1997. 225 p.
22. Amiji M, Park GS. Surface modification of polymeric biomaterials with poly(ethylene oxide), albumin, and heparin for reduced thrombogenicity. J Biomater Sci, Polym Edn 1993;4:217–234.
23. Galletti PM. Thrombosis in extracorporeal devices. In: Leonard EF, Turitto VT, Vroman L, editors. Blood in contact with natural and artificial surfaces. New York: Ann NY Acad Sci 1987; 516:679–682.
24. Harris JM. Introduction to biotechnological and biomedical applications of polyethylene glycol. Polym Preprints 1997;38:520–521.
25. Lee JH, Lee HB, Andrade JD. Blood compatibility of poly(ethylene oxide) surfaces. Prog Polym Sci 1995;20:1043–1079.
26. Sofia SJ, Premnath V, Merrill EW. Poly(ethylene oxide) grafted to silicon surfaces: Grafting density and protein adsorption. Macromolecules 1998;31:5059–5070.
27. Thom V, Jankova K, Ulbricht M, Kops J, Jonsson G. Synthesis of photoreactive α-4-azidobenzoyl-ω- methoxy-poly(ethylene glycol)s and their end-on photo-grafting onto polysulfone ultrafiltration membranes. Macromol Chem Phys 1998;199:2723–2729.
28. Azzam RMA, Bashara NM. Ellipsometry and polarized light. Amsterdam: Elsevier Science Publishers; 1987. 530 p.
29. Arnebrant T. Proteins at the metal/water interphase in relation to interfacial structure [PhD Thesis]. Lund, Sweden: Lund University; 1987.
30. Altankov G, Groth T. Reorganization of substratum-bound fibronectin on hydrophilic and hydrophobic materials is related to biocompatibility. J Mater Sci: Mater Med 1994;5:732–737.
31. Grinnell F. Focal adhesion sites and the removal of substratum-bound fibronectin. J Cell Biol 1986;103:2697–2706.
32. Zhang M, Desai T, Ferrari M. Proteins and cells on PEG-immobilized silicon surfaces. Biomaterials 1998;19:953–960.
33. Grinnell F. Fibronectin adsorption on material surfaces. In: Leonard EF, Turitto VT, Vroman L, editors. Blood in contact with natural and artificial surfaces. New York: Ann NY Acad Sci; 1987. 280 p.
34. Groth T, Altankov G. Studies on cell–biomaterial interactions: Role of tyrosine phosphorylation during fibroblast spreading on surfaces varying in wettability. Biomaterials 1996;17:1227–1234.
35. Faucheux N, Warocquier–Clerout R, Duval JL, Haye B, Nagel MD. cAMP levels in cells attached to AN69 and Cuprophan: cAMP dependence on cell aggregation and the influence of serum. Biomaterials 1999;20:159–165.
36. Altankov G, Groth T, Krasteva N, Albrecht W, Paul D. Morphological evidence for a different fibronectin receptor organization and function during fibroblast adhesion on hydrophilic and hydrophobic glass substrata. J Biomater Sci, Polym Edn 1997;8:721–740.
37. Neff JA, Caldwell KD, Tresco PA. A novel method for surface modification to promote cell attachment to hydrophobic substrates. J Biomed Mater Res 1998;40:511–519.
38. Massia SP, Hubbell JA. An RGD spacing of 440 nm is sufficient for integrin $\alpha_5\beta_3$- mediated fibroblast spreading and 140 nm for focal contact and stress fiber formation. J Cell Biol 1991;114: 1089–1100.
39. Ito Y, Chen G, Imanishi Y. Artificial juxtacrine stimulation for tissue engineering. J Biomater Sci, Polym Edn 1998;9:879–890.

Publikation 13

Thomas Groth und Wolfgang Wagenknecht (2001)

Anticoagulant potential of regioselective derivatized cellulose.

Biomaterials, **20**, 2719-2729.

ELSEVIER

Biomaterials 22 (2001) 2719–2729

Biomaterials

www.elsevier.com/locate/biomaterials

Anticoagulant potential of regioselective derivatized cellulose

Thomas Groth[a,*], Wolfgang Wagenknecht[b]

[a]Department of Membrane Research, Institute of Chemistry, GKSS Research Center, Kantstrasse 55, D-14513 Teltow, Germany
[b]Fraunhofer Institute of Applied Polymer Research, Kantstrasse 55, D-14513 Teltow, Germany

Received 21 June 1999; accepted 8 January 2001

Abstract

Regioselective derivatization was carried out introducing sulfate, phosphate or quaternary ammonia groups in C2-, C3- and C6-position of the anhydroglycose unit of cellulose. The anticoagulant potential of these derivatives was estimated with common clotting assays, such as thrombin time and partial thromboplastin time. It was found that a pronounced anticoagulant activity of cellulose derivatives could be achieved if the degree of substitution (DS) with sulfate was above 1.0. The anticoagulant activity was maximal at a DS of about 1.5 and then decreased again. Further, it was detected that particularly sulfation in C2-position resulted in a pronounced anticoagulant activity of cellulose derivatives. Development and application of assays specific for thrombin and factor Xa indicated that the anticoagulant potential of these cellulose derivatives was mainly due to anti-thrombin activity. The comparison of cellulose sulfates and cellulose derivatized with phosphate and quaternary ammonium groups demonstrated that the negative charge and type of the substituent is an important prerequisite for the anticoagulant activity of cellulose derivatives. Indeed, derivatization with sulfate produced superior activity in comparison with phosphate.

Keywords: Cellulose sulfates; Regioselective derivatization; Clotting times; Thrombin assay; Factor Xa assay; Heparinoid activity

1. Introduction

Extracorporal blood purification during the treatment of end-stage renal failure has proven to be successful in saving the lives of numerous patients over many years. The benefit has resulted from the use of membranes prepared from natural and synthetic polymers that accomplish the controlled removal of solutes and water from blood. In recent years many types of membranes made of synthetic polymers were developed that seemed to be advantageous with respect to permeability and biocompatibility in comparison with membranes based on cellulose [1,2]. On the other hand, the apparent lower biocompatibility of cellulosic membranes is discussed controversially, negative impacts on the patients health state with deleterious consequences have also been observed for synthetic membranes [3,4]. There is increasing evidence that dialyzers based on cellulose may have per se the same clinical outcome [5], or are even advantageous under specific conditions [6], but reduce considerably the cost of dialysis treatment [5]. Dialysis related problems of bioincompatibility can be expected because of the large contact area between flowing blood and a foreign surface that may lead to the activation of different defense systems of the organism [7,8]. Particularly significant during hemodialysis are the activation of the complement, and coagulation system, as well as the activation of platelets and leukocytes [8–10]. The activation of coagulation during hemodialysis is prevented by administering heparin as anticoagulant. However, heparin not only prevents the onset of coagulation in the extracorporal circuit, but may also lead to bleeding with fatal consequences for the patient [11]. To overcome the difficulties with systemic application of heparin, local anticoagulation in the extracorporal circuit seems to be a promising approach [11–13]. This can be achieved by the adsorption, introduction in the polymer bulk, or covalent binding of heparin or heparinoid substances that leads to an improved thromboresistance of the device [13–16].

Naturally occurring sulfated polysaccharides like heparin and heparan sulfate show anticoagulant activity that is attributed to a pentasaccharide sequence with N- and O-sulfate groups forming the binding site for

* Corresponding author. Fax: +49-3328-352460.
E-mail address: thomas.groth@gkss.de (T. Groth).

0142-9612/01/$ - see front matter
PII: S0142-9612(01)00013-8

antithrombin III (AT III) [17,18]. The anticoagulant action of heparin is due to a 1000-fold increase in the affinity of AT III for thrombin and factor Xa [19,20]. Moreover, heparin not only causes the necessary conformational change of AT III, but also forms a catalytic surface to which both thrombin and AT III bind [21]. The specific interaction between AT III and heparin is because of the electrostatic interaction of positively charged amino acids in the heparin binding pocket of AT III with negatively charged sulfate residues [22,23]. It has been shown that chemical sulfation of low affinity heparin leads to an enhanced anticoagulant action of the modified heparin [24].

Artificial heparinoids may be synthesized on the basis of polysaccharides (i.e., dextrans) that are sulfated [15,25,26]. These compounds might be used for blends with cellulose for membrane formation and applied in hemodialysis. Since heparin is sulfated in distinct positions of the sugar residues [17], the question remains if stochastic or regioselective sulfation of cellulose is able to provoke a substantial heparinoid activity, and what degree of substitution is necessary for the achievement of a sufficient anticoagulant potential.

In this study we have prepared cellulose derivatives by homogeneous regioselective derivatization with sulfate, phosphate, and quaternary ammonium groups. The distribution of the substituents was investigated by ^{13}C-NMR-studies. Clotting assays that were recently successfully used for the estimation of anticoagulant action of immobilized heparin [27] were also applied in this investigation. Further, specific assays for factor IIa (thrombin) and factor Xa were applied to find out the mechanism of the anticoagulant action. Details are reported herein.

2. Materials and methods

2.1. Synthesis of cellulose derivatives

Synthesis and chemical analysis of cellulose derivatives have been presented in more detail by us [28,29] and will be briefly described here. The substances were named later in the result section according to the route of derivatization, e.g. synthesis via cellulose acetate (CA), the type of substituents, e.g. sulfate (S) and the degree of substitution (DS) as for example CA-S_{DS}.

Most experimental work was performed with commercial cellulose acetates with degree of substitution (DS) of 1.9, 2.4 and 2.9, respectively. For regioselective deacetylation of cellulose triacetate (CTA, DS = 2.9), a 5–10% by weight solution of the polymer was prepared in dimethylsulfoxide (DMSO) at 100°C. After cooling to 80°C 2.3 mol hexamethylene diamine per mol anhydroglucose unit (AGU) with 22 mol H_2O per mol AGU were added, and the reaction mixture was stirred at 80°C for 1–24 h, arriving at a DS between 2.4 and 0.7. After neutralization with glacial acetic acid, the polymer product was precipitated in water, subsequently washed with water, and finally dried at 60°C in vacuum. In the low DS-range of one or less, the precipitation was achieved by ethanol in order to avoid a too extensive swelling of the precipitate.

Sulfation of the various partially substituted cellulose acetates (CA-S) was performed with sulfamic acid at 80°C after dissolving or suspending the cellulose acetate in dry dimethylformamide (DMF) to a 5–10% by weight solution or suspension (see Fig. 1). An excess of sulfamic acid (2 mol per mol of free OH-groups) was generally employed to esterify as much of the free OH-groups as possible while the acetate groups served as a very effective protecting group. A reaction time of 1.5 h at 80°C was found to be sufficient. The mixed cellulose ester containing acetate and sulfate half ester groups was precipitated in a concentrated solution of sodium acetate in ethanol, and after washing with 4% by weight sodium acetate in ethanol, the product was deacetylated by 4% by weight NaOH in ethanol containing 10% H_2O. The heterogeneous system was reacted for 24 h at room temperature arriving at a negligible residual acetate-DS of less than 0.01 without any significant loss of sulfate half ester groups. The reaction product was further processed by washing with ethanol, and dried at 60°C in vacuum.

For a subsequent phosphatation obtaining cellulose phosphates (CA-P) as shown in Fig. 2, the partially

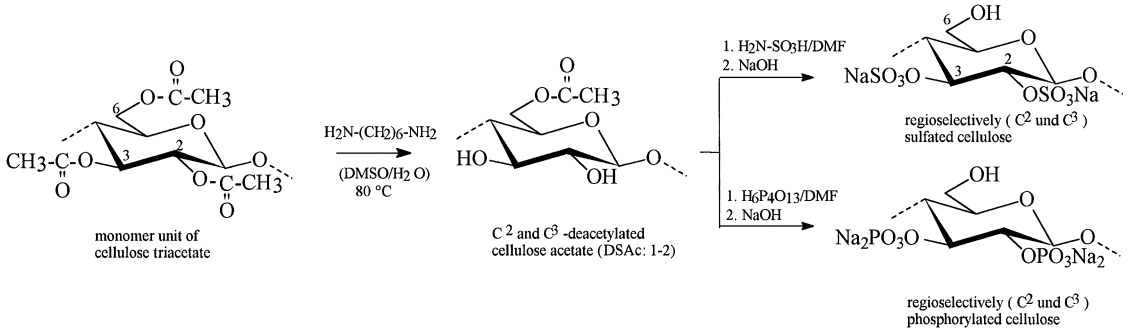

Fig. 1. Scheme of the synthesis of cellulose sulfates and phosphates via cellulose triacetate.

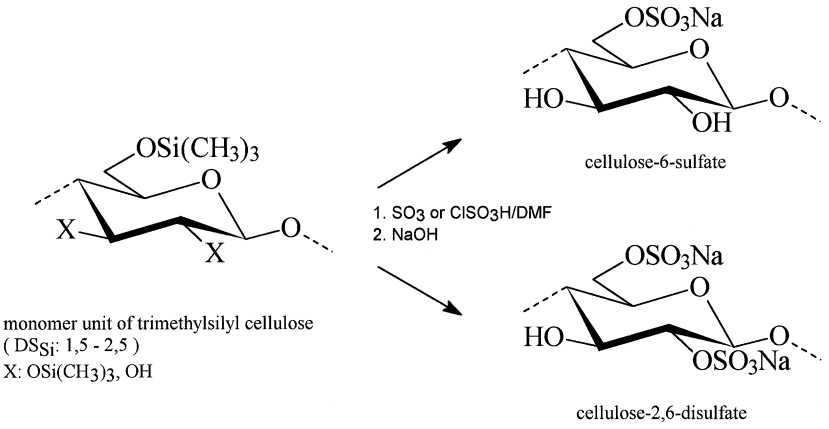

Fig. 2. Scheme of the synthesis of cellulose sulfates via trimethylsilyl cellulose.

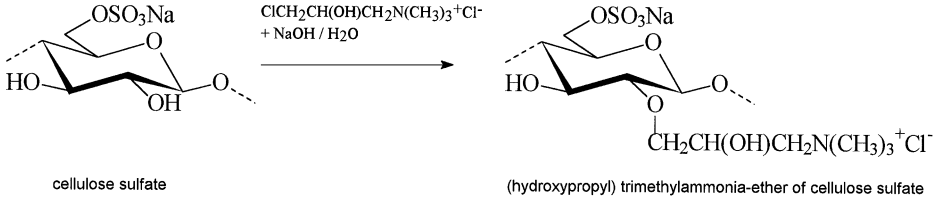

Fig. 3. Scheme of the synthesis of cellulose ampholytes by cationization of cellulose sulfates.

substituted cellulose acetate was dissolved in dry DMF at 120°C to a 5–10% by weight solution. An incomplete dissolution at low DS (<1.0) was not relevant in the subsequent esterification. 4.5 mol of tri-*n*-butylamine per mol AGU was added to the system at 120°C, followed by addition of 1.5 mol tetrapolyphosphoric acid per mol AGU in DMF. After 6 h reaction at 120°C a clear homogeneous system was obtained from which the polymer was precipitated by pouring in 4% by weight NaOH in ethanol. The precipitate was kept for 24 h at room temperature for a complete deacetylation. To remove the residual polyphosphoric acid, the product was suspended subsequently in ethanol at pH 2.0 (adjusted with HCl) and extensively washed with ethanol containing 10% H_2O. After neutralization to pH 7.0 with ethanolic NaOH and washing with pure ethanol, the product was dried at 60°C in vacuum. The obtained samples covered a range of substitution between 0.5 and 1.0 of anionic phosphate groups.

A series of cellulose sulfate esters were prepared via trimethylsilyl cellulose as an intermediate (CSi-S). Silylation was performed according to [29] and is shown in Fig. 2 with trimethylchlorosilane after activation of the cellulose material, usually acetate grade cotton linters with ammonia at low temperature. A 2–3% by weight suspension of dry cellulose was prepared in a saturated solution of NH_3 in DMF or tetrahydrofuran (THF), respectively, at −15°C and activated for 2 h. Then, the suspension was reacted with 2 mol trimethylchlorosilane per mol AGE, first under stirring at −15°C for 2 h and then for further 4 h raising slowly the temperature of the system to 60°C. The reaction mixture was separated from solid NH_4Cl by filtration and used without isolation of the trimethylsilylcellulose for the subsequent sulfation. A DS of silyl groups of about 1.5 was obtained by the DMF procedure, and of about 2.0–2.4 by the THF procedure. The subsequent sulfation was performed with SO_3 in DMF or HSO_3Cl in DMF at room temperatures for 2 h, adjusting the DS by the amount of reagent employed and arriving at a sulfate-DS between 0.9 and 2.2. The chlorosulfonic acid procedure was preferred in the low DS-range, the SO_3 procedure in the high DS-range. The reaction product was precipitated in acetone containing 4% of water and washed extensively with the same mixture. After neutralization with ethanolic NaOH and washing with pure ethanol the samples were dried at 60°C in vacuum.

For introducing quaternary ammonium groups in the partially substituted cellulose sulfates (CA-SK, see Fig. 3) a 10% aqueous solution of the half ester with a DS of 0.25 or 0.45, respectively, was reacted with 3 mol (3-chloro-2-hydroxypropyl)-trimethylammonium chloride per AGU dissolved in water and 4 mol NaOH (aqueous solution) per mol AGU at room temperature for 24 h. The reaction product was precipitated in methanol, and neutralized to pH 7–8 with acetic acid in methanol. Then, it was washed with a methanol/water mixture (80 : 20% by volume) to remove NaCl and excess reagent. Finally,

it was washed with pure methanol and dried at 60°C in vacuum.

2.2. Analytical methods

The DS of the cellulose derivatives finally obtained was characterized by elemental analysis and ^{13}C-NMR spectroscopy. The substituent distribution within the AGU was assessed from the ^{13}C-NMR spectrum of the cellulose derivatives dissolved in D_2O by integrating the signal areas and comparing those of the substituted position to those of the appropriate non-substituted one as described in [30].

2.3. Biological assays

2.3.1. Collection and preparation of blood

Blood was drawn from healthy human volunteers who had no medication for at least 10 days. Blood was anticoagulated with sodium citrate (3.8 g/100 ml). The blood was centrifuged at 2000*g* for 20 min. The supernatant cell free plasma was separated. Plasma samples from 10 different donors were pooled, aliquoted and snap frozen at −70°C. For experimental work plasma was thawed at 37°C and used within 2 h.

2.3.2. Measurement of clotting times

Thrombin time (TT) was measured using 30 IU/ml thrombin (Behring Werke, Germany). Partial thromboplastin time (PTT) was estimated using a commercial test kit (Boehringer Mannheim, Germany). Measurements were carried out with a coagulometer KC 4a (Amelung, Germany). Cellulose derivatives were dissolved in TRIS buffer, pH 7.4. 100 µl pooled plasma were mixed with 50 µl cellulose derivative solution and incubated for 1 min (TT) or 3 min (PTT), respectively. TT was measured after addition of 100 µl thrombin solution (0.3 IU/ml). PTT was estimated after addition of 100 µl kaolin–cephalic solution, followed by the addition of 100 µl 25 mM $CaCl_2$ solution. After the addition of activator the time needed for clotting was measured. If samples did not clot within 10 min it was observed that no clotting occurred afterwards. Therefore, measurements were stopped after 10 min and those samples defined as non-clottable (n.c.). To still obtain visible data points in the graphs these values were set at a clotting time of 600 s. However, it should be kept in mind that these data represent conditions under which the plasma did not clot at all.

2.3.3. Inactivation of thrombin and factor Xa

The anticoagulant potential of the different cellulose derivatives was tested in addition by their ability to support the inactivation of thrombin and factor Xa in the presence of antithrombin III. This was possible by the development of amidolytic assays for thrombin and factor Xa in separate investigations. Cellulose derivatives or reference substances were dissolved in 50 mM Tris-HCl, 175 mM NaCl, 10 mM EDTA, and 0.5 mg/ml human serum albumin [24]. The thrombin assay was carried out mixing 50 µl AT III (activity 0.265 pkat/ml) with 200 µl thrombin (activity 0.53 nkat/ml), and 50 µl of the test substance. After 5 min incubation at 37°C 200 µl chromogenic substrate S-2238 (0.22 mM) was added and the mixture was incubated for 2 min. The conversion of the chromogenic substrate was stopped by the addition of 200 µl acetic acid (20% v/v). The optical density was measured at 405 nm in 96 well plates with a plate reader (Anthos 2001, Austria). A standard curve was obtained under identical conditions for thrombin activities from 0 up to 1.053 nkat/ml and used for the calculation of residual thrombin activity from the measured OD.

The factor Xa assay was performed using 200 µl of factor Xa solution (activity 1.06 nkat/ml), 50 µl AT III solution (activity 0.265 pkat/ml), 50 µl test solution and 200 µl chromogenic substrate S-2222 (0.22 mM). The experiment was carried out in the same manner as the thrombin assay. Residual factor Xa activities were calculated from a standard curve. Thrombin, factor Xa, AT III, and the chromogenic substrates S-2238, and S-2222 were supplied by Chromogenix, Sweden.

2.3.4. Statistics

All experiments were carried out with plasma pooled from 10 different donors. The results represent the means of four independent measurements. Because of the use of pooled plasma during the clotting assays or the use of standardized protein solutions during the Factor IIa and Xa assays standard deviations were too small to be visible in the graphs and are therefore not shown here. Significant differences ($p \leqslant 0.05$) were estimated by Students *t*-test and are shown in the figure captions when applicable.

3. Results

3.1. Cellulose sulfates via cellulose acetate (CA-S)

Table 1 gives an overview of the DS obtained by chemical analysis and ^{13}C-NMR for cellulose sulfates synthesized via cellulose acetate. Table 1 also shows the distribution of the sulfate ester groups with regard to C2-, C3- and C6-position within the AGU. It can be seen that derivatization was performed predominantly in C2-position, although C3- and C6-position were derivatized to some extent as well.

The influence of sulfate content on the heparinoid action of derivatized cellulose was investigated with common clotting assays measuring the action of thrombin (TT), or the contact system (PTT) in pooled plasma. Further direct monitoring of inhibition of active serine

Table 1
Sulfate content and substitution pattern of cellulose sulfate synthesized via cellulose acetate

	DS by chemical analysis	DS by ^{13}C-NMR	Substitution pattern of sulfate		
			C2	C3	C6
CA-$S_{0.26}$	0.35	0.26	0.17	0.08	0
CA-$S_{0.95}$	0.80	0.95	0.55	0.20	0.20
CA-$S_{1.14}$	1.10	1.14	0.74	0.09	0.31
CA-$S_{1.33}$	1.40	1.33	0.76	0.10	0.47
CA-$S_{1.35}$	1.07	1.35	0.67	0.33	0.35

protease was carried out with amidolytic assays specific for thrombin and factor Xa using pure preparations of these clotting factors and antithrombin III.

First, it was observed that the increase of the overall sulfate content enhanced the heparinoid action of cellulose derivatives synthesized via cellulose acetate with predominant derivatization in C2-position (see also Table 1). Fig. 4a and b show that the increase of the degree of sulfation of CA-S prolongs the clotting times TT and PTT. However, it is also visible that particularly thrombin time rises up to a DS of 1.33 and then decreases again. The big difference in the heparinoid activity of CA-$S_{1.33}$ and CA-$S_{1.35}$ indicates some effect of the position of the sulfate groups (see below). At a concentration of CA-S of 25 μg/ml no clotting occurs for a DS $\geqslant$ 0.95 during TT measurements, and for a DS $\geqslant$ 1.15 during PTT measurements.

To figure out whether the anticoagulant action of these heparinoid substances was due to anti-Xa or anti-thrombin activity amidolytic assays have been applied for selected CA-S with low or high DS. Fig. 5a shows that the anti-thrombin activity of CA-$S_{0.26}$ was almost negligible while CA-$S_{1.33}$ caused about 40 per cent inhibition of thrombin activity. It was also observed that the anti-thrombin activity of CA-$S_{1.35}$ was much lower which might be related to the different substitution pattern as shown in Table 1. In comparison, the anti-Xa activity as shown in Fig. 5b was constant for CA-$S_{0.26}$, but was decreased up to 60 per cent for CA-$S_{1.33}$ as well.

3.2. Cellulose sulfates via trimethylsilyl cellulose (CSi-S)

Cellulose sulfate derivatives based on silylated cellulose were predominantly derivatized in C6-position, but also to some extent in C2-, and to a lesser degree in C3-position which is shown in Table 2. Fig. 6a demonstrates that the investigation of clotting times using these substances yielded generally shorter thrombin times as observed for CA-S with comparable DS (see Fig. 4a for a comparison). In contrast, the PTT times of CSi-S derivatives shown in Fig. 6b were in general comparable to that of CA-S derivatives (shown in Fig. 4b). Again it was observed that maximal anticoagulant activity was already achieved at an intermediate DS of about 1.35.

As already shown for CA-S derivatives, factor IIa, and Xa assays were applied for CSi-S derivatives selecting the following materials: CSi-$S_{0.95}$, CSi-$S_{1.35}$, and CSi-$S_{2.18}$. Pronounced concentration-dependent anti-IIa activity was found for CSi-$S_{1.35}$ and CSi-$S_{2.18}$ as shown in Fig. 7a. Indeed, no anti-thrombin activity was observed for the CSi-$S_{0.95}$ sample. The measurement of the anti-Xa activity of the same materials shown in Fig. 7b resulted in a more complicated pattern. Small concentrations of the materials could already cause some general inhibition of the assay which were not concentration dependent for CSi-$S_{0.95}$ and CSi-$S_{1.35}$. A slight concentration-dependent inhibition of factor Xa was found for

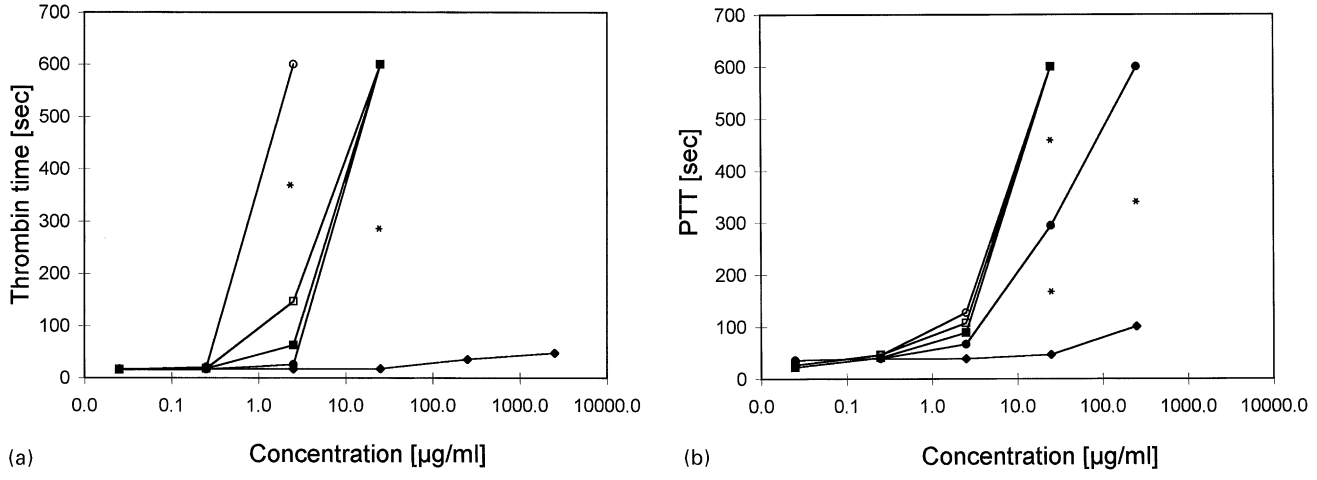

Fig. 4. Thrombin time (a), and partial thromboplastin time (PTT, b) measured in citrate plasma in the presence of increasing concentrations of cellulose sulfates prepared from cellulose acetate (from 0.025 μg/ml up to 2.5 mg/ml) with different degrees of derivatization (DS). (♦)—DS = 0.26; (●)—DS = 0.95; (□)—DS = 1.14; (○)—DS = 1.33; (■)—DS = 1.35. Asterisks in the graph indicate significant differences ($p \leqslant 0.05$).

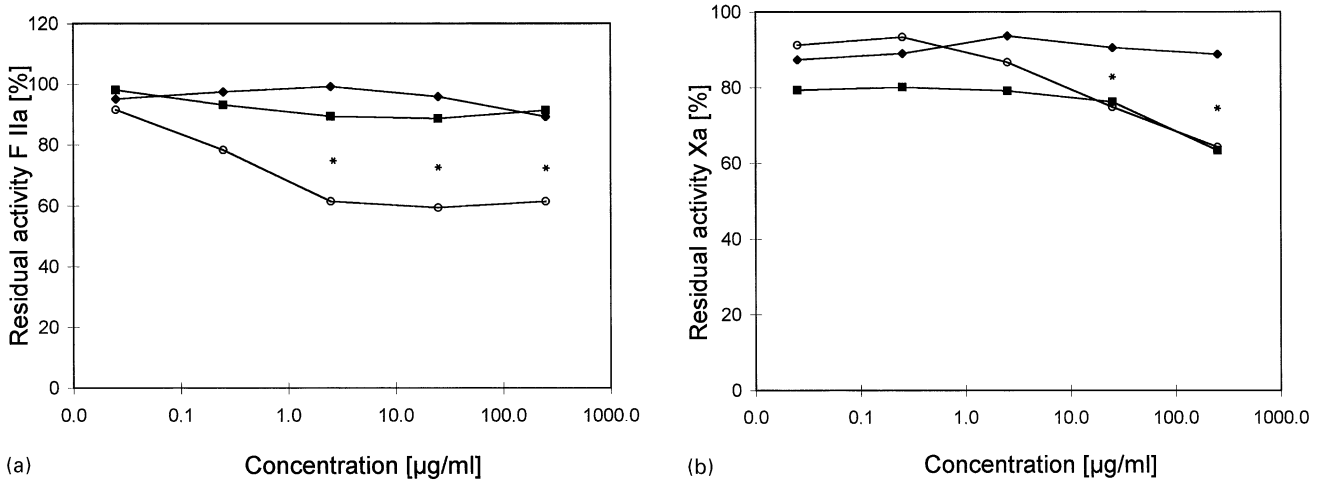

Fig. 5. Residual activity of thrombin (F IIa, a), and factor Xa (F Xa, b) for selected cellulose sulfates prepared from cellulose acetate with different degrees of derivatization (DS). (♦)—DS = 0.26; (○)—DS = 1.33; (■)—DS = 1.35. Asterisks in the graph indicate significant differences ($p \leqslant 0.05$).

Table 2
Sulfate content and substitution pattern of cellulose sulfate synthesized via silyl cellulose

	DS by chemical analysis	DS by ^{13}C-NMR	Substitution pattern of sulfate		
			C2	C3	C6
CSi-$S_{0.95}$	0.98	0.95	0.00	0.00	0.95
CSi-$S_{1.0}$	0.99	1.0	0.35	0.00	0.70
CSi-$S_{1.35}$	1.14	1.35	0.4	0.00	0.95
CSi-$S_{1.5}$	1.74	1.5	0.50	0.20	0.80
CSi-$S_{2.18}$	1.51	2.18	0.88	0.30	1.00

CSi-$S_{2.18}$ indicated by the drop in the residual Xa activity at higher derivative concentrations (above 25 µg/ml). This material actually had the highest DS in the whole study.

3.3. Influence of the overall DS and site of sulfate ester groups on the heparinoid action of derivatives

The general relationship between DS and clotting times is shown in Fig. 8 at a concentration of cellulose derivatives of 2.5 µg/ml. Both clotting times (TT and PTT) increased from the baseline level at a DS of about 1.0 reaching a maximum at a DS of about 1.3. The scattering of the data from different derivatives for the same or similar DS might be attributed to the different distribution of the sulfate half ester groups in the AGU.

Therefore, further investigations were devoted to the influence of the position of the sulfate half ester group on the anticoagulant potential of the cellulose derivatives. Table 3 shows the overall DS and the substitution pattern of sulfate. Fig. 9a compares the thrombin times after addition of cellulose derivatives with a DS = 0.95 where derivatization was carried out predominantly in C2-position (CA-S_{regio}), exclusively in C6-position (CSi-S), or to the same extent in C2-, C3- and C6-position (CA-S_{stat}). It is evident that predominant sulfation in C2-position caused a superior anticoagulant activity compared to C6-position, and statistical derivatization with respect to thrombin time because plasma did not clot in the presence of CA-S_{regio} above a concentration of 2.5 µg/ml. On the other hand, the C3-position seems to play an important role for the partial thromboplastin time as demonstrated in Fig. 9b since CA-S_{regio} had an increased clotting time in comparison with CSi-S.

Further insight into the mechanism of anticoagulant action of the different cellulose sulfate derivatives was obtained by plotting the DS of the different positions (C2, C3, C6) versus the clotting times for CA-S and CSi-S derivatives. Fig. 10 shows that the degree of sulfation in C2-position increased both with thrombin time and partial thromboplastin time showing a dependence of the anticoagulant activity of cellulose sulfates on derivatization in C2-position. However, no correlation was observed between the degree of sulfation in C3-, or C6-position and the clotting times (not shown here).

3.4. Cellulose phosphate (CA-P)

Further investigations were carried out to study the effect of negatively charged substituents other than sulfate on the heparinoid action of cellulose derivatives. For this purpose cellulose acetate was substituted after deacetylation with phosphate groups in C2- and C6-position with a $DS_{phosphate}$ up to 0.96. The distribution of the phosphate groups in the AGU is shown in Table 4. As shown in Table 5 there was no significant prolongation of thrombin time below a $DS_{phosphate}$ of about 1. Only for

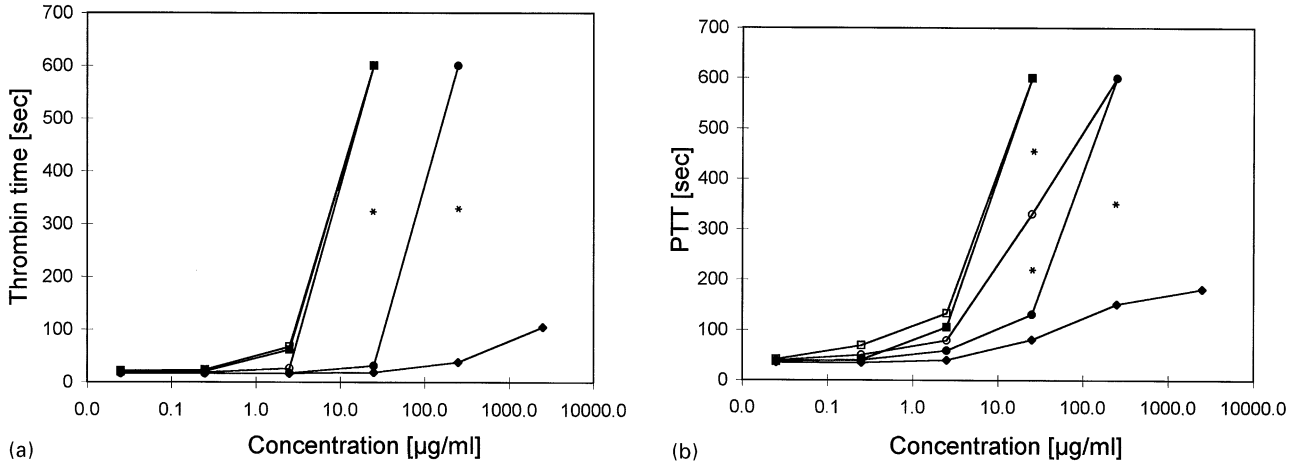

Fig. 6. Thrombin time (a), and partial thromboplastin time (PTT, b) measured in citrate plasma in the presence of increasing concentrations of cellulose sulfates prepared from silyl cellulose (from 0.025 µg/ml up to 2.5 mg/ml) with different degrees of derivatization (DS). (♦)—DS = 0.95; (●)—DS = 1.0; (□)—DS = 1.35; (○)—DS = 1.5; (■)—DS = 2.18. Asterisks in the graph indicate significant differences ($p \leqslant 0.05$).

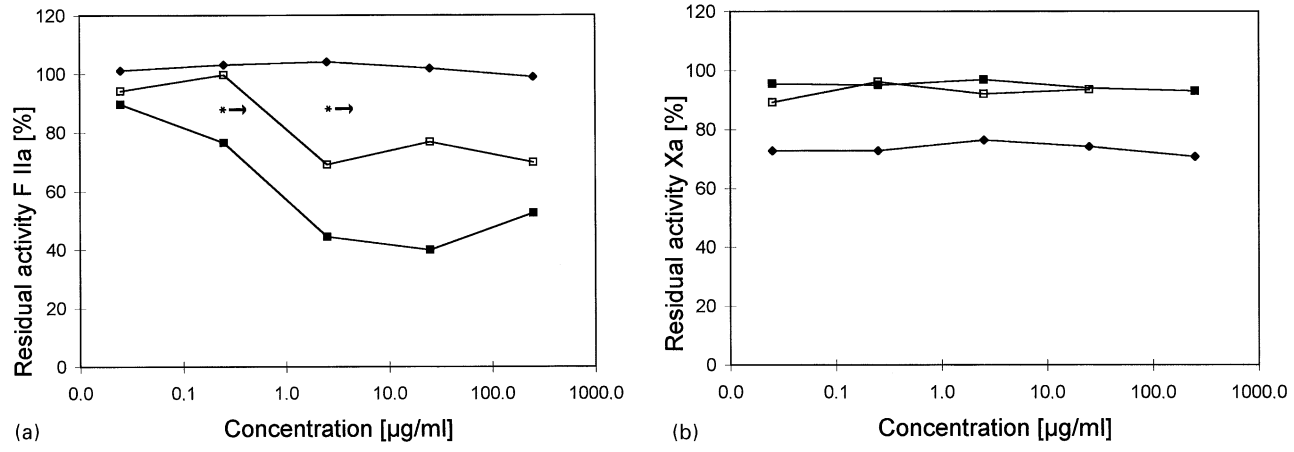

Fig. 7. Residual activity of thrombin (F IIa, a), and factor Xa (F Xa, b) for selected cellulose sulfates prepared from silyl cellulose with different degrees of derivatization (DS). (♦)—DS = 0.95; (□)—DS = 1.35; (■)—DS = 2.18. Asterisks in the graph indicate significant differences ($p \leqslant 0.05$).

$DS_{phosphate} = 0.96$ plasma did not clot at concentrations $\geqslant 250$ µg/ml. The measurement of partial thromboplastin time (see Table 6) yielded some prolongation of clotting time at higher concentrations (2.5 mg/ml) which was much lower than the observed inhibition by CA-S or CSi-S derivatives.

3.5. Cellulose ampholytes

Cationic (2-hydoxylpropyl)-trimethyl ammonium substituents were introduced in low substituted cellulose sulfates to test further the role of charges on the anticoagulant potential of cellulose derivatives. Two different compounds with DS for sulfate groups of 0.45 and 0.25 and DS for quaternary amino groups of 0.23 and 0.53, respectively, were selected. With these compounds it was shown that there was obviously no heparinoid activity. Table 7 shows the result of thrombin time measurements which are similar to partial thrombin time estimates (not shown here) exhibiting that there was no significant prolongation of clotting times in the presence of ampholytic cellulose.

3.6. Low molecular weight (LMW) and non-fractionated heparin

To obtain insight into the mechanism of the activity of cellulose sulfates, F IIa (thrombin) and Xa assays were carried out in the presence of LMW and non-fractionated heparin. It is shown in Fig. 11 that non-fractionated heparin caused a very strong inhibition of F IIa and only little inhibition of F Xa while LMW heparin exhibited stronger anti-Xa activity and less inhibition of thrombin.

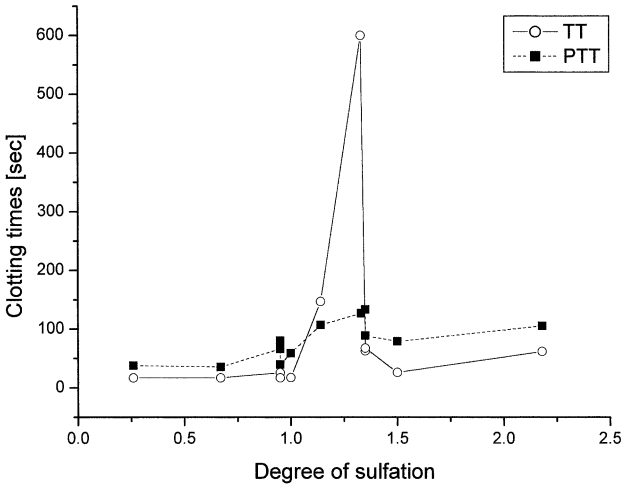

Fig. 8. Thrombin time (○), and partial thromboplastin time (■) plotted versus degree of substitution (DS) of cellulose sulfates at a sample concentration of 2.5 μg/ml.

Table 3
Cellulose sulfates with different substitution patterns but same DS

	DS by chemical analysis	DS by ^{13}C-NMR	Substitution pattern of sulfate		
			C2	C3	C6
CSi-S	0.98	0.95	0.00	0.00	0.95
CA-S_{stat}[a]	0.92	0.95	0.30	0.30	0.35
CA-S_{regio}[b]	0.80	0.95	0.55	0.20	0.20

[a]Statistical derivatization.
[b]Regioselective derivatization.

4. Discussion

In this study we presented a chemistry for regioselective derivatization of cellulose with sulfate or other functional groups. We were able to show that the type and distribution of substituents on cellulose derivatives play a crucial role for the anticoagulant potential of the substances using general clotting assays, such as measurement of thrombin time and partial thromboplastin time. By the application of amidolytic assays for thrombin and factor Xa it was found that cellulose sulfates predominantly substituted in C2-position expressed an anticoagulant potential that seems to be mainly due to anti-thrombin activity. Moreover analysis of the dependence of clotting times on overall DS indicated that sulfation of about 1.5 resulted in the greatest degree of anticoagulation. Sulfated poly- and oligosaccharides with anticoagulant and anti-viral activity have been developed so far based on sulfated dextran, xylan, chitosan, and others (reviewed in [31]). The anticoagulant properties of sulfated polysaccharides have been known for a long time (see for example [32]); however, because of the inherent toxicity of many of these materials they could not enter clinical practice as anticoagulants. More recent investigations tried to highlight the role of substitution sites in cellulose sulfates with regard to clotting of whole blood on foreign surfaces in the presence of these substances [33]. However, no information about the mechanism of anticoagulant action was provided and the process of derivatization did not allow a precise regioselective derivatization. In this and our previous papers [28–30] we introduced regioselective derivatization of cellulose and explored its mode of anticoagulant action.

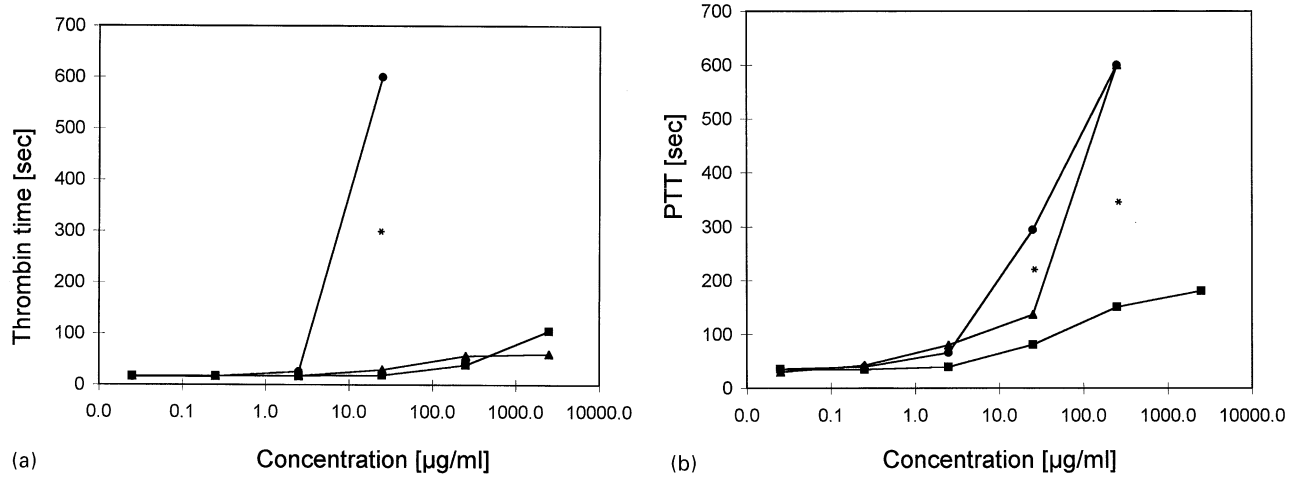

Fig. 9. Thrombin time (a), and partial thromboplastin time (PTT, b) of cellulose sulfates with DS = 0.95, but different sites of substitution: (●)—derivatization predominantly in C2 position; (■)—derivatization only in C6 position, and (◆)—derivatization to the same extent in C2-, C3-, and C6-position. Asterisks in the graph indicate significant differences ($p \leqslant 0.05$).

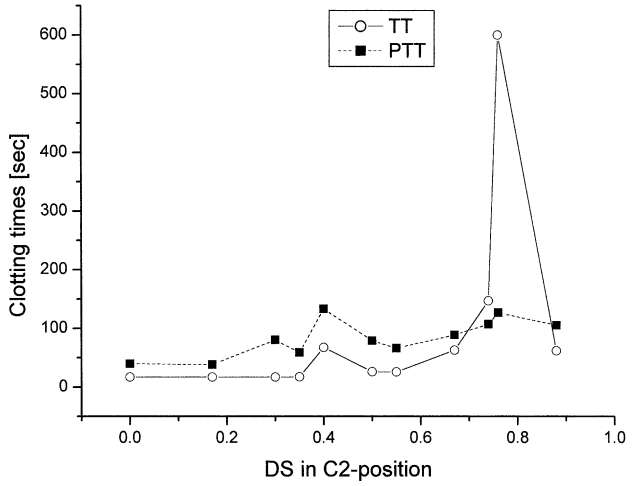

Fig. 10. Thrombin time (○), and partial thromboplastin time (■) plotted versus degree of substitution (DS) at the C2-position of cellulose sulfates at a sample concentration of 2.5 μg/ml.

Table 4
Substitution pattern of cellulose phosphates (CA-P)

	DS by chemical analysis	DS by ^{13}C-NMR	Substitution pattern of phosphate		
			C2	C3	C6
CA-$P_{0.44}$	0.77	0.44	0.11	0.00	0.29
CA-$P_{0.51}$	0.70	0.51	0.23	0.00	0.28
CA-$P_{0.96}$	1.16	0.96	0.77	0.00	0.19

Table 5
Thrombin time as a function of concentration of cellulose phosphates (CA-P_{DS}) with different degrees of derivatization

Con. (μg/ml)	0.025	0.25	2.5	25	250	2500
	Thrombin time in s					
CA-$P_{0.44}$	18.4	18.4	18.4	20.7	35.7	49.4
CA-$P_{0.51}$	20.8	20.0	21.9	24.0	36.3	59.6
CA-$P_{0.96}$	21.4	21.4	25.6	110.5	n.c.[a]	n.c.[a]

[a]No clotting after 10 min.

Table 6
Partial thromboplastin time as a function of concentration of cellulose phosphates (CA-P_{DS}) with different degrees of derivatization

Con. (μg/ml)	0.025	0.25	2.5	25	250	2500
	Partial thromboplastin time in s					
CA-$P_{0.44}$	35.0	35.1	35.7	36.5	45.7	96.5
CA-$P_{0.51}$	36.9	37.6	37.6	39.5	45.7	89.7
CA-$P_{0.96}$	35.0	35.5	36.1	38.6	77.0	360.0

Table 7
Thrombin time as a function of concentration (C) of ampholytic cellulose (CA-SN) with degree of derivatization (DS) for nitrogen

Con. (μg/ml)	0.025	0.25	2.5	25	250	2500
	Thrombin time in s					
CA-$SN_{0.45/0.23}$	18.6	18.6	18.6	18.0	19.6	23.7
CA-$SN_{0.25/0.45}$	19.1	19.1	19.1	17.4	17.5	19.0

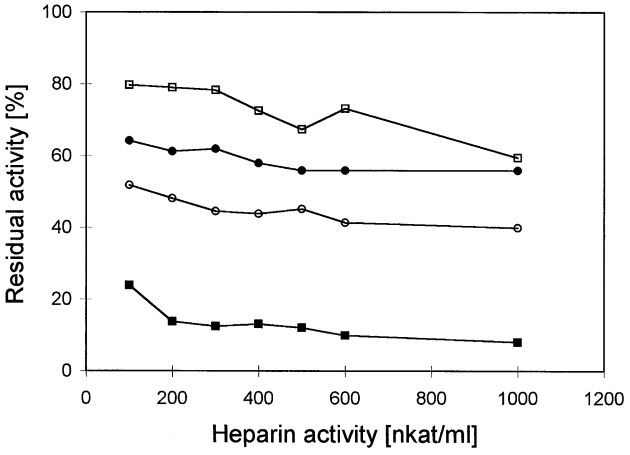

Fig. 11. Residual activity of thrombin (F IIa, black symbols), and factor Xa (F Xa, empty symbols) in dependence on the concentration of fractionated LMW heparin (circles), and unfractionated heparin (squares).

The anticoagulant activity of heparin is due to the interaction with antithrombin III which increases in the affinity for thrombin, but also for other active serine proteases, such as factor Xa [17–20,34]. Heparin has also some direct inhibitory effect on thrombin which accounts for about 2 per cent of the enhancement [34]. The minimal AT III binding sequence in heparin is $GlcNSO_3 6SO_3$–GlcA–$GlcNSO_3 3,6SO_3$–IdoA2SO_3–Gl$cNSO_3 6SO_3$ with Glc as D-glucosamine, GlcA as D-glucuronic, IdoA as L-idouronic [15,35]. The anticoagulant activity of heparin was described to be highly dependent on the presence of sulfate esters in C3-position of GlcN [15,35,36]. However, sulfates in the C2-position of IdoA are also important for the conformation of the polysaccharide chain resulting in a high affinity for AT III [35,37]. In this study we achieved a high anticoagulant activity with a derivatization of cellulose with sulfates predominantly in C2-position. Most of the derivatives had only moderate or no substitution with sulfate

in C3-position. However, by comparison of CA-$S_{1.33}$ with CA-$S_{1.35}$ and CSi-$S_{1.35}$, CSi-$S_{1.5}$ having some sulfate content in C3-position it was evident that derivatization in C2 resulted in a higher anticoagulant potential than sulfation in C3-position. On the other hand, comparison of derivatization in C3- and C6-position revealed that sulfation in C3-position resulted in the expected higher anticoagulant potential. This was evident by a comparison of CA-S_{stat} with CSi-S both having a DS of 0.95 where the latter was only sulphated in C6-position. It can therefore be concluded that derivatization in C6-position has only a minor effect on the anticoagulant potential of cellulose sulfates. The relatively high anticoagulant potential of cellulose sulfates based on silylated cellulose seemed to be therefore based on the content of sulfate in C2-position and some derivatization in C3-position.

Interestingly, the analysis of the relation between thrombin time and partial thromboplastin time with the overall DS in sulfate at a concentration of 2.5 μg/ml resulted in a peak of anticoagulant activity below a DS of 1.5. This was also evident from the graphs in Figs. 4 and 6 showing that a DS of 1.35 resulted in the greatest clotting times. Since optimum activity is a common feature in enzymological observations when enzymes and ligands interact according to a key–lock principle this result indicates specifity of interaction between regioselective derivatized cellulose sulfates and AT III. In fact, such a relationship was described recently by Jozefowicz and Jozefonvicz as biospecifity of randomly functionalized polymers for different biological systems, such as clotting or complement factors, DNA, etc. [38]. The observations in this paper on the anticoagulant activity of cellulose sulfates confirm the J and J principle [38] for a further class of functionalized polymers. While such a biospecifity peak was visible in Fig. 8, it was not possible to obtain such a clear relationship for the DS in C2-position though there was a similar trend which indicated such a dependence.

Interaction between heparin and AT III has a strong electrostatic component which occurs between the negatively charged sulfate residues in heparin and positively charged lysine residues in the allosteric center of AT III [17–20,33,34]. To test if other charged substituents than sulfate may provoke an anticoagulant activity, derivatization with phosphate and quaternary ammonia was performed. Although phosphates as negatively charged substituents expressed some anticoagulant potential it was much lower than that of sulfated cellulose at comparable DS. This is evident by comparison of CA-$P_{0.96}$ and CA-$S_{0.95}$ where the latter had a much higher anticoagulant activity. In contrast, introduction of positively charged substituents, such as quaternary ammonium groups abolished anticoagulant action completely. This underlines the important role of sulfate groups for the heparinoid action of polysaccharides. Evidence for the important role of sulfates can be drawn not only from the chemical structure of heparin and other polysaccharides with anticoagulant activity, but also from increased anticoagulant action after chemical oversulfation of these compounds [24].

Investigations on the mechanism of anticoagulant action of sulfated cellulose were carried out with amidolytic assays for thrombin and factors Xa in the presence of AT III. Experiments with HCII-mediated thrombin inhibition were not carried out although recent papers revealed that other glycoside-bearing polymers may function by exerting anticoagulant action via this pathway [39]. For both CA-S and CSi-S with higher DS a clear concentration-dependent inhibition of thrombin activity was found. Results of experiments with factor Xa did not show such a clear relationship although CA-S with high DS caused some inhibition of factor Xa activity. It was also observed that most derivatives caused a general inhibition of the factor Xa assay which was probably overlapping concentration effects. Overall, it might be concluded that the cellulose sulfates synthesized in this study have a higher anticoagulant activity towards thrombin than factor Xa. To further explore the possible mode of action and the applicability of the amidolytic assays used in this study comparative experiments with non-fractionated and LMW heparin have been carried out. There it was found that in the presence of AT III non-fractionated heparin had a superior inhibiting effect on thrombin and LMW heparin on factor Xa which is also in agreement with general findings about the activity of different heparins [40]. Thus, the proposed mechanism of anticoagulant action of the cellulose sulfates predominantly derivatized in C2-position could be similar to non-fractionated heparin building a ternary complex between AT III and thrombin [19–24,34,35].

There are a number of attempts to improve the hemocompatibility of dialysis membranes based on cellulose by the covalent immobilisation of heparin [12,13,41]. This could allow a reduced anticoagulation with heparin during hemodialysis and would diminish undesirable side effects. Unfortunately, covalent binding of heparin negatively influenced the permeability of membranes [13]. Possible applications for the cellulose sulfates with high anticoagulant activity as prepared in this study could be their use as blends with cellulose prior to membrane formation or for grafting material surfaces by covalent attachment improving the hemocompatibility of dialysis membranes or other biomaterials.

Acknowledgements

This work was supported by BMBF, Grant No. BEO 22-0310375A. The technical assistance of Mrs. Schenker and Ruth Hesse is gratefully acknowledged. We are indebted to Prof. Philipp for helpful discussions.

References

[1] Henderson LW, Cheung AK, Chenoweth DE. Choosing a membrane. Am J Kidney Dis 1983;3:5–20.

[2] Putz D, Barnas U, Luger A, Mayer G, Woloszuk W, Graf H. Biocompatibility of high-flux membranes. Int J Artif Organs 1992;15:456–560.

[3] Johnson RJ. Complement activation during extracorporal therapy: biochemistry, cell biology and clinical relevance. Nephrol Dial Transplant 1994;9(Suppl 2):36–45.

[4] Parnes EL, Shapiro WB. Anaphylactoid reactions in hemodialysis patients treated with the AN 69S dialyser. Kidney Int 1991;40:1148–52.

[5] Bonomini V, Coli L, Feliciangeli G, Mosconi G, Scolari MP. Long-term results: cellulosic vs. synthetic membranes. Contrib Nephrol 1995;113:120–34.

[6] Klinkmann H, Vienken J. Membranes for dialysis. Nephrol Dial Transplant 1995;10(Suppl 3):39–45.

[7] von Sengbusch G, Bowry S, Vienken J. Focusing on Membranes. Artif Organs 1992;17:244–53.

[8] Courtney JM, Lamba NMK, Sundaram S, Forbes CD. Biomaterials for blood-contacting applications. Biomaterials 1994; 15:737–44.

[9] Lindhout T. Biocompatibility of extracorporal blood treatment. Selection of haemostatic parameters. Nephrol Dial Transplant 1994;9(Suppl 2):83–9.

[10] Vanholder R. Biocompatibility issues in hemodialysis. Clin Mater 1992;10:87–133.

[11] Lazarus JM. Complications of hemodialysis. Kidney Int 1980; 18:783–96.

[12] Shiomo T, Satoh M, Miya M, Imai K, Akasu H, Othake K. Binding of heparin onto ethylene-vinyl alcohol copolymer membrane. J Biomed Mater Res 1988;22:269–80.

[13] Hinrichs WLJ, ten Hopen HW, Engbers GH, Feijen J. In vitro evaluation of heparinized Cuprophan hemodialysis membranes. J Biomed Mater Res 1997;35:443–50.

[14] Eloy R, Belleville J, Paul J, Pusineri C, Baguet J, Rissoan M-C, Cathignol D, Ffrench P, Ville D, Tartullleri M. Thromboresistance of bulk heparinized catheters in human. Thromb Res 1987;45:223–33.

[15] Josefonvicz J, Jozefowicz M. Interactions of biospecific functional polymers with blood proteins and cells. J Biomater Sci Polym Edn 1990;1:147–66.

[16] Seifert B, Romaniuk P, Groth Th. Bioresorbable, heparinized polymers for stent coating: in vitro studies on heparinization efficiency, maintainance of anticoagulant properties and improvement of stent haemocompatibility. J Mater Sci Mater Med 1996;7:465–9.

[17] Lindahl U, Kjellén L. Heparin or heparan sulfate—what is the difference? Thromb Haemostas 1991;66:44–8.

[18] Choay J. Chemically synthesized heparin-derived oligosaccharides. Ann N Y Acad Sci 1989;556:61–74.

[19] Choay J, Petitou M, Lormeau JC, Sinay P, Casu B, Gatti G. Structure-activity relationship in heparin: a synthetic pentasaccharide with high affinity for antithrombin III and eliciting high anti-factor Xa activity. Biochem Biophys Res Commun 1983; 116:492–9.

[20] Atha DH, Lormeau JC, Petitou M, Rosenberg RD, Choay J. Contribution of 3-O- and 6-O-sulfated glucosamine residues in the heparin-induced change in antithrombin III. Biochemistry 1987;23:6454–61.

[21] Danielsson A, Raub E, Lindahl U, Björk I. Role of ternary complexes, in which heparin binds both antithrombin and proteinase, in the acceleration of the reactions between antithrombin and thrombin or factor Xa. J Biol Chem 1986;261:15467–73.

[22] Carrell RW, Christey PB, Boswell DR. Serpins: antithrombin and other inhibitors of coagulation and fibrinolysis. Evidence from amino acid sequences. In: Verstraete M, Vermylen J, Lijnen R, Arnout J, editors. Thrombosis and haemostasis. Leuven: Leuven University Press, 1987. p. 1–15.

[23] Hurst RE, Menter JM, West SS, Settine JM, Coyne EH. Structural basis for anticoagulant activity of heparin. 1. Relationship to the number of charged groups. Biochemistry 1979;18: 4283–7.

[24] Schoen P, Wielders S, Petitou M, Lindhout T. The effect of sulfation on the anticoagulant and antithrombin III-binding properties of a heparin fraction with low affinity for antithrombin III. Thromb Res 1990;57:415–23.

[25] Hatanaka K, Yoshida T, Miyahara S, Sato T, Ono F, Uryu T, Kuzuhara H. Synthesis of new heparinoids with high anticoagulant activity. J Med Chem 1987;30:810–5.

[26] Hatanaka K, Hirobe T, Yoshida T, Yamanaka M, Uyru T. Synthesis and sulfation of branched dextrans. Polym J 1990;22:435–41.

[27] Rhodes NP, Williams DF. Plasma recalcification as a measure of contact phase activation and heparinization efficiacy after contact with biomaterials. Biomaterials 1994;15:35–7.

[28] Phillip B, Klemm D, Wagenknecht W. Regioselektive Veresterung und Veretherung von Cellulosederivaten. Das Papier 1995;28(2):58–64.

[29] Wagenknecht W, Nehls I, Stein A, Klemm D, Phillip B. Synthesis and substituent distribution of Na-cellulose sulfates via O-trimethylsilyl cellulose as intermediate. Acta Polym 1992;43: 266–9.

[30] Wagenknecht W, Nehls I, Phillip B. Studies on the regioselectivity of cellulose sulfation in the N_2O_4-N,N-dimethlyformamide cellulose system. Carbohydr Res 1993;240:245–52.

[31] Uryu T. Artificial polysaccharides and their biological activities. Prog Polym Sci 1993;18:717–61.

[32] Husemann E, Pfannemüller B, Schill H, Hertlein W. Über die blutgerinnungs-hemmende Wirkung und Speicherung von Amylose-Schwefelsäureestern. Z Naturforsch 1957;12:427–33.

[33] Okajima K, Kamide K, Matsui T. Cellulose sulfate having anticoagulant action and process for preparing same. European Patent Application 1982, Publication No. 0053473, 39pp.

[34] Rosenberg RD. Role of heparin and heparinlike molcules in thrombosis and atherosclerosis. Fed Proc 1985;44:404–9.

[35] Casu B. Protein-binding domains of heparin and other sufated glycosaminoglycans. Carbohydrates in Europe 1994. p. 18–21.

[36] Razi N, Lindahl U. Biosynthesis of heparin/heparan sulfate. The D-glucosaminyl 3-O-sulfotransferase reaction: target and inhibitor saccharides. J Biol Chem 1995;270:11267–75.

[37] Cros S, Petitou M, Sizun P, Perez S, Imberty A. Combined NMR and molcular modelling study of an ioduronicacid-containing trisaccharide related to antithrombotic heparin fragments. Bioorg Med Chem 1997;5:1301–9.

[38] Jozefowicz J. Jozefonvicz, Randomness, biospecifity: random copolymers are capable of biospecific molcular recognition in living systems. Biomaterials 1997;18:1633–43.

[39] Onishi M, Miyashita Y, Motomura T, Yamashita S, Sakamoto N, Akashi M. Anticoagulant and antiprotease activities of a heparinoid sulfated glucoside-bearing polymer. J Biomater Sci Polym Edn 1998;9:973–84.

[40] Stiekema JCJ. Heparin and its biocompatibility. Clin Nephrol 1986;1:3–8.

[41] Erdtmann M, Keller R, Baumann H. Photochemical immobilization of heparin, dermatan sulfate, dextran sulfate and endothelial cell surface heparan sulfate onto cellulose membranes for the preparation of athrombogenic and antithrombogenic polymers. Biomaterials 1994;15:1043–8.

Publikation 14

Barbara Seifert, Thomas Groth, Kerstin Herrmann, Paul Romaniuk (1995).

Immobilisation of heparin on polylactide for application to degradable biomaterials in contact with blood.

Journal of Biomaterials Science – Polymer Edition **7**, 277-287.

J. Biomater. Sci. Polymer Edn, Vol. 7, No. 3, pp. 277–287 (1995)

Immobilization of heparin on polylactide for application to degradable biomaterials in contact with blood

B. SEIFERT[1], TH. GROTH[2]*, K. HERRMANN[2] and P. ROMANIUK[1]

[1]*Institute of Roentgendiagnostics, Department of Interventional Radiology,*
[2]*Biomaterials Research Unit, School of Medicine (Charité), Humboldt University Berlin, Schumannstrasse 20/21, 10098 Berlin, Germany*

Received 10 November 1994; accepted 8 December 1994.

Abstract—The poly-(D, L-lactide) RESOMER® R208 (Boehringer-Ingelheim, Germany) was modified with heparin to improve the blood contacting properties of the material. The immobilization of herapin was carried out by covalent binding with glutaraldehyde as the coupling agent. The reaction conditions, such as temperature and time, were varied to optimize the binding of herapin. The efficiency of the immobilization was monitored with respect to the total amount of coupled herapin with a toluidine blue assay and the anticoagulant activity of immobilized heparin with a factor Xa assay. The hemocompatibility of the modified polylactide was estimated after blood-material contact by the activation of platelets measured with an enzyme immuno assay for GMP140. Immobilization at ambient temperature and a reaction time of 2 h resulted in maximal heparin binding, high anticoagulant activity, and low thrombogenicity. Since the remaining unsaturated aldehyde groups of the coupling agent may cause a low hemocompatibility of the material, washing of the heparinized polylactide was carried out with ethanol. However, it was shown that washing diminished the anticoagulant activity of heparin and increased the thrombogenicity. The prolonged storage of heparinized polylactide in phosphate buffered saline for 8 days demonstrated that small quantities of herapin were released but the hemocompatibility was further improved, indicated by an increasing anticoagulant potential and a decrease in platelet activiation with incubation time. A comparison of polylactide, heparinized polylactide, polypropylene, and Pellethane® with respect to platelet activation by GMP140 assay and scanning electron microscopy, revealed that the heparinization of polylactide substantially improved the hemocompatibility of RESOMER® R208, making the material comparable to Pellethane®.

Key words: Polylactide; heparin immobilization; toluidine blue assay, factor Xa assay, platelet activation.

INTRODUCTION

Aliphatic polyesters of α-hydroxy acid derivatives like polyglycolic acid or polylactic acid are biodegradable and bioresorbable materials [1]. *In vivo*, they are cleaved by hydrolytic deesterification into glycolic and lactic acid, respectively, during time periods of up to several months. The degradation products are incorporated into metabolic pathways and excreted as water and carbon dioxide. Thus these materials do not remain in the body as foreign materials over a long time period [2]. Because of the biocompatibility, degradability and mechanical properties, polylactides are predominantly used for hard tissue replacement such as rods, screws, and plates in bone restoration, as artificial tendons, in drug delivery systems, or as suture material [3,4].

The biocompatibility of polylactides *in vitro* was investigated by cell proliferation studies in contact with these materials [5, 6]. Although polylactide monomers that might

* To whom correspondence should be addressed at: GKSS Forschungszentrum Geesthacht GmbH, Abt. Membranforschung, Kantstrasse 55, 14513 Teltow-Seehof, Germany.

be released during degradation may possess a certain cytotoxic potential [7], the biocompatibility of polylactides *in vivo* was found to be good [1, 8, 9]. So far, little is known about the blood contacting properties of polylactides. Despite good biocompatibility in contact with bone and other tissue, the hemocompatibility of polylactides might be low. It is well known that the physicochemical properties of the biomaterial surface such as chemical composition, surface free energy, surface charge, and surface structure including polymer chain mobility, porosity, and roughness rule the interaction with the plasma proteins and blood cells [10]. One possible complication during blood–biomaterial contact is the activation of the intrinsic system of the clotting cascade leading finally to fibrin polymerization and thrombus formation [11, 12]. On the other hand, platelet adhesion and activation occur predominantly after deposition of fibrinogen and other attachment proteins and may also lead to the development of a thrombus on the material surface [13, 14]. Since many polymeric materials possess a certain thrombogenic potential it cannot be ruled out that polylactides in contact with flowing blood may cause thrombus formation and embolism.

An improvement of the performance of biomaterials in contact with blood can be achieved by the immobilization of physiologically active substances such as heparin via covalent binding [15–17]. Heparin is a linear polysaccharide composed of repeating units of uronic acid and D-glucosamine. Due to its unique structure and surface charge distribution, heparin is able to interact with several different proteins such as blood-clotting factors and human serum lipoproteins [18]. The action of immobilized heparin can be directed vs the clotting cascade by an enchancement of the effect of antithrombin III and the prevention of platelet activation. The antithrombin III–heparin complex predominantly inhibits the activity of factor Xa and thrombin [19–21].

It was the aim of this study to develop a biodegradable material with improved hemocompatibility on the base of polylactide and heparin with glutaraldehyde (GA) as the coupling agent. It was therefore investigated how the reaction conditions influenced the quantities of attached heparin on the polylactide and its anticoagulant potential. The hemocompatibility of different samples was evaluated by testing the activation of platelets on the polymer surface.

MATERIALS AND METHODS

Polylactide sheets and reference materials

A commercial poly-(D, L-lactide) (RESOMER® R208; Boehringer-Ingelheim, Germany) was selected as the material for the immobilization of heparin. Cast sheets of the polymer were prepared from a 5% solution of poly-(D, L-lactide) dissolved in chloroform after evaporation of the solvent. The reference materials polypropylene and Pellethane® 2363-80 AE were kindly supplied by Dr. W. Lemm (Free University Berlin, Klinikum Charlottenburg), the coordinator of the EUROBIOMAT research program of the European Communities.

Heparin immobilization

The immobilization of heparin was carried out using porcine mucosa heparin (Serva Biochemistry, Germany, 174 I U mg^{-1} with GA (Sigma, USA) as the coupling agent using a modification of the method of Peppas and Merrill [22]. A mixture of 12% aqueous solution of heparin and 6% aqueous solution of GA (1:1) adjusted with 0.1 M sulphuric

acid to pH 5.2 was incubated with the polymer sheets for the time and at the temperature indicated. The polymer sheets were then washed thoroughly with distilled water.

Toluidine blue assay

The estimation of the total amount of surface immobilized heparin was measured by a modified toluidine blue colorimetric method [23]. The method was performed incubating polymer sheets of 1 cm^2 into 0.5 ml phosphate buffered saline (PBS) (140 mM NaCl, 10 mM Na_2HPO_4, pH 7.4) and 0.5 ml 0.005% aqueous toluidine blue solution (TB) (Sigma, USA). After shaking the vials for 5 min, 1 ml hexane was added. After mixing for 30 s, separation of hexane and the aqueous phase followed. TB and bound heparin formed a complex at the polymer surface and as a result, a decolorization of the aqueous phase took place. The optical density (O.D.) of the aqueous phase was measured at 631 nm (SPEKOL 220, Carl Zeiss Jena, Germany). The amount of coupled heparin was then quantified by comparison with a standard curve of known concentrations of heparin and given in IU cm^{-2}.

Factor Xa assay

Since covalently immobilized heparin may not be completely anticoagulant-active control of the biological function of heparin is necessary. For this purpose a factor Xa chromogenic assay was developed that measures the anticoagulant effect of heparin via antithrombin III (AT III) on the inhibition of factor Xa. Polymer sheets (diameter 11 mm) were incubated in 0.075 ml AT III (0.04 IU ml^{-1}) for 5 min. Factor Xa (0.3 ml, 0.32 IU ml^{-1}) was then added and the mixture incubated for 5 min. Thereafter, the chromogenic substrate S-2222 (0.3 ml, 0.55 mM, Haemochrom Diagnostica, Germany) was added. The hydrolysis of S-2222 was stopped with 0.3 ml 20% acetic acid after 2 min. The resulting chromophore was measured spectrophotometrically at 405 nm (SPEKOL 220, Carl Zeiss Jena, Germany). A comparison with a standard of known activities of heparin was used to estimate the amount of immobilized biologically-active heparin per surface area.

Enzyme immuno assay for GMP140

Adhesion and subsequent activation of platelets on biomaterials result from the undesired interactions between blood and biomaterials. To test the potential thrombogenicity of the different materials, the platelet activation was monitored by the presence of GMP140 on the platelet membrane. For this purpose a recently developed enzyme immuno assay (EIA) for GMP140 was applied [24, 25]. Briefly, after 30 min contact of platelet rich plasma with the materials, the amount of GMP140 was estimated using the monoclonal mouse antibody CD 62 (Immunotech S.A., France) and the polyclonal sheep anti-mouse IgG peroxidase conjugated antibody (Sigma Immuno Chemicals, St. Louis, USA). *O*-phenylene diamine and a 1:1 mixture of 2 M H_2SO_4 and 0.1 M Na_2SO_3 were used as the chromogenic substrate and stopping reagent, respectively. Aliquots of the substrate were measured at 492 nm (Anthos Plate Reader, Austria). The measured O.D. refers to the degree of platelet activation, i.e. a low O.D. indicates a low activation of platelets.

Scanning electron microscopy

To investigate the number and morphology of adhering platelets on the different materials, qualitatively scanning electron microscopy was used. Sheets of the materials were placed

in an adhesion chamber and incubated with platelet-rich plasma for 30 min. After that the materials were washed with PBS and fixed in 2% glutaraldehyde solution in PBS at 4°C for 24 h. The samples were then dehydrated in rising ethanol concentrations and air dried. After sputtering with gold the samples were examined with a scanning electron microscope Leica S 360 (Leica Cambridge Ltd., UK).

RESULTS

First, it was investigated how the duration of the immobilization procedure influences the binding of heparin and its biological function. It was found that the overall binding of heparin to the RESOMER® R208 measured with TB was maximum at 2 h (see Fig. 1). However the anticoagulant activity and the activiation of platelets were not significantly different for 1, 2, or 3 h reaction time (data not shown). All further immobilization procedures were carried out over a 2-h reaction time.

The temperature of the reaction was a second parameter of heparin immobilization. Figure 2a demonstrates that the total binding of heparin to the RESOMER® R208 was significantly higher at 37°C in comparison to the ambient temperature (AT) (22°C) or 50°C ($p \leq 0.05$, t-test). However, if the anticoagulant potential of the immobilized heparin was tested with the factor Xa assay (see Fig. 2b), the activity decreased significantly from 22 > 37 > 50°C (≤ 0.05, t-test). Also, the thrombogenicity indicated by the presence of GMP140 shown in Fig. 2c increased with the reaction temperature and was significantly lower at 22°C ($p \leq 0.05$, t-test). Thus, all further experiments were carried out with polylactide heparinized at the AT for 2 h.

The modified polylactide was washed and stabilized with ethanol (80% aqueous solution) to try to eliminate possibly-existing thrombogenic aldehyde groups at the polymer surface after heparin immobilization with GA. It is shown in Table 1 that washing with ethanol resulted in a significant reduction of total heparin content ($p \leq 0.05$, t-test) whilst the anticoagulant activity did not change significantly. In contrast, a decreasing hemocompatibility was observed after washing with ethanol, indicated by a significant increase of platelet activation measured by the GMP140 assay ($p \leq 0.05$, t-test).

The hemocompatibility of non-modified and heparin-modified RESOMER® R208 was compared with two reference materials: polypropylene and Pellethane®. Figure 3 shows

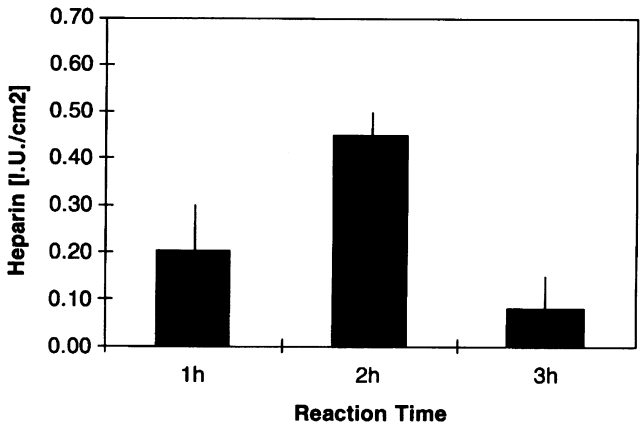

Figure 1. Total content of immobilized heparin on RESOMER® R208 with respect to reaction time measured by the toluidine blue assay (means ± S.E.M., $n = 5$).

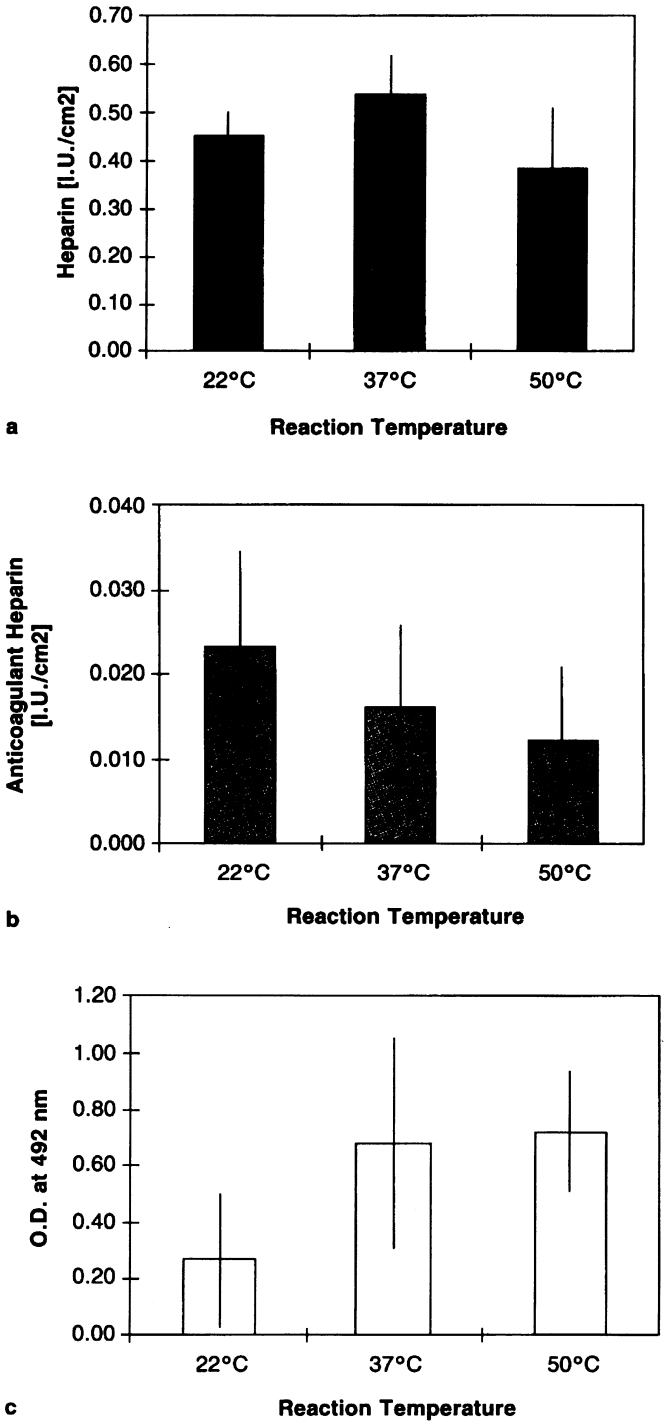

Figure 2. (a) Total heparin content, (b) anticoagulant activity of immobilized heparin, and (c) hemocompatibility of heparin-modified RESOMER® R208 with respect to reaction temperature (means ± S.E.M., $n = 5$).

Table 1.
Total heparin content, anticoagulant activity of immobilized heparin, and hemocompatibility of heparin-modified RESOMER® R208 after washing with ethanol (means ± S.E.M., $n = 5$)

	Total heparin content Toluidine blue assay (IU cm^{-2})	Anticoagulant active heparin Factor Xa assay (IU cm^{-2})	Hemocompatibility GMP140 assay (O.D. at 492 nm)
distilled water	0.44 ± 0.24	0.023 ± 0.012	0.27 ± 0.20
1 h ethanol	0.18 ± 0.10	0.020 ± 0.018	0.58 ± 0.13

the results of these experiments. The pure R208 seemed to be more hemocompatible than polypropylene and less than Pellethane®, indicated by the results of the GMP140 assay. However, the hemocompatibility of R208 was substantially improved after binding of heparin, indicated by the low platelet activation on this surface. In Fig. 4, the scanning electron microscope images of platelets on the reference materials and the non-modified and heparinized RESOMER® R208 are shown. On the more thrombogenic materials, polypropylene (Figure. 4a) and non-modified polylactide (Fig. 4b), a high number of platelets were adhered and activated. It is shown that most of the adhering platelets were completely spread although the extent of surface coverage was smaller on R208. To a certain extent the aggregation of platelets was observed. In contrast to these materials, Pellethane® showed only a moderate adhesion of platelets (Fig. 4c). Further, platelets were still in the early phases of activation indicated by the start of pseudopodia formation. The heparin-modified R208 (Fig. 4d) showed the smallest extent of platelet adhesion with almost no pseudopodia formation. Spreading of platelets was not observed.

The permanence of immobilized heparin on the polyactide surface was studied by incubating samples in PBS at AT for 1–8 days. The system was placed in an orbital shaker to prevent concentration gradients and the supernatant changed at defined intervals. The following quantities were estimated: the amount of heparin released into the supernatant (Fig. 5a); the surface concentration of heparin measured by TB (Fig. 5b); the anticoagulant activity by the factor Xa assay (Fig. 5c); and the thrombogenicity by the GMP140 assay (Fig. 5d). In Fig. 5a it is shown that decreasing amounts of heparin were released into the supernatant for up to 7 days. After 8 days an increase of the released heparin was observed. Accordingly, the amount of detectable heparin on th polylactide surface, measured by

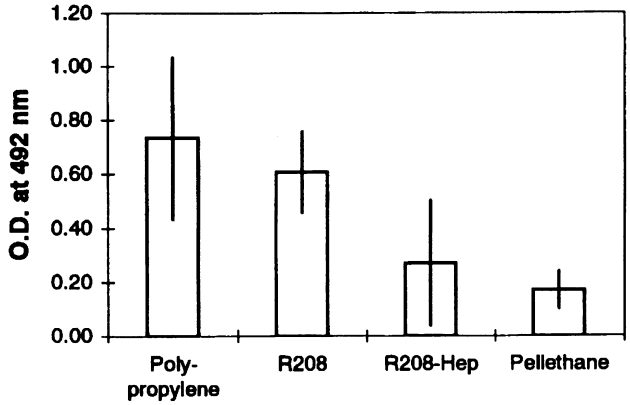

Figure 3. Comparison of platelet activation on polypropylene, Pellethane®, and non-modified and heparin-modified RESOMER® R208 (2 h, 22°C) measured by GMP140 assay (means ± S.E.M., $n = 5$).

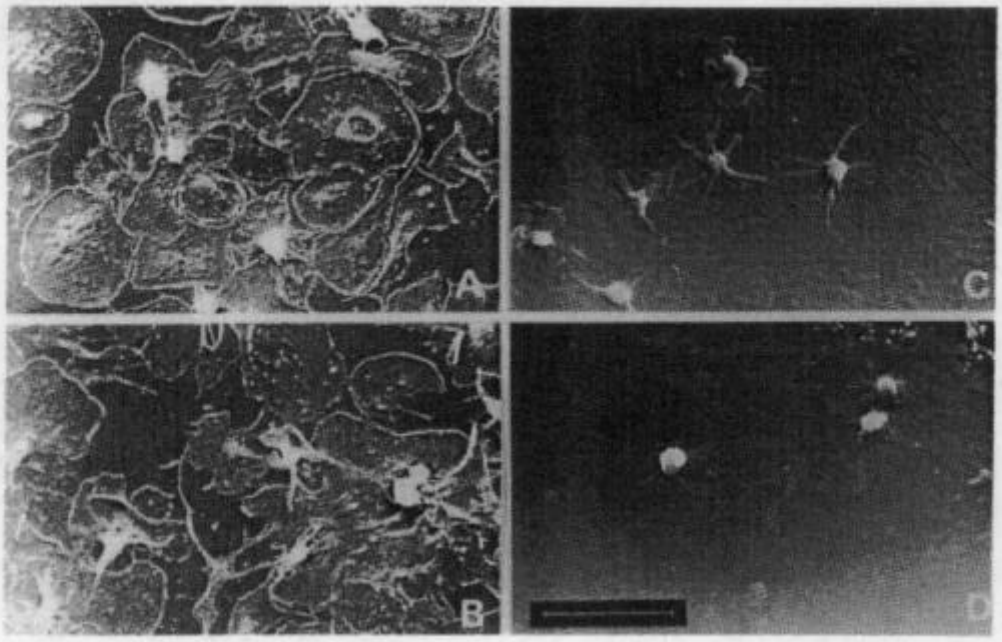

Figure 4. Scanning electron microscope images of: (a) polypropylene; (b) non-modified RESOMER® R208; (c) Pellethane®; and (d) heparin-modified R208 (2 h, 22°C) after contact with platelet rich plasma for 30 min (bar: 10 μm).

TB, decreased with incubation time (Fig. 5b). In contrast to these results the anticoagulant potential (Fig. 5c) and the hemocompatibility (Fig. 5d) improved with incubation time.

DISCUSSION

It was shown in this study that an improvement in hemocompatibility of RESOMER® R208 can be achieved by the covalent binding of heparin. An immobilization product with maximum binding of heparin and good hemocompatibility was obtained after 2 h heparinization at the AT. In the case of RESOMER® R208 a total heparin content of about 0.5 IU cm^{-2} or 2.9 µg cm^{-2}, respectively, was achieved.

After the increase of heparin binding with a rise in reaction temperature from the AT to 37°C, a further temperature increase from 37 to 50°C resulted in a decrease of immobilized heparin. A possible reason is that at temperatures near the glass transition temperature of the polylactide RESOMER® R208 (T_G ~ 50°C), rearrangement of macromolecule chains in the polymer decreased the concentration of polarizable groups on the polymer surface [26]. In contrast to the overall binding of heparin, the anticoagulant potential and the hemocompatibility decreased with an increase of the reaction temperature. It seems to be reasonable that the rise in reaction temperature might increase the efficiency of the coupling reaction of GA and heparin [22], resulting in a multi-point attachment of the heparin molecule inhibiting the biological function of heparin [19]. Moreover it is probable that cross-linking of heparin by GA occurs to a certain degree, diminishing the biological activity of bound heparin. Therefore, the availability of free essential functional groups of heparin and the flexibility of the heparin molecule itself may be reduced. This decrease in flexibility may negatively influence the interaction of heparin with ATIII, thrombin, and

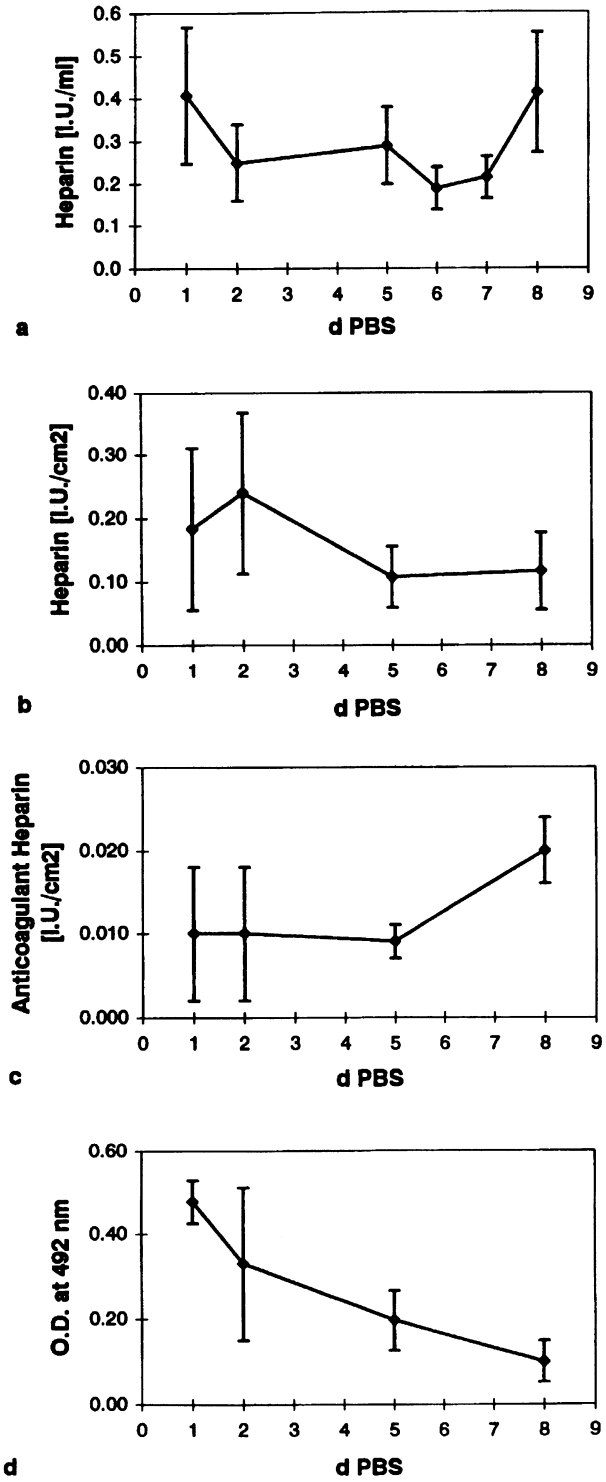

Figure 5. Total heparin content of: (a) supernatant; (b) polymer sheet; (c) anticoagulant activity of immobilized heparin; and (d) hemocompatibility of heparin-modified RESOMER® R208 after incubation with phosphate buffered saline up to 8 days (means ± S.E.M., $n = 5$).

platelets [20]. To promote the binding of non-cross-linked heparin, this substance was added to the reaction mixture in excess.

Surprisingly, washing of heparinized RESOMER® R208 with ethanol did not improve the hemocompatibility of the heparinized polylactides. The washing procedure was supposed to reduce any remaining unsaturated aldehyde groups that might possess a certain thrombogenic potential. However, it was found that the washing procedure with ethanol reduced the total heparin content. Nevertheless, although the content of anticoagulant active herapin was obviously not changed, the hemocompatibility was impaired. Therefore, washing of the heparinized polylactides with ethanol, as suggested by Peppas and Merrill [22], was not further carried out.

The permanence of immobilized heparin and its anticoagulant properties on the RESOMER® R208 surface studied in contact with a fluid (PBS) for up to 8 days was good. The heparin was gradually released into the fluid and might be physiologically active in the blood stream. It was concluded from this result that apart from covalent binding heparin was also immobilized by simple physical adsorption or entrapment into the polymer matrix. This is also in accordance with the results of Peppas and Merrill [22], who found that there was about one fifth on initial heparin content present on the polymer surface after elution of heparinized polymer for 4 days. On the other hand the significant increase of the heparin release after 8 days might be connected not only with a breakdown of acetal bridges at the spacer molecules, but also with the beginning of the degradation of the polylactide surface. The observed increased anticoagulant activity (factor Xa assay) and improved hemocompatibility (GMP140 assay) also indicate that degradation of polylactide RESOMER® R208 has actually been started [27–30]. During this process the molecular weight of the polylactide chains first decreases [27] which might lead to a better molecular mobility of the heparin molecules still attached. The polylactide chain might act as a 'spacer', thus leading to better anticoagulant and non-thrombogenic properties as known from other papers [20]. This is in accordance with the assumption that the action of heparin platelet adhesion is mainly due to the steric repulsion excerted by the heparin molecule itself [21]. Moreover, the results of the elution experiments suggest that the hemocompatibility of the heparinized polylactide surface *in vivo* may improve during prolonged blood–material contact. Both the release of adsorbed heparin and reactivation of covalently bound heparin by the break-down of acetal bridges or polymer degradation may lead to better blood contacting properties of the biomaterials during a possible application, preventing platelet activation and thrombus formation.

The comparison of non-modified and heparinized RESOMER® R208 with two reference materials demonstrated that the pure polylactide R208 has a comparable hemocompatibility to other blood contacting materials (e.g., polypropylene). Moreover, it was shown by quantitative analysis via the cell-EIA for GMP140 and qualitative analysis via scanning electron microscopy that the heparinized product of RESOMER® R208 has excellent blood contacting properties.

Heparinized polylactides might be applied in the cardivascular system for the construction of artificial vessels or intravascular stents. Vascular prosthesis should possess a certain porosity in order to develop the ingrowth of vascularized perigraft tissue and endothelial cells [31]. The application of biodegradable polymers as one material of a two-component prosthesis may produce an increasing mural porosity with prolonged application [32]. As a result, the loss of blood may be minimized and the healing properties improved. The use of intravascular stents is often complicated by thrombus formation and vascular restenosis from after a few weeks up to 3 months [33]. The process of restenosis is mainly attributed

to the myointimal hyperplasia as well as thrombus formation where platelets may also contribute due to the release of platelet derived growth factors (PDGF), thrombin, and other compounds [33, 34]. This event does not occur after the complete ingrowth of the stent, usually made of metal alloys [34]. Therefore, the coating of a stent with biodegradable material such as polylactide may improve the biocompatibility of metal stents maintaining the necessary mechanical propertied thus preventing thrombus formation and decreasing possible restenosis.

Acknowledgements

This work is partially supported by the Bundesministerium für Forschung und Technologie, Germany (Grant Nr. FKZ 01ZZ9101) and the School of Medicine (Charité) at Humboldt University, Berlin.

REFERENCES

1. M. Vert, S. M. Li, G. Spenlehauer and P. Guerin, *J. Mater. Sci. Mater. Med.* **3**, 432 (1992).
2. R. K. Kulkarni, K. C. Pani, C. Neumann and F. Leonhard, *Arch. Surg.* **93**, 839 (1966).
3. P. U. Rokkanen, *Ann. Med.* **23**, 109 (1991).
4. O. Laitinen, I. Alitalo, T. Toivonen, J. Vasenius, P. Törmälä and S. Vainionpää, *J. Mater. Sci. Mater. Med.* **4**, 547 (1993).
5. A. van Sliedregt, A. M. Radder, K. De Groot and C. A. van Blitterswijk, *J. Mater. Sci. Mater. Med.* **3**, 365 (1992).
6. A. van Sliedregt, K. De Groot and C. A. van Blitterswijk, *J. Mater. Sci. Mater. Med.* **4**, 213 (1993).
7. A. van Sliedregt, J. A. van Loon, J. van der Brink, K. de Groot and C. A. van Blitterswijk, *Biomaterials* **15**, 251 (1994).
8. C. M. Agrawal, K. F. Haas, D. A. Leopold and H. G. Clark, *Biomaterials* **13**, 176 (1992).
9. H. Saitoh, T. Takata, H. Nikai, H. Shintani, S.-H. Hyon and Y. Ikada, *J. Mater. Sci. Mater. Med.* **5**, 194 (1994).
10. J. D. Andrade and V. Hlady, *Prog. Surf. Sci.* **79**, 1 (1986).
11. C. F. Scott, *J. Biomater. Sci. Polymer Edn.* **3**, 173 (1991).
12. Th. Groth, K. Derdau, F. Strietzel, F. Foerster and H. Wolf, *ATLA* **20**, 390 (1992).
13. Th. Groth, K. Klosz, E. J. Campbell, R. R. C. New, B. Hall and H. Goering, *J. Biometer. Sci. Polymer Edn.* **6**, 497 (1994).
14. Th. Groth, A. Podias and Y. Missirlis, *Colloids Surfaces B: Biointerfaces* **3**, 241 (1994).
15. S. W. Kim and J. Feijen, *CRC Crit. Rev. Biocompatibility* **1**, 229 (1985).
16. J. D. Andrade and V. Hlady, *Adv. Polymer Sci.* **79**, 1 (1986).
17. N. A. Plate and L. I. Valuev, *Adv. Polymer Sci.* **79**, 96 (1986).
18. P. Schoen, The anticoagulant activity of heparin biochemical studies in purified system, Maastricht (1991). Rijksuniversiteit Limburg, Maastricht, The Netherlands.
19. R. Larsson, O. Larm and P. Olsson, *Ann. N. Y. Acad. Sci.* **516**, 102 (1987).
20. S. W. Kim, H. Jacobs, J. Y. Lin, C. Nojori and T. Okano, *Ann. N. Y. Acad. Sci.* **516**, 116 (1987).
21. M. Amiji and K. Park, *J. Biomat. Sci. Polymer Edn.* **4**, 217 (1993).
22. N. A. Peppas and E. W. Merrill, *J. Biomed. Mater. Res.* **11**, 423 (1977).
23. P. K. Smith, A. K. Mallia and G. T. Hermanson, *Analyt. Biochem.* **109**, 466 (1980).
24. E. J. Campbell, R. R. C. New and S. A. Charles, in: *MRS Symp. Proc. Tissue-Inducing Biomaterials*, p. 229 L. G. Cima and E. S. Ron (Eds.). (1992).
25. Th. Groth, A. Gronert, S. Ziemer and R. Hesse, in: *The Reference Materials of the European Communities*, p. 183, W. Lemm (Ed.). Kluwer, Amsterdam (1992).
26. S. L. Cooper and G. M. Estes, *ACS* **176**, 643 (1979).
27. RESOMER®-Resorbierbare Polyester, Boehringer Ingelheim, (1993).
28. K. H. Lam, P. Nieuwenhuis, I. Molenaar, H. Esselbrugge, J. Feijen, P. J. Dijkstra and J. M. Schakenraad, *J. Mater. Sci. Mater. Med.* **5**, 181 (1994).
29. C. Migliaresi, L. Fambri and D. Cohn, *J. Biomat. Sci. Polymer Edn.* **5**, 591 (1994).
30. S. S. Shah, K. J. Zhu and C. G. Pitt, *J. Biomat. Sci. Polymer Edn.* **5**, 421 (1994).
31. K. M. Sedlarik, P. B. van Wachem, H. Bartels and J. M. Schakenraad, *Biomaterials* **11**, 4 (1990).

32. D. Cohn, *Proc. Biointeractions,* p. 3, Nordwijkerhout, (1993).
33. J. C. Palmaz, *AJR* **160**, 613 (1993).
34. H. M. M. van Beusekom, W. J. van der Giessen, R. J. van Suylen, E. Bos, F. T. Bosman and P. W. Serruys, *JACC* **21**, 45 (1993).

Publikation 15

Barbara Seifert, Paul Romaniuk, Thomas Groth (1997)

Covalent immobilisation of hirudin improves the haemocompatibility of polylactide-glycolide in vitro.

Biomaterials **18**, 1495-1502.

ELSEVIER

PII: S0142-9612(97)00079-3

Biomaterials **18** (1997) 1495–1502

0142-9612/97/$17.00

Covalent immobilization of hirudin improves the haemocompatibility of polylactide–polyglycolide *in vitro*

B. Seifert, P. Romaniuk and Th. Groth*

*Institut für Röntgendiagnostik, Bereich Interventionsradiologie/Angiologie, Universitätsklinikum Charité, Humboldt-Universität zu Berlin, Schumannstrasse 20-21, 10098 Berlin, Germany; *GKSS Forschungszentrum, Institut für Chemie, Abteilung Membranforschung, Kanstrasse 55, 14513 Teltow-Seehof, Germany*

A biodegradable polymer, poly(D,L-lactide-*co*-glycolide) RESOMER® RG756, was modified by surface immobilization of recombinant hirudin (r-Hir) with glutaraldehyde as coupling reagent to improve the blood contacting properties of the polymer. The activity of immobilized hirudin on the polymer was estimated by a chromogenic assay to about 2.5 ATU r-Hir cm^{-2}. The improvement of the haemocompatibility of the modified RG756 was evaluated in terms of platelet adhesion/activation, whole blood clotting times and clot formation rate. Fluorescence microscopy revealed that surface modification with r-Hir resulted in decreased platelet adhesion and activation. An ELISA for P-selectin, a marker of platelet activation, was used to confirm this result. Clotting time experiments demonstrated significantly prolonged non-activated partial thromboplastin times, and a decreased clot formation rate of whole blood in contact with r-Hir modified RG756 compared with the plain polymer. Comparison of immobilized r-Hir with bound heparin yielded equivalent improvement of blood-contacting properties of the investigated polymers. These *in vitro* investigations indicate that the immobilization of r-Hir on RG756 is a useful method to improve the blood contacting properties of polylactides/polyglycolides and other polymers as well. © 1997 Elsevier Science Limited. All rights reserved

Keywords: Polylactide, polyglycolide, hirudin immobilization, haemocompatibility

Received 3 January 1997; accepted 7 May 1997

The use of biodegradable materials has recently been proposed for several applications in contact with blood where temporary reconstruction and/or stabilization of tissue and organs is needed[1,2]. One of these applications is the vascular prosthesis that should possess a certain porosity to support the ingrowth of vascularized perigraft tissue[3]. The application of a biodegradable polymer as one material of a two-component prosthesis may produce an increasing porosity with time. In contrast to current porous prosthesis consisting of woven polymer fibres, bleeding through pores might be minimized and the healing properties improved[1]. Another possible use of degradable polymers in contact with blood is the construction of intravascular stents that have to maintain blood vessels open after balloon dilatation. The use of current metallic intravascular stents is often complicated by thrombosis (despite intensive anticoagulative therapy) and vascular re-stenosis[4]. The process of re-stenosis is attributed to myointimal hyperplasia as well as thrombus formation whereby platelets contribute to both processes by the release of PDGF, thrombin and other substances[4,5]. The use of polymer stents or temporary polymer coatings on metallic stents may enhance the biocompatibility in comparison with plain metal stents[2,6]. The polymers might also be used for the immobilization of drugs with anti-thrombogenic and/or anti-proliferative action[6,7,8]. Degradable polymers like polylactides and polyglycolides are *per se* not haemocompatible, yet investigations on the blood contacting properties of these materials are rarely found[9,10].

Hirudin has been shown to have superior anticoagulant properties versus several heparins. In comparison with heparin, hirudin is not inactivated by platelet factor 4, histidin-rich glycoprotein, or vitronectin. The concentrations of these proteins are increased in some disorders that may lead to heparin resistance. Hirudin has no direct effect on platelets and endothelial cells like heparin, thus decreasing the risk of thrombocytopenia. Moreover, hirudin acts independently of antithrombin III by direct inhibition of thrombin, the central enzyme in thrombosis, in tight stoichiometric relations (for review see Ref. 11). Indeed, thrombin is the most potent platelet activator, stimulating the production of platelet-derived growth factor and the secretion of prostacyclin, platelet-activating factor, and plasminogen-activator inhibitor[12,13]. After complexing with hirudin, thrombin loses its effects on platelets, e.g. the thrombin-induced platelet aggregation and release reactions are prevented[14]. It was shown previously that generation of thrombin on biomaterials has a major impact on downstream thrombus formation[15]. Therefore the immobilization of hirudin

Correspondence to Dr Barbara Seifert.

on degradable polymers seems to be a promising approach for the prevention of thrombus formation on blood-contacting biomaterials.

In this work we have covalently coupled recombinant hirudin on a resorbable polymer showing that immobilization of hirudin reduces significantly the adhesion/activation of platelets, and has an inhibiting influence on the coagulation system. Results are reported herein.

MATERIALS AND METHODS

Materials

Polymers

A commercial biodegradable poly(D,L-lactide-*co*-glycolide) RESOMER® RG756, (Boehringer–Ingelheim, Germany) was selected as material for the immobilization of hirudin. Cast sheets of the polymer were prepared from a 5% solution in chloroform after evaporation of the solvent. Glass coverslips were spin-coated with the same polymer solution using a Convac 1001 device (Convac, Germany).

Blood

Blood was drawn from healthy volunteers who had no medication for at least one week. The blood was collected in sodium citrate (3.13 g/100 ml) at a blood/citrate ratio of 9:1. Platelet rich plasma (PRP) was prepared by centrifugation. Platelet count was adjusted to 200000 μl^{-1}.

Methods

Immobilization of anticoagulants

Recombinant hirudin (HBW023) was a kind of gift from Behringwerke AG (Marburg, Germany) with a specific activity of 16000 ATU mg^{-1}. The immobilization of r-Hir on the polymer surface was performed with glutaraldehyde (GA, Sigma, USA) as coupling agent. The polymer surface was first activated by the incubation with GA in distilled water, followed by an incubation with r-Hir in phosphate buffered saline (PBS, pH 7.4). Subsequent incubation with 1% glycine in PBS was carried out for saturation of remaining free aldehyde groups. Samples were washed thoroughly between the different steps. Incubation times and concentrations were varied as indicated in the results section. All incubation procedures were carried out at 37°C. Heparin immobilization was performed as described previously[10].

AMC assay

For determination of the amount of bound aldehyde groups on the polymer surface an AMC (7-amino-4-methylcoumarin) assay was used. After incubation of surfaces with GA and subsequent washing, 2 ml AMC solution (16.3 mM in methanol/acetic acid 30:5) was added to the polymer samples (22 mm diameter). After 1 h incubation with AMC solution surfaces were washed with methanol. 0.1 M borate buffer (pH 9.7) was added for hydrolysis of AMC-aldehyde groups and the supernatant was measured after 10 min with a Perkin–Elmer fluorescence spectrometer LS 50 B at an excitation wavelength of 370 nm and an emission wavelength of 440 nm. A comparison with a standard curve of known concentrations of AMC was used to estimate the amount of AMC molecules and thus the quantities of aldehyde groups per surface area.

Hirudin assay

The activity of immobilized r-Hir was estimated by the modification of a S-2366 chromogenic assay for soluble hirudin. Samples were incubated with the chromogenic substrate S-2366 (25 mg ml^{-1}) for 2 min followed by the addition of thrombin (1.4 I.U. ml^{-1}). Both chemicals were obtained from Haemochrom Diagnostica (Germany). The hydrolysis of S-2366 was stopped by the addition of 20% acetic acid after 1 min. The optical density (OD) of the resulting chromophore was measured at 405 nm (Spectronic® Genesys™5 spectrophotometer, Milton Roy, USA). A comparison of the sample OD with a standard curve of known activity of r-Hir was used to estimate the specific activity of the immobilized r-Hir per surface area.

Immunofluorescence microscopy of platelets

The degree of platelet adhesion and spreading on the different materials was further investigated with immunofluorescence microscopy. After 30 min contact of PRP with the materials at 37°C, samples were washed with PBS followed by a fixation with 3% paraformaldehyde. Labelling of platelets was performed with a monoclonal mouse antibody CD 41a (Immunotech., S.A., France) followed by polyclonal goat anti-mouse IgG antibody, conjugated with fluorescein (Jackson Immuno Research, USA). Immunofluorescence microscopy was carried out with a Jenamed Fluorescence Microscope (Carl Zeiss, Jena, Germany).

P-selectin assay

The thrombogenicity of pure and anticoagulant-modified RG756 was tested after blood–material contact with an enzyme immuno assay for P-selectin, that is expressed on the surface of activated platelets[16]. Briefly, after 30 min contact of PRP with the samples platelet activation was assessed for P-selectin on adhering platelets using the monoclonal mouse antibody CD 62 (Immunotech S.A., France) and the polyclonal sheep anti-mouse IgG peroxidase-conjugated antibody (Sigma Immuno Chemicals, St. Louis, USA). *O*-phenylene diamine (1 mg ml^{-1}; Sigma) and a 1:1 mixture of 2 M H_2SO_4 and 0.1 M Na_2SO_3 were used as chromogenic substrate, and stopping reagent, respectively. Aliquots of the substrate solution were measured at 492 nm (Anthos Plate Reader, Austria).

Coagulation times

The different modifications of RG756 foils were mounted to a special measuring chamber made of Teflon[16], where the bottom (22 mm diameter) was completely covered by the polymer. One millilitre citrated whole blood was filled into the measuring chamber. The chamber was moved on a orbital shaker at 37°C for 30 min. Thereafter aliquots of 100 μl of whole blood were taken and non-activated partial thromboplastin time (PTT) and thrombin time (TT) estimated. Coagulation times were measured with a coagulometer KC 4A (Amelung, Germany) that measures the clotting time of plasma and whole blood,

respectively. Non-activated PTT was carried out with a PTT kit (Boehringer Mannhein, Germany) without kaolin as activator. For the estimation of TT a kit from Behringwerke (Germany) was used. Both assays were carried out according to the instructions of the supplier.

Clot formation rate

For estimation of whole blood clot formation rate the different modifications of RG756 foils were mounted to a Teflon chamber, where the bottom (11 mm diameter) was completely covered by the polymers. The clot formation rate was measured according to a method by Groth *et al.*[17], which is basically an improved modification of the method from Imai and Nose[18]. Briefly, 150 μl citrated whole blood was filled into the chamber and recalcified with 15 μl calcium chloride solution (25 mM). The extent of a clot formation was then quantified as a function of time by water-induced haemolysis which was achieved by the addition of 1 ml distilled water to the chamber. Red blood cells which were not entrapped within the clot were readily lysed owing to the low osmotic pressure. The supernatant liquid which contained the haemoglobin (0.5 ml) was removed after 30 s. The absorbance (A) of free haemoglobin was quantified photometrically at 545 nm (Spectronic® Genesys™5 spectrophotometer, Milton Roy, USA). The clot formation rate was calculated according to Groth *et al.*[17] as a function of time (t) after the beginning of recalcification

$$\text{Clot formation rate (\%)} = (1 - A_{t=x}/A_{t=0}) \times 100 \quad (1)$$

where $A_{t=0}$ is the absorbance at the beginning and $A_{t=x}$ is the absorbance after time x.

RESULTS AND DISCUSSION

AMC assay

The immobilization of proteins on polymer surfaces has to be carried out at least as a two-step-procedure to avoid possible protein denaturation and excessive protein cross-linking during simultaneous incubation with coupling agents[19]. Therefore, the surfaces were first activated with GA. The quantities of bound aldehyde as a function of GA concentration (0.2 and 2.0%, respectively) and incubation times (0.5–3.0 h) were estimated with the AMC assay. The results in *Figure 1* demonstrate that binding of GA was time dependent with a maximum of free aldehyde groups between 0.5 and 1.0 h. Longer incubation yielded to a decrease in free aldehyde groups, most probably because cross-linking of bound aldehyde to free GA mono- or oligomers. It was also found that a lower GA concentration of 0.2% resulted in an earlier accomplishment of the maximum. This phenomenon might be explained by a higher percentage of GA monomers at lower concentrations that are expected to diffuse, and react more rapidly than larger GA polymers[19]. Indeed, later experiments demonstrated that the platelet adhesion/activation was minimal at a GA concentration of 2.0%, and an incubation time of 1 h. These conditions were thus chosen for the further part of this study.

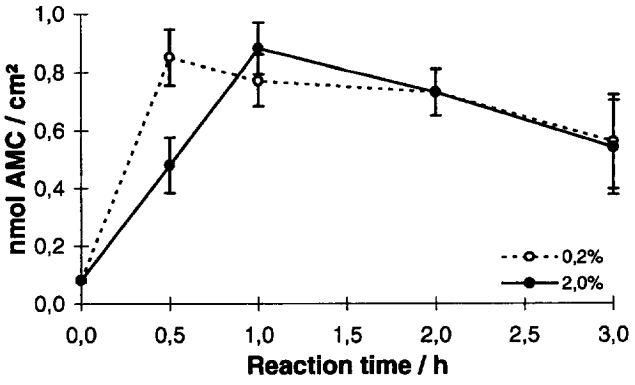

Figure 1 Content of bound aldehyde groups on RESOMER® RG756 after incubation with 0.2 (○) and 2.0% (●) glutaraldehyde as a function of reaction time (means ± S.E.M., $n = 5$).

Immobilization of hirudin

GA-activated samples were incubated with r-Hir solution of different concentrations and for various time periods. The activity of immobilized hirudin was determined by its reaction with thrombin in the presence of the chromogenic substrate S-2366. It is shown in *Figure 2a* that the activity of immobilized r-Hir was maximal after 2 to 3 h incubation (hirudin concentration 200 μg ml^{-1}). The increase of the hirudin concentration in the reaction solution from 200 μg ml^{-1} to 1000 μg ml^{-1} revealed no significant difference in the activity of surface-bound hirudin whether 200 or 1000 μg r-Hir ml^{-1} were applied (*Figure 2b*). Calculation of the activity of surface-bound r-Hir yielded 2.5 ATU r-Hir per cm^2.

Immunofluorescence microscopy

It is known that platelets play a crucial role during thrombus formation on foreign materials[20,21]. Immunofluorescence microscopy was used as a further measure for the optimization of hirudin binding (see *Figures 3* and *4*) using an anti-GP IIb antibody for the visualization of platelet morphology on surfaces. In previous investigations we have shown that immunofluorescence microscopy can be used to study the effect of biomaterial properties on platelets, and these results are related to quantitative methods measuring platelet activation[8,22]. *Figure 3A* and *B* show that the plain RG756 expressed a rather high thrombogenicity indicated by the high number of adherent platelets with formation of pseudopodia, and extensive cell spreading. These results are in agreement with our previous studies[8,10] and results of other investigations[9], demonstrating that polylactides and polyglycolides may cause substantial platelet activation. In general, the immobilization of hirudin resulted in a reduction in platelet adhesion/activation, indicated by the lower number of adhering platelets and reduced spreading of platelets as shown in *Figure 3*. Decreasing adhesion and activation of platelets was observed if the concentration of GA was increased from 0.2 to 2.0% (compare *Figure 3C, E* and *G* with *Figure 3D, F* and *H*), but not if the concentration of r-Hir in the reaction solution was enhanced from 200 μg ml^{-1} (see *Figure 3C* and *D*) to 1000 μg ml^{-1} (see *Figure 3E* and *F*) during the binding procedure. This

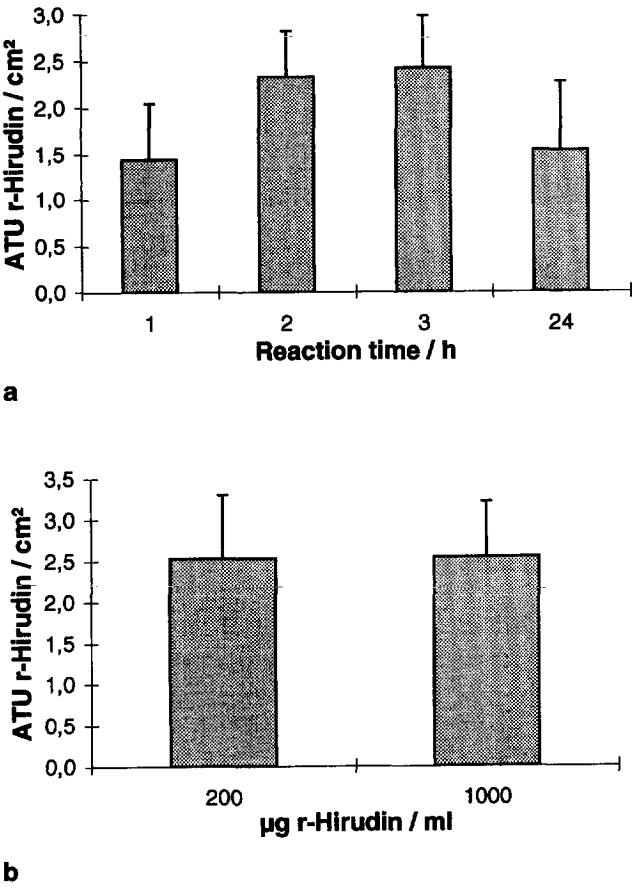

Figure 2 Hirudin activity of r-Hir-modified RESOMER® RG756 with respect to **a**, reaction time and **b**, hirudin concentration in the incubation solution (means ± S.E.M., $n = 5$).

result is also in agreement with the quantitative estimates of r-Hir binding as shown in *Figure 2b*. However, post-treatment with 1% glycine for 1 h (see *Figure 3G* and *H*) further decreased platelet adhesion and formation of pseudopodia indicating that remaining unbound aldehyde groups on the substratum have been responsible for the formation of pseudopodia and platelet aggregates. It is shown in *Figure 2a* that an increase of the r-Hir reaction time up to 3 h increased its binding. To determine how the duration of incubation with r-Hir influences the thrombogenicity, RG756 pre-activated with 0.2% GA (see *Figure 4A, C* and *E*), or 2.0% (see *Figure 4B, D* and *F*) was incubated for 1 h (*Figure 4A* and *B*), 2 h (*Figure 4C* and *D*) or 3 h (*Figure 4E* and *F*) with 200 μg r-Hir ml^{-1}. It is obvious from *Figure 4* that the increase of the incubation time, as well as the increase of GA concentration from 0.2% to 2.0% decreased the amount of adhering platelets, the extent of pseudopodia and aggregate formation. Therefore, an incubation with 200 μg r-Hir ml^{-1} for 3 h seems to be optimal for a very low thrombogenicity of the RG756.

Platelet adhesion and activation (P-selectin assay)

Platelet adhesion/activation was estimated for selected reaction conditions (2% GA; 200 μg r-Hir ml^{-1}; 3 h incubation) with the P-selectin assay and compared with that of non-modified, or heparinized RG756. It is shown in *Figure 5* that the plain RG756 produced the highest activation of platelets indicated by the high OD for P-selectin. The immobilization of hirudin induced a reduction in platelet adhesion/activation in comparison to pure RG756 ($P \leqslant 0.1$) but this was still higher than RG756 modified with heparin ($P \leqslant 0.025$ with respect to RG756). We have shown recently that the immobilization of heparin on polylactide/polyglycolide foils decreases the thrombogenicity indicated by less platelet adhesion and activation[10]. The comparison in *Figure 5* demonstrates a similar inhibiting effect of hirudin on platelet adherence and activation like that of heparin. However, it is apparent that under these experimental conditions heparin has a slightly higher anti-thrombogenic activity than r-Hir. The reason for the better action of heparin with respect to the prevention of platelet adhesion/activation might be that the quantity of immobilized heparin is 3 μg cm^{-2} in comparison with hirudin, which is 0.2 μg cm^{-2} if we assume that the activity of bound r-Hir is equivalent to that of soluble r-Hir. Indeed, the calculation of the catabolic activities of these anticoagulants revealed that heparin has an activity of about 0.5 I.U. cm^{-2}, while hirudin has an activity of about 3.2 ATU cm^{-2}. Nevertheless the units applied (I.U. and ATU) are comparable and suggest a better thromboresistance of hirudin modified surfaces, the kind of action of both anticoagulants is different. Heparin catalyzes the inhibition of thrombin by antithrombin III and is released afterwards[23], while hirudin is directly complexed with thrombin and finally consumed[11]. Clinical studies comparing the anticoagulant action of hirudin and heparin found that almost the same amount of anticoagulant must be applied (0.4 mg kg^{-1} body weight bolus), that equals about 70 I.U. heparin, and 64 000 ATU hirudin, respectively[24]. If we consider these data then it is understandable that the heparinized surface has a slightly better thromboresistance than hirudin-treated RG756.

Coagulation times

Whole blood clotting times have proved to be applicable for testing the haemocompatibility of biomaterials[25]. Non-activated partial thromboplastin time (PTT) and thrombin time (TT) were investigated after 30 min contact with plain and r-Hir-modified RG756 to measure the possible activation of coagulation on the material surface. It is shown in *Figure 6* that the immobilization of r-Hir on RG756 increases both PTT and TT. Since free r-Hir should not be present during the clotting tests, only consumption of coagulation factors and their subsequent inhibition could be responsible for any effect on clotting times. TT was not significantly changed ($P \leqslant 0.15$) most probably because addition of pure thrombin might overlay any slight inhibiting effect of immobilized r-Hir. In contrast, it was found that non-activated PTT was significantly prolonged for increasing r-Hir concentrations. *Figure 6* shows that contact with RG756-1000 μg r-Hir ml^{-1} significantly ($P \leqslant 0.005$) increased the baseline (pure RG756) up to 1.2 fold. This result reflects a possible inhibition of coagulation on the polymer because the PTT test mirrors changes reaching from the contact system of plasmatic coagulation up to the fibrin polymerization[26].

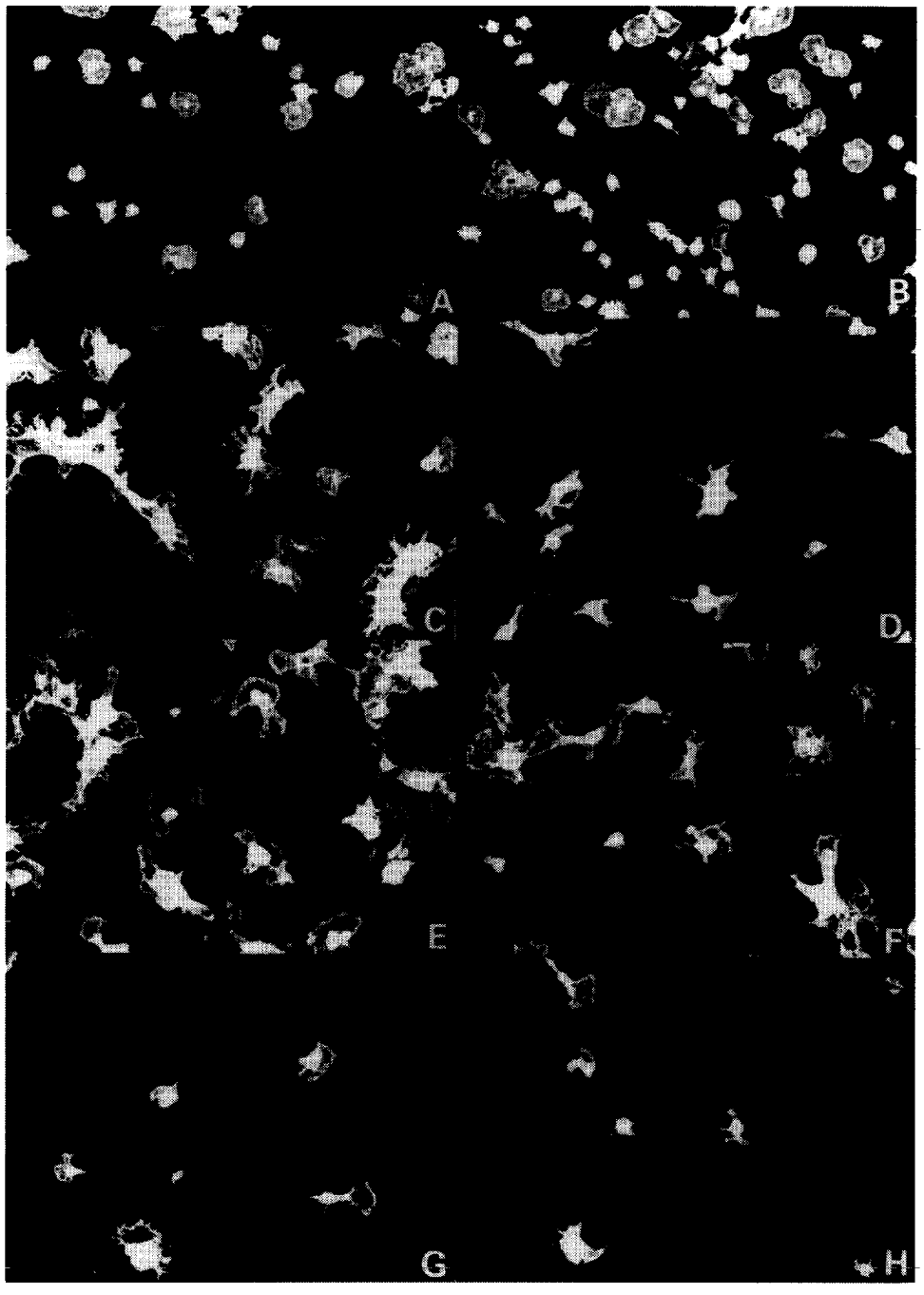

Figure 3 Immunofluorescence micrographs of plain (**A, B**) and r-Hir-modified RESOMER® RG756 with change of glutaraldehyde concentration (**C, E, G,** 0.2% and **D, F, H,** 2.0%), hirudin concentration (**C, D** 200 and **E, F,** 100 μg ml^{-1}, 3 h) and incubation with glycine (**G,** 200 μg r-Hir ml^{-1}, and **H,** 1000 μg r-Hir ml^{-1}) after 30 min contact with platelet rich plasma (original magnification ×320).

Consumption and inhibition in particular of factor Xa on the hirudin modified polymer may lead to prolonged PTT, which was observed and discussed recently for heparinized materials[25].

Clot formation rate

Whole blood clotting assays for the estimation of biomaterial-induced coagulation are carried out after contact of blood with the surface and might be less sensitive for the estimation of surface-related phenomena. Therefore, coagulation was assessed directly on non-modified, heparin- and r-Hir-modified RG756 by the measurement of whole blood clot formation rate up to 120 min after the addition of $CaCl_2$-solution. *Figure 7* shows that the modification of the polymer surface resulted in a significantly decreased clot formation rate on RG756 modified with 200 and 1000 μg r-Hir ml^{-1} during the first 60 min in comparison with non-modified RG756. The clot formation rate on heparin-modified RG756 was also decreased, but to a lower extent than r-Hir-modified RG756. This obviously different behavior, in comparison with platelet activation shown earlier, might be explained by the fact that during the assay faster sedimentation of red blood cells prevents the interaction of platelets with the surface[17]. Therefore, mainly clotting enzymes and red blood cells contact

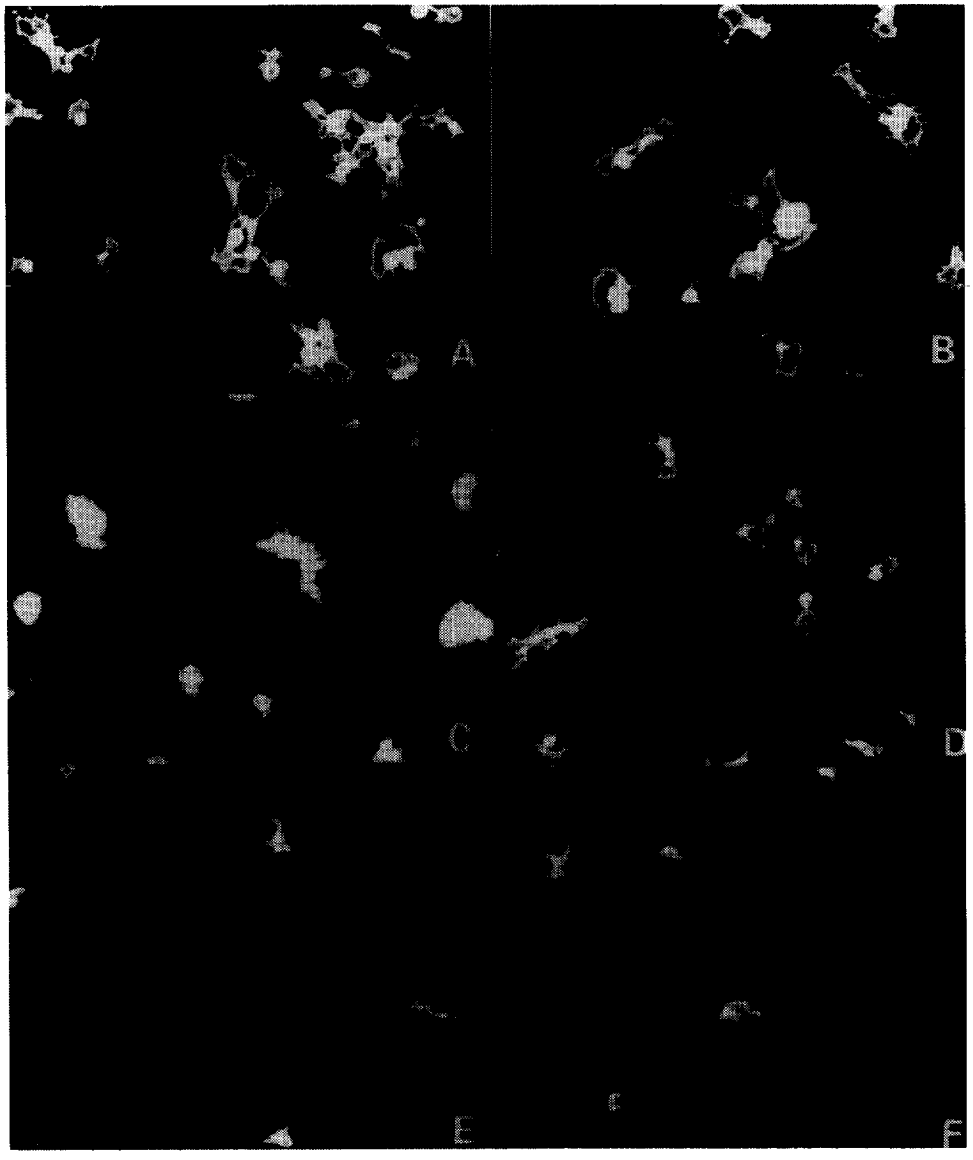

Figure 4 Immunofluorescence micrographs of r-Hir-modified RESOMER® RG756 with change of glutaraldehyde concentration (left lane, 0.2%, and right lane, 2.0%) and incubation time with a 200 μg r-Hir ml^{-1} for 1 h (**A, B**), 2 h (**C, D**), and 3 h (**E, F**) (original magnification ×320).

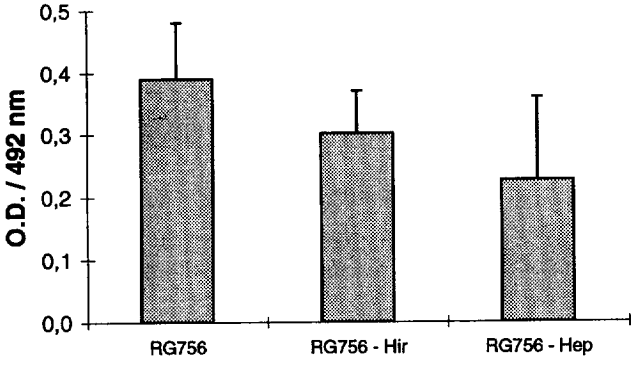

Figure 5 Comparison of platelet activation on non-modified, heparin- and r-Hir-modified RESOMER® RG756 (means ± S.E.M., $n = 5$).

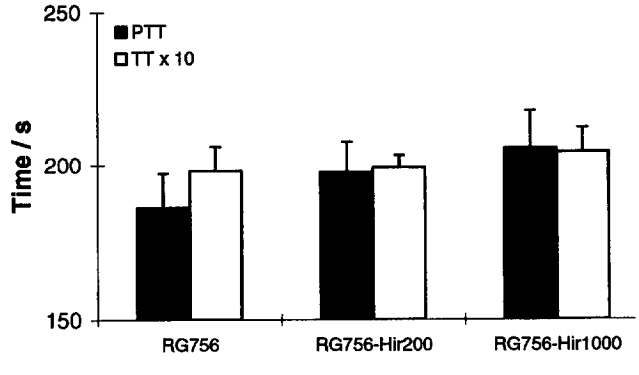

Figure 6 Non-activated partial thromboplastin time (PTT, black columns) and thrombin time (TT times 10, empty columns) of citrated whole blood after contact with non-modified and r-Hir-modified RESOMER® RG756 for 30 min (means ± S.E.M., $n = 5$).

the material surface. Generated thrombin might be bound to immobilized hirudin inhibiting the process of fibrin formation that is measured by the whole blood clot formation rate. In contrast, heparinized surfaces may continuously release AT III-thrombin intermediate complexes[23], resulting in a continuous generation of thrombin on the surface that may partly be involved in fibrin polymerization.

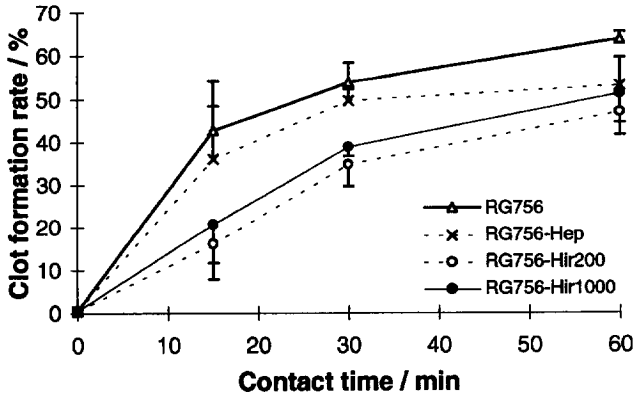

Figure 7 Clot formation rate of whole blood on non-modified (Δ), heparin- (×) and r-Hir-modified (○, 200 $\mu g\,ml^{-1}$; ●, 1000 $\mu g\,ml^{-1}$) RESOMER® RG756 (means ± S.E.M., $n = 5$).

CONCLUSION

It was shown that the immobilization of r-Hir with glutaraldehyde as coupling agent improves the blood-contacting properties of RG756. Optimal conditions for r-Hir binding have been found with 1 h surface activation (2% GA), followed by incubation with 200 μg r-Hir ml^{-1} for 3 h and subsequent saturation with 1% glycine for 1 h. The use of 200 μg r-Hir ml^{-1} incubation solution (3200 ATU ml^{-1}) resulted in a surface concentration of about 2.5 ATU r-Hir cm^{-2}. Immunofluorescence microscopy and ELISA for P-selectin revealed lower platelet adhesion and activation on this surface compared with non-modified RG756. It was further demonstrated that although coagulation times (non-activated PTT and TT) were only slightly prolonged on immobilized r-Hir, the clot formation rate of whole blood has been significantly decreased in comparison with the non-modified polymer. In summary it can be concluded that hirudin is an alternative to the application of heparin for the improvement of blood-contacting properties of biomedical polymers. Indeed, it has to be considered that binding of hirudin to thrombin is irreversible. Thus, the bound hirudin is consumed and not able to bind more thrombin in contrast to heparin which acts catalytically. On the contrary, hirudin immobilization may lead to a passivation of the surface, which is restricted by thrombin generation on the artificial surface. The *in vitro* results of this study indicate a considerable improvement of the haemocompatibility of polymers by immobilized hirudin that make short-term applications of treated biomedical materials reasonable. Moreover, from our results it cannot be ruled out that immobilization of r-Hir may lead to a passivation of surfaces for a longer time period, which remains to be proven in future investigations.

ACKNOWLEDGEMENTS

This work was supported by the BMBF, Germany (Grant Nr. FKZ 01ZZ9101).

REFERENCES

1. Cohn, D., *Proc. 4th International Conference Biointeractions.* Noordwijkerhout, The Netherlands, 1993, p. 3.
2. Agrawal, C.M., Haas, K.F., Leopold, D.A. and Clark, H.G., Evaluation of poly(L-lactid-acid) as a material for intravascular polymeric stents. *Biomaterials*, 1992, **13**, 176–182.
3. Sedlarik, K.M., van Wachem, P.B., Bartels, H. and Schakenraad, J.M., Rapid endothelialization of microporous vascular prostheses covered with meshed vascular tissue: a preliminary report. *Biomaterials*, 1990, **11**, 4–8.
4. Palmaz, J.C., Intravascular stents: tissue–stent interactions and design considerations. *AJR Am. J. Roentgenol.*, 1993, **160**, 613–618.
5. van Beusekom, H.M.M., Serruys, P.W. and van der Giessen, W.J., Coronary stent coatings. *Coron. Artery Dis.*, 1994, **5**, 590–596.
6. McNair, A.M., Novel phosphorylcholine-based hydrogel polymers: developments in interventional cardiology. *Proceedings of Polymers in Medicine and Surgery—PIMS 96.* University of Strathclyde, Glasgow, UK, 1996, pp. 53–59.
7. Herrmann, K., Groth, Th., Seifert, B. and Romaniuk, P., Heparin-modified polylactide as biodegradable hemocompatible biomaterial. *J. Mater. Sci. Mater. Med.*, 1994, **5**, 728–731.
8. Seifert, B., Romaniuk, P. and Groth, Th., Bioresorbable, heparinized polymers for stent coating: *in vitro* studies on heparinization efficiency, maintenance of anticoagulation properties and improvement of stent haemocompatibility. *J. Mater. Sci. Mater. Med.*, 1996, **7**, 465–469.
9. Klee, D., Thissen, H., Thelen, H., Severich, B., Hoffmeister, K., vom Dahl, J., Hanrath, P. and Höcker, H., Surface modification of bioresorbable polymers to improve the antithrombogenic properties. *Proceedings of Polymers in Medicine and Surgery—PIMS 96.* University of Strathclyde, Glasgow, UK, 1996, pp. 87–93.
10. Seifert, B., Groth, Th., Herrmann, K. and Romaniuk, P., Immobilization of heparin on polylactide for application of degradable biomaterials in contact with blood. *J. Biomater. Sci. Polymer Edn*, 1995, **7**, 277–287.
11. Markwardt, F., Hirudin and derivatives as anticoagulant agents. *Thromb. Haemos.*, 1991, **66**, 141–152.
12. Gentry, P.A., The mammalian blood platelet: its role in haemostasis, inflammation and tissue repair. *J. Comp. Pathol.*, 1992, **107**, 243–270.
13. Serruys, P.W., Herrman, J.P.R., Simon, R., Rutsch, W., Bode, C., Laarman, G.J., van Dijk, R., van den Bos, A.A., Umans, V.A.W.M., Fox, K.A.A., Close, P. and Deckers, J.W., A comparison of hirudin with heparin in the prevention of restenosis after coronary angioplasty. *N. Engl. J. Med.*, 1995, **333**, 757–763.
14. Reilly, T.M., Knabb, R.M., Hassell, S.M., Bozarth, J.M., Forsythe, M.S., Mayo, M.C., Racanelli, A.L. and Mousa, S.A., Effect of thrombin inhibitors on platelet functions: comparative analysis of Dup 714 and hirudin. *Blood Coagul. Fibrinolysis*, 1992, **3**, 513–517.
15. Hubbell, J.A., and McIntire, L.V.C., Visualization and analysis of mural thrombogenesis on collagen, polyurethane and nylon. *Biomaterials*, 1986, **7**, 354–363.
16. Groth, Th., Campbell, E.J., Herrmann, K. and Seifert, B., Application of enzyme immunoassays for testing haemocompatibility of biomedical polymers. *Biomaterials*, 1995, **16**, 1009–1015.
17. Groth, T., Derdau, K., Strietzel, F., Foerster, F. and Wolf, H., The haemocompatibility of biomaterials *in vitro*: investigations on the mechanism of the whole-blood clot formation test. *ATLA*, 1992, **20**, 390–395.
18. Imai, Y. and Nose, Y., A method for evaluation of antithrombogenicity of materials. *J. Biomed. Mater. Res.*, 1972, **6**, 165–172.
19. Ruijgrok, J.M., de Wijn, J.R. and Boon, M.E., Optimizing glutaraldehyde crosslinking of collagen: effects of time, temperature and concentration as measure by

shrinkage temperature. *J. Mater. Sci. Mater. Med.*, 1994, **5**, 80–87.

20 Courtney, J. M., Lamba, N. M. K., Sundaram, S. and Forbes, C. D., Biomaterials for blood-contacting applications. *Biomaterials*, 1994, **15**, 737–744.

21. Missirlis, Y. F. and Wautier, J. L., *The role of platelets in blood–biomaterial interactions*. Kluwer, Dordrecht, 1993.

22. Mitzner, E. and Groth, Th., Modification of poly(ether urethane)elastomers by incorporation of poly(isobutylene)glycol. Relation between polymer properties and thrombogenicity. *J. Biomater. Sci. Polym. Edn*, 1996, **7**, 1105–1118.

23. Schoen, P., The anticoagulant activity of heparin. Thesis, Rijks University Limburg, Maastricht, 1991, p. 159.

24. Turpie, A. G. G., Weitz, J. I. and Hirsh, J., Advances in antithrombotic therapy: novel agents. *Thromb. Haemost.*, 1995, **74**, 565–571.

25. Rhodes, N. P. and Williams, D. F., Plasma recalcification as a measure of contact phase activation and heparinization efficacy after contact with biomaterials. *Biomaterials*, 1994, **15**, 35–37.

26. Lane, D. A. and Bowry, S. K., The scientific basis for selection of measures of thrombogenicity. *Nephrol. Dial. Transplant.*, 1993, **9(suppl. 2)**, 18–28.

Publikation 16

Barbara Seifert, Georgios Mihanetzis, Thomas Groth, Wolfgang Albrecht, Klaus Richau, Yannis Missirlis, Dieter Paul, Günter von Sengbusch (2002).

Polyetherimide – a new membrane forming polymer for biomedical applications.

Artificial Organs **26**, 189-199.

Artificial Organs
26(2):189–199, Blackwell Publishing, Inc.

Polyetherimide: A New Membrane-Forming Polymer for Biomedical Applications

*B. Seifert, †G. Mihanetzis, *T. Groth, *W. Albrecht, *K. Richau, †Y. Missirlis, *D. Paul, and *G. von Sengbusch

**Institute of Chemistry, Department of Biomaterials, GKSS Research Center Geesthacht GmbH, Teltow, Germany; and †Department of Mechanical Engineering, Biomedical Engineering Laboratory, University of Patras, Rion, Patras, Greece*

Abstract: Membranes for biohybrid organs such as the biohybrid liver support system have to face 2 different environments, namely blood and tissue cells. Accordingly, the respective membrane surfaces must have optimal properties in terms of biocompatibility for blood or tissue. Flat membranes prepared by a phase inversion process from polyetherimide were modified by binding of tris-(hydroxymethyl)-aminomethane to obtain a surface with hydroxyl groups by binding of polyethylene imine to attach a hydrophilic macromolecule with amine groups useful as a spacer for later bonding of further ligands and by attachment of heparin. The binding of the different ligands was successful as monitored by different physicochemical methods. The blood response of plain polyetherimide was comparable to that of polyacrylonitrile, and it could be further improved by the binding of heparin. The tissue compatibility of polyetherimide and its different modifications was compared with commercial cell culture substrate membranes (Millicell) and found to be comparable for polyetherimide and even better after the modification with tris-(hydroxymethyl)-aminomethane. In conclusion, polyetherimide seems to be an interesting material for the production of membranes for application in biohybrid organ systems. **Key Words:** Biohybrid organs—Membranes—Polyetherimide—Surface functionalization—Biocompatibility.

Membranes with specific transport properties are widely used in different types of separation processes for technical, biotechnological, and biomedical applications (1). In the field of medicine, membranes are applied for blood detoxification and oxygenation (1–3). A well known example is hemodialysis in cases of end-stage renal disease to replace a part of the kidney function by using flat membrane or hollow fiber dialyzers to eliminate excess water, salts, and excreted products of metabolism, e.g., urea (2,3). One of the problems of current artificial organ therapies is that the device can replace only a part of the organ's function. This can lead to an increased morbidity and mortality of the patient, as is known from long-term dialysis patients, or in cases of fulminant hepatic failure using adsorption technologies (5,6). Hence, efforts have been made to combine the physical performance of polymer materials, such as the capacity of particles for adsorption or the ability of membranes for filtration, with the activity of living cells originating from the organ to be replaced (7,8). The biohybrid liver support system, which is probably one of the most advanced systems in this respect, is an example of the combination of polymer membranes and living cells (9–11).

Membranes for hemodialysis have been optimized by appropriate bulk composition or surface properties to minimize the interactions with different humoral and cellular components of blood such as the clotting system and platelets or the complement system and leukocytes (2,3). Accordingly, most of them are not optimal for the immobilization of tissue cells, which makes them less favorable as host materials in biohybrid organs (12). On the other hand, membranes developed as substrata in biotechnological or tissue engineering applications that are optimized to host adhesion-dependent cells may be strong activators of blood components (13,14). Since patients suf-

Received May 2001.
Presented in part on the 65th birthday of Prof. Dr. Horst Klinkmann on May 7, 2000, Rostock, Germany.
Address correspondence and reprint requests to Dr. Thomas Groth, GKSS Research Center Geesthacht GmbH, Institute of Chemistry, Kantstr. 55, 14513 Teltow, Germany. E-mail: Thomas.Groth@gkss.de

fer normally from lack of viable and functional autologous cells in the respective organ, xeno or allogenic cells are used in biohybrid organs (15). These cells must be protected against the immune system of the patient. This is possible by adjustment of the membrane permeability (7). Hence, the development of membranes for biohybrid organs faces very complex requirements. Existing prototypes of biohybrid organ support systems use mostly commercial materials such as polycarbonate, polysulfone, polypropylene membranes and others (16), which must be considered as one of the reasons for the limited lifetime of the devices (12).

So far, polyimide materials such as polyetherimide (PEI) have not been frequently applied as biomaterials. Recent investigations on their biocompatibility have shown that polyimides do not exert any significant level of cytotoxicity or hemolysis and allow the attachment and growth of cells (16–18). Therefore, it was anticipated that PEI is a candidate for biomedical applications for parts of intraocular lenses, biosensors, oxygenators, or neuroprostheses (19,20). PEI also possesses considerable mechanical strength and thermal stability as shown recently (21). This should make PEI suitable for steam sterilization. Furthermore, PEI has very good membrane-forming properties (22,23). The polymer backbone of PEI possesses functional groups that are accessible for a wet chemistry modification to adapt the resulting membrane material to a specific application such as contact with blood or tissue cells. Consequently, PEI represents a very interesting material for the preparation of membranes for application in conventional artificial organs such as hemodialyzers but more particularly in biohybrid organs.

Membranes in biohybrid organs have to contact blood for oxygenation, nutrition, and detoxification from one side and the organ cells from the other side. Surface modification of PEI could be used to produce bifunctional membranes with a blood as well as a tissue compatible side. Therefore, in this study, we tried to immobilize different ligands on PEI membranes and to investigate the blood and tissue response of these materials with regard to the type of ligand and duration of functionalization. In more detail, the following surface modifications were performed. First, hydroxyl groups were introduced by the modification with tris-(hydroxymethyl)-aminomethane (Tris). This surface modification was expected to provide a more hydrophilic surface that could improve the blood response of the material (24). Second, introduction of secondary and primary amine groups was provided by the covalent binding of polyethylene imine. This hydrophilic macromolecule may be used subsequently as a spacer for the immobilization of other bioactive ligands to modulate the blood or tissue response of the membrane. Third, binding of heparin to the membrane surface also was included in this study to improve the blood response of PEI membranes.

The hemocompatibility of these surfaces was assessed in vitro by measuring the activation of the clotting and complement system and the adhesion of platelets. The tissue compatibility was determined by the estimation of tissue cell growth on the membranes, using human fibroblasts as a general model. Results are reported herein.

MATERIALS AND METHODS

Polymers

Polyimides are polymers that normally consist of aromatic rings coupled by imide linkages, that is, linkages in which 2 carbonyl (C=O) groups are attached to the same nitrogen (N) atom. In the PEI (Ultem 1000, General Electric, Schenectady, NY, U.S.A.) used here as polymer for membrane formation, ether groups are inserted into the polyimide backbone (Fig. 1, top). The carbonyl groups adjacent to the imide nitrogen are used for binding modifying groups and ligands.

Membrane formation

Flat membranes with a low porosity were prepared from PEI by a conventional phase inversion process. The PEI polymer was disolved in *N*-methylpyrrolidone for 2 h at 80°C with a concentration of

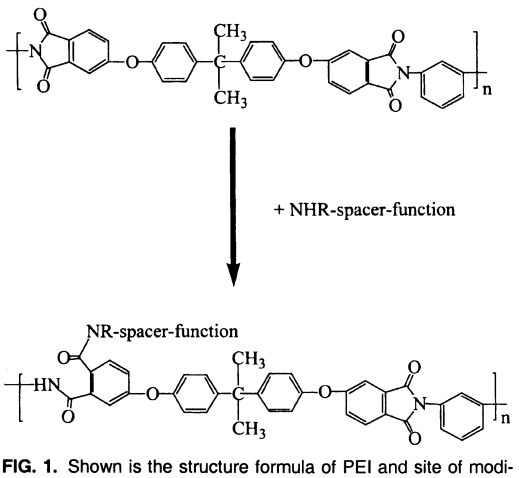

FIG. 1. Shown is the structure formula of PEI and site of modification with a modificator containing an amine group with a residue (hydrogen, alkyl, or aryl group) (NHR) (NR, bound amine group with residue), a spacer, and functional groups (function).

25 wt% polymer in solvent. The membranes were formed with 250 μm casting slit width at a drawing speed of 2 m/min. The solution was at room temperature. After casting the polymer solution to a thin film on a steel band, the polymer film was placed in the water precipitation bath at room temperature. After intensive rinsing with water, the membranes were tempered for 10 min at 90°C, dried at room temperature, and stored in the dry state. Pure polyacrylonitrile (PAN) membranes also were prepared by a phase inversion process and used as a reference material in the blood compatibility studies. In contrast to the PEI membranes, the PAN membrane was stored in the wet state until further investigation.

Membrane modification

Surface modification of PEI membranes by wet chemistry was used to produce amine functionalized, hydroxylated, or heparinized surfaces. The carbonyl group of the imide backbone part was used for the binding of an amine group of the modifying substance (Fig. 1, bottom). The general method for this modification was incubation of the PEI membranes in an aqueous solution of modifying substance (2% modificator in solution) in 1-propanol/water (1:1) at 70°C for the time given (1 or 10 min). The modifying substances were polyethylene imine (molecular weight 25,000 daltons, PEI-NH1 and 10), Tris (PEI-OH1 and 10), and heparin sodium salt (170 IU/mg, all Sigma-Aldrich, Taufkirchen, Germany; PEI-Hep1 and 10). Modified membranes were intensively washed with distilled water after modification and stored in the wet state until further investigations.

Contact angle

For estimating the wettability of the membranes, contact angle measurements were made with the captive bubble method using distilled water and equipment produced by Zeiss (Jena, Germany). A strip of the membrane was fixed horizontally in a holder that was immersed upside down into a little glass box filled with distilled water. A curved cannula needle attached to a syringe with a measuring screw was used to apply a bubble of vapor-saturated air below the membrane. The bubble volume was increased and decreased with the help of the screw to generate advancing and receding conditions. The contact angle was measured directly on the bubble with the goniometer telescope.

The receding and advancing angles, i.e., the dewetting and wetting contact angles, were taken after the triple line (contact line of air, water, and membrane) had moved on the solid surface due to increasing and decreasing volume of the air bubble.

Zeta potential

Streaming potential measurements were carried out as described previously with an EKA Electro Kinetic Analyzer (Anton Paar KG, Graz, Austria) (25). A flat plate measuring cell with an electrolyte channel between sample surfaces with an effective area of $2 \times (74 \times 15)$ mm^2 and an effective height in the order of 0.3 mm was used. Measurements were performed at 25.0 ± 0.5°C using aqueous KCl solution ($I = 10^{-3}$ mole^{-1}). The pH value was adjusted with equimolar KOH and HCl solutions, respectively. The zeta potential was calculated while surface conductivity was not taken into account.

Determination of surface functional groups and ligands

Hydroxyl groups

A dansyl chloride assay was used to estimate the content in hydroxyl groups on the modified membrane surface (26). The method was modified because the recommended solvent pyridine dissolved the membranes. Alternatively, diethylether was used as solvent for dansyl chloride (5-dimethylaminonaphtalene-1-sulphochloride, 20 mg/10 ml; Sigma-Aldrich) with addition of diisopropylethylamine (15.3 μl/10 ml; Merck, Darmstadt, Germany). The samples were immersed in this solution for 3 h. After washing, the fluorescence emission spectra of dried membranes were measured with a luminescence spectrometer LS 50 B (Perkin-Elmer Ltd., Beaconsfield, Buckinghamshire, U.K.) at an excitation wavelength of 350 nm and an emission wavelength of 380 to 500 nm.

Fourier-transformed infrared spectra of dry membranes without dansyl chloride labeling were measured with a Magna IR Spectrometer 550 (Nicolet, Madison, WI, U.S.A.) in the attenuated total reflection modus (FTIR-ATR) to detect the functionalization with hydroxyl groups on the membrane surface.

Amine groups

An Acid Orange II assay was used for determining the degree of functionalization, i.e., the density of primary and secondary amine groups on the membrane surface (27).

Samples were immersed into a solution of 500 μ*M* Acid Orange II (Sigma-Aldrich) in distilled water at pH 3 (diluted HCl) at which there is a protonation of amines. After shaking overnight at room temperature, the samples were washed twice with water (pH 3). The amount of bound dye was quantified after detachment in distilled water at pH 12 (diluted NaOH). This was achieved after 15 min shaking at

room temperature when the dye detached because of the deprotonation of amines at the basic pH value. The optical density of the solution was measured spectrophotometrically at 492 nm. The surface density of amine groups was quantified by comparison with a standard curve of known concentrations of Acid Orange II.

Quantification of bound heparin

The estimation of the total amount of surface bound heparin was measured by a modified toluidine blue colorimetric method (28). The method was performed by incubating polymer sheets (size 1.5 cm^2) in 0.7 ml phosphate buffered saline (PBS, 140 m*M* NaCl, 10 m*M* Na_2HPO_4, pH 7.4) and 0.7 ml with 0.005% aqueous toluidine blue solution (TB; Sigma-Aldrich). After shaking the vials for 5 min, 2 ml of hexane was added, followed by mixing for 30 s. Afterwards, the separation of hexane and the aqueous phase took place. TB and bound heparin formed a complex on the polymer surface (or at the interface water-hexane in the case of the standard curve). As a result, the decolorization of the aqueous phase took place. The optical density of the aqueous phase was measured at 620 nm (TECAN Spectro Fluor Plus, Crailsheim, Germany) after dilution with absolute ethanol 1:5 (vol/vol). The amount of coupled heparin then was quantified by comparison with a standard curve of known concentrations of heparin and given in IU/cm^2.

Blood collection and preparation

Fresh blood was obtained from healthy volunteers who had no medication for 1 week. Diatube H CTAD (31.9 mg/ml sodium citrate, blood/citrate ratio 9:1, containing theophylline and dipyridamole; Diagnostica Stago, Parsippany, NJ, U.S.A.) was used as an anticoagulant in all experiments except in the case of kallikrein determination. Here heparinized blood was used (10 IU sodium heparin/ml; Sigma-Aldrich). The blood was centrifuged at 300 *g* for 10 min immediately after collection to obtain platelet rich plasma (PRP). Platelet poor plasma (PPP) was prepared by a further centrifugation at 3,000 *g* for 15 min.

Measurement of plasma kallikrein-like activity

The contact of blood with foreign surfaces causes the activation of factor XII to XIIa, which, through the conversion of plasma prekallikrein to kallikrein, starts the coagulation cascade. The spectophotometric detection of the p-nitroaniline released during the reaction of kallikrein with the chromogenic substrate H–D–Pro–Phe–Arg–NH–Ph–NO_2 is a test suitable to measure the contact activation induced by materials in contact with blood. Kallikrein-like activity was measured with the chromogenic substrate S-2302 (Chromogenix/Haemochrom Diagnostica, Essen, Germany) using a method described in previous studies (29). Heparinized PPP had contact with materials in a Teflon chamber (22 mm diameter wells, 1 ml PPP per well) for 30 and 60 min, respectively. In a 96 well plate, 200 µl of PPP diluted 5 times with Tris-HCl buffer (pH 7.8) was mixed with 100 µl S-2302 (2 m*M*) and incubated at 37°C for up to 20 min. During this time, the reaction kinetics, i.e., the transformation of the chromogenic substrate, were tracked every 2 min at 405 nm (TECAN SPECTRA Plate Reader, Crailsheim, Germany). The slope in the optical density kinetics gives a measure of the kallikrein-like activity.

Activation of the coagulation system: nonactivated partial thromboplastin time

Membrane samples were fixed in a Teflon chamber with a 22 mm well diameter. Six hundred microliters of PPP was added to each well. After 30 min contact time, the PPP was collected, and the nonactivated partial thromboplastin time (nAPTT) was determined by the plasma recalcification technique (30) using a C.K. PREST assay (without activation to avoid masking effects) measuring coagulation time with a ST4 coagulometer, both from Diagnostica Stago. PPP without membrane contact was used as a control sample.

Complement activation (Bb fragment enzyme immunoassay)

Previous studies have shown that classical activation of the complement system is of minor importance in material-contact interactions whereas activation on foreign surfaces via the alternative pathway is an important parameter for hemocompatibility characterization of biomaterials (31,32).

The alternative pathway is initiated with the complement component C3 that is cleaved to release C3b that binds to the activating surface. Covalently bound C3b binds factor B. Within the C3bB complex, factor B is rendered susceptible to cleavage by factor D. A small factor Ba is released whereas Bb remains complexed with C3b on the surface. The assessment of the complement component Bb (as well as other components resulting from further cleavages like C3a, iC3b, and C5a) in blood plasma after blood-material interaction represents a rapid method of evaluating complement-related blood compatibility of biomaterials. Quantification of fragment Bb generation was performed by an enzyme-linked immunosorbent assay (ELISA) provided by Quidel (San Diego, CA, U.S.A.). A contact time of

15 min was selected because the generation of complement fragments can decrease after this period and this may lead to poor resolution results (33,34).

Briefly, the Bb fragment ELISA was determinded in a 96 well plate precoated by Quidel. It was washed thoroughly, and specimen diluent, reconstituted standards, controls, or diluted specimens were added to the assigned wells. The samples were incubated at room temperature for 30 min and washed thoroughly. The Bb conjugate was added and incubated at room temperature for 30 min followed by thorough washing. The substrate solution was added, and after 30 min the reaction was stopped by stop solution. The optical density of the solution was measured at 405 nm (TECAN SPECTRA Plate Reader).

Platelet retention and adhesion

After centrifugation PRP and PPP were mixed in order to obtain a standard initial platelet (PLT) density of 250,000 PLT/μl. Membrane samples were fixed in a Teflon chamber with a 22 mm well diameter and wetted with phosphate-buffered saline (PBS). Six hundred microliters of standardized PRP was added to each well after removing PBS. After 30 min contact time, the PRP was collected, and a platelet count was made with a Coulter Counter Type Z2 (Coulter Corp., Miami, FL, U.S.A.). Comparison with the platelet count before membrane contact yielded the number of retained and adherent platelets, respectively.

Tissue compatibility

For tissue compatibility tests, 3T3 fibroblasts (CCL 163, ATCC, Manassas, VA, U.S.A.) were grown in Dulbecco's modified Eagle's medium (with D-glucose, 1,000 mg/L, L-glutamine, antibiotic, antimycotic solution, 1×, and HEPES buffer, 10 m*M*) containing 10% fetal bovine serum. Cells were passaged at 80% to 90% confluence with 0.05% trypsin–0.02% EDTA (all Sigma-Aldrich) and resuspended at densities of 10^5 cells/ml.

Cell proliferation studies were accomplished with membrane disks (13 mm diameter) in 24 well plates. Sterile samples were seeded with 0.5 ml of cell suspension and incubated for up to 4 days. MTT (3-[4,5-dimethyl-2-thiasolyl]-2,5-diphenyl-2H-tetrazolium-bromide, Merck, Darmstadt, Germany) and LDH (lactate dehydrogenase, Boehringer Mannheim, Penzberg, Germany) tests quantified the cell attachment and growth in terms of activity of mitochondria and content of LDH, respectively. The commercial membrane Millicell-HA (Millipore, Boston, MA, U.S.A.) was used as a reference material.

RESULTS

Membrane formation

The first experimental work dealt with the preparation of flat membranes with low porosity from PEI by the phase inversion process. Figure 2 shows that PEI has excellent membrane forming properties resulting in asymmetric polymer membranes with a dense and smooth separating layer, a sponge-like highly porous transition layer, and a macrovoids-containing support layer. The same polymer also was used to produce hollow fibers that show the known structure of many other membrane materials applied in hemodialysis (not shown here).

Water contact angle and streaming potential measurements

The membranes were characterized by water contact angle and partly by zeta potential measurements. Functionalization with different ligands was assessed by spectroscopic and colorimetric methods.

The water contact angles of the membranes are

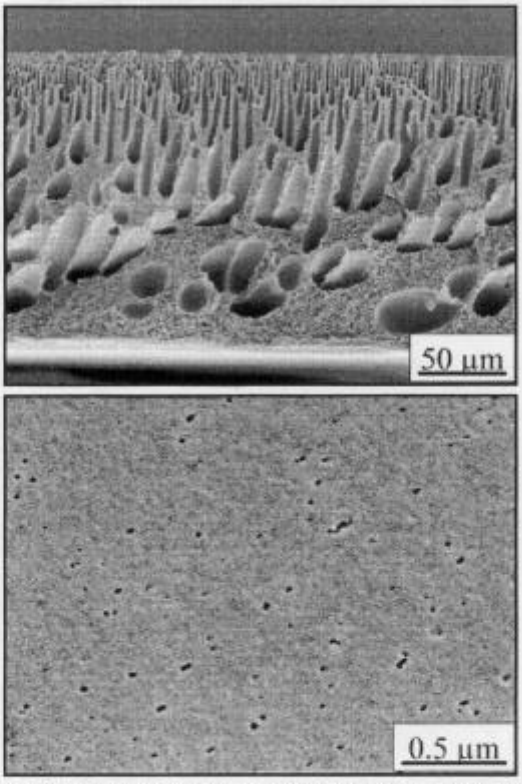

FIG. 2. The scanning electron microscopy images are of the unmodified PEI membrane: cross section (**top**) and surface of the separating layer (**bottom**).

given in Fig. 3. Unmodified PEI in the wet state has an advancing and receding contact angle of 79.5 degrees and 49.0 degrees, respectively. Modification with Tris (PEI-OH) increased advancing only slightly, but caused a higher increase of the receding angle. The hysteresis, meaning the difference between advancing and receding contact angle, decreased however, indicating a more homogenous and/or smoother surface. Modification with polyethylene imine (PEI-NH) and heparin (PEI-Hep) did not result in a significant change of the advancing water contact angles. However, changes were observed for the receding contact angles with functionalization time. Ten minute modification of PEI-NH resulted in lower receding contact angles compared to the unmodified PEI. Small changes in water contact angles only were observed for PEI-Hep. PAN had a much lower advancing and receding water contact angle in comparison to PEI and the different modifications.

Streaming potential measurements were only performed for the non- and amine-modified PEI membranes (Fig. 4). Unmodified PEI membranes showed a zeta potential of about −20 mV at pH 7.0. Binding of amine functions by modification with polyethylene imine resulted in an increase of the zeta potential to positive values of about 16 mV at pH 7.0.

Specific assessment of surface modification by spectroscopy and dye binding assays

The quantification of immobilized hydroxyl groups after functionalization with Tris by binding of dansyl chloride was complicated because the fluorescence emission spectrum of the dye coincided with a fluorescence emission peak of the PEI membranes. However, it was observed that the surface modification with Tris reduced the maximum intensity of PEI concomitantly with the duration of surface modification. Furthermore, a shift of the maximum toward 485 nm indicated dye binding to the hydroxyl groups, mainly at PEI membrane, modified with Tris for 10 min (Fig. 5).

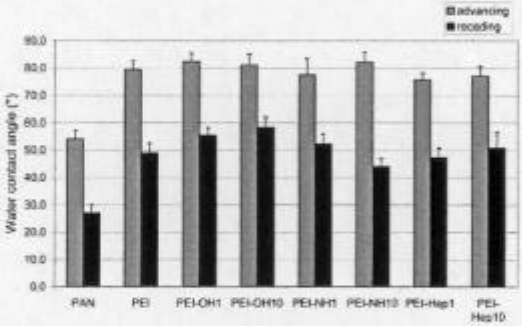

FIG. 3. The chart shows advancing (wetting) and receding (dewetting) water contact angles of unmodified and modified PEI membranes estimated by the captive bubble method (PAN: polyacrylonitrile, PEI: polyetherimide, PEI-OH: modification of PEI with Tris, PEI-NH, with polyethylene imine, and PEI-Hep, with heparin; numbers indicate modification time in minutes).

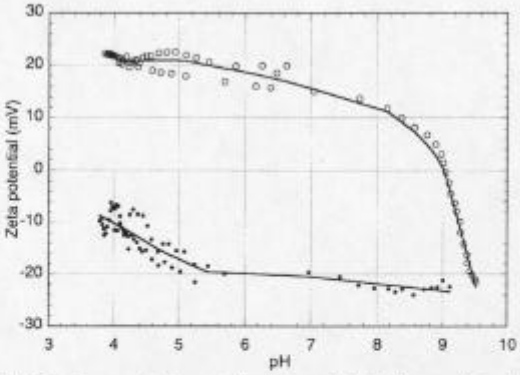

FIG. 4. The graph shows the zeta potential of non- (closed circles) and polyethylene imine-modified (open circles) PEI membranes estimated by streaming potential measurements.

In the FTIR-ATR spectra of Tris-modified PEI membranes, the typical broad absorbance band of O–H valence vibrations characteristic for the presence of hydroxyl groups was found between wave numbers 3,200 and 3,600 cm^{-1} as shown in Fig. 6. For unmodified PEI, this absorbance band was absent. The absorbance bands around 3,070 cm^{-1} origin from C–H valence vibrations on a C double binding and around 3,480 cm^{-1} from N–H valence vibrations. A quantitative evaluation of the spectra was not possible.

The density of amine groups was determined with an Acid Orange II assay and is shown in Table 1. Modification with polyethylene imine for 1 min already immobilized a considerable quantity of amine groups on the membrane's surface. Incubation for 10 min resulted in a surface density of 56.6 nmole/cm^2 with the assumption of a 1:1 binding ratio of Acid Orange II molecules to the amine groups. There was also a certain binding of dye to the unmodified membrane of about 1.1 nmole/cm^2 that was subtracted.

The density of heparin molecules in terms of international units (IU) was determined with a TB assay. Results are also shown in Table 1. After short-time modification for 1 min, already a considerable amount of heparin was immobilized that was further increased by a longer modification time up to 0.234 IU/cm^2 after 10 min. There was also some nonspecific dye binding to the unmodified membrane of about 0.029 IU/cm^2 that was subtracted.

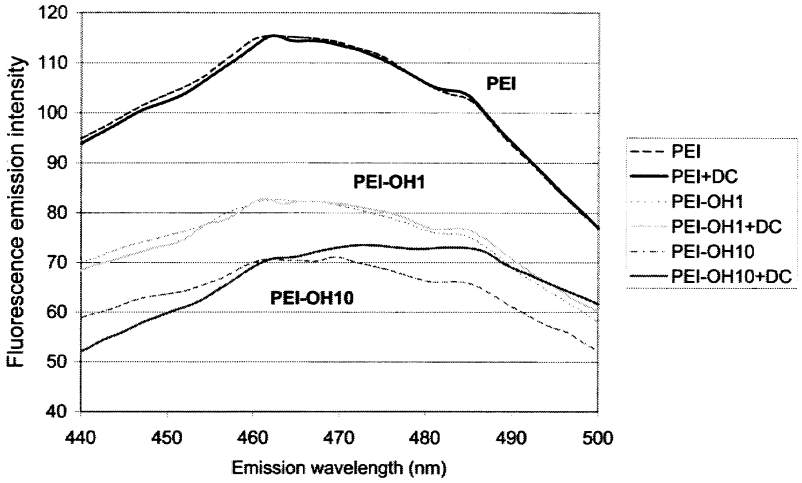

FIG. 5. Shown are fluorescence emission spectra of non- and Tris-modified PEI membranes without and with dansyl chloride (DC) labeling of hydroxyl groups (excitation at 350 nm) (PEI: polyetherimide, PEI-OH: modification of PEI with Tris, numbers indicate modification time in minutes).

Hemocompatibility

The measurement of kallikrein-like activity in PPP after 30 and 60 min contact time was used to estimate the activation of the contact system of the coagulation cascade and is shown in Fig. 7. It was found that kallikrein-like activity was highest on unmodified PEI. Surface modification with the different ligands reduced the kallikrein-like activity significantly ($p < 0.005$) to a level similar to PAN. Interestingly, longer modification with polyethylene imine (PEI-NH) and with heparin reduced the kallikrein-like activity while longer modification with Tris (PEI-OH) enhanced the activity again.

The activation of the coagulation cascade was further determined by nAPTT. Results are shown in Fig. 8. Most of the membranes including plain PEI did not cause any significant changes of the clotting time in comparison to the control PPP. However, 1 min modification with Tris resulted in a reduction of clotting time of about 10%.

Surface modification of PEI membranes also had a reducing effect on the activation of the alternative complement pathway as indicated by the results of measurement of Bb fragment shown in Fig. 9. This was evident by the fact that plain PEI generated the highest Bb fragment quantities comparable to PAN. Short-time modification with Tris (PEI-OH) and heparin (PEI-Hep) reduced the generation of the Bb fragment significantly ($p < 0.025$) although a longer functionalization up to 10 min increased the comple-

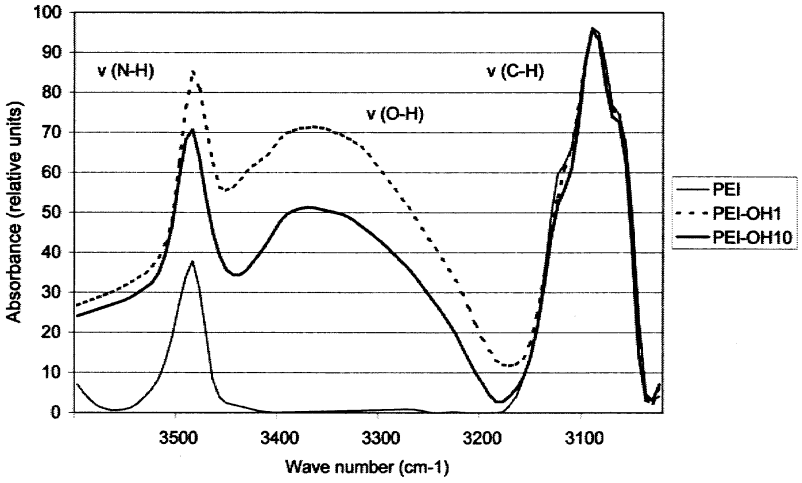

FIG. 6. Shown are FTIR-ATR spectra of non- and Tris-modified PEI membranes in the wave number region characteristic for vibrations of hydroxyl groups (PEI: polyetherimide, PEI-OH: modification of PEI with Tris, numbers indicate modification time in minutes).

TABLE 1. *Density of functional groups and ligands on PEI membranes modified with polyethylene imine and heparin sodium salt*

Membrane	Amine group density (nmol/cm^2)	Heparin density (IU/cm^2)
PEI-NH1	10.4 ± 4.9	
PEI-NH10	56.6 ± 16.0	
PEI-Hep1		0.078 ± 0.003
PEI-Hep10		0.234 ± 0.016

PEI: polyetherimide, PEI-NH: modification of PEI with polyethylene imine, and PEI-Hep, with heparin; numbers indicate modification time in minutes.

ment activation again. Interestingly, an increased content in amine functions seems to have a reducing effect on the complement activation that was visible for PEI-NH10.

Platelet adhesion on the surfaces was determined by counting the platelets before and after contact with the surface. The resulting ratio was defined as the percentage of platelet adhesion and is shown in Fig. 10. The modification with Tris (PEI-OH) seemed to have no influence on platelet adhesion while the modification with polyethylene imine (PEI-NH1 or 10) caused an increase. The immobilization of heparin resulted in a decrease of platelet adhesion particularly at 10 min modification time.

Tissue compatibility

The metabolic activity and growth of 3T3 fibroblasts were studied in direct contact with the membranes by MTT and LDH assay and are shown in Figs. 11 and 12. Millicell membranes as commercial cell culture substrata were included here as a control. Both MTT and LDH tests indicated the best conditions for the growth and function of cells on Tris-modified membranes (PEI-OH). This membrane modification yielded a metabolic activity of cells

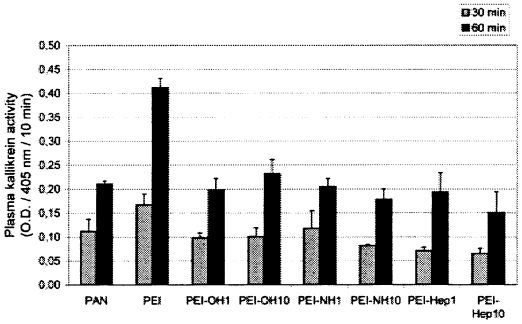

FIG. 7. The chart shows contact activation of PPP after contact to unmodified and modified PEI membranes for 30 and 60 min estimated by plasma kallikrein activity (PAN: polyacrylonitrile, PEI: polyetherimide, O.D.: optical density, PEI-OH: modification of PEI with Tris, PEI-NH, with polyethylene imine, and PEI-Hep, with heparin; numbers indicate modification time in minutes).

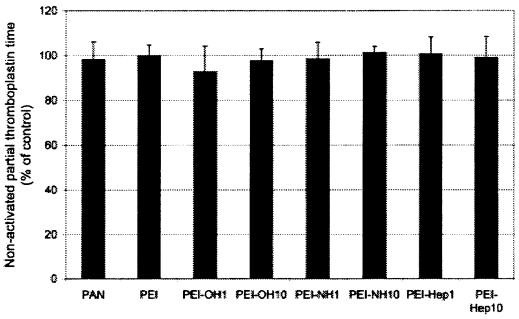

FIG. 8. The chart shows nAPTT of PPP after contact to unmodified and modified PEI membranes for 30 min (PAN: polyacrylonitrile, PEI: polyetherimide, control: plasma without contact to membrane, PEI-OH: modification of PEI with Tris, PEI-NH, with polyethylene imine, and PEI-Hep, with heparin; numbers indicate modification time in minutes).

comparable to and a growth better than on Millicell culture substrata. In contrast, the modifications with polyethylene imine (PEI-NH) and heparin caused a cellular response that was comparable to or even worse than plain PEI. Especially longer time heparinization caused lower growth of 3T3 fibroblasts on the membranes.

DISCUSSION

In this article a technique for rapid surface functionalization of PEI membranes was introduced to accommodate the membrane surface to a specific environment such as blood or tissue contact. The ligands used in this study should demonstrate that surface functionalization is possible with different compounds such as simple low molecular weight molecules such as Tris but also with intermediate or large molecular weight substances such as the polyethylene imine or heparin. On the other hand, it was

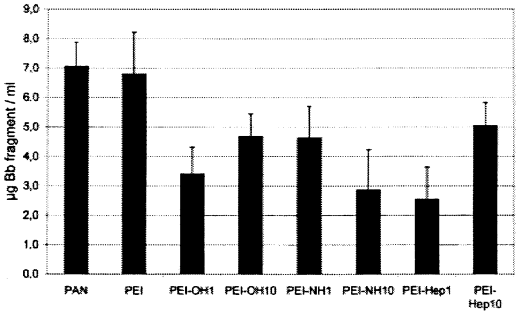

FIG. 9. The chart shows complement activation of PPP after contact to unmodified and modified PEI membranes for 15 min estimated by content of Bb fragment in plasma (PAN: polyacrylonitrile, PEI: polyetherimide, PEI-OH: modification of PEI with Tris, PEI-NH, with polyethylene imine, and PEI-Hep, with heparin; numbers indicate modification time in minutes).

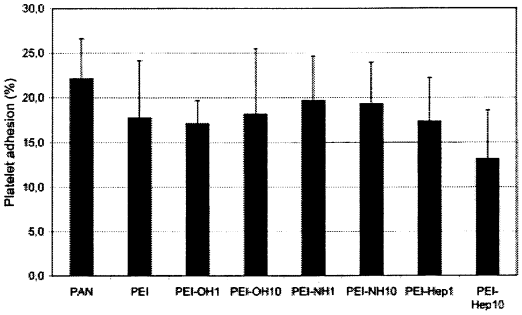

FIG. 10. The chart shows platelet adhesion on unmodified and modified PEI membranes after contact for 15 min estimated by platelet retention (PAN: polyacrylonitrile, PEI: polyetherimide, PEI-OH: modification of PEI with Tris, PEI-NH, with polyethylene imine, and PEI-Hep, with heparin; numbers indicate modification time in minutes).

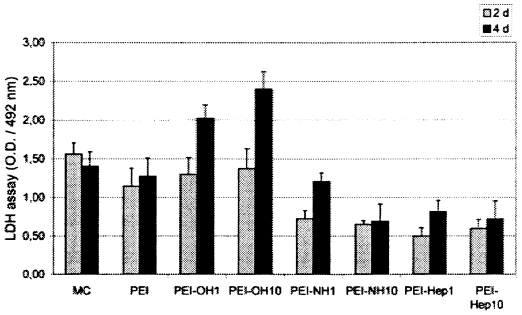

FIG. 12. The chart shows growth of 3T3 fibroblasts after 2 and 4 days of cultivation on unmodified and modified PEI membranes estimated by an LDH assay (PAN: polyacrylonitrile, PEI: polyetherimide, O.D.: optical density, MC: Millicell-HA, PEI-OH: modification of PEI with Tris, PEI-NH, with polyethylene imine, and PEI-Hep, with heparin; numbers indicate modification time in minutes).

also assumed that functionalization with hydroxyl and amine groups or heparin should have a specific effect on the blood or tissue response of the resulting material.

Monitoring the surface modification of PEI by simple water contact angle measurements demonstrated no major changes of the advancing water contact angles, indicating that the underlying polymer still expressed its hydrophobic nature. This indicates that although there was a successful modification (see below), surface coverage with the different ligands was not complete. Changes were found for receding water contact angles, indicating alterations of the surface properties due to the functionalization. Evidence for this assumption was found in the literature (35,36). However, the observed changes did not always meet the expectations.

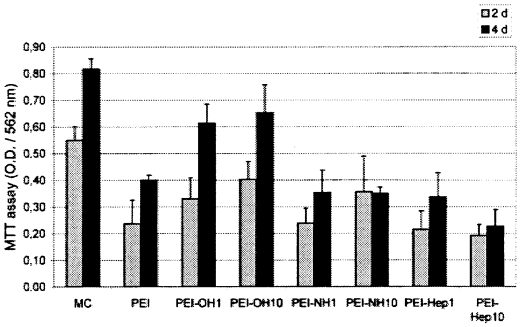

FIG. 11. The chart shows metabolic activity of 3T3 fibroblasts after 2 and 4 days of cultivation on unmodified and modified PEI membranes estimated by a MTT assay for activity of mitochondria (PAN: polyacrylonitrile, PEI: polyetherimide, O.D.: optical density, MC: Millicell-HA, PEI-OH: modification of PEI with Tris, PEI-NH, with polyethylene imine, and PEI-Hep, with heparin; numbers indicate modification time in minutes).

For example, it was supposed that the use of Tris would increase the hydrophilicity of the PEI-OH membrane by the presence of hydroxyl groups. This was observed in some of our previous work on functionalizing glycidyl group carrying surfaces (37). However, it turned out that the material became apparently more hydrophobic as indicated by the increased receding water contact angle. This would indicate some reduction in the surface roughness or porosity of the membrane surface (35) and hence indicates only a limited degree of the functionalization with the ligand. In contrast, the immobilization of polyethylene imine increased the hydrophilicity of the PEI membrane. This was interpreted as a successful surface functionalization with the more hydrophilic macromolecule polyethylene imine. The heparinization did not cause any significant changes of water contact angles. Subsequent investigations by other physicochemical measurements, however, could clearly show qualitatively or quantitatively the presence of the different functional groups such as hydroxyl or amine groups and of heparin on the membrane surface.

The hemocompatibility of plain PEI and the different membrane modifications were investigated in vitro by studying the activation of the coagulation and complement systems and the adhesion of platelets. As a result of these investigations, it was found that PEI seems to be a material with lower blood compatibility in terms of coagulation and complement activation. This was deduced from the generation of kallikrein and the Bb fragment of complement which were highest on plain PEI while all other modifications and partly PAN expressed lower values. The measurement of nAPTT that was suggested as a means to detect an influence of biomaterials on

the coagulation system (32) did not show any significant changes between the materials. According to this and our previous results (29), it seems to be less suitable in comparison to tests measuring the generation of specific activated coagulation factors, such as factor XIIa, kallikrein, or thrombin-antithrombin III complexes (38). Platelets adhered to all these surfaces to almost the same extent except that PAN had higher values here. Only a longer incubation with heparin was able to cause a significant reduction in platelet adhesion on the PEI membrane as it was also observed in our previous work on heparin immobilization (13,14). Considering all experimental results in terms of blood response so far, only immobilization of heparin seems to be a suitable means to further improve the hemocompatibility of PEI to make it more applicable to contact blood, e.g., for dialysis or the blood-contacting side in biohybrid organs.

In contrast to the blood response, the tissue compatibility differed greatly between PEI and some modifications. Comparison was made with Millicell, a commercial microporous membrane material for culture of adhesion dependent cells. It was shown in the Results section that 3T3 fibroblasts number and growth on PEI membranes were comparable to Millicell although the metabolic activity as measured by the MTT assay was significantly reduced on PEI. Immobilization of Tris, however, created a membrane surface (PEI-OH) that was superior to Millicell in terms of cell number and allowed a comparable metabolic activity of cells. The other 2 modifications with polyethylene imine (PEI-NH) and heparin (PEI-Hep), however, caused a reduction in cell number/growth and metabolic activity that makes these types of ligands less favorable for tissue-contacting membranes. Recent investigations have shown that many of the commercially available membranes are not suitable for immobilization of organ cells like hepatocytes (11,12). Our own investigations with PAN and polysulfone have revealed successfully that these materials can be used to some extent for seeding epithelial cell lines (39). However, we have observed also that primary hepatocytes do not attach and function well on these substrata. PEI membranes, however, seem to have per se a good tissue compatibility as found in this study and by others (16–18) that can be improved further by binding of adhesion promoting or biospecific ligands.

In conclusion, PEI can be considered as a promising material for the preparation of membranes for biohybrid organs. The possibility of modifying PEI membranes within short time periods (less than 10 min) provides the possibility of obtaining bifunctional membranes that can have different surface modifications on both sides. In this way, membranes could be prepared for biohybrid organs having blood and tissue compatible sides.

Acknowledgments: The authors gratefully acknowledge the support of A. Podias and N. Katsala in cell culture and blood compatibility experiments. We thank M. Schossig-Tiedemann for making the scanning electron images of PEI membranes. Dr. H. Kamusewitz is gratefully acknowledged for helpful discussions. This work was partly supported by the Federal Ministry for Education and Science (Germany) (BMBF) in the frame of the bilateral scientific and technological cooperation between Greece and Germany (Grant No. GRI 130-97 to T. Groth and Y. Missirlis).

REFERENCES

1. Paul D. Polymermembranen für die Stofftrennung. *Chemie in unserer Zeit* 1998;32:197–205.
2. von Sengbusch G, Bowry S, Viencken J. Focusing on membranes. *Artif Organs* 1993;17:244–53.
3. Klinkmann H, Viencken J. Membranes for dialysis. *Nephrol Dial Transplant* 1995;19(Suppl 3):39–45.
4. Alpard SK, Zwischenberger JB. Adult extracorporal membrane oxygenation for severe respiratory failure. *Perfusion* 1998;13:3–15.
5. Bonomini V, Coli L, Feliciangeli G, Mosconi G, Scolari MP. Long-term results: Cellulosic vs. synthetic membranes. In: Bonomini V, Berland Y, eds. *Dialysis Membranes: Structure and Predictions. Contrib Nephrol Basel* 1995;113:120–34.
6. Hirasawa H, Sugai T, Oda S, Shiga H, Matsuda K, Ueno H, Sadahiro T. Efficacy and limitation of apheresis therapy in critical care. *Ther Apher* 1997;1:223–8.
7. Colton CK. Implantable biohybrid artificial organs. *Cell Transplant* 1995;4:415–36.
8. Rozga J, Demetriou AA. Artificial liver: Evolution and perspective. *ASAIO J* 1995;41:831–7.
9. Wolf CFW, Minick CR, McCoy CH. Morphologic examination of a prototype liver assist device composed of cultured cells and artificial capillaries. *Int J Artif Organs* 1978;1:45–51.
10. Dixit V. Development of a bioartificial liver using isolated hepatocytes. *Artif Organs* 1994;18:371–84.
11. Bader A, Knop E, Fühauf N, Crome,O, Böker K, Christians U, Oldhafer K, Ringe B, Pichlmayr R, Sewing KF. Reconstruction of liver tissue in vitro: Geometry of characteristic flat bed, hollow fiber, and spouted bed reactors with reference to the in vivo liver. *Artif Organs* 1995;19:941–50.
12. Qiang S, Yaoting Y, Hongyin L, Klinkmann H. Comparative evaluation of different membranes for the construction of an artificial liver support system. *Int J Artif Organs* 1997;20: 119–24.
13. Seifert B, Groth T, Herrmann K, Romaniuk P. Immobilisation of heparin on polylactide for application to degradable biomaterials in contact with blood. *J Biomater Sci Polym Ed* 1995;7:227–87.
14. Seifert B, Romaniuk P, Groth T. Covalent immobilisation of hirudin improves the haemocompatibility of polylactide-polyglycolide in vitro. *Biomaterials* 1997;18:1495–502.
15. Jauregui HO, Chowdury NR, Chowdury JR. Use of mammalian liver cells for artificial liver support. *Cell Transplant* 1996; 5:353–67.
16. Imai Y, Watanabe A, Masuhara E, Imai Y. Structure-biocompatibility relationship of condensation polymers. *J Biomed Mater Res* 1983;17:905–12.
17. Richardson RR Jr, Miller JA, Reichert WM. Polyimide as

biomaterials: Preliminary biocompatibility testing. *Biomaterials* 1993;14:627–35.
18. Peluso G, Petillo O, Ambrosio L, Nicolais L. Polyetherimide as biomaterial: Preliminary in vitro and in vivo biocompatibility testing. *J Mater Sci Mater Med* 1994;4:738–42.
19. Kawakami H, Mori Y, Takagi J, Nagaoka S, Kanamori T, Shinbo T, Kubota S. Development of a novel polyimide hollow fiber for an intravascular oxygenator. *ASAIO J* 1997;43: M490–4.
20. Stieglitz T, Meyer JU. Implantable microsystems. Polyimide-based neuroprotheses for interfacing nerves. *Med Device Technol* 1999;10(6):28–30.
21. Le Dû C. Polyetherimide: A resin for the most demanding medical devices. *Medical Device Technology Conference,* Chester UK: Advancestar Communications Inc. March 2–3, 1999.
22. Kneifel K, Peinemann KV. Preparation of hollow fiber membranes from polyetherimide for gas separation. *J Membrane Sci* 1992;65:295–307.
23. Peinemann KV, Maggioni JF, Nunes SP. Poly(etherimide) membranes obtained from solutions in cosolvent mixtures. *Polymer* 1998;39:3411–6.
24. Ikada Y, Iwata H, Horii F, Matsunaga T, Tanigutchi M, Suzuki M, Taki W, Yamagata S, Yonekawa Y, Handa H. Blood compatibility of hydrophilic polymers. *J Biomed Mater Res* 1981;15:697–718.
25. Richau K, Eisold, C, Kudela, V, Schwarz, HH, Paul, D. Electrochemical characterization of charged membranes and membrane systems. *Desalination* 1996;104:19–26.
26. Ivanov VB, Behnisch J, Holländer A, Mehdorn F, Zimmermann H. Determination of functional groups on polymer surfaces using fluorescence labelling. *Surf Interface Anal* 1996; 24:257–62.
27. Uchida E, Uyama Y, Ikada Y. Sorption of low-molecular-weight anions into thin polycation layers onto a film. *Langmuir* 1993;9:1121–4.
28. Smith PK, Mallia AK, Hermanson GT. Colorimetric method for the assay of heparin content in immobilised heparin preparations. *Anal Biochem* 1980;109:466–73.
29. Groth T, Synowitz J, Malsch G, Richau K, Albrecht W, Lange KP, Paul D. Contact activation of plasmatic coagulation on polymeric membranes measured by the activity of kallikrein in heparinised plasma. *J Biomater Sci Polym Ed* 1997;8: 797–807.
30. Rhodes NP, Williams DF. Plasma recalcification as a measure of contact phase activation and heparinisation efficacy after contact with biomaterials. *Biomaterials* 1994;15:35–37.
31. Kazatchkine MD, Nydegger UE. The human alternative complement pathway: Biology and immunopathology of activation and regulation. *Prog Allergy* 1982;30:193–234.
32. Rhodes NP, Wilson DJ, Williams DF. Relationship between leukocyte attachment and complement activation mediated by polymers. *Cellular Engineering* 1997;2:1–6.
33. Ward RA, Klein E, Harding GB, Murchison K. Response of complement and neutrophils to hydrophilised synthetic membranes. *ASAIO Trans* 1988;34:334–7.
34. Schmidt B, Mujais SK. Evaluation of dialysis membrane blood compatibility: Experimental methods. In: Bonomini V, Berland Y, eds. *Dialysis Membranes: Structure and Predictions. Contrib Nephrol* 1995;113:32–44.
35. Kamusewitz H, Possart W, Paul D. The relation between equilibrium contact angle and the hysteresis on rough paraffin wax surfaces. *Colloids and Surfaces A: Physicochemical and Engineering Aspects* 1999;156:271–9.
36. Vienken J, Diamantoglou M, Hahn C, Kamusewitz H, Paul D. Considerations on developmental aspects of biocompatible dialysis membranes. *Artif Organs* 1995;19:398–406.
37. Groth T, Altankov G. Insights into the tissue compatibility of biomaterials. In *Proceedings of the 9th International Conference Polymers in Medicine and Surgery,* London: IOM Communications 2000;205–13.
38. Lindhout T. Biocompatibility of extracorporal blood treatment. Selection of haemostatic parameters. *Nephrol Dial Transplant* 1994;9(Suppl 2):83–9.
39. Fey-Lamprecht F, Groth Th, Albrecht W, Paul D, Gross U. Development of membranes for the cultivation of kidney epithelial cells. *Biomaterials* 2000;21:183–92.

Publikation 17

Thomas Groth, Barbara Seifert, Günter Malsch, Wolfgang Albrecht, Dieter Paul, Anelia Kostadinova, Natalia Krasteva, George Altankov (2002).

Interaction of human skin fibroblasts with moderate wettable polyacrlyonitrile copolymer membranes.

Journal of Biomedical Materials Research **61**, 290-300.

Interaction of human skin fibroblasts with moderate wettable polyacrylonitrile–copolymer membranes

Thomas Groth,[1] Barbara Seifert,[1] Günter Malsch,[1] Wolfgang Albrecht,[1] Dieter Paul,[1] Anelia Kostadinova,[2] Natalia Krasteva,[2] George Altankov[2]

[1]*Department of Biomaterials, Institute of Chemistry, GKSS Research Centre, Kantstrasse 55, D-14513 Teltow, Germany*

[2]*Institute of Biophysics, Bulgarian Academy of Sciences, Str. Acad. G. Bonchev, bl. 21, BG-1113 Sofia, Bulgaria*

Received 28 June 2001;revised12 September 2001; accepted 28 November 2001

Abstract: The development of a bioartificial skin is a step toward the treatment of patients with deep burns or nonhealing skin ulcers. One possible approach is based on growing dermal cells on membranes to obtain appropriate living cellular stroma (sheets) to cover the wound. New membrane-forming copolymers were synthesized, based on acrylonitrile (AN) copolymerization with hydrophilic N-vinylpyrrolidone (NVP) monomer, in different percentage ratios, such as 5, 20, and 30% w/w, and with two other relatively high polar comonomers—namely, sodium 2-methyl-2-propene-1-sulfonic acid (NaMAS) and aminoethylmethacrylate (AeMA). All these copolymers were characterized for their bulk composition and number average molecular weight, and used to prepare ultrafiltration membranes. Water contact angles and water uptake were estimated to characterize the wettability and scanning force microscopy to visualize the morphology of the resulting polymer surface. Cytotoxicity was estimated according to the international standard regulations, and the materials were found to be nontoxic. The interaction of the membranes with human skin fibroblasts was investigated considering that these cells are among the first to colonize membranes upon implantation or with prolonged external contact. The overall cell morphology, formation of focal adhesion contacts, and cell proliferation were estimated to characterize the cell material interactions. It was found that the pure polyacrylonitrile homopolymer (PAN) membrane provides excellent conditions for seeding with fibroblasts, comparable only to a copolymer containing AeMA. In contrast, the presence of NaMAS with acidic ionic groups decreased both the attachment and proliferation of fibroblasts. Low content of NVP in the copolymer, up to about 5%, still enabled good attachment and spreading of cells, as well as subsequent proliferation of fibroblasts, but higher ratios of 20 and 30% resulted in a significant decrease of these cellular activities. © 2002 Wiley Periodicals, Inc. J Biomed Mater Res 61: 290–300, 2002

Key words: acrylonitrile copolymers; hydrophilic; hydrophobic; human skin fibroblasts; tissue engineering

INTRODUCTION

Many tissue-engineered products are based on *in vitro* cultivation and propagation of cells derived from natural tissues.[1] They have to be specifically shaped to provide mechanical support to replace part of the tissue or organ. Therefore, the cells are usually cultured on synthetic or natural scaffolds. The basic requirement of these scaffolds is their high porosity allowing sufficient delivery of nutrients and oxygen, as well as removal of metabolites.[2] In this respect, the application of synthetic membranes recently has been considered to be very prospective, as their chemical composition and mechanical properties can be easily modified according to specific needs.[3–6] The first tissue-engineered organ, processed from the lab for the first accepted patients' care, was skin.[7] Currently, there is a huge number of patients with deep burns or nonhealing skin ulcers, and many of them would benefit from a large-scale production of bioartificial skin.[8] The common tissue engineering technologies are based on the creation of living stroma of fibroblasts and/or keratinocytes, which have been cultured to obtain sufficient cell numbers.[9–11] Conventional monolayer cell culture systems, however, do not provide the normal cellular environment for large-scale production and may enhance dedifferentiation of cells.[12,13] Moreover, under such conditions the cells may suffer from insufficient delivery of oxygen and nutrients. Furthermore, the mechanical stability of these skin substitutes, as well as their method of application to the wound, suf-

Correspondence to: Thomas Groth; e-mail: Thomas.Groth@gkss.de or George Altankov; e-mail: altankov@obzor.bio21.bas.bg

Contract grant sponsor: NATO; contract grant number: LST 975147

Contract grant sponsor: European Communities; contract grant number: BE 97-432

fer from technical problems,[11] which still are not completely resolved. Thus, the implementation of a bioengineered skin consisting of cultured dermal cells on polymer membranes may be considered as one step toward the treatment of wounds and for the substitution of large areas of skin.

Attachment, proliferation, and function of anchorage-dependent cells are greatly dependent on the surface properties of the underlying substratum.[12,14] Fibroblasts, as highly motile and adhesive mesenchymal cells, are among the first cells to colonize implants. These cells can proliferate and produce significant amounts of extracellular matrix (ECM), which opsonize the foreign material that might be important for subsequent interaction with epithelial cells.[15] In general, fibroblasts attach and grow better on hydrophilic, as well as moderately wettable surfaces, accompanied by the development of sufficient cell spreading, arrangement of focal adhesion contacts and actin cytoskeleton.[16] Subsequently, these cells synthesize and organize extracellular matrix, a process also dependent on the wettability of substrata.[17] The type of functional groups exposed on the surface also influences cellular behavior. For example, from our experiments,[18] and that of others[19] it became evident that fibroblasts grow and function better on functionalized amine groups than on surfaces containing acidic ionic groups.

Fibroblasts are an essential constituent for the construction of skin substitutes consisting of dermal and epidermal components. Hence, in this study, we have tried to highlight the role of the chemical composition of polymer membranes for the attachment, morphology and growth of human skin fibroblasts. We have applied a polyacrylonitrile (PAN) homopolymer and three new membrane-forming copolymers based on acrylonitrile (AN) copolymerization with hydrophilic N-vinylpyrollidone (NVP) monomer, in different percentage ratios—5, 20, and 30%—or with two other relatively polar comonomers—namely, sodium 2-methyl-2-propene-1-sulfonic (NaMAS) and aminoethylmethacrylate (AeMA). All these copolymers were characterized and used to prepare relatively dense membranes with ultrafiltration properties. These dense membranes with pores in the nanometer scale should avoid any topographical influence in discovering only the effect of polymer composition. Fibroblast morphology was studied with confocal laser scanning microscopy because of their high fluorescent background and relatively low transparency. We found that an increasing amount of NVP comonomer reduced the attachment, spreading, and proliferation of cells. In contrast, PAN homopolymer and amine groups containing AN-copolymer P(AN-AEMA) expressed considerably better properties with regard to fibroblast interactions. Details of this study are reported herein.

MATERIALS AND METHODS

Polymer synthesis

The copolymers studied comprise three polyacrylonitrile derivatives functionalized by (1) the nonionic, but strong hydrophilizing comonomer NVP, (2) the primary amine group containing comonomer AeMA, and (3) the anionic comonomer NaMAS. The introduction of these monomers was achieved by a free-radical random copolymerization technique to obtain copolymers with graduated compositions and excellent membrane-forming properties. Homopolymerized PAN was included as reference material (Fig. 1). The synthesis is described below.

The basic AN monomer (Merck, >99% purity) was distilled before use, whereas the other comonomers, such as NVP (Aldrich; 99% purity), AeMA (Polyscience, Inc.), and NaMAS (Aldrich; 98% purity) were used without further purification. Dimethylformamide (DMF) (Aldrich; 99.8% purity) was distilled at 40 mbar/60°C before application as an aprotic solvent in polymer synthesis. 2,2′-azoisobutyronitrile (AIBN) (recrystallized twice from water at 30°C) was used as free radical initiator in the case of AN homopolymerization and ammonium peroxide sulfate (APS) (fractionally crystallized from ethanol at 40°C) for AN copolymerization, respectively. The solution polymerization was carried out by filling the reactor with DMF, adding AN followed by the comonomer, and finally the initiator. The reaction times listed in Table I reached from about 60 min for NVP up to 1440 min for NaMAS to obtain the required conversions *U*. In the case of APS-initiated copolymerization, the temperature was adjusted to 50°C, except for the NaMAS copolymer (45°C). In the case of AIBN-initiated AN

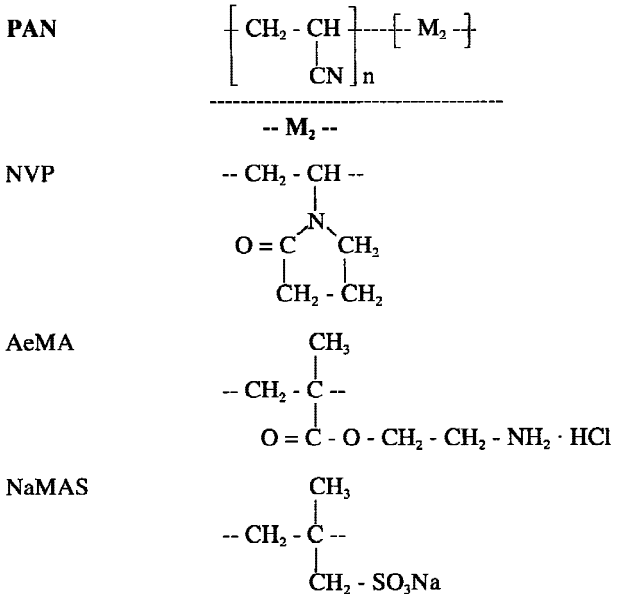

Figure 1. Structure formulas of polyacrylonitrile and the comonomers (PAN: polyacrylonitrile; M_2: second monomer or comonomer; NVP: N-vinylpyrrolidone; AeMA: aminoethyl-methacrylate; NaMAS: sodium 2-methyl-2-propene-l-sulfonic acid).

TABLE I
Polymer Synthesis Parameters and Characteristics[a]

			Synthesis Parameters			Polymer Characteristics	
	Polymerization Pattern	Comonomer	$X_{com.}$ (mol %)	t (min)	U (%)	$X_{com.in\ polym.}$ (mol %)	$M_{n,Osm.}$ (10^3 g/mol)
PAN	PAN	—	—	360	28.6	—	48.5
NVP5	P(AN-NVP5)	N-vinylpyrrolidone	2.0	120	26.5	4.8	38.8
NVP20	P(AN-NVP20)	N-vinylpyrrolidone	9.9	60	26.9	20.9	37.5
NVP30	P(AN-NVP30)	N-vinylpyrrolidone	21.6	90	44.5	31.1	105.0
AeMA	P(AN-AeMA)	Aminoethyl-methacrylate	1.0	360	20.6	5.2	57.0
NaMAS	P(AN-NaMAS)	Sodium 2-methyl-2-propene-1-sulfonic acid	1.03	1440	42.1	1.9	19.6

[a] $X_{com.}$: Comonomer concentration in reaction mixture; t: reaction time; U: conversion; $X_{com.in\ polym.}$: comonomer content in copolymer; $M_{n,\ Osm}$: number average molecular weight determined osmometrically.

homopolymerization the temperature was 54°C as in previous experiments.

The applied total monomer concentration ([M] = 3.8 mol/L) included well-graduated molar ratios of the comonomer in the feed, ranging from zero for PAN up to 31.1 mol % for the NVP-enriched feed. In the case of NVP, the initial monomer feed composition was calculated from our own predetermined AN/NVP monomer that which were predicted to be 5, 20, and 30 mol % NVP, respectively. On the other hand, in the case of the AeMA copolymer series, this monomer reactivity ratio was still unknown and the initially applied feed compositions of 0.05, 0.1, and 1.0 mol % AeMA, respectively, were chosen to obtain copolymers with significant lower comonomer content than in the case of the NVP copolymers. For further experimental work, only the copolymer with the highest AeMA content was applied in this study. Finally, in the case of NaMAS copolymer, only the comonomer molar ratio of 1.0 mol % NaMAS in the feed was applied as an example for low-density charged copolymers.

At the end of the reaction, the polymer solutions were poured into a large excess of ethanol. The precipitated polymer was filtered, washed, and rinsed with dehydrated ethanol and dried in vacuum.

Polymer characterization

The polymer samples were characterized by chemical composition and molecular weight analysis, respectively. In the case of the molecular weight determination, osmotic pressure measurements were carried out with an automatic membrane osmometer-type Osmomat 090 (Gonotec GmbH, Berlin, Germany) to obtain the average molecular weight values M_n. The measurements of osmotic pressure were carried out at 45°C. The average molecular weight was calculated by linear regression using a pressure–concentration plot.

Chemical composition analysis was performed with an EA 1110 automatic elemental analyzer (CE Instruments, Rodano, Italy). Based on the installed carbon, hydrogen, nitrogen, and sulfur (CHNS) version, a simultaneous determination of these elements was possible. The obtained data for S and N were used to calculate the molar fraction compositions of the different copolymers.

Membrane formation

Flat ultrafiltration membranes with an asymmetric pore structure across the wall were prepared by a conventional phase inversion process on a nonwoven support (Histar 100). The polymers were dissolved in DMF at concentrations between 15 and 40% polymer depending on the viscosities of the polymer solutions. The polymer solution had a temperature of 1–2°C and was spread as a solution film onto the surface of nonwoven supports continuously drawn into a water precipitation bath with a drawing speed of 4 m/min. After annealing in water for 10 min at 65 and 90°C, respectively, to remove residual solvent, the membranes were stored in distilled water containing 0.02 NaN_3. For all experiments, membranes were washed thoroughly with distilled water to remove NaN_3.

Contact angle measurements

Contact angles (CA) were measured using the captive bubble method, where an air bubble is injected from a syringe with a stainless steel needle onto the inverted sample surfaces immersed into ultra pure Milli-Q water. The diameter of the contact area between surface and bubble was always greater than 3 mm. Advancing and receding contact angle measurements were performed with a goniometer (Carl Zeiss, Jena, Germany) by stepwise withdrawing/adding of air from/to the captured bubble. Contact angle measurements were carried out with membranes and spin-coated films of the polymers. At least ten measurements of different bubbles, on at least three different locations, were averaged to calculate one CA value.

Water uptake

The water uptake was estimated to characterize the hydrophilicity of the polymer bulk phase. Membranes were not used because of their porosity, which could influence the water content. Hence, dense polymer films were prepared in Petri dishes (diameter 5 cm) from 10 mL of 2 wt % polymer

solutions solved in DMF. After evaporation of solvent, the resulting films were cut into 3 pieces. These parts were immersed in distilled water for 24 h at room temperature. The surface-bound water was lightly dabbed with tissue. The weight loss with drying was measured in a HR73 moisture analyzer (Mettler-Toledo GmbH, Giessen, Germany) and used to calculate the water uptake.

Scanning force microscopy (SFM)

The surface topography of membranes was investigated with scanning force microscopy. A multimode scanning force microscope (NanoScope IIIa, Digital Instruments, Inc., Santa Barbara, CA, USA) was used in contact mode with a commercial silicon cantilever to analyze the membrane surface under contact with distilled water.

Cell culture

Human skin fibroblasts (Cell lining GmbH, Berlin, Germany) were grown in Dulbecco's modified Eagle's medium (DMEM), supplemented with 10 m*M* *N*-(2-hydroxyethyl)piperazine-*N*′-ethanesulfonic acid (HEPES) buffer (Biochrom KG, Berlin, Germany), antibiotic/antimycotic solution (Sigma-Aldrich, Taufkirchen, Germany), and 10% fetal bovine serum (FBS) (Biochrom KG, Berlin, Germany). Cells were harvested at 80–90% confluence with 0.05% trypsin–>0.02% ethylenediaminetetraacetic acid (EDTA) (Sigma-Aldrich, Taufkirchen, Germany).

Membrane disks (diameter 13 mm) were sterilized with 70% ethanol in 24-well cell culture plates. The membranes were fixed with special Teflon rings (inner diameter 11 mm, outer diameter 15 mm) to the bottom of culture plates to avoid floating. The cell suspension was added to each well (1 mL per well) at a final density of 5×10^4 cells/well and incubated at 37°C in 5% CO_2 for the times indicated.

Cytotoxicity

The 3T3 fibroblasts (3T3, ATCC CCL 163) grown in DMEM containing 10% FBS were used for cytotoxicity testing. Cells were harvested at 80–90% confluence with 0.05% trypsin–>0.02% EDTA and seeded at densities of 10^4 cells per well in 96-well plates. After 24 h the medium was replaced by extracts prepared from membranes and cultured again for 24 h. Extracts were prepared by incubating 5 cm^2 of membranes in 8 mL DMEM at 37°C for up to 7 days. The metabolic activity of cells after incubation with the extracts was measured with the XTT assay (Boehringer Mannheim, Penzberg, Germany) based on the conversion of the tetrazolium salt sodium 3′-[1-(phenylaminocarbonyl)-3,4 tetrazolium]-bis(4-methoxy-6-nitro)benzene-sulfonate (XTT). The neutral red assay (NR) was used to detect possible changes of cell viability and membrane integrity as a result of cytotoxicity of membranes.[20] Brass was used as positive (cytotoxic), and pure DMEM solution as negative, controls.

Visualization of cell morphology and spreading

Overall morphology of living fibroblasts was visualized with fluorescein diacetate (FDA) (Sigma-Aldrich, Taufkirchen, Germany) staining. Cells were seeded on the various membranes and cultured for 72 h. Then 5 μL FDA stock solution (1 mg/mL in acetone) was added to 500 μL medium supernatant. After 5 min staining with FDA, the solution was exchanged by fresh medium. The membranes were mounted in a drop of medium to glass slides and investigated immediately with a confocal laser scanning microscope LSM 510 (Carl Zeiss, Jena, Germany). The obtained images were further processed with the image analyzing software KS 300 (Carl Zeiss Vision, Eching, Germany) to estimate the spread area and form factor of adhering cells.

Vinculin staining

Immunofluorescence staining of vinculin to visualize focal adhesions was carried out after 24 h of incubation. The cells were fixed with 3% paraformaldehyde, permeabilized for 10 min with 0.5% Triton-X 100, and saturated with 1% bovine serum albumin (BSA) for 15 min. Then, cells were incubated for 45 min at 37°C with a monoclonal antivinculin antibody (Sigma-Aldrich, Taufkirchen, Germany) followed by 30 min incubation with Cy3-conjugated goat-antimouse immune globulin G (Jackson Immuno Research Laboratories, Inc., USA) as secondary antibody. Finally, the samples were mounted to glass slides and studied with confocal laser scanning microscopy.

Cell proliferation

The proliferation of fibroblasts was determined at 1, 2, and 4 days of incubation by lactate dehydrogenase (LDH) assay. The LDH assay reflects the activity of cytosolic lactate dehydrogenase, which can be used to estimate the number of cells.[21] The assay kits were obtained from Boehringer Mannheim (Penzberg, Germany) and used as suggested by the manufacturer. Each experiment was performed in quadruplicate.

RESULTS

Chemical composition and molecular weight characteristics of polymers

The chemical composition of the resulting copolymers was estimated by elemental analysis and is

shown as x_{com} (molar comonomer content) in Table I. In the case of NVP copolymer synthesis, the predicted compositions of about 5, 20, and 30 mol % NVP could be achieved well, using the calculated NVP feed compositions with x_{feed} = 2.0, 9.9, and 21.6 mole % NVP, respectively. These copolymers were classified according to their actual NVP content and named as NVP5, 20, or 30. The comonomer content of the amine containing copolymer was found to be about 5 mol % and was named AeMA. The sulfone group containing polymer contained about 2 mol % comonomer and was named NaMAS.

Water contact angles and water uptake

PAN was found to be a moderately wettable polymer membrane with water contact angles of about 60° for the advancing (wetting) and about 43° for the receding (dewetting) mode (Fig. 2). Copolymerization of AN with NVP resulted in only minor changes of wettability displayed by a small decrease in the receding water contact angles. The expected higher hydrophilicity of NVP containing membranes was not observed, indicating some influence of the membrane formation process on water contact angles. Only dense films of the polymers, which were prepared by spin coating on glass slides, showed decreasing water contact angles with increasing NVP content (Fig. 2). The largest change of wettability was found for NaMAS where both advancing and receding contact angles decreased to about 18° and 16°, respectively, indicating a highly hydrophilic membrane surface. Interestingly, the spin-coating film of NaMAS had much higher water contact angles than the membrane. The AeMA copolymer membrane had a higher advancing contact angle and hence represented a more hydrophobic surface when compared to the pure PAN membrane. It is noteworthy that the receding water contact angle decreased for all copolymer membranes studied when compared to pure PAN.

Water uptake was estimated to further characterize the interaction of the different copolymers with an aqueous environment. As shown in Fig. 3, the water uptake of copolymer films increased with increasing content of NVP. A particularly high water uptake, which led to an increase in weight of about 40 and 50%, was observed for NVP20 and NVP30, respectively. This is a strong indication for swelling of these polymers. NaMAS also has been shown to be a highly hydrophilic surface according to the water contact angle measurements; a rather high water uptake comparable to that of NVP20 was observed. On the other hand, water uptake of pure PAN, NVP, and AeMA was about 20%.

Scanning force microscopy

Scanning force micrographs of the polymer membrane surface are shown in Figure 4. The images obtained via SFM analysis were also quantified to yield the average surface roughness (Table II). It is evident that in the 1 μm region NaMAS had the smoothest surface together with NVP20 and NVP30. At this scale, the reduced surface roughness of membranes with higher NVP content was probably determined by swelling of the polymers. PAN, NVP5, and AeMA had visibly comparable surface roughness. Because of the similarities in surface roughness, only PAN, NVP5, NVP20, and NVP30 are shown in Figure 4.

Overall cell morphology

The overall cell morphology was estimated after 72 h by staining with FDA. Striking differences were observed between the membranes with higher content of

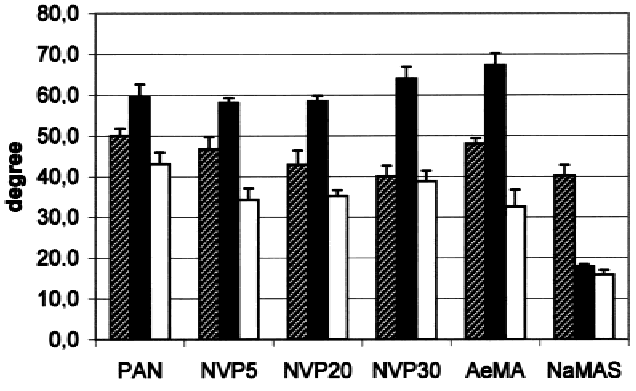

Figure 2. Advancing (wetting, black/shaded columns) and receding (dewetting, white columns) water contact angles of polyacrylonitrile and the copolymers as films (shaded columns) and membranes (black/white columns).

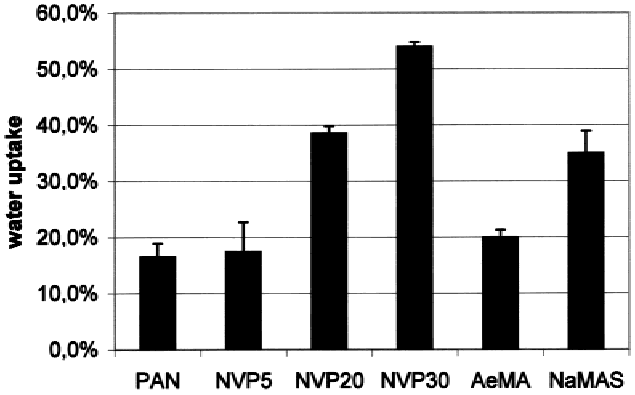

Figure 3. Water uptake of polyacrylonitrile and the copolymer films after 24 h incubation in distilled water at room temperature.

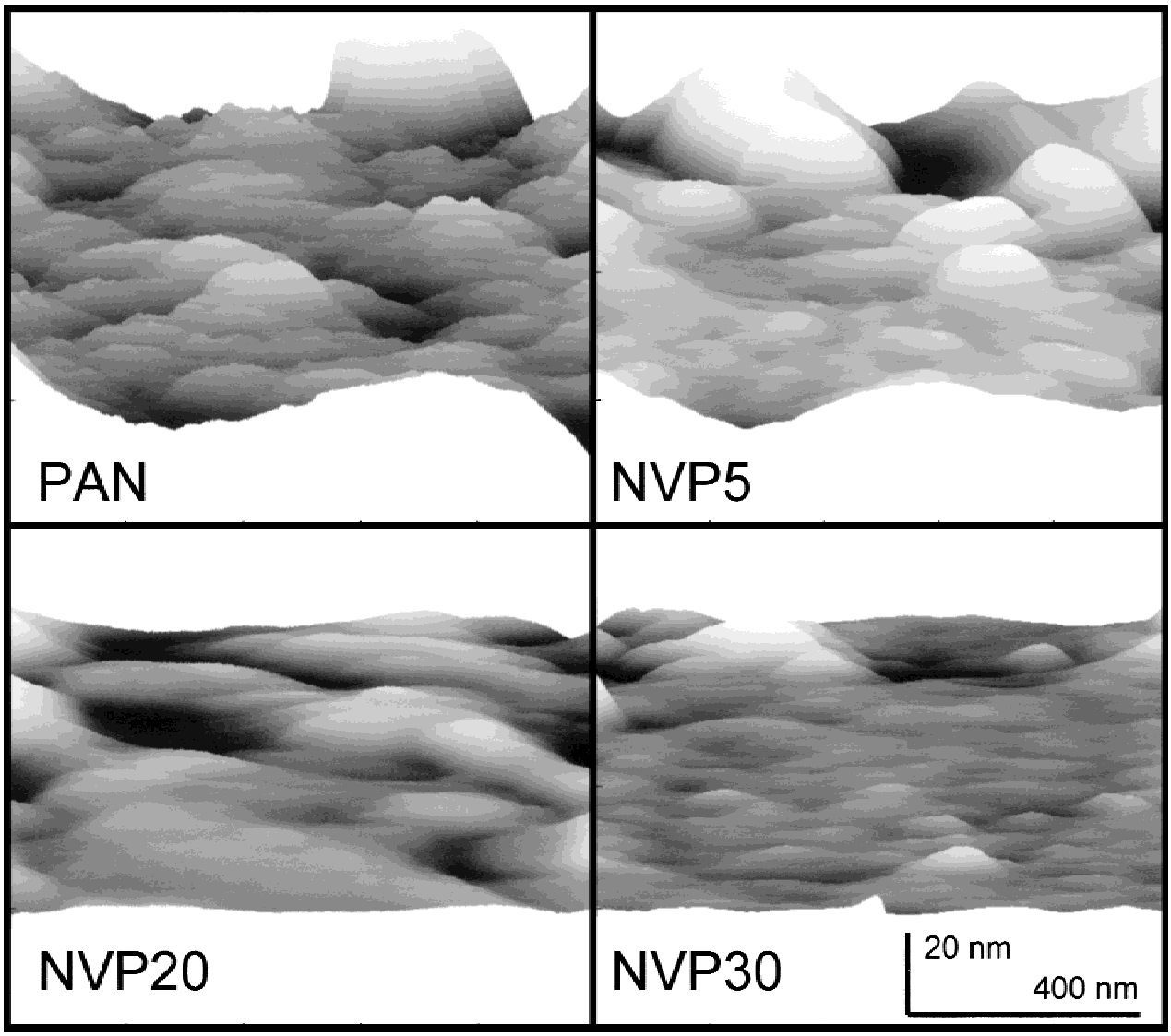

Figure 4. Fluid-mode scanning microscopy images of the polymer membrane surfaces. The views depict the topography of a square area, 1 μm wide, as would be seen from the front with a 30° pitch.

NVP and the other materials as shown in Figure 5. The cell layer on PAN was almost confluent (a) while the increasing NVP content caused a reduction in cell number and change of cell shape [Fig. 5(b–d)]. Fibroblasts plated on AeMA grew to a similar extent as on PAN [compare Fig. 5(a) and Fig. 5(e)]. However, it seemed that they were more spread in comparison to cells grown on NaMAS [Fig. 5(f)].

TABLE II
Average Surface Roughness of Polyacrylonitrile and the Copolymer Membranes Estimated by Scanning Force Microscopy for a Scanning area of 1 μm × 1 μm

Membrane	Average Surface Roughness (nm)
PAN	2.59
NVP5	2.70
NVP20	1.40
NVP30	0.90
AeMA	2.09
NaMAS	1.23

To compare the differences in cell shape and spreading quantitatively, image analysis was performed. The results shown in Table III demonstrate a strong decrease of the spread area for NVP20 and NVP 30. The spread area of fibroblasts grown on PAN, NVP5, and AeMA was comparable while some slight reduction was observed for NaMAS. The calculation of the form factor, which can range from 1 (circular shape) to about 0 (linear shape), was only elevated for NVP20 and NVP30, which goes along with the observation that round cells were detected on these materials.

Vinculin staining

Focal adhesions were visualized by vinculin (Fig. 6). On all membranes, except on NVP30, the focal adhe-

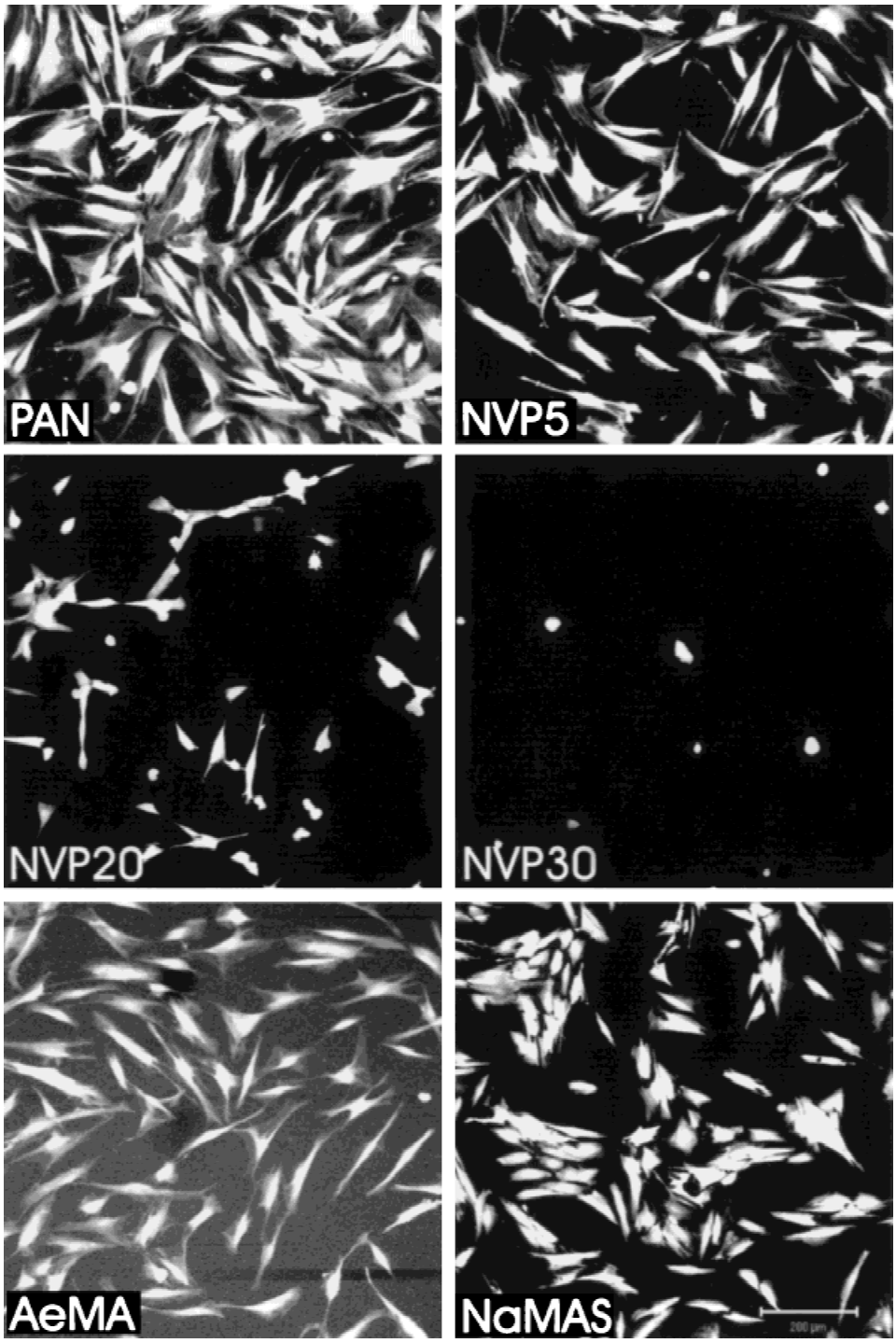

Figure 5. Visualization of cell morphology by vital stain (FDA) after 72 h of incubation of human fibroblasts on membranes of polyacrylonitrile and the copolymers (bar 200 μm).

sion contacts were visible. The strongest expression of focal adhesions was observed in cells plated on PAN and NVP5 [Fig. 6(a) and Fig. (b)]. Further increase in the amount of NVP, however, clearly disturbed the formation of the focal adhesion plaques since they became shorter and less intense on NVP20 and disappeared on NVP30 [Fig. 6(c,d)]. Fibroblasts with high spreading on the support like PAN and NVP5 [Fig. 6(a,b)], developed focal adhesions organized in long stripes toward the direction of cell polarization, while slightly reduced interaction of cells with AeMA and NaMAS [Fig. 6(e,f)] was indicated by shorter and dot-like clusters of vinculin.

Cytotoxicity and proliferation assays

No cytotoxicity of membrane extracts was detected by the application of XTT and NR tests. Figure 7

TABLE III
Average Spread Area and Form Factors of Human Fibroblasts After 72 h on Polyacrylonitrile and the Copolymer Membranes Estimated by Image Analysis After Vital Staining (FDA) and Immunofluorescence Imaging with a Confocal Laser Scanning Microscope

Membrane	Average Spread Area ($\mu m)^2$	Form Factor
PAN	3678 ± 1427	0.303 ± 0.125
NVP5	3018 ± 1281	0.294 ± 0.107
NVP20	1104 ± 585	0.428 ± 0.200
NVP30	518 ± 232	0.739 ± 0.099
AeMA	3080 ± 1635	0.324 ± 0.138
NaMAS	1681 ± 664	0.346 ± 0.139

shows the result of XTT test as an example. It is clear that none of the membrane materials caused a strong reduction of the metabolic activity of 3T3 fibroblasts in comparison to DMEM as negative control. On the other hand, extracts prepared from brass that served as cytotoxic control caused a total inhibition of cell metabolism. Since results of the NR test were quite similar, they are not shown here.

The adhesion and growth of human fibroblasts on membranes were assessed up to 4 days with the LDH assay (Fig. 8). After 24 h the highest number of attached cells was found on PAN and NVP5 , while on NVP20 the lowest attachment was observed. During the next 24 h a significant increase in the number of cells was observed for all membranes except on NVP30 where only a slight increase in LDH activity of cells was found. After 4 days cell proliferation was highest on PAN, NVP5 and AeMA. A reduced growth of cells was detected on NVP20 followed by NVP30. Also, NaMAS diminished the proliferation of fibroblasts in comparison to PAN, NVP5, and AeMA.

DISCUSSION

In this paper we studied the influence of copolymer composition including the effect of hydrophilizing the primary amine or ionic sulfone group containing comonomers on the attachment, morphology, and proliferation of human skin fibroblasts. All materials were nontoxic as tested with mouse 3T3 fibroblasts.[22] The basic observation was that an increase in the hydrophilizing NVP comonomer content above 5% w/w had a negative impact on the attachment and growth of fibroblasts. A similar result was obtained for acidic sulfone groups, while in contrast, pure PAN and the presence of primary amine functions resulted in a better cellular response.

Synthesis of these polymers was aimed at obtaining materials with good membrane forming properties and tissue compatibility. The requirement useful in preparing phase inversion membranes was successfully tested in previous investigations.[23,24] Preparation of dense membranes should avoid any influence of membrane topography on the interaction with fibroblasts. This was concluded from recent studies that have shown an effect of membrane pores on the response of cells, only if pores have diameters in the micrometer scale.[25,26] In fact, the membranes used in this study possessed average pore sizes smaller than 10 nm. This was evident from water permeation studies (not shown here) and the SFM investigations indicating that all membrane surfaces studied were relatively smooth in a scale up to 1 μm. Water contact angle measurements showed that PAN possessed a moderately wettable surface, eliciting the most positive response to fibroblasts in terms of cell attachment, spreading, and proliferation. Surprisingly, the increase in hydrophilizing NVP content was not accompanied by decreasing membrane water contact angles. However, when spin-coated films of these polymers were prepared, a decrease of the advancing water contact angle with increasing NVP content was observed. A similar observation was made for NaMAS, as these membranes had very low advancing and receding water contact angles, while contact angles of spin-coated films were only a little different from PAN. This indicates some influence of the membrane formation process on the surface wettability of these polymers.[27,28] Since the differences in wettability between the membranes were rather small (except NaMAS), particularly for NVP containing copolymers, we decided to characterize the hydrophilicity of these polymers further by their water uptake to explain some of the results obtained in the biological experiments. Here it was observed that copolymers with 20 and 30 mol % NVP had a tremendous water uptake in comparison to the other materials. This clearly indicates a swelling of these membranes, and because of the stronger hydration, it must reflect their ability to host cells. A similar high water uptake was also observed for NaMAS. However, since this material possesses ionic sulfone groups, stronger attractive forces for proteins and cells can be anticipated[29] that result in a different biological response (see below). Scanning force microscopy of fully hydrated membranes provided some further evidence that membranes with higher water uptake had a reduced surface roughness thus indicating their swelling.

When the fibroblast attachment was investigated after 24 h, before proliferation had begun, the differences between the biological properties of materials were obvious. Staining for vinculin showed that attachment and spreading of fibroblasts was decreased on NVP20 and NVP30. Focal adhesion became shorter and disappeared completely at a NVP content of 30%, which points to the lower adhesive potential of these materials. This decrease in cell adhesion can be explained by the higher water uptake of these polymers, probably reducing adsorption of attachment proteins

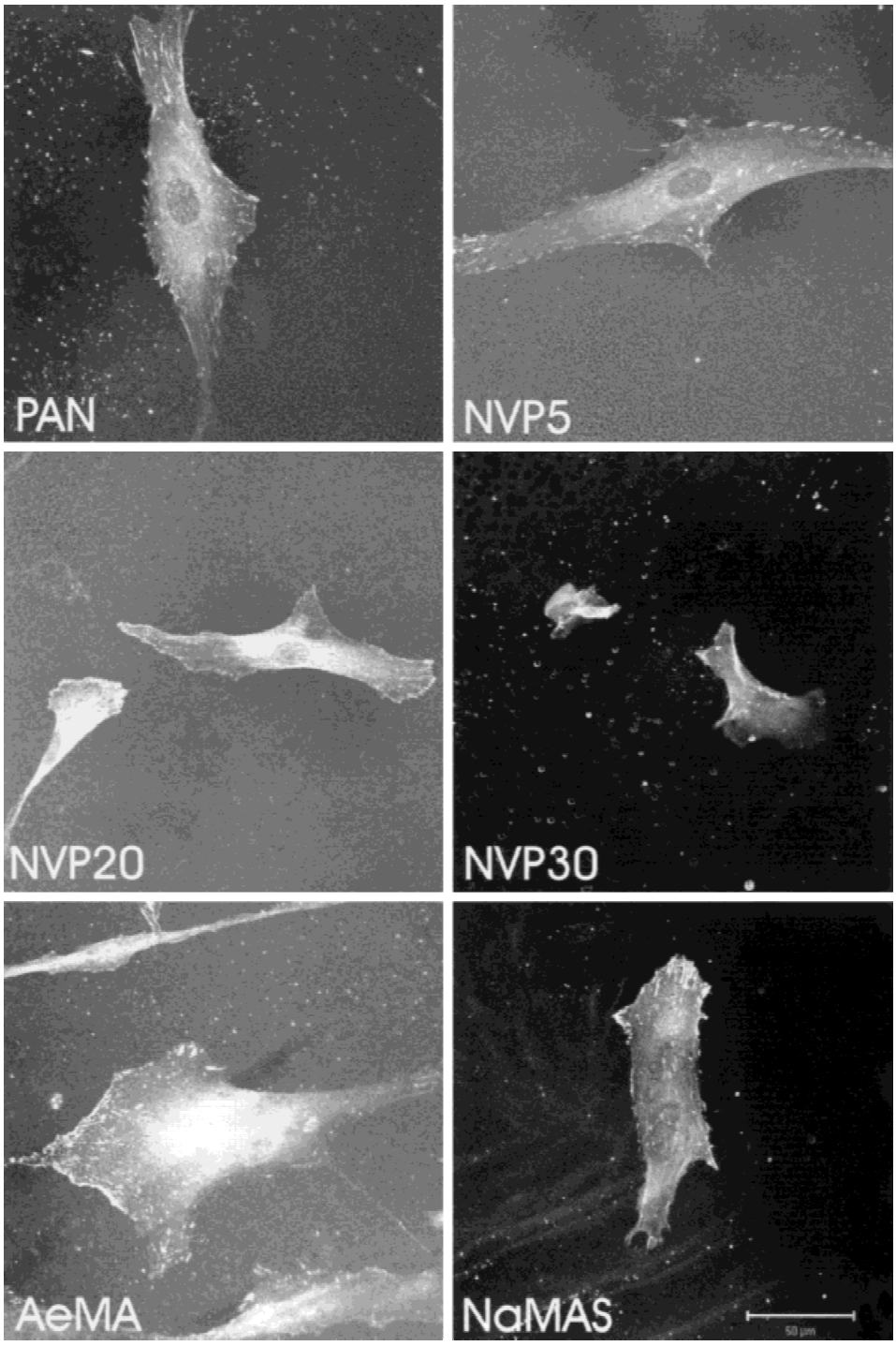

Figure 6. Visualization of focal adhesion sites by labeling of vinculin after 24 h of incubation of human fibroblasts on membranes of polyacrylonitrile and the copolymers (bar 50 μm).

that was shown for hydrogels[30] and polyvinylpyrrolidone coated substrata.[31] On the other hand, more cells with stronger focal adhesions were observed on PAN and NVP5, and a slightly reduced focal adhesion formation on AeMA and NaMAS, i.e., on membranes that had basic or acidic surface functionalities. The promoting role of polar surface functionalities for cell adhesion was shown recently, particularly for amine and sulfone functionalized silane surfaces.[32] Differences between the materials became stronger after 72 h, when proliferation of cells took place. Only a few cells could be detected on NVP30. Cell growth on NVP20 was also reduced in comparison to the other materials. These cells showed a reduced spread area, were easily detachable, tended to grow in islands, and many were round-shaped. On the other hand, signifi-

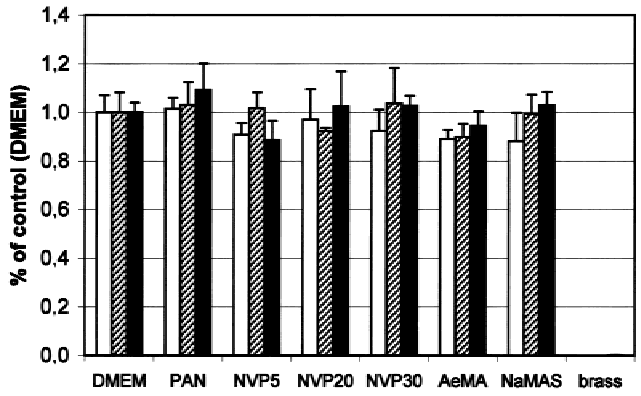

Figure 7. XTT test on cytotoxicity of polyacrylonitrile and the copolymer membranes with 3T3 fibroblasts after contact with extracts produced during 1 (white columns), 3 (shaded columns), and 7 days' (black columns) incubation with materials (DMEM—negative control; brass—positive control).

cantly higher cell proliferation was observed on PAN, NVP5, and AeMA. These cells were more spread and had an elongated triangular morphology typical for fibroblast. Indeed, some reduction of cell proliferation and spreading was observed for NaMAS, which might be due to the presence of negatively charged sulfone groups having a negative impact on the proliferation of cells.[33] It is noteworthy, however, that these results concern only the fibroblast interaction while other cell types may behave differently on these substrata.[34] Our recent results suggest that the application of membranes and scaffolds based on hydrophilic copolymers containing NVP could be beneficial for the culture and functional activity of epithelial cells.[24,35] Moreover, we have shown that these materials also have a good hemocompatibility.

In summary, regarding a possible application of these membranes as culture substrata and for the development of an artificial skin PAN, NVP5, and AeMA can be considered materials suitable for the immobilization of fibroblasts. The presence of amine

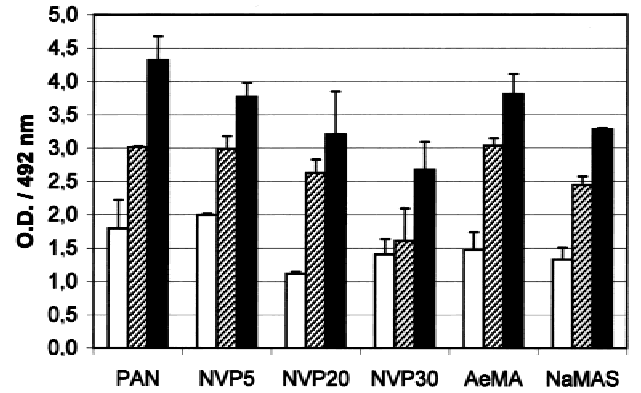

Figure 8. Quantity of human fibroblasts after 1 (white columns), 2 (shaded columns), and 4 days' (black columns) of growth on polyacrylonitrile and the copolymer membranes estimated by lactate dehydrogenase test.

functions on AeMA can be an advantage since biologically active ligands, such as adhesive proteins, signal peptides, and growth factors, can be covalently coupled via a simple wet chemistry. On the other hand, if a direct culture of keratinocytes on the above membranes is considered, a growth inhibition of skin fibroblasts on NVP-containing substrata could provide favorable conditions for epidermis formation. This will be studied in future investigations.

This work was supported in the frame of a NATO linkage grant LST 975147 to T. Groth and G. Altankov, and the Brite/EuRam project BE 97-4329 funded by the European Communities. Mrs. Ruth Hesse is gratefully acknowledged for technical assistance.

References

1. Vacanti JP, Vacanti CA. The challenge of tissue engineering. In: Lanza RP, Langer R, Chick WL, editors. Principles of tissue engineering. Austin, TX: Landes Bioscience; 1997. pp 1–6.
2. Yannas IV. In vivo synthesis of tissues and organs. In: Lanza RP, Langer R, Chick WL, editors. Principles of tissue engineering. Landes Bioscience, Austin, TX: Landes Bioscience; 1997. pp 169–178.
3. Gogolewski S, Pineda, L, Busing, CM. Bone regeneration in segmental defects with resorbable polymer membranes IV. Does the polymer composition affects the healing process? Biomaterials 2000;21:2513–2520.
4. Kuroyanagi Y. Advances in cultured skin substitutes. Jpn J Plastic Reconstr Surg 2000;43:571–580.
5. Legallais C, David B, Doré E. Bioartificial livers (BAL): Current technological aspects and future developments. J Membrane Sci 2000;181: 81–95.
6. Fey-Lamprecht F, Groth Th, Albrecht W, Paul D, Gross U. Development of membranes for the cultivation of kidney epithelial cells. Biomaterials 2000;21: 183–192.
7. Bell F, Rehrlich P, Butte DJ, Nakatsuji T. Living tissue formed in vitro and accepted as skin equivalent of full thickness. Science 1981;221:1052–1054.
8. Sabolinski ML, Alvarez O, Auletta M, Mulder G, Parentau NL. Cultured skin as a smart material healing wounds: Experience in venous ulcers. Biomaterials 1996;17:311–320.
9. Rheinwald JG. Methods for clonal growth and serial cultivation of normal human epidermal keratinocytes and mesothelial cells. In: Baserga R, editor. Cell growth and division, A practical approach. New York: Oxford University Press; 1989. pp 81–94.
10. Naughton GK. Skin and epithelia. In: Lanza RP, Langer R, Chick WL, editors. Principles of tissue engineering. Landes Bioscience, Austin, TX: Landes Bioscience; 1997. pp 169–178.
11. Kuroyanagi Y. Advances in wound dressings and cultured skin substitutes. J Artif Organs1999;2:97–116.
12. Anselme K. Osteoblast adhesion on biomaterials. Biomaterials 2000;21:667–681.
13. Minuth WW, Schumacher K, Strehl R, Kloth S. Physiological and cell biological aspects of perfusion culture techniques employed to generate differentiated tissues for long term biomaterial testing and tissue engineering. J Biomater Sci—Polym Ed 2000;11:495–522.
14. Grinnell F. Cellular adhesiveness and extracellular substrata. Int Rev Cytol 1978;53: 65–144.
15. Clark RAF. Wound repair: lessons for tissue engineering, In:

In: Lanza RP, Langer R, Chick WL, editors. Principles of tissue engineering. Landes Bioscience, Austin, TX: Landes Bioscience; 1997. pp 1–6.
16. Altankov G, Grinnell F, Groth Th. Studies on the biocompatibility of materials: Fibroblast reorganization of substratum-bound fibronectin on surfaces varying in wettability. J Biomed Mater Res 1996;30:385–391.
17. Altankov G, Groth Th. Fibronectin matrix formation by fibroblasts on surfaces varying in wettability. J Biomater Sci—Polym Ed 1997;8:299–310.
18. Groth Th, Altankov G. Insights into the tissue compatibility of biomaterials. Proceedings of 9th International Conference on Polymers in Medicine and Surgery 2000.
19. Biran R, Noble MD, Tresco PA. Characterisation of cortical astrocytes on materials of differing surface chemistry. J Biomed Mater Res 1999;46:150–159.
20. Groth Th, Falck P, Miethke RR. Cytotoxicity of biomaterials—Basic mechanisms and in vitro test methods: A review. ATLA 1995;23:790–799.
21. Tamada Y, Kulik EA, Ikada Y. Simple method for platelet counting. Biomaterials 1995;16:259–261.
22. Anonymous. ISO 10993-5, Biological evaluation of medical devices—Part 5: Tests for cytotoxicity: in vitro methods. International Standard Organisation, 1999.
23. Groth TH, Seifert B, Albrecht W, Malsch G. German Patent Application: Membranes made from P(AN-NVP)-copolymers with both haemo and tissue compatibility. Az: DE 100 30 307.2.
24. Krasteva N, Harms U, Albrecht W, Seifert B, Hopp M, Altankov G, Groth Th. Membranes for biohybrid liver support systems—Investigations on hepatocyte attachment, function and growth. Biomaterials 2002. In press.
25. Evans MDM, Dalton BA, Steele JG. Persistent adhesion of epithelial tissue is sensitive to polymer topography, J Biomed Mat Res 1999;46:485–493.
26. Dalton BA, Evans MDM, McFarland GA, Steele JG, Modulation of corneal epithelial stratification by polymer surface topography. J Biomed Mat Res 1999;45:384–394.
27. Kamusewitz H, Possart W, Paul D. The relation between equilibrium contact angle and the hysteresis on rough paraffin wax surfaces. Coll Surf A: Physicochem Eng Asp 1999;156:271–279.
28. Kamusewitz H, Ulbricht M, Thom V, Riedel M, Paul D. The calculation of thermodynamic quantities by means of wetting experiments on different polymeric surfaces. Proc Interfacial Phenomena in Composite Materials, Berlin 1999, p 29.
29. Norde W, Lyklema J, Why proteins prefer interfaces. J Biomater Sci— Polym Ed 1991;2:183–202.
30. Tamada Y, Ikada Y. Fibroblast growth on polymer surfaces and biosynthesis of collagen. J Biomed Mater Res 1994;28:667–675.
31. Defife KM, Shive MS, Hagen KM, Clapper DL, Anderson JM. Effects of photochemically immobilized polymer coatings on protein adsorption, cell adhesion, and the foreign body reaction to silicone rubber. Inc J Biomed Mater Res 1999;44:298–307.
32. Groth T, Altankov G. Insights into the tissue compatibility of biomaterials. Proceedings of the 9th International Conference Polymers in Medicine and Surgery, IOM Communications 2000, pp 205–213.
33. Mestries P, Borchiellini, Barbaud C, Duchesnay A, Escartin Q, Barritault D, Caruelle JP, Kern P. Chemically modified dextrans modulate expression of collagen phenotype by cultured smooth muscle cells in relation to the degree of carboxymethyl, benzylamide, and sulfation substitutions. J Biomed Mater Res 1998;42:286–294.
34. Webb K, Hlady V, Tresco PA. Relationships among cell attachment, spreading, cytoskeletal organization, and migration rate for anchorage-dependent cells on model surfaces. J Biomed Mater Res 2000;49:362–368.
35. Fey-Lamprecht F, Albrecht W, Groth Th, Weigel T, Gross U. Morphological studies on the culture of kidney epithelial cells in a fibre-in-fibre bioreactor design using hollow fiber membranes. J Biomed Mater Res 2002. In press.

Publikation 18

Natalia Krasteva, Ulrike Harms, Wolfgang Albrecht, Barbara Seifert, Michael Hopp, George Altankov, Thomas Groth (2002).

Membranes for biohybrid liver support systems – investigations on hepatocytes attachment, morphology and growth.

Biomaterials **23**, 2467-2478.

ELSEVIER

Biomaterials 23 (2002) 2467–2478

Biomaterials

www.elsevier.com/locate/biomaterials

Membranes for biohybrid liver support systems—investigations on hepatocyte attachment, morphology and growth

Natalia Krasteva[a], Ulrike Harms[b], Wolfgang Albrecht[b], Barbara Seifert[b], Michael Hopp[c], George Altankov[a], Thomas Groth[b,*]

[a] *Institute of Biophysics, Bulgarian Academy of Sciences, Str. Acad. G. Bonchev, bl. 21, BG-1113 Sofia, Bulgaria*
[b] *Department of Biomaterials, Institute of Chemistry, GKSS Research Centre, Kantstrasse 55, D-14513 Tetlow, Germany*
[c] *Clinic of Dental Prosthetics, Faculty of Medicine Charité, Humboldt University, Schumannstrasse 20-22, D-10177 Berlin, Germany*

Received 10 March 2001; accepted 28 October 2001

Abstract

The biological properties of four different membranes were studied regarding their possible application in biohybrid liver support systems. Two of them, one made of polyetherimide (PEI), and a second based on polyacrylonitrile-*N*-vinylpyrollidone co-polymer (P(AN-NVP)), were recently developed in our lab and studied for the first time. Together with pure polyacrylonitrile (PAN) membranes, the three preparations were characterised as ultra-filtration membranes. Their ability to support cell attachment, morphology, proliferation and function of human hepatoblastoma C3A cells was studied. The role of surface morphology for the interaction with hepatocytes was highlighted using a commercial, moderately wettable polyvinylidendifluoride (PVDF) membrane with micro-filtration properties. Comparative investigations showed strongest interaction of C3A cells with PAN membranes, as the focal adhesion contacts were more expressed and cell growth was also high. However, the functional activity in terms of albumin synthesis was reduced. Very similar results were obtained with the most hydrophobic PEI membrane. In contrast, the most hydrophilic membrane P(AN-NVP) was found to provoke stronger homotypic adhesion (E-cadherin expression) of C3A cells and less substratum attachment (focal adhesions), but enhanced albumin secretion. However, proliferation of C3A cells was lowered. Micro-porous PVDF membrane showed very good initial attachment, but the resulting cell material and cell–cell interaction were relatively poor developed. Among four membranes tested, PEI seems to be the most attractive membrane for biohybrid liver devices, as it provides good surface properties for hepatocytes interaction, but in addition it is highly thermostable, which would permit steam sterilisation. No simple relationship, however, between the wettability of the membranes and their ability to support hepatocyte adhesion and function was found in this study. © 2002 Published by Elsevier Science Ltd.

Keywords: Polymer membranes; Surface properties; Hepatoblastoma cells; Cell–biomaterial interaction; Biohybrid liver

1. Introduction

Since synthetic membranes were introduced in extracorporal treatment of kidney failure, significant efforts were made to develop membranes with better haemocompatibility [1,2]. In general, polymer membranes must posses specific functional characteristics to be used in extracorporal devices for haemodialysis, like selective permeability, biostability and low interactions with proteins and cells [1–3]. Hence, most of the membranes developed for conventional blood-contacting biomedical applications are optimised to be inert and non-interacting with the blood proteins, as well as, with cells. In contrast, membranes considered for the immobilisation of tissue cells, like hepatocytes, ought to support cell attachment and promote proliferation and function of these cells. Biohybrid liver support systems are based on the immobilisation of hepatocytes on membranes, which should function over distinct periods of time to replace the liver function in cases of fulminant hepatic failure [4–6]. Membranes developed for haemodialysis have been tested previously as a culture substratum for hepatocytes [7], but most of them expressed poor characteristics regarding cellular interaction and function.

*Corresponding author. Department of Membrane Research, Institute of Chemistry, GKSS Research Center, Kantstrasse 55, D-14513 Tetlow, Germany. Fax: +49-3328-46452.

E-mail addresses: altankov@obzor.bio21.bas.bg (G. Altankov), thomas.groth@gkss.de (T. Groth).

0142-9612/02/$ - see front matter © 2002 Published by Elsevier Science Ltd.
PII: S0142-9612(01)00381-7

Adhesion, proliferation and function of anchorage dependent cells were shown to be highly dependent on the surface properties of biomaterials [8–12]. It is well accepted that the physicochemical properties of the material surface determine the adsorption of proteins and subsequent cellular interaction [8–12]. Particularly important for cell adhesion is the adsorption of attachment proteins, like fibronectin (FN), vitronectin (VN) and others [6,9,13,14]. Numerous investigations were devoted to compare the impact of different surface properties on cellular interactions, such as wettability, presence of charges and specific functional groups, amorphous versus crystalline domains, etc. [15–18]. However, it must be noted here that many of these investigations were carried out with selected types of cells, mostly derived from connective tissue. For example, it is well established that fibroblasts grow and function better on hydrophilic surfaces [19,20]. Tresco et al., however, have shown that the behaviour of cells on a specific biomaterial surface may vary greatly with the type of cell investigated [21]. It can therefore be anticipated that hepatocytes may behave in a different way compared with fibroblasts. In fact, it is known from recent investigations that spreading of hepatocytes on hydrophilic surfaces is accompanied by an altered cell function [22]. On the other hand, the functional activity of these cells may be enhanced if they are cultured in aggregates [23]. For instance, under these circumstances hepatocytes maintained their functionality over longer periods of time in contrast to the conditions when they are attached and spread [22]. This is also the case after plating hepatocytes on different matrix proteins, like FN, VN or collagen [24]. Our Investigations have shown that hepatocytes tend to have a stronger homotypic adhesion on hydrophobic surfaces, which may be an indication for a better functionality [25]. Hence, in this study, it was interesting to learn how the wettability of membranes influences the attachment, growth and function of this type of cells.

Polyacrylonitrile (PAN) is one of the standard materials for the preparation of haemodialysis membranes [1,2]. PAN has a good biocompatibility for blood-contacting applications [1,2] and was also reported to support the attachment of hepatocytes [7]. In addition, it has good membrane forming properties and can be easily co-polymerised with a variety of co-monomers [26]. Here we studied the biological properties of PAN and one new membrane material, based on polyacrylonitrile-*N*-vinylpyrollidone co-polymer (P(AN-NVP)), which was recently developed in our lab [26] to render the membrane surface more hydrophilic. In contrast, polyimides such as polyetherimide (PEI) are more hydrophobic and still not frequently applied as biomaterials. Recent investigations, however, show that polyimides are not cytotoxic and allow the attachment and growth of cells [27–29]. On the other hand, PEI has a considerable mechanical strength and thermal stability as it was shown recently [30]; which should make it suitable for steam sterilisation. Moreover, PEI has good membrane forming properties [31,32] and its polymer backbone possesses functional groups to be used for a wet chemistry modification to adapt the resulting membrane material for simultaneous contact with blood and tissue cells [33].

In this study, we investigated the capability of membranes made of PAN, P(AN-NVP) and PEI to support the attachment, proliferation and function of human hepatoblastoma C3A cells. These cells were chosen as they possess functional features of normal hepatocytes and are able to continuously proliferate in vitro, in contrast to primary hepatocytes. Moreover, C3A cells were shown to be applicable in biohybrid liver support systems [6]. All these three types of membranes (PEI, PAN and P(AN-NVP)) have been designed as ultra-filtration membranes. Thus, they possess similar smooth surfaces. As we were further interested to learn more about the role of surface topography in hepatocyte behaviour we employed in this study another, moderately wettable and commercially available polyvinylidendifluoride (PVDF) membrane, which has micro-, instead of ultra-filtration properties. To characterise the hepatocyte interactions with the different membranes, we studied the initial cell attachment, the overall cell morphology, focal adhesion formation and cell growth. The functionality of adhering cells was characterised by the metabolic activity and protein synthesis, as well as, the expression of intercellular junctions. Details of this investigation are reported herein.

2. Materials and methods

2.1. Materials

Pure PAN and P(AN-NVP) were synthesised as described in a previous paper [26]. Briefly, acrylonitrile (AN) monomer (MERCK; >99% purity) and NVP (ALDRICH; 99% pure) were used for co-polymerisation. Dimethylformamide (DMF; ALDRICH; 99.8% pure.) was applied as solvent and 2,2′-azoisobutyronitrile (AIBN, recrystallised twice from water at 30°C) as free radical initiator in the case of PAN polymerisation and ammonium peroxide sulphate (APS, fractional crystallised from ethanol at 40°C) for AN co-polymerisation with NVP. The solution polymerisation was carried out under nitrogen by filling DMF in the reactor, adding AN followed by the NVP, and finally the initiator. The concentration of the AN monomer was 3.8 mol/l. 9.9 mol% NVP was added in the case of P(AN-NVP) polymerisation. The reaction time was 360 min for the PAN polymerisation and 60 min for NVP co-polymerisation. The reaction temperature was

adjusted to about 50°C. At the end of the reaction, the polymer solutions were poured into a large excess of ethanol. The precipitated polymer was filtered, washed and rinsed with dehydrated ethanol and dried in vacuum. The molecular weight of the obtained polymers measured by membrane osmometry was about 0.005 g/mol for PAN and about 0.004 g/mol for P(AN-NVP).

Polyimides are polymers that usually consist of aromatic rings coupled by imide linkages—that is, linkages in which two carbonyl groups are attached to the same nitrogen atom. In the PEI (Ultem 1000, General Electrics) used as polymer for membrane formation ether groups are inserted into the polyimide backbone.

Furthermore, commercial hydrophilised PVDF membranes (Millipore, Ireland) were used as obtained from the producer. The chemical structure of the different polymers is shown in Fig. 1.

2.2. Membrane formation

Flat PAN membranes were prepared by a conventional phase inversion process using a belt-casting machine. The PAN polymer was dissolved in *N*,*N*-dimethylformamide and low molecular weight additive for 2 h at 80°C to a concentration of 17 wt%. After cooling the solution to room temperature (RT) it was degassed and cast as a thin solution film onto a steel belt. The steel belt, and therefore the solution film, is transported with a drawing speed of 2 m/min in a coagulation bath consisting of pure water at RT. The

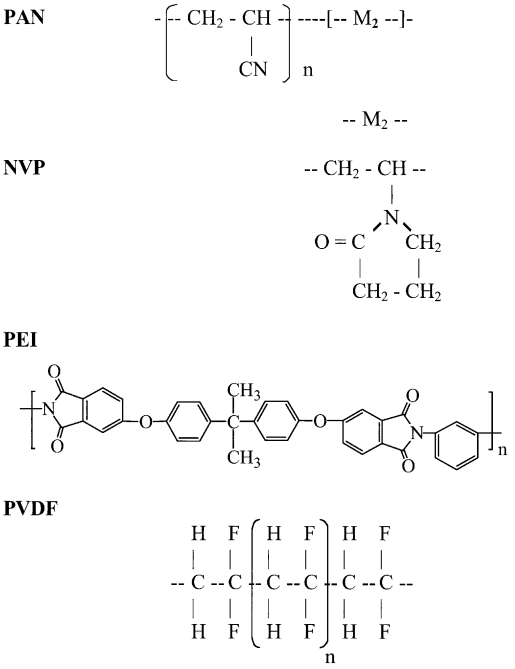

Fig. 1. Chemical structure of polymers, such as PAN (homo-polymer), P(AN-NVP) with M2 as NVP co-monomer, PEI and PVDF used for the formation of membranes investigated in this study.

casting slit width was 300 μm. After rinsing the membrane with water free of solvent and additive, the membrane was post-treated 10 min at 90°C in an annealing device and stored until use in an aqueous 0.02 wt% sodium acid solution.

The same procedure was applied to form PEI membranes using a 25 wt% PEI solution in *N*-methyl pyrollidone as solvent. The casting slit width was 250 μm.

P(AN-NVP) membranes were formed from an 18 wt% polymer solution in DMF and low molecular weight additive on a glass support in a lab scale using a doctor knife to form the solution film. The solution film was coagulated in water, extensively washed with distilled water and stored until use in an aqueous 0.02 wt% sodium acid solution.

2.3. Measurement of the membrane pore characteristics

Permeabilities and rejections of PAN and P(AN-NVP) membranes were determined at 0.05 MPa in a stirred ultra-filtration cell (Amicon, Type 8010). The ultra-filtration experiments were carried out first with distilled water, then with a solution of a test substance mixture (0.1 wt% aqueous solution of a dextran mixture with molecular weights from 650 to 215,000 Da). The molecular size distribution of dextrans in permeates, in retentates and in original solutions was determined using gel permeation chromatography (GPC). From the results of GPC the average pore diameter (D_{50}), the maximal pore diameter (D_{100}) and the separating curve were calculated by assuming a logarithmic normal distribution of the pore size. The cut-off D_{100} corresponds to the value of the inflectional tangent of the logarithmic normal distribution extrapolated to a rejection of 100%.

The PEI membrane was characterised only by water flux since the permeability was too low for solute rejection technique.

The PVDF micro-filtration membrane was characterised by bubble point technique using a Coulter Porometer 2 (Beckman & Coulter Electronics, UK) and Porofil (Coulter) as displacement liquid. The bubble point technique is based on the liberation of a pressured gas through the liquid saturated membrane and another through the dry membrane. The Young–Laplace theorem gives the relation between the pressure the gas needs to pass the membrane and the diameter of the pores. The evaluation was carried out according to the solute rejection technique.

2.4. Scanning electron microscopy (SEM) of membranes

The wet membrane samples were dehydrated in graded ethanol 50, 70, 80, 90 and 96 vol%, twice with absolute ethanol and finally with ether. Such treated flat

membranes are fractured in liquid nitrogen and coated with a gold/palladium (80/20) layer. Samples were investigated in JSM 6400-F field emission scanning electron microscope (Joel, Japan) at an acceleration voltage of 5 kV.

2.5. Contact angle measurements

Contact angles (CA) were measured using the captive bubble method, where an air bubble is injected from a syringe with a stainless steel needle onto the inverted sample surfaces immersed into ultra-pure Milli-Q water. The diameter of the contact area between surface and bubble was always >3 mm. Advancing and receding CA measurements were realised with a goniometer fitted with a tilting stage (Carl Zeiss, Germany) by stepwise withdrawing/adding air from/to the captured bubble. At least 10 measurements of different bubbles, on at least three different locations, were averaged to yield one CA value.

2.6. Cell culture

C3A cells (a human hepatoblastoma cell line, supplied by ATCC, USA) were grown in Eagle MEM (Sigma Chemical Co., St. Louis, MO, USA) supplemented with 10% foetal bovine serum (FBS) (Sigma), 1% HEPES, 1% sodium pyruvate (Sigma), and 1% antibiotic/antimycotic solution (Sigma) in a humidified incubator at 37°C in the presence of 5% CO_2. For the experiments, cells were plated at a density of 5×10^4 cells per well, using 24-well tissue culture plates (Costar), containing membranes. Flat sheets of membranes were cut into 13 mm-diameter disks and were tightly wedged into the culture wells, resulting in a flat, even-bottomed surface. To avoid floating in the presence of medium, O-rings of Teflon tubing were used to wedge the membranes to the bottom.

2.7. Initial cell attachment

5×10^4 cells per well were incubated for 2, 4, 6, 8 and 22 h in 24-well tissue culture plates containing the membranes. After the incubation, the supernatants were removed and the number of non-attached cells was counted in Burger's haemocytometer chamber and compared with the number of cells seeded. The percentage of adhering cells was calculated from quadruplicated experiments.

2.8. Actin staining

Immunofluorescence microscopy for the visualisation of cellular structures, such as actin, vinculin and E-cadherin (see below) was carried out after 3 d of culture to allow the growth of cells and establishment of larger cell aggregates.

To visualise the actin cytoskeleton, the samples were fixed with 3% para-formaldehyde, permeabilised for 5 min with 0.5% Triton-X 100 and incubated for 40 min with 5 U/ml fluorescein-conjugated phalloidin (Sigma). Then, the samples were washed in PBS and mounted with Mowiol. Because of the high auto fluorescence of membrane samples all morphological investigations (see also below) were performed with a confocal laser scanning microscope type LSM 510 with Axiovert 510 optics (Carl Zeiss, Jena, Germany).

2.9. Vinculin and E-cadherin staining

Cells were fixed and permeabilised as describe above and then saturated with 1% BSA. To detect focal adhesions, samples were incubated for 30 min at 37°C with a monoclonal anti-vinculin antibody (Sigma), followed by 30 min incubation with Cy3 conjugated goat anti-mouse IgG (Jackson Immuno Research Laboratories, Inc. USA) used as secondary antibody.

To visualise cell–cell contacts, samples were incubated with monoclonal anti-E-cadherin antibody (Dianova, Germany) for 30 min and further processed with the same secondary antibody. Finally, the samples were mounted and studied as above.

2.10. SEM of hepatocytes attached to membranes

Hepatocytes were cultured for 3 d on the membranes, washed with medium and fixed with 2.5% glutaraldehyde (Sigma). Samples were then dehydrated by washing in increasing ethanol concentrations and then air-dried. Samples were sputtered with platinum and investigated with a scanning electron microscope Cambridge 360 S (Leica, UK).

2.11. Proliferation assays

The proliferation of C3A cells was determined after 1, 3, and 7 d of incubation using two colourimetric assays. An MTT assay, which assesses the rate of mitochondrial reduction of MTT, was used to measure the metabolic activity of cells. An LDH assay, which measures the activity of cytosolic lactate dehydrogenase after cell lysis was used to estimate the number of cells [34]. Both assays were obtained from Boehringer Mannheim (Penzberg, Germany) and used as suggested by the producer. Each experiment was quadruplicated.

2.12. Measurement of human serum albumin synthesis

Cells were seeded as described above. Before the day of protein secretion measurements, wells were washed with serum-free medium and finally 500 μl medium

without FBS were added. This medium was withdrawn after 24 h and the amount of secreted protein was determined. Albumin production was estimated by ELISA via a standard antibody-capture immunoassay as described previously [25]. Each experiment was quadruplicated.

3. Results

Figs. 2 and 3 show the morphology of the different membranes, characterised by SEM. PEI (see Fig. 2A and B), PAN (see Fig. 2C and D) and P(AN-NVP) (see Fig. 3A and B) have a typical asymmetric morphology with a more dense, smooth separating layer (see right panel) and a highly porous supporting layer (see left panel). The top view on the surface of these membranes (right panel) reveals visible pores in the separating layer, which are in the nanometer scale. In contrast, the PVDF membrane (see Fig. 3C and D) shows features of a typical homogenous micro-filtration membrane visible in the cross-section (Fig. 3C) with a highly porous and rough surface (see the top view Fig. 3D). The surface pores of this membrane are in a micrometric scale ($\sim$1 μm and more).

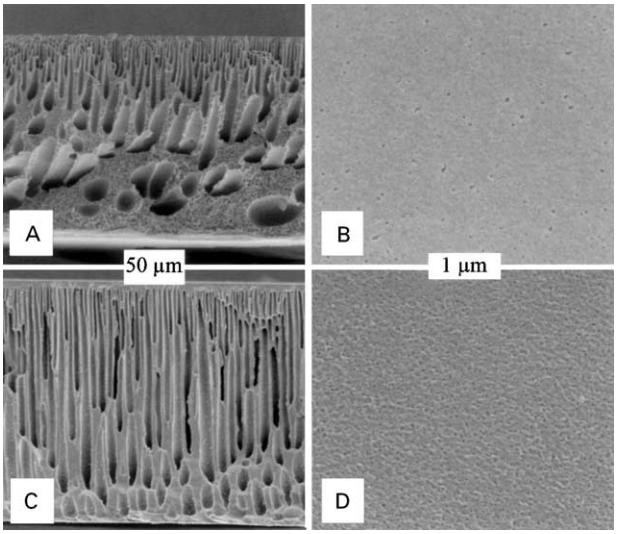

Fig. 2. Scanning electron micrograph of PEI (A and B) and PAN (C and D) with cross section (left panel) and top view (right panel).

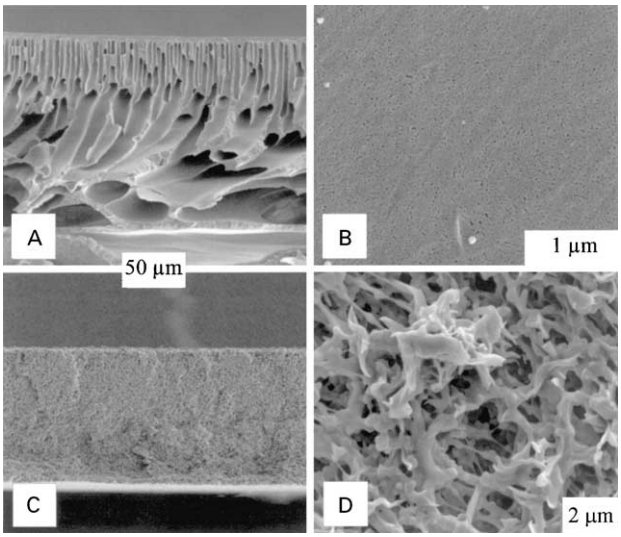

Fig. 3. Scanning electron micrograph of P(AN-NVP) (A and B) and PVDF (C and D) with cross section (left panel) and top view (right panel).

The investigation of transport properties by water permeation measurements (see Table 1) revealed that pure PAN and PEI membranes were typical ultra-filtration membranes. PVDF membranes demonstrated a very high water permeability indicating that the cut-off was much greater. The pore characteristics estimated by the bubble point technique resulted in average pore sizes of about 0.5 μm representing not surface but passage pores within the membrane. P(AN-NVP) possessed higher water permeability than PAN and PEI in particular, and had also quite high molecular cut-off. Thus, it has properties, which are more close to micro-filtration membranes. In Fig. 4, the separating curves of the investigated membranes, except PEI membrane, are presented for a direct comparison of the pore structures between the membranes. Besides the different average pore diameter of the membranes, the symmetrically structured PDVF membrane possesses a steeper separating curve than the PAN or P(AN-NVP) membranes that are asymmetrically structured.

The results from water CA measurements are shown in Table 2. Among all membranes tested PEI was most hydrophobic, with an advancing water CA of 79.5°. PVDF and PAN had similar intermediate wettabilities, with advancing CA of 67.2° and 63.2°, respectively. The P(AN-NVP) membrane was the most hydrophilic with an advancing CA of 53.0°.

C3A cells were seeded on the membranes and the amount of non-attached cells was examined at different time points. The calculated values of cell adhesion (in %) are shown in Fig. 5. In general, C3A cells attached slowly on the membranes and reached about 90% attachment after 20–24 h of incubation. Initial adhesion at 2 h was obviously better on the moderately wettable membranes PAN, P(AN-NVP) and PVDF in comparison to the hydrophobic PEI membrane. P(AN-NVP) showed a tendency for lower attachment at the beginning in contrast to the PVDF membrane. If we consider also the surface structure of the membranes, then it seems that the different surface topography of PVDF membranes which resulted from the higher porosity was advantageous for the initial adhesion of C3A cells.

Table 1
Permeability characteristics and pore structure data of membranes

Membrane	Water permeability (l/m/h/kPa)	Pore characteristics		
		D_{50} (nm)	D_{100} (nm)	Cut-off (kDa)
PAN	0.02	2.3	9.8	40
P(AN-NVP)	6.46	10.1	40.6	900
PEI	<0.001	<1.0[a]	<2.0[a]	<5.0[a]
PVDF	63.9	430	500	—[b]

[a] Not determinable with dextran solutions because of the low permeability, assessed on the basis of water permeability.
[b] Calculation of cut-off not possible for micro-porous membranes.

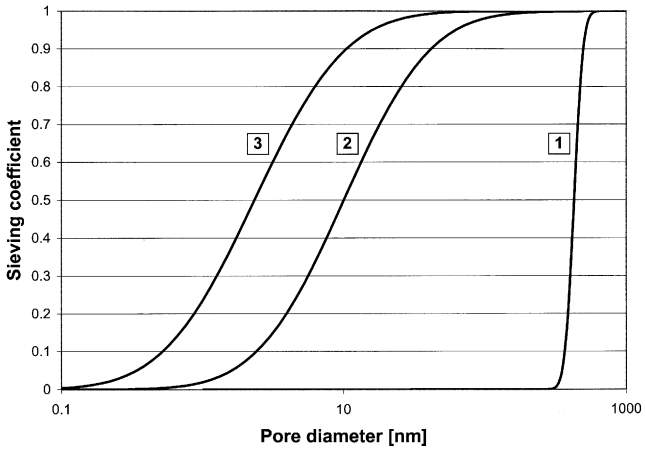

Fig. 4. Separation curves for PVDF [1], P(AN-NVP) [2] and PAN [3] obtained by the measurement of the molecular size distribution of dextrans in permeates (see materials ans methods section) plotting sieving coefficients versus pore diameters.

Table 2
Water CA of membranes

	Advancing angle (°)	Receding angle (°)
PAN	63.2	28.0
P(AN-NVP)	53.0	44.6
PEI	79.5	49.0
PVDF	67.1	27.7

SEM studies revealed that C3A cells not only attach slowly to the membranes but also tend to form aggregates (homotypic adhesion) when grown on membranes. It is demonstrated in Fig. 6A and C that cells grew in larger flattened aggregates on PAN and PEI. In contrast, the size of aggregates was much smaller on P(AN-NVP) with the tendency of round shaped cells (see Fig. 6B and E) while small aggregates were also observed on PVDF (Fig. 6D). It is interesting to note that cells cultured on PVDF tended to develop pseudopodia, which were anchored in the pores of the micro-filtration membrane as visible in Fig. 6F.

The staining for actin (see Fig. 7) shows clear differences in the overall morphology of cells residing in aggregates and in the organisation of their actin cytoskeleton. Hepatocytes cultured on PAN were more spread and often possessed longitudinal stress fibres, as shown in Fig. 7A. Similar observations were made for PEI (see Fig. 7C), though here actin was more condensed, especially in the centre of aggregates. However, completely different results were obtained for P(AN-NVP) and PVDF membranes that are shown in Fig. 7B and D, respectively. Hepatocytes cultured on these membranes developed only a limited number of longitudinal stress fibres. Most of the actin was condensed and tended to organise circumferentially along the cell edges.

Staining of vinculin again yielded the best formation of focal adhesion complexes in cells cultured on PAN (see Fig. 8A). Structures resembling focal adhesions were found not only at the periphery of aggregates, like on P(AN-NVP) and PEI (see Fig. 8B and C), but also over the entire ventral surface of cells in aggregates. In some regions, vinculin tended to be organised in the areas of cell–cell contacts as well (see Fig. 8A). Less staining for vinculin was observed on the ventral surface of cells grown on PEI. A very special finding in these preparations was the intense nuclear staining of hepatocytes (Fig. 8C), probably due to the non-specific entrapment of secondary antibody used in immunofluorescence visualisation. When C3A cells were cultured on P(AN-NVP) they formed smaller aggregates with a weak staining for vinculin, mostly along the periphery of aggregates (see Fig. 8B). In contrast, on PVDF membranes staining for vinculin resulted in a punctuate distribution of antibody as demonstrated in Fig. 8D. Presumably, these structures represented insertions of the parts of cell body in the membrane pores (approximate size of 1 μm and more).

E-cadherin as major protein of the adherens junctions in epithelia was also studied by immunofluorescence to look for a possible promotion of cell–cell interactions on the membranes. Fig. 9 shows that E-cadherins were localised expectably in the area of cell–cell contacts, and these were mostly pronounced on PAN (Fig. 9A).

E-cadherins were also expressed on PEI, but much less organised. Moreover, it seemed that their distribution did not follow the whole area of cell–cell contacts as shown in Fig. 9C. In contrast, hepatocytes cultured on P(AN-NVP) (see Fig. 9B) expressed an intense staining over the entire area of cell–cell contacts. Diffuse punctual staining associated with membrane pores was observed again in cells on PVDF membranes as demonstrated in Fig. 9D.

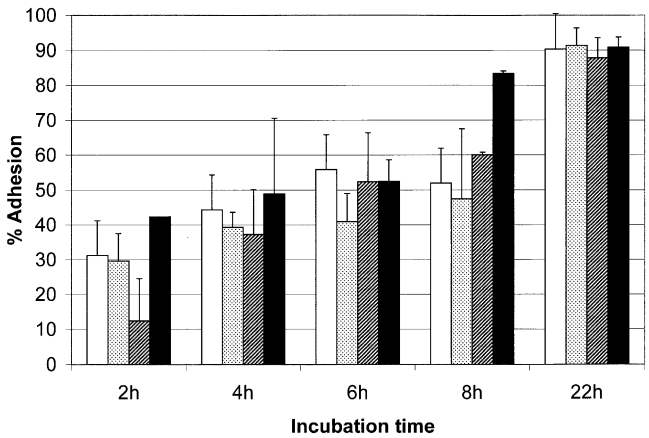

Fig. 5. Adhesion kinetics of C3A cells adhering on PAN (empty bars), P(AN-NVP) (dotted bars), PEI (shaded bars) and PVDF (black bars). Adhesion (means ± SD) was measured by counting non-attached cells and calculating the percentage of adhesion from cell count at the beginning.

The metabolic activity and growth of C3A cells on the various membranes were investigated over a period of 7 d using two standard assays, MTT and LDH, respectively (see Fig. 10a and b). A typical increase in cell-associated signals was observed for both MTT and LDH assays during the culture of cells due to the increasing cell number. However, no significant differences were found for the different membranes over the entire culture period, except for P(AN-NVP), where the cell number quantified by LDH assay was significantly lower after 7 d ($p < 0.05$).

The functional activity of hepatocytes cultured on the membranes was assessed additionally by measuring the secretion of albumin, as a function of time. The results are shown in Fig. 11. Secretion of albumin measured by ELISA, did not show significant differences on the days 1 and 3 between the membranes. However, after 7 d cells cultured on P(AN-NVP) secreted the highest amount of albumin, followed by PEI, PVDF and PAN.

4. Discussion

This paper shows a relationship between the morphology of human hepatoblastoma C3A cells in terms of

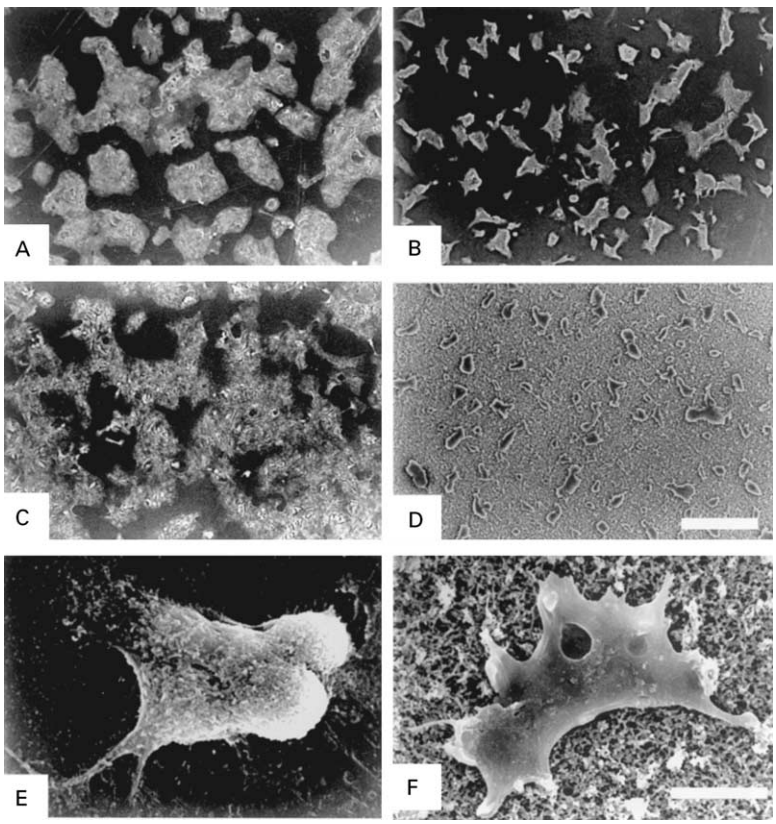

Fig. 6. Scanning electron micrographs of C3A cells cultured for 3 d on PAN (A), P(AN-NVP) (B), PEI (C) and PVDF (D). Bar corresponds to a length of 200 μm. High magnifications of cells are shown for P(AN-NVP) (E) and PVDF (F). Bar corresponds to a length of 20 μm.

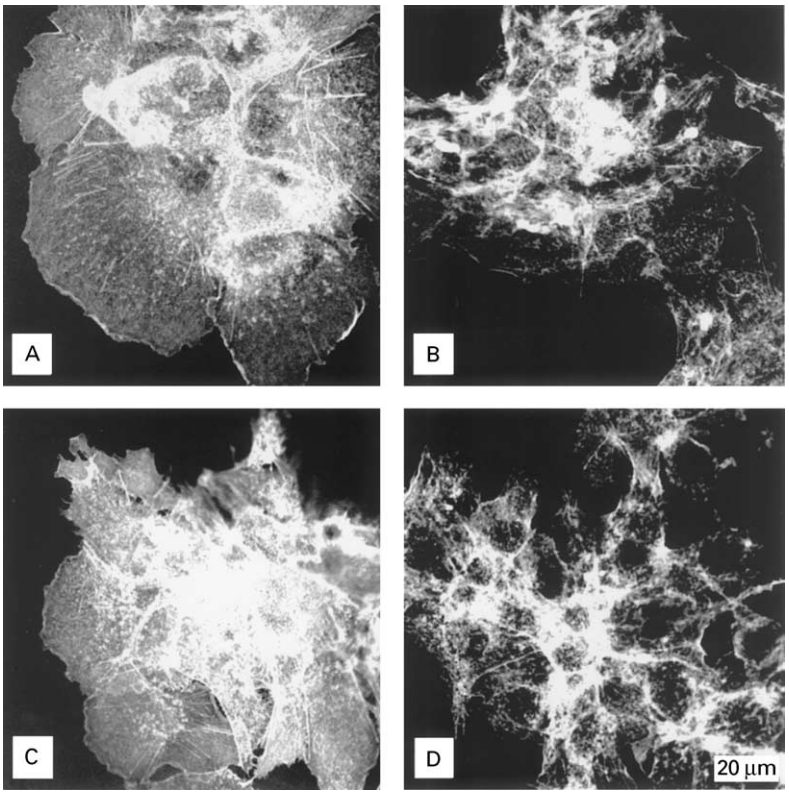

Fig. 7. Organisation of actin cytoskeleton of C3A cells on PAN (A), P(AN-NVP) (B), PEI (C) and PVDF (D). Bar corresponds to a length of 20 μm.

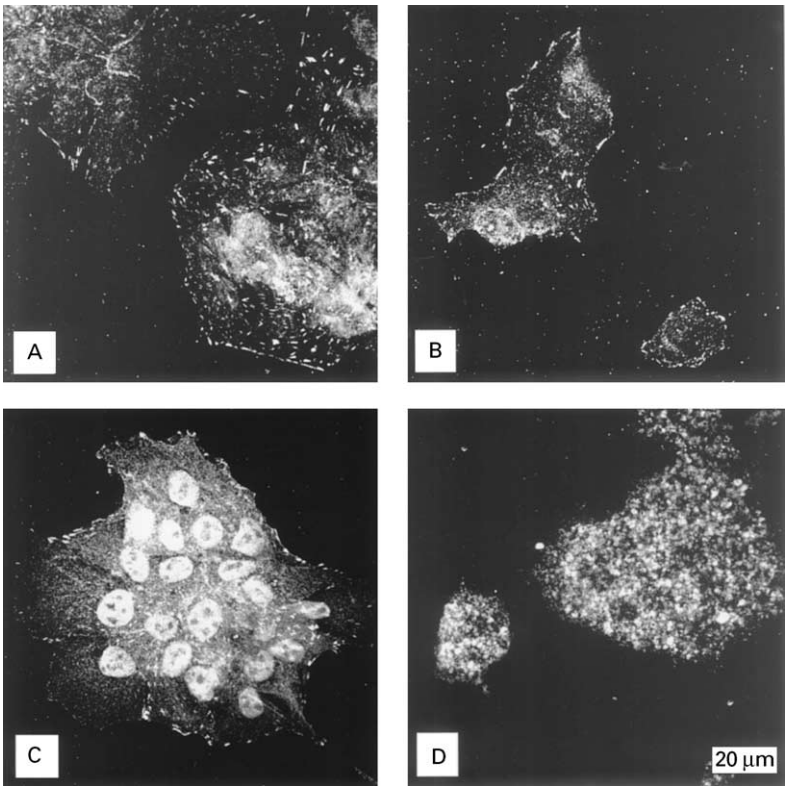

Fig. 8. Vinculin distribution in C3A cells on PAN (A), P(AN-NVP) (B), PEI (C) and PVDF (D). Bar corresponds to a length of 20 μm.

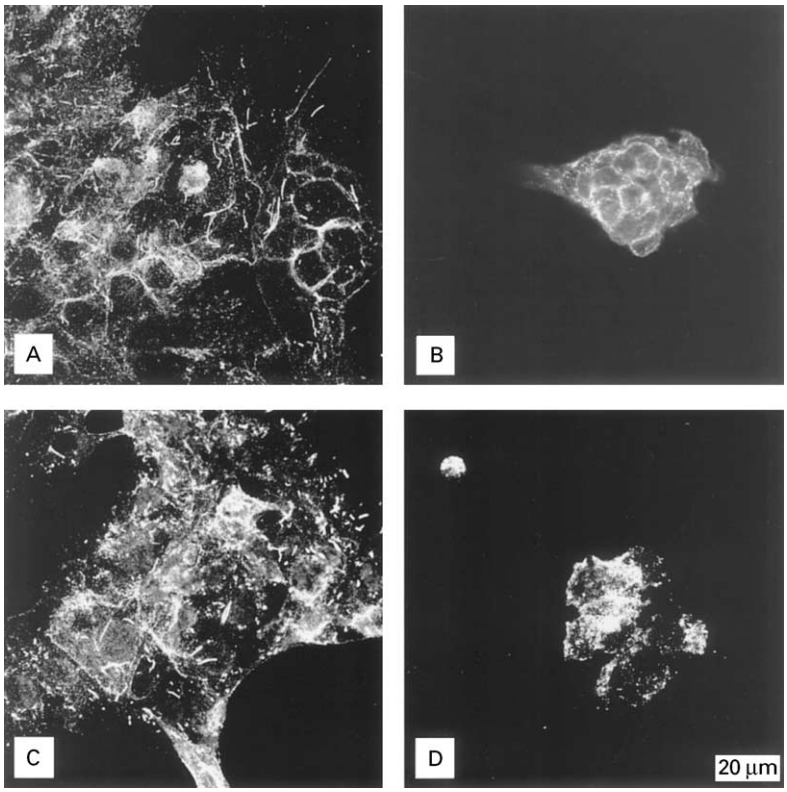

Fig. 9. Distribution of E-cadherin in C3A cells cultured on PAN (A), P(AN-NVP) (B), PEI (C) and PVDF (D). Bar corresponds to a length of 20 μm.

overall cell morphology, actin cytoskeleton and focal adhesion formation, and cell–cell contacts and their ability to grow and secrete proteins, such as human serum albumin on different polymer membranes. The synthetic membranes employed in this study are potential materials for biohybrid liver support systems. They had a different polymer composition, P(AN-NVP), PAN and PVDF as moderate wettable materials and PEI as a hydrophobic membrane.

The results show that C3A cells attach slowly to these membranes and tend to make aggregates. The kinetics of cell attachment showed that even after 8 h the number of adhering cells did not exceed 60% and sufficient adhesion of about 90% was measured at the next day. Interestingly, initial adhesion at 2 and 4 h tends to follow the general rule that cells adhered less efficiently on hydrophobic surfaces [8–11,15], since adhesion was lower on the PEI membrane in comparison with the more wettable PAN and P(AN-NVP) membranes. Then, already after 6 h these differences disappeared almost completely which might be due to the fact that cells start to secrete proteins and modify the underlying substratum [35]. The surface morphology, however, seemed to play a role as well [36], since the micro-porous PVDF membrane allowed a quite high cellular attachment until 8 h incubation, although it has almost the same wettability as PAN. On the other hand, P(AN-NVP) membranes showed a tendency to reduced initial attachment, up to 8 h incubation, which might be explained with the ability of this co-polymer to take up water making the membrane hydrogel-like [37]. It is known that adsorption of proteins and adhesion of cells is reduced on these types of surfaces [38,39].

Nevertheless, it was shown recently that the wettability of substrata has an influence on hepatocyte morphology, viability and function [25,40], such a simple relationship was not established here. The results from actin and vinculin staining show that cells growing on PAN possessed mostly longitudinal organised cytoskeleton and developed a higher number of focal adhesion complexes. Although growing in aggregates, the cells in the periphery were more spread than on the other membranes, which correlated with the moderate wettability of the PAN membrane. These results are in agreement with our previous observations with human fibroblasts when cell spreading and formation of focal adhesion plaques were better on moderately wettable model substrata (see for example [11,19]). However, a quite similar morphology of C3A cells was observed on the hydrophobic PEI membrane. Although actin was more condensed (in the middle of aggregates) the hepatocytes looked well-spread and developed sufficient

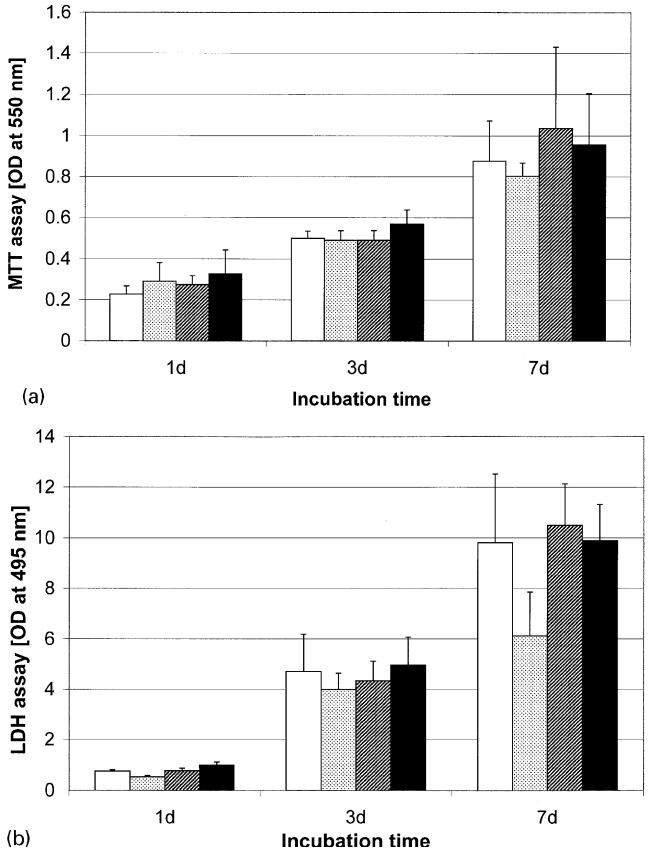

Fig. 10. MTT assay for metabolic (a) and LDH assay for cell number (b) measured as optical density (OD, means ± SD) function of culture time on PAN (empty bars), P(AN-NVP) (dotted bars), PEI (shaded bars) and PVDF (black bars).

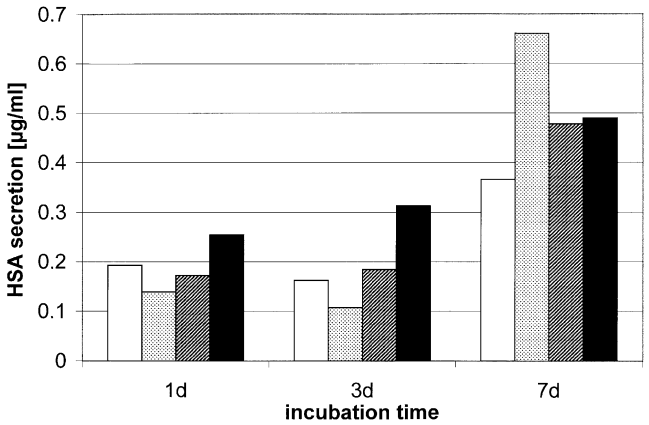

Fig. 11. Secretion human serum albumin by C3A cells measured by ELISA technique in supernatants of culture wells as a function of time on PAN (empty bars), P(AN-NVP) (dotted bars), PEI (shaded bars) and PVDF (black bars). Values are given in means ± SD.

amount of focal adhesion contacts, in comparison with cells grown on the relatively hydrophilic P(AN-NVP) and PVDF membranes. This rather strong interaction of hepatocytes with the hydrophobic PEI membrane was surprising on the base of our previous data [25] and also results of others [40]. One possible explanation is that PEI membranes tend to adsorb higher amounts of proteins from surrounding media [41] that could have a beneficial effect on the attachment and spreading of C3A cells. The investigations with SEM supported these observations. Hepatocytes grew in larger more spread aggregates on PAN and PEI while smaller aggregates were observed on P(AN-NVP) and PVDF. Moreover, high magnification images revealed that aggregates on P(AN-NVP) contained round-shaped cells while cell pseudopodia entered the micro-pores on PVDF membranes. In fact, growth of C3A cells on the different substrata as measured by the LDH assay was not different during the first 3 d of culture. However, after 7 d it was obvious that cells were not able to grow to the same extent on P(AN-NVP). The lowered growth of cells on this substratum should be related to its hydrophilic character and may have implications for a better functionality of hepatocytes on this substratum as discussed below.

It is well known that C3A cells have a quite reduced ability to synthesise urea and low activity for xenogenic metabolism [42] but can secrete considerable amounts of proteins [43]. In this respect, it was interesting to learn that C3A cells having a lower potential to grow on P(AN-NVP) had a superior ability to secrete proteins on this substratum, particularly if we take into account the lower number of cells. In contrast, cells on PAN, and partly on PVDF membranes grew well, but had a comparatively diminished ability to secrete proteins. This may be attributed to the fact that cells undergoing proliferation have a limited capability to fulfil their function [44]. In this respect, PEI can be considered as a promising material also, because of the relatively good hepatocyte growth and functional activity on this substratum.

The development of cell–cell contacts might be considered as an additional measure for cell functionality. E-cadherins, which stain the adherens junctions in epithelia, were pronouncedly expressed in C3A cells cultured on PAN. It is noteworthy, however, that the best cell–substratum interaction was also observed here. On the other hand, no complete staining of the entire cell borders was observed on the hydrophobic PEI membrane, which was also found to be a useful substratum for hepatocyte adhesion and function. This points to the possibility that a very strong interaction of hepatocytes with the underlying substratum might result in the reduction of their ability to make cell–cell contacts. In contrast, cells growing in aggregates on the most hydrophilic P(AN-NVP) containing mostly round cells, expressed both strongly actin and E-cadherins, which were clearly aligned in the areas of cell–cell contact. A possible positive effect of this morphology on cell functionality in terms of protein

synthesis was discussed above and was also found by others [22,23].

The peripheral distribution of both actin and E-cadherins indicates a strong homotypic cell adhesion [45]. In the light of the above discussion concerning the effect of PAN on hepatocytes, it might be speculated that the weaker cell–substratum interaction on P(AN-NVP) could promote stronger cell–cell interactions. This might reduce the ability of cells to proliferate but seems to have a positive impact on some functional features of cells, such as their ability to synthesise proteins. The micro-porous PVDF membrane showed dot like staining for all proteins tested, indicating that part of the cells entered the pores of the membrane which was also shown by SEM. E-cadherin staining here was also poorly organised, that points to weak cell–cell contacts. Other authors recently discussed a possible strong effect of the porosity of track-etched membranes with the finding that larger pores, as we observed for the PVDF membranes, might have an inhibiting effect on proliferation and function of epithelial cells [46,47]. We will publish a more detailed analysis of the effect of membrane pores on the proliferation and function of hepatocytes in a forthcoming paper. If we compare the morphological observations with the growth of cells, then it seems that cells, which spread well on membranes, received stronger signals that promotes their proliferation. Hence, cell growth was higher on PAN and PEI in comparison to P(AN-NVP). On the other hand, when hepatocytes had a weak contact with the substratum they may survive by anchoring to each other, forming tight cell–cell contacts, which may also provide better conditions for some cellular functions, such as protein synthesis.

In summary, we found no simple relations between the wettability of the membranes and their ability to support cell adhesion and function. However, a clear relation between the morphology of adhering cells and their functional behaviour was found. According to the needs of biohybrid liver devices, PEI seems to be an attractive membrane material. It provides good surface properties for hepatocyte interaction as PAN membranes, but in addition it is highly temperature stable, which would permit steam sterilisation. On the other hand, new materials like P(AN-NVP) can also be considered as an interesting substrata if sufficient numbers of hepatocytes are seeded to promote a sufficient functionality of biohybrid liver support system.

Acknowledgements

The programme WTZ of BMBF for the bilateral co-operation between Germany and Bulgaria, Grant No. BUL 98-001, supported this work. Dr G. Malsch is gratefully acknowledged for the delivery of PAN polymers. We are thankful to Mrs Ruth Hesse and Mr Schossig-Tiedemann for technical assistance.

References

[1] von Sengbusch G, Bowry S, Viencken J. Focusing on membranes. Artif Organs 1993;17(4):244–53.
[2] Klinkmann H, Viencken J. Membranes for dialysis. Nephrol Dial Transplant 1995;19(suppl 3):39–45.
[3] Paul D. Polymermembranen für die Stofftrennung. Chem Unserer Zeit 1998;32:197–205.
[4] Bader A, Knop E, Böker K, Frühauf N, Schüttler W, Oldhafer K, Burkhard R, Pichelmayr R, Sewing K-F. A novel bioreactor design for in vitro reconstruction of in vivo liver characteristics. Artif Organs 1995;30:368–74.
[5] Gerlach JC. Development of a hybrid liver support system. A review. Int J Artif Organs 1996;19:645–54.
[6] Hughes RD, Williams R. Assessment of bioartificial liver support in acute liver failure. Int J Artif Organs 1996;19:3–6.
[7] Qiang S, Yaoting Y, Hongyin L, Klinkmann H. Comparative evaluation of different membranes for the construction of an artificial liver support system. Int J Artif Org 1997;20(2):119–24.
[8] Grinnell F, Milam M, Spree PA. Attachment of normal and transformed hamster kidney cells to substrata varying in chemical composition. Biochem Med 1973;7:87–90.
[9] Steele JG, McFarland C, Dalton BA, Johnson G, Evans MD, Howlett CR, Underwood PA. Attachment of human bone cells to tissue culture polystyrene and to unmodified polystyrene: the effect of surface chemistry upon initial cell attachment. J Biomater Sci Polym Ed 1993;5:245–57.
[10] Webb K, Hlady V, Tresco PA. Relative importance of surface wettability and charged functional groups on NIH 3T3 fibroblast attachment, spreading, and cytoskeletal organization. J Biomed Mater Res 1998;41:422–30.
[11] Groth T, Altankov G. Cell-surface interactions and the tissue compatibility of biomaterials. In: Harris PI, Chapman D, editors. New biomedical materials—basic and applied studies, biomedical and health research, vol. 16. Amsterdam: IOS Press, 1998. p. 12–23.
[12] Anselme K. Osteoblast adhesion on biomaterials. Biomaterials 2000;21:667–81.
[13] Juliano DJ, Saavedra SS, Truskey GA. Effect of the conformation and orientation of adsorbed fibronectin on endothelial cell spreading and the strength of adhesion. J Biomed Mater Res 1993;27:1103–13.
[14] Grinnell F, Feld MK. Adsorption characteristics of plasma fibronectin in relationship to biological activity. J Biomed Mater Res 1981;15:363–81.
[15] Ruardy TG, Moorlag HE, Schakenraad JM, Van der Mei HC, Busscher HJ, Underwood A, Elwing H, Lee HB. Detachment of human endothelial cells under flow from wettability gradient surfaces with different functional groups. Cells Mater 1997;7:123–33.
[16] Biran R, Noble MD, Tresco PA. Characterisation of cortical astrocytes on materials of differing surface chemistry. J Biomed Mater Res 1999;46:150–9.
[17] Culp LA, Sukenik CN. Cell type-specific modulation of fibronectin adhesion functions on chemically derivatized self-assembled monolayers. J Biomater Sci Polym Ed 1998;9:1161–76.
[18] Park A, Griffith Cima L. In vitro response to differences in poly L-lactide crystallinity. J Biomed Mater Res 1996;31:117–30.
[19] Altankov G, Grinnell F, Groth Th. Studies on the biocompatibility of materials: fibroblast reorganization of substratum-bound fibronectin on surfaces varying in wettability. J Biomed Mater Res 1996;30:385–91.

[20] Wachem van PB, Beugling T, Feijen J, Detmers JP, Aken van WG. Interaction of cultured human endothelial cells with polymeric surfaces of different wettabilities. Biomaterials 1985;6:403–8.
[21] Webb K, Hlady V, Tresco PA. Relationships among cell attachment, spreading, cytoskeletal organisation and migration rate for anchorage-dependent cells on model surfaces. J Biomed Mater Res 2000;49:362–8.
[22] Sawamoto K, Takahashi N. Modulation of hepatocyte function by changing the cell shape in primary culture. In Vitro Cell Dev Biol—Animal 1997;33:569–74.
[23] Gerlach J, Koppel K, Schauwecker HH, Tauber R, Muller C, Bücherl ES. Use of hepatocytes in adhesion and suspension culture for liver support bioreactors. Artif Organs 1989;12:788–92.
[24] te Velde AA, Ladiges NCJJ, Flendrig LM, Chamuleau RAFM. Functional activity of isolated pig hepatocytes attached to different extracellular matrix substrates. Implication for application of pig hepatocytes in a bioartificial liver. J Hepatol 1995;23:184–92.
[25] Krasteva N, Groth Th, Fey-Lamprecht F, Altankov G. The role of surface wettability for hepatocyte adhesive interaction and function. J Biomater Sci Polym Ed 2001;12(6):613–27.
[26] German patent: Mit Blut und Gewebe Verträgliche Membranen aus P(AN/NVP)-Mischpolymeren und deren Anwendung im medizinischen Bereich, DE-Az 100 30 307.2-44.
[27] Imai Y, Watanabe A, Masuhara E, Imai Y. Structure-biocompatibility relationship of condensation polymers. J Biomed Mater Res 1983;17(6):905–12.
[28] Richardson Jr RR, Miller JA, Reichert WM. Polyimide as biomaterials: preliminary biocompatibility testing. Biomaterials 1993;14(8):627–35.
[29] Peluso G, Petillo O, Ambrosio L, Nicolais L. Polyetherimide as biomaterial: preliminary in vitro and in vivo biocompatibility testing. J Mater Sci Mater Med 1994;4:738–42.
[30] Le Dû C. Polyetherimide: a resin for the most demanding medical devices. Medical Device Technology Conference, London, March 2–3, 1999.
[31] Kneifel K, Peinemann KV. Preparation of hollow fiber membranes from polyetherimide for gas separation. J Membr Sci 1992;65:295–307.
[32] Peinemann KV, Maggioni JF, Nunes SP. Poly(etherimide) membranes obtained from solutions in cosolvent mixtures. Polymer 1998;39:3411–6.
[33] Seifert B, Mihanetzis G, Groth Th, Albrecht W, Richau K, Missirlis Y, Paul D, von Sengbusch G. Polyetherimide—a new membrane forming polymer for biomedical applications. Artif Organs, in press.
[34] Tamada Y, Kulik EA, Ikada Y. Simple method for platelet counting. Biomaterials 1995;16:259–61.
[35] Altankov G, Groth Th. Fibronectin matrix formation by human fibroblasts on surfaces varying in wettability. J Biomater Sci Polym Ed 1996;8:299–310.
[36] Deligianni DD, Katsala ND, Koutsoukos PG, Missirlis YF. Effect of surface roughness of hydroxyapatite on human bone marrow cell adhesion, proliferation, differentiation and detachment strength. Biomaterials 2001;22:87–96.
[37] Groth Th, Seifert B, Malsch G, Albrecht W, Paul D, Kostadinova A, Krasteva N, Altankov G. Dependence of human skin fibroblast growth on the composition of moderate wettable polyacrylonitrile co-polymers, in press.
[38] Tamada Y, Ikada Y. Fibroblast growth on polymer surfaces and biosynthesis of collagen. J Biomed Mater Res 1994;28:667–75.
[39] Griffith LG. Polymeric biomaterials. Acta Mater 2000;48:263–77.
[40] Catapano G, di Lorenzo MC, della Volpe C, de Bartolo L, Migliaresi M. Polymeric membranes for biohybrid liver support devices: the effect of membrane surface wettability on hepatocyte viability and functions. J Biomater Sci Polym Ed 1996;7:1017–27.
[41] Tsoneva R, Groth Th, Albrecht W, Altankov G, Paul D. Plasma protein adsorption on polymer membranes. Abstr XVth Aachener Colloq Biomater, 2001. p. 84.
[42] Tagaki M, Fukuda N, Yoshida T. Comparison of different hepatocyte cell lines for use in a hybrid artificial liver model. Cytotechnology 1997;24:39–45.
[43] Uludag H, Sefton MV. Microencapsulated human hepatoma (HepG2) cells: in vitro growth and protein release. J Biomed Mater Res 1993;27:1213–24.
[44] Ingber DE. Mechanochemical switching between growth and differentiation by extracellular matrix. In: Lanzer R, Langer R, Chick W, editors. Principles of tissue engineering. Austin, TX, USA: R.G. Landes Company, 1997. p. 89–109.
[45] Gumbiner BM. Regulation of cadherin adhesive activity. J Cell Biol 2000;148:399–403.
[46] Evans MDM, Dalton BA, Steele JG. Persistent adhesion of epithelial tissue is sensitive to polymer topography. J Biomed Mater Res 1999;46:485–93.
[47] Dalton BA, Evans MDM, McFarland GA, Steele JG. Modulation of corneal epithelial stratification by polymer surface topography. J Biomed Mater Res 1999;45:384–94.

8. Publikationsliste des Authors

1. Richter R, Groth Th, Halle W (1986) The membrane potential of pig aortic endothelial cells, Biomedica Biochimica Acta. **45(7),** 897 – 902.
2. Herrmann A, Groth Th, Lassmann G, Ladhoff A-M,Hillebrecht B (1986) Structural alterations of the human erythrocyte membrane upon influenca virus attachment, Bioscience Report **6 (1)**, 45 – 55.
3. Herrmann A, Lassmann G, Groth Th, Donath E, Hillebrecht B (1986) Conformational alterations within the glycocalyx of erythrocyte membranes studied by spin labelling. Biochimica Biophysica Acta **861**, 111 – 121.
4. Donath E, Herrmann A, Coakley WT, Groth Th, Egger M, Taeger M (1987) The influence of the antiviral drugs amantadine and rimantadine on erythrocyte and platelet membranes and its comparison with that of tetracaine, Biochemical Pharmacology **36 (4)**, 481 – 487.
5. Hermann A, Pritzen C, Palesch A, Groth Th (1988) The influenca virus-induced fusion of erythrocyte ghosts does not depend on osmotic forces. Biochimica Biophysica Acta **943**, 411 – 418.
6. Wolf H, Karwath R, Groth Th (1988) Interaction of blood with biomedical polymers - some basic aspects. In: Advances in Biomedical Measurements (Carson ER, Kneppo P und Krekule I, Hrsg.), Plenum Press, New York und London, 133 – 142.
7. Altankov G, Smilenov L, Groth Th, Wolf H (1989) On the adhesion of lymphocytes on fibronectin coated glass surfaces - column bead method. Comptes rendue de l'Academie bulgares des Sciences **42 (5)**, 117 – 120.
8. Groth Th, Wolf H, Vassilieff Chr (1989) The spiral method as a novel measuring principle for quantitative evaluation of in vitro hemocompatibility of polymers. Proceedings VIth International Conference PIMS, Polymers in Medicine and Surgery Leeuwenhorst, Holland, 18/1 - 18/5.
9. Wolf H, Groth Th, Karwath R, Mientus W, Trommler A (1989) Stand und Perspektiven der Entwicklung und Testung von Biomaterialien für die Medizin. Charité - Annalen **9**, 127 – 135.
10. Groth Th, Vassilieff Chr, Wolf H, Kuhn H (1990) Investigation of blood-biomaterial interactions by means of a new quantitative dynamic measuring principle. Biomaterials, Artificial Cells and Artificial Organs, **18 (4)**, 517 – 522.

11. Altankov G, Groth Th, Kostadinova A, Förster F, Wolf H, Nikolaeva N (1990) A novel spectrophotometrical method for quantification of lymphocyte adhesion onto different solid surfaces. Comptes rendue de l'Academie bulgares des Sciences **43 (6)**, 107 – 110.

12. Groth Th (1991) Die Hämokompatibilität von Biomaterialien in vitro - Aufbau von Methoden zur Bestimmung der Adhäsion von Blutzellen an Fremdoberflächen. Dissertation A - Humboldt-Universität zu Berlin.

13. Klosz K, Groth Th, Olschewski M, Becker R (1991) Die Hämokompatibilität von Polyurethanen: I. Charakterisierung physikochemischer Materialeigenschaften, Biomedizinische Technik, **36 (Ergänzungsband)**, 322 – 323.

14. Groth Th, Klosz K, Strietzel F, Richter G, Becker R (1991) Die Hämokompatibilität von Polyurethanen: II. Untersuchung der in vitro Hämokompatibilität, Biomedizinische Technik, **36 (Ergänzungsband)**, 324 – 325.

15. Groth Th, Vassilieff Chr, Wolf H, Richter G, Förster F (1992) Developement of a new dynamic method for quantitative evaluation of in vitro hemocompatibility of biomedical materials, Journal of Biomaterials Science, Polymer Edition **3 (4)**, 285 – 300.

16. Vassilieff Chr, Groth Th, Petsev D, Kostadinov A, Nikolaeva N, Altankov G, Tenchov B, Wolf H (1992) Cell adhesion to protein covered glass surfaces. Annuaire de l'Universite de Sofia **82**, 201 – 206.

17. Groth Th, Mihanetzis G, Missirlis Y, Wolf H (1992) The interrelationship between platelet adhesiveness and released platelet factors during standardized in vitro blood/biomaterial contact. In: Biomaterial-Tissue Interfaces, P.J. Doherty et al. (Eds.), Advances in Biomaterials **10**, 247 - 251

18. Groth Th, Gronert A, Ziemer S, Hesse R (1992) The hemocompatibility of reference materials in vitro - comparative investigation of platelet adhesion/activation and platelet aggregability. In: The reference materials of the European Communities, W. Lemm (ed.), 183 – 192.

19. Groth Th, Derdau K, Strietzel F, Förster F, Wolf H (1992) The hemocompatibility of biomaterials in vitro - Investigations on the mechanism of the whole blood clot formation test. ATLA - Alternatives to Laboratory Animals **20**, 390 – 395.

20. Podias A, Groth Th, Missirlis Y (1994) The effect of shear rate on the adhesion/activation of human platelets in flow through a closed-loop polymeric tubular system. Journal of Biomaterials Science - Polymer Edition **6**, 399-410.

21. Groth Th, Altankov G, Klosz K (1994) Adhesion of human peripheral blood lymphocytes is dependent on surface wettability and protein preadsorption, Biomaterials **15(6)**, 423-428.

22. Groth Th, Herrmann K, Campbell EJ, New RRC, Hall B, Hesse R, Goering H (1994) Protein adsorption, lymphocyte adhesion and platelet adhesion/activation on polyurethane ureas is related to hard segment content and composition. Journal of Biomaterials Science - Polymer Edition **6**, 497-510.

23. Groth Th, Podias A, Missirlis Y (1994) Platelet adhesion and activation under static and flow conditions. Colloids and Surfaces B. Biointerfaces **3**, 241-249.

24. Altankov G, Groth Th (1994) Reorganization of substratum bound fibronectin on hydrophilic and hydrophobic materials is related to biocompatibility. Journal of Materials Science - Materials in Medicine **5**, 732-737.

25. Herrmann K, Groth Th, Seifert B, Romaniuk P (1994) Heparin-modified polylactide as biodegradable hemocompatible biomaterial. Journal of Materials Science - Materials in Medicine **5**, 728-731.

26. Groth Th, Zlatanov I, Altankov G (1994) Adhesion of human peripheral lymphocytes on biomaterials preadsorbed with fibronectin and vitronectin, Journal of Biomaterials Science - Polymer Edition **6**, 729-739.

27. Seifert B, Herrmann K, Groth Th, Romaniuk P (1994) Heparinisierte Polylaktide als bioresorbierbare, hämokompatible Biomaterialien. Biomedizinische Technik **39 (suppl.)**, 103-104.

28. Groth Th, Campbell E, Herrmann K, Seifert B (1995) Application of enzyme immuno assays for testing haemocompatiblity of biomedical polymers. Biomaterials, **16**, 1009-1015.

29. Seifert B, Groth Th, Herrmann K, Romaniuk P (1995) Immobilization of heparin on polylactide for application to degradable biomaterials in contact with blood. Journal of Biomaterials Science - Polymer Edition **7**, 277-287.

30. Groth Th, Altankov G (1995) Fibroblast spreading and proliferation on hydrophilic and hydrophobic surfaces is related to tyrosine phosphorylation in focal contacts. Journal of Biomaterials Science - Polymer Edition **7**, 297-305.

31. Groth Th, Falck P, Miethke R-R (1995) Cytotoxicity of biomaterials - basic mechanisms and in vitro test methods: a review. ATLA **23**, 790-799.

32. Altankov G, Grinnell F, Groth Th (1986) Studies on the biocompatibility of materials: Fibroblast reorganization of substratum-bound fibronectin on surfaces varying in wettability. Journal of Biomedical Materials Research **30**, 385-391.

33. Groth Th, Altankov G (1996) Studies on the cell-biomaterial interaction: Role of tyrosine phosphorylation during fibroblasts spreading on surfaces varying in wettability. Biomaterials **17**, 1227-1234.

34. Seifert B, Romaniuk P, Groth Th (1996) Bioresorbable, heparinized polymers for stent coating: In vitro studies on heparinization efficiency, maintenance of anticoagulant properties and improvement of stent haemocompatibility. Journal of Materials Science - Materials in Medicine **7**, 465-469.

35. Altankov G, Groth Th (1996) Fibronectin matrix formation and the biocompatibility of materials. Journal of Materials Science - Materials in Medicine **7**, 425-429.

36. Darkow R, Groth Th, Albrecht W, Paulke B-R, Paul D (1996) Synthetic microparticles with pseudobiological ligands for endotoxin removal. Proceedings of Polymers in Medicine and Surgery PIMS `96, University of Strathclyde, Glasgow, 113-120.

37. Mitzner E, Groth Th (1996) Modification of poly(ether urethane)elastomers by incorporation of poly/isobutylene)glycol. Relation between polymer properties and thrombogenicity. Journal of Biomaterials Science - Polymer Edition **7**, 1105-1118.

38. Altankov G, Groth Th (1997) Fibronectin matrix formation by fibroblasts on surfaces varying in wettability. Journal of Biomaterials Science - Polymer Edition **8**, 299-310.

39. Groth Th, Synowitz J, Malsch G, Richau K, Albrecht W, Lange K-P, Paul D (1997) Contact activation of plasmatic coagulation on polymeric membranes measured by the activity of kallikrein in heparinized plasma. Journal of Biomaterials Science - Polymer Edition **8**, 797-808.

40. Altankov G, Groth Th, Krasteva N, Albrecht W, Paul D (1997) Morphological evidence for a different fibronectin receptor organization and function during fibroblast adhesion on hydrophilic and hydrophobic glass substrata. Journal of Biomaterials Science - Polymer Edition **8**, 721-740.

41. Seifert B, Groth T, Romaniuk P (1997) Covalent immobilization of hirudin improves the haemocompatibility of polylactide-polyglycolide in vitro. Biomaterials **18**, 1495-1502.

42. Groth Th, Altankov G (1998) Reorganization of fibronectin by fibroblasts and signaling via integrins are related to the biocompatibility of materials. In: Frontiers in biomedical polymer applications. Vol. 1., R. Ottenbrite (ed.), Technomics Publisher, 43-58.

43. Groth Th, Altankov G (1998) Cell-surface interactions and the tissue compatibility of biomaterials. In: New Biomedical Materials, (Harris PI and Chapman D, eds.), IOS Press, Amsterdam, 12-23.

44.Fey-Lamprecht F, Gross U, Groth Th, Albrecht W, Paul D, Fromm M, Gitter AH (1998) Functionalitiy of MDCK kidney tubular cells on flat polymer membranes for biohybrid kidney. Journal of Materials Science - Materials in Medicine **9**, 711-715.

45.Groth Th, Altankov G, Kostadinova A, Krasteva N, Albrecht W, Pau D (1999) Altered vitronectin receptor (alpha v integrin) function in fibroblasts adhering on hydrophobic glass. Journal of Biomedical Materials Research **44**, 341-351.

46.Mullaney M, Groth Th, Darkow R, Hesse R, Albrecht W, Paul D, von Sengbusch G (1999) Investigation of plasma protein adsorption on functionalized nanoparticles for application in apheresis. Artificial Organs **23**, 87-97.

47.Darkow R, Groth Th, Czipull K, Albrecht W, Paul D (1999) Functionalized nanoparticles for endotoxin binding in aqueous solutions. Biomaterials **20**, 1277-1283.

48.Fey-Lamprecht F, Groth Th, Albrecht W, Paul D, Gross U (2000) Development of membranes for the cultivation of kidney epithelial cells. Biomaterials **21(2)**, 183-192.

49.Thom V, Altankov G, Groth Th, Jankova K, Jonsson G, Ulbricht M (2000) Optimizing Cell-Surface Interactions by Photo-Grafting of Poly(Ethylene Gylcol) (PEG). Langmuir, **16(6)**, 2756-2765.

50.Thom V, Altankov G, Groth Th, Jankova K, Jonsson G, Ulbricht M (2000) Modulating the biocompatibility of polymer surfaces with Poly(Ethylene Gylcol) (PEG) – Effects of fibronectin. Journal of Biomedical Materials Research **52(1)**, 219-230.

51.Groth, Th., Altankov G (2001) Insights into the tissue compatibility of biomaterials. Proceedings of 9th International Conference on Polymers in Medicine and Surgery, IOM Publications, London, 205-213.

52.Hopp M, Groth Th, Rogaschewski S (2001) Magenetwerkstoffe im Zellkulturtest. In: Magnete in der Zahnmedizin,Blankenstein F (Ed.), Flohr Verlag Rottweil, 28-38.

53.Groth Th, Wagenknecht W (2001) Anticoagulant potential of regioselective derivatized cellulose. Biomaterials, **20(22)**, 2719-2729.

54.Hopp M, Rogaschewski S, Groth Th (2001) Auswirkungen magnetischer Korrosionsprodukte. In: Restaurative Zahnmedizin 200x, J. Wirz (Herausgeber), Quintessenz-Verlag Berlin, 142-173.

55. Krasteva N, Groth Th, Fey-Lamprecht F, Altankov G (2001) The role of surface wettability for hepatocyte adhesive interactions and function. Journal of Biomaterials Science - Polymer Edition **12(6)**, 613-627.

56. Hilke R, Albrecht W, Weidemann S, Groth Th, Weigel T, Plagge A, Paul D (2001) A new module arrangement for plasma apheresis. Transfusion and Apheresis Science **25**, 5-15.

57. Seifert B, Mihanetzis G, Groth Th, Albrecht W, Richau K, Missirlis Y, Paul D, von Sengbusch G (2002). Polyetherimide – a new membrane forming polymer for biomedical applications. Artficial Organs, **26(2),** 189-199.

58. Krasteva N, Harms U, Albrecht W, Seifert B, Hopp M, Altankov G, Groth Th (2002) Membranes for biohybrid liver support systems – investigations of hepatocyte attachment, morphology and growth, Biomaterials **23(12)**, 2467-2478.

59. Groth Th, Seifert B, Malsch G, Albrecht W, Paul D (2002) Dependence of human skin fibroblast growth on the chemical composition of moderate wettable polyacrylonitrile copolymer membranes. Journal of Biomedical Materials Research **61,** 290-300.

60. Fey-Lamprecht F, Albrecht W, Groth Th, Weigel T, Gross U (2002) Morphological studies on the culture of kidney epithelial cells in a fibre-in-fibre bioreactor design using hollow fibre membranes. Journal of Biomedical Materials Research, **im Druck**.

61. Albrecht W, Weigel T, Groth Th, Hilke R, Paul D (2002) Formation of porous bilayer hollow fibre membranes. Macromolecular Symposia, **im Druck**.

62. Tzoneva R, Heuchel M, Groth T, Altankov G, Albrecht W, Paul D (2002) Fibrinogen adsorption and platelet interactions on polymer membranes. Journal of Biomaterials Science - Polymer Edition, **im Druck**.

63. Groth Th (2002) Novel polymer membranes for biohybrid organ technology. Business Briefing: Medical Device Manufacturing & Technology**, im Druck**.

64. Hopp M, Rogaschewski S, Groth Th, Testing the cytotoxicity of metal alloys used as magnetic prosthetic devices. Journal of Materials Science - Materials in Medicine, **im Druck**.

65. Krasteva N, Seifert B, Hopp M, Malsch G, Albrecht W, Altankov G, Groth Th, Membranes for biohybrid liver support – behaviour of C3A cells is dependent on the composition of acrylonitril copolymers, **eingereicht**.

66. Tzoneva R, Groth Th, Altankov G, Paul D, remodeling of fibrinogen by endothelial cells in dependence on fibronectin matrix assembly. Effect of substratum wettability. Journal of Materials Science – Materials in Medicine, **eingereicht**.

9. Literatur

Alcantar NA, Aydil ES, Israellachvili JN (2000) Polyethylene glycol-coated biocompatible surfaces. Journal of Biomedical Materials Research **51**, 343-351.

Alpard SK, Zwischenberger JB (1998) Adult extracorporal membrane oxygenation for severe respiratory failure. Perfusion **13**, 3-15.

Altankov G, Grinnell F (1995) Fibronectin receptor internalization and AP-2 complex reorganization in potassium-depleted fibroblasts. Experimental Cell Research **216**, 299-307.

Alvarez V, Pulido R, Campanero MR, Paraiso V, de Landazuri MO, Sanchez-Madrid F (1991) Differentially regulated cell surface expression of leukocyte adhesion receptors on neutrophils. Kidney International **40**, 899-905.

Anderheiden D, Klee D, Heller B, Richter H, Mittermayer Ch, Höcker H (1990) Surface modification of a biocompatible polymer based on polyurethane for artificial blood vessels. Proceedings of BIOMAT 90 “Polymers and immobilized cells or biomolecules”, Bordeaux, Frankreich.

Andrade JD (1992) Needs, problems, and opportunities in biomaterials and biocompatibility. Clinical Materials **11**, 19-23.

Andrade JD, Lee HB, Jhon MS, Kim SW, Hibbs JB (1973) Water as a biomaterial. Transactions of the American Society of Artificial Internal Organs **19**, 1-7.

Andrade JD, Hlady V (1986) Protein adsorption and materials biocompatibility: A tutorial review and suggested hypothesis. In: Progress in Surface Science **79**, 1 – 63.

Andrade JD, Herron J, Hlady V, Horsley D (1987) Simulation of protein adsorption. The denaturation correlation. Croatica Chemica Acta **60**, 495-503.

Andrade JD, Hlady V (1991) Vroman effects, techniques, and philosophies. Journal of Biomaterials Science – Polymer Edition **2**, 161 – 172.

Anonymus (1992) ISO 10993: Biological evaluation of medical devices. London, International Standard Organisation.

Anonymus (1992) ISO 10993–4: Biological evaluation of medical devices. Part 4: Selection of tests for interaction with blood. London, International Standard Organisation.

Arnander C, Dryjski M, Larsson R, Olsson P, Swedenborg J (1986) Thrombin uptake and inhibition on endothelium and surfaces with a stable heparin coating: A comparative in vitro study. Journal of Biomedical Materials Research **20**, 235-246.

Bardwaj S, Henze U, Klein B, Zwadlo-Klarwasser G, Klinge U, Mittermayer Ch, Klosterhalfen B (1997) Monocyte-biomaterial interaction inducing phenotypic dynamics of monocytes: a possible role of monocyte subsets in biocompatibility. Journal of Materials Science – Materials in Medicine **8**, 737-742.

Baier RE, Meier AE (1988) Implant surface preparation. The International Journal of Oral & Maxillofacial Implants **3**, 9-20.

Baier RE (1984-1985) Adhesion in the biological environment. Biomaterials Medical Devices and Artificial Organs **12**, 133-159.

Baier RE (1999) Physical and biomechanical issues in graft design. Seminars in Vascular Surgery **12**, 8-17.

Bamford CH, Al-Lamee KG (1992) Chemical methods for improving the haemocompatibility of synthetic polymers. Clinical Materials **10**, 243-261.

Bauer TW, Schils J (1999) The pathology of total joint arthroplasty. II Mechanisms of implant failure. Skeletal radiology **28**, 483-497.

Becker GW (1983) Polyurethane In: Kunststoff-Handbuch, Bd. Polyurethane, Oertel G (Hrsg.) Hanser Verlag München.

Bell GI, Dembo M, Bongrand P (1984) Cell adhesion – Competition between nonspecific repulsion and specific bonding. Biophysical Journal **45**, 1051-1064.

Bervers EM, Comfurius P, Zwaal RF (1996) Regulatory mechanisms in the maintainance and modulation of transmembrane lipid asymmetry: pathophysiological implications. Lupus **5**, 480-487.

Benesch J, Svedhem S, Svensson SCT, Valiokas R, Liedberg B, Tengvall P (2001) Protein adsorption to oligo(ethylene glycol) self assembled monolayers : Experiments with fibrinogen, heparinised plasma and serum. Journal of Biomaterials Science – Polymer Edition **12**, 581-597.

Besseling NAM (1997) Theory of hydration forces between surfaces. Langmuir **13**, 2113-2122.

Billmeyer FW Jr. (1971) Textbook of polymer science – Second Edition. Wiley Interscience, New York, 598 S.

Black J (1992) Biological Performance of Materials: Fundamentals of Biocompatibility, 2nd Edition, New York, M. Dekker.

Boffa GA, Lucien N, Faure A, Boffa MC (1977) Polytetrafluoroethylene-N-vinylpyrrolidone graft copolymers: affinity with plasma proteins. Journal of Biomedical Materials Research **11**, 317-337.

Bongrand P, Capo C, Depieds R (1982) Physics of cell adhesion. Progress in Surface Science **12**, 217-286.

Bonomini V, Coli L, Feliciangeli G, Mosconi G, Scolari MP (1995). Long-term results: Cellulosic vs. synthetic membranes. In: Bonomini V, Berland Y, (Hrsg.), Dialysis membranes: Structure and predicitions. Contrib Nephrol Basel: Karger **113**, 120-134.

Bos GW, Scharenborg NM, Poot AA, Engbers GHM, Beugeling T (1999) Proliferation of endothelial cells on surface-immobilised albumin-heparin conjugate loaded with basic fibroblasts growth factor. Journal of Biomedical Materials Research **44**, 330-340.

Bots JG, van der Does L, Bantjes A (1986) Small diameter blood vessel prostheses from blends of polyethylene oxide and polypropylene oxide. Biomaterials **7**, 393-399.

Bowry SK, Courtney JM, prentice CRM, Douglas JT (1984) Utilization of the platelet release reaction in the blood compatibility assessment of polymers. Biomaterials **5**, 289-292.

Brash JL, Ten Hove P (1984) Effect of plasma dilution on adsorption of fibrinogen to solid surfaces. Thrombosis and Haemostasis **51**, 326-330.

Brash JL (1990) Studies of protein adsorption relevant to blood compatible materials. In: Modern Aspects of Protein Adsorption on Biomaterials, (Missirlis YF und Lemm W, Hrsg.), Kluwer Academic Publisher, Dordrecht, 39-48.

Braun D, Cherdron H, Ritter H (1999) Praktikum der makrokolekularen Stoffe. Wiley-VCH, Weinheim, 346 Seiten.

Breuers W, Klee D, Plein P, Richter HA, Menges G, Mittermayer Ch, Höcker H (1987) Modifizieren von Polyetherurethan-Folien für medizinische Anwendungen. Kunststoffe **77**, 1273-1276.

Bruck SD, (1980) Properties of Biomaterials in the Physiological Environment, Boca Raton, CRC Press.

Brooks PC, Montgomery AMP, Rosenfeld M, Reisfeld RA, Hu T, Klier G, Cheresh DA (1994) Integrin ?v?3 antagonists promote tumor regression by inducing apoptosis of angiogenic blood vessels. Cell **79**, 1157-1164.

Burridge K, Turner CE (1992) Tyrosine phosphorylation of Paxillin and pp 125 FAK accompanies cell adhesion to extracellular matrix: A role in cytoskeletal assembly. Journal of Cell Biology **119**, 893-903.

Carlos TM, Harlan JM (1994) Leukocyte-endothelial adhesion molecules. Blood **84**, 2068-2101.

Casu B (1990) Protein-binding domains of heparin and other sulfated glycosaminoglycans. Carbohydrates in Europe **11**, 18-21.

Chen JH, Wei J, Chang CY, Laiw RF, Lee YD (1998) Studies on segmented polyetherurethane for biomedical application: effects of composition and hard-segment content on biocompatibility. Journal of Biomedical Materials Research **41**, 633-48.

Chenoweth DE (1987) Complement activation in extracorporal circuits. Annals of the New York Academy of Sciences **516,** 306-313.

Cheung AK (1994) Complement activation as indices of haemodialysis membrane haemocompatibility: The choice of methods and assays. Nephrology Dialysis Transplantation **9 [suppl.2]**, 96-103.

Christensen K, Larsson R, Emanuelsson H, Elgue G, Larsson A (2001) Heparin coating of the stent graft – effects on platelets, coagulation and complement activation. Biomaterials **22**, 349-355.

Choay J, Petitou M, Lormeau JC, Sinai P, Casu B, Gatti G (1983) Structure-activity relationship in heparin: a synthetic pentasccharide with high affinity for antithrombin III and eliciting high anti-factor Xa activity. Biochemical Biophysical Research Communication **116**, 492-499.

Christopher RA, Kowalczyk AP, McKeown-Longo PJ (1997) Localization of fibronectin matrix assembly sites on fibroblasts and endothelial cells. Journal of Cell Science **110**, 569-581.

Clark RAF (1997) Wound repair: lessons for tissue engineering. In: Principles of tissue engineering (Lanza RP, Langer R, Chick WL Hrsg.), Landes Bioscience, Georgetown, Texas, S. 737-782.

Cobb RR, Molony JL (1996) Interleukin 1ß expression is induced by adherence and is enhanced by Fc-receptor binding to immune complex in THP-1 cells. FEBS Letters **396**, 241-246.

Coleman RW (1969) Activation of plasminogen by plasma Kallikrein. Biochemical Biophysical Research Communication **351**, 273-281.

Coppolino MG, Dedhar S (2000) Bi-directional signal transduction by Integrin receptors. The International Journal Of Biochemistry & Cell Biology **32**, 171-188.

Cozens-Roberts C, Quinn JA, Lauffenburger DA (1990) Receptor-mediated adhesion phenomena. Biophysical Journal **58**, 107-125.

Craddock PR, Fehr J, Dalmasso AP, Brigham KL, Jacob HS (1977) Hemodialysis leukopenia. Pulmonary vascular leukostasis resulting from complement activation by dialyzer cellophane membranes. Journal Clinical Investigation **59**, 879-888.

Danielsson A, Raub E, Lindahl U, Björk I (1986) Role of ternary complexes in which heparin binds both antithrombin and proteases, in the acceleration of the reactions between antithrombin and thrombin or factor Xa. Journal of Biological Chemistry **261**, 15467-15473.

Darnell J, Lodish H, Baltimore D (1994) Molekulare Zellbiologie. Walter de Gruyter Verlag, Berlin-New York, 1277 S.

Defife KM, Hagen KM, Clapper DL, Anderson JM (1999) Photochemically immobilised polymer coatings. Effects on protein adsorption, cell adhesion and leukocyte activation. Journal of Biomaterials Science – Polymer Edition **10**, 1063-1074.

Denstedt JD, Reid G, Sofer M (2000) Advances in ureteral stent technology. World Journal of Urology **18**, 237-242.

Dewez J-L, Lhoest J-B, Detrait E, Berger V, Dupont-Gillain CC, Vincent LM, Schneider Y-J, Bertrand P, Rouxhet PG (1998) Adhesion of mammalian cells to polymer surfaces: from physical chemistry of surfaces to selective adhesion on defined patterns. Biomaterials **19**, 1441-1445.

Dieterich D (1987) Polyurethane In: Methoden der organischen Chemie. Houben-Weyl, **Band E20**, S. 1561.

Dinarello CA (1989) Interleukin-1 and its biologically related cytokines. Advances in Immunology **4**, 153-205.

Dinarello CA (1991) Interleukin-1 and interleukin-1 antagonism. Blood **77**, 1627-1652.

Dinarello CA (1992) Cytokines: Agents provocateurs in hemodialysis. Kidney International **41**, 683-694.

Duan X, Lewis RS (2002) Improved haemocompatibility of cysteine-modified biomaterials via endogenous nitric oxide. Biomaterials **23**, 1197-2003

Duncan AC, Sefton MV, Brash JL (1997) Effect of C4-, C8- and C18-alkylation of poly(vinyl alcohol) hydrogels on the adsorption of albumin and fibrinogen from buffer and plasma: limited correlation with platelet interactions. Biomaterials **18**, 1585-1592.

Duncan R, Kopecek J (1984) Soluble synthetic polymers as potential drug carriers. Advances in Polymer Science **57**, 51-96.

Dvorankova B, Smetana K, Königova R, Singerova H, Vacik J, Jelinkova M, Kapounkova Z, Zahradnik M (1998) Cultivation and grafting of human keratinocytes on a poly(hydroxyethyl methacrylate) support to the wound bed: a clinical study. Biomaterials **19**, 141-146.

Eberhardt RC, Munro MS, Frautschi JR, Lubin M, Clubb FJ, Miller CW, Sevastianov VI (1987) Influence of endogenous albumin binding on blood-material interactions. Annals of the New York Academy of Sciences **516**, 78-95.

Eloy R, Belleville J, Paul J, Pusineri C, Baguet J, Rissoan M-C, Cathignol D, Ffrench P, Ville D, Tartulier D (1987) Thromboresistance of bulk heparinised catheters in human. Thrombosis Research **45**, 223-233.

Fabricius-Homan DJ, Cooper SL (1991) A comparison of the adsorption of three adhesive proteins to biomaterial surfaces. Journal of Biomaterials Science – Polymer Edition **3**, 27-47.

Falck P (1994) Activation of human neutrophils by organic polymer surfaces. Journal of Materials Science – Materials in Medicine **29**, 4007-4012.

Falck P (1995) Characterization of human neutrophils adherent to organic polymers. Biomaterials **16**, 61-66.

Faruqi RM, DiCorleto PE (1993) Mechanisms of monocyte recruitment and accumulation. British heart Journal **69[suppl]**, S19-S29.

Fasman GD (1986) Handbook of Biochemistry and Molecular Biology 3rd Edition, Proteins Volume II, CRC Press, Boca Raton.

Feng L, Andrade JD (1994) Protein adsorption on low temperature isotropic carbon: I. Protein conformational change probed by differential scanning calorimetry. Journal of Biomedical Materials Research **28**, S. 735 –

Fey-Lamprecht F, Groth Th, Albrecht W, Paul D, Gross U (2000) Development of membranes for the cultivation of kidney epithelial cells. Biomaterials **21(2)**, 183-192.

Garcia AJ, Boettiger D (1999) Integrin-fibronectin interactions at the cell-material interface: initial integrin binding and signaling. Biomaterials **20**, 2427-2433.

Geiger B, Bershadsky A, Pankov R, Yamada KM (2001) Transmembrane extracellular matrix – cytoskeleton crosstalk. Nature Reviews – Molecular Cell Biology **2**, 793-805.

Gentry PA (1992) The mammalian blood platelet – its role in hemostasis, inflammation and tissue repair. Journal of Comparative Pathology **107**, 243-270.

George JN, Nurden AT, Phillips DR (1984) Molecular defects in interaction of platelets with the vessel wall. New England Journal of Medicine **311**, 1084-1096.

Gerlach J, Koppel K, Schauwecker HH, Tauber R, Muller C, Bücherl ES (1989) Use of hepatocytes in adhesion and suspension culture for liver support bioreactors. Artificial Organs **12**, 788-792.

Gerlach JC (1996) Development of a hybrid liver support system. A review. International Journal of Artificial Organs **19,** 645-654.

Gilmore AP, Burridge K (1996) Regulation of Vinculin binding to talin and actin by phosphatidylinositol-4-5-bisphosphate. Nature **381**, 531-535.

Ginsberg MII, Du X, Plow EF (1993) Inside-out signaling. Current Opinion in Cell Biology **4**, 766-771.

Grasel TG, Cooper SL (1986) Surface properties and blood compatibility of polyurethaneureas. Biomaterials **7**, 315-328.

Griffith L (2000) Polymeric biomaterials. Acta Materialia **48**, 263-277.

Grinnell F, Milam M, Spree P (1973) Attachment of normal and transformed hamster kidney cells to substrata varying in chemical composition. Biochemical Medicine **7**, 87-90.

Grinnell F, Feld MK (1981) Adsorption characteristics of plasma fibronectin in relationship to biological activity. Journal of Biomedical Materials Research **15**, 363-381.

Grinnell F (1986) Focal adhesion sites and the removal of substratum-bound fibronectin. Journal of Cell Biology **103**, 2697-2706.

Grinnell F (1987) Fibronectin adsorption on material surfaces. Annals of New York Academy of Sciences **516,** 280-290.

Gross UM (1988) Biocompatibility – the interaction of biomaterials and host response. Journal of Dental Education **52**, 798-803.

Groth Th, Falck P, Miethke R.-R (1995) Cytotoxicity of biomaterials – Basic mechanisms and in vitro test methods: A review. Alternatives to Laboratory Animals **23**, 790 – 799.

Groth Th, Altankov G (1998) Cell-surface interactions and the tissue compatibility of biomaterials. In: New Biomedical Materials, (Harris PI and Chapman D, Hrsg.), IOS Press, Amsterdam, 12-23.

Groth, Th., Altankov G (2001) Insights into the tissue compatibility of biomaterials. Proceedings of 9th International Conference on Polymers in Medicine and Surgery, IOM Publications, London, 205-213.

Groth Th, Seifert B, Albrecht W, Malsch G (2002) Mit Blut und Gewebe verträgliche Membranen aus P(AN-NVP) Mischpolymeren und deren Anwendung im medizinischen Bereich. Offenlegunsschrift DE 100 30 307 A1.

Hamburger SA, McEver RP (1990) GMP-140 mediates adhesion of stimulated platelets to neutrophils. Blood **75**, 550-554.

Harker LA, Fuster V (1986) Pharmakology of platelet inhibitors. Journal of the American College of Cardiology **8**, 21b-32b.

Harris PI, Chapman D (1998) New biomaterials based on mimicry of biomembrane components. In: New Biomedical Materials (Harris PI, Chapman D, Hrsg.), IOS Press, Amsterdam, 24-31.

Hayward JA, Chapman D (1984) Biomembrane surfaces as models for polymer design – the potential for haemocompatibility. Biomaterials **5**, 135-142.

Helmus MN, Hubbell JA (1993) Materials selection. Cardiovascular Pathology **2[suppl]**, 53S-71S.

Hern DL, Hubbell JA (1998) Incorporation of adhesion peptides into nonadhesive hydrogels useful for tissue resurfacing. Journal of Biomedical Materials Research **39**, 266-267.

Himmelfarb J, Lazarus JM, Hakim R (1991) Reactive oxygen species production by monocytes and polymorphonuclear leukocytes during dialysis. American Journal of Kidney Disease **17**, 271-276.

Hirasawa H, Sugai T, Oda S, Shiga H, Matsuda K, Ueno H, Sadahiro T (1997) Efficacy and limitation of apheresis therapy in critical care. Therapeutical Apheresis **1**, 228-223.

Hocking DC, Smith RK, McKeown-Longo PJ (1996) A novel role for the Integrin-binding III-10 module in fibronectin matrix assembly. Journal of Cell Biology **133**, 431-444.

Hoenich NA, Woffindin C, Mathews JNS, Viencken J (1995) Biocompatibility of membranes used in the treatment of renal failure. Biomaterials **16**, 587 – 592.

Hoffman AS (1986) Letter to the editor: A general classification scheme for “hydrophilic” and “hydrophobic” biomaterial surfaces. Journal of Biomedical Materials Research **20**, ix-xi.

Hoffman AS (1987) Modification of material surfaces to affect how they interact with blood. Annals of the New York Academy of Sciences **516**, 96-101.

Hoffman (2001) Hydrogels for biomedical applications. Annals of the New York Academy of Sciences **944**, 62-73.

Hoffmann A und Markwardt F (1984) Inhibition of the thrombin-platelet reaction by Hirudin. Hemostasis **14**, 164-169.

Horbett TA (1984) Mass action effects on competitive adsorption of fibrinogen from hemoglobin solutions and from plasma. Thrombosis and Haemostasis **51**, S. 174 –181.

Horbett TA, Schway MB (1988) Correlations between mouse 3T3 cell spreading and serum fibronectin adsorption on glass and hydroxymethylmethacrylate-ethylmethacrylate copolymers, Journal of Biomedical Materials Research **22**, 763-793.

Horbett TA (1993) Principles underlying the role of adsorbed plasma proteins in blood interactions with foreign materials. Cardiovascular Pathology **2 [suppl],** 137S-148S.

Huang S, Ingber DE (1999) The structural and mechanical complexity of cell growth control. Nature Cell Biology **1**, E131-E138.

Hubbell JA (1998) Synthetic biodegradable polymers for tissue engineering and drug delivery. Current Opinion in Solid State & Materials Science **3**, 246-251.

Huber AR, Kunkel SL, Todd RF, Weiss SJ (1991) Regulation of transendothelial neutrophil migration by endogenous interleukin-8. Science **254**, 99-102.

Hudson TW, Evans GR, Schmidt CE (2000) Engineering strategies for peripheral nerve repair. Orthopedic Clinics of North America **31**, 485-498.

Hughes RD, Williams R (1996) Assessment of bioartificial liver support in acute liver failure. International Journal of Artificial Organs **19**, 3-6.

Huisveld IA, Haspers H, Van Heeswijk GM, Bernink MJE, Erich WBM, Bouma BN (1985) Contribution of contact activation factors to urokinase-related fibrinolytic activator in whole plasma. Thrombosis and Haemostasis **54**, 102-113.

Humes HD (2000) Bioartificial kidney for full renal replacement therapy. Seminars in Nephrology **20**, 71-82.

Hurst RE, Menter JM, West SS, Settine JM, Coyne EH (1979) Structural basis for anticoagulant activity of heparin. 1. Relationship to the number of charged groups. Biochemistry **18,** 4283-4287.

Hyde JAJ, Chinn JA, Phillips RE Jr. (1999) Polymer heart valves. Journal of Heart Valve Disease **8**, 331-339.

Hynes RO (1987) Integrins: a family of cell surface receptors. Cell **48**, 549-554.

Hynes RO (1992) Integrins: versatility, modulation, and signalling in cell adhesion. Cell **69**, 11-25.

Ingber D (1998) In search of cellular control: signal transduction in context. Journal of Cellular Biochemistry Supplements **30/31**, 232-237.

Ishihara K, Nomura H, Mihara T, Kurita K, Iwasaki Y, Nakabayashi N (1998) Why do phospholipids reduce protein adsorption ? Journal of Biomedical Materials Research **39**, 323-330.

Ishihara K, Ishikawa E, Iwasaki Y, Nakabayashi N (1999) Inhibition of fibroblast cell adhesion on substrate by coating with 2methacrylooxyethyl phosphorylcholine polymers. Journal of Biomaterials Science – Polymer Edition **10**, 1047-1061.

Iwasaki Y, Ijuin M, Mikami A, Nakabayashi N, Ishihara K (1999) Behavior of blood cells in contact with water-soluble phospholipid polymer. Journal of Biomedical Materials Research **46**, 360-367.

Jacobs AA, Ward RA, Wellhausen SR, McLeish KR (1989) Polymorphonuclear leukocyte function during hemodialysis. Relationship to complement activation. Nephron **52**, 119-124.

Johnson RJ (1994) Complement activation during extracorporal therapy: biochemistry, cell biology and clinical relevance. Nephrology Dialysis Transplantation **9 [suppl. 2]**, 36-45.

Juliano RL, Haskill S (1993) Signal transduction from the extracellular matrix. Journal of Cell Biology **120**, 577-585.

Juliano DJ, Saavedra SS, Truskey GA (1993) Effect of the conformation and orientation of adsorbed fibronectin on endothelial cell spreading and the strength of adhesion. Journal of Biomedical Materials Research **27**, 1103-1113.

Kaelble DH, Moacanin J (1979) Surface energetics analysis of artificial blood substitutes. Medical Biology Engineering and Computing **17**, 593-601.

Kao WJ, Hubbell JA, Anderson JM (1999) Protein-mediated macrophage adhesion and activation on biomaterials: A model for modulating cell behavior. Journal of Materials Science - Materials in Medicine **10**, 601-605.

Kapur R, Lilien J, Black J (1993) Field-dependent fibroblast orientation on charged surfaces is independent on polarity and adsorbed serum proteins. Biomaterials **14**, 854-860.

Kaplan AP, Silverberg M (1987) The coagulation-kinin pathway of human plasma. Blood **70**, 1-15.

Katz B-Z, Zamir E, Bershadsky A, Kam Z, Yamada KM, Geiger B (2000) Physical state of the extracellular matrix regulates the structure and molecular composition of cell-matrix adhesions. Molecular Biology of the Cell **11**, 1047-1060.

Kawakami H, Mori Y, Takagi J, Nagaoka S, Kanamori T, Shinbo T, Kubota S (1997) Development of a novel polyimide hollow fiber for an intravascular oxygenator. ASAIO Journal **43**, M490-494.

Kiefer N (1993) Structure and function of platelet membrane gylcoproteins. In: The role of platelets in blood-biomaterial interactions. (Missirlis YF und Wuatier J-L, Hrsg.), Kluwer Academic Publishers, Dordrecht, 15-33.

Kim SW, Jacobs H, Lin JY, Nojori C, Okano T (1987) Nonthrombogenic bioactive surfaces. Annals of the New York Academy of Sciences **516**, 116-130.

Kirkpatrick CJ, Mittermayer C (1990) Theoretical and practical aspects of testing potential biomaterials in vitro. Journal of Materials Science – Materials in Medicine **1**, 9 – 13.

Kirkpatrick CJ, Bittinger F, Wagner M, Köhler H, van Kooten TG, Klein CL, Otto M (1998) Current trends in biocompatibility testing. Proceedings of the Institution of Mechanical Engineers Part H-Journal of Engineering in Medicine **212 [Part H]**, 75 – 84.

Kirkpatrick CJ, Wagner M, Köhler H, Bittinger F, Otto M, Klein CL (1997) The cell and molecular biological approach to biomaterial research: a perspective. Journal of Materials Science – Materials in Medicine **8**, 131 – 141.

Klinkmann H, Wolf H, Schmitt E (1984) Definition of biocompatibility. Contributions in Nephrology **37**, 70-77.

Klinkmann H, Viencken J (1995) Membranes for dialysis. Nephrology Dialysis Transplantation **10 [Suppl. 3]**, 39-45.

Klinkmann H (1995) Clinical relevance of biocompatibility – the necessity of a systems approach. Proceedings of 5th Dresden Polymer Discussion, Königstein, 38-52.

Kloczewiak M, Timmons S, Bednarek A, Sakon M, Hawinger J (1989) Platelet receptor recognition domain on the ?-chain of human fibrinogen and its synthetic peptide analogues. Biochemistry **28**, 2915-1919.

Klosz K (1993) Beziehungen zwischen chemischer Struktur, hydrophilem Verhalten und in vitro Hämokompatibilität von Polyurethan-Harnstoff-Elastomeren. Dissertation, Freie Universität Berlin.

Kolff WJ, Berk HT (1943) De kunstmatige nier, een dialysator met groot opperlak. Ned Tijdschr Geneeskd **87**, 1684-1688.

Koshikawa N, Gianelli G, Cirulli V, Miyazaki K, Quaranta V (2000) Role of cell surface metalloprotease MT1-MMP in epithelial cell migration over laminin-5. Journal of Cell Biology **148**, 615-624.

Kumaki T, Sisido M, Imanishi Y (1985) Antithrombogenicity and oxygen permeability of block and graft copolymers of polysimethylsiloxane and poly(a-amino acid). Journal of Biomedical Materials Research **19**, 785-811.

Kumaki T, Sisido M, Imanishi Y (1985) Antithrombogenicity and oxygen permeability of block and graft copolymers of polydimethylsiloxane and poly(?-amino acids). Journal of Biomedical Materials Research **19**, 785-811.

Kunz R, Anders C, Gersonde K (1998) Principles for the reduction of bacterial adhesion to surface-modified polymers. In: New Biomedical Materials (Harris PI, Chapman D, Hrsg.), IOS Press, Amsterdam, 115-121.

Kurz H, Lerner RG, Weseley S, Nelson JC (1985) Changes in fibrinolytic activity during a course of a single haemodialysis session. Clinical Nephrology **24**, 1-4.

Laemmel E, Penhoat J, Warocquier-Clerout R, Sigot-Luizard M-F (1998) Heparin immobilized on proteins usable for arterial prosthesis coating: Growth inhibition of smooth-muscle cells. Journal of Biomedical Materials Research **39**, 446-452.

Lahann J, Klee D, Pluester W, Hoecker H (2001) Bioactive immobilization of r-hirudin on CVD-coated metallic implant devices. Biomaterials **22**, 817-826.

Lamba NA, Courtney JM, Gaylor JD, Lowe GD (2000) In vitro investigation of the blood response to medical grade PVC and the effect of heparin on the blood response. Biomaterials **21**, 89-96.

Lane DA, Bowry SK (1994) The scientific basis for selection of measures of thrombogenicity. Nephrology Dialysis Transplantation **9 [suppl. 2]**, 18-28.

Larson E, Celi A, Gilbert GE, Furie BC, Erban JK, Bonfanti R, Wagner DD, Furie B (1989) PADGEM protein: A receptor that mediates the interaction of activated platelets with neutrophils and monocytes. Cell **59**, 305-312.

Leckband D, Sheth S, Halperin A (1999) Grafted poly(ethylene oxide) brushes as nonfouling surface coatings. Journal of Biomaterials Science – Polymer Edition **10**, 1125-1147.

Lee JH, Lee HB (1998) Platelet adhesion onto wettability gradient surfaces in the absence and presence of plasma proteins. Journal of Biomedical Materials Research **41**, 304-311.

Lee JH, Yoon JY, Kim WS (1998) Continuous separation of serum proteins using a stirred cell charged with carboxylated and sulfonated microspheres. Biomedical Chromatography **12**, 330-334.

Legallais C, David B, Doré E (2000) Bioartificial livers (BAL): current technological aspects and future developments. Journal of Membrane Science **181**, 81-95.

Lendlein A (1999) Polymere als Implantatwerkstoffe. Chemie in unserer Zeit **33**, 279-295.

Lelah MD, Grasel TG, Pierce JA, Cooper SL (1986) Ex vivo interactions and surface property relationships for polyetherurethanes. Journal of Biomedical Materials Research **20**, 433-468.

Li J-S, Ito Y, Zheng J, Takahashi T, Imanishi Y (1997) Enhancement of artificial juxtacrine stimulation of insulin by co-immobilisation with adhesion factors. Journal of Biomedical Materials Research **37**, 190-197.

Lindhout T (1994) Biocompatibility of extracorporal blood treatment. Selection of haemostatic parameters. Nephrology Dialysis Transplantation **9 [suppl. 2]**, 83-89.

Lindhout T, Blezer R, Hemker HC (1990) The anticoagulant mechanism of action of recombinant Hirudin (CGP 39393) in plasma. Thrombosis and Haemostasis **64**, 464-468.

Lyklema J (1985) Surface and Interfacial Aspects of Biomedical Polymers, Band 1, (Andrade JD, Hrsg.), Plenum Press, New York, 293 S.

Lyman DJ, Knutson K, McNeill B, Shibatini K (1975) The effects of chemical structure and surface properties of synthetic polymers on the coagulation of blood IV. The relation between polymer morphology and protein adsorption. Transactions American Society of Artificial Internal Organs **21**, 49-57.

Mandle RJ Jr, Kaplan AP (1977) Hageman factor substrates: II. Human plasma kallikrein. Mechanism of activation by Hageman factor and participation in Hageman factor-dependent fibrinolysis. Journal of Biological Chemistry **252**, 6097-7004.

Manning D, Brass L (1991) The role of GTP-binding proteins in platelet activation. Thrombosis and Haemostasis **66**, 393-399.

Markus AJ, Safier LB, Ullman HL, Islam N, Broekman MJ, Falck JR, Fischer S, Schacky C (1987) Cell-cell interactions in the eicosanoid pathway. The Annals of the New York Academy of Sciences **516**, 407-411.

Markwardt F (1991) Hirudin and derivatives as anticoagulant agents. Thrombosis and Haemostasis **66**, 141-152.

Massia SP, Hubbell J (199o) Covalent surface immobilization of Arg-Gly-Asp and Tyr-Ile-Gly-Ser-Arg containing peptides to obtain well-defined cell-adhesive substrata. Analytical Biochemistry **187**, 292-301.

Massia SP, Stark J, Letbetter DS (2000) Surface-immobilised dextran limits cell adhesion and spreading. Biomaterials **21**, 2253-2261.

Mateo C, Fernandez-Lorente G, Abian O, Fernandez-Lafuente R, Guisan JM (2000) Multifunctional epoxy supports: a new tool to improve the covalent immobilization of proteins. The promotion of physical adsorptions of proteins on the supports before their covalent linkage. Biomacromolecules **1**, 739-745.

Matsuda T, Takano H, Hayashi K, Taenaka Y, Takaichi S, Umezu I, Nakamura T, Iwata H, Nakatani T, Tanaka T (1984) The blood interface with segmented polyurethanes: multilayered protein passivation mechanism. Transactions of the American Society for Artificial Organs **30**, 353-358.

Matsuo M, Sagaye S (1971) Micromorphology – property relationships in graft and block copolymers. In: Colloidal and morphological behaviour of block and graft copolymers, Molau GE (Hrsg.) New York Plenum press, 1-13.

McDonalds JA (1988) Extracellular matrix assembly. Annual Review in Cell Biology **4**, 183-207

McEver RP (1991) Leukocyte interactions mediated by selectins. Thrombosis and Haemostasis **66**, 80-87.

McFarland CD, DeFillipis C, Jenkins M, Tunstell A, Rhodes NP, Williams DF, Steele JG (1998) Albumin-binding surfaces: in vitro activity. Journal of Biomaterials Research – Polymer Edition **9**, 1227-1239.

McNally AK, Anderson JM (1994) Complement C3 participation in monocyte adhesion to different surfaces. Proceedings of the National Academy of Sciences USA **91,** 10119-10123.

Merrill EW, Salzman EW, Wan S, Mahmud N, Kushner L, Lindon JN, Curme J. Platelet-compatible hydrophilic segmented polyurethanes from polyethylene glycols and cyclohexane diisocyanate. Transactions of the American Society of Artifical Internal Organs **28**, 482 - 487.

Missirlis YF, WautierJ-L (1993) The role of platelets in blood-biomaterial interactions. Kluwer Academic Publishers, Dordrecht, 216 S.

Morra M, Cassinelli C (1999) Non-fouling properties of polysaccharide-coated surfaces. Journal of Biomaterials Science – Polymer Edition **10**, 1107-1121.

Muller-Eberhard HJ (1992) Complement: chemistry and pathways. In: Inflammation (Gallin JI, Goldstein IM, Snyderman R, Hrsg.) Raven Press, New York, 33-62.

Mulzer SR, Brash JL (1989) Identification of plasma proteins adsorbed to hemodialyzers during clinical use. Journal of Biomedical Materials Research **23**, 1483 – 1504.

Munro MS, Eberhardt RC, Maki NJ, Brink BE, Fry WJ (1981) Alkyl substituted polymers with enhanced albumin affinity. Transactions of American Society for Artificial Internal Organs **27**, 499-503.

Nagahara S, Matsuda T (1996) Cell-substrate and cell-cell interactions differentially regulate cytoskeletal and extracellular matrix protein gene expression. Journal of Biomedical Materials Research **32**, 677-686.

Nedelmann H, Weigel T, Hicke HG, Müller J, Paul D (1999) Microwave plasma polymerization of acrylic acid on poly(ethylene terephthalate) track-etched membranes. Surface & Coatings Technology **119**, 973-980

Nimni ME (1997) Polypeptide growth factors: targeted delivery systems. Biomaterials **18**, 1201-1225.

Norde W (1986) Adsorption of proteins from solution at the solid-liquid interface. Advances in Colloid and Interface Science **25**, 267-340.

Norde W, Lyklema J (1991) Why proteins prefer interfaces. Journal of Biomaterials Science – Polymer Edition **2**, 183 – 202.

Nydegger U, Rieben R, Lammle B (1996) Biocompatibility in transfusion medicine. Transfusion Science **17**, 481-488.

Okano T, Nishiyama S, Shinohara I, Akaike T, Sakurai Y (1978) Interaction between plasma protein and microphase separated structure of copolymer. Polymer Journal **10**, 223-228.

Okano T, Uruno M, Sugiyama N, Shimida M, Shinohara I, Kataoka K, Sakurai Y (1986) Supression of platelet activity on microdomain surfaces of 2-hydroxyethyl methacrylate-polyether block copolymers. Journal of Biomedical Materials Research **20**, 1035-1047.

Okkema AZ, Cooper SL (1991) Effect of carboxylate and/or sulphonate ion incorporation on the physical and blood-contacting properties of a polyetherurethane. Biomaterials **12**, 668-678.

Österberg E, Bergström K, Holmberg K, Schuman TP, Riggs JA, Burns NL, Van Alstine JM, Harris JM (1995) Protein-rejecting ability of surface-bound dextrans in end-on and side-on configuration: Comparison to PEG. Journal of Biomedical Materials Research **29**, 741-747.

Ostuni E, Chapman RG, Holmlin RE, Takayama S, Whitesides GM (2001) A survey of structure-property relationships of surfaces that resist the adsorption of protein. Langmuir **17**, 5605-5620.

Otey CA, Pavalko FM, Burridge K (1990) An interaction between ?-actinin and the ?1 subunit in vitro. Journal Cell Biology **111**, 721-729.

Otsuka H, Nagasaki Y, Kataoka K (2000) Surface characterization of functionalized polylactide through the coating with heterobifunctional poly(ethylene glycol)/polylactide block copolymers. Biomacromolecules **1**, 39-48.

Owen DR, Chen CM, Oschner JA, Zone RM (1985) Interaction of plasma proteins with selective artificial surfaces. Transactions American Society for Artificial Internal Organs **31**, 240-243.

Palmaz AJR (1993) Intravascular stents – tissue-stent interactions and design considerations. American Journal of Roentgenology **160**, 613-618.

Pankov R, Cukierman E, Katz B-Z, Matsumoto K, Lin DC, Lin S, Hahn C, Yamada KM (2000) Integrin dynamics and matrix assembly: Tensin-dependent translocation of ?5?1-Integrin promotes early fibronectin fibrillogenesis. Journal Cell Biology **148**, 1075-1090.

Park JB (1995) Biomaterials – Introduction, In: The Biomedical Engineering Handbook (Bronzino JD, Hrsg.), CRC Press, Boca Raton, 530 – 536.

Parnes E, Shapiro W (1991) Anaphylactoid reactions in haemodialysis patients treated with AN 69S dialysers. Kidney International **40**, 1148 – 1152.

Parzer S, Balcke P, Mannhalter C (1993) Plasma protein adsorption to hemodialysis membranes: Studies in an in vitro model. Journal of Biomedical Materials Research **27**, 455-463.

Peinemann KV, Maggioni JF, Nunes SP (1998) Poly(etherimide) membranes obtained from solutions in cosolvent mixtures. Polymer **39**, 3411-3416.

Pereira BJG, Dinarello CA (1994) Production of cytokines and cytokine inhibitor proteins in patients on dialysis. Nephrology Dialysis Transplantation **9 [suppl.2]**, 60-71.

Petitt DK, Hoffman AS, Horbett TA (1994) Correlation between corneal epithelial outgrowth and monoclonal antibody binding to the cell-binding domain of adsorbed fibronectin. Journal of Biomedical Materials Research **28**, 685-691.

Prime KL, Whiteside GMJ (1993) Adsorption of proteins onto surfaces containing end-attached oligo(ethylene oxide) – a model system using self-assembled monolayers. Journal of the American Chemical Society **115**, 10714-10721.

Prokop A, Hunkeler D, Di Mari S, Haralson MA, Wang TG (1998) Water soluble polymers for immunoisolation. I: complex coacervation and cytotoxicity. Advances in Polymer Science **36**, 1-51.

Qiang S, Yaoting Y, Hongyin L, Klinkmann H. (1997) Comparative evaluation of different membranes for the construction of an artificial liver support system. International Journal of Artificial Organs **20**, 119-124.

Rapoza RJ, Horbett TA (1990) Postadsorptive transitions in fibrinogen : influence of polymer properties. Journal of Biomedical Materials Research **10**, 1263-1287.

Rasmont A, Leclere P, Doneux C, Lambin G, Tong JD, Jerome R, Bredas JL, Lazzaroni R (2000) Microphase separation at the surface of block copolymers, as studied with atomic force microscopy. Colloids and Surfaces B: Biointerfaces **19**, 381-395.

Ratner BD, Hoffman AS, Hanson SR, Harker LA, Whiffen JD (1979) Blood compatibility – water-content relationships for radiation-grafted hydrogels. Journal of Polymer Science – Part C: Polymer Symposium **66**, 363-375.

Ratner BD (1985) Graft copolymer and block-copolymer surfaces. In: Surface and Interfacial Aspects of Biomedical Polymers. (Andrade JD, Hrsg.) Plenum Press, New York 373-394.

Ratner BD (1993[a]) The blood compatibility catastrophe. Journal of Biomedical Materials Research 27, 283-287.

Ratner BD (1993[b]) New ideas in biomaterials science – a path to engineered biomaterials. Journal of Biomedical Materials Research **27**, 837-850.

Rau DC, Parsegian VA (1990) Direct measurement of forces between linear polysaccharides Xanthan and Schizophyllan. Science **249**, 12-78-1281.

Richardson RR Jr, Miller JA, Reichert WM (1993) Polyimide as biomaterials: preliminary biocompatibility testing. Biomaterials **14**, 627-635.

Ruoslahti E, Pierschbacher MD (1986) Arg-Gly-Asp: A versatile cell recognition signal. Cell **44**, 517-518.

Ruoslahti E (1996) RGD and other recognition sequences for integrins. Annual Review in Cell Biology **12**, 697-715.

Ruoslahti E (1997) Integrins as signaling molecules and targets for tumor therapy. Kidney International **51**, 1413-1417.

Ruoslahti E, Reed JC (1994) Anchorage dependence, integrins and apoptosis. Cell **77**, 477-478.

Salama A, Hugo F, Heinrich D (1988) Deposition of terminal C5b-9 complex on erythrocytes and leukocytes during cardiopulmonary bypass. New England Journal of Medicine **318**, 408-414.

Salzman EW, Lindon L, McManama G, Ware AJ (1987) Role of fibrinogen in activation of platelets by artificial surfaces. Annals of the New York Academy of Sciences **516**, 184-195.

Sato GH (1997) Regulation of Cell behavior by extracellular proteins. In: Principles of tissue engineering. (Lanza RP, Langer R, Chick RW, Hrsg.), Landes Bioscience, Austin, Texas, 11-132.

Sawamoto K, Takahashi N (1997), Modulation of hepatocyte function by changing the cell shape in primary culture. In Vitro Cellular & Developmental Biology – Animal **33**, 569-574.

Schmid-Schönbein H, Born GVR, Richardson PD, Cusack N, Rieger H, Forst R, Rohling-Winkel I, Blasberg P, Wehmeyer A (1981) Rheology of thrombotic processes in flow: The interaction of erythrocytes and thrombocytes subjected to high flow forces. Biorheology **18**, 415-444.

Scott CF (1991) Mechanism of the participation of the contact system in the Vroman effect. Review and summary. Journal of Biomaterials Science – Polymer Edition **2**, 173 – 181.

Seyfert S, Voigt A, Kabbeck-Kupijai D (1995) Adhesion of leukocytes to microscope slides as influenced by electrostatic interaction. Biomaterials **16**, 201-208.

Sharma CP, Essel RM, Arnaout MA (1995) Direct interaction of filamin (ABP-280) with the ?2-integrin subunit. Journal Immunology **154**, 3461-3470.

Shalaby SW, Hoffman AS, Ratner BD, Horbett TA (Hrsg,) (1986) Polymers as biomaterials. Plenum Press, New York.

Sharkey PF, Hozack WJ, Dorr LD, Maloney WJ, Berry D (2000) The bearing surface in total hip arthroplasty: evolution or revolution. Instrumentation Course Lectures **49**, 41-56.

Sigal GB, Mrksich M, Whitesides GM (1998) Effect of surface wettability on the adsorption of proteins and detergents. Journal American Chemical Society **120**, 3464-3473.

Silverberg M, Diehl SV (1987) The activation of the contact system of human plasma by polysaccharide sulfates. Annals of the New York Academy of Science **516**, 268 – 279.

Sims PJ, Ginsberg MH, Plow EF, Shattil SJ (1991) Effect of platelet activation on the conformation of the plasma membrane glycoprotein IIb-IIIa complex. Journal of Biological Chemistry **266**, 7345-7352.

Slack SM, Cui Y, Turitto VT (1993) The effects of flow on blood coagulation and thrombosis. Thrombosis and Haemostasis **70**, 129-134.

Snyderman R, Goetzl J (1981) Molecular and cellular mechanisms of leukocyte chemotaxis. Science **213**, 830-837.

Sofia SJ, Premnath V, Merrill EW (1998) Poly(ethylene oxide) grafted to silicon surfaces: grafting density and protein adsorption. Macromolecules **31**, 5059-5070.

Springer TA (1994) Traffic signals for lymphocyte recirculation and leukocyte emigration: The multistep paradigm. Cell **76**, 301-314.

Steele JG, Johnson G, McFarland C, Dalton BA, Gengenbach TR, Chatelier RC, Underwood PA, Griesser HJ (1994) Roles of serum vitronectin and fibronectin in initial attachment of human vein endothelial cells and dermal fibroblasts on oxygen- and nitrogen-containing surfaces made by radiofrequency plasmas. Journal of Biomaterials Science – Polymer Edition **6**, 511-532.

Takahara A, Jo NJ, Kajiyama T (1989) Surface molecular mobility and platelet reactivity of segmented poly(etherurethaneureas) with hydrophilic and hydrophobic soft segment components. Journal of Biomaterials Science – Polymer Edition **1**, 17-29.

Tamada Y, Ikada Y (1994) Fibroblast growth on polymer surfaces and the biosynthesis of collagen. Journal of Biomedical Materials Research **28**, 783-789.

Tang L, Eaton JW (1993) Fibrin(ogen) mediates acute inflammatory response to biomaterials. Journal of Experimental Medicine **178**, 2147-2156.

Tans G, Rosing J (1987) Structural and functional characterization of factor XII. Seminars in Thrombosis and Hemostasis **13**, 1-14.

Tickner JA, Schettler T, Guidotti T, McCally M, Rossi M (2001) Health risks posed by use of Di-2-ethylhexyl phthalate (DEHP) in PVC medical devices: a critical review. American Journal of Industrial Medicine **39**, 100 – 111.

Tielemanns C, Madhoun P, Lenaers M, Schandande L, Goldman M, Vanherweghem J (1990) Anaphylactoid reactions during haemodialysis on AN 69S membranes in patients receiving ACE inhibitors. Kidney International **38**, 982 – 984.

Tzoneva R, Heuchel M, Groth T, Altankov G, Albrecht W, Paul D (2002) Fibrinogen adsorption and platelet interactions on polymer membranes. Journal of Biomaterials Science - Polymer Edition, **im Druck**.

Turner CE (2000) Paxillin and focal adhesion signalling. Nature Cell Biology **2**, E231-E236.

Ulbricht M, Riedel M (1998) Ultrafiltration membrane surfaces with grafted polymer tentacles: preparation, characterization and application for covalent protein binding. Biomaterials **19**, 1229-1237.

Unanue ER, Allen PM (1987) The basis for the immunoregulatory role of macrophages and other accessory cells. Science **236**, 551-557.

Underwood PA, Bennett FA (1993) The effect of extracellular matrix molecules on the in vitro behavior of bovine endothelial cells. Experimental Cell Research **205**, 311-319.

Van Beusekom HMM, Van der Giesen WJ, Van Suylen RJ, Bos E, Bosman FT, Serruys PW (1993) Histology after stenting of human saphenous-vein bypass grafts - observations from surgically excised grafts 3 to 320 days after stent implantation. Journal of the American College of Cardiology **21**, 45-54.

Van Wachem PB, Vreriks CM, Beugeling T, Feijen J, Bantjes A, Detmers JP (1987) The influence of protein adsorption on interactions of cultured human endothelial cells with polymers. Journal of Biomedical Materials Research **21**, 701-718.

Van Wagenen RA, Andrade JD (1980) Flat plate streaming potential investigations: Hydrodynamics and electrokinetic equivalency. Journal of Colloid and Interface Science **76**, 305-314.

Veresen L, Waer M, Vanrenthergem M, Michielsen P (1990) Angiotensin-converting enzyme inhibitors and anaphylactoid reactions to high flux membranes. Lancet **336**, 1360 – 1362.

Vogler EA (1998) Structure and reactivity of water at biomaterial surfaces. Advances in Colloid and interface science **74**, 69 – 117.

Vogler EA, Graper JC, Harper GR, Sugg HW, Lander LM, Brittain WJ (1995), Contact activation of the plasma coagulation cascade. I. Procoagulant surface chemistry and energy. Journal of Biomedical Materials Research **29**, 1005-1016.

von Sengbusch G, Bowry S, Viencken J (1993) Focusing on membranes. Artificial Organs **17**, 244-253.

Vroman L, Adams AL (1969)[a], Findings with the recordings ellipsometer suggesting rapid exchange of specific plasma proteins at liquid/solid interfaces. Surface Science **16**, 438 – 446.

Vroman L, Adams AL (1969)[b], Identification of adsorbed protein films by exposure to antisera and water vapor. Journal of Biomedical Materials Research **3**, 669 – 681.

Ward RA (1994) Phagocytic cell function as an index of biocompatibility. Nephrology Dialysis Transplantation **9 [suppl. 2]**, 46-56.

Wary KK, Mainiero F, Isakoff SJ, Marcantonio EE, Giancotti FG (1996) The adaptor protein Shc couples a class of integrins to the control of cell cycle progression. Cell **87**, 733-743.

Webb DJ, Parsons JT, Horwitz AF (2002) Adhesion assembly, disassembly and turnover in migrating cells – over and over and over again. Nature Cell Biology **4**, E97-E100.

Webb K, Hlady V, Tresco PA (1998) Relative importance of surface wettability and charged functional groups on NIH 3T3 fibroblast attachment, spreading, and cytoskeletal organization. Journal of Biomedical Materials Research **41**,422-430.

Webb K, Hlady V, Tresco PA (2000) Relationships among cell attachment, spreading, cytoskeletal organization, and migration rate for anchorage-dependent cells on model surfaces. Journal of Biomedical Materials Research **49**, 362-368.

Weiss HJ, Turitto VT, Baumgartner HR (1986) Platelet adhesion and thrombus formation on subendothelium in platelets deficient in glycoproteins IIb-IIIa, Ib and storage granules. Blood **67**, 322-330.

Werner C, Körber H, Zimmermann R, Dukhin S, Jacobasch H-J (1998) Extended electrokinetic characterisation of flat solid surfaces. Journal of Colloid and Interface Science **208**, 329-346.

Wennerberg K, Lohikangas L, Gullberg D, Pfaff M, Johansson S, Fässler R (1996) ?$_1$ Integrin-dependent and -independent polymerization of fibronectin, Journal Cell Biology **132**, 227-238.

Wetzels GMR, Koole LH (1999) Photoimmobilisation of poly(N-vinylpyrrolidone) as a means to improve haemocompatibility of polyurethane biomaterials. Biomaterials **20**, 1879-1887.

Wheeler JC, Woods JA, Cox MJ, Cantrell RW, Watkins FH, Edlich RF (1996) Evolution of hydrogel polymers as contact lenses, surface coatings, dressings, and drug delivery systems. Journal of Long Term Effects of Medical Implants **6**, 207-217.

White JD (1987) Platelet structural physiology: the ultrastructure of adhesion, secretion, and aggregation in arterial thrombosis. Cardiovascular Clinic **18**, 13-33.

Williams DF (1986) Definitions in Biomaterials. In: Proceedings of a Consensus Conference of the European Society of Biomaterials, Elsevier, Amsterdam, 3 – 5.

Williams DF, Black J und Doherty PJ (1992) Second Consensus Conference on definitions in biomaterials. In: Advances in Biomaterials, Vol. 10: "Biomaterials-Tissue Interfaces, (Doherty PJ, Williams RL, Williams DF, Lee AJC, Hrsg.), Elsevier, Amsterdam, 525-533.

Wolf H, Karwath R, Groth Th (1988) Interaction of blood with biomedical polymers – some basic aspects. In: Advances in Biomedical Measurements (Carson ER, Kneppo P und Krekule I, Hrsg.), Plenum Press, New York und London, 133 – 142.

Yasuda H, Gazicki M (1982) Biomedical applications of plasma polymerization and plasma treatment of polymer surfaces. Biomaterials **3**, 68-77.

Young BR, Pitt WG, Cooper SL (1988) Protein adsorption on polymeric biomaterials. II. Adsorption kinetics. Journal of Colloid and Interface Science **125**, 246-260.

Zamir E, Katz M, Posen Y, Erez N, Yamada KM, Katz B-Z, Lin S, Lin DC, Bershadsky A, Kam Z, Geiger B (2000) Dynamics and segregation of cell-matrix adhesions in cultured fibroblasts. Nature Cell Biology **2**, 191-196.

Zardeneta G, Mukai H, Marker V, Milam SR (1996) Protein interactions with particulate Teflon: implications for the foreign body response. Journal of Oral and Maxillofacial Surgery **54**, 873-883.

Zdrahala RJ, Zdrahala IJ. Biomedical applications of polyurethanes: a review of past promises, present realities, and a vibrant future. Journal of Biomaterials Application **14**, 67-90.

Zwaal RFA, Hemker HC (1982) Blood cell membrane and hemostasis. Haemostasis **11**, 12-39.